

# Journal of ARACHNOLOGY

PUBLISHED BY THE AMERICAN ARACHNOLOGICAL SOCIETY



# JOURNAL OF ARACHNOLOGY

**EDITOR-IN-CHIEF:** Deborah Roan Smith, University of Kansas

**MANAGING EDITOR:** Richard S. Vetter, University of California–Riverside

**SUBJECT EDITORS:** *Ecology*—Martin Entling, University of Koblenz-Landau, Germany; *Systematics*—Mark Harvey, Western Australian Museum and Michael Rix, Queensland Museum, Australia; *Behavior*—Thomas C. Jones, East Tennessee State University; *Morphology and Physiology*—Peter Michalik, Ernst Moritz Arndt University, Greifswald, Germany

**EDITORIAL BOARD:** Alan Cady, Miami University (Ohio); Jonathan Coddington, Smithsonian Institution; William Eberhard, Universidad de Costa Rica; Rosemary Gillespie, University of California, Berkeley; Charles Griswold, California Academy of Sciences; Marshal Hedin, San Diego State University; Marie Herberstein, Macquarie University; Yael Lubin, Ben-Gurion University of the Negev; Brent Opell, Virginia Polytechnic Institute & State University; Ann Rypstra, Miami University (Ohio); William Shear, Hampden-Sydney College; Jeffrey Shultz, University of Maryland; Petra Sierwald, Field Museum; Søren Toft, Aarhus University; I-Min Tso, Tunghai University (Taiwan).

The *Journal of Arachnology* (ISSN 0161-8202), a publication devoted to the study of Arachnida, is published three times each year by *The American Arachnological Society*. **Memberships (yearly):** Membership is open to all those interested in Arachnida. A subscription to the *Journal of Arachnology* and annual meeting notices are included with membership in the Society. Regular, \$55; Students, \$30; Institutional, \$125. Inquiries should be directed to the Membership Secretary (see below). **Back Issues:** James Carrel, 209 Tucker Hall, Missouri University, Columbia, Missouri 65211-7400 USA. Telephone: (573) 882-3037. **Undelivered Issues:** Allen Press, Inc., 810 E. 10th Street, P.O. Box 368, Lawrence, Kansas 66044 USA.

## THE AMERICAN ARACHNOLOGICAL SOCIETY

**PRESIDENT:** Marshal Hedin (2015–2017), San Diego State University, San Diego, California, USA.

**PRESIDENT-ELECT:** Richard Bradley (2015–2017), The Ohio State University, Columbus, Ohio, USA.

**MEMBERSHIP SECRETARY:** L. Brian Patrick (appointed), Department of Biological Sciences, Dakota Wesleyan University, Mitchell, South Dakota, USA.

**TREASURER:** Karen Cangialosi, Department of Biology, Keene State College, Keene, New Hampshire, USA.

**SECRETARY:** Paula Cushing, Denver Museum of Nature and Science, Denver, Colorado, USA.

**ARCHIVIST:** Lenny Vincent, Fullerton College, Fullerton, California, USA.

**DIRECTORS:** Charles Griswold (2015–2017), J. Andrew Roberts (2015–2017), Eileen Hebets (2016–2018)

**PARLIAMENTARIAN:** Brent Opell (appointed)

**HONORARY MEMBER:** C.D. Dondale

---

*Cover photo:* Logo of the 20th International Congress of Arachnology, held in Golden, Colorado USA, July 2–9, 2016.

---

Publication date: 13 December 2017

Ⓢ This paper meets the requirements of ANSI/NISO Z39.48-1992 (Permanence of Paper).





## Sand transport and burrow construction in sparassid and lycosid spiders

Rainer Foelix<sup>1</sup>, Ingo Rechenberg<sup>2</sup>, Bruno Erb<sup>3</sup>, Andrea Albín<sup>4</sup> and Anita Aisenberg<sup>4</sup>: <sup>1</sup>Neue Kantonsschule Aarau, Biology Department, Electron Microscopy Unit, Zelgli, CH-5000 Aarau, Switzerland. Email: r.foelix@gmx.ch; <sup>2</sup>Technische Universität Berlin, Bionik & Evolutionstechnik, Sekr. ACK 1, Ackerstrasse 71-76, D-13355 Berlin, Germany; <sup>3</sup>Kilbigstrasse 15, CH-5018 Erlinsbach, Switzerland; <sup>4</sup>Laboratorio de Etología, Ecología y Evolución, Instituto de Investigaciones Biológicas Clemente Estable, Avenida Italia 3318, CP 11600, Montevideo, Uruguay

**Abstract.** A desert-living spider sparassid (*Cebrennus rechenbergi* Jäger, 2014) and several lycosid spiders (*Evipponna rechenbergi* Bayer, Foelix & Alderweireldt 2017, *Allocosa senex* (Mello-Leitão, 1945), *Geolycosa missouriensis* (Banks, 1895)) were studied with respect to their burrow construction. These spiders face the problem of how to transport dry sand and how to achieve a stable vertical tube. *Cebrennus rechenbergi* and *A. senex* have long bristles on their palps and chelicerae which form a carrying basket (psammophore). Small balls of sand grains are formed at the bottom of a tube and carried to the burrow entrance, where they are dispersed. Psammophores are known in desert ants, but this is the first report in desert spiders. *Evipponna rechenbergi* has no psammophore but carries sand by using a few sticky threads from the spinnerets; it glues the loose sand grains together, grasps the silk/sand bundle and carries it to the outside. Although *C. rechenbergi* and *E. rechenbergi* live in the same environment, they employ different methods to carry sand. *Geolycosa missouriensis* lives in a moister habitat and produces solid sand pellets in which sand grains are caked together (without silk threads); the compact pellets are flung away from the burrow entrance by a rapid extension of the first legs. The spiders stabilize the developing tube inside by repeatedly adding silk rings, while digging down. This wall is very thin, consisting of only a few layers of crisscrossing silk threads. An excavated burrow collapses immediately, indicating that the stability is not due to the silk. Instead, the tight interconnection of neighboring sand grains—as in a vault—yields the necessary solidity to the burrow.

**Keywords:** Desert spiders, functional morphology, sand digging

Many ground-living spiders dig burrows into the soil, which they line with silk on the inside. This behavior is widespread among different spiders—in the ancient Mesothelae and Mygalomorphae as well as in the more modern Araneomorphae (e.g., in Eresidae, Filistatidae, Lycosidae, Zodariidae). Although there are several descriptions on burrow construction for certain lycosid and sparassid spiders (Gertsch 1949; Henschel 1990, 1997, 1998; Birkhofer & Moldrzyk 2003; Aisenberg & Peretti 2011; Suter et al. 2011), some aspects of the burrowing behavior and tube construction have received less attention. In particular, the question of how the soil material (mostly sand) is transported to the outside of the burrow has rarely been considered. Whereas digging in moist sand and carrying it away hardly poses a problem, it is a real challenge to transport dry sand grains. We here report how spiders living in the same habitat have solved this problem. Another difficulty for spiders living in dry sand is: how can the burrow wall be sufficiently stabilized to provide a solid tube for housing the spider? We have focused on these questions primarily in two desert spiders from Morocco (*Cebrennus rechenbergi* Jäger, 2014, Sparassidae; *Evipponna rechenbergi* Bayer, Foelix & Alderweireldt, 2017, Lycosidae) which build vertical tubes in dry sand dunes (Foelix et al. 2016; Rechenberg, unpublished data). For comparison, we also looked at some other tube-dwelling lycosids from North and South America: *Geolycosa missouriensis* (Banks, 1895) and *Allocosa senex* (Mello-Leitão, 1945). It turned out that the problem of building burrows in dry sand has been solved in different ways by different spiders.

### METHODS

Spiders were observed, photographed and filmed under natural conditions in the field (*C. rechenbergi*: sand dunes of

the Erg Chebbi desert in northern Morocco, in 2014; *A. senex*: coastal sand dunes near Salinas, Uruguay, in 2016) and additionally in the laboratory; only in the case of *G. missouriensis* did we rely on previous descriptions in the literature (Emerton 1912; Gertsch 1949; Suter et al. 2011). For morphological studies, alcohol-fixed material and exuvia were examined with light (LM) and scanning electron microscopy (SEM) (Zeiss DSM-950). Specimens were dehydrated in acetone and HMDS (hexa-methyl-di-silazane), air-dried and sputtered with gold before inspection. Small pieces of the burrow walls were inspected from the internal and the external side to understand the interactions between sand grains and silk lines. Isolated deposits of dug-out sand either in the form of sand/silk bundles (*E. rechenbergi*) or compact pellets (*G. missouriensis*) were studied with the SEM. Voucher specimens of *A. senex* were deposited in the collection of sección Entomología, Facultad de Ciencias, Uruguay (FCE Ar from 7776 to 7780), those of *C. rechenbergi* at the Senckenberg Museum Frankfurt, Germany (59794-133).

### RESULTS

When spiders are digging vertical tubes into sandy soil, they need to carry away small portions of sand all the time. This is usually done with the pedipalps and chelicerae, but different techniques are used in doing that. We first describe the method of sand transport for the sparassid *C. rechenbergi* and then compare it to the lycosid *E. rechenbergi*, which shares the same habitat in the Moroccan Erg Chebbi dunes (in a northern extension of the Sahara). For comparison, we also report our observations of some additional lycosids, namely *A. senex* from South America (Uruguay), and *G. missouriensis* from North America (Mississippi).



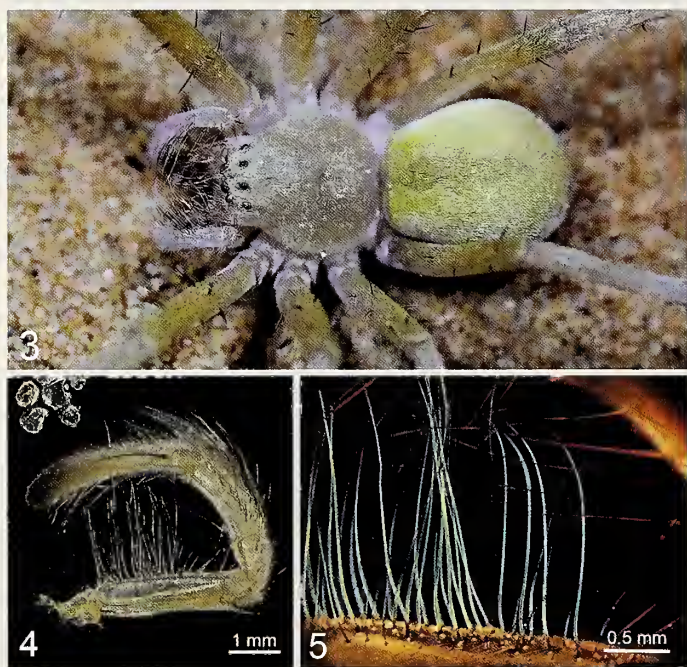


Figures 1–2.—Sand transport in the sparassid *C. rechenbergi*. 1. Spider just coming out of its burrow, carrying a load of sand. 2. Dispersing the dry sand load close to the burrow entrance. Note that the seemingly compact ball of sand disintegrates into single sand grains.

**Sand transport in the sparassid *Cebrennus rechenbergi*.**—*C. rechenbergi* (body length 2 cm) is a recently discovered desert spider that is renowned for a rapid wheeling locomotion that is used when disturbed or threatened (Rast et al. 2015; Rechenberg, unpublished data). When this spider has found a suitable spot for its burrow in a sand dune, it will turn around several times and then push together small amounts of sand with the pedipalps. A little heap of sand is thus formed that needs to be carried away (Figs. 1, 2). However, this poses a problem because the sand is absolutely dry and the sand

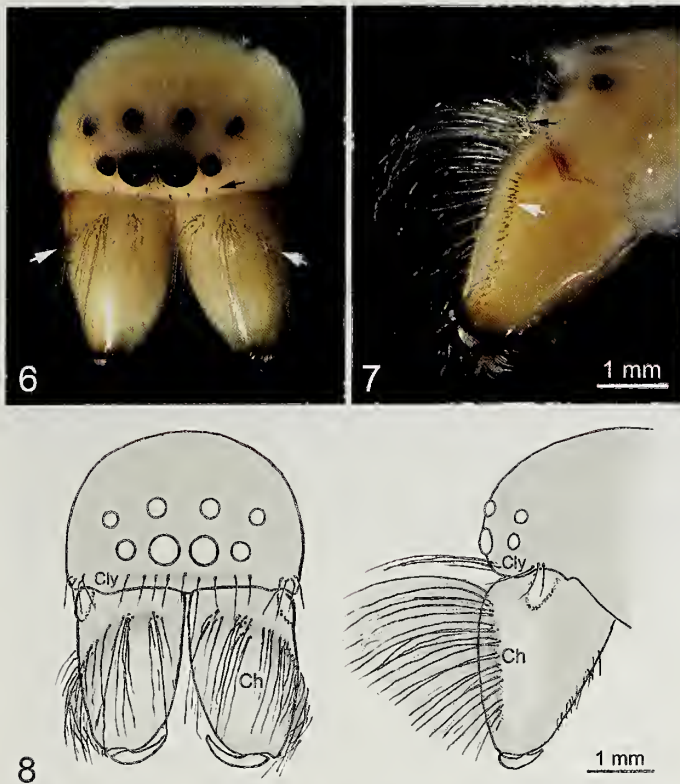
grains do not stick together. How can the spider turn the loose sand grains into a “ball” that will not fall apart during transport? A closer look at the pedipalps and chelicerae suggests an answer: long, curved bristles extending 2 mm from the dorsal and ventral sides of the pedipalps and from the frontal side of the chelicerae form a basket-like structure (Fig. 3). In particular, a bristle row on the femur of the palp overlaps a ventral bristle row of the tibia (Figs. 4, 5), thus forming a fine meshwork that is narrow enough to hold tightly the relatively large sand grains (0.3–0.6 mm). Often these long bristles also bear thousands of small surface rugosities along the hair shaft (Foelix et al. 2015), which probably enhance friction with the sand grains and thus ensure a better grip (Duncan et al. 2007). The long bristles on the pedipalps represent the lower and the lateral walls of a carrying basket, but there are similar bristles on the chelicerae and the clypeus forming an additional, inner basket (Figs. 6–8). The few bristles on the clypeus stick out horizontally (Figs. 7, 8) and can be considered as the “roof” of the carrying basket. The many long bristles on the chelicerae are arranged in three clusters of 5, 10 and 30 bristles respectively; together they form an arc that begins medially and continues downward to the lower lateral margins of the basal segments of the chelicerae (Figs. 6, 8). The spider scoops up the loose sand at the bottom of a developing tube with its pedipalps, then turns around and carries the sand load to the entrance and flicks it away. Video recordings show clearly how the “ball” of sand disintegrates immediately into single sand grains (Fig. 2), which proves that the sand grains are completely dry. The diameter of such a sand “ball” measures about 6 mm; its volume can thus be calculated as 0.1 ml. Since the average burrow of *C. rechenbergi* (2 cm diameter, 25 cm depth, see Fig. 23) has a volume of about 80 ml, this means that the spider has to make 800 runs for the construction of a single tube. This is accomplished at night and is completed in less than two hours.

**Sand transport in the lycosid *Evippomma rechenbergi*.**—Although the exact taxonomic position of this wolf spider (Fig. 9) is still under study, the genus *Evippomma* Roewer, 1959 seems fairly certain, as indicated by the typical white scales covering most of the body (Alderweireldt 1992; Figs. 10,



Figures 3–5.—Pedipalps of *C. rechenbergi*. 3. Dorsal view of a female spider showing long white bristles on chelicerae and palps, which together form a carrying basket (Photo: Bastian Rast). 4. Isolated palp with long bristles on femur and tibia. A few sand grains are pictured on the upper left for size comparison. 5. Femoral bristles (blue) overlap with tibial bristles (red) forming a narrow mesh work (Polarized light microscopy).





Figures 6–8.—Carrying basket on chelicerae and clypeus. 6. Frontal view of carapace and chelicerae. A single row of bristles is seen on the clypeus (black arrow), while several groups of long bristles form an arc on the anterior side of the chelicerae (white arrows). 7. As Fig. 6, but lateral view. 8. Summarizing drawing of figures 6 and 7. Cly, clypeus; ch, chelicerae.

11). This spider species has now been described in a paper in the same issue of this journal (Bayer et al. 2017).

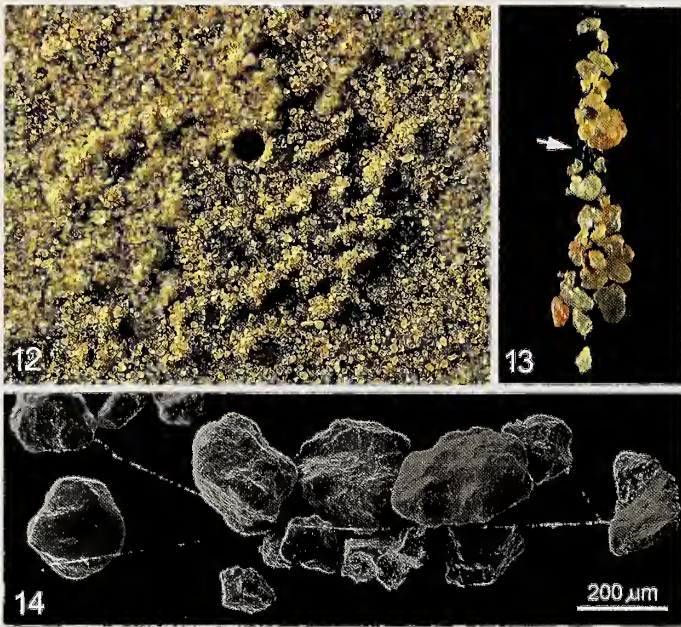
The medium-sized *E. rechenbergi* (1.5 cm body length; Fig. 9) lives in the same habitat as *C. rechenbergi* and also digs vertical burrows in the dry sand dunes. Therefore, we expected to find the same method of carrying sand as in *C. rechenbergi*. However, the pedipalps of *E. rechenbergi* do not have any long, curved bristles that could serve as a carrying basket. How then can *E. rechenbergi* solve the problem of transporting dry sand? When inspecting the immediate surrounding of its burrow entrance, small, indistinct heaps of sand become evident (Fig. 12). Carefully picking up such heaps with forceps reveals that individual sand grains are connected by fine silk threads (Fig. 13). A direct observation of the initial phases of the burrow construction shows how those silk threads come about: the spider stands above the loose sand and dabs its spinnerets briefly onto the sand grains. Then, after turning around, the front legs grab a sand/silk bundle which is quickly transported upwards and deposited around the burrow entrance. It is quite remarkable that only a few thin silk threads are needed to hold the sand grains together (Fig. 14). The connecting strands are strong enough that even large bundles can be carried away, which is often seen in immature spiders.

**Sand transport in the lycosid *Allocosa senex*.**—*Allocosa senex* is a medium-sized wolf spider (1–2 cm body length; Fig. 15) that builds vertical tubes in coastal sand dunes of South America (Aisenberg et al. 2007). Although humidity is very high in this environment, the top sand layer is usually quite dry due to the exposure to the blazing sun. Male spiders are larger than females and build deeper burrows (Aisenberg & Peretti 2011; De Simone et al. 2015). The cast of a male's



Figures 9–11.—The tube-dwelling lycosid spider *Evippomma rechenbergi*. 9. Female spider sitting in the sand of the Erg Chebbi desert in Morocco. 10. Portrait of *Evippomma rechenbergi*. Most of the body is covered with white scales. 11. Single scale under high magnification (oil immersion). Note the internal cuticular mesh work.





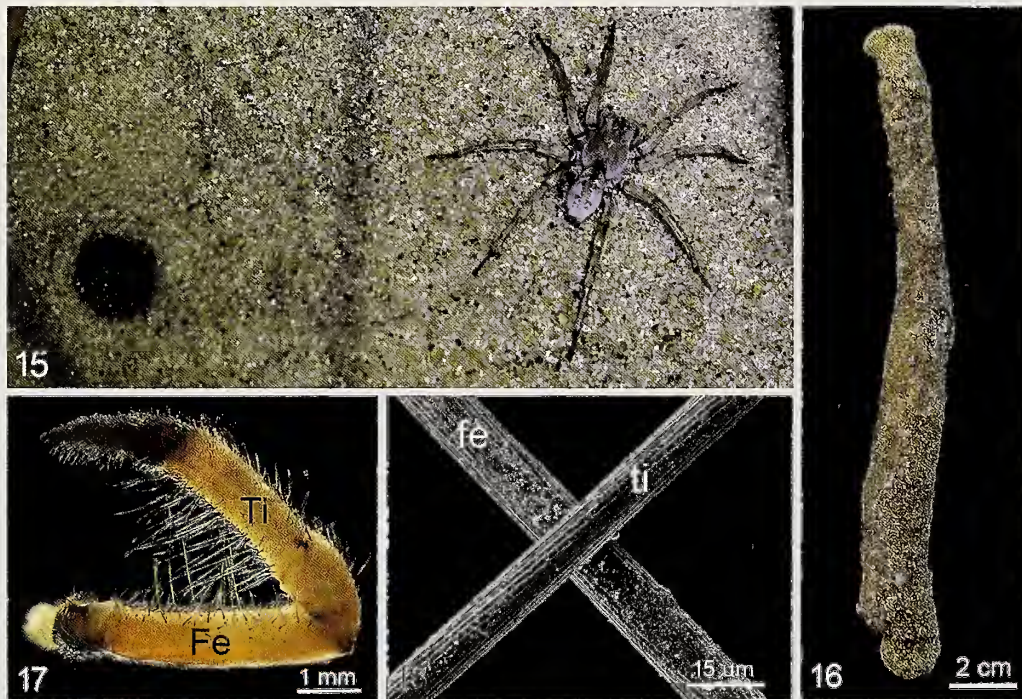
Figures 12–14.—Deposits of dug-out sand grains in *Evippomma rechenbergi*. 12. Burrow entrance with many bundles of sand and silk mixtures. 13. The silk threads become visible (arrow) when those bundles are lifted with forceps. 14. The SEM reveals how few silk lines are used to bind the dry sand grains together.

burrow shows a length of approximately 20 cm and a diameter of 1 cm at the entrance, but almost 2 cm at the bottom (Albin et al. 2015; Fig. 16). This may be of advantage when the spider needs to turn inside its tube, for instance while digging and

transporting sand or during mating, which takes place inside the male's burrow (Aisenberg et al. 2007). The morphology of the pedipalps is very similar to that described for *C. rechenbergi*, i.e., there are also long bristles (2 mm) on the femur and tibia, which overlap at almost right angles, thus forming a good meshwork for a carrying basket (Figs. 17, 18). There are also a few long bristles present on the basal segments of the chelicerae, but they are not arranged in an arc as in *C. rechenbergi* and thus cannot function as an inner carrying basket. The clypeus does not bear any long bristles.

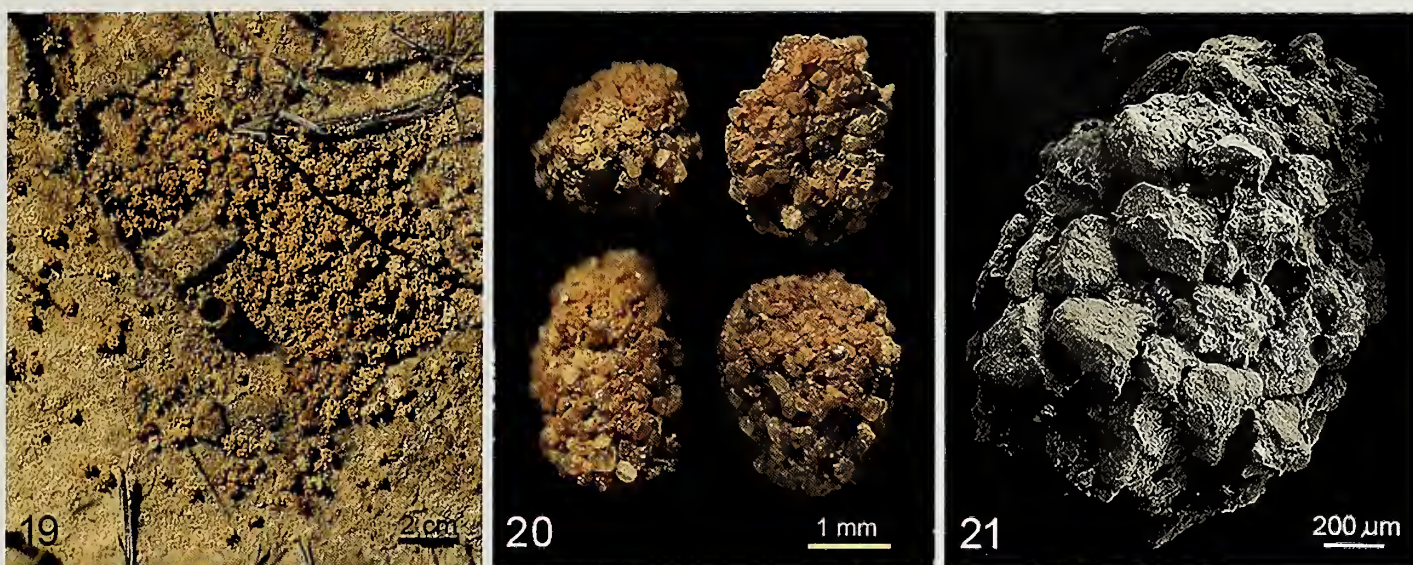
Video recordings of the beginning of a tube's construction show strong scratching movements of the front legs and then a scooping up of the loose sand with the pedipalps. At least in the initial stages, the spider moves up backward, then swings laterally and drops the sand held between the pedipalps very close to the entrance. There are no heaps of sand deposited as in *E. rechenbergi* and only occasionally are sand grains found interconnected by silk. In these rare cases, silk lines were probably added later outside the burrow entrance, but not initially for the transport of sand grains.

**Sand transport in the lycosid *Geolycosa missouriensis*.**—This medium-sized wolf spider (body length 1.5–2.2 cm) also builds vertical tubes in sandy or loamy soil, usually with a short elevated burrow entrance ("turret"; Fig. 19). In contrast to the tube-dwelling lycosids described above, *G. missouriensis* is not dealing with strictly dry sand. The surface of those sand grains is often covered with small (clay?) particles which under moist conditions probably cause sand grains to stick together. At least, this is evident in the solid pellets which *G. missouriensis* produces during burrow construction (Fig. 20). Under higher magnification, most sand grains appear to be caked together



Figures 15–18.—The tube-dwelling wolf spider *A. senex*. 15. Female spider close to a male's burrow (Photo: Marcelo Casacuberta). 16. Cast of a burrow, after filling the tube with bee's wax. Note the larger diameter of the tube at the bottom. 17. Isolated pedipalp of a male spider showing long bristles on femur (Fe) and tibia (Ti), forming a carrying basket. 18. Overlapping femoral (fe) and tibial (ti) bristles on the palp. The contact zone shows some abrasion of the femoral bristle.





Figures 19–21.—Solid sand pellets made by the wolf spider *G. missouriensis*. 19. Burrow entrance, slightly raised into a turret, surrounded by hundreds of discarded pellets (Photo: Gail Stratton). 20. Four sand pellets collected around the burrow entrance. 21. SEM-picture of a pellet, showing that sand grains are caked together but lack connecting silk threads.

by some material filling the interspaces (Fig. 21). More important, no silk threads are seen connecting the sand grains. Because we did not have access to live *G. missouriensis* spiders, we do not know exactly how these solid pellets are formed, whether it is the moisture within the tube that causes the sand grains to turn into a compact bolus, or whether the spider adds some secretion from its mouth parts. A close inspection of the pedipalps and chelicerae reveals many short hairs and bristles; however, these are not arranged as a distinct carrying basket as in *C. rechenbergi*. Still, the hairy pedipalps apparently serve well to hold a compact pellet securely, so it can be transported to the burrow entrance. Interestingly, as video-footage by Suter et al. (2011) shows,

these pellets are not simply dropped at the entrance, but are either silked into the turret or flicked far away. This is accomplished by a rapid extension (1 m/s) of the first legs that causes the pellets to fly in a long arc over a distance of 10–50 cm (Fig. 22; Suter et al. 2011).

**Vertical burrows and their construction.**—Carrying sand away is, of course, only a part in the construction process of a burrow. In the following section, we describe how such a tube is actually built and how it can be turned into a relatively stable structure that will withstand the lateral pressure from the surrounding sand. Because digging a new tube usually takes place at night and mostly below the surface, direct observations are difficult. Only the initial phases can be followed under natural conditions, later phases of the tube construction can sometimes be studied in a terrarium, if the spider happens to dig along a glass wall. We will present a general picture of tube construction based on our observations on *C. rechenbergi* but also point out differences in other tube-dwelling spiders, if known.

Any spider trying to dig a vertical tube into dry sand faces the problem that even the first shallow excavation will not be a cylinder, but inevitably a funnel, due to the loose and sliding sand grains. In order to stop the trickling of sand grains *C. rechenbergi* soon applies a ring of silk threads at the top (the later tube entrance). This ring measures about 2 cm in diameter and reaches only 1–2 mm down. The spider then scoops up a load of dry sand from the bottom of that funnel with its pedipalps and carries it quickly to the outside. After 5 to 6 of such runs, another silken ring will be added below the first one. This pattern of alternating sand transport and silk ring construction will then be repeated for about two hours until the tube has extended to a depth of 20–25 cm (Fig. 23). The consecutive addition of silk rings is still visible in a finished burrow as a fine horizontal striation of the tube wall (Figs. 24, 25). In *C. rechenbergi*, the tube always goes straight down and does not change in diameter; in contrast, in *A. senex*

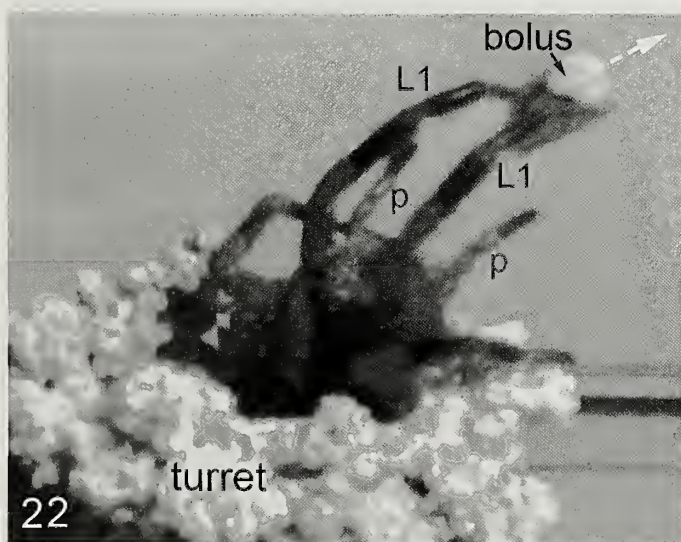
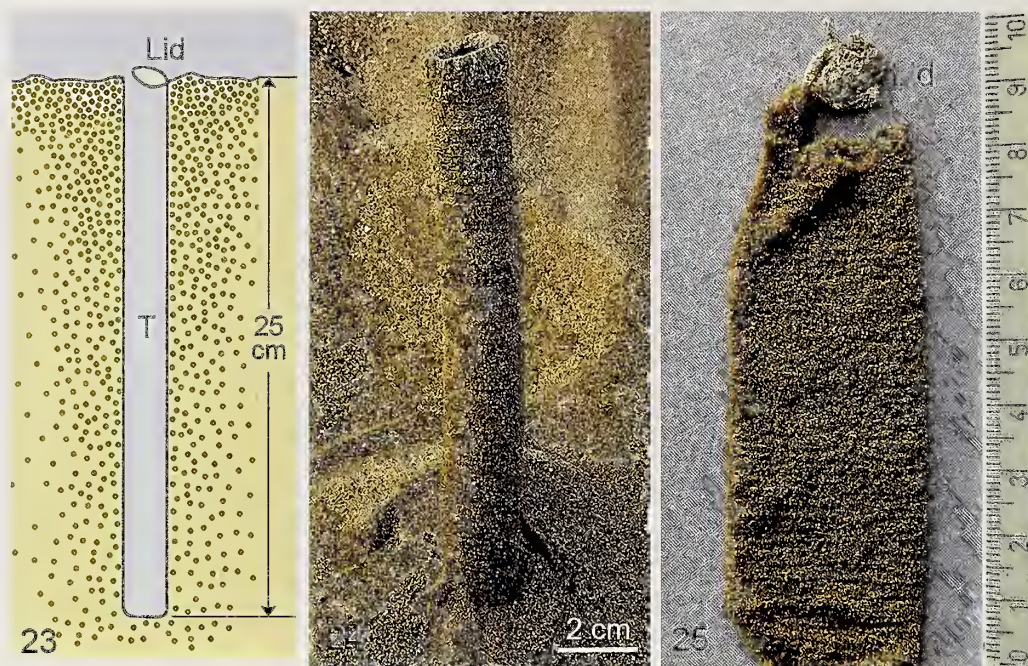


Figure 22.—Single frame from a video-film showing a *G. missouriensis* at the tube entrance (turret) throwing away a sand bolus with the front legs (L1), while the palps (p) have already released their lateral hold (Courtesy of R. Suter).





Figures 23–25.—Vertical burrow of the sparassid *C. rechenbergi*. 23. Diagram of the tube (T), which extends about 25 cm into dry sand and is covered by a thin lid. 24. This vertical burrow had been filled with dry sand, before the surrounding sand was carefully removed. This procedure was chosen to provide mechanical stability for the tube. 25. If a tube is excavated normally, as here, it will collapse immediately. Note the horizontal striation of the tube wall, which results from successively adding small silk rings during tube construction.

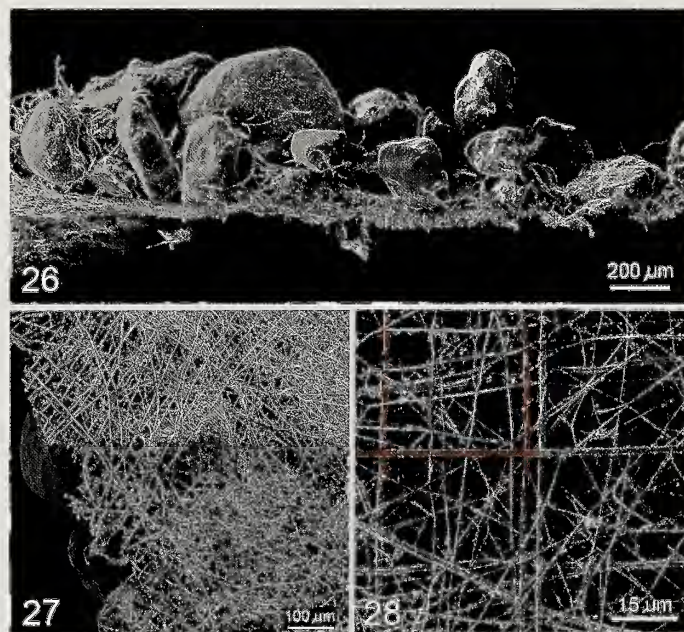
and *G. missouriensis* the tube may bulge toward the bottom (Fig. 16; Suter et al. 2011; Albin et al. 2015).

After the vertical tube is completed, *C. rechenbergi* returns to the entrance and begins the construction of a lid (Fig. 23). While the spider faces down into the tube entrance, its hind legs are stretched outside radially and then bent to pull sand grains toward the spinnerets. Long spigots apply many fine threads to weave a small blanket that is studded on top with 1–2 layers of sand grains (Fig. 26). Eventually a circular platelet (a bit less than 2 cm diameter) is formed that is hinged to the rim of the tube opening. This lid closes the burrow effectively, mostly to prevent sand from being blown into the tube, but also to keep enemies like hunting wasps outside (Stanley et al. 2013).

Under the SEM, the outside of the burrow wall shows mostly plain sand grains and only very few silk threads, whereas the inside exhibits many silk lines covering the surface of the sand grains (Figs. 27, 29–31). This silk lining is extremely thin (a few  $\mu\text{m}$ ) and each underlying sand grain can still be discerned (Fig. 27). The individual silk fibers are also of rather small diameter, ranging from 0.3–3  $\mu\text{m}$ . The thicker threads are often the result of several thinner threads fusing with each other, but that may not always be the case. In *C. rechenbergi*, it is easy to differentiate thinner and thicker threads (Figs. 28, 29), whereas the tube wall in *E. rechenbergi* consists only of thin fibers (Fig. 30). This may explain why the burrow wall is more frail in *E. rechenbergi* than it is in *C. rechenbergi*. It is difficult to say whether the structure of the tube wall has a specific pattern of silk lines or not. The basic design consists of diagonally crisscrossing silk fibers that are overlain by a large meshwork of thick fibers and a less conspicuous meshwork of thin fibers (Fig. 28). When two fibers cross each other, it seems that they are fused at the

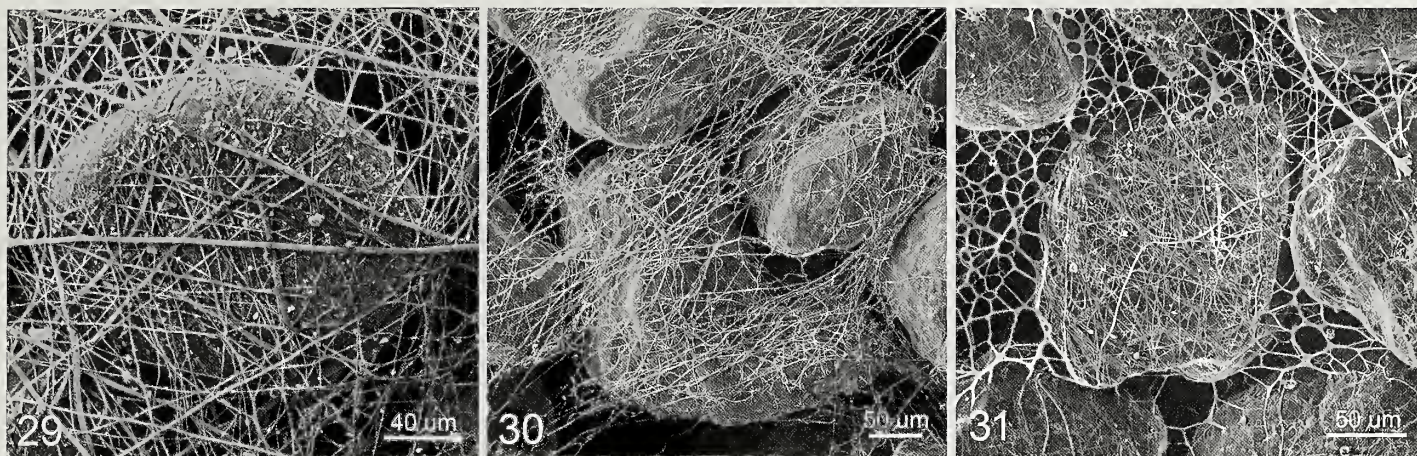
points of contact (Foelix et al. 2016), probably due to some sticky substance coating the surface of those threads.

When observing *C. rechenbergi* individuals directly while they are weaving near the tube entrances, all six spinnerets



Figures 26–28.—Structure of the burrow wall in *C. rechenbergi*. 26. Cross section of the lid in lateral view. Note that only 1–2 layers of sand grains are attached to the thin silk mat. 27. Inside of the burrow wall showing fine silk threads crossing several sand grains. 28. A high magnification of the silk lining reveals a mesh of thick fibers (marked in red) overlying a fine mesh of thin fibers (in blue).



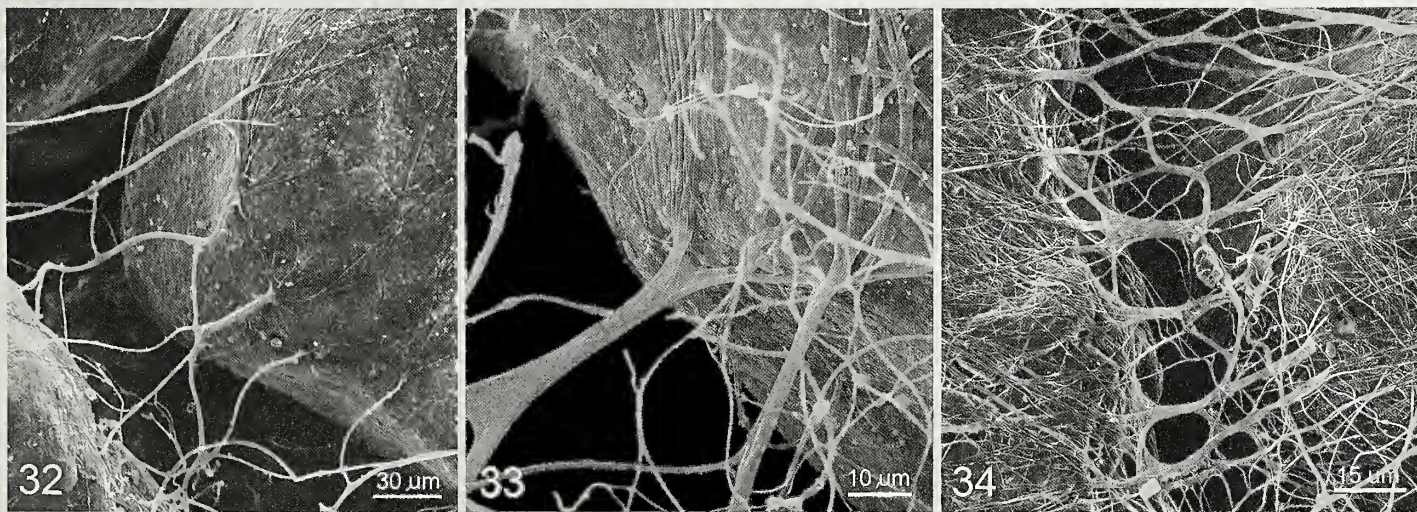


Figures 29–31.—Structure of the inner burrow wall in different spiders. 29. Tube wall of *C. rechenbergi*: thick and thin silk lines crisscross a single sand grain. 30. Tube wall of *Evippomma rechenbergi*: Mostly thin silk lines cover adjacent sand grains. 31. Tube wall of *A. senex*: The coarser webbing in the interspaces between sand grains is probably caused by moisture, which causes the threads to clump together.

seem to be in action. It was not possible, however, to determine which spinnerets or spigots produce which kinds of threads. Using video footage, it is clearly seen that the spinnerets are spread apart and pushed into the loose sand grains; and many fine silk threads seem to be squeezed out actively. It is at this moment that neighboring sand grains become interconnected. Since most spigots are rather long (500  $\mu\text{m}$ ), they can easily reach in between sand grains and thus make lateral connections (Figs. 32–34). Typically, many thin silk lines cover the surface of a sand grain but then combine into a thicker “cable” that crosses the gap to the adjacent sand grain (Fig. 33). We assume that these lateral connections are most important for providing a certain stability to the tube. It must be stressed though, that the silken burrows are very delicate, flimsy structures. The tube is most “solid” in *C. rechenbergi* (although it collapses immediately when excavated), and more frail in *E. rechenbergi*, and even more so in *A. senex*. So the question remains how any of these silken tubes can be stable enough to withstand the lateral

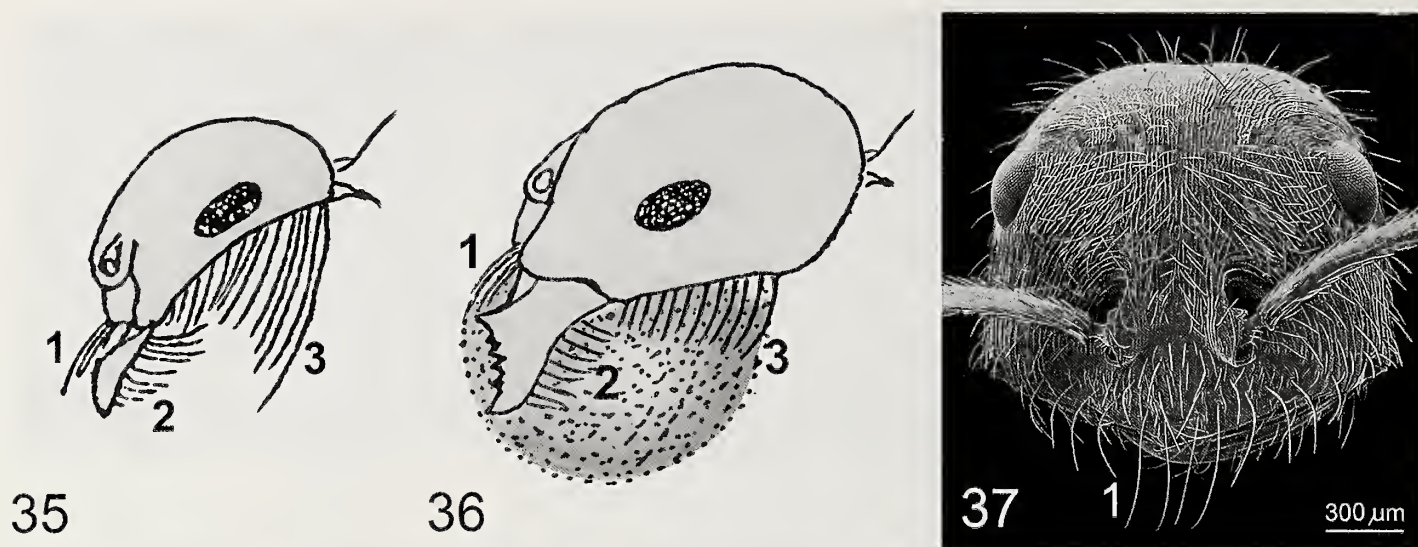
pressure from the surrounding sand, and how a spider can climb up and down such a delicate tube wall.

Some experiments with Moroccan desert sand probably provide the right answer: an aluminum rod (15 mm diameter) was covered with thin (10  $\mu\text{m}$ ) household foil and then gently pushed vertically into the dry sand to a depth of 20 cm. When this rod was carefully pulled out, the remaining foil soon became compressed due to the lateral pressure of the surrounding sand. In a second experiment, a diluted solution of wallpaper glue was thinly brushed onto the outer surface of the foil before the rod was pushed into the soil. After several hours the glue had hardened and when the rod was now withdrawn, the tube (foil) was perfectly stable. Even when the surrounding sand was removed, the foil tube stood free as a vertical cylinder (compare Fig. 24), only covered by a single layer of sand grains on its surface. This means that the mechanical stability of the tube is not due to the foil but to the interconnected sand grains around the tube (similar to the stones in a vault). By analogy, we conclude that the silk tube



Figures 32–34.—Silk fibers connecting neighboring sand grains arise from very fine threads on the surface of a sand grain, which then coalesce into thicker fiber bundles. 32. Tube wall of *C. rechenbergi*. 33. Same as in Fig. 25, but in higher magnification (Photo: A. C. Joel). 34. Tube wall of *A. senex*.





Figures 35–37.—Sand carrying baskets (psammophores) in African desert ants. 35. The harvester ant *Messor caviceps* (Forel, 1902) bears long bristles on the clypeus (1), mandibles (2) and inferior side of its head (3), which together form a basket. 36. *Messor arenarius* (Fabricius, 1787), carrying a pellet of moist sand (after Santschi 1909). 37. Portrait of the Namibian desert ant *Ocymyrmex robustior* (Stitz, 1923) showing the clypeal bristles (1) of its psammophore. Figures 35 and 36 modified after Santschi (1909).

of sand-dwelling spiders likewise owes its stability to the continuously connected sand grains on the outside of the tube, but not to the silk tube itself.

## DISCUSSION

Our study of how sand-dwelling spiders can transport sand during burrow construction has yielded several interesting results: (1) Some species (*C. rechenbergi*, *A. senex*) developed long curved bristles on the pedipalps and chelicerae which together act as a carrying basket for dry sand. (2) Another species (*E. rechenbergi*) lacks such a basket but uses silk threads to connect sand grains before transporting the resulting sand/silk bundles. (3) Still another species (*G. missouriensis*) produces solid sand pellets, probably caked together by moisture, that are flung away from the burrow entrance (Emerton 1912; Suter et al. 2011). Thus, different methods apparently evolved in different spiders, even in exactly the same habitat (Erg Chebbi dunes, Morocco) and even within the same family (Lycosidae). It is remarkable, that on one hand the same method of sand transport (i.e., connecting sand grains with silk lines) evolved independently in sparassids and lycosids and, on the other hand, three kinds of sand transport developed within the lycosids.

There are few descriptions of other sand-dwelling spiders in the literature. The sparassids *Cebrennus villosus* (Jézéquel & Junqua, 1966) and *May bruno* Jäger & Krehenwinkel, 2015 seem to use a “sand basket” (Jäger 2000, 2014; Jäger & Krehenwinkel 2015) very similar to that described above for *C. rechenbergi*. The South American wolf spider *A. senex*, which digs vertical tubes in coastal sand dunes (Aisenberg et al. 2007; Aisenberg & Peretti 2011; De Simone et al. 2015), has a “sand basket” like *C. rechenbergi*, yet less developed (cheliceral bristles are reduced). In contrast, the large sparassid species *Cerbalus* Simon, 1897, which also live in tubes in sand deserts, lack such a carrying basket, but carry sand/silk

bundles to the outside (Henschel 1998; Rechenberg, unpublished data).

It should be mentioned that very similar “sand baskets” (psammophores) are known from certain sand-digging insects, e.g., in ants (Wheeler 1907; Santschi 1909) and in wasps (Evans & West-Eberhard 1970). Initially, Wheeler had suggested that the long curved bristles on the ant’s mouthparts would serve to transport liquid droplets, but then Santschi could prove that they enclosed little sand pellets (Figs. 35–37). In fact, it was Santschi who coined the term *psammophores* for such miniature sand-carrying devices. Whereas Santschi claimed that harvester ants would carry little pellets (“*boulettes*”) of moist sand, it was later shown that psammophores work even better when transporting dry sand (Porter & Jorgensen 1990). To our knowledge our study is the first to demonstrate the presence of psammophores in spiders; it seems they are mainly adapted for handling dry sand. A comparison of the psammophore in a spider (Fig. 8) and an ant (Figs. 34, 35) also shows how the long curved bristles occur in similar positions, each group forming one wall of the “sand basket”. The interesting point is that such psammophores have evolved independently in insects and in spiders.

After having found a psammophore in *C. rechenbergi*, we expected the same method for carrying dry sand in *E. rechenbergi*, since it lives in the same environment. Surprisingly, however, *E. rechenbergi* does not have any specialized pedipalps (“sand baskets”) but uses a completely different technique, namely connecting loose sand with a few silk threads; the resulting sand/silk bundles are then carried to the outside of the burrow. It is amazing how little silk is needed to bind several sand grains together – even under the microscope, it is difficult to detect the few silk lines (Figs. 13, 14). Incidentally, we were not the first to discover this unusual technique: Emerton (1912) gave a detailed description for several species of *Geolycosa*: “...The digging is done by covering the sand with silk enough to hold the grains together



and it is then gathered into pellets of convenient size and carried in the mandibles to the mouth of the burrow, where it is thrown outward by the ends of the front feet. . .". Unfortunately, after looking at those pellets of *G. missouriensis* with the SEM, we did not find any connecting silk lines (Fig. 21); instead, neighboring sand grains seemed to be caked together by some clay material. For producing rather solid pellets, some moisture seems necessary, but we do not know whether it stems from moisture inside the tube or whether the spider adds some liquid from its mouth parts. Although the latter possibility is a tempting idea, this is not very likely considering that *G. missouriensis* produces over 900 pellets when excavating a single tube (Suter et al. 2011). It remains a bit puzzling though that Emerton described quite correctly the flicking away of the pellets from the burrow entrance (Suter et al. 2011) but claimed that silk threads were holding the sand grains together. Perhaps Emerton studied wolf spiders that were living in a rather dry habitat and eventually those used the same technique as *E. rechenbergi*. The palps of *G. missouriensis* do not have a distinct psammophore, i.e., they lack the long curved bristles. This is understandable because this spider carries the sand as solid pellets rather than loose and dry sand grains.

The construction of the vertical silk tube could only be studied in its initial phases when the spider is still visible close to the surface. Most observations were made on the sparassid *C. rechenbergi* but probably also apply to lycosids. The typical technique starts with a silken ring laid down at the later tube entrance, then carrying out several loads of sand from the bottom of the pit to the surface, followed by another silken ring added at a slightly deeper level. From video-films, we gain the impression that all spinnerets are involved in weaving the silken tube. It is noteworthy that the spigots located terminally on each spinneret can spread like a fan while at the same time squeezing out many fine threads. Most likely this is done by a hydrostatic pressure increase inside the opisthosoma. Due to the considerable length of most spigots (500 µm) they can reach deep between the sand grains and thus make strong lateral connections (Figs. 32–34). Most likely those “bridging threads” are responsible for the mechanical stability of a burrow. The many fine threads making up the inner silken lining must also provide some strength but probably serve more to facilitate the spider’s climbing up and down the burrow wall.

It has been pointed out that rather little silk is used for the silken tube (Marshall 1995); and indeed a macroscopic inspection reveals only a very thin silk mat. However, under the SEM even the most delicate silk tubes (Figs. 30, 31) reveal easily a hundred thin threads covering a single sand grain. Whether weaving an entire silken tube is a costly process in terms of energy, is hard to say, because physiological data are lacking. In *C. rechenbergi*, a newly built tube lasts for about one month, before it is replaced; if it is damaged, e.g., due to a sand storm, the spider readily and quickly repairs its tube, or will build a new one. In *G. missouriensis*, it is assumed that the spider stays practically all her life in the same burrow (Wallace 1942) and only maintains and enlarges the tube; the energy expense for silk production thus seems limited.

There are, of course, many other tube-dwelling spiders that have hardly been studied with respect to their tube construction and their method of carrying sand. For example, *Lutica*

Marx, 1891 (Zodariidae) living in the coastal sand dunes of California also builds silk-lined tubes (Ramirez 1995), but little is known about its sand transport and tube construction. It would be quite interesting to find out whether it uses the same—or different—methods as *A. senex* inhabiting the sand dunes of the Atlantic coast in South America (Aisenberg & Peretti 2011; De Simone et al. 2015). Even more interesting would be to find out whether environmental factors (e.g., soil humidity) could determine which sand carrying technique is used, or if the same species can employ different methods when faced with different environmental conditions.

## ACKNOWLEDGMENTS

We are grateful to several colleagues and institutions who supported this study: Robert Suter and Gail Stratton supplied us with data and *Geolycosa* material from Mississippi, USA, and Yael Lubin with *Lycosa* sp. from Israel. Abdullah Regabi El Khayari was very supportive in the field studies in the Moroccan sand dunes and Miguel Simó and Rodrigo Postiglioni likewise with *Allocosa* material in Uruguay. Steffen Bayer, Mark Alderweireldt and Luis Piacentini gave good advice with respect to the taxonomic position of *Evippomma*; Rüdiger Wehner and William Eberhard drew our attention to the psammophores in desert ants and wasps; Jerome Rovner and Wolfgang Schröer critically read our manuscript; and the Neue Kantonsschule Aarau granted free access to their electron microscopes. A. Aisenberg acknowledges funding by PEDECIBA and SNI (ANII), Uruguay.

## LITERATURE CITED

- Aisenberg, A. & A.V. Peretti. 2011. Male burrow digging in a sex-role reversed spider inhabiting water-margin environments. *Bulletin of the British Arachnological Society* 15:201–204.
- Aisenberg, A., C. Viera & F.G. Costa. 2007. Daring females, devoted males, and reversed sexual size dimorphism in the sand-dwelling spider *Allocosa brasiliensis* (Araneae, Lycosidae). *Behavioral Ecology and Sociobiology* 62:29–35.
- Albin, A., M. Simó & A. Aisenberg. 2015. Characterisation of burrow architecture under natural conditions in the sand-dwelling wolf spider *Allocosa brasiliensis*. *Journal of Natural History* 50:201–209.
- Alderweireldt, M. 1992. A taxonomic revision of the African wolf spider genus *Evippomma* Roewer, 1959 (Araneae, Lycosidae). *Journal of African Zoology* 106:153–167.
- Bayer, S., R. Foelix & M. Alderweireldt. 2017. An unusual new wolf spider species from the Erg Chebbi Desert in Morocco (Araneae: Lycosidae: Evippinae). *Journal of Arachnology* 45:344–355.
- Birkhofer, K. & U. Moldrzyk. 2003. Burrow construction in three Tunisian desert spiders (Araneae: Sparassidae, Lycosidae, Filistatidae). *Kaupia Darmstädter Beiträge zur Naturgeschichte* 121:111–118.
- De Simone, G.A., A. Aisenberg & A.V. Peretti. 2015. Female and juvenile burrow digging in *Allocosa brasiliensis*, a South American sand-dwelling wolf spider. *Arachnology* 16:276–280.
- Duncan, R.P., K. Autumn & G.J. Binford. 2007. Convergent setal morphology in sand-covering spiders suggests a design principle for particle capture. *Proceedings of the Royal Society of London B* 274:3049–3056.
- Emerton, J.H. 1912. Four burrowing *Lycosa* (*Geolycosa* Montg., *Scaptocosa* Banks) including one new species. *Psyche* 19:25–36.
- Evans, H.E. & M.J. West-Eberhard. 1970. *The Wasps*. The University of Michigan Press, Ann Arbor.
- Foelix, R., I. Rechenberg, B. Erb & A.C. Joel. 2015. Zum Sandtran-



- sport der Radlerspinne *Cebrennus rechenbergi* (Jäger 2014). *Arachne* 20:14–21.
- Foelix, R., I. Rechenberg, B. Erb & A.C. Joel. 2016. Über den Bau der Wohnröhren bei wüstenlebenden Spinnen. *Arachne* 21:4–17.
- Gertsch, W.J. 1949. *American Spiders*. D. van Nostrand Co., Toronto, New York, London.
- Henschel, J.R. 1990. The biology of *Leucorchestris arenicola* (Araneae: Heteropodidae), a burrowing spider of the Namib dunes. Pp. 115–127. *In* Namib Ecology 25 Years of Namib Research. (M.K. Seely, ed.). Transvaal Museum Monograph No. 7 Transvaal Museum, Pretoria.
- Henschel, J.R. 1997. Psammophily in Namib desert spiders. *Journal of Arid Environments* 37:695–707.
- Henschel, J.R. 1998. Dune spiders of the Negev desert with notes on *Cerbalus psammodes* (Heteropodidae). *Israel Journal of Zoology* 44:243–251.
- Jäger, P. 2000. The huntsman spider genus *Cebrennus*: four new species and a preliminary key to known species. *Revue Arachnologique* 13:163–186.
- Jäger, P. 2014. *Cebrennus* Simon, 1880 (Araneae: Sparassidae): a revisionary up-date with the description of four new species and an updated identification key for all species. *Zootaxa* 3790:319–356.
- Jäger, P. & H. Krehenwinkel. 2015. *May* gen. n. (Araneae: Sparassidae): a unique lineage from Southern Africa supported by morphological and molecular features. *African Invertebrates* 56:365–392.
- Marshall, S.D. 1995. Natural history, activity patterns, and relocation rates of a burrowing wolf spider: *Geolycosa xera archboldi* (Araneae, Lycosidae). *Journal of Arachnology* 23:65–70.
- Porter, S.D. & C.D. Jorgensen. 1990. Psammophores: Do harvester ants (Hymenoptera: Formicidae) use these pouches to transport seeds? *Journal of the Kansas Entomological Society* 63:138–149.
- Ramirez, M.G. 1995. Natural history of the spider genus *Lutica* (Araneae, Zodariidae). *Journal of Arachnology* 23:111–117.
- Rast, B., I. Wendt, G. Ackermann & M. Hüsler. 2015. *Cebrennus rechenbergi* – Akrobatik in der Wüste. *Arachne* 20:4–13.
- Santschi, F. 1909. Sur la signification de la barbe des fourmis arénicoles. *Revue Suisse de Zoologie* 17:449–458.
- Stanley E., C. Toscano-Gadca & A. Aisenberg. 2013. Spider hawk in sand dunes: *Anoplus bichuctus* (Hymenoptera: Pompilidae), a parasitoid wasp of the sex-role reversed spider *Allocosa brasiliensis* (Araneae: Lycosidae). *Journal of Insect Behavior* 26:514–524.
- Suter, R.B., G.E. Stratton & P.R. Miller. 2011. Mechanics and energetics of excavation by burrowing wolf spiders, *Geolycosa* spp. *Journal of Insect Science* 11:22 doi:10.1673/031.011.0122
- Wallace, H.K. 1942. A revision of the burrowing spiders of the genus *Geolycosa* (Araneae, Lycosidae). *American Midland Naturalist* 27:1–62.
- Wheeler, W.M. 1907. On certain modified hairs peculiar to the ants of arid regions. *The Biological Bulletin* 13:185–202.

*Manuscript received 2 September 2016, revised 29 November 2016.*



## Exploring the chemo-textural familiarity hypothesis for scorpion navigation

Douglas D. Gaffin and Brad P. Brayfield: Department of Biology, University of Oklahoma, Norman, OK 73019 USA;  
E-mail: ddgaffin@ou.edu

**Abstract.** The navigation by scene familiarity hypothesis provides broad explanatory power for how bees and ants navigate from the hive to distant food sources and back. The premise is that the visual world is decomposed into pixelated matrices of information that are stored and readdressed as the insects retrace learned routes. Innate behaviors in these insects (including learning walks/flights and path integration) provide the important goal-directed views to allow the initial retracing (i.e., the insect must learn the scene while moving toward the goal because everything looks different while moving away). Scorpion navigation may use a similar premise, with the chemical and textural features of the environment substituting for visual input. Scorpion pectines support thousands of chemo- and mechano-sensitive units called peg sensilla, each containing at least 10 energetically expensive sensory neurons. We have long wondered why pectines have so many pegs and associated neurons. Many sand scorpions emerge onto the surface from their home burrows at night to pursue insect prey and somehow find their way back to their burrows. Based on the measured resolution of peg sensilla, we have calculated that sufficient information exists in sand's texture to enable scorpions to retrace previously experienced paths with little to no chance of confusion. Preliminary evidence of learning walks and path integration in scorpions is also congruent with the navigation by chemo-textural familiarity hypothesis.

**Keywords:** Behavior, electrophysiology, homing, sensory, pectines

Scorpion pectines are ornate, ground-facing chemosensory appendages (Cloudsley-Thompson 1955) that support tens of thousands of chemo-tactile sensilla called “pegs” (Foelix & Müller-Vorholt 1983; Gaffin & Brownell 1997, 2001; Wolf 2008). A lingering question is: Why are there so many pegs? Here, we offer a novel chemo-textural familiarity hypothesis for pecten function. We propose that scorpions may use their pectines to acquire and process ground-based chemical and textural information and use it to recapitulate learned routes to their home burrows.

We derived this idea from the *Navigation by Scene Familiarity Hypothesis* (NSFH) proposed for homing insects (Baddeley et al. 2012). The premise is that a foraging animal, such as a bee or an ant, uses its compound eyes to acquire matrices of visual information while moving toward a goal. Then, during retracing runs, the animal moves in a direction that minimizes the pixel-by-pixel difference between its current retinal view and the views it previously stored in memory. This simple behavioral rule is elegant and congruent with the limited neural capacity of an insect's brain. The animal is not burdened with memorizing long sequences of scenes. Rather, it exploits the inherent stability and visual richness of natural scenes to help it retrace its original path (Gaffin et al. 2015).

Similarly, we suggest that scorpions might use their pectines to acquire and store matrices of chemical and textural information during homebound journeys and use these memories to retrace paths by moving in a direction that minimizes differences between current pecten “glimpses” and those in memory. However, for this mechanism to be viable, three prerequisites should be met. First, the scorpion needs sufficient sensory receptors to detect and encode appropriate environmental complexity. Second, the environment needs to be sufficiently complex to not confuse the animal in areas with similar patterns. And finally, the animal must have a way to acquire goal-directed information, such as through innate behaviors like path integration (Müller & Wehner 1988) and/or learning walks (Wehner et al. 2004). Here we draw parallels

between what is known for insect navigation by visual familiarity and mounting evidence suggesting that scorpions might navigate by chemo-textural familiarity.

**Sufficient sensory receptors.**—For the NSFH to be plausible, sensor resolution must suit the complexity of the animal's environment. In insects, dense packing of light-sensing units called ommatidia enable high resolution. Each ommatidium is directed at its own blurred piece of the visual world; together, ommatidia give the compound eyes a semi-panoramic view of the world (Seidl & Kaiser 1981). The number of ommatidia per eye is impressive. Desert ants have about ~500 (Schwarz et al. 2011), houseflies ~3500 (Sukontason et al. 2008), honeybees ~5,500 (Seidl & Kaiser 1981), and dragonflies ~24,000 ommatidia in each eye (Pritchard 1966)! Consider a desert ant and the 1000 ommatidia that combine to compose her two eyes. If each ommatidium is configured to respond in only two states—“off” if its face is mostly dark and “on” if mostly light—then the number of uniquely detectable patterns is  $2^{1000}$ . Of course, this number of patterns would multiply significantly if the number of detectable states extends to multiple gray levels and/or to colors.

A legitimate question would be how this pattern-detection potential compares to the number of scenes an insect experiences. Worker ants forage for a couple of months. If we assume an individual forages full time (day and night), and her eyes capture frames at 60 per second (Srinivasan & Lehrer 1984), she would experience about 300 million glimpses in her lifetime (24 h/day  $\times$  60 min/h  $\times$  60 s/min  $\times$  60 glimpses/s). Simply put, the pattern detection potential of an ant's eyes is hundreds of orders of magnitude greater than the number of scenes she experiences.

Scorpion pectines also possess a high degree of sensor resolution. The pectines are divided into a species-dependent number of teeth, ranging from a half dozen in some members of the Chactidae (Swoveland 1978) to nearly 40 in some male Vaejovidae (Gaffin & Brownell 2001). Each tooth supports an array of minute, chemo-tactile sensitive peg sensilla on its



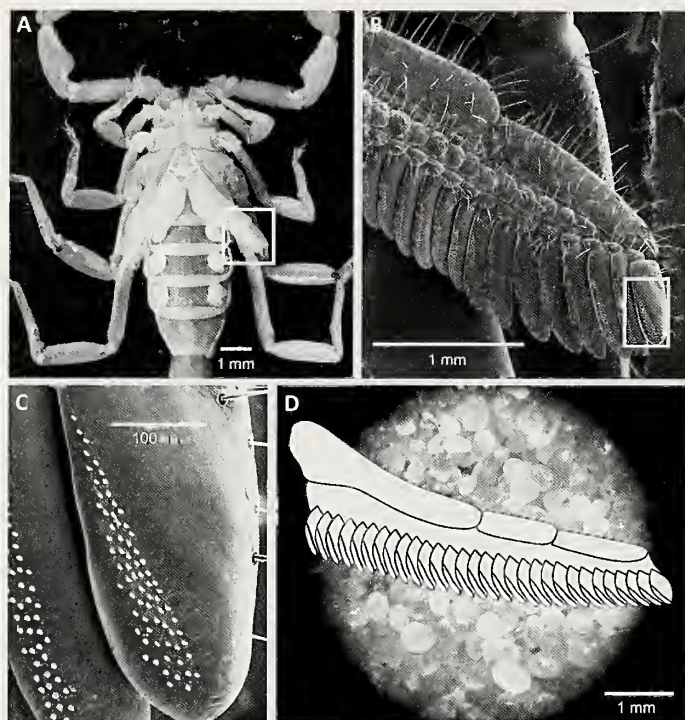


Figure 1.—Scorpion pectines have sufficient sensory receptors. (A) Ventral view of a male *P. utahensis* shows the paired pectines extending laterally from the ventral mesosoma. (B) Expanded view from (A); each pecten is composed of a series of teeth. (C) Expanded view from (B); each tooth has dense patches of minute peg sensilla. (D) Size of a male *P. utahensis* pecten relative to sand grains from the animal's native west Texas habitat. [1(B) and 1(C) provided by Elise Knowlton.]

distal, ground-directed surface (Fig. 1). Like the ommatidia of insect eyes, the number of peg sensilla on pectinal teeth is impressive. The number of pegs varies by species from tens to hundreds per tooth and from hundreds to tens of thousands across the two pectines (Gaffin & Brownell 2001). We have estimated that female *Paruroctonus utahensis* (Williams, 1968) have approximately 12,500 pegs/mm<sup>2</sup>, which translates to tens to hundreds of pegs per grain of sand in the perceived environment (Gaffin & Walvoord 2004).

The pegs are richly innervated by populations of sensory neurons. Each peg contains at least one mechanosensitive neuron that responds to peg deflection (Hoffmann 1964; Foelix & Müller-Vorholt 1983; Gaffin & Brownell 1997; Gaffin 2002; Melville 2000). Most peg neurons (10 or more) have typical chemosensory characteristics based on morphological accounts (Foelix & Müller-Vorholt 1983). Judged by their single, slit-shape terminal pore, peg sensilla are best classified as contact chemoreceptors. Peg neurons show broad response profiles to near-range stimulation by a variety of volatile organic compounds (Gaffin & Brownell 1997) or by direct contact of chemicals with the peg tip (Knowlton & Gaffin 2011). In short, scorpion pectines have the neural potential to detect enormous numbers of unique chemotextural surface patterns.

If we are to understand how information is relayed and processed in the scorpion brain, it will be useful to develop electrophysiological techniques to record along specific parts

Table 1.—Potential number of unique response patterns of scorpion pectines, given various numbers of teeth and neural response states ( $n$  = no. of teeth).

# of teeth / pecten	# of teeth / 2 pectines	Number of unique patterns at 2, 10, & 100 response states		
		2 states (2 <sup>n</sup> )	10 states (10 <sup>n</sup> )	100 states (100 <sup>n</sup> )
20	40	~10 <sup>12</sup>	10 <sup>40</sup>	10 <sup>80</sup>
25	50	~10 <sup>15</sup>	10 <sup>50</sup>	10 <sup>100</sup>
30	60	~10 <sup>18</sup>	10 <sup>60</sup>	10 <sup>120</sup>
35	70	~10 <sup>21</sup>	10 <sup>70</sup>	10 <sup>140</sup>
40	80	~10 <sup>24</sup>	10 <sup>80</sup>	10 <sup>160</sup>

of the pectinal neural pathway. Currently, we hypothesize that the unit of information is the individual pectinal tooth rather than the individual peg. Morphological tracings of pectinal neurons to the scorpion's subesophageal ganglion show that a topological arrangement is maintained at that level (Brownell 1998). That is, the order of the teeth on each pecten spine appears to be preserved in the brain, where the pectinal nerve terminates prior to subsequent secondary neural processing. Enormous amounts of information are still available, even if peg responses are averaged across the breadth of each tooth, and such blurring of resolution could help compensate for environmental disturbance. Table 1 shows sample combinations of pecten tooth configurations and different assumptions for neural response states (2, 10, and 100 states) in the brain. For example, an animal with only 20 teeth per pecten (i.e., 40 teeth across both pectines) and a simple all-or-none (2-state) response rule, can detect 10<sup>12</sup> different patterns. If the number of response states increases to 10, then the number of resolvable patterns grows to 10<sup>40</sup>. Eighty pectinal teeth and 100 response states could accommodate 10<sup>160</sup> different patterns!

**Sufficient environmental complexity.**—For accurate navigation by scene familiarity to be plausible, the environment must contain enough information that the animal will not get lost or confused by moving toward a similar-looking (or similar-tasting) but incorrect scene. When natural scenes (be they visual, chemical, or textural) are transformed to pixelated matrices, the chance that any two scenes will be alike must be extremely remote.

When considered from the pixelated matrices of an insect's eye, the world is rich in visual information. This content can be assessed by transforming scenes to matrices of various dimensions and calculating the summed absolute pixel-by-pixel differences among the scenes (Zeil et al. 2003; Baddeley et al. 2012; Narendra et al. 2013; Gaffin et al. 2015; Gaffin & Brayfield 2016). An individual scene compared to all other scenes produces a volcano-shaped plot. The focal scene forms the volcano's pit (subtracting a matrix of pixels from itself yields zero) and the summed difference values that vary directly with distance, form the caldera's slopes (Zeil et al. 2003; Narendra et al. 2013). Extending this type of analysis to a path of images produces a canyon-shaped plot, where the river bottom reflects the self-subtraction of the path scenes and the slopes reflect the increasing differences with distance from the path. Using this information, autonomous agents can be



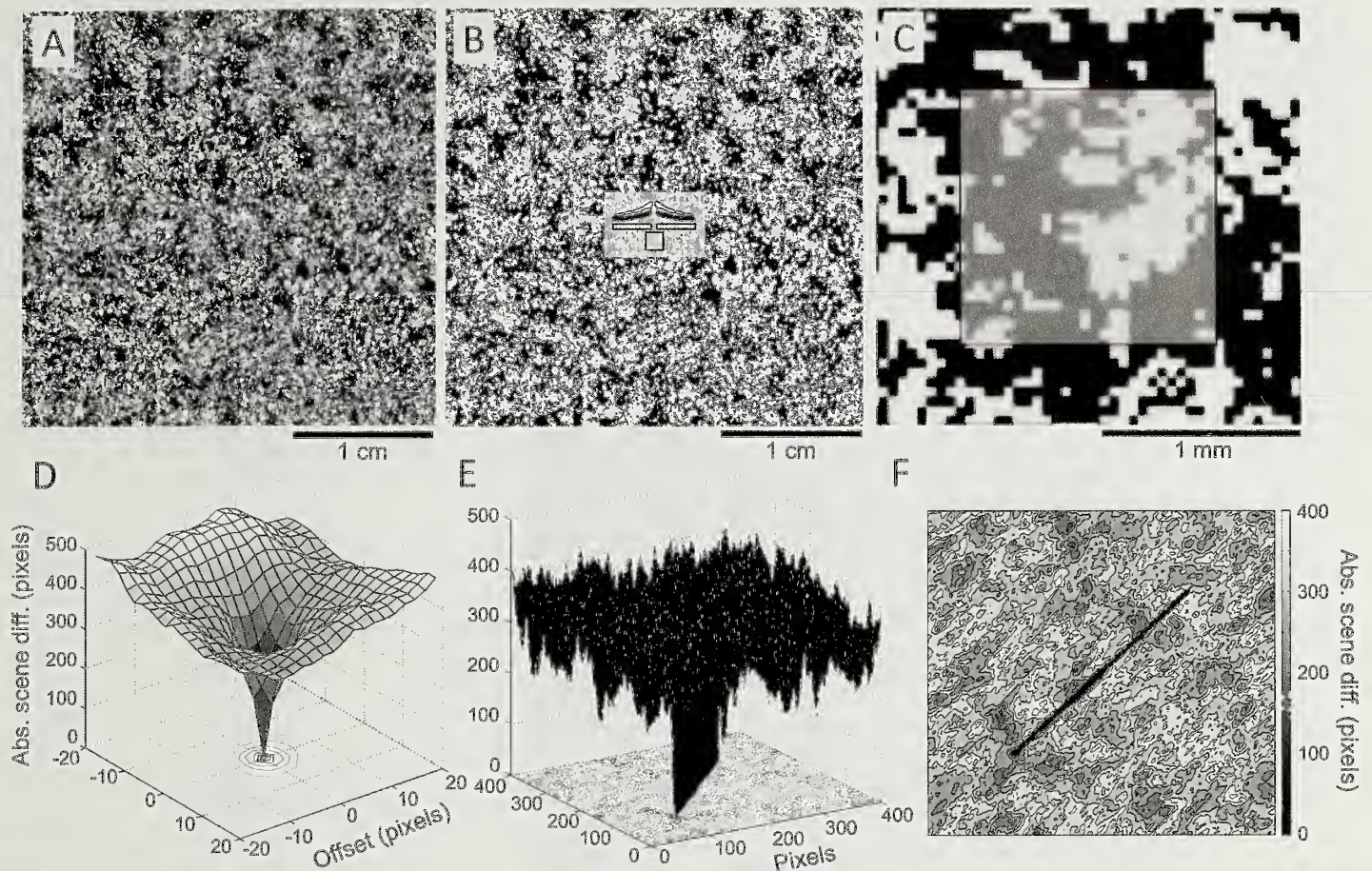


Figure 2.—Analysis of textural information content. (A) High contrast photography was used to estimate sand textural information. Sand from Monahans State Park (TX) was placed in a Petri dish and illuminated by light directed from the side at  $30^\circ$  to the sand surface. We took 100 random photographs of the sand using a 40x power dissecting scope. We used a MATLAB script to import, turn to gray, crop to squares representing 3x3 mm of sand surface, enhance the contrast, and reduce the resolution to 335x335 pixels for each of the 100 images. This resolution value was derived by multiplying the peg sensilla density of 12,500 per  $\text{mm}^2$  (Gaffin & Walvoord 2004) by  $9 \text{ mm}^2$  and taking the square root. We randomly rotated and concatenated the squares to produce a  $10 \times 10$  matrix of these images composed of 11,222,500 pixels in a 3350x3350 square. Using a value of eight pegs for chemical discrimination (Knowlton & Gaffin 2011), the number of pixels was reduced to 1,402,813 in the square ( $11,222,500/8$ ). The square root of this number produces a matrix of 1184 pixels on each side. (B) We changed the image to black and white and superimposed a drawing of the pectines to show relative scale. The two rectangles indicate the area of the peg fields, and these have been combined into the square below (area  $\sim 1.5 \text{ mm}^2$ ). (C) Expansion of area around the square from (B). This square is 30 pixels on a side, which represents our sensor resolution based on the resolving power of peg sensilla. (D) Image difference volcano indicates that the focal scene is different from all other scenes in a 1600-pixel area. Surface (E) and contour (F) plots of difference information for a 200-pixel-long diagonal training path across a 400x400 (160,000 pixels) piece of the sand landscape.

programed to use these catchment areas to navigate based on scene familiarity alone (Baddeley et al. 2012; Gaffin et al. 2015; Gaffin & Brayfield 2016).

What about the chemo-textural landscape that scorpion pectines encounter? While the exact composition, concentration, and placement of naturally occurring chemicals on sand is beyond our reach, we can estimate textural information using high contrast photography. To do this, we placed sand from the scorpion's habitat in a Petri dish, directed a light from the side, and took 100 random photographs of the sand under a 40x scope. We then wrote a MATLAB script to import, crop, turn to gray, enhance the contrast, randomly rotate, and stitch together the photos to create a proxy for the sand's textural landscape (Fig. 2A). We then reduced the resolution of this landscape based on the measured chemical-resolving power of the pegs. We have estimated that it requires

at least eight pegs to discern two chemicals based on the response of individual pegs to pure stimuli and the time that the pegs are close enough to the ground during a "pectinal sniff" to register a response (Knowlton & Gaffin 2011). To further simplify the landscape and to be as conservative as possible for this simulation, we converted the image to black and white (shown in Fig. 2B). This modified image represents the details of the textural world from the pectines' point of view. We then calculated the area of the ground-contacting surfaces of pectinal teeth and generated a square of the same area (see the small square below the superimposed pectines in Fig. 2B). Figure 2C shows an expanded sample of the textural landscape relative to this square to highlight what the patterns look like at that level.

By comparing individual pecten-sized squares in the sand landscape to all other possible squares, we generated



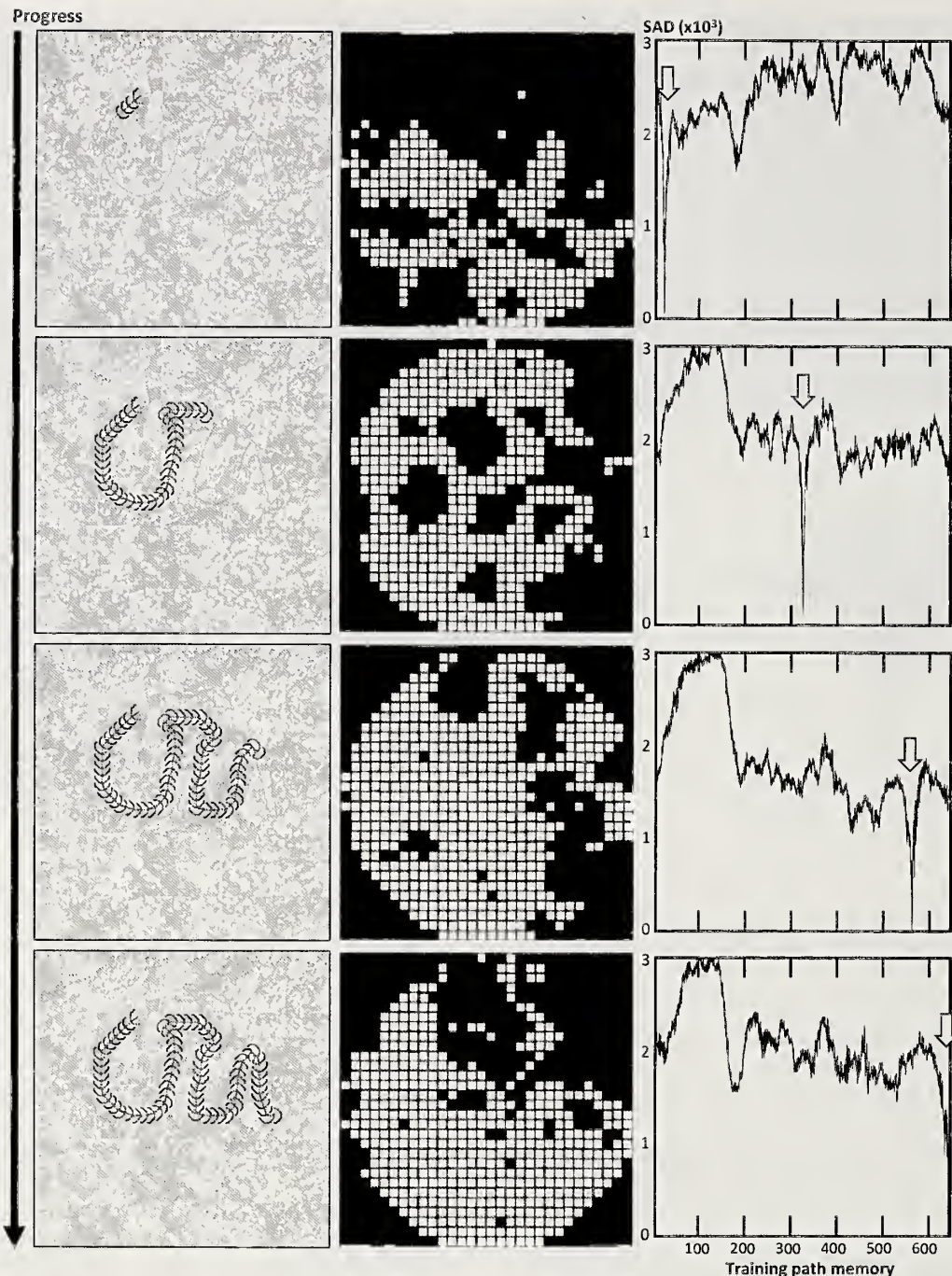


Figure 3.—Auto-tracking of a sample training path. A complex training path was drawn over the sand textural landscape (from Fig. 2(B)) to initiate the simulation. In this example, approximately 700 pecten-sized “scenes” were pixelated (30x30), circularized and stored to memory. The circularization simplifies rotational comparisons of samples. The agent is placed near the beginning of the training path and an arc of samples is taken to mimic an animal’s saccade. Each test scene matrix is rotated and compared (non-sequentially) to all scene matrices in memory based on the sum of the absolute pixel differences (SAD). The agent selects and uses the rotational angle of the best matched test scene as its bearing for its next forward step (based on a pre-defined length). It takes a step and the saccade and testing procedure repeats. The four horizontal panels of this simulation show the progress of the agent as it successfully navigates the training path. Within each horizontal panel, the current progress of the agent (left image), the current pecten-sized pixelated “view” of the sensor (middle image), and an activity monitor that plots the SAD of the current scene compared to all scenes in memory (right image) are displayed. Note how the trough (lowest SAD) in the plot (indicated by arrow) moves in register with the progress of the agent along the training path.

a plot that resembles a volcano, similar to the one described for visual information. This plot demonstrates that each pecten-sized square is distinct from all other squares (Fig. 2D). Further, when we compared a contig-

uous line of these squares (analogous to a training path) to all other squares, the plot resembled a steep-walled canyon (Fig. 2E, F) with a distinct catchment area relative to the referenced squares.



We have extended this analysis to produce simulations of autonomous agents that retrace paths drawn over our sand texture landscape. Figure 3 shows an example of a familiarity-based tracking algorithm (using vision as a proxy for texture) retracing a complex path (adapted from Gaffin et al. 2015; see figure legend for details of how the algorithm works). The simulation shows that the inherent information content of our simplified sand texture landscape is sufficient for an analog of the pectines to navigate the training path. Of note, see the activity plots on the right of each of the four panels. The arrow in each plot highlights the trough in the sum of the absolute pixel differences (SAD) of each test scene as compared to all training scenes in memory. This again shows the catchment area that exists around each considered point relative to the entire set of training path images (as discussed in Fig. 2). This type of simulation allows us to test the interplay of sensor resolution and environmental complexity on tracking performance.

**Behaviors for acquiring goal-directed information.**—Based on sensor and environmental complexity, it is plausible that scorpions could use at least textural familiarity to retrace previously experienced paths. However, an important premise of the NSFH is that scenes are retraced in the same goal-directed orientations that they were first acquired; no scene will match when the animal is moving away from the goal. Bees and ants acquire their first set of training images via path integration and learning flights or walks.

**Path integration:** Path integration (PI) allows animals to estimate the angle and distance of displacement from their home nests during outbound excursions. Displacement studies have been used to assess PI. In a classic example, researchers caught a desert ant that stumbled on a feeder and then displaced the ant to a distant release point (Müller & Wehner 1988). The ant walked in a straight line before making tight turning movements; the direction and length of the straight segment was approximately the same as the original direction and distance to the nest from the feeder. Desert ants appear to retrace familiar visual paths learned during training excursions that were produced initially by PI (Collett & Collett 2000; Wehner & Srinivasan 2003; Wittlinger et al. 2006; Baddeley et al. 2012). Consistent with the familiarity hypothesis, PI allows the individual to acquire a goal-directed set of images for subsequent retracing.

We have seen some examples of apparent PI in scorpions in the field. In these cases, we dragged a small stick across the sand to entice a scorpion from its burrow and onto a small cutting board buried just under the sand. We displaced the scorpion by carefully sliding the board 20–50 cm further from its burrow. In each case, the initial movement of the animal was to a point where the burrow would have been had the animal not been displaced. This straight segment was followed by looping patterns of movement. The tight turns and loops are similar to those observed in nest-searching ants (Wehner & Srinivasan 1981).

**Learning walks/flights:** Bees do an interesting set of orientation flights during their first excursions from the hive (Zeil et al. 1996; Palikij et al. 2012). They back away from the hive and make short swooping arcs while facing the hive. They then return to the hive and make additional, wider sets of arcs before setting off on their first foraging trip. It is thought that

they are widening the visual target for their hive, broadening the visual catchment area of familiarity that will lead them home. Similarly, desert ants do learning walks around their nests prior to setting out on their initial foraging ventures (Wehner et al. 2004).

We have, on occasion, observed what appear to be learning walks by scorpions during our scorpion hunts. Sometimes, during early evening, we have noticed animals making short looping movements away from their burrows and back. We have also captured several examples of this behavior during long-term video recordings in the lab. The movements range from tight backing movements near the burrow to looping movements that take the animal approximately 15 cm from the burrow before returning. If we are to fully characterize the use of PI and learning walks in scorpions, we need to document many additional examples of these behaviors in the field. It is also crucial to develop carefully controlled behavioral assays in the lab (Vinnedge & Gaffin 2015) to precisely map PI and learning walks and to explore the use of previously experienced chemo-textural patterns during home-bound journeys.

**Conclusions.**—In summary, several tantalizing clues allow us to think about the pectines in relation to chemo-textural familiarity navigation. Pectines are replete with thousands of chemo-tactile peg sensilla, and a conservative estimate of environmental texture indicates abundant information content based on measured sensilla resolution. There are also hints of innate path integration and learning walk behaviors that generate initial sets of goal-directed images. Still, more research is necessary to test this hypothesis properly. We need carefully controlled behavioral studies examining the use of previously experienced chemo-textural patterns during homing runs and an assay that teases apart the contributions of PI, familiarity, and other potential mechanisms (vision, chemical trails) for homing.

## ACKNOWLEDGMENTS

We thank Mariëlle Hoefnagels for her valuable review of this manuscript. We also thank Andrew Philippides, Paul Graham, Alex Dewar, and Arthur Gaffin for important discussions on visual familiarity, Bob Suter for informal conversations about these ideas and for technical assistance, and Kendall Hughes for additional feedback on the narrative. Finally, we thank the Life Fund of the University of Oklahoma Foundation and professional funds from the University of Oklahoma Presidential Teaching Fellowship in the Honors College for financial support.

## LITERATURE CITED

- Baddeley, B., P. Graham, P. Husbands & A. Philippides. 2012. A model of ant route navigation driven by scene familiarity. *PLoS Computational Biology* 8:1–16 e1002336.
- Brownell, P.H. 1998. Glomerular cytoarchitectures in chemosensory systems of arachnids. *Annals of the New York Academy of Science* 855:502–507.
- Cloudsley-Thompson, J.L. 1955. On the function of the pectines of scorpions. *Annals & Magazine of Natural History* 8:556–560.
- Collett, T.S. & M. Collett. 2000. Path integration in insects. *Current Opinion in Neurobiology* 10:757–762.
- Foelix, R.F. & G. Müller-Vorholt. 1983. The fine structure of



- scorpion sensory organs. II. Pecten sensilla. Bulletin of the British Arachnological Society 6:68–74.
- Gaffin, D.D. 2002. Electrophysiological analysis of synaptic interactions within peg sensilla of scorpion pectines. Microscopy Research and Technique 58:325–334.
- Gaffin, D.D. & B.P. Brayfield. 2016. Autonomous visual navigation of an indoor environment using a parsimonious, insect inspired familiarity algorithm. PLoS ONE 11(4): e0153706. doi:10.1371/journal.pone.0153706
- Gaffin, D.D. & P.H. Brownell. 1997. Response properties of chemosensory peg sensilla on the pectines of scorpions. Journal of Comparative Physiology A 181:291–300.
- Gaffin, D.D. & P.H. Brownell. 2001. Chemosensory behavior and physiology. Pp. 184–203. In Scorpion Biology and Research. (P.H. Brownell & G.A. Polis, eds.). Oxford University Press, New York, New York.
- Gaffin, D.D. & M.E. Walvoord. 2004. Scorpion peg sensilla: are they the same or are they different? Euscorpius 17:7–15.
- Gaffin, D.D., A. Dewar, P. Graham & A. Philippides. 2015. Insect-inspired navigation algorithm for an aerial agent using satellite imagery. PLoS ONE 10(4): e0122077. doi:10.1371/journal.pone.0122077
- Hoffmann, C. 1964. Zur funktion der kammförmigen organ von skorpionen. Naturwissenschaften 7:172.
- Knowlton, E.D. & D.D. Gaffin. 2011. Functionally redundant peg sensilla on the scorpion pecten. Journal of Comparative Physiology A 197:895–902.
- Melville, J. 2000. The pectines of scorpions: Analysis of structure and function. Ph.D. Thesis, Oregon State University, Corvallis, OR.
- Müller, M. & R. Wehner. 1988. Path integration in desert ants, *Cataglyphis fortis*. Proceedings of the National Academy of Science 85:5287–5290.
- Narendra, A., S. Gourmaud & J. Zeil. 2013. Mapping the navigational knowledge of individually foraging ants, *Myrmecia croslandi*. Proceedings of the Royal Society B 280:20130683.
- Palikij, J., E. Ebert, M. Preston, A. McBride & R. Jander. 2012. Evidence for the honeybee's place knowledge in the vicinity of the hive. Journal of Insect Physiology 58:1289–1298.
- Pritchard, G. 1966. On the morphology of the compound eyes of dragonflies (Odonata: Anisoptera), with special reference to their role in prey capture. Proceedings of the Royal Entomological Society of London A 41:1–8.
- Schwarz, S., A. Narendra, A. & J. Zeil. 2011. The properties of the visual system in the Australian desert ant *Melophorus bagoti*. Arthropod Structure & Development 40:128–134.
- Seidl, R. & W. Kaiser. 1981. Visual field size, binocular domain and the ommatidial array of the compound eyes in worker honey bees. Journal of Comparative Physiology A 143:17–26.
- Srinivasan, M.V. & M. Lehrer. 1984. Temporal acuity of honeybee vision: behavioural studies using moving stimuli. Journal of Comparative Physiology A 155:297–312.
- Sukontason, K.L., T. Chaiwong, S. Piangjai, S. Upakut, K. Moophayak & K. Sukontason. 2008. Ommatidia of blow fly, house fly, and flesh fly: implication of their vision efficiency. Parasitology Research 103:123–131.
- Swoveland, M.C. 1978. External morphology of scorpion pectines. Master's thesis, California State University, San Francisco.
- Vincedge, J. & D.D. Gaffin. 2015. Determination of in-lab site fidelity and movement patterns of *Parmoctonus utahensis*. Journal of Arachnology 43:54–58.
- Wehner, R. & M.V. Srinivasan. 1981. Searching behaviour of desert ants, genus *Cataglyphis* (Formicidae, Hymenoptera). Journal of Comparative Physiology 142:315–338.
- Wehner, R. & M.V. Srinivasan. 2003. Path integration in insects. Pp. 9–30. In The Neurobiology of Spatial Behaviour. (K.J. Jeffery, ed.). Oxford University Press, New York, New York.
- Wehner, R., C. Meier & C. Zollikofer. 2004. The ontogeny of foraging behavior in desert ants, *Cataglyphis bicolor*. Ecological Entomology 29:240–250.
- Wittlinger, M., R. Wehner & H. Wolf. 2006. The ant odometer: stepping on stilts and stumps. Science 312:1965–1967.
- Wolf, H. 2008. The pectine organs of the scorpion, *Vaejovis spinigerus*: structure and (glomerular) central projections. Arthropod Structure & Development 37:67–80.
- Zeil, J., M.I. Hofmann & J.S. Chahl. 2003. Catchment areas of panoramic snapshots in outdoor scenes. Journal of the Optical Society of America A 20:450–469.
- Zeil, J., A. Kelber & R. Voss. 1996. Structure and function of learning flights in bees and wasps. Journal of Experimental Biology 199:245–252.

*Manuscript received 30 September 2016, revised 19 May 2017.*



## Retreat availability and social influences on retreat sharing in group-living huntsman spiders, *Delena lapidicola* and *Delena cancerides* (Araneae: Sparassidae)

Cameron Jones<sup>1,2</sup> and Linda S. Rayor<sup>1</sup>: <sup>1</sup>Department of Entomology, Cornell University, Ithaca, NY 14853;

<sup>2</sup>Department of Neurobiology, Physiology and Behavior, Animal Behavior Graduate Group, University of California, One Shields Avenue, Davis, CA 95616; E-mail: LSR1@cornell.edu

**Abstract.** Retreat selection is critical for animals that spend much of their diel cycle in retreats. At issue is how retreat availability and social dynamics interact to influence whether retreats are defended from or shared with conspecifics. The prolonged subsocial huntsman spider, *Delena lapidicola* (Hirst 1991, Sparassidae), lives in family groups under rock retreats which are relatively abundant on granite headlands in Western Australia. Their more social congener, *D. cancerides* (Walckenaer, 1837), lives in rare retreats under the bark of trees in southern Australia. We tested retreat sharing patterns with kin and non-kin in *D. lapidicola*, and of unrelated adult female *D. cancerides* using laboratory assays. For each trial, two spiders were introduced 12-hr apart in a large arena with two retreats and given 24-hr to share a retreat or occupy their own retreat. Aggression and mortality were recorded. In this study, 42% of *D. lapidicola* shared retreats regardless of kinship, age, sex, mass or natal colony. Even adult females shared retreats peacefully. Aggression only occurred once. In stark contrast, no *D. cancerides* adult females shared retreats and 36% of the trials resulted in mortality or serious injury. Our results support the hypothesis that an abundance of retreats in *D. lapidicola* habitats reduces pressure to defend and allows sharing with little discrimination of kinship, while the rarity of retreats in *D. cancerides* habitats results in aggressive defense.

**Keywords:** Retreat site selection, saxicolous ectotherm, kin recognition, habitat saturation, sociality

Many animals spend long portions of their day hidden in diurnal or nocturnal retreats. These retreats are critical, valuable resources that impact all aspects of an organism's fitness, as the retreats provide protection from a wide array of abiotic and biotic selective forces (Berryman & Hawkins 2006). Abiotic forces include temperature, humidity, and wind, while biotic forces include dynamics such as intraspecific attraction or competition, interspecific competition, or predation risk (Langkilde & Shine 2004; Croak et al. 2008). These forces are particularly salient to animals that live on open rock outcrops where vegetation does not provide a buffer for abiotic forces, and where competition for a limited number of available retreats under rocks can be intense (Langkilde & Shine 2004). Evidence suggests that saxicolous (or rock-dwelling) ectotherms such as spiders, lizards, and snakes are extremely particular in their choice of retreat site selection, clearly preferring certain thermal, spatial, and other microclimate features of the specific rock retreats (Huey et al. 1989; Goldsbrough et al. 2004; Croak et al. 2008), as well as where the retreat is positioned in the overall landscape (Croak et al. 2012).

Social dynamics and retreat availability interact to determine whether rock retreats are defended or shared with conspecifics in group-living, saxicolous animals (Pike et al. 2011). Intersecting factors likely influence decisions to share retreats. (1) Individuals may compete for optimal retreats and expend energy to maintain solo occupancy of that retreat, particularly if suitable retreats are rare. (2) Relatively abundant retreats may mean that individual retreats are temporarily shared because they are not worth defending. (3) Relatively abundant retreats may mean that individuals never need to share retreats. (4) There are benefits to sharing retreats even when they are relatively abundant. (5) In social species, individuals tolerate retreat sharing with other conspecifics, but

whether there are preferences for kin or for specific age-sex classes may vary with the species.

In a laboratory study, we explored which of these situations best describes the retreat sharing behavior of a nocturnally active, exclusively saxicolous prolonged subsocial spider, *Delena lapidicola* (Hirst, 1991) (previously, *Eodelena lapidicola*; see Agnarsson & Rayor 2013). In this group-living spider species, potential retreats are relatively abundant in the wild (Rayor 2016). Our goal was to determine whether the spiders would defend or share retreats with conspecifics, and whether there were behavioral differences in retreat sharing between non-kin and among various age-classes. As a contrast, we compared patterns of retreat sharing in the same experimental design with its more social sister species, *Delena cancerides* (Walckenaer, 1837), which lives under the bark of trees in retreats which are exceedingly rare (Yip et al. 2012), and which have been demonstrated to discriminate who share their retreats based on kinship and the age-class of the conspecifics (Yip et al. 2009). All evidence indicates that retreat sharing in *D. cancerides* is best described as a situation where individuals actively compete to maintain occupancy of rare retreats but readily share retreats with kin or colony mates and younger animals (Yip et al. 2009; Yip & Rayor 2011; Rayor 2016).

*Delena lapidicola* live in crevices under exfoliated rocks exclusively on granite headlands in SW Western Australia (Agnarsson & Rayor 2013). The nocturnally active spiders remain under the rock retreats during the day, foraging at night from the edge of the rock or in the open. Although potential retreats appear plentiful, quantitative analysis demonstrates that there are clear preferences for rocks of certain sizes, composition, crevice size, and thermal properties, which may reduce the actual number of potential retreats (Rayor, van den Berg, and Hurst, unpublished data). Recent discoveries suggest these spiders live in matrilineal family groups with up to three cohorts of siblings remaining under



the rock retreat with their mother (Rayor 2016). Offspring remain with their mothers under the natal rock until at least the 5<sup>th</sup> or 7<sup>th</sup> instar out of 10 or 11 instars. Patchily distributed colonies of *D. lapidicola* are often found in ‘neighborhoods’, where occupied retreats are within ~10m of one another. A particularly dense neighborhood may include several retreats occupied by an adult female with her offspring, several male:female pairs, and mature, penultimate, or (rarely) 5<sup>th</sup> or 6<sup>th</sup> instar solitary individuals. Within this area, spiders without young may move between retreats. Therefore it is probable that (1) individuals from different colonies interacted on occasion while foraging at night or visited each other’s rock retreats to assess the age, sex, receptivity, or holding power of the resident, and (2) that at least some of the neighboring colonies were occupied by kin who had spread outward from their natal colony. These expectations are supported by evidence from extensive studies on reptiles, particularly velvet geckos (*Oedura lesueurii*: Gekkonidae) and, to a lesser extent, broad-headed snakes (*Hoplocephalus bungaroides*: Elapidae) which live exclusively on rock outcrops. These species largely remain in their natal area and do not move widely between rocky outcrops (Dubey et al. 2011, 2012).

Social factors and kin recognition may also affect retreat sharing. In the subsocial and prolonged subsocial spider species where a single female remains in association with her offspring for prolonged periods (see Yip & Rayor 2014), there is increasing evidence that many of these species exhibit kin or colony mate discrimination, are resistant to accepting non-kin into their webs or retreats, and are less likely to share prey with those individuals (Evans 1999; Bilde & Lubin 2001; Beavis et al. 2007; Schneider & Bilde 2008; Yip et al. 2009; Grinstead et al. 2011; Ruch et al. 2015). Compared to the more social cooperative and colonial social spider species which remain in their natal colony and show little evidence of nepotism, these subsocial species are more likely to encounter non-kin and to live in smaller groups where there may be greater costs to accepting non-kin into groups (Auletta & Rayor 2011; Berger-Tal et al. 2015). This appears to be particularly true of the prolonged subsocial huntsman species which, instead of constructing webs, must search for retreats of limited size and availability (Yip et al. 2012; Rayor 2016). These small discrete retreat sites may increase both intraspecific competition for occupancy of the retreats and the benefits of discriminating kin from non-kin (Yip et al. 2009, 2012).

Based on previous experiments on *D. cancerides*, we hypothesized that when given the choice of sharing or choosing an empty retreat, *D. lapidicola* would aggregate with kin from the same colony, younger animals, or the opposite sex, but prefer to be alone in a retreat if the introduced animal did not fit these criteria. We hypothesized that adult or penultimate females would be extremely unlikely to share retreats, and, if they shared, they would do so only with colony mates. Additionally, we predicted that aggression, possibly leading to mortality, would be higher between older animals and non-kin. These two predictions fit with previous studies on their sister group, *D. cancerides*, which aggressively defend retreats from potential reproductive competitors (Yip et al. 2009; Yip & Rayor 2011). Similarly, we hypothesized that spiders whose natal colonies in the wild were closer together were more likely to be related than individuals from

colonies found great distances from one another, and that spiders from proximate colonies might share retreats more frequently. To directly compare the patterns of retreat sharing and aggression found in *D. lapidicola* with *D. cancerides*, we used the same experimental protocol to determine rates of retreat sharing and aggressive interactions between unrelated penultimate and adult female *D. cancerides*. This allowed us to examine how retreat sharing behavior differs between two species where the potential costs associated with accepting non-colony mates is similar, but the abundance of suitable retreats in their native habitat is markedly different.

## METHODS

**Study organisms.**—In 2014, *D. lapidicola* [Sparassidae: Deleninae] were collected from under exfoliated rocks in granite headlands along the southern coast of Two People’s Bay National Park, Western Australia, Australia. Colony demographics were noted and location of sites recorded on GIS. Prior to the start of experiments, individuals were maintained in family groups or mated pairs at Cornell University, New York, USA, in covered glass arenas (45 × 35 × 30 cm tall) under light:dark 18:6 cycles at 23°C. Spiders were given water and fed house crickets, *Acheta domesticus*, *ad libitum*. *Delena lapidicola* used in this study included adult females and subadults (between 7<sup>th</sup> to 9<sup>th</sup> instar, where adults are the 10<sup>th</sup> instar.) The second huntsman species, *D. cancerides*, was collected from Canberra, ACT, Australia in 2014. Prior to experiments, individual adult female *D. cancerides* were housed in 41 × 20 × 26 cm glass terrariums with artificial bark (Plexiglas sheets each attached with Velcro) providing ~1cm deep retreats along the long sides of the arena (see Yip et al. 2009 for details).

**Retreat size preference.**—In the field, *D. lapidicola* use horizontally-oriented retreats under rocks that have an average area of ~8 cm<sup>2</sup> with ~1 cm crevice entrances (Rayor, van den Berg, & Hurst, unpublished data). To test preferences for rock retreat size in the lab, rock retreats of two different sizes were placed at each end of a large terrarium (91 × 45 × 40 cm) and a water dish was placed equidistant from the two potential retreats. Retreats were made with commercial 9.5 × 20 cm ceramic tiles placed on top of each other with a front crevice of ~1 cm and back of the tiles touching. Rock widths were divided into three categories: small (9.5 × 20 cm), medium (19 × 20 cm) or large (28.5 × 20 cm). Preliminary tests revealed that spiders always moved into a retreat during the experiment, and would occupy all three rock sizes in the absence of an alternative retreat. Preference tests were conducted between different sizes of rock retreats: small vs. medium ( $n = 10$ ), small vs. large ( $n = 10$ ), and medium vs. large ( $n = 18$ ). One *D. lapidicola* spider was used per preference trial and each individual was tested only once. We recorded the sex, mass, carapace width, length of femur of the second leg and length of the tibia and tarsus of the second leg. Spiders were introduced in front of the water dish in late afternoon, and left overnight to allow them to adjust to the arena and choose a rock retreat. After ~12 hours, the location of the spider and the rock size was recorded. After each trial, the terrarium, water dish, and rocks were thoroughly washed with warm water. Tiles that were reused were randomly paired with other tiles and placed in switched positions.



**Social interaction trials.**—We added two individuals to the arena on subsequent days and allowed them to remain together overnight to assess whether the choice to join another animal in one retreat or to choose a solo retreat was based on the individual *D. lapidicola*'s colony, age, or sex. Retreat sizes that were favored in the rock size preference trials were used in the social interaction trials. Each trial consisted of two retreats of the same size placed at opposite ends of a covered glass arena with dimensions (91 × 45 × 40 cm) with a water dish equidistant between the two retreats. One pair of *D. lapidicola* was used per trial and consisted of either individuals from different colonies or from the same colony. The first specimen of each trial ("Resident") was lightly anesthetized with CO<sub>2</sub>, marked with Testors enamel paint, and its sex, mass, carapace width, length of femur of the second leg and length of the tibia and tarsus of the second leg was recorded. These measurements were used to infer instar of each individual. Due to the strong correlation between these measurements within *D. lapidicola*, we will henceforth refer to mass as the size of each specimen. The resident was then placed within the testing arena in front of the water dish and given >12 hours to occupy a retreat. On the second day, a second specimen ("Introduced") of similar size from either the same or different colony was similarly marked and measured before being placed in the arena. Differences in size between the resident and introduced species were minimal ( $X \pm SE = 0.52 \pm 0.06$  cm). The arena was monitored for 10 min following the introduction of the introduced specimen to record any signs of aggression, before the two spiders were left overnight for >12 hours. In all 48 trials, spiders had moved into a retreat overnight. We recorded which retreat the resident and introduced spiders were in, along with any evidence of aggressive encounters (injury to a spider, missing legs, or death). Due to the limited availability of *D. lapidicola* for these experiments, some individuals were used several times but always in different permutations: Adult females from separate colonies  $n = 12$ , trials  $n = 18$ ; Subadults from separate colonies  $n = 39$ , trials  $n = 20$ ; Subadults from the same colonies  $n = 19$ , trials  $n = 10$ . No individual was used more than twice in different pairs after a minimum period of 48 hours post trial and any individuals injured during a trial were removed from the rest of the study. Pair composition and determination of which individual was used as "Resident" or "Introduced" was random. After each trial, the arena, rocks and water dishes were washed and replaced.

For comparison, we analyzed the behavior of 15 adult female *D. cancerides* from different colonies in 30 introduction trials to assess the propensity to share retreats and relative aggression. Individuals were retested several times, but they were always in different permutations and injured spiders were never retested. Only large retreats were used and, because this species is less dorso-ventrally flattened than *D. lapidicola*, the crevice size was doubled. Although *D. cancerides* primarily use retreats under bark, they readily occupy retreats under rocks, roofs, or shutters if other retreats are unavailable.

**Colony separation distance.**—To evaluate the possibility that spiders either remembered individuals from neighboring colonies or that colony mates or kin were distinguishable by olfactory cues on their cuticle (Grinsted et al. 2011), we calculated the distances between the capture sites of the

Table 1.—Factors determining propensity of *D. lapidicola* to share retreats (48 trials on 70 individuals).

Random effects	Variance	LRT	<i>P</i>	
ID	0.029	0.006		0.938
Fixed effects	B	SE	<i>z</i>	<i>P</i>
Intercept	0.244	0.619	0.395	0.693
Same region	-0.652	0.862	-0.757	0.449
Colony	-0.262	0.891	-0.294	0.767
Female	-0.103	0.516	-0.200	0.842
Adult	-1.094	0.649	-1.672	0.095
Distance	-0.131	0.394	-0.332	0.740
Mass	0.391	0.295	1.322	0.186
Large Rock	0.157	0.579	0.271	0.786
Initial Rock left	0.076	0.491	0.154	0.877
Marginal R	0.085			
Conditional R	0.093			
AIC	142.6			
Deviance	122.6			
Residual df	86			

individual's natal retreat in the wild. We predicted that *D. lapidicola* spiders collected from neighboring colonies were more likely to be more closely related than spiders living significantly greater distances apart or from entirely separate granite headlands. Therefore to assess whether the colony distance at which the spiders had been collected had any effect on propensity to aggregate, we measured the distance between natal colonies of each spider. In this study, individuals from 21 different colonies ranging from 4 to 710 meters apart with an average distance of 286 meters were used. GPS coordinates for each of these colonies were obtained by Rayor, van den Berg, & Hurst (unpublished data). Distances between colonies were measured between them using Google Earth (Google Inc).

**Statistical tests.**—All statistical tests were conducted in the statistical software package R version 3.3.1 (R Core Team 2014). We performed a Chi-square test to determine retreat size preference. The results from this test indicated that there were two favorable retreat sizes, medium and large (see Results), which we then used for the social interaction trials. We analyzed propensity of individuals to share retreats using generalized linear mixed modeling (GLMM) techniques. Our response variable (whether spiders shared retreats or not) was modeled with a binomial distribution and logit link function and spider ID as a random effect. We compared a fully parameterized model with individual ID as a random effect to a model without it, while keeping the fixed effect structure, using a likelihood ratio test (1 degree of freedom [df], (Pinheiro & Bates 2000), to test for significant consistent individual differences in propensity to share retreats. We did not detect any consistent differences among individuals in tendency to share retreats in *D. lapidicola* (Table 1). To avoid redundancy in our models predicting propensity to share retreats, we continued our analyses using generalized linear models without a random effect.

To determine what factors predicted propensity to share retreats, we utilized an information theoretic approach to discern which variable best predicted the number of retreats shared. The model set included only models with a single main effect. Therefore we had eight models with effects of size, sex,



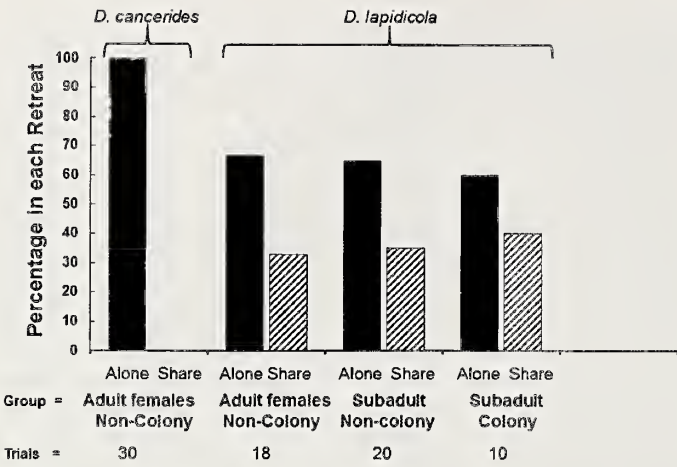


Figure 1.—Percentage of trials where spiders settled into retreats by themselves (Alone) or with the other individual in the experiment (Share) for *Delena cancerides* and *D. lapidicola*. Results for *D. lapidicola* trials were separated based on the experimental animals' age-class and whether they came from the same colony or from different colonies (non-colony). There were no significant differences in the percentage of retreats shared and alone in different *D. lapidicola* groups, but *D. cancerides* were alone significantly more than all *D. lapidicola*.

colony distance, whether spiders were from the same colony, size of rocks in trials (medium or large), the retreat (left or right) initially occupied by the resident, whether pairs originated from the same region, and an additional null model.

We also constructed binomial GLMMs to determine how retreat-sharing patterns and aggression differed between adult female *D. lapidicola* and *D. cancerides*. Both aggression and retreat sharing response variables were coded as binomial responses. The model sets included only models with a single fixed effect and individual ID as a random effect. Including the null model, there were 8 models with effects of all size measurements, size of rocks in trials (medium or large), the retreat (left or right) initially occupied, and the species (*D. lapidicola* or *D. cancerides*). All GLMMs were fitted using the LME4 package (Bates et al. 2015) and were compared using Akaike's Information Criteria with a small sample size correction (AICc). We also calculated Akaike weight using the BBMLE package (Bolker 2017),  $\omega_i$ , to estimate the probability of one model being the best fit for the data, relative to all other compared models. Models within two  $\Delta$  AIC were deemed to have equivalent fits (Burnham & Anderson 2002).

Table 2.—Top three generalized linear models for predicting propensity of *D. lapidicola* to share retreats as indicated by AICc model selection procedures. AICc: Akaike's Information Criterion corrected for small sample size;  $\omega_i$ : Akaike weight.

	Shared Retreats ~ 1			Shared Retreats ~ Left rock initially occupied			Shared Retreats ~ same colony		
	$\beta$	SE	P	$\beta$	SE	P	$\beta$	SE	P
Intercept	-0.601	0.3018	0.0465	-0.319	0.4647	0.493	-0.654	0.3419	0.0558
Initial Occupied Rock	-	-	-	-0.48	0.614	0.434	-	-	-
Colony	-	-	-	-	-	-	0.2485	0.7305	0.7338
	AICc=64.399 $\omega_i=0.295$			AICc=65.788 $\Delta$ AICc=1.6 $\omega_i=0.134$ $R^2_{adj}=0.009$ and $F_{1,46}=0.61$ , $p=0.43$			AICc=66.284 $\Delta$ AICc=2.1 $\omega_i=0.105$ $R^2_{adj}=0.002$ and $F_{1,46}=0.11$ , $p=0.74$		

RESULTS

**Retreat size preference.**—When given a choice of retreats of different sizes, *D. lapidicola* preferred larger retreats over smaller retreats. Medium sized retreats were preferred over small ( $n = 10$ ,  $\chi^2 = 10$ ,  $df = 1$ ,  $P = 0.002$ ), and large over small ( $n = 10$ ,  $\chi^2 = 10$ ,  $df = 1$ ,  $P = 0.002$ ). There was no difference in preference between medium and large retreats ( $n = 18$ ,  $\chi^2 = 2.29$ ,  $df = 1$ ,  $P = 0.13$ ).

**Retreat sharing in *Delena lapidicola*.**—Forty-two percent of the trials resulted in individuals sharing retreats irrespective of which colony they originated from (Fig. 1). Using a model comparison approach, we did not find any variable that was successful in predicting retreat sharing patterns, as the best fit model was the null, intercept-only model ( $\omega_i = 0.295$ ; Table 2). The second and third best fit models included which retreat (left or right) was initially occupied by the resident and whether spiders in a trial were from the same colony or from different colonies, respectively. However, neither of these models contained a significant effect on propensity to share retreats and only carried a combined 24% of the total weight. These results imply that among other factors, neither sex, nor age, nor colony, nor distance between colonies of origin influence retreat sharing behavior in *D. lapidicola*.

**Retreat sharing in *Delena cancerides*.**—*Delena cancerides* never shared retreats with conspecifics from other colonies. As such, the best model identified species as the best predictor for sharing retreats, with trials conducted with *D. cancerides* occupying separate retreats ( $\Delta$ AICc to next model = 3.8, and weight  $\omega_i = 0.8119$ ; Table 3). A likelihood ratio test revealed that there were no individual differences across adult females of either species in propensity to share retreats ( $X^2 = 0.442$ ,  $df = 1$ ,  $P = 0.506$ ).

**Rates of conflict.**—The levels of aggression in *D. lapidicola* and *D. cancerides* in social interaction trials was also dramatically different. Only one aggressive encounter occurred in *D. lapidicola* trials, when a resident adult female attacked and killed the adult female intruder immediately upon introduction. In contrast, 11 of the 30 trials with *D. cancerides* resulted in either lost limbs or mortality. As such, the best-fit model for predicting aggression identified species as the best predictor ( $\Delta$ AICc to next model = 29.3, and weight,  $\omega_i = 1$ ; Table 4). Furthermore, in trials with aggression in *D. cancerides*, a likelihood ratio test between models with and without individual ID as a random effect revealed among-individual differences in female aggression ( $X^2 = 5.82$ ,  $df = 1$ ,  $P = 0.016$ ).



Table 3.—The best-fit model predicting propensity of adult females to share retreats in trials conducted with all *D. cancerides* and trials conducted with all *D. lapidicola* as indicated by AICc model selection procedures. AICc: Akaike's Information Criterion corrected for small sample size;  $\omega_i$ : Akaike weight.

Random effects	Estimate			
ID	0.640			
Fixed Effects	$\beta$	SE	Z	P
Intercept	-21.62	211.24	16.999	0.918
Lapidicola	20.58	211.24	3.495	0.922
Marginal R <sup>2</sup>	0.962			
Conditional R <sup>2</sup>	0.968			

## DISCUSSION

Our *a priori* predictions about the propensity of *Delena lapidicola* to share retreats based on the traits observed in *D. cancerides* were almost uniformly incorrect. When given a choice between sharing retreats and occupying a retreat solitarily, the prolonged subsocial *Delena lapidicola* shared retreats 42% of the time regardless of the spider's age, colony, or distance between colonies of origin in our experiments. Notably, the percentage of adult females who shared was similar to that of the other age-classes and non-colony mates pairs. This is particularly surprising considering that adult females were not found sharing any retreats with other adult females in the wild (field data 2008 and 2014:  $n = 26$  rock retreats that had an adult female plus other individuals, Rayor, unpublished data). Moreover, with the exception of a single mortality event between adult females, there was no evidence of aggression between these spiders in our experiments. None of the adult females we used in this experiment were on the verge of laying eggs, so more aggression might be anticipated by those females. This level of tolerance and tendency to aggregate in *D. lapidicola* was completely unexpected.

The most probable explanation for our observations of frequent retreat sharing and the lack of aggression in *D. lapidicola* is that there may be limited selection for active defense of rock retreats. The natural rock retreats for *D. lapidicola* are relatively abundant, with the number of potential retreats vastly exceeding the number of colonies in the habitat (Rayor 2016). Even minor shifts in the positions of rock retreats dramatically impact acceptability to reptiles for retreats on rock outcrops (Croak et al. 2008), so our assessment of abundance of suitable retreats may be an overestimate but there were likely more potential retreats than spiders in all areas. Most *D. lapidicola* do not lay down silk or put other investment into improving the rock retreat, with the exception of adult females that put down silk bands around their egg sacs to protect from predators and parasites. Therefore, because the retreats are apparently plentiful and require little investment, their low value likely reduces the need for defense from other individuals. Simultaneously, tolerance toward conspecifics may be beneficial because social aggregations of marbled geckos (*Christinus marmoratus*), which appear to be both predators and prey of the spiders, are potential competitors for the same retreat rocks (Kearney et al. 2001; Rayor unpublished

Table 4.—The best-fit model predicting aggression within adult females in trials conducted with all *D. cancerides* and trials conducted with all *D. lapidicola* as indicated by AICc model selection procedures. AICc: Akaike's Information Criterion corrected for small sample size;  $\omega_i$ : Akaike weight.

Random effects	Estimate			
ID	0.640			
Fixed Effects	$\beta$	SE	Z	P
Intercept	71.38	713.04	0.100	0.920
Lapidicola	-85.93	714.04	-0.121	0.904
Marginal R <sup>2</sup>	0.124			
Conditional R <sup>2</sup>	0.999			

data). Thus, our data suggest that with more abundant retreat options, *D. lapidicola* more closely fit the situation where individuals more readily share retreats because there are few benefits to defending the retreat and potential benefits to sharing.

In contrast, *Delena cancerides* adult females never shared retreats and serious aggression was commonplace, aligning with previous studies suggesting that rare retreats require active defense, particularly for females who need sole ownership of a retreat to reproduce. In *D. cancerides* conspecific competition for retreats is intense, the retreats require active effort to securely attach the bark to the tree, and the spiders are intolerant and aggressive toward unrelated conspecifics (Yip et al. 2009, 2012). This environmental constraint of a limited number of available retreats is hypothesized to drive selection for sociality within *D. cancerides*, with offspring remaining in their natal colony with their mother until they are physically able to compete for rare retreats. The contrast between *D. lapidicola* and *D. cancerides* social tolerance and willingness to share retreats is an illustration of how differences in retreat availability and investment in maintaining the retreat may influence social dynamics in social spiders.

Social factors must influence retreat sharing decisions in these prolonged subsocial spiders, but our results do not demonstrate whether or not kin recognition is found in *D. lapidicola*. There is strong evidence of kin discrimination in *D. cancerides* and other subsocial species where spiders respond to kin and non-kin differentially based on chemosensory cues, even if the spiders are familiar with non-kin (Beavis et al. 2007; Schneider & Bilde 2008; Grinsted et al. 2011; but see Auletta & Rayor 2011). In this study, we assessed whether retreat sharing with non-colony members exhibited a neighborhood effect, with rock-sharing occurring more frequently between *D. lapidicola* from colonies of origin in proximity (<50 m) with one another. Distance between colonies had no effect on spiders' propensity to share retreats, with sharing occurring even between spiders from distant granite headlands. Further investigation will be needed to determine whether *D. lapidicola* are capable of discriminating kin or colony mates, or whether their tendency to aggregate in retreats makes kin recognition unimportant. Differences in retreat availability in their native habitat appear to drive the two sister spider species' response to retreat sharing.



## ACKNOWLEDGMENTS

We greatly appreciated the assistance of Francesca T. van den Berg (University of Sydney/ Macquarie University), Jacob Hurst (Cornell, Fresno State University), Two-People's Bay Ranger Mark True, and Dr. Mark Harvey (Western Australia Museum) in collecting and studying the field biology of *D. lapidicola*. Francesca van den Berg, Erie Yip, Cole Gilbert, Orr Spiegel and anonymous reviewers provided invaluable input on the manuscript. Financial support was provided by Hunter Rawlings Cornell Presidential Research Scholars of Cornell University for Cameron Jones.

## LITERATURE CITED

- Agnarsson, I. & L.S. Rayor. 2013. A molecular phylogeny of the Australian huntsman spiders (Sparassidae, Deleninae): Implications for taxonomy and social behavior. *Molecular Phylogenetics and Evolution* 69:895–905.
- Auletta, A. & L.S. Rayor. 2011. Preferential prey sharing among kin not found in the social huntsman spider, *Delena cancerides* (Sparassidae). *Journal of Arachnology* 39:258–262.
- Bates, D., M. Mächler, B. Bolker & S. Walker. 2015. Fitting linear mixed-effects models using lme4. *Journal of Statistical Software* 67:1.
- Beavis, A.S., D.M. Rowell & T. Evans. 2007. Cannibalism and kin recognition in *Delena cancerides* (Araneae: Sparassidae), a social huntsman spider. *Journal of Zoology* 271:233–237.
- Berger-Tal, R., Y. Lubin, V. Settepani, M. Majer, T. Bilde & C. Tuni. 2015. Evidence for loss of nepotism in the evolution of permanent sociality. *Scientific Reports* 5:13284.
- Berryman, A. & B. Hawkins. 2006. The refuge as an integrating concept in ecology and evolution. *Oikos* 115:192–196.
- Bilde, T. & Y. Lubin. 2001. Kin recognition and cannibalism in a subsocial spider. *Journal of Evolutionary Biology* 14:959–966.
- Bolker, B. 2017. Tools for General Maximum Likelihood Estimation. Online at <https://cran.r-project.org/web/packages/bbmle/bbmle.pdf>
- Burnham, K. & D. Anderson. 2002. *Model Selection and Multimodel Inference: A Practical Information-Theoretic Approach*. Springer, New York.
- Croak, B., D. Pike, J. Webb & R. Shine. 2008. Three-dimensional crevice structure affects retreat site selection by reptiles. *Animal Behaviour* 76:1875–1884.
- Croak, B., D. Pike, J. Webb & R. Shine. 2012. Habitat selection in a rocky landscape: Experimentally decoupling a retreat site attributes from that of landscape features. *PloS ONE* 7(6):e37982.
- Dubey, S., B. Croak, D. Pike, J. Webb & R. Shine. 2012. Phylogeography and dispersal in the velvet gecko (*Oedura lesueurii*), and potential implications for conservation of an endangered snake (*Hoplocephalus bungaroides*). *BMC Evolutionary Biology* 12:67.
- Dubey, S., J. Sumner, D. Pike, J.S. Keogh, J. Webb & R. Shine. 2011. Genetic connectivity among populations of an endangered snake species from Southeastern Australia (*Hoplocephalus bungaroides*, Elapidae). *Ecology and Evolution* 1:218–227.
- Evans, T.A. 1999. Kin recognition in a social spider. *Proceedings of the Royal Society of London B: Biological Sciences* 266:287–292.
- Goldsbrough, C., D. Hochuli & R. Shine. 2004. Fitness benefits of retreat-site selection: Spiders, rocks, and thermal cues. *Ecology* 85:1635–1641.
- Grinstead, L., T. Bilde & P. d'Ettorre. 2011. Cuticular hydrocarbons as potential kin recognition cues in a subsocial spider. *Behavioral Ecology* 22:1187–1194.
- Huey, R., C. Peterson, S. Arnold & W. Porter. 1989. Hot rocks and not-so-hot rocks: retreat-site selection by garter snakes and its thermal consequences. *Ecology* 70:931–944.
- Kearney, M., R. Shine, S. Comber & D. Pearson. 2001. Why do geckos group? An analysis of “social” aggregations in two species of Australian lizards. *Herpetologica* 57:411–422.
- Langkilde, T. & R. Shine. 2004. Competing for crevices: interspecific conflict influences retreat-site selection in montane lizards. *Oecologia* 140:684–691.
- Pike, D., J. Webb & R. Andrews. 2011. Social and thermal cues influence nest-site selection in a nocturnal gecko, *Oedura lesueurii*. *Ethology* 117:796–801.
- Pinhairo, J. & D. Bates. 2000. *Mixed-Effects Models in S and S-PLUS*. Springer Science and Business Media.
- R Core Team. 2014. *R: A language and environment for statistical computing*. R Foundation for Statistical Computing, Vienna, Austria. Online at <http://www.R-project.org/>
- Rayor, L.S. 2016. How habitat and retreat limitation influence sociality in prolonged subsocial spiders. *Denver Museum of Nature & Science Reports* 3:158–159.
- Ruch, J., M. Dumke & J.M. Schneider. 2015. Social network structure in group-feeding spiders. *Behavioral Ecology and Sociobiology* 69:1429–1436.
- Schneider, J. & T. Bilde. 2008. Benefits of cooperation with genetic kin in a subsocial spider. *Proceedings of the National Academy of Sciences USA* 105:10843–10846.
- Yip, E.C. & L.S. Rayor. 2011. Do social spiders cooperate in predator defense and foraging without a web? *Behavioral Ecology and Sociobiology* 65:1937–1945.
- Yip, E.C. & L.S. Rayor. 2014. Maternal care and subsocial behavior in spiders. *Biological Reviews* 89:427–449.
- Yip, E.C., S. Clarke & L.S. Rayor. 2009. Aliens among us: Nestmate recognition in the social huntsman spider, *Delena cancerides*. *Insectes Sociaux* 56:223–231.
- Yip, E.C., D.M. Rowell & L.S. Rayor. 2012. Behavioral and molecular evidence for selective immigration and group regulation in the social huntsman spider, *Delena cancerides* (Araneae: Sparassidae). *Biological Journal of the Linnean Society* 106:749–762.

*Manuscript received 30 September 2016, revised 11 August 2017.*



## Effect of seasonal photoperiod on molting in *Loxosceles reclusa* and *Loxosceles laeta* spiders (Araneae: Sicariidae)

Richard S. Vetter<sup>1</sup>, Linda M. Penas<sup>2</sup> and Mark S. Hoddle<sup>1</sup>: <sup>1</sup>Department of Entomology, University of California, Riverside, CA 92521. E-mail: rick.vetter@ucr.edu <sup>2</sup>Department of Statistics, University of California, Riverside, CA 92521

**Abstract.** During the winter of 2014–15 in southern California, attempts were made to accelerate immature brown recluse spiders, *Loxosceles reclusa* Gertsch & Mulaik, 1940, to maturity for a pest control experiment in early spring. Despite food offerings, spiders stopped molting after October although they were maintained at 25° C and had swollen, well-nourished abdomens. It was surmised that decreased filtered daylight from a paper-covered window might be suppressing molting. Feeding was halted in January 2015; 88 spiderlings were checked weekly for molts. Molting resumed during late March 2015 and continued through May 2015 despite no feedings. To more thoroughly elucidate photoperiod effects on molting, during the week of the September 2015 equinox, three cohorts of 10 immatures of both brown and Chilean recluses, *L. laeta* (Nicolet, 1849), were exposed to three light regimes: 14:10 L:D, natural, 10:14 L:D. Through November 2015 to late March 2016 for brown recluses, there was no molting in the 10:14 regime, 3 of 10 spiders molted in the natural light regime, and 8 of 10 spiders molted in the 14:10 L:D regime. Additionally, fifteen newly-emerged brown recluse spiderlings split into three cohorts of 5 spiders each in November exhibited more molting in the 14:10 L:D compared to natural and 10:14 L:D light cycles. Chilean recluses showed no differences in molting across the three photoperiod regimes. This species difference may be explained in that brown recluses are native to temperate zones where winters can be fatal; Chilean recluses are tropical where short photoperiods may have little significance for survival.

**Keywords:** Life history traits, urban entomology, urban pest, development, recluse spiders

Spider life-history traits are often influenced by abiotic variables such as temperature, humidity, and photoperiod. Even when brought into the laboratory and exposed to conditions that are considered favorable for continued growth, seasonal cessation of development has been noted for a variety of spider taxa such as *Pardosa astrigera* L. Koch, 1878 (Miyashita 1969), *Pisaura mirabilis* (Clerck, 1757) (Dondale & Legendre 1971), *Parasteatoda tepidariorum* (C.L. Koch, 1841) (Tanaka 1991, 1992) and thomisids (Schick 1965). This cessation can be labeled diapause or quiescence depending on the conditions. Diapause requires an environmental trigger such as non-adverse temperature and seasonal light cycle changes to initiate and terminate this condition, which involves endocrinology and synthesis or reduction of specific compounds (Saunders 2002). Quiescence is merely a short period of inactivity instigated by unfavorable conditions, which can be immediately reversed upon return to normal environmental factors (Saunders 2002).

The brown recluse spider, *Loxosceles reclusa* Gertsch & Mulaik, 1940, was not known to be medically important in North America until 1957 (Atkins et al. 1957); soon after this date, there was a rush to present biological and medical information on the spider. Extensive life history work was documented by Hite et al. (1966) and Horner & Stewart (1967). However, one area that has yet to be investigated is the effect of seasonal photoperiod on *Loxosceles* molting. Instigated by a serendipitous observation, herein we examine the response of brown recluse spiders and their tropical relatives, the Chilean recluse spider, *L. laeta* (Nicolet, 1849) to different photoperiod regimes in the laboratory.

### METHODS

**Spiders.**—Brown recluse spiders were taken from a colony that was initiated with specimens collected in Columbia,

Missouri in 1995, with occasional genetic infusion from spiders collected in Russellville, Arkansas and Lenexa, Kansas. Chilean recluses originated from a colony that was started from specimens collected in San Gabriel (Los Angeles County) California in 2003 and had been in captivity since then without genetic infusion.

**General procedures.**—In all experiments, spiderlings were maintained individually in 3½ to 40 dram vials (13 to 150 ml) with plastic snap-on lids; vial volume corresponded with spiderling size. A piece of paper towel was placed inside the vial such that it covered the inner half of the vial's circumference, providing a surface for silk deposition to aid in molting as well as prey capture. When being fed, each spiderling was offered a single German cockroach, *Blattella germanica*, approximately the same body length as that of the spiderling.

**Initial observation that instigated the study.**—In the autumn of 2014, more than 100 brown recluse spiderlings emerged from egg sacs and were separated into individual 3½ dram vials. Each was offered a small German cockroach twice a month, which is sufficient for growth (i.e., recluse spiders fed twice a month undergo molting), in the expectation that the spiderlings would mature by early spring for an unrelated, large-scale mating experiment. Although spiderlings were not being specifically monitored, it was observed that they ceased molting after October. None were dying and their abdomens were very well distended, similar to spiders capable of molting. These spiderlings were maintained in a room in the University of California-Riverside (UCR) Insectary and Quarantine facility that had diffuse natural lighting. The window to this room was located under a large overhang of the insectary, was covered with brown butcher paper, never received direct sunlight and was used continuously for recluse spider maintenance for several years with spiders readily molting to maturity. When molting was still not occurring by the end of



January despite prey offerings on a twice-monthly basis, it was surmised that cessation of development might be due to the decreased natural winter light cycle.

Therefore, in attempt to determine whether molting was influenced by photoperiod, at the end of January, 88 spiderlings in their individual vials were haphazardly chosen from the cohort of 100+. Prey offerings ceased and vials were checked once a week from 8 February 2015 until the first molt was observed (30 March 2015), after which they were checked twice a week until 31 May 2015, when this portion of the study was terminated. When a spiderling molted, it was removed from the pool because we wanted to document the first post-winter molting of each spiderling. Spiderlings were in their second to fourth instars at the initiation of the experiment in early February. Room temperature was maintained at approximately 25° C year-round, but not recorded.

**Effect of photoperiod on molting.**—In September 2015, immature brown and Chilean recluse spiders ( $n = 30$  of each species) were arranged from smallest to largest in approximate size within each species and assigned to three cohorts via numbers randomly generated in triplets (i.e., 213, 132, 312, etc.) so that each experimental cohort within each species would have an approximately similar range of spider sizes and, hence, approximately the same demographics of instars. Penultimate males were not used. Based on experience in rearing hundreds of recluses from egg sacs, it was estimated that the spiderlings ranged from the third to seventh instars. This spectrum was chosen in order to have representatives from various instars involved in the bioassay instead of biasing it toward one particular instar; in insects, different instars within a species can have differential proclivity to entering diapause (Tauber et al. 1986). For each species, one cohort of ten spiderlings was assigned to a 14:10 L:D light cycle exposure, the second to a 10:14 L:D light cycle and the third to a natural light cycle through a brown paper-covered window. The UCR campus where experiments were conducted is located at 33° 57' N latitude and approximately experiences seasonal 14:10 and 10:14 photoperiod extremes. Prior to the start of the experiment, spiderlings were maintained in a room in the Insectary and Quarantine Facility at UCR with an ambient photoperiod and offered *B. germanica* about once a month. The last pre-assay meal occurred between 11 to 13 September 2015 when spiderlings were transferred to clean vials.

The photoperiod experiment was initiated on 26 September 2015, 5 days after the autumn equinox when the light cycle was approximately 12:12 L:D, at which point, spiderlings were offered *B. germanica* again and assigned to one of the three experimental cohorts. The 14:10 and 10:14 L:D cohorts were placed inside plywood boxes, 45 cm height x 45 cm width by 60 cm length with a piece of white opaque plastic (3 mm thick) placed at the 45 cm mark inside the box, constituting the back wall, and covered with a lid (Fig. 1). A light socket with a 4-watt frosted nightlight bulb (EverydayLiving, Kroger Co., Cincinnati OH) was positioned behind the plastic on the posterior 15 cm of the box such that light passing through the plastic was diffuse. Light levels during the day were 145 lux in the 14:10 and 10:14 L:D boxes and varied in the natural box from 44 lux on an overcast morning to 145 lux on a sunny afternoon as measured with a light meter (Gossen Luna-Pro

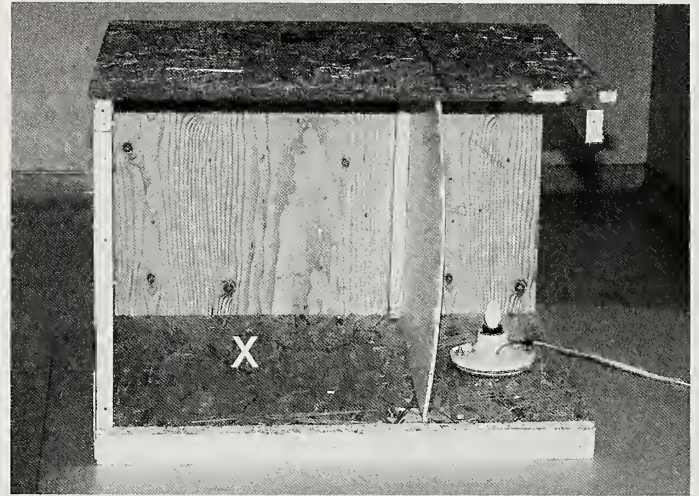


Figure 1.—View of the plywood box that housed either the 14:10 or 10:14 light cycle cohorts of spiders. The right wall of the box (facing the camera) is removed for photographic purposes. The light was placed outside of the area of the box housing the spiders and was open to the back. Spiders, in vials, were placed near the “X”.

SBC, Manfrotto Distribution, Upper Saddle River, NJ). During the day, room contents were readily visible, whereas at night, the room was completely dark to the human eye, hence, providing a definite day/night cycle.

The box fronts faced each other such that light at the back of each box was emitted toward a wall covered with black construction paper, reducing reflected light, which was further obstructed with pieces of cardboard so that light should not have been visible to spiderlings in the other boxes. On the day the experiment was initiated, timers (Woods model 50008 indoor 7-day timer 2-C, Coleman Cable, Waukegan, Illinois) programmable to the minute, provided one cohort of each *Loxosceles* species with 12¼ hours of light, increasing the light period by 15 minutes per week until reaching the 14:10 L:D level at week 7 (14 November 2015), while, conversely, a second cohort of each species was initially provided with 11¼ hours of light, decreasing the light period by 15 minutes per week until the 10:14 L:D level was reached also on 14 November 2015. These light levels were then maintained until the experiment was terminated on 28 May 2016. The two cohorts (one each of *L. reclusa* and *L. laeta*) receiving natural light were placed in a cardboard box positioned flush against the paper-covered window. The room temperature was  $24.8 \pm 0.35^\circ \text{C}$  for the duration of the experiment. Vials were checked for remnant exuviae each week from 3 October 2015 until 28 May 2016. Spiderlings were offered *B. germanica* every week for the first 3 weeks and then at 2-week intervals for the remainder of the experiment. If a cockroach was still alive at the subsequent prey offering, the spiderling was not offered additional prey. Likewise, a spiderling was not offered prey if its legs were dark (indicating that molting was imminent within a few days), or if its legs were pale in the presence of a recently shed skin (indicating it had molted in the previous 2 days) as it could be vulnerable to roach predation (Vetter & Rust 2010). On 27 November 2015, all spiderlings were transferred to clean vials with new pieces of paper toweling because of the buildup of shed skins, silk and dead roaches; if



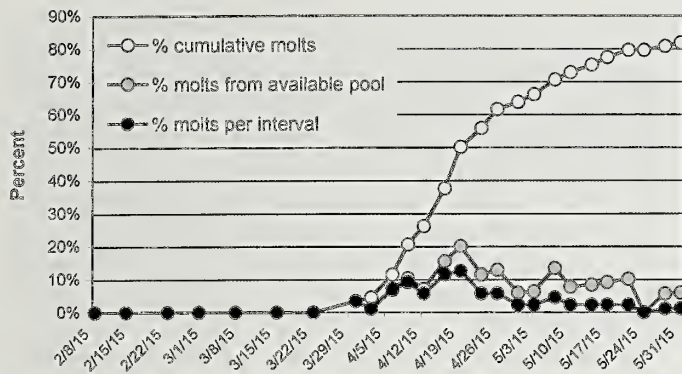


Figure 2.—Molting phenology of a pool of 88 brown recluse spiderlings exposed to a natural light cycle. The spiderlings had not molted from November 2014 to January 2015 despite being offered prey, then were not fed from February 2015 onward. Spiderlings were checked weekly until the first molt occurred on 30 March 2015, thereafter checked twice weekly through the end of May 2015. Molts per interval (%) and cumulative molts (%) are in reference to the original 88 spiderlings.

warranted due to growth via molting, spiderlings were transferred to larger vials (i.e., the diameter of the vial to which the spider was transferred was noticeably larger than the leg span of the spider such that it should not have been cramped for space). This movement of spiderlings to clean vials and new paper towels was subsequently performed on 23 January and 19 March 2016 (during a week between prey offerings). When males matured, they were removed from the experiment as they had reached their terminal life stage; suspected mature females were left in the experiment in case they were still penultimates.

**Source of additional spiderlings.**—Spiderlings emerged from one brown recluse egg sac during the week ending on 14 November 2015. Fifteen second-instar spiderlings were individually transferred to 3½ dram vials on 17 November 2015, were randomly separated into three cohorts of five spiderlings each the next day and added to the 14:10, natural and 10:14 light cycle boxes. They were offered roaches for the first time on 21 November 2015 during the regular feeding week for the *Loxosceles* spiderlings described in the previous photoperiod experiment and, thereafter, each was offered a cockroach

every two weeks, similar to the spiders in the assay above. These additional spiderlings were similarly checked for molting once a week. These spiderlings were of interest because they had not experienced the normal seasonal light cycle after emerging from the egg sac in comparison to the spiderlings in the previous experiment which experienced several weeks at an ambient light cycle leading up to the autumn equinox on 21 September 2015.

**Statistics.**—Data regarding differences among the numbers of spiders molting in the three light cycle regimes were analyzed with Fisher's Exact Test because of the large percentage of small expected frequencies; hence, only *P* values are reported. Data were analyzed using the statistical package SAS.

## RESULTS

**Initial observation that instigated the study.**—Spiderlings exposed to a natural light cycle and with termination of feeding at the end of January 2015 were first detected to molt on 30 March 2015 when exuviae were noted in three vials (Fig. 2). At least one newly-molted spiderling was detected at every twice-weekly check until 24 May 2015 when the pool of potential molters had decreased from 88 to 18. The highest level of molting occurred during a 7-day period (12–19 April 2015) where 21 spiderlings molted (32.3% of the spiderlings in the potential pool at week's start). When this bioassay was terminated at the end of May 2015, 17 spiderlings (19.3%) had yet to molt. Of the original 88 spiderlings, none died during this bioassay because of unsuccessful molting or starvation despite the lack of prey for those who had not eaten for up to 4 months.

**Effect of photoperiod on molting in brown recluse spiders.**—In October 2015, the first full month under the three different light cycles (the manipulated light cycles were still being increased in the 14:10 L:D regime and decreased in the 10:14 L:D regime), there was no statistical difference among brown recluses in regard to the number of spiders molting ( $P = 0.89$ , Fig. 3a, Table 1). However, during the period from November 2015 through February 2016, eight brown recluses in the 14:10 L:D photoperiod molted 10 times (6 once, 2 twice), 3 of 10 from the natural light cycle molted once and no moltings

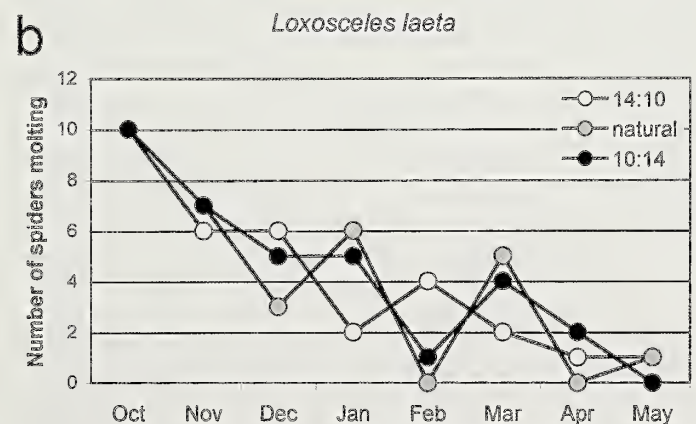
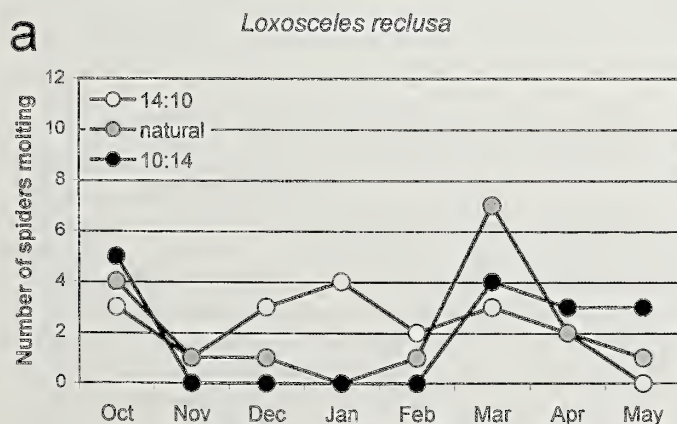


Figure 3.—(a) The number of brown recluse spiders molting each month from October 2015 through May 2016 under three light cycle regimes. (b) The number of Chilean recluse spiders molting each month from October 2015 through May 2016 under three light cycle regimes.



Table 1.—The number of brown and Chilean recluse spiders molting in October 2015 and in November 2015 through February 2016 across three photoperiod regimens. Sample size was 10 for all cohorts except for the *L. reclusa* 10:14 L:D light cycle from November to February, which was nine because of the death of one spider through incomplete molting in October. In parentheses is the number of molts undergone by the spiders in the cohort during that period.

	Oct 2015	Nov 2015 to Feb 2016
<i>Loxosceles reclusa</i>		
14:10 L:D	3 (3)	8 (10)
natural light cycle	4 (4)	3 (3)
10:14 L:D	5 (5)	0
<i>Loxosceles laeta</i>		
14:10 L:D	10 (11)	9 (18)
natural light cycle	10 (10)	10 (16)
10:14 L:D	10 (10)	10 (18)

occurred in the nine brown recluses in the 10:14 L:D light cycle. (The tenth spider in this last cohort died while molting in October.) This difference in the number of individual brown recluses molting in the three light regimes during November 2015–February 2016 is statistically significant ( $P < 0.001$ , Table 1). However, one curious result was that for the natural and 10:14 L:D cycles, there was a spike in molting in March 2016 (Fig. 3).

Second instar spiderlings that emerged from an egg sac in November and were introduced into the three photoperiod regimes 4 days later showed a significant effect of light cycle exposure on molting ( $P = 0.001$ , Fig. 4). The five spiderlings in the 14:10 L:D light cycle each molted twice during the winter (December to February) whereas there was no molting by the spiderlings in the natural and 10:14 L:D light cycles during the same period. Spiderlings kept at the natural light cycle had two molts to the third instar detected on each of 26 March and 9 April 2016, and the 10:14 L:D light cycle had two molts detected to the third instar on each of 9 and 23 April 2016. At the termination of the experiment, the 14:10 L:D cohort

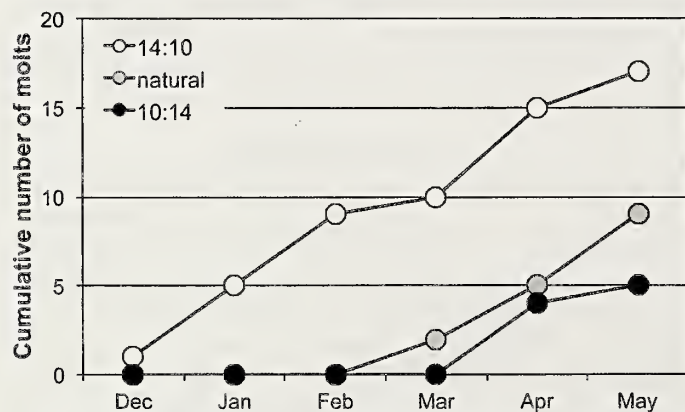


Figure 4.—The cumulative number of molts for 15 spiderlings which emerged from the same egg sac in November 2016. Within 4 days post-emergence, they were split into three cohorts of five spiderlings each, and each cohort was placed into one of the three experimental photoperiod regimes. The ordinate axis is in units of five such that each horizontal separation correlates exactly to a specific instar.

Table 2.—The number of brown and Chilean recluse spiders molting a specific number of times in November 2015 through February 2016 across three different photoperiod regimens. The potential sample size was 10 for all cohorts except for the *L. reclusa* 10:14 L:D light cycle, which was nine because of the death of one spider through incomplete molting in October.

	Number of spiders molting a specific number of times			
	zero	once	twice	three time
<i>Loxosceles reclusa</i>				
14:10 L:D	2	6	2	0
natural light cycle	7	3	0	0
10:14 L:D	9	0	0	0
<i>Loxosceles laeta</i>				
14:10 L:D	1	2	5	2
natural light cycle	0	4	6	0
10:14 L:D	0	3	6	1

consisted of two 6<sup>th</sup> instars and three 5<sup>th</sup> instars, the natural light cycle cohort consisted of four 4<sup>th</sup> instars and one 3<sup>rd</sup> instar and the 10:14 L:D cohort consisted of four 3<sup>rd</sup> instars with one death going into the 3<sup>rd</sup> instar (Fig. 4).

**Effect of photoperiod on molting in Chilean recluse spiders.**—In contrast to brown recluses, Chilean recluses continued to molt throughout the winter regardless of light cycle although they did so at a decreased rate from October, when every spider molted at least once (Table 1). No significant differences were detected among the three light cycles, with 29 of the 30 spiders molting at least once from November to February ( $P = 1$ , Table 1, Fig. 3b). Likewise, for the Chilean recluses the pool of potential molters decreased with time as spiders matured. There was also a spike in molting in the natural and 10:14 L:D spiders in March 2016 similar to that observed for the brown recluses.

**Comparison of the two recluse spider species.**—In the period from November 2015 to February 2016, there were no differences in the number of brown and Chilean recluses molting a specific number of times (none, once, twice, or three times) in the 14:10 L:D light cycle ( $P = 0.131$ , Table 2). However, a significantly greater number of Chilean recluses molted more often than brown recluses in the natural ( $P = 0.001$ , Table 2) and 10:14 L:D light cycles ( $P < 0.0001$ , Table 2).

## DISCUSSION

Molting by brown recluse spiders appears to be influenced by seasonal photoperiod with decreased daylight suppressing this life history trait. In the initial experiment with exposure to natural light, spiderlings did not molt during the winter despite being sufficiently nourished to do so (Fig. 2). Molting did not initiate until soon after the last week in March where the molters endured a 2- to 4-month period without food. If molting were strongly dependent upon food availability, spiders should have continued molting throughout the winter. Instead, molting was initiated during the period when food was not offered. Recluse spiders are well known for surviving long periods without food (Eskafi et al. 1977; Lowrie 1980) and most of the spiderlings retained sufficient body stores



during this period of prey absence not only to survive but molt to the next instar.

In the second bioassay with the three photoperiod regimes, brown recluses did not molt from November 2015 through February 2016 when kept at the 10:14 L:D photoperiod in comparison to a significantly higher number molting at the 14:10 L:D light regime for the same period (Fig. 3). Of interest, there were spikes of molting in the natural light regime in March 2016 corroborating the timing of the post-winter molting initiation of the first experiment. Curiously, there was also a spike during this same period by spiders in the 10:14 L:D light regime which continued into April and May 2016. Schaefer (1987) mentions that endogenous rhythms may play a role in seasonal initiation of spider development so even short photoperiods may not be sufficient to permanently suppress molting. This is corroborated in insects which lose sensitivity to photoperiod as diapause progresses (Tauber et al. 1986).

The most compelling evidence for effects of seasonal light was observed when brown recluse spiderlings were introduced to differing photoperiods soon after emergence from the egg sac. All five spiderlings in the 14:10 L:D photoperiod molted at least twice during the winter before any molting occurred in the natural or 10:14 L:D photoperiod (Fig. 4). The cohort of five spiderlings in the natural light cycle did not exhibit their first molt until the end of March 2016, the same time of year as the cohort of 88 spiderlings first molted in the previous year, corroborating the stimulus of the natural light level around the time of the spring equinox. Both of these experiments are consistent with the observations of behavioral cessation in a synanthropic population of brown recluses in an unheated Illinois garage where spiders were not actively seen from mid-October to mid-May (Cramer 2015). In comparison, molting in the Chilean recluse is much less affected by photoperiod as they continued to molt throughout the winter months albeit at a lower rate than in October (Fig. 3).

Although this experiment did not detect a significant effect of light cycle on the Chilean recluse, it is possible that this was due to small sample size. In addition, there is the confounding factor that these spiders also molted more frequently in winter than brown recluses, and because of the experimental design of using a range of ages, some *L. laeta* spiders molted to maturity during the course of the experiment, removing themselves from the sample pool. As an artificial exploratory exercise, if the number of *L. laeta* spiders that molt per month from November to February is doubled (data not shown), a statistically significant relationship emerges. However, the criss-crossing pattern of the three photoperiod lines in Fig. 3b does not indicate much of a conspicuous trend in any direction.

Nonetheless, if there is a difference in response to seasonal photoperiod by these two species, there may be a valid evolutionary basis for it. Gertsch (1967) shows the distribution of *L. laeta* in South America to be predominantly from the Equator to about 34° south latitude. Much of this region encompasses tropical climates where seasonal photoperiod and temperature fluctuations are minor and prey are likely available year round. Hence, there would be no reason for cessation of activity in the “winter” months of reduced photophase for a species that evolved in the tropics.

Additionally, only the spiders at the southernmost portion of its range would experience a 10:14 photoperiod which still would place them in regions with moderate winter temperatures. In contrast, Gertsch & Ennik (1983) show the indigenous distribution of *L. reclusa* to occur from approximately 28° to 41° north latitude in North America. Therefore, areas of dense brown recluse habitat are subject to predictable extreme winter conditions with snow cover and subfreezing temperatures in many portions of their natural range, such that the winter light cycle suppresses molting, in contrast to the tropical Chilean recluse which may be active year-round. Somewhat similarly, Tanaka (1992) demonstrated that subtropical *Parasteatoda tepidariorum* spiders from a lower latitude in Japan readily molted to maturity at a photoperiod with decreased light levels that inhibited development in the same species collected from a more temperate and higher latitude location.

In comparison to spiders, diapause in insects has been so well studied for decades that books have been dedicated to the topic (e.g., Brown & Hodek 1980; Tauber et al. 1986; Saunders 2002). Years ago, authors documented the growing number of insect species that underwent diapause but that gave way to an acceptance that almost every insect exhibited diapause, and it was the rare creature that did not (Saunders 2002). Most insect diapause seems to be tied to light cycle, which is a reliable seasonal indicator, but diapause can also be modified or influenced by temperature, humidity or rainfall. Diapause even occurs to some degree for insects near the equator, where light cycle does not vary much from 12:12 L:D; here diapause may be significantly influenced by seasonal rainfall patterns (Tauber et al. 1986; Saunders 2002). Photoperiod influences pre-diapause factors such as fat deposition and accumulation of cryoprotectants, which occurs well before induction initiates (Adedokun & Denlinger 1985; Denlinger 2002).

With the voluminous insect literature, it is possible to find almost every permutation of diapause factors. Examples include: (1) induction and/or termination by photoperiod, which can be dictated by the absolute photoperiod length; (2) induction by photoperiod, which can be dictated by the degree of change in photoperiod regardless of actual light cycle; (3) induction by photoperiod but termination requiring a specific number of days at low temperatures at critical periods of diapause; (4) induction by photoperiod but endogenous termination instigated after a specific time period, even when held under conditions that induce diapause initially; (5) stage of development (egg, larva, pupa) where some insects have differential susceptibility to diapause depending upon which instar is exposed to the critical conditions. In gene regulation, diapause silences many genes while conversely, some genes are only uniquely expressed at this time; expression of some of these genes can increase or decrease only hours before or after environmental factors trigger diapause induction or termination (Denlinger 2002).

Several studies have shown the effect of photoperiod on spider behavior. Similar to insects, factors other than light (e.g., temperature) likely play a contributory role in observed behaviors (Baert 1978; Schaefer 1987). Kurihara (1979) collected egg sacs of *Agelena limbata* Thorell, 1897 in late September and transferred them from natural conditions to the laboratory (20° C, 70% RH). On the first day that molting



to the second instar was noticed as the spiderlings were entering winter diapause, the egg sacs were assigned to seven light regimes, varying from 10 to 16 hours of light. Ninety-five to 100% of sacs maintained at  $\geq 13\frac{1}{2}$  hours of light per day had spiderling emergence within 26 to 39 days, whereas egg sacs maintained at  $\leq 13$  hours of light had only 5% to 31% emergence after 140 to 165 days. Short day light cycles can inhibit female reproductive development in spiders, which can be reversed by exposure to long-day light cycles or cold temperatures (Schaefer 1987). Miyashita (1969) collected *Pardosa astrigera* (cited as *Lycosa T-insignita*) in Japan from November to March; those spiders collected later in this period were able to molt to maturity in the laboratory sooner after long photoperiod exposure than spiders collected earlier. This long photoperiod was purported to break winter diapause and enhance progression to the mature molt by spiders that were starting to respond to longer natural daylength. Tanaka (1991) demonstrated that *Parasteatoda tepidariorum* spiderlings developed faster under long photoperiods than short ones with a comparatively greater delay in the ultimate molt to maturity in the short photoperiod. Response to seasonal photoperiod may be species specific where several (e.g., *Pholcus phalangioides* (Fuesslin, 1775), *Bathypantes gracilis* (Blackwall, 1841), *Pachygnatha clercki* Sundevall, 1823) show similar rates of development regardless of photoperiod regime. In contrast, postembryonic development in others (e.g., *Pirata piraticus* (Clerck, 1757), *Tetragnatha montana* Simon, 1874, *Oedothorax retusus* (Westring, 1951)) is retarded by short photoperiods (Schaefer 1976 as cited in Schaefer 1987).

The information provided by this study may be useful beyond extending our academic knowledge on the life history of recluse spiders. The motivation for this work was to generate a large number of mature spiders by the early part of their active season in order to conduct experiments. This may not be possible if photoperiod in the laboratory is not manipulated appropriately. Researchers using recluse spiders, especially brown recluses, should consider the effect of photoperiod on colony growth and subsequent maintenance.

#### ACKNOWLEDGMENTS

We thank Imad Bayoun and Serguei Triapitsyn (UCR Entomology) for allowing the use of the UC Riverside Insectary and Quarantine Facility where the assays were run. Thanks also to Ruth Amrich (UCR Entomology) for assistance in the experiments.

#### LITERATURE CITED

Adedokun, T.A. & D.L. Denlinger. 1985. Metabolic reserves associated with pupal diapause in the flesh fly, *Sarcophaga crassipalpis*. *Journal of Insect Physiology* 31:229–233.  
 Atkins, J.A., C.W. Wingo & W.A. Sodeman. 1957. Probable cause of necrotic spider bite in the Midwest. *Science* 126:73.  
 Baert, L. 1978. Influence de la photopériodicité sur la maturation ovarienne chez *Gongylidium rufipes* (Sundevall) (Araneae, Linyphiidae). *Revue Arachnologique* 2:23–27.

Brown, V.K. & I. Hodek. 1980. Diapause and Life Cycle Strategies in Insects. Dr. W. Junk Publishers, The Hague, The Netherlands.  
 Cramer, K.L. 2015. Activity patterns of a synanthropic population of the brown recluse spider, *Loxosceles reclusa* (Araneae: Sicariidae), with observations on feeding and mating. *Journal of Arachnology* 43:67–71.  
 Denlinger, D.L. 2002. Regulation of diapause. *Annual Review of Entomology* 47:93–122.  
 Dondale, C.D. & R. Legendre. 1971. Winter diapause in a Mediterranean population of *Pisaura mirabilis* Clerck. *Bulletin of the British Arachnological Society* 2:6–10.  
 Eskafi, F.M., J.L. Frazier, R.R. Hocking & B.R. Norment. 1977. Influence of environmental factors on longevity of the brown recluse spider. *Journal of Medical Entomology* 14:221–228.  
 Gertsch, W.J. 1967. The spider genus *Loxosceles* in South America (Araneae, Scytodidae). *Bulletin of the American Museum of Natural History* 136:117–174.  
 Gertsch, W.J. & F. Ennik. 1983. The spider genus *Loxosceles* in North America, Central America, and the West Indies (Araneae, Loxoseelidae). *Bulletin of the American Museum of Natural History* 175:264–360.  
 Hite, J.M., W.J. Gladney, J.L. Lancaster & W.H. Whitcomb. 1966. The biology of the brown recluse spider. University of Arkansas, Fayetteville. Agricultural Experiment Station Bulletin No. 711, 26pp.  
 Horner, N.V. & K.W. Stewart. 1967. Life history of the brown spider, *Loxosceles reclusa* Gertsch and Mulaik. *Texas Journal of Science* 19:334–347.  
 Kurihara, K. 1979. Photoperiodic regulation of winter diapause in the grass spider. *Experientia* 35:1479–1480.  
 Lowrie, D.C. 1980. Starvation longevity of *Loxosceles laeta* (Nicolet) (Araneae). *Entomological News* 91:130–132.  
 Miyashita, K. 1969. Seasonal change of population density and some characteristics of overwintering nymph *Lycosa T-insignita* Boes. et Str. (Araneae: Lycosidae). *Applied Entomology and Zoology* 4:1–8.  
 Saunders, D.S. 2002. *Insect Clocks*. 3<sup>rd</sup> ed. Elsevier, Amsterdam, The Netherlands.  
 Schaefer, M. 1976. Experimentelle Untersuchungen zum Jahreszyklus und zur Überwinterung von Spinnen (Araneida). *Zoologische Jahrbücher Abteilung für Systematik Ökologie und Geographie der Tiere* 103:127–289.  
 Schaefer, M. 1987. Life cycles and diapause. Pp. 331–347. *In* *Ecophysiology of Spiders*. (W. Nentwig, ed.). Springer-Verlag, Berlin Heidelberg.  
 Schick, R.X. 1965. The crab spiders of California (Araneae, Thomisidae). *Bulletin of the American Museum of Natural History* 129:1–180.  
 Tanaka, K. 1991. Diapause and seasonal life cycle strategy in the house spider, *Achaearanea tepidariorum* (Araneae, Theridiidae). *Physiological Entomology* 16:249–262.  
 Tanaka, K. 1992. Photoperiodic control of diapause and climatic adaptation of the house spider, *Achaearanea tepidariorum* (Araneae, Theridiidae). *Functional Ecology* 6:345–352.  
 Tauber, M.J., C.A. Tauber & S. Masaki. 1986. *Seasonal Adaptations of Insects*. Oxford University Press, New York.  
 Vetter, R.S. & M.K. Rust. 2010. Periodicity of molting and resumption of post-molt feeding in the brown recluse spider, *Loxosceles reclusa* (Araneae: Sicariidae). *Journal of the Kansas Entomological Society* 83:306–312.

*Manuscript received 21 June 2017, revised 12 February 2017.*



## In the spider nursery: indifference, cooperation or antagonism?

Susan E. Riechert<sup>1</sup>, Jonathan Pruitt<sup>2</sup> and Jennifer Bosco<sup>1</sup>: <sup>1</sup>Department of Ecology and Evolutionary Biology, University of Tennessee, Knoxville TN 37996-1610, USA; E-mail: riechert@utk.edu; <sup>2</sup>Department of Ecology, Evolution and Marine Biology, University California-Santa Barbara, Santa Barbara, CA 93160, USA

**Abstract.** Based on studies of adult behavior, the desert spider *Agelenopsis aperta* (Gertsch, 1934) is considered exemplary of a species exhibiting an aggressive syndrome. This study offers a first examination of the nature of interactions that juvenile *A. aperta* engage in during the period when sibs are clustered on a group web. We test the hypothesis that early instar *A. aperta* lack the aggressiveness noted for older instars. Our data set is comprised of observations of five weekly feedings offered to 818 sibling pairs, constituting an average of 4.6 replicate sib pairs from each of 174 families. At each weekly feeding, a worker termite was offered to each sib in the shared container in which they had built web retreats. We observed no cooperative foraging during the course of these feedings. Rather, most families exhibited a mix of independent foraging and non-injurious contests over prey. We present a brief overview of the occurrence and initiation of contests over prey, with particular reference to the weekly feeding in which contests first occur versus the feeding in which a seminal contest takes place (i.e., where sibs earn permanent winner versus loser status).

**Keywords:** *Agelenopsis aperta*, sibling interactions, feeding bouts

In arthropods such as spiders, there is a gregarious phase in the life cycle when the young are clustered in the confined space of a silk nest or web. During this period, indirect fitness effects among sibs are likely to occur, in which the behavior of an individual not only influences its own future reproductive success but that of its sibs as well. For example, cooperation in prey capture not only offers positive benefits to sibs that engage in the capture of a prey item, but also to sibs that participate only in feeding on that prey (e.g., *Amaurobius ferox* (Walckenaer, 1830) (Kim et al. 2005). Alternatively, negative indirect effects are expected when resources available to clustered sibs are limited. Both exploitative (independent foraging for prey) and interference competition (agonistic interactions over prey) may produce these indirect negative fitness effects (Keddy 1989).

In this study, we examine sibling interactions of early instar *Agelenopsis aperta* (Gertsch, 1934) during the gregarious phase in the life cycle that takes place in the absence of the mother. *Agelenopsis aperta* is a desert species, which is known for the competitive behavior it exhibits over websites as late instars and adults (e.g., Riechert 1981). Our focal question is whether the agonistic behavior that later instars exhibit towards conspecifics is exhibited at this early stage in the life cycle when cooperative behavior or independent feeding might be favored.

We, thus, examined sib-sib pair behavior during five weekly feedings to establish whether early instars of this species exhibit resource exploitation (independent foraging), contest competition (agonistic interactions over prey), cooperation (joint capture and feeding) or some combination of these three resource utilization strategies. The nature of contest initiation is additionally outlined herein.

### METHODS

**Test system.**—*Agelenopsis aperta* is an arid-lands spider that occupies the full range of habitat types found at elevations below 1800 m in the southwestern United States and Mexico. This species' web is comprised of a non-sticky sheet upon

which prey capture and agonistic interactions occur. There is also a silk-lined funnel retreat that leads into a protected area, such as a crevice or under a rock or stump. Extensive work by Riechert and colleagues over the past forty years has led to a wealth of information regarding the ecology and behavior of this species as well as the role of population ecology in behavioral differentiation (See reviews in Riechert 1993, 1999, Riechert et al. 2001).

As spiderlings emerge from the egg case they lay down silk, forming a communal web. Individuals produce silk retreats within this web structure and begin feeding on prey within 10 days of emergence (Riechert, personal observations). This communal web is occupied for several weeks. As individuals begin dispersing from it, they build individual webs nearby (Riechert 1974). The high density of siblings through the first month following emergence from the egg case offers the opportunity for cooperative foraging as well as for agonistic encounters over prey. This forms the impetus for our study of *A. aperta* interactions at this stage of the life cycle.

**Collection and pair establishment.**—Gravid females from two arid west Texas locations—a mesquite-dominated flat just west of the town Balmorhea in Reeves County (30.97°N, 103.75°W) and a cactus scrub hillside just east of the Big Bend National Park in Brewster County, TX (29.32°N 103.14°W)—provided the source of F2 offspring of 174 F1 generation females. As we found no size biases among spiderlings within a clutch (Fisher Scientific accu-124D balance mass determinations), we randomly assigned sibs from each family to pairs. The number of replicates initially established depended on clutch size, with a maximum of ten pairs from any one family. We marked each sib in a pair with fluorescent powder of a different color before releasing them into a plastic container measuring 3.5 cm in dia and 1 cm in height. We refurbished the respective color markings as necessitated by molts.

**Weekly staged feedings.**—At each of five weekly feedings, we simultaneously dropped a worker termite (*Reticulitermes flavipes* (Kollar, 1837)) at the funnel entrances of the two sibs sharing a container. (Note that one termite is approximately three times the mass of an early instar *A. aperta* (Mean termite



mass =  $1.89 \pm 0.03$  mg; mean *A. aperta* spiderling mass =  $0.54 \pm 0.01$  mg). Subsequently, we scored the behavior of the sibs for a five-min period or until prey capture activities had ended. We revisited each sib pair ~30mins later to record the feeding status of each sib (i.e., did the respective sibs each have a termite secured at its web funnel, were both sibs feeding on the same termite, or did one sib have control of both termites introduced into the shared container?).

A contest over prey in a particular weekly feeding was declared "seminal" when it led to a clear resolution of each individual's competitive status relative to its sib for that and all subsequent weekly feeding bouts. In this study, there were two potential contest outcomes. Competitive interactions could end in a "draw" or with the identification of a distinct contest "winner" and "loser". The outcome "draw" leads to subsequent independent foraging by the paired sibs. (Each sib attacks and feeds only on the termite offered to it at its funnel entrance, without respect to what its sib is doing.) On the other hand, "winners" of seminal contests tend to monopolize future prey offerings, while "losers" defer to their winning sib in subsequent feeding opportunities. The winner/loser seminal contest outcome can lead to marked differences in the growth rates of the paired sibs, particularly when contest resolution occurs early in the series of five weekly feedings (a topic of a later paper on this system).

**Analyses.**—Our final data set consisted of 818 surviving sib pairs with a mean number of  $4.6 \pm 0.04$  replicates/family and a total of 4,090 feeding bouts. We used the statistical package JMP<sup>®</sup> Pro version 12.0 (SAS Institute Inc) in the completion of these analyses. Chi square tests were applied to simple frequency questions and logistic regression applied in examining the potential influences of family and population on juvenile behavioral type representation.

## RESULTS

**Satiation prey levels.**—Our test for the assumption that a single termite prey offers food greater than what an early instar *A. aperta* can consume is substantiated by 162 observations of different individuals feeding on a termite offered the previous week. No significant relationship exists between an individual's size relative to its sib and its propensity to feed on an old prey item ( $X^2_2 = 0.79$ ,  $P = 0.37$ ,  $n = 162$ ). Further, feeding on a prey item remaining from past feedings occurs randomly across the five weekly feedings ( $X^2_3 = 7.04$ ,  $P = 0.07$ ).

**Foraging strategy representation.**—Sixty-five percent of sib pairs engaged in contest competition during at least one weekly feeding trial. Thirty-five percent of sibling pairs never engaged in contest competition and demonstrated only independent foraging. None of the sibling pairs demonstrated cooperative foraging. The significant whole model test result ( $X^2_{165.816} = 264.67$ ,  $P < 0.001$ ) reflects a significant family effect only. No significant population (collection locality) effect is present ( $X^2 = 0.12$ ,  $P = 0.72$ ). Inspection of the data indicates that most families exhibit some mix of sibs that forage only independently and those that contest prey in the paired sib context. We did find, however, that all sib pairs contested prey at least once in 24.5% of the families, while all sib pairs foraged independently in another 5% of the families (Fig. 1).

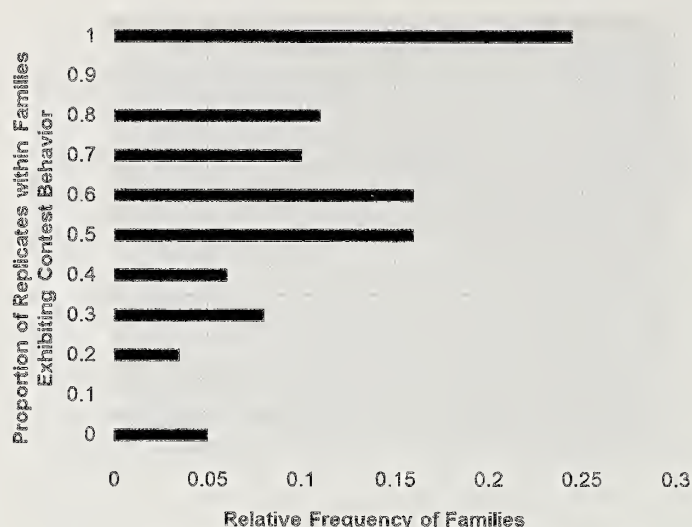


Figure 1.—Family distribution of proportions of replicate sib pairs exhibiting contest competition during at least one feeding bout during the 5 weeks of the experiment.

**Contests over prey.**—Contests between sibs over prey offered in a weekly feeding occur when an individual ignores (78.2%,  $n = 471$ ) or abandons (21.8%,  $n = 131$ ) the termite offered at its own funnel entrance, and encroaches on the termite offered to its sib. A total of 531 of the 818 sibling pairs demonstrated contest competition in at least one of the five weekly feedings. The average number of weekly feedings in which a pair of sibs contested prey equaled  $1.52 \pm 0.04$ , and only 3% of sib pairs engaged in contests over prey in more than three of the five weekly feedings (Table 1). Although there was a familial effect on *whether or not* sibs contested prey in at least one of the weekly feedings (Fig. 1), no familial effect was found in the *number* of weekly feedings in which sib pairs contested prey ( $F_{ratio} = 1.08$ ,  $P = .47$ ).

Table 1 presents data on the timing of contests over prey over the course of the five weeks of the experiment. Table 1(A) shows the proportion of all contest events, sib-pairs' first contest events and sib-pairs' seminal contests (establishing ultimate winner/loser status) that took place during each of the five weekly feedings.

Table 1(B) presents summary statistics for three categories of contests experienced by sib pairs (all contests, first contest and seminal contest). Mean first contest is the average of the week numbers (1 through 5) in which sib pairs experienced their first contest over prey. Mean seminal contest is the average of the week numbers in which each sib pair experienced a contest that established a winner and loser in that contest and all subsequent contests. Mean for all contests indicates the average week number in which any contest over prey took place.

Although first contests may prove to be seminal contests, on average the seminal contest occurs after the first contest. The timing of first contests (mean week =  $2.13 \pm .06$ ) and seminal contests (mean week =  $2.67 \pm .06$ ) over the five weekly feedings differ significantly ( $X^2 = 45.1$ ,  $P < 0.00001$ ). Standard errors are measures of the accuracy with which a sample represents a "population". The small standard errors reflect the large sample sizes (number of sib pairs) and thus, high



Table 1.—Timing of sib-sib contests over prey, over five weekly feedings. (A) Distribution of three types of contest events across five weekly feedings. Each sib pair can experience one “first contest” and no more than one seminal contest (see text); a first contest may prove to be a seminal contest. “Total contests” refers to all contests (first, seminal or other) a sib pair engages in over the course of five weekly feedings. Figures indicate the proportion of each type of contest event (first, seminal or total contests) that occurred during each weekly feeding period. (B) Summary statistics. Means are calculated as the average weekly feeding period (1 through 5) in which each sib pair experienced any contest over prey, in which each sib pair’s first contest occurred, and in which a seminal contest occurred. The low standard error values reflect the fact that the mean parameter estimates are accurate indicators of the true weekly distribution of the respective contest types.

A. Weekly Feeding	Proportion of total contests	Proportion of all 1 <sup>st</sup> contests	Proportion of all seminal contests
1ST	0.621	0.44	0.28
2ND	0.283	0.26	0.23
3RD	0.064	0.13	0.20
4TH	0.016	0.09	0.15
5TH	0.016	0.08	0.14
B. Summary Statistics	All contests	1 <sup>st</sup> contests	Seminal contests
Mean week in which sib groups experienced contests of each type	1.52	2.13	2.67
Standard Error	0.04	0.06	0.06
Sample Size (# sib pairs)	531	531	529*

\* Two contests unresolved during course of five weekly feedings.

accuracy of the mean estimates provided for the three aspects of contest timing with respect to the five weekly feedings.

Note that only two of the 531 sib pairs followed in this study failed to establish draw/winner/loser status over the course of the five weekly feedings. Further, there were only 24 contests that ended in a draw, with individuals subsequently foraging independently. Thus, the vast majority of the seminal contests (95.1%) led to distinct winner/loser designations for the paired sibs.

Contest-initiating acts can be broadly differentiated as being prey-directed versus sib-directed. Prey-directed actions consist of joining in the capture of a termite that has been offered to its sib or carrying off a termite that has already been secured by its sib. These prey takeovers account cumulatively for only 27% of the behavioral acts that initiate sib-sib contests over prey. The majority of the contest initiating acts are sib-directed such as blocking the sib from reaching its prey item and shoving or chasing it away from it. Chase sib from its prey (33%) and lunge at sib (25%) are prominent sib directed contest initiating acts. The distribution of behavioral acts sibs engage in differs significantly between 1<sup>st</sup> interactions and seminal interactions ( $X^2 = 20.95$ ,  $P < 0.001$ ,  $df = 9$ ). (Note that 1<sup>st</sup> interactions that are also seminal interactions were excluded from this analysis.) First interaction deviations from expectations contributed most to the significant test result. This included lower than expected incidences of the initial act involving prey take away, blocking sib from/shoving sib off prey, threats directed towards sib, hovering by a sib in possession of a termite and following of the sib with bumping

of it. On the other hand, there was more sib following, sib chase away from prey and grappling between sibs as the interaction initiating behavior in 1<sup>st</sup> interactions than expected.

## DISCUSSION

**Foraging strategy representation.**—We argue that our experiment is biased towards cooperative foraging over independent foraging and competition. This is because a worker termite is ~three times the mass of an early instar *A. aperta*. It takes much silk investment to secure a worker termite, which also offers more mass than can be consumed in a feeding bout. Nevertheless, no sib pairs were observed to share in the capture and feeding on a termite in this study. This result is indicative of early (constitutional) determination of behavioral temperament.

While we did not observe any instances of cooperative foraging, we did detect significant levels of both familial and within clutch variation in behavioral tendencies of early instar *A. aperta*. The phenotype mix (24.5% of the families at the aggressive end and 5% at the passive end of a continuum in behavioral temperament) is potentially reflective of the meta-population structure of *A. aperta* in the desert southwest US. Here small patches of riparian habitat are interspersed within an arid-land habitat matrix with much gene flow particularly from arid adapted into riparian local populations (Riechert et al., 2001). Low aggressiveness is the prominent phenotype in riparian habitats offering abundant prey, but also where predation pressure by birds is quite high (e.g., Hammerstein & Riechert 1988; Riechert & Hall 2000). High aggressiveness is the prominent phenotype in more arid areas, reflecting competition for web sites offering both maximum foraging time and prey capture success with encountered insect prey (Riechert & Tracy 1975; Riechert 1976).

**Fitness implications.**—Contest competition is, in a sense, a “bet hedge” against harsh environments. Under conditions with limited resources, scramble competition (independent foraging) is more likely to lead to volatile boom-and-bust population dynamics and population die-offs (after Hassell 1975; Lomnicki 2009). Contest competition, in contrast, allows winners/dominants to emerge and potentially reach the body size thresholds required to reproduce (Sharpe & Avilés 2016). Given the harsh arid environmental conditions typically experienced by *A. aperta*, and the expected indirect fitness benefits of insuring the survival of some individuals within a family, contest competition might well be expected to prevail in sib-sib interactions during the aggregative phase of the life cycle. It provides insurance that the better competitors within a family gain contest experience and potential greater access to prey during times when food is limiting. Full treatment of contest structure and the fitness consequences of contesting prey at this stage of the life cycle is beyond the scope of this short conference proceedings and will be presented elsewhere.

## ACKNOWLEDGMENTS

This work was supported by NSF grant # 0315901. Special thanks to Nadia Ayoub for her assistance in the field



collections of the parental populations under the auspices of a collecting permit from the Texas Parks & Wildlife Department. We would also like to thank Stephanie Duncan for overseeing the F1 generation rearings and matings and set-up of the replicate pairs for each family. The following undergraduates assisted in the lab F1 rearings, matings, mass determinations, and data spreadsheet entry: Nilton Baretto, Sarah Duncan, Nicole Halloy, David Herzof, Sarah Beam Post and Jamie Troupe.

#### LITERATURE CITED

- Hammerstein, P. & S.E. Riechert. 1988. Payoffs and strategies in spider territorial contests: ESS-analyses of two ecotypes. *Evolutionary Ecology* 2:115–138.
- Hassell, M.P. 1975. Density-dependence in single-species populations. *Journal of Animal Ecology* 44:283–295.
- Keddy, P.A. 1989. *Competition*. Chapman and Hall, London.
- Kim, K.W., B. Krafft & J.C. Choe. 2005. Cooperative prey capture by young subsocial spiders. *Behavioral Ecology and Sociobiology* 59:92–100.
- Lomnicki, A. 2009. Scramble and contest competition, unequal resource allocation, and resource monopolization as determinants of population dynamics. *Evolutionary Ecology Research* 11:371–380.
- Riechert, S.E. 1974. The pattern of local web distribution in a desert spider: mechanisms and seasonal variation. *Journal of Animal Ecology* 43:733–745.
- Riechert, S.E. 1976. Web-site selection in a desert spider, *Agelenopsis aperta* (Gertsch). *Oikos* 27:311–313.
- Riechert, S.E. 1981. The consequences of being territorial: spiders, a case study. *American Naturalist* 117:871–892.
- Riechert, S.E. 1993. The evolution of behavioral phenotypes: lessons learned from divergent spider populations. *Advances in Animal Behaviour* 22:103–134.
- Riechert, S.E. 1999. The use of behavioral ecotypes in the study of evolutionary processes. Pp. 3–32. *In* *Geographic Variation in Behavior: Perspectives on Evolutionary Mechanisms*. (S. Foster, J. Endler, ed.). Oxford University Press, U.K.
- Riechert, S.E. & R.F. Hall. 2000. Local population success in heterogeneous habitats: reciprocal transplant experiments completed on a desert spider. *Journal of Evolutionary Biology* 13:1–10.
- Riechert, S.E. & C.R. Tracy. 1975. Thermal balance and prey availability: bases for a model relating web-site characteristics to spider reproductive success. *Ecology* 56:265–284.
- Riechert, S.E., F.D. Singer & T.C. Jones. 2001. High gene flow levels lead to gamete wastage in a desert spider system. *Genetica* 112/113:297–319.
- Sharpe, R.V. & L. Avilés. 2016. Prey size and scramble vs. contest competition in a social spider: implications for population dynamics. *Journal of Animal Ecology* 85:1401–1410.

*Manuscript received 29 September 2016, revised 3 April 2017.*



## A new *Liphistius* species (Mesothelae: Liphistiidae: Liphistiinae) from Thailand, with notes on its natural history

Varat Sivayyapram<sup>1</sup>, Deborah Roan Smith<sup>2</sup>, Suthon Weingdow<sup>3</sup> and Natapot Warrit<sup>1</sup>: <sup>1</sup>Center of Excellence in Entomology and Department of Biology, Faculty of Science, Chulalongkorn University, Bangkok 10330, Thailand. E-mail: natapot.w@chula.ac.th <sup>2</sup>Department of Ecology and Evolutionary Biology, University of Kansas, Lawrence, Kansas 66045, USA; <sup>3</sup>Mae Wong National Park, Klonglan District, Kamphaeng Phet 62180, Thailand

**Abstract.** A new species of trapdoor spider of the genus *Liphistius* Schiödte, 1849 (Mesothelae: Liphistiidae) is described from specimens collected from Mae Wong National Park, Klonglan district, Kamphaeng Phet province, Thailand. This *Liphistius* species belongs to the *bristowei* species-group based on the elevated cumulus and the distinct embolic part, and resembles *L. yamasakii* Ono, 1988. Diagnostic characters of the male and female are discussed, and a map is provided for the type localities of the 32 previously described *Liphistius* species in Thailand. This is the first record of a *Liphistius* species in the *bristowei* species-group that builds a T- or Y-shaped burrow with two trapdoor openings.

**Keywords:** Systematics, checklist, conservation, spider

<http://zoobank.org/?lsid=urn:lsid:zoobank.org:pub:B1E4838E-2650-4896-88FB-E764C86B1F27>

The segmented trapdoor spiders of the Family Liphistiidae are the sister group to all other extant spiders. They bear many plesiomorphic characters, including the presence of abdominal tergal plates and the position of the spinnerets on the median area of the opisthosoma (Platnick & Gertsch 1976; Haupt 2003; Xu et al. 2015). Two allopatric subfamilies are included in the family: Liphistiinae Thorell, 1869 and Heptathelinae Kishida, 1923. The Liphistiinae includes a single genus, *Liphistius* Schiödte, 1849, found in Laos, Thailand, peninsular Malaysia, Myanmar and the Indonesian island of Sumatra (World Spider Catalogue 2017). The Heptathelinae includes the remaining seven genera of liphistiids, whose members are distributed in China, Japan and Vietnam. Heptathelinae can be distinguished from Liphistiinae by the absence of a male tibial apophysis and by the female internal genitalia (Platnick & Sedgwick 1984; Haupt 2003; Xu et al. 2015), and by differences in burrow construction (see below).

The genus *Liphistius* includes more than 50 described species, and in Thailand, 32 *Liphistius* species have been recorded from 22 provinces throughout the country (Fig. 1, Table 1), demonstrating a high level of diversity and endemism (Platnick & Sedgwick 1984; Schwendinger 1987, 1990, 1995, 1996, 1998, 2009, 2013; Ono 1988a, b; Ono & Schwendinger 1990; Sedgwick & Schwendinger 1990). The group is well known for its limited dispersal ability, and most *Liphistius* species described in Thailand have been recorded only from their type localities. Currently, only seven Thai *Liphistius* species are known to occur outside of their type localities: *L. bicoloripes* Ono, 1988, *L. bristowei* Platnick & Sedgwick, 1984, *L. isan* Schwendinger, 1998, *L. lahu* Schwendinger, 1988, *L. lannaianus* Schwendinger, 1990, *L. pusohm* Schwendinger, 1996, and *L. thaleban* Schwendinger, 1990. However, the apparently limited distributions of many *Liphistius* species could also be a result of insufficient sampling, habitat alteration, and deforestation.

Schwendinger (1990) classified *Liphistius* into three species-groups: the *bristowei* species-group, the *birmanicus* species-group, and the *trang* species-group, based on characters of the

male pedipalp—particularly the cumulus and the embolic parts—and the female genitalia. Based on a review of the literature, the number of species in each species-group in Thailand is as follows: *bristowei*-group (4 species), *birmanicus*-group (1 species), *trang*-group (26 species), and one *incertae sedis* species, *L. jarujini* Ono, 1988 (Fig. 1, Table 1). *Liphistius* habitats include sloped soil banks on man-made roads or paths cut into mountains or small hills (Haupt 2003). Other *Liphistius* species dwell in caves and among boulders. Three types of *Liphistius* burrows have been documented thus far; however, burrow types do not correspond with species-group classification. These are: (1) the more or less straight undivided terrestrial tube with one trapdoor opening equipped with silk “signal lines” for prey capture; (2) the T- or Y-shaped terrestrial burrow with two trapdoors, one equipped with signal lines, the other lacking signal lines; and (3) the sac-like retreat on the surface of a cave wall or boulder, without a burrowing tube structure but with a trapdoor equipped with signal lines (Platnick & Sedgwick 1984; Schwendinger 1990). Unlike *Liphistius*, members of the Heptathelinae do not construct signal lines.

Until now, only one *Liphistius* species, *L. kanthan* Platnick, 1997, from Perak, Malaysia, has been evaluated and designated as a critically endangered species under the IUCN (2017), showing the possibility of extinction in this group of spiders due to restricted ranges, habitat destruction and human exploitation. In August 2015, the authors (VS and NW) discovered an aggregation of *Liphistius* burrows along a man-made road cutting during a spider collecting expedition to Mae Wong National Park, Thailand. Here, we describe this species for the purpose of further ecological studies and for conservation assessment.

## METHODS

Spiders were collected in Mae Wong National Park, Klonglan district, Kamphaeng Phet province, Thailand (16°05.67'N, 99°07.436'E) on a man-made road cutting (Fig.



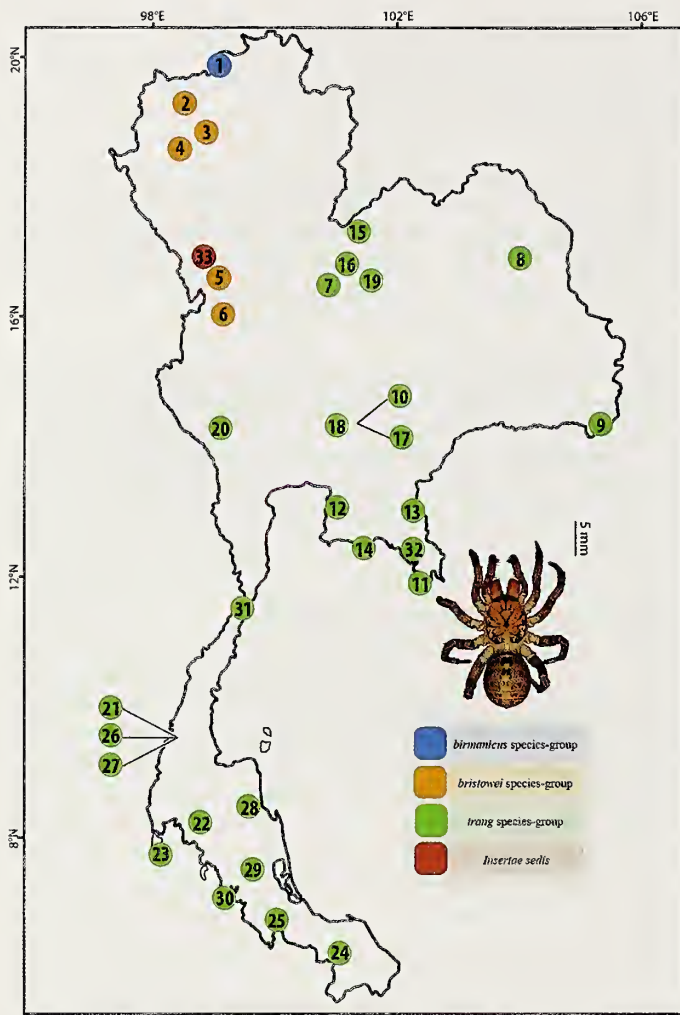


Figure 1.—Type localities of 33 described *Liphistius* species in Thailand based on descriptions from Platnick & Sedgwick (1984), Schwendinger (1987, 1990, 1995, 1996, 1998, 2009), Ono (1988a, b), Ono & Schwendinger (1990), and Sedgwick & Schwendinger (1990). See Table 1 for type locality information regarding each species. The species displayed is a female *L. erawan* Schwendinger, 1996 (dorsal view).

2). An estimated 300+ burrows were present on the banks at the time of discovery (August 2015). We excavated a subset of the burrows using forceps and collected 15 specimens (7 ♀, 8 subadults). Trapdoor width and length, and burrow depth were measured for each specimen using digital calipers (Mitutoyo). Numbers of signal lines were also recorded. One of the subadult specimens collected molted into an adult male on 30 October 2015 (this specimen is designated as the holotype). In late December 2015, we returned to the initial collecting site and discovered two additional collecting localities 1 km east and west of the original location (16°05.333'N, 99°07.88'E; 16°05.334'N, 99°07.88'E) and collected an additional 31 specimens (17 ♀, 14 subadults). Eleven egg sacs were also recovered from the female burrows. All live specimens were transported back to the Department of Biology, Chulalongkorn University, and reared until 1

November 2015 (for specimens collected in August 2015) and until 25 December 2015 (for specimens collected in December 2015) before being preserved in 95% ethanol.

Measurements are reported in millimeters and were obtained using a Zeiss Stemi DV4 stereomicroscope with ocular micrometer, or with digital calipers. Total length (with and without chelicerae length) does not include the anal tubercle. Appendage measurements were based on the left appendages. Pedipalp and leg lengths include the lengths of the femur, patella, tibia, metatarsus, and tarsus. The female genital area was removed from the specimens and cleared using 5% potassium hydroxide. Terminology of genital characters follows Schwendinger (1987, 1990, 1995, 1996, 1998, 2009) and Schwendinger & Ono (2011). The abbreviations used here are as follows: ALE, anterior lateral eye; AME, anterior median eye; CL, carapace length; CW, carapace width; EL, palpal coxal length; EW, palpal coxal width; LL, labium length; LW, labium width; OL, ocular tubercle length; OW, ocular tubercle width; PME, posterior median eye; PLE, posterior lateral eye; SL, sternum length; SW, sternum width; TL<sub>1</sub>, total length with chelicerae; TL<sub>2</sub>, total length without chelicerae.

## SYSTEMATICS

Family Liphistiidae Thorell, 1869

Subfamily Liphistiinae Thorell, 1869

Genus *Liphistius* Schiödte, 1849

*Liphistius maewongensis* sp. nov.

<http://zoobank.org/?lsid=urn:lsid:zoobank.org:act:93009B75-A775-4376-B2AF-C8C4210F1F15>

(Figs. 2–6)

**Type material.**—*Holotype male*. THAILAND: *Kamphaeng Phet*: Klonglan District, Mae Wong National Park, 16°05.67'N, 99°07.436'E, 1266 m, 23 December 2015, V. Sivayyapram (CUMZ-AR-ARA-Lip.2017.1).

**Paratypes.** THAILAND: *Kamphaeng Phet*: 1 ♀ allotype, same data as holotype except 6 August 2015 (CUMZ-AR-ARA-Lip.2017.2); 1 ♀, same data (CUMZ-AR-ARA-Lip.2017.3); 1 ♀, same data except 23 December 2015 (CUMZ-AR-ARA-Lip.2017.4); 1 ♀, same data (CUMZ-AR-ARA-Lip.2017.5); 1 ♀, same data (CUMZ-AR-ARA-Lip.2017.6).

**Other material examined.**—THAILAND: *Kamphaeng Phet*: 5 ♀, 7 subadult juveniles, Klonglan District, Mae Wong National Park, 16°05.67'N, 99°07.436'E, 1266 m, 6 August 2015, V. Sivayyapram (CUMZ-AR-ARA-Lip.2017.7–18); 14 ♀, 12 subadult juveniles, same data except 16°05.333'N, 99°07.88'E, 1193 m, 23 December 2015 (CUMZ-AR-ARA-Lip.2017.19–44); 2 subadult juveniles, same data except 1218 m (CUMZ-AR-ARA-Lip.2017.45–46).

**Etymology.**—The specific epithet refers to the type locality, Mae Wong National Park, an important tiger sanctuary in Southeast Asia.

**Diagnosis.**—*Liphistius maewongensis* sp. nov. is similar to *L. yamasakii* Ono, 1988, but can be distinguished from the latter by its smaller size, by the distinct shape of the embolus, which has a slender tip (Fig. 4b), by the less prominent sharp distal edge of the contrategulum (Fig. 4a), by the narrower paracymbium (Fig. 4a, b), by the less prominent cumulus



Table 1.—Synopsis of 33 described *Liphistius* species from Thailand. Type localities are provided verbatim from their original descriptions. Remarks are our interpretation and additions. *Liphistius* species-group classification is based on Schwendinger (1990). The species numbers correspond to Figure 1.

No.	Species	Type Locality	Type Locality Remarks	Original Description	Species-group
1	<i>L. lahn</i>	“Doi Angkhang (19°57'N, 99°05'E), 1500 m alt., Fang District, Chiang Mai Province, northern Thailand.”		Schwendinger (1998)	<i>birmanicus</i>
2	<i>L. lamaianus</i>	“Thailand: Huay Nam Dang and Doi Chang”	Doi Chang is the highest peak in Huai Nam Dang National Park (1,962 m), Mae Taeng District, Chiang Mai province	Schwendinger (1990)	<i>bristowei</i>
3	<i>L. bristowei</i>	“Doi Suthep mountain, 1,100 m alt., Chiang Mai, Thailand”		Platnick & Sedgwick (1984)	<i>bristowei</i>
4	<i>L. yamasakii</i>	“Doi Inthanon, 1,700 m alt. between Maeo Khun Klang and Mae Chaem, Chiang Mai, Thailand”		Ono (1988a)	<i>bristowei</i>
5	<i>L. marginatus</i>	“Thailand: Lan Sang National Park”	Lan Sang National Park, Mucang District, Tak province	Schwendinger (1990)	<i>bristowei</i>
6	<i>L. maewongensis</i> n. sp.	Kamphaeng Phet province, Klonglan District, Mae Wong National Park (16° 05.670'N, 99° 07.436'E), elevation 1266 meter		Sivayyapram et al. (2017)	<i>bristowei</i>
7	<i>L. owadai</i>	“Thung Salaeng Luang, 550 m alt., Phitsanulok Province, Thailand”		Ono & Schwendinger (1990)	<i>trang</i>
8	<i>L. isan</i>	“Phu Phan National Park (16°43'N, 103°51'E), 520 m, Kut Bak District, Sakon Nakhon Province, northeastern Thailand.”		Schwendinger (1998)	<i>trang</i>
9	<i>L. dangrek</i>	“Phu Chong Nayoi National Park (14°18'N, 105°10'E), 300 m, Nam Yun District, Ubon Ratchathani Province, northeastern Thailand.”	Schwendinger (1996) indicated that <i>L. dangrek</i> is found only in the surrounding of Tham Bak Tew Waterfall in the NP. Currently, this waterfall has changed its name to “Huai Luang Waterfall”	Schwendinger (1996)	<i>trang</i>
10	<i>L. suwat</i>	“Heo Suwat Waterfall (14°21'N, 101°29'E), 580 m, Khao Yai National Park, Pak Chong District, Nakhon Ratchasima Province, northeastern Thailand.”		Schwendinger (1996)	<i>trang</i>
11	<i>L. nesiotiens</i>	“Ko Chang National Park (12°01'N, 102°19'E), 50 m, Laem Ngop District, Trat Province, southeastern Thailand.”	Koh Chang district was separated from Laem Ngop district in 2007 and is the type locality of <i>L. nesiotiens</i>	Schwendinger (1996)	<i>trang</i>
12	<i>L. sayam</i>	“Khao Khieo Wildlife Sanctuary (13°10'N, 100°58'E), 110 m, Si Racha District, Chon Buri Province, central Thailand”		Schwendinger (1998)	<i>trang</i>
13	<i>L. ornatus</i>	“Khao Soi Dao Wildlife Sanctuary, 300–400m alt., Chanthaburi Province, Thailand”		Ono & Schwendinger (1990)	<i>trang</i>
14	<i>L. phileion</i>	“Ao Phrao (=Coconut Bay), 10 m, Samet Island (12°33'N, 101°26'E), Khao Laem Ya & Mu KO Samet National Park, Rayong District and Province, southeastern Thailand.”		Schwendinger (1998)	<i>trang</i>
15	<i>L. ochraceus</i>	“Phu Rua National Park, 1,200m alt., Loei Province, Thailand”		Ono & Schwendinger (1990)	<i>trang</i>
16	<i>L. onoi</i>	“Phu Hin Rongkla National Park (16°52'N, 101°03'E), 1200 m, Nakhon Thai District, Phitsanulok Province, northeastern Thailand”		Schwendinger (1996)	<i>trang</i>



Table 1.—Continued.

No.	Species	Type Locality	Type Locality Remarks	Original Description	Species-group
17	<i>L. thoranie</i>	"Kong Kao Waterfall (14°21'N, 101°25'E), 680 m, Khao Yai National Park, Pak Chong District, Nakhon Ratchasima Province, northeastern Thailand."		Schwendinger (1996)	<i>trang</i>
18	<i>L. tham</i>	"Thailand, Tham Suan Hin"	"Tham Suan Hin" described by Sedgwick and Schwendinger (1990) is currently known as Lumphinee Suan Hin cave, Wat Tham Phra Phothisat monastery, Kaeng Khoi District, Saraburi province (Ellis 2012)	Sedgwick & Schwendinger (1990)	<i>trang</i>
19	<i>L. pusohm</i>	"Nam Nao National Park (16°44'N, 101°32'E), 800 m Lom Sak District, Phetchabun Province, northeastern Thailand."		Schwendinger (1996)	<i>trang</i>
20	<i>L. erawan</i>	"Erawan Waterfall and National Park (14°25'N, 99°03'E), 100 m, Bo Phloi District, Kanchanaburi Province, western Thailand"		Schwendinger (1996)	<i>trang</i>
21	<i>L. schwendingeri</i>	"Khlong Nakha, 50m alt., Ranong, South Thailand"	Khlong Na Kha Wildlife Sanctuary, Suk Samran district, Ranong province	Ono (1988b)	<i>trang</i>
22	<i>L. fuscus</i>	"Khao Phanom Bencha National Park (8°12'N, 98°56'E), 280 m, Krabi District, Krabi Province, Thailand."		Schwendinger (1995)	<i>trang</i>
23	<i>L. phuketensis</i>	"Tone Sai Waterfall, Khao Phra Thaco Non-hunting Area (8°02'N, 98°22'E), 100 m, Thalang District, Phuket Island and Province, southern Thailand."		Schwendinger (1998)	<i>trang</i>
24	<i>L. rufipes</i>	"Than To Waterfall (6°2'N, 101°10'E), 150 m, Banglang National Park, Than To District, Yala Province, Thailand."		Schwendinger (1995)	<i>trang</i>
25	<i>L. thaleban</i>	"Thailand: Thaleban National Park"	Thale Ban National Park, Wang Prachan, Khuan Don District, Satun province	Schwendinger (1990)	<i>trang</i>
26	<i>L. bicoloripes</i>	"Khlong Nakha, 50m alt, Ranong, South Thailand"	Khlong Na Kha Wildlife Sanctuary, Na Kha, Suk Samran District, Ranong province	Ono (1988b)	<i>trang</i>
27	<i>L. castaneus</i>	"Khlong Nakha Wildlife Sanctuary, 30 m, Kapoe District, Ranong Province, Thailand."	Schwendinger (1995) might have erred in stating that Khlong Nakha WS is in Kapoe district, since this WS is located in Suk Samran district	Schwendinger (1995)	<i>trang</i>
28	<i>L. niphanae</i>	"Khao Luang National Park, 120 m alt., Nop Pitam, Tha Sala, Nakon Si Thammarat, South Thailand"		Ono (1988b)	<i>trang</i>
29	<i>L. trang</i>	"Krachong Forest, 100 m. near Trang, Thailand"	Krachong Forest, Na Yong District, Trang Province	Platnick & Sedgwick (1984)	<i>trang</i>
30	<i>L. thaleri</i>	"Ko (= Island) Libong (also called Ko Talibong), near Ao Tokae (= Gekko Bay) (7°16'04"N, 99°22'38"E), 30 m"		Schwendinger (2009)	<i>trang</i>
31	<i>L. albipes</i>	"Khao Luang, Nam Tok Huay Yang National Park (11°38'N, 99°33'E), 550 m, Thap Sakae District, Prachuab Khiri Khan Province, Thailand."		Schwendinger (1995)	<i>trang</i>
32	<i>L. tenuis</i>	"Nam Tok Phliu-Khao Sabap National Park (12°32'N, 102°12'E), 100 m, Chanthaburi District and Province, southeastern Thailand."		Schwendinger (1996)	<i>trang</i>
33	<i>L. jarujini</i>	"Taksin Maharat National Park, 950 m alt, ca 30 km W of Tak, Muzng, Thailand"		Ono (1988a)	<i>Incertae sedis</i>



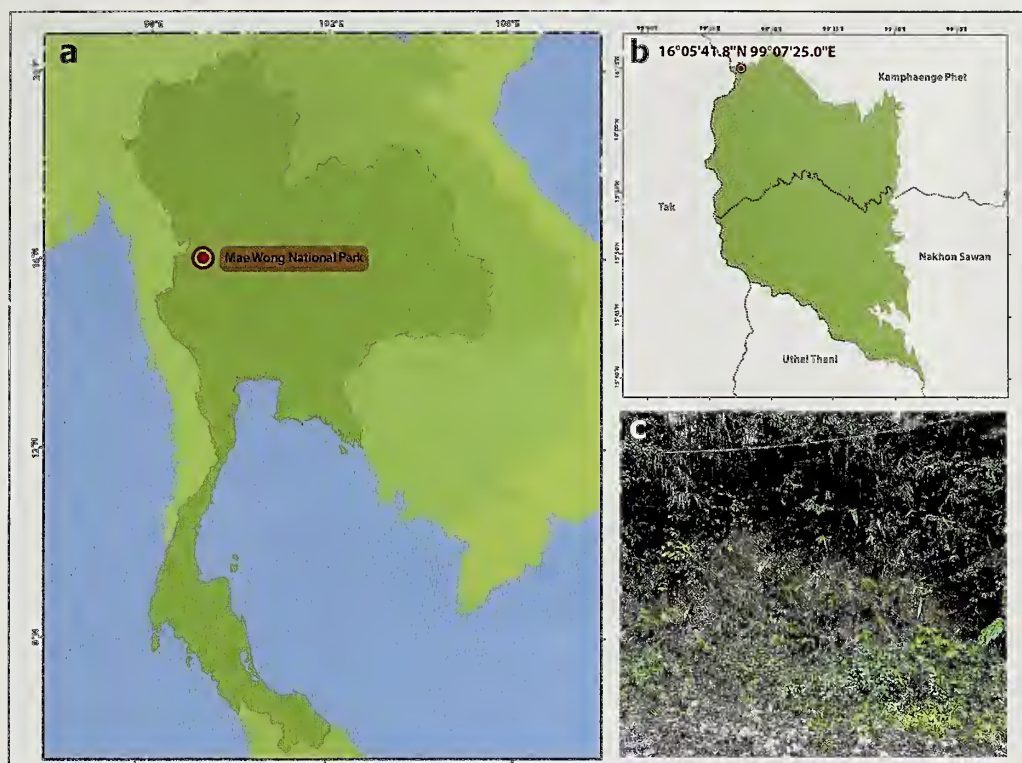


Figure 2.—Type locality of *Liphistius maewongensis* sp. nov. in Mae Wong National Park (a, b), Klonglan District, Kamphaeng Phet province, Thailand; (c), a man-made road cutting hill slope where *L. maewongensis* burrows were found.



Figure 3.—Dorsal habitus of *Liphistius maewongensis* sp. nov. Adult male (left) and female (right). Note the darker coloration of the male specimen.



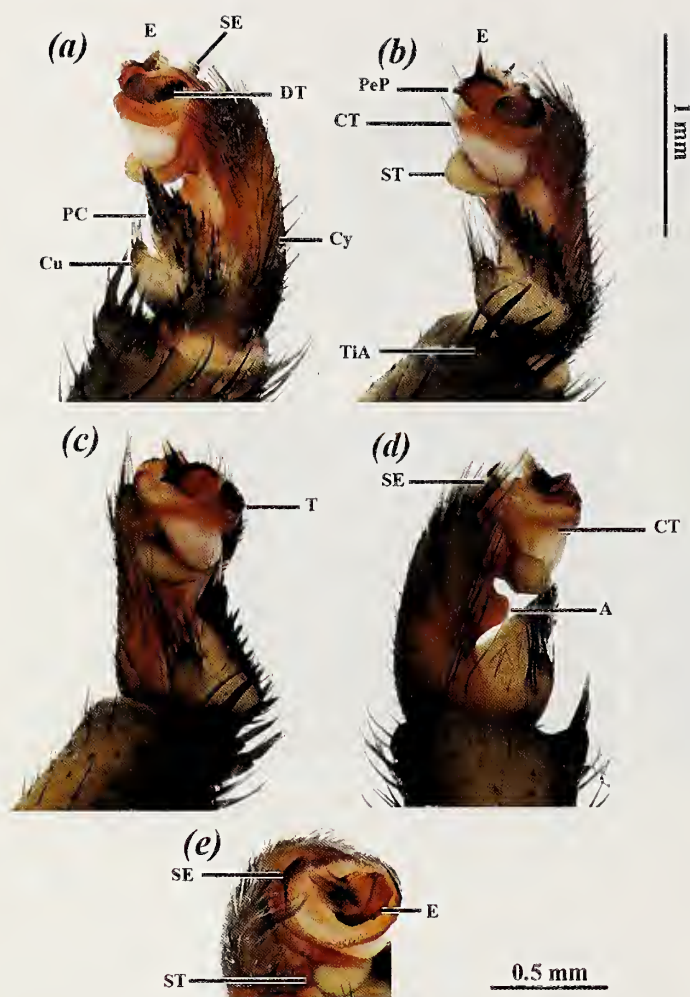


Figure 4.—Male pedipalp of *Liphistius maewongensis* sp. nov. (holotype: CUMZ-AR-ARA-Lip.2017.1): (a) retrolateral view; (b) retroventral view; (c) ventral view; (d) proventral view; (e) distal view. A = alveolar apophysis; CT = contrategulum; Cu = cumulus; Cy = cymbium; DT = dorsal extension of terminal apophysis of tegulum; E = embolus; PC = paracymbium; PeP = paraembolic plate; SE = sharp distal edge of contrategulum; ST = subtegulum; TiA = tibial apophysis.

(Fig. 4a, b), and by the distinct subtegular apophysis (Fig. 4b, c) (see also Ono 1988a). The female *L. maewongensis* has larger medium-sized pores on the pore plate that lead to the ampulliform vesicles, and a distinct genital atrium and arrangement of the receptacular cluster (Fig. 5).

**Description.**—Male holotype (CUMZ-AR-ARA-Lip.2017.1). Color (live specimens): carapace black, paler in median area; opisthosoma black, abdominal tergites darker than other areas; chelicerae black, paler in proximal portion; leg and pedipalp pale yellow with black annulations; palpal coxa, leg coxae, labium and sternum black (Fig. 3). Total length: TL1 16.3, TL2 14.7. Carapace: CL 6.75, CW 6.25. Ocular tubercle: OL 0.99, OW 1.17. Eye sizes and interdistances: AME 0.9, ALE oval shape 0.18 and 0.75, PME oval shape 0.42 and 0.33, PLE oval shape 0.18 and 0.48; AME-AME 0.15, AME-ALE 0.18, PME-PME 0.03, PME-PLE 0.09,

AME-PME 0.09, ALE-PLE 0.06. Labium: LL 0.72, LW 1.36. Sternum: SL 3.08, SW 0.96. Palpal coxa: EL 1.96, EW 1.60. Chelicerae with 11 promarginal teeth. Paired tarsal claws with 4 teeth, unpaired tarsal elaw with 1 small denticle. Pedipalp and leg measurements: pedipalp length: 11.36 (3.60+2.08+3.68+2.00), leg I: 17.12 (4.88+2.56+3.68+3.92+2.08), leg II: 15.00 (2.28+2.56+3.52+4.40+2.24), leg III: 19.92 (5.28+2.56+3.44+5.54+2.80), leg IV: 25.12 (6.32+2.88+4.96+7.12+3.84). Pedipalp with four tapering spines on short truncate tibial apophysis, paracymbium protruding and narrow bearing numerous short strong spines, cumulus elevated bearing several long hairs, alveolar process well developed, subtegular apophysis slightly elevated, tegulum narrow with dentate dorsoproximal edge of tegulum, contrategulum broad with dentate ventral ridge, small paraembolic plate. Embolus short, adjoining sclerotized embolic parts with two longitudinal ridges that reach to tip (Fig. 4).

Female allotype (CUMZ-AR-ARA-Lip.2017.2). Color (live specimens): carapace orange-brown with thick black markings along the margins which radiate to thoracic groove; opisthosoma orange-brown with black spot on lateral surface, abdominal tergites orange-brown with black pattern in the middle and lateral margins (Fig. 3); chelicerae brown proximally, black distally; leg and pedipalp light-brown with black annulations; palpal coxa, leg coxae, labium, and sternum black. Total length: TL1 12.38, TL2 10.63. Carapace: CL 5.88, CW 5.38. Ocular tubercle: OL 0.88, OW 0.88, clypeus narrow. Eye sizes and interdistances: AME 0.09, ALE oval shape 0.51 and 0.15, PME 0.39, PLE oval shape 0.42 and 0.12, AME-AME 0.06, AME-ALE 0.12, PME-PME 0.03, PME-PLE 0.06, ALE-PLE 0.09. Labium: LL 0.76, LW 1.12. Sternum: SL 3.04, SW 1.32. Palpal coxa: EL 1.92, EW 1.16. Chelicerae with 12 promarginal teeth. Paired tarsal claws with 3 teeth, unpaired tarsal claw with 1 small denticle. Pedipalp and leg measurements: pedipalp length: 10.56 (3.68+1.92+2.40+2.56), leg I: 13.36 (4.48+2.08+2.72+2.56+1.52), leg II: 13.52 (4.40+2.08+2.80+2.64+1.60), leg III: 14.64 (4.40+2.08+2.88+3.36+1.92), leg IV: 20.80 (5.68+2.56+4.08+5.60+2.88). Vulva: anterodorsal poreplate rectangle, wider than long, anterior and lateral lips thick without distinct lobe, large ventral vesicle (Fig. 5). Receptacular cluster racemose, well develop. Genital atrium wide, sclerotized portion well developed, with W-shaped posterior margin, connected to lateral margin of atrium.

**Variation.**—Pedipalp and leg measurements for nine adult female specimens (individuals with egg sacs collected on 23 December 2015) are provided in Table 2.

**Remarks.**—*Liphistius maewongensis* belongs to the *bristowei* species-group *sensu* Schwendinger (1990), based on the elevated cumulus (Figs. 4a–d) and the two longitudinal ridges on the sclerotized part of the embolie parts that reach the tip (Fig. 4e). Thus, the *bristowei* species-group of *Liphistius* is currently comprised of *L. bristowei*, *L. lannaianus*, *L. marginatus* Schwendinger, 1990, *L. yamasakii*, and *L. maewongensis*. Despite the similarity between *L. yamasakii* and *L. maewongensis*, the male pedipalp shapes are grossly different (see Diagnosis, above).

**Distribution, burrows and natural history.**—*Liphistius maewongensis* is found only in the area surrounding the type locality in Mae Wong National Park, which spans an area of approximately 2–3 km<sup>2</sup> within an altitudinal range of 1193–



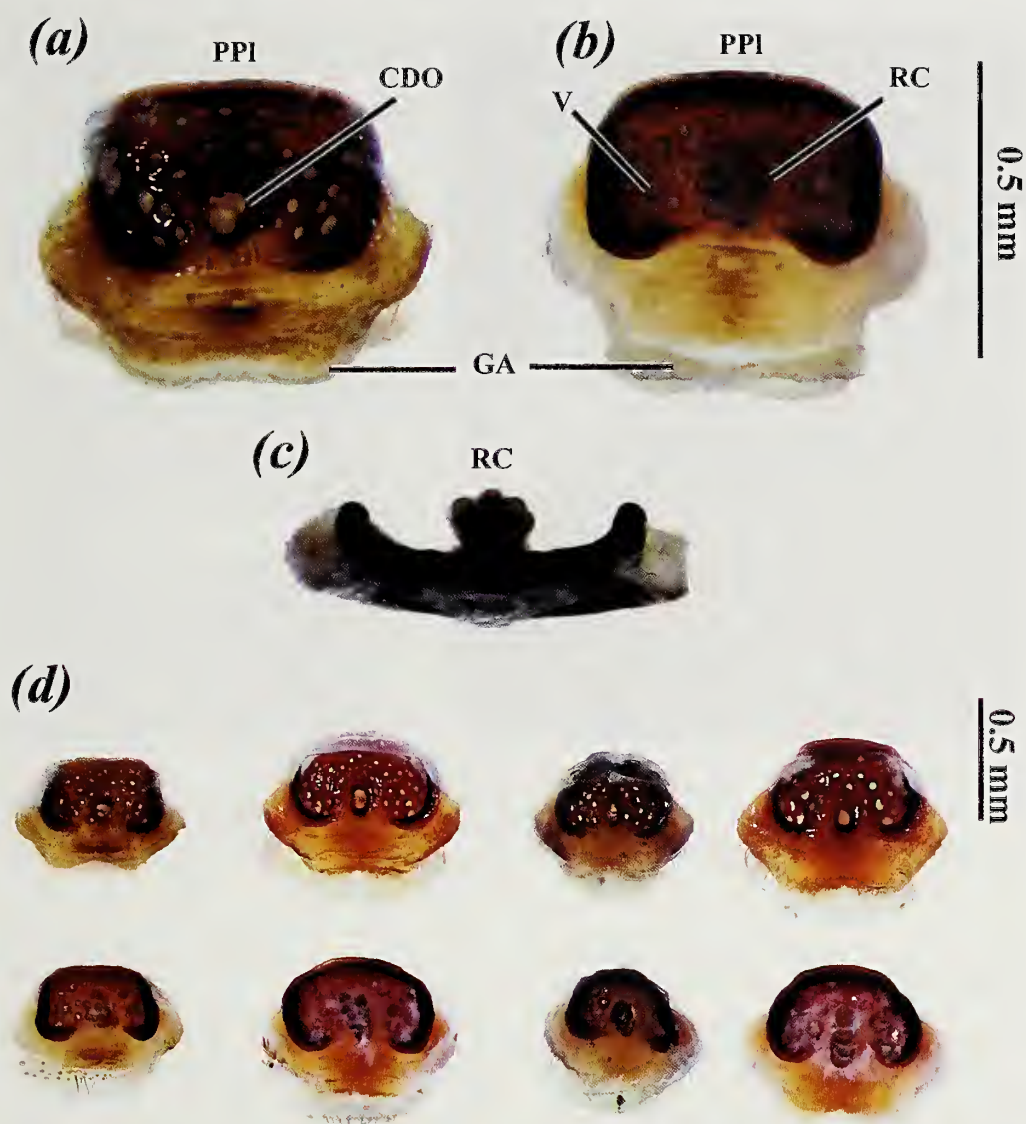


Figure 5.—Female vulvae of *Liphistius maewongensis* sp. nov. (a–c) Allotype (CUMZ-AR-ARA-Lip.2017.2): (a) dorsal view; (b) ventral view; (c) distal view; (d) Variations in four female paratype vulvae (upper row, dorsal view; lower row, ventral view), from left to right (CUMZ-AR-ARA-Lip.2017.3–6, respectively). CDO = central dorsal opening; GA = genital atrium; PPI = poreplate; RC = receptacular cluster; V = ampulliform vesicle.

1266 m. No additional individuals were found beyond 10 km from the type locality. *Liphistius maewongensis* was found in soil burrows on man-made road cuttings with a gentle surface inclination of 68.2–87.1 degrees measured from ground level. All burrows, regardless of size, had a trapdoor. Two types of burrows were observed, the simple straight burrow with a single opening (with signal lines) ( $n = 21$ ) and the T- or Y-shaped burrow ( $n = 25$ ) with two openings (one trapdoor is equipped with signal lines, whereas the other is not) (Fig. 6). The number of signal lines on trapdoors ranged from 4–8 ( $n = 46$ ). Straight burrows had an average number of signal lines of  $5.86 \pm 1.01$  (4–7;  $n = 21$ ), whereas T- or Y-shaped burrows had an average number of signal lines of  $6.24 \pm 0.88$  (5–8;  $n = 25$ ). The shape of trapdoors with signal lines was more or less oval with an average width of  $11.17 \pm 4.03$  mm (4.6–24 mm;  $n = 46$ ), an average length of  $16.42 \pm 5.21$  mm (7–28 mm;  $n =$

46), and an average depth of  $69.02 \pm 23.84$  mm (24.66–144.5 mm;  $n = 46$ ). The shape of trapdoors of straight burrows with signal lines was more or less oval with an average width of  $10.02 \pm 4.97$  mm (4.6–24 mm;  $n = 21$ ), an average length of  $14.84 \pm 6.37$  mm (7–28 mm;  $n = 21$ ), and an average depth of  $70.26 \pm 21.02$  mm (40–105.1 mm;  $n = 21$ ). The shape of trapdoors of T- or Y-shaped burrows with signal lines was more or less oval with an average width of  $12.14 \pm 2.77$  mm (8.1–17.9 mm;  $n = 25$ ), an average length of  $17.74 \pm 3.63$  mm (12.3–27.3 mm;  $n = 25$ ), and an average depth of  $67.97 \pm 27.74$  mm (27.6–144.5 mm;  $n = 25$ ). The shape of trapdoors of T- or Y-shaped burrows without signal lines was more or less oval with an average width of  $9.6 \pm 2.42$  mm (5.1–15.5 mm;  $n = 25$ ) and an average length of  $12.92 \pm 2.67$  mm (9.5–18.8 mm;  $n = 25$ ). In the field, we observed that while excavating for individual spiders in a T- or Y-shaped burrow through its trapdoor with





Figure 6.—Burrow types of *Liphistius maewongensis* sp. nov.: (a) two trapdoor openings of a T- or Y-shaped burrow (note the opening without signal lines used as escape door; yellow arrow); (b) a cross-sectional sketch of a T- or Y-shaped burrow; (c) an opening of a trapdoor of a simple horizontal burrow with signal lines; (d) a cross-sectional sketch of a simple horizontal burrow.

signal lines, the spider frequently escaped through the second trapdoor without signal lines. We speculated that one of the functions for the second trapdoor is that it is used as an “escape door” (Fig. 5a). This is the first report of a T- or Y-shaped burrow found in a species belonging to the *bristowei* species-group, since Schwendinger (1990) earlier reported that such a burrow characteristic is usually only found in the *birmanicus*- and *trang* species-groups.

The number of eggs per egg sac was between 31–52 eggs ( $n = 11$ ). Since one male of *L. maewongensis* molted to an adult in October, and high numbers of female egg sacs were found in December and not in August, we inferred that the mating period is likely to be around October–December. This annual cycle concurs with the findings of Schwendinger (1990) for species of the *bristowei* and *birmanicus* species-groups, which also have mating seasons during this time in Thailand.

## ACKNOWLEDGMENTS

The authors are grateful to the assistance in the field provided by the park rangers at Mae Wong National Park. Our colleagues, Nontawat Chatthanabun, Narin Chomphuphuang, Sirat Lertjintanakit, Pakorn Nalinrachatakan and Chaowalit Songsangchote assisted us during intensive field collecting throughout the study. Peeranat Bokorane and Puttita Pasukdee assisted us with the figures of the male and female genitalia and the Thailand map. We also greatly appreciate Michael Rix, Peter Schwendinger and an anonymous reviewer for providing useful comments to improve the manuscript. This research is supported by the 90<sup>th</sup> Anniversary of Chulalongkorn University Scholarship (GCUGRI125601047M) and the Graduate School scholarship, Chulalongkorn University to commemorate the 72<sup>nd</sup> anniversary of his Majesty King Bhumibol Adulyadej. The Center of Excellence in Biodiversity, Office of Higher Education

Table 2.—Pedipalp and legs measurements of nine adult females of *Liphistius maewongensis* sp. nov. collected on 23 December 2015. All measurements (mean  $\pm$  s.d.) are given in millimeters.

	Femur	Patella	Tibia	Metatarsus	Tarsus	Total length
<b>Pedipalp</b>	3.34 $\pm$ 0.52	1.73 $\pm$ 0.41	2.34 $\pm$ 0.44	-	2.35 $\pm$ 0.40	9.76 $\pm$ 1.69
<b>Leg I</b>	4.06 $\pm$ 0.57	2.07 $\pm$ 0.30	2.51 $\pm$ 0.43	2.38 $\pm$ 0.40	1.38 $\pm$ 0.18	12.39 $\pm$ 1.81
<b>Leg II</b>	4.10 $\pm$ 0.62	2.04 $\pm$ 0.32	2.53 $\pm$ 0.43	2.54 $\pm$ 0.36	1.42 $\pm$ 0.30	12.64 $\pm$ 1.92
<b>Leg III</b>	4.06 $\pm$ 0.59	2.06 $\pm$ 0.33	2.64 $\pm$ 0.41	2.96 $\pm$ 0.67	1.74 $\pm$ 0.25	13.45 $\pm$ 2.17
<b>Leg IV</b>	5.17 $\pm$ 0.77	2.39 $\pm$ 0.32	3.60 $\pm$ 0.47	5.09 $\pm$ 0.82	2.54 $\pm$ 0.36	18.79 $\pm$ 2.68



Commission, Thailand also provided partial funding for this work (PERDO-BDC: BDC-PG2-159009/1).

#### LITERATURE CITED

- Ellis, M. 2012. The Caves of Saraburi, Thailand. Takobi Limited, Somerset, UK.
- Haupt, J. 2003. The Mesothelae – monograph of an exceptional group of spiders (Araneae: Mesothelae) (Morphology, behaviour, ecology, taxonomy, distribution and phylogeny). *Zoologica* 154:1–102.
- IUCN 2017. The IUCN Red List of Threatened Species. Version 2017–1. Online at <http://www.iucnredlist.org>
- Ono, H. 1988a. Liphistiid spiders (Araneae, Mesothelae) of northwest Thailand. *Bulletin of the National Museum of Nature and Science Tokyo (A)* 14:35–41.
- Ono, H. 1988b. Liphistiid spiders (Araneae, Mesothelae) of south Thailand. *Bulletin of the National Museum of Nature and Science Tokyo (A)* 14:145–150.
- Ono, H. & P.J. Schwendinger. 1990. Liphistiid spiders (Araneae, Mesothelae) from central and eastern Thailand. *Bulletin of the National Museum of Nature and Science Tokyo (A)* 16:165–174.
- Platnick, N.I. & W.J. Gertsch. 1976. The suborders of spiders: a cladistic analysis (Arachnida, Araneae). *American Museum Novitates* 2607:1–15.
- Platnick, N.I. & W.C. Sedgwick. 1984. A revision of the spider genus *Liphistius* (Araneae, Mesothelae). *American Museum Novitates* 2781:1–31.
- Schwendinger, P.J. 1987. On the male of *Liphistius trang* (Araneae: Mesothelae) with notes on the natural history of the species. *Natural History Bulletin of the Siam Society* 35:9–25.
- Schwendinger, P.J. 1990. On the spider genus *Liphistius* (Araneae: Mesothelae) in Thailand and Burma. *Zoologica Scripta* 19:331–351.
- Schwendinger, P.J. 1995. New *Liphistius* species (Araneae, Mesothelae) from southern Thailand and northern Malaysia. *Zoologica Scripta* 24:143–156.
- Schwendinger, P.J. 1996. New *Liphistius* species (Araneae, Mesothelae) from western and eastern Thailand. *Zoologica Scripta* 25:123–141.
- Schwendinger, P.J. 1998. Five new *Liphistius* species (Araneae, Mesothelae) from Thailand. *Zoologica Scripta* 27:17–30.
- Schwendinger, P.J. 2009. *Liphistius thaleri*, a new mesothelid spider species from southern Thailand (Araneae, Liphistiidae). *Contributions to Natural History* 12:1253–1268.
- Schwendinger, P.J. 2013. On two *Liphistius* species (Araneae: Liphistiidae) from Laos. *Zootaxa* 3702:51–60.
- Schwendinger, P.J. & H. Ono. 2011. On two *Heptathela* species from southern Vietnam, with a discussion of copulatory organs and systematics of the Liphistiidae (Araneae: Mesothelae). *Revue suisse de Zoologie* 118:599–637.
- Sedgwick, W.C. & P.J. Schwendinger. 1990. On a new cave-dwelling *Liphistius* from Thailand (Araneae: Liphistiidae). *Bulletin of the British Arachnological Society* 8:109–112.
- World Spider Catalog. 2017. World Spider Catalog. Version 18.0. Natural History Museum, Bern. Online at <http://www.wse.nmbe.ch>
- Xu, X., F. Liu, J. Chen, H. Ono, D. Li & M. Kuntner. 2015. A genus-level taxonomic review of primitively segmented spiders (Mesothelae, Liphistiidae). *ZooKeys* 488:121–151.

*Manuscript received 4 April 2017, revised 13 July 2017.*



## Revision of *Misumessus* (Thomisidae: Thomisinae: Misumenini), with observations on crab spider terminology

G. B. Edwards: Curator Emeritus, Arachnida & Myriapoda, Florida State Collection of Arthropods, Gainesville, FL 32608, USA. E-mail: gb.edwards@freshfromflorida.com

**Abstract.** The widespread and previously monotypic genus *Misumessus* Banks, 1904 from North America is found to consist of at least seven species. The type species, *M. oblongus* (Keyserling, 1880), occurs from Ontario, Canada, to eastern Texas and ranges over most of the eastern and mideastern United States. *Misumessus lappi* sp. nov. has a midwestern range and is known from central Texas to eastern Colorado. *Misumessus dicaprio* sp. nov. is recorded from western North America from California, Utah and western Colorado, south to Arizona, New Mexico, and southwest Texas. *Misumessus tami* sp. nov. occurs in the southern half of peninsular Florida. *Misumessus quintero* sp. nov. is circum-Caribbean, with records from Mexico to Panama, Trinidad, and the Greater and Lesser Antilles. Another Antillean species, *M. bishopae* sp. nov., is known from Puerto Rico, Dominica, and possibly the Grenadines. *Misumessus blackwalli* sp. nov. is known from Bermuda from a single male; it is unlikely that this species represents *Thomisus pallens* Blackwall, 1868, a *nomen dubium* based on a juvenile female, and the only thomisid previously reported from Bermuda. This name has not been used since the 19<sup>th</sup> century other than in catalogs and checklists, and since its retention could potentially create a homonym, it is declared a *nomen oblitum*. The epigynal ‘hood’ of thomisids is considered misnamed, as it engages the retrolateral tibial apophysis (RTA), and is renamed the ‘coupling pocket’ as in other RTA elade members. A hood is herein considered to be a general term that refers to an epigynal outgrowth partly enclosing a depression that engages a structure on the palpal bulb rather than the palpal tibia.

**Keywords:** *Mecaphesa*, *Misumena*, *Misumenoides*, *Misumenops*, new species

<http://zoobank.org/?lsid=urn:lsid:zoobank.org:pub:55E1EEAE-25FC-4A00-B45F-64D21BABD4AA>

The genus *Misumessus* Banks, 1904 is one of five genera of Misumenini presently known from North America (Lehtinen 2004; Lehtinen & Marusik 2008). The others are *Mecaphesa* Simon, 1900, *Misumena* Latreille, 1804, *Misumenoides* F. O. Pickard-Cambridge, 1900, and *Misumenops* F. O. Pickard-Cambridge, 1900. *Misumessus* long was considered a synonym of *Misumenops* (Petrunkévitch 1911; Gertsch 1939), or a subgenus of *Misumenops* (Schick 1965). *Misumenops* was re-diagnosed by Lehtinen & Marusik (2008), resulting in the establishment of *Mecaphesa* and *Misumessus* as valid genera. Unfortunately the justification for elevating *Misumessus* was based only on analysis of female characters (Lehtinen & Marusik, 2008), which are re-evaluated herein, and the quite different male characters are analyzed as well.

Until now, *Misumessus* had been considered monotypic, with its type species, *M. oblongus* (Keyserling, 1880), reported as widespread from Canada to Guatemala, and also reported from the island of St. Vincent in the Lesser Antilles (World Spider Catalog 2017). Among collections examined are continental specimens from as far south as Panama, and from various islands including Bermuda, Trinidad, and the Greater and Lesser Antilles. The genus is not only more widespread than previously reported, but good evidence exists that there is not just one, but at least seven species of *Misumessus*.

The most conspicuous evidence for multiple species of *Misumessus* is found in the structure of the male palp. As in salticid genera with circular tegula (Maddison 2015) and as observed for some other Misumenini (Lehtinen & Marusik 2008), different species of *Misumessus* have the embolus beginning at different points on the circumference of the tegulum. In *Misumessus*, the starting position of the widened embolus base can be compared to hours on a clock face, as in

Lehtinen & Marusik (2008), or given in degrees of a circle with zero degrees in the 12:00 position.

A second piece of evidence for multiple species is the location of each type of male in its own distinctive geographic range, in most cases with little to no overlap between species (Fig. 1, distribution map). This is especially evident where there are major geographic divides like north-south oriented mountain ranges, such as the Rocky Mountains, between species.

Conversely, females are difficult to separate by genital structure; external intraspecific variation is great with considerable apparent interspecific overlap, and species-specific differences are subtle. However, these differences do exist, in the form of scape length, scape shape, modifications to the edges of the scape tip, and especially in the shape and size of the coupling pocket (‘hood’). Among some species it is clear that there are differences in the length of the epigynal copulatory ducts, but in other species, this is more difficult to evaluate due to the convoluted course of the ducts. Given that there are differences in embolus length among species, it would be expected that copulatory duct length would also vary among species. However, other differences exist as well, such as the amount of coiling and the placement of the wider section of the duct that enters the spermatheca.

**Observations on terminology and the phylogenetic relationships of thomisids.**—It is necessary here to address some terms in the family Thomisidae before proceeding further, which requires a summary of the phylogenetic position of the family. Although other hypotheses have been proposed, for the most part, thomisids have been considered to be related to one of two groups: either part of the Dionycha close to the Salticidae (Lehtinen 1967; Loerbroeks 1984; Edwards 2004; Ramírez



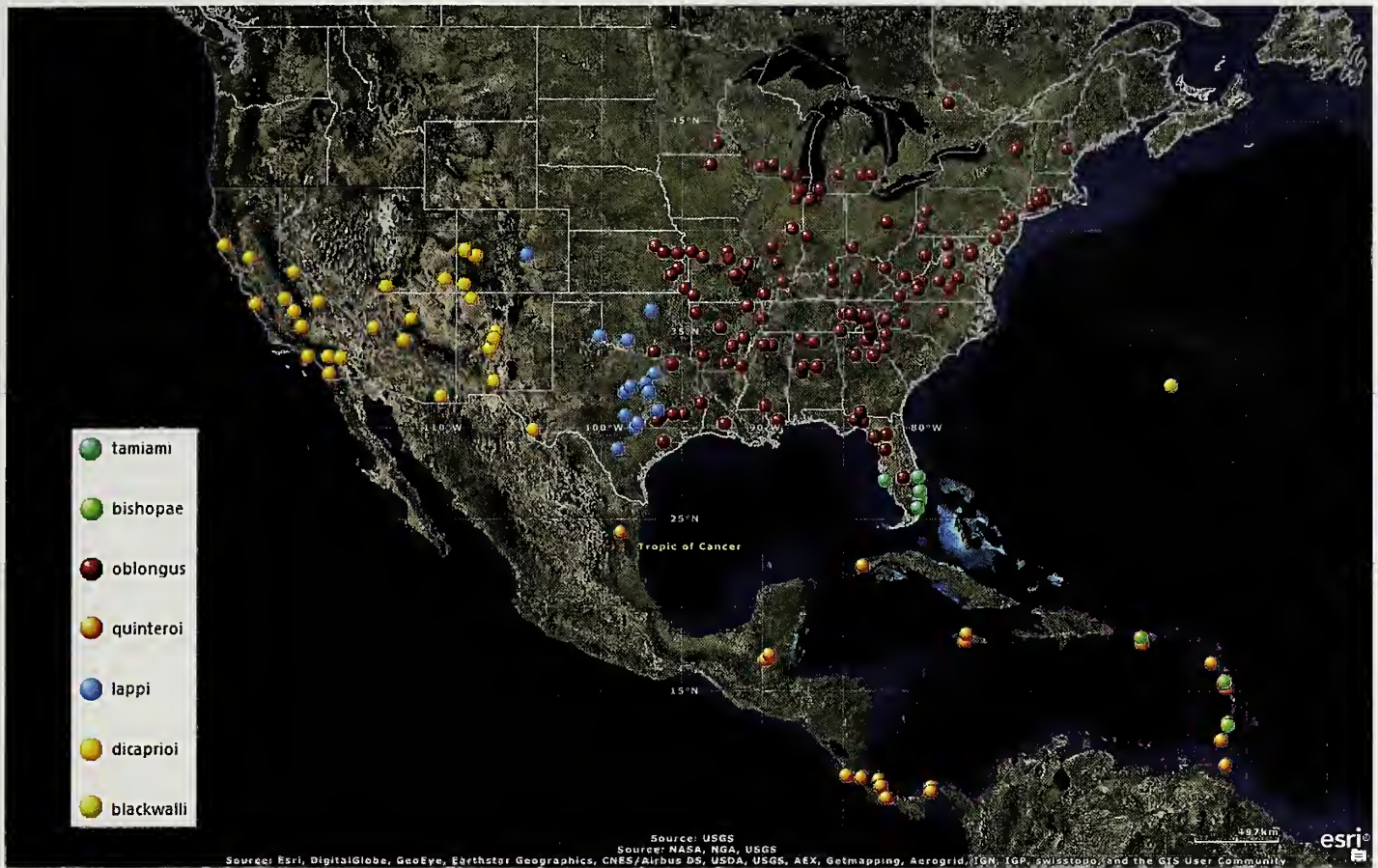


Figure 1.—Distribution of *Misumessus* species, with species denoted on map legend.

2014), with a retinal mosaic similar to salticids in the Australian thomisid *Hedana* sp. (Blest & O'Carroll 1989); or belonging to the Lycosoidea (Homann 1975; Corronca & Terán 1997, 2000; Ramírez 2014 as an alternate possibility). The most recent evidence based on molecular data favors lycosoids (Moradmand et al. 2014; Polotow et al. 2015; Garrison et al. 2016; Wheeler et al. 2016). While Garrison et al. (2016) indicated that the Lycosoidea and Dionycha were sister groups, with thomisids basal in the lycosoids, a similar study by Polotow et al. (2015; see also the morphological study by Ramírez 2014) analyzing a greater diversity of pertinent taxa, showed that the Dionycha were sister to a larger group known as the 'oval calamistrum clade' that included the Lycosoidea. They also indicated an immediate sister-group relationship of thomisids with oxyopids. Wheeler et al. (2016), in the most comprehensive review of spider phylogeny to date, gave a lycosoid phylogeny more consistent with Garrison et al. (2016). Here the thomisids were weakly associated with the Psecridae, and these families together were sister to a clade consisting of (in order) core Ctenidae, Oxyopidae (associated with Senoculidae), and the higher lycosoids.

In all of these cases, thomisids are part of the RTA clade, i.e., the palps each have a retrolateral tibial apophysis (RTA), with some exceptions (e.g., RTA lost in Lycosidae). Although morphological phylogenetic studies tend to weight male palps more than they do female epigyna due to the greater average

number of visible characters on the palps, epigyna should have corresponding characters to the functional parts of the palps. In this case, the RTA has a corresponding epigynal feature that has been known by several different names. Edwards (2015) gave it the functional name of 'coupling pocket' in salticids, which will be used here.

Many Thomisidae have a usually anterior epigynal structure that has been known as a hood. However, since this 'hood' engages the male retrolateral tibial apophysis, it is in fact a coupling pocket [e.g., *Ebrechtella tricuspidata* (Fabricius, 1775), "The more pointed and sclerotized tip of the rta ... is inserted into a median hood of the epigyne..."; Huber 1995: 155, as *Misumenops tricuspidatus*]. Hoods as they exist in other families (e.g., Salticidae in the Dionycha, Lycosidae in the Lycosoidea) are extrusions of the anterior edge of the epigynal plate; like a coupling pocket, they partially enclose a depression, which is the source of confusion. Even though both are engaged as intersexual copulatory mechanisms, there is a functional difference between them, as a hood (as defined here) engages part of the palpal bulb, while the coupling pocket engages the retrolateral tibial apophysis. In lycosids, it is the median apophysis (Dondale & Redner 1978a); in salticids, it is apparently a type of highly modified guide to brace the embolus (Edwards 2015). In addition, although many salticine salticids have posterior coupling pockets, others (e.g., some Freyina and Plexippini) have anterior coupling pockets like thomisids. This similar epigynal



structure, along with a similar palpal structure in basal salticids, may in part explain why thomisids and salticids have been thought to be related.

Another possible reason for this similarity is that if thomisids are basal lycosoids, and if lycosoids were directly sister to the Dionycha, then it is not unlikely that thomisids would have more in common with dionychans than would other lycosoids, due to shared symplesiomorphies. The simplified phylogeny illustrated by Garrison et al. (2016) suggested this relationship, and although the salticids alone were not likely to be the most basal group in dionychans, there was supporting evidence that they belonged to a near basal clade of families within that group (Ramírez 2014; Polotow et al. 2015), and thus might make a viable representative of what could be similar among basal dionychans and basal lycosoids. Ironically, the possibility that thomisids and oxyopids are sister groups would not negate this general idea, as oxyopids also have been thought to be related to salticids (Jackson 1986 and references therein). However, Wheeler et al. (2016) placed salticids in a terminal position in the Dionycha part B, much more distant from the thomisids; and since the lycosoids apparently are not direct sisters of dionychans nor basal in the oval calamistrum clade (Polotow et al. 2015), nor are thomisids alone basal in the lycosoids (Wheeler et al. 2016), there appear to be several other steps between dionychans and lycosoids that have yet to be shown to maintain morphological consistency in important structures like genitalia.

An offshoot of the revelation that thomisids are lycosoids is that there no longer seems to be any justification for using special color pattern terminology in thomisids, i.e., the carapace alatal bands (Schick 1965) can be referred to simply as submarginal bands as in lycosids (e.g., Dondale & Redner 1978a; Wallace & Exline 1978). However, the soma macrosetae designations of Schick (1965) seem to be useful and are utilized herein.

## METHODS

**Material examined.**—The following institutions and individuals provided loans of types and other specimens: American Museum of Natural History (AMNH), New York, NY; British Natural History Museum (BNHM), London, United Kingdom; California Academy of Sciences (CAS), San Francisco, CA; Canadian National Collection (CNC), Ottawa, Canada; Denver Museum of Nature and Science (DMNS), Denver, CO; Field Museum of Natural History (FMNH), Chicago, IL; Florida State Collection of Arthropods (FSCA), Gainesville, FL; Hank Guarisco collection (HGC), Lawrence, KS; Museum of Comparative Zoology (MCZ), Cambridge, MA; Wild Basin Wilderness Preserve, Saint Edwards University (SEU), Austin, TX; Smithsonian Institute, United States National Museum (USNM), Washington D.C.; Texas A & M University Insect Collection (TAMU), College Station, TX; Biodiversity Collections, University of Texas at Austin (UTA), Austin, TX; University of Vermont (UVT), Burlington, VT. In addition, Joe Lapp and Leslie Bishop donated specimens to the FSCA (see Acknowledgments).

**Morphological methods and abbreviations.**—Specimens were examined in 75–80% ethanol, and sorted with Omana and

Leica MS5 microscopes. Photos were taken by J. T. Lapp with a Canon EOS T3i on a Zeiss Stemi 2000C microscope and stacked with Helicon Focus, and by GBE with an AxioCam HRc on a Zeiss V20 microscope using Zen stacking software. The map was created in ArcGIS, while figure plates were assembled in Corel Paintshop Pro X2. For localities, latitude and longitude coordinates as given on the collection label are recorded if present, otherwise county or other centroid lat/long coordinates are used to approximate the location. Measurements are in millimeters and are given as ‘mean (range),’ or ‘type (range)’ for designated types of new species (H = holotype, A = allotype);  $n = 5$  for all species and available sexes except  $n = 2$  for male *M. tamiami* sp. nov. and  $n = 1$  for male *M. blackwalli* sp. nov. Obviously large and small adult specimens were included in the measurements in an attempt to sample the true size range for a species when available specimens exceeded five samples for each sex. The left palp is referenced for palp characters (right palp mirror-imaged if necessary). Specific references to eyes refer to the eye lenses. Introductory bibliographic citations in species accounts may have an exclamation point after a citation, indicating the author has examined the type(s) of the referenced species described therein, a commonly used convention in entomological taxonomic literature.

Individual scale bars are shown on images taken with Zen software, but other images lack scale bars. Due to the similar sizes of each species, images lacking scale bars can be assumed to approximate similar images with scale bars, or extrapolations can be made based on mean body size, given with each species description. BugGuide references are available online at <http://bugguide.net/node/view/15740> (use search for specific image numbers); the iNaturalist references are available online at <https://www.inaturalist.org/observations/7239942>

Abbreviations used in figures and descriptions are: A1, A2, S1, named carapace spiniform setae; ALE, anterior lateral eye; AME, anterior medial eye; CD, copulatory duct; Cl, clypeus; CO, copulatory opening; CP, coupling pocket [on posterior end of scape]; EB, embolus base; E, embolus; EGW, eye group width (measured at PLE); ET, embolus tip; ITA, intermediate tibial apophysis; PLE, posterior lateral eye; PME, posterior median eye; RTA, retrolateral tibial apophysis; S, spermatophore; Sc, scape [includes the coupling pocket]; Sp, spermathecae; Tg, tegulum; VTA, ventral tibial apophysis. Setal types: ‘clavate’ denotes relatively short, black, on body, similar to spiniform except the distal tip is broader than the base and flattened; ‘filiform’ denotes short, pale, slender and hair-like, on body and legs; ‘macroseta’ denotes relatively long, thick, dark, on legs (typically on true ventral surface); ‘spiniform’ denotes relatively short, black, on body and legs, with narrow conical slightly attenuate rounded tip (same as ‘rigid setae’ of Lehtinen & Marusik 2008). Clavate and spiniform setae can be thought of as types of soma macrosetae, versus typical ventral leg macrosetae, although they may also occur on the dorsal and lateral surfaces of the legs.

## TAXONOMY

**Family Thomisidae** Sundevall, 1833  
**Subfamily Thomisinae** Sundevall, 1833



**Tribe Misumenini Dahl, 1913**  
**Genus *Misumessus* Banks, 1904**

*Misumessus* Banks, 1904: 112.

**Type species.**—*Misumena oblonga* Keyserling, 1880: 79, by monotypy.

**Diagnosis.**—*Misumessus* is considered a valid genus with the following presumed synapomorphies: female—epigynal scape present (Figs. 3f, i, 4g, 5e, 7f, 8g, 9a, e, g), coupling pocket more posteriorly placed than in related genera (on posterior end of scape), and coupling pocket miniaturized (Figs. 3h, 4h, 5e, 7h, 8h); male—embolus exceeding 360 degrees around tegulum (Figs. 3a, 4b, 5b, 7e, 10c, h, 11d, g, 12d), and RTA extended dorsally from a short base with a blunt tip curved in a distal direction (Figs. 3c, 4d, 5c, 7d, 10e, j, 11e, h, 12f).

**Description.**—*Females*: Body length 4–8 mm (with gravid females at upper end of range), with much greater body mass than males. In life, body typically pale green in color. Dorsal abdomen often has noticeable faint reticulation due to subdermal deposition of guanine, which may make most of abdominal dorsum appear white. Freshly preserved specimens appear white or pale yellow, but longer preserved specimens have darker yellowish brown carapace with large median pale patch of variable size and shape posterior to eye group; there are subtle differences in patch shape that may be species specific. Each lateral edge of carapace has row of short pale filiform setae. Carapace length and width nearly equal, but average slightly wider than long (usually less than 0.1 mm). Most species with clypeus slightly sloping forward from dorsal to ventral. Most species lack patterns on chelicerae. Sternum typically white.

All eyes ('eye group') continuously connected by surrounding white pigment; underlying retinæ individually encased in black pigment, usually not apparent (other than through the transparent but apparently 'black' lenses) unless preservation is suboptimal. Eye lenses all small, but ALEs noticeably largest; other lenses subequal in size, although AMEs typically slightly wider than posterior eyes, i.e., ALE >> AME > PLE = PME in most species. Distance between PMEs wider than between AMEs, so medial eyes form a trapezoid wider posteriorly. Posterior eye row wider than anterior eye row.

Face with distinctive pigmentation, including amount of pigment below eye group on clypeus, and presence/absence and orientation of minute gray or tan lines within pigmented eye group area. These lines may be due to patterns of reduced white pigmentation, therefore line color could be influenced by underlying integument color; or they may be darker pigmented areas. Females entirely lack dorsal spiniform setae on body, or on carapace may have some or all of A1, A2, or S1 spiniforms around lateral edge of eye group (see Schick 1965, fig. 1; Fig. 10a); otherwise with sparse filiform setae on dorsum.

Females have 3–5 spiniforms on prolateral and dorsal surfaces of all femora. Ventral surfaces of legs I and II have 4–5 large pairs of macrosetae on tibiae (sometimes 5<sup>th</sup> pair, if present, is smaller than others), and 6 pairs on metatarsi. Venter of femora of legs I–II in preserved females with broad white band, at least in *M. obscurus*, *M. quintero* sp. nov., and *M. tamiami* sp. nov.

Abdomen significantly longer than wide, or may be of roughly equal dimensions (e.g., in gravid females). Epigyne

with median extension directed posteriorly and positioned in the approximate middle of the epigyne; this is considered a scape (in the general sense) that is variable in length, width, and ventral profile (convex laterally or parallel-sided); the posterior edge may appear bilobed, convex, or truncate. Miniaturized coupling pocket at posterior end of scape. In posterior view, coupling pocket cavity can be seen (Figs. 3g, 4j, 5h, 7g, 8i).

Copulatory openings located on each side of coupling pocket in posterior view (Fig. 3g), in anterior part of posteriorly-placed atrium. Each of these opens directly into narrow copulatory duct that makes wide lateral spiral of about 1.5 revolutions whose circumference narrows on last half turn. Narrow section connects to wider section of duct that has sinuate shape, usually lateral to widest section of duct, until widest part enters anteromedial area of spermatheca. There may be small coils or partial loops in the wider section of the duct. Fertilization duct emerges from medial face of spermatheca.

*Males*: Body length 1.9–4.2 mm. In life, usually with yellow to reddish carapace, sternum yellow, and yellow abdomen often with white anterolateral bands or with medial darker pigment; femora of legs I and II, and all legs III and IV, pale green. Legs I and II with red or reddish brown bands on distal ends of femora, patellae, tibiae, metatarsi, and tarsi, and on proximal end of tibiae; otherwise distal segments yellow. Preserved males with darker carapace and eye group pigment as in females; legs III and IV translucent white with little or no pigment, or yellow. With full complement of spiniforms around and within eye group, and two rows of posterior carapace spiniforms, a subposterior row with four spiniforms on each side, and a posterior row with two spiniforms on each side. Legs I and II with inconspicuous ventral leg macrosetae, but like females, have row of 3–5 spiniforms on prolateral and dorsal surfaces of all femora. Abdomen dorsally noticeably covered with short dark regularly-spaced spiniforms, and sometimes seems to have a weakly sclerotized median scutum. Venter off white to pale yellow, usually without darker markings.

Embolus exceeds 360 degrees in rotation around tegulum. Species separated by location of embolus base origin and by amount of separation of embolus origin from embolus tip (measured in degrees herein). Lightly sclerotized embolus base, of characteristic elongate curved teardrop shape, is smoothly integrated along outer edge of tegulum. Embolus tip in slight groove on retrolateral edge of cymbium and generally emerges between 90 and 135 degrees.

There are species-specific differences in RTA shape, especially relative length of basal part, and amount and direction of curvature of distal part (see retrolateral and dorsal views of palps). Approximately basal third of RTA extends distally, is flattened cylindrical in shape, and is shallowly concave at distal end. Dorsal edge of RTA strongly developed, begins as continuation of concave distal surface that is diverted in a dorsal direction, and is curved to a stout tip, more or less pointing distally. Where dorsal edge diverted dorsally, retrolateral edge narrowed and slightly projects outward, which might be interpreted as small intermediate tibial apophysis (ITA). All species of *Misumessus* also have a small curved ventral tibial apophysis (VTA).



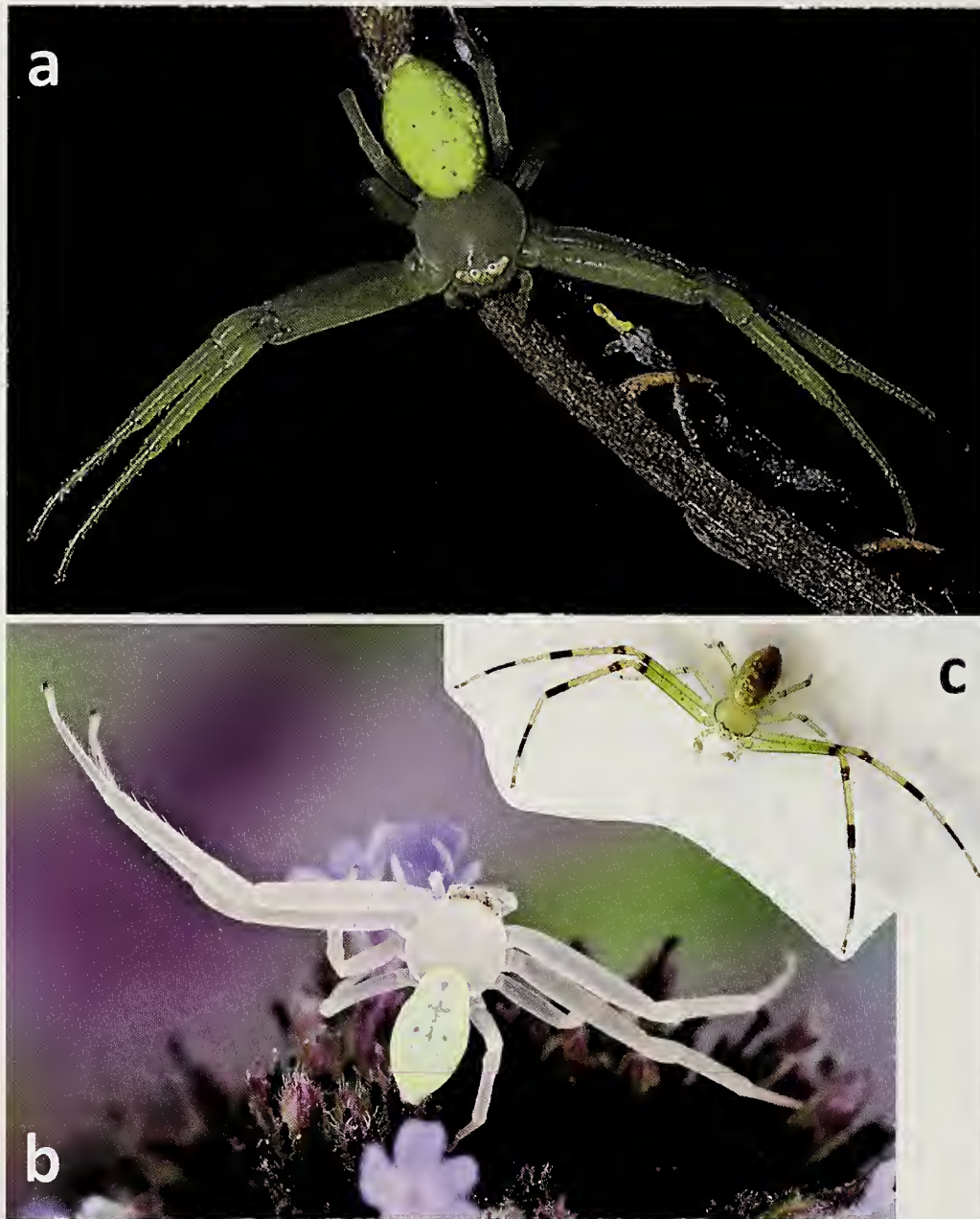


Figure 2.—*Misumessus oblongus* (Keyserling, 1880), live images. a, typical female from Florida; b, white form female from North Carolina; c, male from Kansas with maximum abdominal pigment. Photo credits: a by Daniel D. Dye II; b by Colin Hutton; c by Hank Guarisco.

**Variation.**—Notable exceptions to the general generic description are given here (also if pertinent included with individual species). Eye group pigment sometimes pink in part or entirely, or yellow in part or entirely. The AME of *M. lappi* sp. nov. are smaller than the posterior eyes. Female body color in life occasionally whitish or yellow; white in female and most male *M. lappi* sp. nov., amber to brown in *M. quintero* sp. nov. A pair of narrow yellow to red anterolateral abdominal bands occasionally are present, and rarely may be continuous anteriorly. Shape of posterior end of scape may in part be a function of how much separation there is between the scape and body (affecting the corresponding viewing angle of the observer). Males, especially smaller individuals, may have a

reduced number of spiniforms on the carapace; *M. blackwalli* sp. nov. lacks spiniforms on the abdomen. Gertsch (1939) noted other variations, including extra pairs of macrosetae on the metatarsi of legs I and II.

**Notes.**—According to Schick (1965: 111), “Guide pocket not present; instead, large tongue-like flap developed in anterior portion of epigynum; intromittent orifice obscure, situated at base of flap.” In fact, the guide pocket, what is named here the coupling pocket, is present, and the ‘flap’ is considered a scape, in agreement with Lehtinen & Marusik (2008). The copulatory openings are correctly indicated by Schick as near the base of the scape.



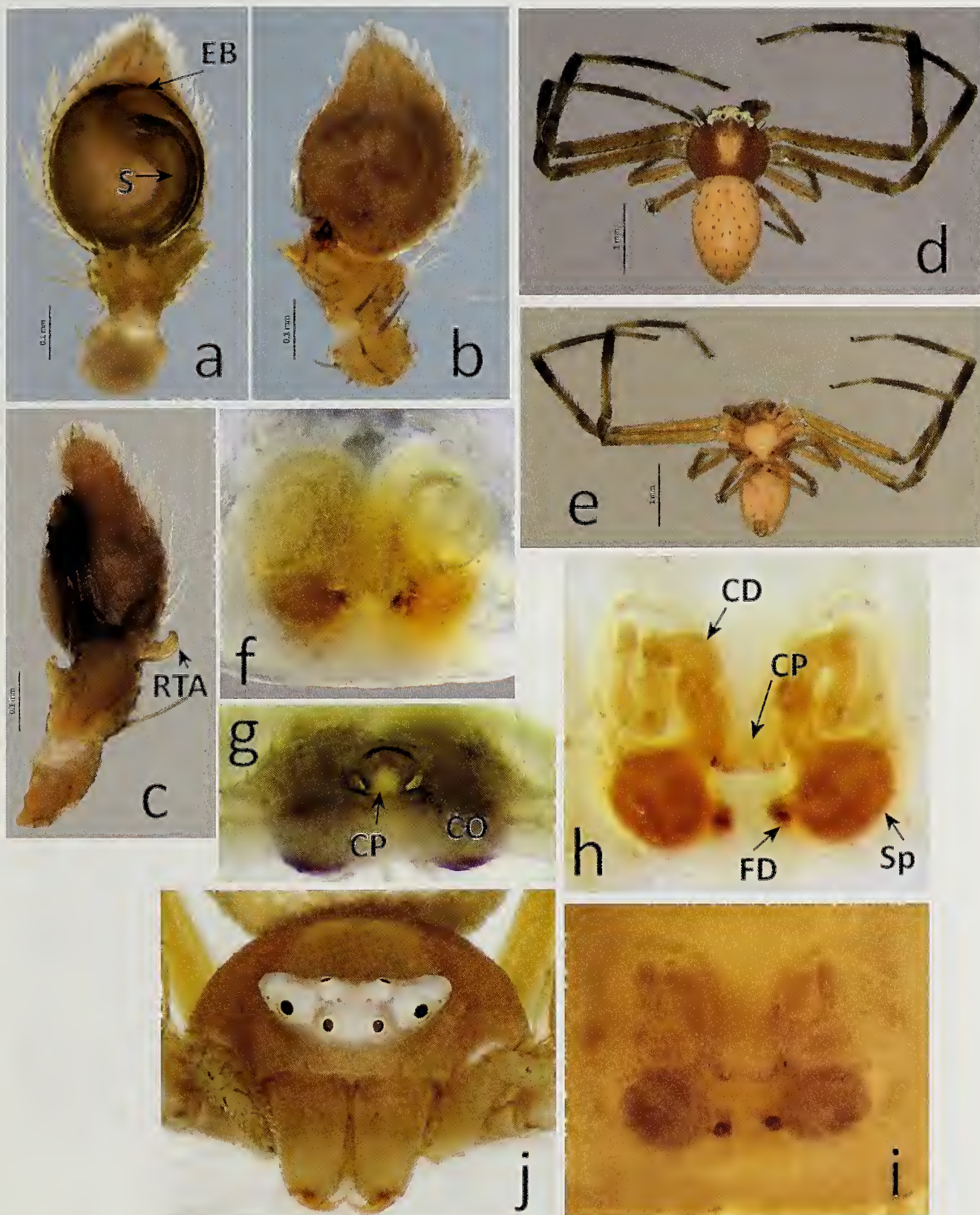


Figure 3.—*Misumessus oblongus* (Keyserling, 1880). a–e, Male from Florida: a, ventral palp; b, dorsal palp; c, retrolateral palp; d, dorsum; e, venter. f, Female from Texas, ventral epigyne cleared. g–j, Female from Wisconsin: g, posterior epigyne cleared; h, dorsal epigyne cleared; i, ventral epigyne; j, face. Photo credits: f–i by Joe Lapp.



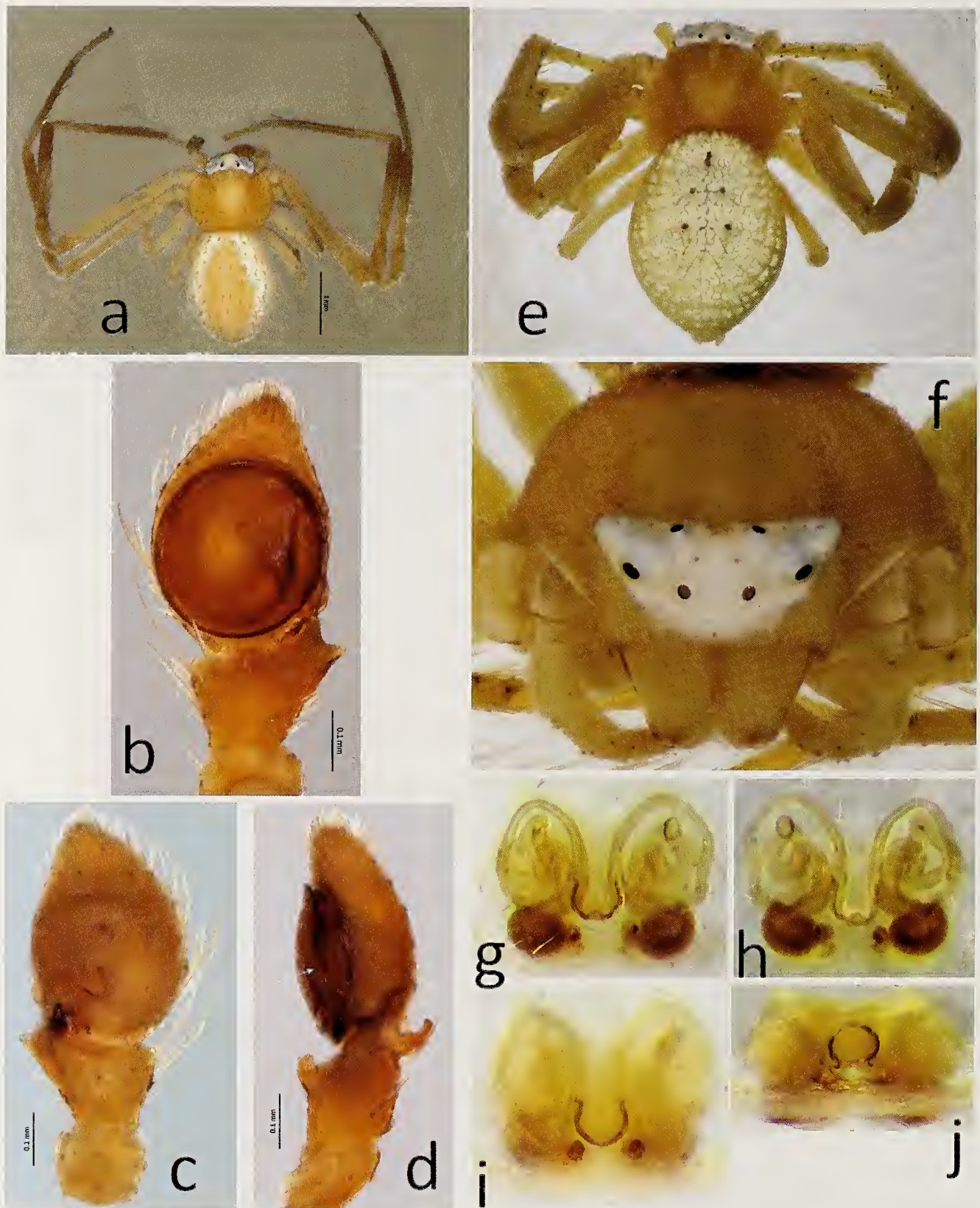


Figure 4.—*Misumessus dicaprioi* sp. nov. a–d, Male from California: a, dorsum; b, ventral palp; c, dorsal palp; d, retrolateral palp, arrow to transitional dark area between embolus base and spermophore. e–j, Female from Arizona: e, dorsum; f, face with extra clypeal pigment; g, ventral epigyne cleared; h, dorsal epigyne cleared; i, ventral epigyne; j, posterior epigyne cleared. Photo credits: e–j by Joe Lapp.



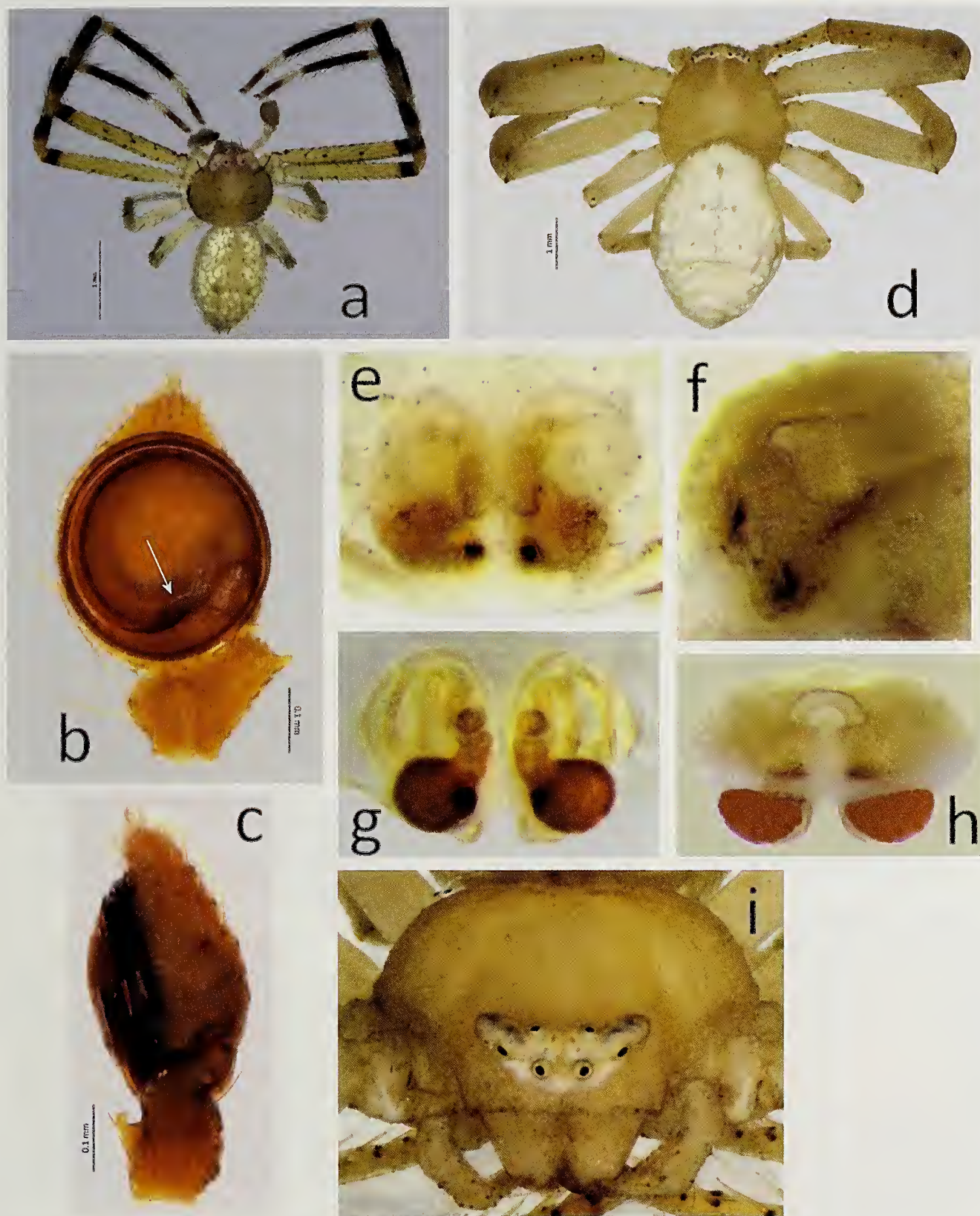


Figure 5.—*Misumessus tamiami* sp. nov. from Florida. a–c: Male: a, dorsum; b, ventral palp, arrow to transitional dark area between embolus base and spermophore; c, retrolateral palp. d–i, Female: d, dorsum; e, ventral epigyne; f, postero-ventrolateral epigyne showing scape elevation; g, dorsal epigyne cleared; h, posterior epigyne cleared; i, face. Photo credits: d–i by Joe Lapp.



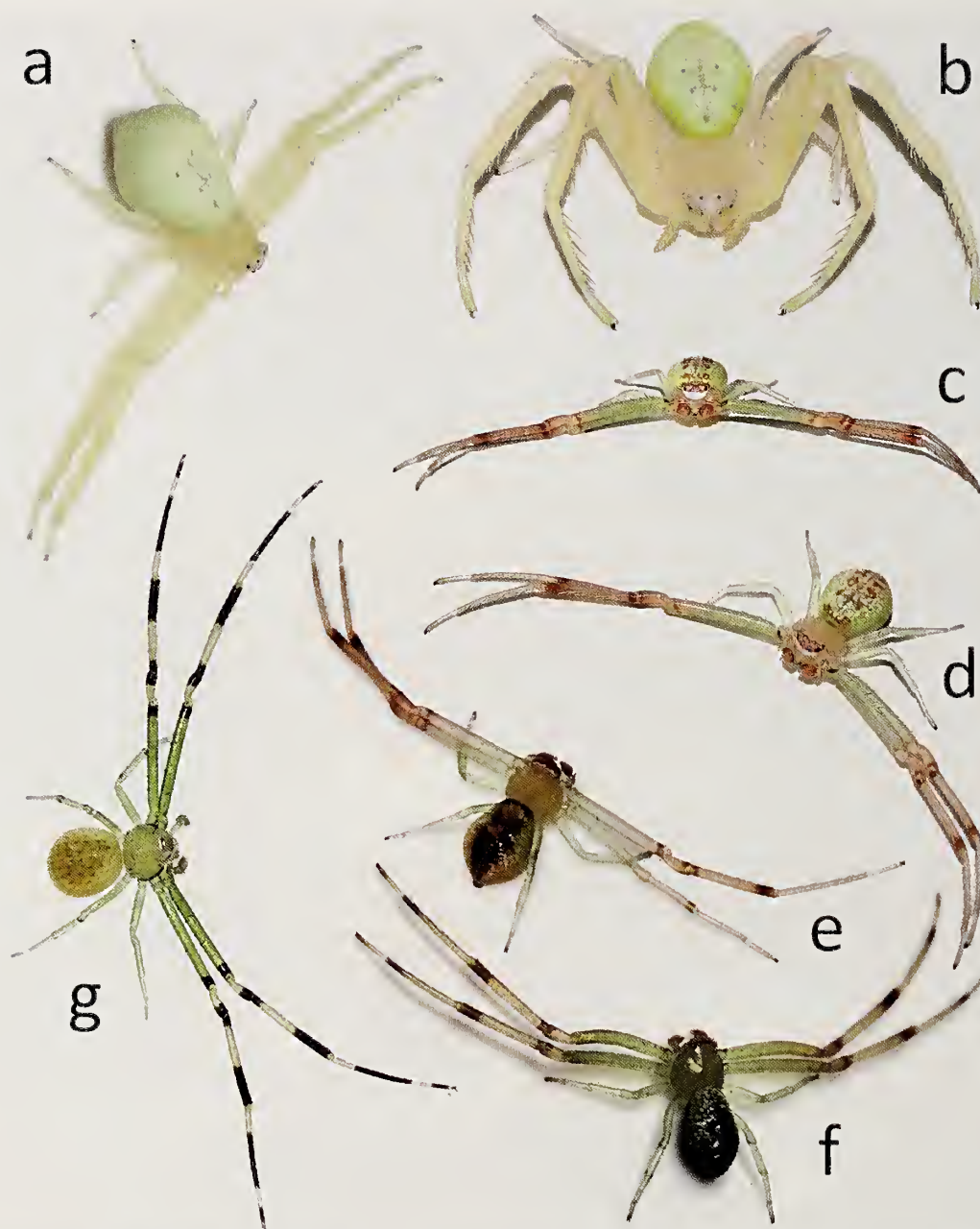


Figure 6.—*Misumessus lappi* sp. nov. from Texas, live images: a, penultimate female; b, adult female; e–f, adult males; c, d, holotype male, form with only red spots; e, form with additional red between red spots; f, dark green form; g, live male *Misumessus oblongus* (Keyserling, 1880) from Wisconsin. Note the proportionately longer legs I and II of *M. oblongus* compared to *M. lappi* sp. nov. Photo credits: a–f by Joe Lapp; g by Ilona Loser.

*Misumessus oblongus* (Keyserling, 1880)  
(Figs. 2, 3, 6g)

*Misumena oblonga* Keyserling, 1880: 79 (Dm). Emerton, 1892: 371!

*Misumena americana* Keyserling, 1880: 85. (Df). Synonymized by Banks, 1893: 125. Simon, 1897: 876.

*Misumenops oblongus* (Keyserling): F. O. P.-Cambridge, 1900: 144; Gertsch, 1939: 319; Chickering, 1940: 197; Kaston, 1948: 415; Schick, 1965: 111; Dondale & Redner, 1978b: 141; Breene et al., 1993: 78.

*Misumessus oblongus* (Keyserling): Banks, 1904: 112; Lehtinen & Marusik, 2008: 195.

**Type material.**—*Syntype males* (of *M. oblonga*). UNITED STATES: *Maryland and Illinois*: I examined three male syntypes from Peoria, Illinois, deposited in the BNHM (BM1890.7.1.3682–4).

*Syntype females* (of *M. americana*): *Maryland and Illinois*: see Gertsch (1939) (not examined).

**Other material examined.**—CANADA: *Ontario*: 11 ♀, Farran Pt., Walton, 45.8208°N, 78.5443°W, D.C. Lowrie



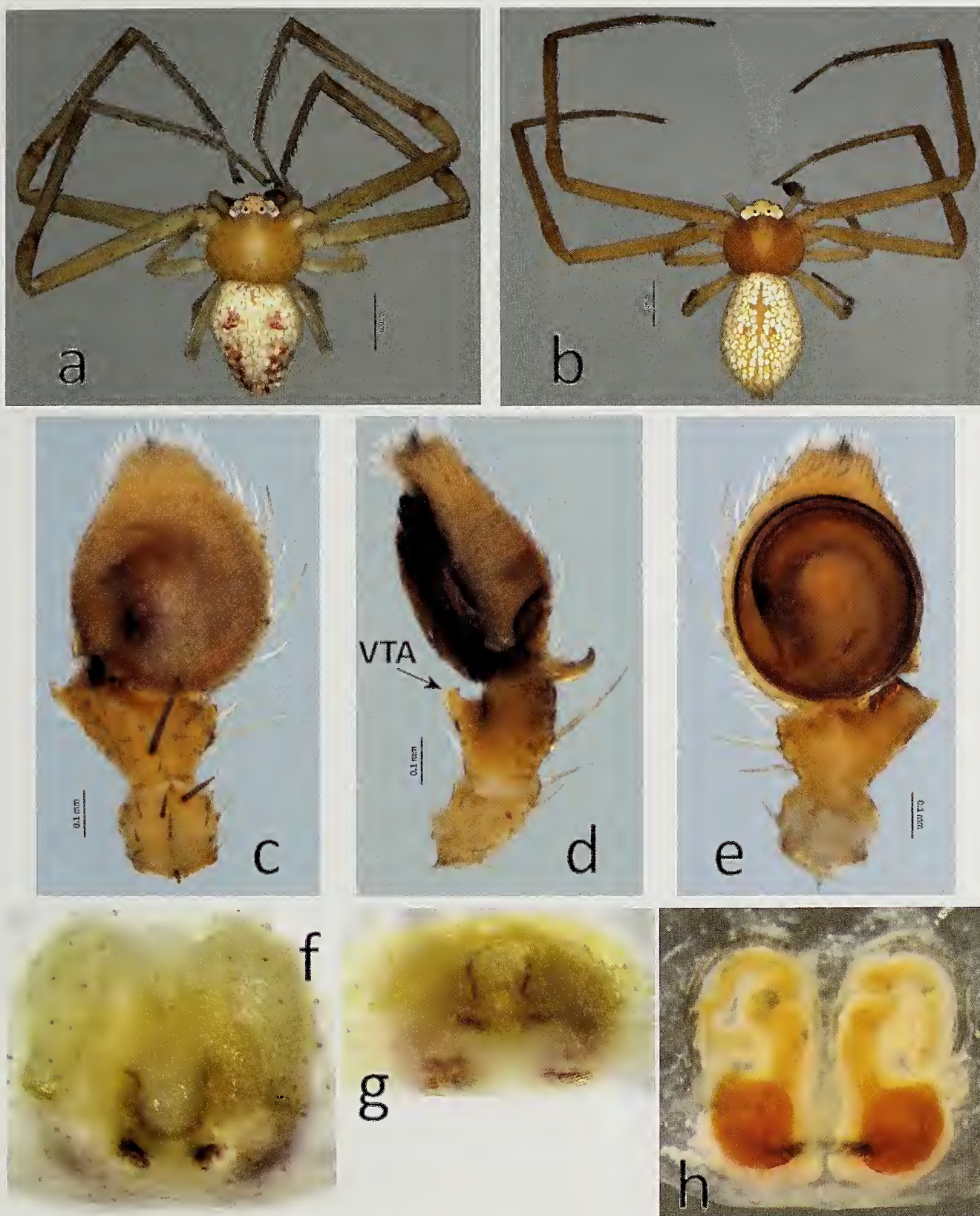


Figure 7.—*Misumessus lappi* sp. nov. from Texas. a–e, Males: a, paratype male dorsum, preserved one year; b, holotype male dorsum, preserved five years (compare to Fig. 6c, d); c, dorsal palp; d, retrolateral palp; e, ventral palp. f–h, Female: f, ventral epigyne; g, posterior epigyne cleared; h, dorsal epigyne cleared. Photo credits: f–h by Joe Lapp.



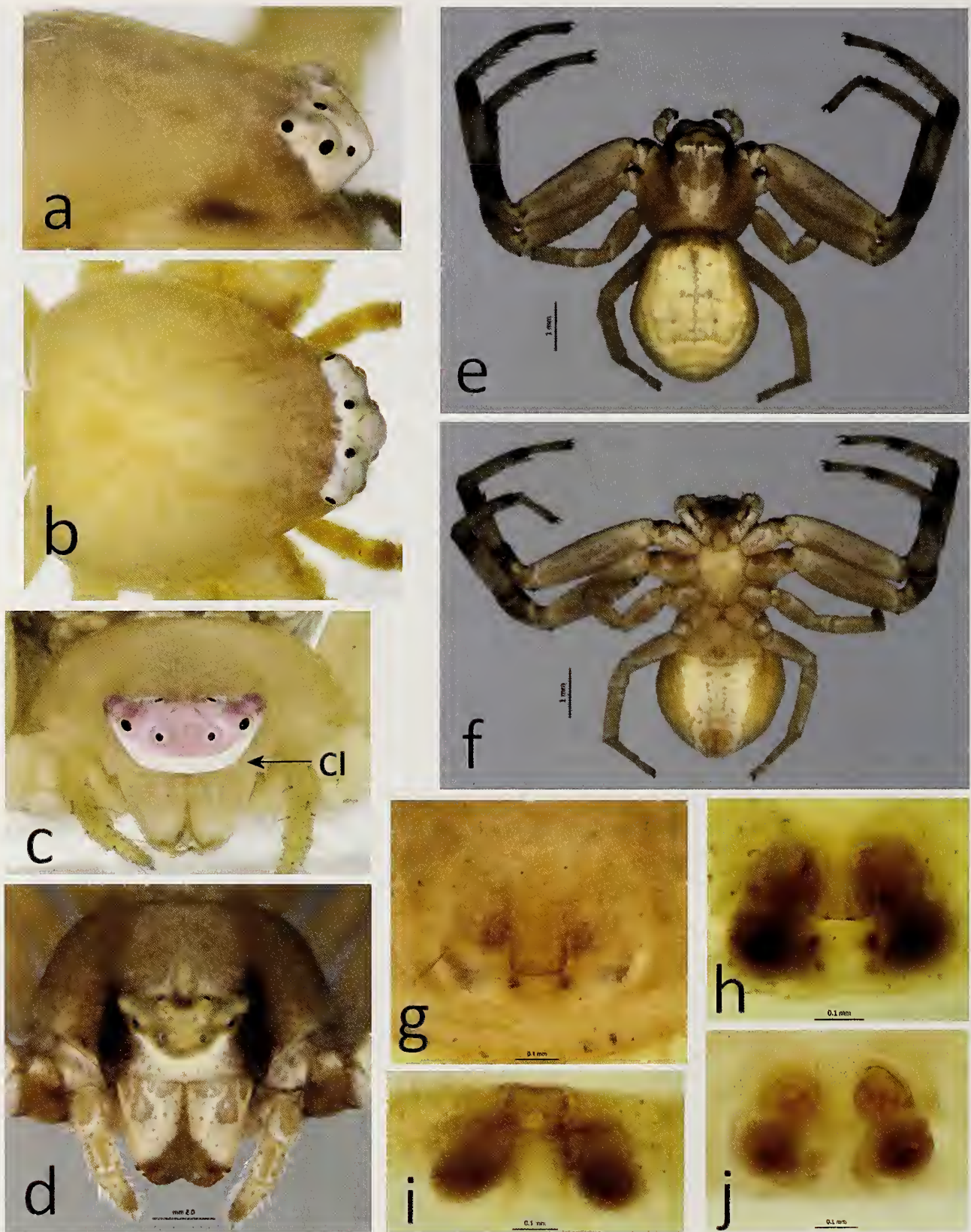


Figure 8.—*Misumessus* species. a–c, Female *M. lappi* sp. nov. from Texas: a, lateral carapace; b, dorsal carapace; c, face. d–j, Female *Misumessus quinteroi* sp. nov. from Puerto Rico: d, face; e, dorsum; f, venter; g, ventral epigyne; h, ventral epigyne cleared; i, posterior epigyne cleared; j, dorsal epigyne cleared. Photo credits: a–c by Joe Lapp.



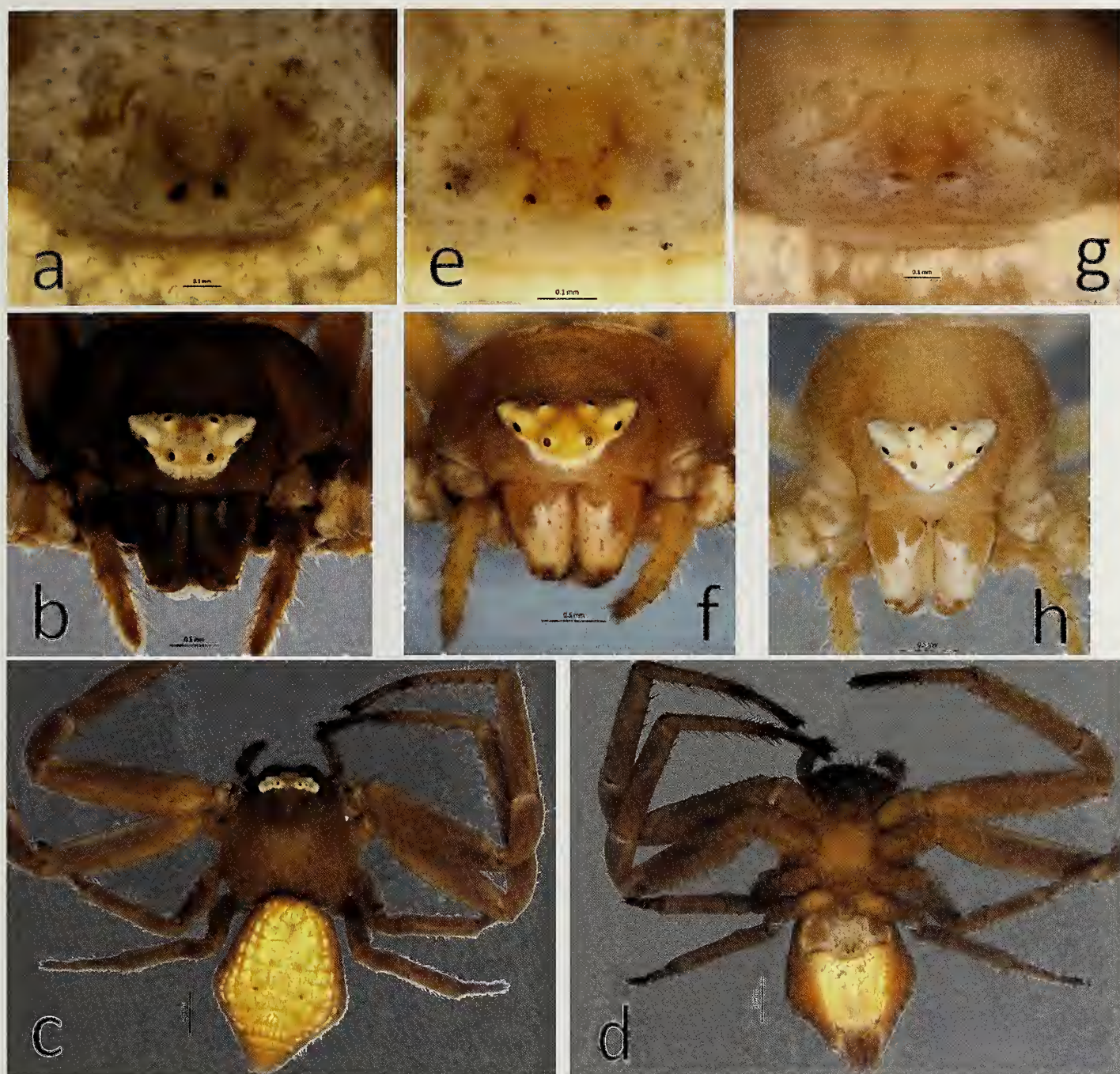


Figure 9.—*Misumessus quinteroi* sp. nov. a–d, Female from Costa Rica: a, ventral epigyne; b, face; c, dorsum; d, venter. e–f, Female from Jamaica: e, ventral epigyne; f, face. g–h, Female from Dominica: g, ventral epigyne; h, face.

(FMNH). UNITED STATES: *Alabama*: 1 ♀, Colbert Co., Wilson Dam, 34.7140°N, 87.7610°W, 1 August 1953, R. Schick (AMNH); 1 ♀, Hale Co., Moundville, 32.9906°N, 87.5834°W, 1 August 1939 (AMNH); 3 ♀, 2 penultimate ♀, Morgan Co., Decatur, 34.4954°N, 86.8811°W, 30 May 1939, A.F. Archer (AMNH); 1 ♀, Shelby Co., Oak Mt. St. Pk., 33.2601°N, 86.6702°W, July–August 1940, A.F. Archer (AMNH); 1 ♀, Tuscaloosa Co., Tuscaloosa, 33.2589°N, 87.5258°W, 22 April 2005 (AMNH). *Arkansas*: 1 ♂, 1 ♀, Bradley Co., 33.4746°N, 92.1961°W, 12 May 1964, W.H.

Whitcomb (CAS 9068465); 1 ♀, Chicot Co., 33.3088°N, 91.3136°W, soybeans, 11 July 1962, Boyer (CAS 9068448); 1 ♀, Conway Co., 35.2714°N, 92.6767°W, 5 July 1963 (CAS 9068459); 1 ♂, same data except 3 July 1964, B.A. Dumas (CAS 9068456); 1 ♂, same data except Morrilton, pitfall trap, 23 May 1964 (CAS 9068451); 2 ♀, same data except Plumerville, 35.2714°N, 92.6767°W, alfalfa, 18 June 1957, L. Moore (MCZ 72853); 1 ♀, Hempstead Co., 33.7892°N, 93.6823°W, cotton, 2 September 1960 (CAS 9068445); 1 ♂, 2 ♀, Jefferson Co., 34.2954°N, 91.9289°W, rice, 26–27 July 1963,



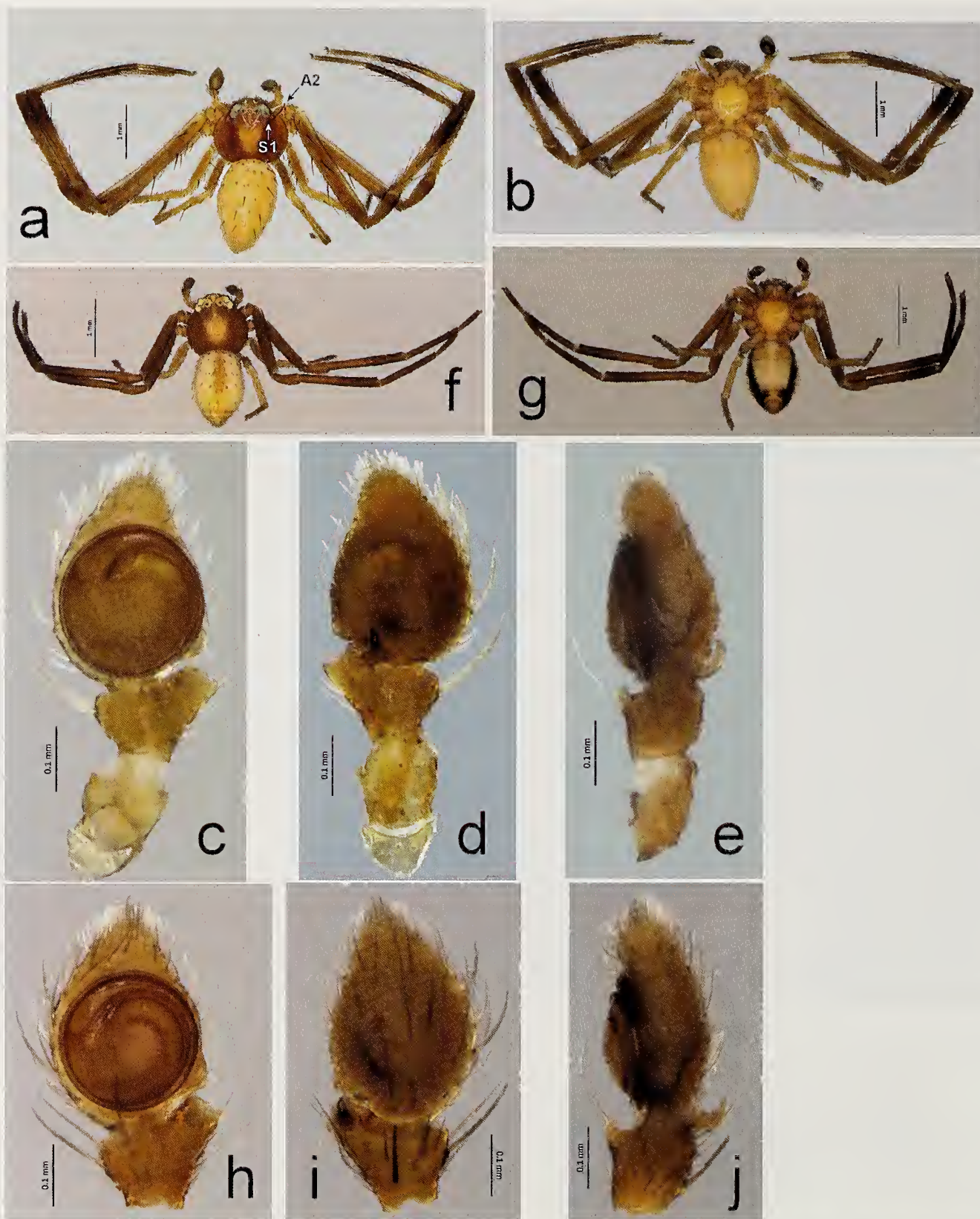


Figure 10.—*Misumessus quinteroi* sp. nov. a–e, Holotype male from Panama: a, dorsum, arrows to labeled elongate earapae spiniforms; b, venter; c, ventral palp; d, dorsal palp; e, retrolateral palp. f–j, Male from Dominica: f, dorsum; g, venter; h, ventral palp; i, dorsal palp; j, retrolateral palp.



- J. Guerra (CAS 9068446); 2 ♂, 3 ♀, same data except weeds, 25 June 1963, J. Guerra, (CAS 9068474); 1 ♀, same data except 1 July 1963, J. Guerra (CAS 9068464); 1 ♂, Mississippi Co., 35.7101°N, 90.0505°W, cotton, 18 August 1966 (CAS 9068437); 1 ♂, same data except 4 June 1966, W. Peck (CAS 9068442); 2 ♀, Monroe Co., 34.7134°N, 91.2149°W, 18 July 1963, W.H. Whitcomb (CAS 9068453); 1 ♂, 3 ♀, Randolph Co., 36.3494°N, 90.9710°W, 10 July 1963, I. Brown (CAS 9068449); 7 ♂, 1 ♀, Washington Co., Cove Creek Valley, 15 mi S Prairie Grove, Boston Mts, 35.9756°N, 94.1936°W, el. 1000', June 1957 (MCZ 72852). *Connecticut*: 1 ♂, Fairfield Co., Norwalk, 41.2272°N, 73.3775°W, 23 June 1933, Gertsch (AMNH); 1 ♀, same data except 22 October 1935, B.J. Kaston (AMNH); 1 ♀, same data except 4 July 1935, Gertsch (AMNH); 1 penultimate ♂, 1 juvenile ♀, 10 June 1933, Gertsch (AMNH); 1 ♂, Hartford Co. New Britain, 41.7936°N, 72.7305°W, 30 July 1948, B.J. Kaston, (USNM 2074581); 1 ♀, same data except 12 October 1949, B.J. Kaston (USNM 2074581); 1 penultimate ♀, Middlesex Co.: 41.4626°N, 72.5347°W, Middlefield, 30 June 1935, H.L. Johnson (AMNH); 1 ♀, same data except Middletown, 1 August 1935, H.L. Johnson (USNM 2074581); 1 ♂, New Haven Co., 41.3919°N, 72.9411°W, 19 July 1938, D.S. Riggs (USNM 2074581); 1 ♀, same data except Branford, 12 September 1935, B.J. Kaston (AMNH); 1 ♂, same data except Orange, 28 June 1935, B.J. Kaston (USNM 2074581); 1 ♀, same data except Westville, 15 April 1905, B.J. Kaston (USNM 2074581). *Delaware*: 1 ♂, New Castle Co., Hockessin, 39.6260°N, 75.6087°W, June 1988, P. Sierwald (FMNH 0000 044 881). *Florida*: 1 ♂ Alachua Co., 29.6943°N, 82.3797°W, 4 October 1934, H.K. Wallace 320 (FSCA); 1 ♂, same data except 18 April 1935, H.K. Wallace 395 (FSCA); 4 ♀, same data except Micanopy, 5 mi E, 29.6943°N, 82.3797, Bridge over River Styx in sphecid mud nest, 13 August 1963, K. Stone (FSCA); 1 ♀, same data except 14 August 1963, K. Stone (FSCA); 1 ♀, same data except 15 August 1963, K. Stone (FSCA); 5 ♂, 1 ♀, same data except Gainesville, *Albizia julibrissin* (in bloom), 26 June 1984, M. Plagens (FSCA); 2 penultimate ♀, same data except 12 June 1935, Gertsch (AMNH); 1 ♀, Citrus Co., 28.8583°N, 82.4609°W, *Salvia lyrata*, 21 April 1987, R. Dudley (FSCA); 1 ♀, Dixie Co., Old Town, 4 mi N, 29.5546°N, 83.1068°W, mesophytic understory, 23 May 1979, G.B. Edwards (FSCA); 1 ♀, same data except 5 April 1980, G.B. Edwards (FSCA); 1 ♂, Highlands Co., 27.3603°N, 81.3398°W, 22 August 1989, J. Bennett (FSCA); 9 ♂, Jefferson Co., 30.3658°N, 83.8529°W, 1 July 1968 Whitcomb (MCZ 72859); 4 ♂, 2 ♀, same data except 17 July 1968, Whitcomb (MCZ 72858); 2 ♂, Leon Co., Tall Timbers Res. Sta., 30.4645°N, 84.2918°W: wooden bridge, prey of *Trypargilum clavata*, 18 July 1974, G.B. Edwards (FSCA); 1 ♀, same data except on magnolia, 12 June 1981, G.B. Edwards (FSCA); 3 ♀, Martin Co., Port Sewall, 27.1464°N, 80.3148°W, 27 December 1938 & 8–12 February 1939 (AMNH); 1 ♀, Sarasota Co., Myakka River State Park, 27.2051°N, 82.4330°W, 6 April 1938, Gertsch (AMNH). *Georgia*: 1 ♂, 3 ♀, 1 juvenile, Fulton Co., 33.8302°N, 84.3152°W, May 1899, J.H. Emerton (AMNH); 1 juvenile, Habersham Co., 34°36'N, 83°31'W, 27 April 1943, W. Ivie (AMNH); 1 ♂, Oglethorpe Co., East of Lexington, 33°50'N, 83°03'W, 22 April 1943, W. Ivie (AMNH); 1 ♂, Rayburn Co., Rayburn Bald, 34.9656°N, 83.2999°W, 8 August 1957, (CNC); 1 ♂, Thomas Co., Bar M Ranch, S of Boston, 30.8992°N, 83.9360°W, 25 June 1978, H., L. & F. Levi (MCZ 72855); 1 ♂, same data except 25 June 1978, H., L. & F. Levi (MCZ 72857). *Iowa*: 1 ♂, Cerro Gordo Co., McIntosh Woods nr. Clear Lake, 43.0933°N, 93.2575°W, woods, 14 June 1961, H. Levi (MCZ 72848). *Illinois*: 1 ♀, Champaign Co., 40.1233°N, 88.1872°W, on wild cherry-eating caterpillars, (AMNH); 1 ♂, Cook Co., Palos Park, 41.8783°N, 87.7460°W, 30 May 1911, A.B. Wolcott (FMNH); 4 ♀, Marion Co., Centralia, 38.4586°N, 89.1679°W, mud dauber nest, N. Banks (MCZ 72481); 2 ♂, Montgomery Co., Farmersville, 39°25'N, 89°40'W, 10 June 1933, W. Ivie (AMNH); 1 ♂, Pope Co., Kaskaskia experimental forest (within Shawnee National Forest), 37.4948°N, 88.8008°W, 7 May 1968, (AMNH); 1 ♂, Will Co., New Lenox, 41.4886°N, 87.9885°W, 8 July 1933, D.C. Lowrie (FMNH). *Indiana*: 2 ♂, La Porte Co., Smith, 41.5267°N, 86.7413°W, 23 May 1936, D.C. Lowrie (FMNH); 1 ♀, same data except 41.4586°N, 87.0940°W, 21 May 1938, D.C. Lowrie (FMNH); 1 ♂, Parke Co., 39.7557°N, 87.2493°W, 19 May 1965, Lillian Ross (FMNH Z 15 735); 1 ♂, Porter Co., Dune Acres, 41.4586°N, 87.0940°W, 6 June 1936, D.C. Lowrie (FMNH). *Kansas*: 1 ♂, Anderson Co., Garnett, 38.2107°N, 95.2858°W, 10 August 1989, H. Guarisco (HGC); 1 ♂, Cherokee Co., KSU pecan experimental field, 37.1857°N, 94.8142°W, 1 August 1984, H. Guarisco (HGC 6631); 1 ♂, same data except 5 June 1986, H. Guarisco (HGC 6643); 1 ♂, same data except 4 June 1987, H. Guarisco (HGC 8459); 1 ♂, same data except 22 May 1986, H. Guarisco (HGC 6625); 2 ♂, same data except 19 June 1986, H. Guarisco (HGC 6621); 1 ♂, same data except 22 May 1986, H. Guarisco (HGC 6633); 1 ♂, same data except 11 June 1985, H. Guarisco (HGC 6629); 1 ♂, Douglas Co., Baldwin City, 38.9040°N, 95.2907°W, mud dauber nest, 19 June 1991, H. Guarisco (HGC 4767); 1 ♂, same data except Fitch Nat Hist Res., 38.9040°N, 95.2907°W, 15 July 1987, H. Guarisco (HGC 2429); 1 ♀, same data except 1 August 1989, H. Guarisco (HGC 311); 1 ♂, Riley Co., Konza Prairie, 39°05'27"N, 96°35'09"W, 12–15 June 2001, H. Guarisco (HGC 4643); 1 ♂, Webaunsee Co., Lake Webaunsee, 38.9515°N, 96.1913°W, 22 July 2015, H. Guarisco (HGC 8734); 9 ♀, Woodson Co., Toronto St Pk, 37.9030°N, 95.7010°W, 4 September 1980, H. Guarisco (HGC 8583). *Kentucky*: 1 ♂, Jefferson Co., Louisville, 38.2046°N, 85.6788°W, 18 July 1933, Gertsch (AMNH); 1 ♂, LaRue Co., Sonora, 1 mi E, 37.4945°N, 85.6742°W, 5 July 1985, H.A. Dean (TAMU); 1 ♂, Madison Co., 37.7041°N, 84.2627°W, 6 July 1985, H.A. Dean (TAMU). *Louisiana*: 1 ♀, Acadia Parish, 30°N, 92°W, 30 August 1933 (AMNH). *Maryland*: 1 ♀, Montgomery Co., Plummer's Island, 39.1168°N, 77.1587°W, 11 July 1956, K.V. Krombein (USNM 2074581). *Michigan*: 1 ♂, Barry Co., Gun Lake, 42.6223°N, 85.3158°W, 30 June 1970, N.P. (AMNH); 1 ♂, Berrien Co., Sawyer, 41.9646°N, 86.5062°W, cultivated blueberry plants, 22 July 1964, T. Burger (CAS 9068472); 1 ♀, Livingston Co., E.S. George Reserve, 42.5695°N, 83.8984°W, 7 July 1951, H.K. Wallace (AMNH); 1 ♂, Oakland Co., Royal Oak, 42.6116°N, 83.3279°W, 16 July 1936, M.H. Hatch (CAS 9068454). *Minnesota*: 1 ♂, Dodge Co., Claremont, 3 mi NE, 44.0366°N, 92.8563°W, sweeping herbs, 25 June 1966, D.T. Jennings (DMNS 23397). *Missouri*: 1 ♀, Boone Co.,



Columbia, 38.9625°N, 92.2633°W, 9 July 1966, Bayer (UTA 61585); 1 ♂, same data except 38°N, 92°W, Jun (AMNH); 1 ♂, Cole Co., Jefferson City, 38.6431°N, 92.1130°W, 21 August 1945, W.W. Dowdy (USNM 2074581); 1 ♀, Crawford Co., Merimac River, 37.9424°N, 91.3218°W, 25 August 1962, D.L. & H.E. Frizzell, B. Vogel (CAS 9068457); 1 ♀, Dent Co., Hobson, 37.6111°N, 91.5194°W, 7 July 1959, H.E. Frizzell, V. Baird (CAS 906847); 1 ♀, Franklin Co., W of Jewith Hwy, 38.4260°N, 91.0186°W, 12 August 1979, S. Parshall (FMNH 0000 073 950); 1 ♀, Jackson Co., 39.0239°N, 94.4190°W, 25 June 1975, Dondale (CNC); 1 ♂, 1 ♀, same data except Sibley, Fort Osage, 39.0239°N, 94.4190°W, sweeping herbaceous vegetation near deciduous woods, 25 June 1975, B. Cutler, D. T. Jennings (AMNH); 1 ♂, Johnson Co., Warrensburg, 38.7192°N, 93.7787°W, sweep sun low veg, 2 June 1965, D.L. Frizzell (CAS 9068406); 2 ♂, same data except sweeping upland shrubs, 27 May 1962, W. Peck (CAS 9068432); 1 ♂, same data except 1 June 1963, W. Peck (CAS 9068405); 1 ♂, same data except on web hanging from tree, 19 August 1961, W. Peck (CAS 9068455); 1 ♀, same data except 9 September 1961, W. Peck, D.L. & H.E. Frizzell (CAS 9068458); 1 ♂, Newton Co., Newtonia, 36.8905°N, 94.2853°W, open field, tall grass, 30 May 1962, W. Peck (CAS 9068467); 1 ♂, Phelps Co., Beaver Creek, 10 mi. S of Rolla, 37.8597°N, 91.7734°W, 11 June 1950, H.E. & D.L. Frizzell (CAS 9068435); 2 ♀, Rolla Co., Dry Fork Creek, 38.7629°N, 93.7361°W, 15 July 1951, H.E. & D.L. Frizzell (CAS 9068471); 2 ♀, same data except 15 July 1951, H.E. & D.L. Frizzell (CAS 9068463); 1 ♀, 1 ♂, same data except 23 June 1949, H.E. & D.L. Frizzell, E.S.L.? (CAS 9068439); 1 ♀, same data except 1 June 1951, D.L. Frizzell (CAS 9068447); 1 ♀, same data except 9 October 1950, H.E. & D.L. Frizzell (CAS 9068441); 1 ♀, same data except Rolla, 20 July 1967, D.L. Frizzell (CAS 9068469); 1 ♀, Stoddard Co., Ardeola, 36.9122°N, 89.9298°W, 22 July 1950, H.E. & D.L. Frizzell (CAS 9068466); 1 ♀, same data except Bloomfield, 9 mi. N, 22 July 1950, D.L. & H.E. Frizzell (CAS 9068444). *Mississippi*: 1 ♀, 1 juvenile, Harrison Co., Gulfport, 30.4336°N, 89.0753°W, 28 August 1933, W. Ivie (AMNH); 2 ♂, Lafayette Co., Oxford, 34.3457°N, 89.4808°W (AMNH); 2 ♂, Marion Co., Columbia, 31.1971°N, 89.8893°W, (AMNH); 1 ♂, Panola Co., 34.3549°N, 89.9762°W, 6–9 Sept 1962, H.E. & D.L. Frizzell, L. Sardis (CAS 9068468). *North Carolina*: 1 ♂, Buncombe Co., Montreat, 35.5972°N, 82.5293°W, 12 June 1953, R.D. Barnes (AMNH); 2 ♀, 1 penultimate ♀, same data except Black Mts, Beutenmuller (AMNH); 1 ♂, Durham Co., Duke Forest, 36.0362°N, 78.8792°W, 13–18 June 1933, A.M. Chickering (MCZ 72851); 1 ♀, Lincoln Co., Lincolnton, 35.4810°N, 81.2233°W, L. Cobb (USNM 2074581); 1 ♀, Macon Co., 35°06'17"N, 83°17'14"W, beating, 16 July 1998, I. Agnarsson (USNM 2074581); 1 ♀, same data except 35.0959°N, 83.3700°W, beating, 14 July 1998, I. Agnarsson (USNM 2074581); 1 ♂, same data except Wayah Bald, 10 August 1957, Maconlo (CNC); 2 ♂, 13 July 1957 (CNC); 1 ♂, Swain Co., Great Smoky Mt Natl Pk, Indian Gap, 35.4301°N, 83.4457°W, 2 July 1957, J.R. Vockeroth (CNC). *New Hampshire*: 1 ♂, Carroll Co., West Ossipee, 43.7726°N, 71.1918°W, 1 August 1936, S. Mulaik (AMNH). *New Jersey*: 4 ♀, Hunterdon Co., Lambertville, 40°22'N, 74°56'W, 26 July 1953, W. Ivie (AMNH); 3 juveniles, same data except 1 June 1953, W. Ivie (AMNH); 2 ♀, same data except 1 July 1953, W.

Ivie (AMNH); 1 ♂, Somerset Co., Bedminster, 40.5683°N, 74.6167°W, sweep misc. veg., 14 July 1991, D.A. Dean (TAMU). *New York*: 1 ♀, Essex Co., Adirondack Mountains, 44.1282°N, 73.8692°W, 31 July 1893 (USNM 2074581). *Ohio*: 1 penultimate ♀, Hamilton Co., Cincinnati, 39.1705°N, 84.5222°W, 22 June 1980, G.B. Edwards (FSCA); 1 ♂, 2 ♀, Knox Co., Gambier, 40.3820°N, 82.3815°W (AMNH). *Oklahoma*: 1 ♀, Marshall Co., Lake Texoma, Oklahoma Univ. Biological station, 33.9944°N, 96.7373°W, 1 June 1963, C.S. Lin (AMNH). *Pennsylvania*: 1 ♀, Bucks Co., NE of Jamison, nr Furlong, 40.3101°N, 75.0735°W, 1 June 1957, W. Ivie (AMNH); 4 ♂, 5 penultimate ♀, 1 juvenile, same data except Horseshoe Bend, Neshaminy Creek, 40°16'N, 75°3'W, 1 June 1954, W. Ivie (AMNH); 1 ♂, same data except E of Jamison, Neshaminy Creek, 33°16'N, 75°03'W, 8 June 1963, W. Ivie (AMNH); 2 ♂, Butler Co., Slippery Rock, 5 mi SE, 40.9168°N, 79.9103°W, 28 June 1967, B. Vogel (DMNS 2053); 1 ♀, Washington Co., 40.1368°N, 80.1875°W, 15 August 1979 (AMNH). *South Carolina*: 1 ♀, Abbeville Co., 34.2572°N, 82.4672°W, 20 November 1953, Lillian Ross (FMNH Z 15 733); 1 ♀, 1 penultimate ♀, Greenville Co., Greenville, 34.8817°N, 82.3996°W, 16 June 1980, R.S. Peigler (TAMU). *Tennessee*: 1 ♀, Blount Co., Hatcher Mountain, 35.7391°N, 83.9528°W, 4 July 1978, V. McNeilus (UTA 1701); 3 ♀, same data except Great Smoky Mountains, 35.8470°N, 83.5440°W, 8 July 1933, Gertsch (AMNH); 3 ♂, same data except Great Smoky Mt. NP, Chestnut Ridge Trail, 35.7391°N, 83.9528, 4 June 1978, V. McNeilus (UTA 1697); 1 ♂, Cumberland Co., Crossville, 2 mi N, 35.9576°N, 84.9742°W, 23 July 1978, V. McNeilus (UTA 1702); 1 ♂, Hamilton Co., Chattanooga, 35.1221°N, 85.2167°W, 28 May 1987, H.A. Dean (TAMU); 1 ♂, 3 ♀, Knox Co., Knoxville, 35.9845°N, 83.9516°W, 7 July 1933, W.J. Gertsch (USNM 2074581); 1 ♂, same data except 14 May 1975, Kronk (UTA 7399); 1 ♂, same data except North Shore Dr., 14 June 1977, V. McNeilus (UTA 1699); 7 ♀, Roane Co., Kingston, 35.9073°N, 84.5337°W, 2 July 1933, Gertsch (AMNH); 1 ♂, Sevier Co., Elkmont, 35.8517°N, 83.5720°W, 11 June 1939, Kaston (AMNH). *Texas*: 1 ♂, Brazos Co., 30.6404°N, 96.3379°W, suction trap, 2 August 1979, D.A. Dean, J. Taylor (TAMU voucher specimen #585); 1 ♀, same data except mud dauber nest, 8 October 1985, D.A. Dean (TAMU); 1 ♂, Burleson Co., Adriance Orchard, 30.4473°N, 96.5939°W, from pecan, 7 May 1992, T.Y. Li (TAMU); 1 ♀ 1 ♂, Comanche Co., 32.0789°N, 98.4708°W, fogging in pecan at night, 17 July 2001, A. Calixto, A. Knutson (TAMU); 1 ♂, Delta Co., 33.3691°N, 95.6552°W, D Vac cotton, 10 August 1983, D.A. Dean (TAMU); 1 ♂, Polk Co., 30.7790°N, 94.8875°W, 22 May 1984, J.B. Woolley (TAMU); 17 ♂, Robertson Co., 30.748°N, 96.551°W, fogging in pecan at night, 7 July 2001, A. Calixto, A. Knutson (TAMU); 1 ♂, same data except 1 June 2001, A. Calixto, A. Knutson (TAMU); 1 ♀, 1 ♂, same data except 14 August 2001, A. Calixto, A. Knutson (TAMU); 1 ♂, same data except 30°44'54.5"N, 96°33'19.1"W, cardboard bands in pecan, 9 July 2001, A. Calixto (TAMU); 1 ♂, Sabine Co., 31.3242°N, 93.8283°W, flight intercept trap, beech magnolia forest, 25 Aug–10 September 1989, R.E. Anderson, E. Morris (TAMU 930); 1 ♂, Travis Co., Austin, 30.3152°N, 97.7561°W, (AMNH); 1 ♂, same data except 21 July 1947, H.E. & D.L. Frizzell (CAS 9068433); 1 ♂, Walker Co.,



30.7590°N, 95.5445°W, Ellis Prison Unit, 18 August 1980, D.A. Dean (TAMU); 1 ♂, same data except cotton, 9 May 1978, D.A. Dean (TAMU 245); 1 ♀, same data except 5 July 1978, D.A. Dean (TAMU 495); 1 ♀, same data except 30 August 1978, D.A. Dean (TAMU 678); 1 ♀, same data except 12 June 1978, D.A. Dean (TAMU 520); 1 ♀, same data except 16 May 1978, W.L. Sterling (TAMU 306); 1 ♂, Wharton Co., 29.3056°N, 96.1737°W, D-Vac cotton, 8 July 1983, D.A. Dean (TAMU). *Virginia*: 1 ♀, Amherst Co., Geo. Washington National Forest, 37.5434°N, 79.1032°W, 21 June 1982, G.B. Edwards (FSCA); 3 ♂, 12 ♀, Arlington Co., Arlington, 38.8751°N, 77.1001°W, July 1956, K.V. Krombein (USNM 2074581); 3 ♂, 1 juvenile, Craig Co., Potts Mountain, 37.4936°N, 80.1805°W, 3 July 1946, H.K. Wallace 1212A (FSCA); 1 ♂, Fairfax Co., Falls Church, 38.8400°N, 77.2635°W (AMNH); 3 ♂, 1 juvenile, Giles Co., 37.3566°N, 80.5376°W, 22 June 1946, H.K. Wallace 1196 (FSCA); 2 ♂, same data except Mountain Lake, 3 July 1946, H.K. Wallace 1211A (FSCA); 1 ♂, Goochland Co., 37.7375°N, 77.8987°W, 6 July 1987, H.A. Dean (TAMU); 1 ♂, Hampshire Co., Capon Bridge, 39.3349°N, 78.5661°W, 9 June 1985, J. Coddington, C. Sobrevila (USNM 2074581); 1 ♀, Montgomery Co., Radford, 37.1562°N, 80.3856°W, 7 July 1934, W.J. Gertsch (USNM 2074581); 2 ♀, Page Co., Shenandoah National Park, E. of Luray, 38.6635°N, 78.3720°W, 5 July (AMNH); 3 ♂, same data except 38.4512°N, 78.5150°W, 14 June 1982, H. Goulet (CNC); 1 ♀, 1 penultimate ♀, Prince Edward Co., Hampden Sydney, 37.2593°N, 78.4300°W, 20 June 1982, G.B. Edwards (FSCA); 1 ♀, same data except Rice, 37.0277931°N, 78.289494°W, on purple *Buddleia*, 27 August 2012, M. Green (FSCA); 1 ♀, Randolph Co., Spruce Knob Lake, 38.8093°N, 80.0088°W, 17 July 1988, G.F. & J.F. Hevel (USNM 2074581); 17 ♀, Smyth Co., Marion, 36.8517°N, 81.5454°W, 6 July 1934, Gertsch (AMNH). *Washington, D.C.*: 1 ♀, 38.9072°N, 77.0369°W, 1956–1957, J. Dante (CAS 9068473). *Wisconsin*: 1 ♂, Dane Co., Madison, 43.0788°N, 89.4027°W, 17 November 1962, Baerwald (UTA 1700); 1 ♀, same data except Univ. Wisc. campus, 20 November 1967, S. Hunsaker (UTA 7703); 1 ♀, Iowa Co., 42.9933°N, 90.1429, T8N, R5E, S9S W1/4, 12 October 1995, S. Delaney (UTA 1692); 1 ♀, Kenosha Co., Kenosha, 42.5602°N, 87.9975°W, 12 June 1970, J. Litsinger (UTA 53027); 1 ♂, Walworth Co., Lake Geneva, Williams Bay, 42.6307°N, 88.5260°W, 5 July 1949, D.C. Lowrie (FMNH); 1 ♂, same data except Wychwood, 29 June 1938, D.C. Lowrie (FMNH). *West Virginia*: 1 ♂, Raleigh Co., 37.7672°N, 81.2519°W, 8 July 1987, H.A. Dean (TAMU); 1 ♂, Wayne Co., 38.2077°N, 82.4573°W, 10 June 1987, H.A. Dean (TAMU).

**Diagnosis.**—Males can be distinguished from other species of *Misumessus* by the position of the embolus base, which starts in the range 11:00–12:30 (330–15 degrees), with a median of about 12:00 (Fig. 3a). Females can be distinguished in cleared ventral view by the minute conical median coupling pocket with an outline shape of an equilateral triangle (approximately as long as wide) (Fig. 3h).

**Description.**—*Female*: BL = 5.08 (4.45–6.01), CL = 2.17 (1.76–2.44), CW = 2.25 (1.90–2.63), EGW = 1.08 (0.94–1.21). General appearance as in genus description. Typical females light green in color when alive (Fig. 2a), without any markings. Newly preserved female specimens white, but

long-preserved specimens have carapace as in male. Eye group with pigment divided by diagonal gray stripe between AME and ALE, closer to AME, that curves dorsally over AME, nearly joining medially and isolating AME; another gray line between ALE and PME connected to curved line (Fig. 3j). Epigyne with scape, variable in ventral and posterior aspect, and in length, ranging from about 2.5 x longer than wide (Fig. 3f) to about 2.5 x wider than long (Fig. 3i); the latter is more prevalent. Scape slightly converging toward its tip (where the coupling pocket is located; Fig. 3i). Copulatory ducts long and convoluted, with median coil or half loop in most medial section of wider part of duct (Fig. 3h).

*Male*: BL = 2.70 (2.56–2.96), CL = 1.16 (1.13–1.21), CW = 1.25 (1.21–1.32), EGW = 0.70 (0.65–0.75). General appearance as in genus description. Males in life typically with green carapace, green legs III and IV, green femora of legs I and II with distal reddish brown leg bands, and yellow abdomen, with variable amount of yellow brown pigment medially on dorsal abdomen. At its maximum, pigment appears as broad median stripe (Fig. 2c), that seems to define boundaries of weakly sclerotized scutum. Typically long-preserved males have yellowish brown cephalothorax, with distinctive but slightly diffuse pale mark in middle of carapace, the rest of body light yellow to amber, with yellow femora and without other markings except leg banding (Fig. 3d). Embolus base beginning near 12:00 position (range 11:00 to 12:30). Embolus completely encircles tegulum, then continues another 95–110 degrees to tip (Fig. 3a); smaller males typically toward higher end of range of embolus base placement (12:30), therefore have shorter embolus.

**Distribution.**—Eastern NA from Ontario, Canada on the north to eastern Texas and the northern two-thirds of peninsular Florida on the south, with a western border at approximately 98°W longitude, roughly equivalent to the eastern edge of the Great Plains. The distribution given by Lehtinen & Marusik (2008) as “Mexico to southern Canada” is not supported, as the only Mexican record I have seen, from Tamaulipas, is *M. quintero* sp. nov. I also have been unable to corroborate a Guatemala record as reported by the World Spider Catalog (2017), although it is possible that this species extends along the eastern coast of Mexico to eastern parts of Central America. If indeed a *Misumessus*, it is more likely that the Guatemala record represents *M. quintero* sp. nov. as well, as there are verified records of *M. quintero* sp. nov. from eastern Guatemala.

Furthermore, Gertsch (1939) noted that Pickard-Cambridge (1900) mistakenly synonymized *Misumenops pallens* (Keyserling, 1880) with *Misumena americana* (= *M. oblongus*). Combining the information from Gertsch (1939) and Pickard-Cambridge (1900), it is apparent that there were two epigynal forms, one associated with *M. americana*, and one with *M. pallens*, and the Guatemala record matched the *M. pallens* form. Gertsch did not include this record in his distribution of *M. oblongus*. Therefore the Guatemala record of *M. oblongus* is considered erroneous.

**Notes.**—Sometimes in life, the cephalothorax or the abdomen of *M. oblongus* females is white (e.g., Fig. 2b), but both body sections white together has not been seen. Female green body pigment (becoming white) and male green leg pigment (becoming yellow or white) in preserved specimens



are lost (the green pigment apparently is quickly denatured in alcohol). Gertsch (1939) stated that occasionally there were red [antero-] lateral abdominal bands, but I have only seen yellow anterolateral bands in preserved specimens; this might also be due to denatured pigment. A photo that appears to be of a live female *M. oblongus* from Ohio with a complete red anterior abdominal band was recently posted on iNaturalist, available online at <https://www.inaturalist.org/observations/7239942>

The syntypes of *Misumena oblonga* (males) and *M. americana* (females) are all from the northern central and northeastern United States, so there does not seem to be any question that they are synonymous, and the name *M. americana* is unavailable for another species. Therefore Simon's (1900) identification of *M. americana* from St. Vincent likely was erroneous, and the specimens he saw were probably one of the Antillean species.

*Misumessus dicaprio* sp. nov.

<http://zoobank.org/?lsid=urn:lsid:zoobank.org:act:DB790A80-AB2D-4424-AAC2-02E4F928D3F6>

(Fig. 4)

*Misumenops (Misumessus) oblongus* (Keyserling): Schick, 1965: 7, 108 (in part; misidentification).

**Type material.**—*Holotype male*. United States: *California*: Riverside County, Riverside, 13 June 1963, D. Miller (CAS).

**Other material examined.**—UNITED STATES: *Arizona*: 1 ♂, Cochise Co., Chiricahua Mts., South Fork Cave Creek, 31.7513°N, 109.9384°W, 13 June 1958, Alexander (AMNH); 1 ♀, Coconino Co., Grand Canyon, 35.7231°N, 111.8218°W, 24 July 1934, Lutz (AMNH); 7 ♂, same data except Sitgreaves NF, Chevelon Rd Ranger Station, T13N R13E, el. 7000', sweeping yellow blossom clover, 10 June 1969, D.T. Jennings (DMNS 24770); 1 ♀, same data except 11 June 1969, D.T. Jennings (DMNS 24752); 3 ♂, same data except 11 June 1969, D.T. Jennings, DMNS, 24753; 1 ♂, Mohave Co., Yavapai Mt. Park, 35.2787°N, 114.1155°W, el. 5,000', 20 June 1968, L.D. Mikelson (CAS 9068462); Yavapai Co., Prescott, 3 mi. E at Granite Dells, 34.6279°N, 112.3162°W, el. 5,280', 22 June 1968, 1 ♀ L.D. Mikelson (CAS 9068461). *California*: 1 ♀, Fresno Co., Fresno, 8 mi W, 36.7391°N, 119.7007°W, 23 August 1956, R.O. Schuster (AMNH); 1 ♂, Inyo Co., Bishop, 36.5847°N, 117.5806°W, 26 June 1941, W.M. Pearce (AMNH 1012); 2 ♂, 4 ♀, same data except Silver Canyon, 27 June 1941, W.M. Pearce (AMNH 1018); 3 ♂, 2 ♀, Kern Co., Road's End, Kern River, 35.3523°N, 118.6461°W, 3 July 1956, V. Roth, W. Gertsch (AMNH); 1 ♀, Los Angeles Co., Coldbrook Campground, San Gabriel Mts., 33.8004°N, 118.2793°W, riparian woodland, reared, 1962–1963, R.X. Schick 250 (CAS 9053576); 1 ♂, same data except 19 June 1963, R.X. Schick 250 (CAS 9053613); 1 ♀, same data except Coldbrook Campground, 2 mi. N on State Rd 39, San Gabriel Mts., chaparral, reared, 1962–1963, R.X. Schick 246 (CAS 9053630); 1 ♀, same data except San Gabriel Canyon, 14 April–10 June 1958, J.H. Pumphrey (AMNH); 1 ♀, same data except Sunland, 10 August 1951, T. Tice (AMNH); 1 ♀, Mendocino Co., Hopland, 39.3267°N, 123.4891°W, 23 July 1953, W. J. & J. W. Gertsch, AMNH; 8 ♂, 1 ♀, Mono Co., Benton Station, 38.0278°N, 119.1236°W, 10 July 1941, W.M.

Pearce (AMNH 855); 1 juvenile, Monterey Co., Greenfield, 4 mi. W at junction of Greenfield Arroyo Seco and Arroyo Seco Roads, 36.4505°N, 121.4724°W, scrub, reared, 1963–1964, R. X. Schick 307 (CAS 9053540); 1 ♂, same data except Hastings Natural History Res., 36°22'N, 121°33'W, 6 July 1940, J.M. Linsdale (CAS 9053508); 2 ♀, Riverside Co., San Jacinto, 33.7955°N, 116.9617°W, el. 4,600', 1 July 1958, C.P. Alexander (AMNH); 1 ♂, same data except San Jacinto Mts., Herkey Creek, 33.7409°N, 116.2024°W, 20 June 1939, E.S. Ross (CAS 9053545); 4 ♂, 3 ♀, same data except Herkey Creek Camp, 12–23 June 1959, R. Schick, D. Verity (AMNH 117); 3 ♀, San Diego Co., Cleveland Nat. Forest, nr Henshaw Res., 32.9300°N, 116.9509°W, 30 July 1956, V. Roth, W. Gertsch, AMNH; 1 ♀, same data except 5 mi W Lake Henshaw, 15 July 1958, W. J. & J. W. Gertsch (AMNH); 1 ♀, same data except Lakeview District, 20 July 1948 (AMNH 1753); 3 ♀, same data except Pine Valley, 10 July 1953, W. J. & J. W. Gertsch (AMNH); 1 ♂, same data except Santa Ysabel, 1 August 1947, W.M. Pearce (AMNH 1646); 1 ♀, Yolo Co., Davis, 38.6953°N, 121.9051°W, trap in carrot plots, 10 July 1957, E. C. Garlson (AMNH). *Colorado*: 2 ♂, 2 ♀, Delta Co., Cedaredge, 38°53'03"N, 107°55'43"W, el. 6,200', beat sheet *Rhus trilobata*, 3 July 2001, F. Fraser (DMNS 5750); 1 ♂, 1 ♀, Mesa Co., Grand Junction, 39°02'12"N, 108°37'56"W, el. 4,585', beat sheet flowers, 8 August 2001, L. Seidman (DMNS 5152); 1 ♀, Montezuma Co., Mesa Verde Natl. Mon., Mancos River, 37.4169°N, 108.5914°W, 19 July 2001, K. Uziel (DMNS, 6466). *New Mexico*: 1 ♂, Bernalillo Co., Sandia Mountains, nr Albuquerque, 35.0723°N, 106.6064°W, 14 July 1982, C.W. Agnew (TAMU); 1 ♀, Doña Ana Co., Aguirre Springs, 32.4936°N, 106.7252°W, beating manzanita, 17 July 1991, B. Cutler (DMNS 31498); 1 ♂, San Juan Co., Fruitland, 36.7099°N, 108.1336°W, sweeping alfalfa, 23 July 1969, D.C. Heninger (DMNS 23704); 1 ♂, Socorro Co., Magdalena Mts., Cibola NF, Water Canyon Campground, W of Socorro, 34.2041°N, 106.9795°W, el. 6,800', sweeping *Acer negundo*, 25 October 1964, D.T. Jennings (DMNS 23969); 1 ♀, Valencia Co., Manzano Mts., Trigo Cañon, J.F. Kennedy Campground, 34.7200°N, 106.7356°W, beating *Quercus grisea* foliage, 12 September 1975, D.T. Jennings, M.E. Toliver (DMNS 24427). *Texas*: 3 ♂, Presidio Co., Candelario, 29.9529°N, 104.2911°W, on willow, 27 April 2004, A. Knutson, M. Muegge (TAMU 102); 2 ♂, same data except A. Knutson, M. Muegge (TAMU 101.3); 1 ♂, same data except A. Knutson, M. Muegge (TAMU 102.1). *Utah*: 1 ♀, San Juan Co., Bluff, 37.6468°N, 109.7514°W, 5 September 1937, G.F. Knowlton (AMNH); 1 ♂, Washington Co., Hurricane, 4 mi. E on State Hwy 15, 37.2781°N, 113.4208°W, scrub, reared, 1964–1965, R.X. Schick 406 (CAS 9068440); 1 ♂, same data except Zion National Park, scrub, reared, 1964–1965, R.X. Schick 405 (CAS 9068452); 1 ♀, same data except Interstate 15, 6 mi. W Santa Clara, 1964–1965, R.X. Schick 407 (CAS 9068434).

**Etymology.**—This species is named in honor of Leonardo DiCaprio, for his efforts to raise awareness about global warming.

**Diagnosis.**—Males can be distinguished from other species of *Misumessus* by the position of the embolus base, which starts in the range 1:00–2:30 (30–75 degrees), with a median of about 2:00 (Fig. 4b). This species is similar to *M. oblongus*



except for the embolus base, which begins farther to the retrolateral side and has less separation from the embolus tip. This species is also similar to *M. blackwalli* sp. nov. in the position of the embolus base, but lacks carapace tubercles, and the embolus is a little longer. Females can be distinguished by having a coupling pocket that is about as wide as or slightly wider than long, proportionately similar to *M. oblongus*, but much smaller in absolute size (about one quarter total volume of coupling pocket of *M. oblongus*) (Fig. 4g).

**Description.**—*Females*: BL = 5.33 (4.03–6.98), CL = 1.91 (1.69–2.17), CW = 2.01 (1.82–2.32), EGW = 1.04 (0.97–1.12). General appearance as in genus description. In life, females entirely pale green, or abdomen silvery white (Schick 1965). Carapace in preserved specimens brownish with large pale median trapezoidal patch narrowing posteriorly (Fig. 4e). Oblique lines on face between AMEs and ALEs either absent or present as nearly straight lines that converge at the posterior edge of eye group pigment, and may have another line between ALE and oblique line (not reaching AME lens); also a curved line between ALE and PME each side as in *M. oblongus* (Fig. 4f). Some populations have ventral extension of white eye group pigment, but less than occurs in *M. lappi* sp. nov. (Fig. 4f). Scape usually about as wide as long or wider than long, parallel-sided or convex laterally with widest point about mid-length, and posterior end truncate or broadly rounded (Fig. 4i). Copulatory ducts long and convoluted, lacking median coil or half loop in most medial section of wider part of duct; transition to wider part of duct anterior to widest medial section (Figs. 4g, h).

*Males*: BL = H2.86 (2.69–3.05), CL = H1.22 (1.06–1.30), CW = H1.30 (1.21–1.35), EGW = H0.75 (0.66–0.81). General appearance as in genus description. In life, males have orange-red carapace with green femora, and light green abdomen with white anterolateral bands (Schick 1965). Preserved specimens with carapace as in female; median area of dorsal abdomen pale, but white lateral bands of abdomen visible (Fig. 4a). Embolus base origin in range 1:00–2:30, median 2:00; embolus with complete revolution around tegulum, and additional 60–90 degrees from beginning of embolus base to embolus tip (Fig. 4b).

**Distribution.**—California, Utah, and western Colorado from the west side of the Rocky Mountains, south and east through Arizona and New Mexico to western Texas, and probably northwest Mexico, as there are several records just on the United States side of the border from Texas to California.

**Notes.**—The clypeal face pigment appears as a transverse elongate narrow extension of the white pigment extending from the ventral edge of the white eye group pigment (Fig. 4f). This extra pigment extends ventrally little more than half the height of the clypeus, although this is variable. Specimens from the northern part of the range generally lack this extra white pigment, and there are mixed populations with or without extra pigment in northern Arizona. There are also intermediate specimens with some irregular white pigment in the area where a fully-developed extension would be. Schick's (1965) comments would imply that males have a more darkly pigmented carapace than some other species.

It is somewhat surprising that Schick (1965) did not recognize the California populations of this species as

undescribed, but likely this was due to the embolus base position being nearly a continuation of the position variability that occurs in *M. oblongus*, and the difficulty in diagnosing differences in females.

*Misumessus tamiami* sp. nov.

<http://zoobank.org/?lsid=urn:lsid:zoobank>.

org:act:959C9957-3BF6-4A37-AA52-B6243409DF40

(Fig. 5)

**Type material.**—*Holotype male*. United States: Florida: Sarasota Co., North Port, 27.2051°N, 82.4330°W, on *Spondias mombin*, 25 April 1989, K. Jenkins (FSCA).

**Other material examined.**—UNITED STATES: Florida: 1 ♂, Broward Co., 26.1422°N, 80.2761°W, on a citrus plant, 25 June 1976, P. Karayeanes (FSCA); 1 ♀, same data except on *Citrus sinensis*, 15 July 1980, C. Culbreth (FSCA); 1 ♀, Miami-Dade Co., 25.6480°N, 80.4312°W, on *Cordia sebestena*, 2 April 1984, P. Perum (FSCA); 1 ♀, same data except on *Bucida bucerus*, 6 May 2010, O. Garcia (FSCA); 1 ♀, same data except on hibiscus, 26 September 2006, M. Francois (FSCA); 1 ♀, 1 juvenile, same data except on cypress and roadside weeds, 22 June 1964, K. Stone (FSCA); 1 ♀, same data except along trail in lush hammock, 21 June 1964, K. Stone (FSCA); 1 ♀, same data except on *Quercus* sp., 11 April 2011, M. Hernandez (FSCA); 1 ♀, same data except on *Nerium oleander*, 10 April 2008, M. Hernandez, FSCA; 1 ♀, same data except on *Persea americana*, 26 October 2009 (FSCA); 1 ♀, 3 juveniles, same data except roadside canal banks, heavy cutgrass and ragweed growth, 25 June 1964, K. Stone (FSCA); 1 ♀, same data except 28 December 1940, A. F. Archer (AMNH); 3 ♀, Palm Beach Co., 26.5879°N, 80.2843°W, Royal Palm Park, 5–8 December 1938, Watson, Sanford (AMNH); 1 ♀, Saint Lucie Co., 27.3816°N, 80.3923°W, on *Eupatorium capillifolium*, 18 October 1982, K. Hibbard (FSCA); 1 ♀, same data except on *Persea americana*, 8 September 1982, K. Hibbard (FSCA).

**Etymology.**—A noun in apposition that is an allusion to the southern peninsular range of this species in south Florida, including along the Tamiami Trail.

**Diagnosis.**—Males can be distinguished from other species of *Misumessus* by the position of the embolus base, which starts in the range 3:30–4:30 (105–135 degrees) (Fig. 5b). Females can be distinguished by the very wide triangular coupling pocket, which is about twice as wide as long (Fig. 5e).

**Description.**—*Female*: BL = 5.88 (5.25–7.34), CL = 2.27 (2.12–2.45), CW = 2.39 (2.19–2.53), EGW = 1.08 (1.03–1.12). General appearance as in genus description. Living females apparently light greenish yellow. Preserved specimens with brownish white cephalothorax with nearly square pale mark in middle of carapace (Fig. 5d). Face with oblique gray line lacking, rather AME and ALE connected by narrow, roughly horizontal line from dorsal side of AME to ventral side of ALE (Fig. 5i). There also may be broad gray band between AMEs (Fig. 5i). Epigynal scape short, at least 2 x wider than long, with very wide triangular coupling pocket, about twice as wide as long (Fig. 5e). Posterior end of scape equal to or slightly wider than attachment point. Copulatory ducts long, sinuate section narrow in anterior half, wider part with three tight coils just prior to entering spermathecae (Fig. 5g).



**Male:** BL = H2.30 (2.18–2.30), CL = H0.99 (0.97–0.99), CW = 1.12 (1.12–1.15), EGW = 0.67 (0.63–0.67). General appearance as in genus description. Carapace color in preserved specimens as in female; abdomen with pale median area surrounded by white pigment (Fig. 5a). Distal segments of palps and legs III and IV with gray pigment. Embolus base in range 3:30–4:30 (105–135 degrees), mean 4:00 (two males); embolus with two complete revolutions around tegulum and a bit more (about 30 degrees) to tip (Fig. 5b). First revolution consists of embolus base plus an extended transitional section that is slightly thicker than filamentous part that completes a little more than another revolution.

**Distribution.**—Southern peninsular Florida from Sarasota County to St. Lucie County and southward, but not yet recorded from the Florida Keys. Possibly absent from the central ridge, where *M. oblongus* occurs at least as far south as Highlands County, so this may be a species that only occurs in southern coastal and Everglades habitats.

**Notes.**—For color of live female, see BugGuide image # 873506 of a presumed female of this species from Miami-Dade County, Florida; the image color is accurate per the photographer (Seth Ausubel, pers. comm. 2016).

*Misumessus lappi* sp. nov.

<http://zoobank.org/?lsid=urn:lsid:zoobank.org:act:C7BFA4EE-29BA-4BCB-9B47-0A734A312CD2>

(Figs. 6a–f, 7, 8a–c)

**Type material.**—*Holotype male*. UNITED STATES: *Texas*: Travis Co., Austin, Zilker Nature Preserve, on *Malvaviscus arboreus* var. *drummondii*, 2 July 2011, J. T. Lapp, collected as penultimate, matured 26 July 2011, BugGuide photo # 605882 of adult by J. T. Lapp (FSCA).

**Paratypes.** United States: *Texas*: 2 ♂, 1 ♀, Travis Co., Austin, 6841 Raccoon Run, shaken from mature live oak, 9 July 2015, J. T. Lapp, collected as penultimates, all matured by 23 July 2015 (FSCA); 1 ♀, Hays Co., Wimberley, EmilyAnn Theatre and Gardens, from Ashe juniper, 13 May 2011, J. T. Lapp, collected as subadult and reared, BugGuide photo # 605893 of adult by J. T. Lapp (FSCA).

**Other material examined.**—UNITED STATES: *Colorado*: 2 ♂, 1 ♀, El Paso Co., 38°43'22"N, 104°49'36"W, el. 6190', sweep in shortgrass meadow, 27 July 2001, P. E. Cushing (DMNS 5149). *Oklahoma*: 1 ♂, Comanche Co., Fort Sill, West Range, rocky outcrop N. of Man Dam Pond, 34°43'28"N, 98°33'50"W, el. 1560', under rocks, 10 July 2004, P. E. Cushing (DMNS 7093); 1 ♀, Payne Co., Stillwater, 36.1094°N, 96.9690°W, Summer 1931, R.W. Macy (AMNH). *Texas*: 1 ♂, Collingsworth Co., Salt Fork of Red River, N. of Wellington, 34.8559°N, 100.1778°W, 6 July 1939, L.I. Davis (AMNH); 2 ♂, Comanche Co., 32.0789°N, 98.4708°W, fogging in pecan at night, 21 August 2001, A. Calixto, A. Knutson (TAMU); 1 ♂, same data except Comanche, 15 mi NE, 31.9692°N, 98.5313°W, 14 July 1936, Davis (AMNH); 4 ♂, 5 penultimate ♀, 3 juveniles, Dallas Co., Dallas, 32.8972°N, 96.7369°W, 17 July 1936, L.I. Davis (AMNH); 1 ♀, Erath Co., 32.2308°N, 98.2018°W, 12 August 1982, C.W. Agnew (TAMU); 1 ♀, same data except peanuts, 26 August 1981, C.W. Agnew (TAMU 582); 1 ♂, same data except sweeping woods, 11 August 1983, C.W. Agnew (TAMU); 4 ♂, 2 penultimate ♀, same data except mud dauber nest, 30 July

1983, C.W. Agnew (TAMU); 1 ♂, same data except suction trap, 28 July 1983, C.W. Agnew (TAMU); 1 ♂, same data except 7 July 1982, C.W. Agnew (UTA 7704); 1 ♂, Frio Co., 28.9141°N, 99.0511°W, D-Vac cotton, 23 June 1983, D.A. Dean (TAMU); 1 ♂, Hill Co., 31.9768°N, 97.0875°W, D-Vac cotton, 9 August 1983, D.A. Dean, TAMU; 1 ♂, Johnson Co., Alvarado, 32°N, 97°W, 2 September 1933, W. Ivie (AMNH); 1 ♂, Llano Co., 30.7410°N, 98.5398°W, 1 August 1935, L.I. Davis (AMNH); 1 ♂, same data except 10–12 July 1936, L.I. Davis (AMNH); 1 ♂, Robertson Co., 30.748°N, 96.551°W, fogging in pecan at night, 19 September 2001, A. Calixto, A. Knutson (TAMU); 4 ♂, Travis Co., 30°25'58"N, 97°52'01"W, beating trees, 23 July 1994, Dunlap, Quinn, Seale, Woolley (UTA 33733); 10 ♂, same data except 13–14 July 1994, Cate, Dunlap, Quinn, Wharton (TAMU); 13 ♂, same data except 30°27'43"N, 97°52'19"W, 17 July 1993, (TAMU); 1 ♂, same data except Austin, 30.3152°N, 97.7561°W, 7 July 1947, H.E. Frizzell (CAS 9068438); 2 ♂, same data except 30°27'43"N, 97°52'19"W, Long Hollow Creek, 2 August 1993 (TAMU).

**Etymology.**—This species is named in honor of Joseph T. Lapp of Austin, Texas, who first recognized specimens he collected as a new species, and who provided various types of logistical assistance as well as many of the images used in this revision.

**Diagnosis.**—Males can be distinguished from other species of *Misumessus* by the position of the embolus base, which starts in the range 7:30–8:30 (225–255 degrees) (Fig. 7e), and in life with paired spots on the abdomen (Figs. 6c–f). Females can be distinguished by the presence of a coupling pocket that is twice as long as wide (Fig. 7h). Both sexes also with distinctive anterior projection in front of AMEs, and AMEs smaller than posterior eyes (Figs. 8a, b).

**Description.**—*Female*: BL = 6.76 (6.23–7.86), CL = 2.68 (2.19–2.97), CW = 2.59 (2.28–2.79), EGW = 1.21 (1.05–1.30). General appearance as in genus description. Living females white with light green abdomen that has yellow anterolateral bands (Fig. 6b). Preserved females off white with white and/or pink pigment in eye group (Figs. 8a–c). Face with shallow broad anterior projection in front of AMEs, clypeus slightly receding posterior to projection in lateral view (Fig. 8a). AMEs smaller than posterior eyes (Fig. 8a), unique for genus, seemingly correlated with anterior face projection. All eyes, projection, and clypeus below eyes to carapace margin encased in white and/or pink pigment. Eye group with diagonal stripes between AMEs and ALEs extending in a straight line. Scape slightly longer than wide, lobe-like, and slightly convex in all aspects laterally and posteriorly from ventral view (Fig. 7f). Coupling pocket narrow and about twice as long as wide (Fig. 7h). Copulatory ducts with two tight coils or a half loop in anterior part of broader section connecting to spermathecae; first bend in wider part of duct absent, instead duct transition is from a more medial position (Fig. 8j).

**Male:** BL = H3.48 (3.29–4.15), CL = H1.63 (1.61–1.77), CW = H1.69 (1.61–1.75), EGW = H0.89 (0.83–0.90). General appearance as in genus description. In most living specimens, the carapace is off white in color, and may have a slight reddish tint. Preserved specimens have light brown cephalothorax with pale quadrangular median spot that has short anterior and posterior median extensions. Dorsal abdomen in



living and freshly preserved specimens with double row of paired red spots submedially (Fig. 7a); long preserved specimens lacking spots or with pale remnants of spots present, otherwise abdomen mostly a white mosaic of guanine deposits (Fig. 7b). Embolus base origin in range 7:30–8:30 (225–255 degrees), median at 8:00. Embolus completely encircles tegulum from its point of origin, then about an additional 210–270 degrees (Fig. 7e).

**Distribution.**—Central Texas from the eastern edge of the Edwards Plateau, northwest to eastern Colorado, on the east side of the Rocky Mountains.

**Notes.**—Specimens seem to be restricted to trees or to shrubs and other understory plants under trees. Some reared females had white abdomens, but wild caught females and subadult females had a mostly or entirely green abdomen (J. T. Lapp, pers. comm. 2016). Both sexes are variable in color. Females are mostly white, but the abdominal dorsum may be white with green anterolateral bands, pale green with yellow anterolateral bands (Fig. 6b), or simply pale green (Fig. 6a). Possibly the version with yellow bands is the normal color, as penultimate males also are this color (see below). Males have two submedial rows of variably red spots on the abdomen, with the dorsum otherwise off white, although some have the area between the spots red, and one specimen had the abdomen dark green but with darker abdominal spots still visible, and with paler olive green anterolateral abdominal bands, carapace, femora, and hind legs (Figs. 6c–f).

The holotype specimen collected in 2011 no longer has visible spots (see BugGuide photo referenced above that shows these were present at time of maturation, also compare Figs. 6c, d to Fig. 7b). Other specimens collected at earlier dates all lack spots or have only faint pale pigment spots on an otherwise silvery-white dorsum, so it appears that these markings do not persist in alcohol. Also, photos of the holotype male as a penultimate (e.g., BugGuide photo # 605890) show that it lacks spots and has an abdominal color very much like a presumed typical adult female (green with yellow anterolateral bands). Therefore the dark spots only occur in the living and recently preserved adult males.

*Misumessus quinteroi* sp. nov.

<http://zoobank.org/?lsid=urn:lsid:zoobank.org:act:AE28A00D-FEAB-4A57-BC7E-DD1E94CDC9F5>

(Figs. 8d–j, 9, 10)

**Type material.**—*Holotype male*. PANAMA: *Chiriqui*: Puerto Armueñas, 13 July 1981, G. B. Edwards (FSCA).

**Paratypes.** PANAMA: *Chiriqui*: 2 ♂, same data as holotype (FSCA). *Bocas del Toro*: 1 ♀ (allotype), Changuinola, 1 August 1981, G. B. Edwards (FSCA).

**Other material examined.**—COSTA RICA: *Cartago*: 1 ♀, Cartago, 9.8638°N, 83.9162°W, 1400–1500 m, 9 August 1975, N.L.H. Krauss (AMNH). *Limón*: 1 ♀, Talamanca Canton of Limón, Cahuita, 9.7348°N, 82.8452°W, 4 August 1981, G.B. Edwards (FSCA); 1 ♂, same data except Sixaola, 4 August 1981 (FSCA). *Puntarenas*: 1 ♀, Golfito, 9.9845°N, 84.8300°W, el. 400 m, 26 July 1981, G.B. Edwards (FSCA). CUBA: *Pinar del Rio*: 1 ♂, Soledad (a barrio in Consolación), 22.4225°N, 83.8490°W, 1–11 August 1934, P.F. Darlington (MCZ 71306). DOMINICA: 1 ♂, Central Reserve, 15.2445°N, 61.2735°W: general sweep, 28 May 2003, L. Bishop (FSCA); 1 ♀, same

data except Freshwater Lake, 2 June 2003, J. Mutti (FSCA); 2 ♀, 1 juvenile ♀, same data except Portsmouth, 15.5562°N, 61.4581°W, el. 0–100 m, July 1979, N.L.H. Krauss (AMNH, in 3 vials); 1 ♀, same data except Tarrou Cliff, beach seagrasses, 30 May 2003, Bishop et al. (FSCA). GRENADA: 1 ♀, Grenville, 12.1243°N, 61.6239°W, 13 September 1967, N.L.H. Krauss (AMNH). GUATEMALA: *Petén*: 1 ♀, Santa Elena, 16.9181°N, 89.8926°W, el. 120–160 m, August 1976, N.L.H. Krauss (AMNH). *Tikal*: 1 ♀, El Petén, 17.2249°N, 89.6110°W, 23–24 September 1959, O. & I. Degener (AMNH). JAMAICA: *Manchester*: 1 ♀, Grove Place, 18.0322°N, 77.5084°W, 15 July 1960, Vauries (AMNH). *St. Ann Parish*: 1 ♀, Discovery Bay, 18.4582°N, 77.3985°W, 20–21 March 1955, A.M. Nadler (AMNH). MEXICO: *Tamaulipas*: 1 ♂, 1 ♀, Tempoal, 1 mi. S, 24.3185°N, 98.8496°W, tropical forest, 18 July 1965, R.X. Schick, D.A. Schroeder (CAS 9068443). MONTSERRAT: 1 ♀, Plymouth, 16.7065°N, 62.2157°W, el. 100 m, August 1971, N.L.H. Krauss (AMNH); 1 ♀, same data except, 0–200 m, July 1972, N.L.H. Krauss (AMNH). PANAMA: *Canal Zone*: 1 ♀, Madden Dam area, 9.2318°N, 79.5772°W, Jun–July 1960, Lundy (AMNH); 1 ♀, same data except Balboa, 8.9614°N, 79.5632°W, May–June 1960, Lundy (AMNH). PUERTO RICO: 1 ♀, Isla Caja de Muertos, 17.8951°N, 66.5179°W, 24 June 1959, Medina, Martorell (AMNH). ST. VINCENT (W.I.): 1 ♀, Kingstown, 13.1600°N, 61.2248°W, October 1967, N.L.H. Krauss (AMNH); 1 ♀, same data except 1 September 1967, N.L.H. Krauss (AMNH). TRINIDAD & TOBAGO: *Trinidad*: 1 ♂, 1 ♀, 2 juvenile, Tunapuna Piarco, Piarco, 10.6027°N, 61.3327°W, 23 February 1959, A.M. Nadler (AMNH).

**Etymology.**—This species is named in honor of Diomedes Quintero, Panamanian arachnologist, for his cooperation with ongoing work on Panamanian spiders.

**Diagnosis.**—Males can be distinguished from other species of *Misumessus* by the position of the embolus base, which starts in the range 9:00–10:30 (270–315 degrees) (Figs. 10c, h). Females can be distinguished by the presence of a coupling pocket that is narrow and about 25% longer than wide, between that of *M. dicaprio* (about as long as wide), and *M. lappi* (about twice as long as wide) (Fig. 8h). The epigynal scape of *M. quinteroi* reaches the greatest separation from the abdomen subdistally. On the face, a horizontal dark line is present between each ALE–AME pair similar to *M. tamiami*, along with a complex branched pale marking on the anterior face of the chelicerae (Figs. 8d, 9b, f, h). Extra face pigment on the clypeus is similar to some specimens of *M. dicaprio*. Tibiae I and II with only 2–3 pairs of ventral macrosetae, other species with 4–5 pairs.

**Description.**—*Female*: BL = A4.85 (4.85–7.31), CL = A2.17 (2.17–2.39), CW = A2.18 (2.18–2.56), EGW = A1.03 (1.03–1.12). General appearance as in genus description. Preserved specimens with cephalothorax brownish white to medium brown (Figs. 8d, e, 9b, c, f, h), pale quadrangular patch in middle of carapace (Fig. 9c). Chelicerae with pale strongly angulate patches (Figs. 8d, 9b, f, h). Usually with extra face pigment below eyes on clypeus (Figs. 8d, 9b, f, h). Face has strongly curved gray or brown lines nearly isolating all individual eyes except AME, including horizontal lines between each set of ALE and AME connected by curved line below AME, and sometimes dark pigment between the AMEs



(Fig. 9b), but also with a broad curved line between ALE and PME that goes around most of the ALE (Fig. 8d). Eye group pigment white or yellow. Abdomen mostly white to dark yellow dorsally (Figs. 8e, 9c). Abdominal venter broadly white to yellow medially but often with narrow median area defined by double row of pigmented small spots, and area between spots may be filled in with gray pigment, creating a narrow median stripe (Fig. 8f); larger median pale area usually bordered by pale to dark yellowish brown laterally (Figs. 8f, 9d). Ventral tibiae I and II with 2–3 pairs of macrosetae. Epigynal scape unique in reaching greatest separation from body subdistally; posterior end of scape curves slightly back toward body. Widened section of copulatory duet mostly anteromedial to spermatheca with single coil about midway on widest medial part leading directly into spermatheca.

**Male:** BL = H2.93 (1.93–2.93), CL = H1.25 (0.93–1.29), CW = H1.38 (0.96–1.38), EGW = H0.71 (0.66–0.71). General appearance as in genus description. Preserved males similar to females in color variability. Extraordinarily long spiniforms on legs, abdomen, and two long pairs (S1, A2) near the eye group (Fig. 10a). Proximal tibial and distal femoral leg bands apparently missing, but integument in general is darker than other species, so banding may be obscured. Abdominal venter as in female except black laterally in one male (Fig. 10g). Embolus base origin in range 9:00–10:30 (270–315 degrees), median near 9:00, with complete revolution around tegulum, and additional 150–225 degrees to embolus tip (Figs. 10c, h).

**Distribution.**—Circum-Caribbean, with continental records from Mexico, Guatemala, Costa Rica, and Panama, and island records from Cuba, Jamaica, Puerto Rico, several islands in the Lesser Antilles, and Trinidad (Trinidad & Tobago). The latter record makes this the only known *Misumessus* species from South America, as Trinidad is a continental island.

**Notes.**—In very dark individuals, the cheliceral pattern may be hard to see, but the dark color itself is a species indicator.

There is a female specimen of *M. quinteroi* in the AMNH collection with the following two labels [labels separated by semicolon]: 27Bc. N37:W112; Mp.aba. Assuming part of this refers to latitude: longitude, this would place the specimen in Utah, which is highly unlikely unless transported there. If this label interpretation is correct, then the specimen is likely mislabeled.

*Misumessus bishopae* sp. nov.

<http://zoobank.org/?lsid=urn:lsid:zoobank.org:act:567B4924-E28C-4E0F-9040-CAB0F0B6F4E7>

(Fig. 11)

**Type material.**—*Holotype male*. DOMINICA: Springfield Plantation Garden, looking down, 29 May 2003, J. Mutti (FSCA).

**Paratypes.** DOMINICA: 2 ♂, same data as holotype except 17 May 2003, L. Bishop, A. Moore (FSCA); 1 ♂, Wotten Waven Sulfur Springs, 6 January 2003, Bishop et al. (FSCA).

**Other material examined.**—DOMINICA: 1 penultimate ♂, Springfield Plantation Garden, beatsheet, 17 May 2003, J. Jamison, J. Mutti (FSCA). PUERTO RICO: 2 ♂, Cayo Norte (off Culebra), 18.2345°N, 66.5935°W, 14 April 1965, H. Heatwole, F. MacKenzie (AMNH). GRENADINES: 1 juvenile ♀ (species uncertain), Bequia, 13.0220°N,

61.2354°W, el. 170 m, cinnamon-garpoan dry scrub, 5 May 2013, Team CarBio (UVT CarBio 075).

**Etymology.**—This species is named in honor of Leslie Bishop, for the work of her and her students on Dominican spiders.

**Diagnosis.**—Males can be distinguished from other species of *Misumessus* by the position of the embolus base, which starts in the range 5:00 to 7:30 (180–225 degrees).

**Description.**—*Male:* BL = H2.18 (2.00–2.28), CL = H1.04 (0.94–1.04), CW = H1.03 (0.94–1.04), EGW = H0.66 (0.61–0.66). General appearance as in genus description. Preserved males with brown cephalothorax and pale pentagonal mark in middle of carapace (Fig. 11a); abdominal dorsum yellow, venter gray. Embolus base origin with median about 6:30, range 5:00 to 7:30 (180–225 degrees), although males at 5:00 and 5:30 are only from Puerto Rico (see Notes).

**Distribution.**—Puerto Rico, Dominica, Grenadines(?).

**Notes.**—No females were found that matched with the small males of this species. There is one Dominican female assigned to *M. quinteroi* that has an almost entirely white abdomen, but it also has the cheliceral color pattern, darker narrow median ventral abdominal stripe, and one of the epigynal variations typical for *M. quinteroi* (Figs. 9g, h).

A white juvenile specimen from the Grenadines with pink eye pigment and no cheliceral pattern included here seems more likely to represent this species than *M. quinteroi*. This would suggest that *M. bishopae* is distributed primarily in the Lesser Antilles, but occurring also in Puerto Rico, the easternmost island of the Greater Antilles.

The two Puerto Rico males have a longer embolus base than the Dominican males, starting about 5:00–5:30, but the remainder of the palpal bulb appears to be the same (Fig. 11g). The embolus base of the Dominican males starts at 6:00–7:30 (Fig. 11d). The latter record was an outlier that matched the lower end of the embolus base position range of *M. lappi*, which otherwise is quite different and occurs in the midwestern United States.

*Misumessus blackwalli* sp. nov.

<http://zoobank.org/?lsid=urn:lsid:zoobank.org:act:D1E01218-839B-4B79-83CA-5F1ADFC65483>

(Fig. 12)

**Type material.**—*Holotype male*. BERMUDA: 32.3093°N, 64.7503°W, 1 July 1905, T. Kincaid (CAS; only specimen known).

**Etymology.**—This species is named in honor of John Blackwall, early British pioneer in arachnology and author of the family Salticidae, whose taxonomic concepts and illustrations were far advanced for his time.

**Diagnosis.**—Male has an embolus base beginning at 2:00, like *M. dicaprio*. However, this species can be distinguished from other species of *Misumessus* by a pair of small carapace tubercles, the very short RTA base, and filiform abdominal setae.

**Description.**—*Male holotype:* BL = 2.91, CL = 1.13, CW = 1.22, EGW = 0.75. General appearance as in genus description. Preserved male has brown carapace with pale quadrangular mark in center, legs and abdomen brownish yellow except darker brown leg banding.



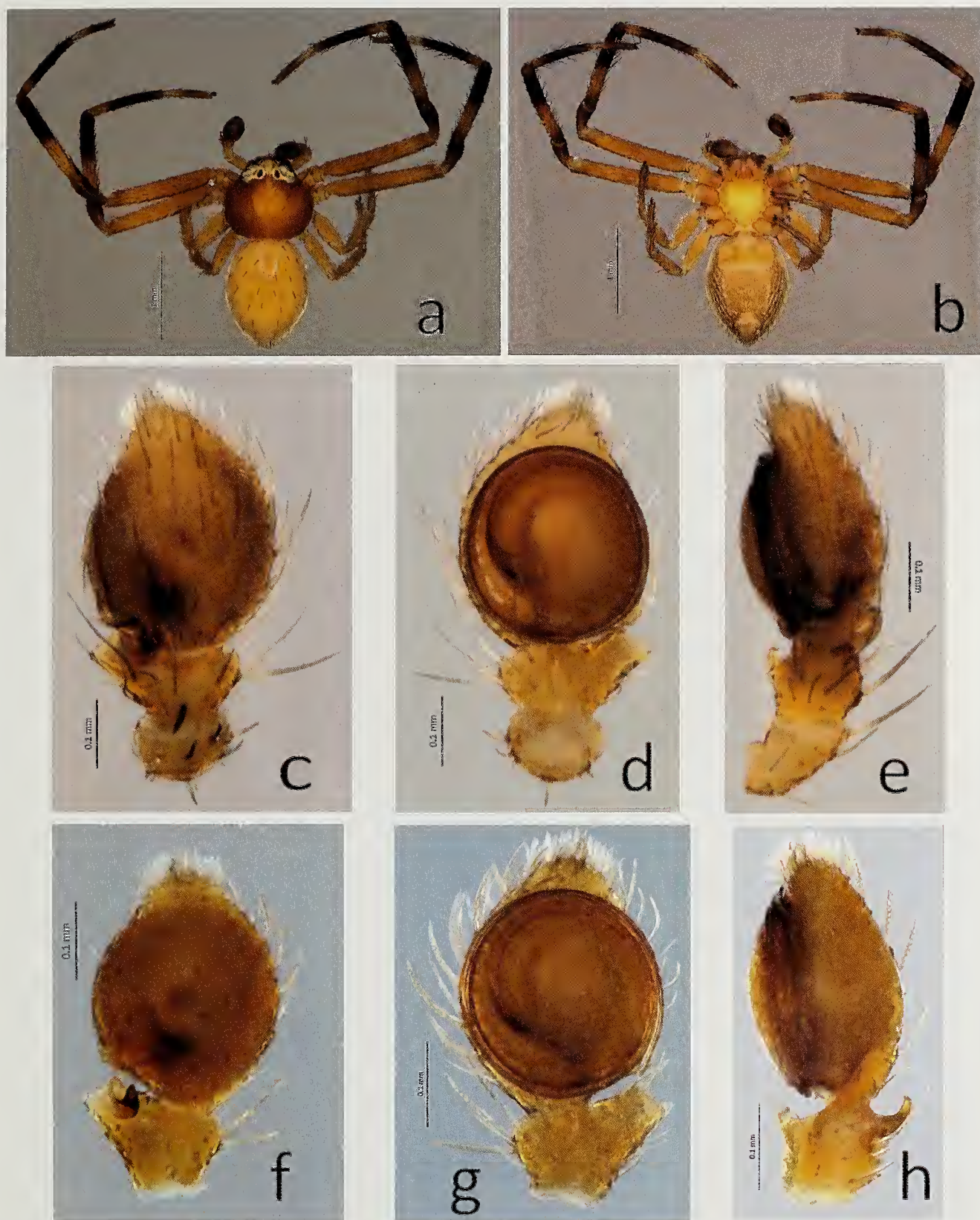


Figure 11.—*Misumessus bishopae* sp. nov. a–e, Holotype male from Dominica: a, dorsum; b, venter; c, dorsal palp; d, ventral palp; e, retrolateral palp. f–h, Male from Puerto Rico: f, dorsal palp; g, ventral palp; h, retrolateral palp.



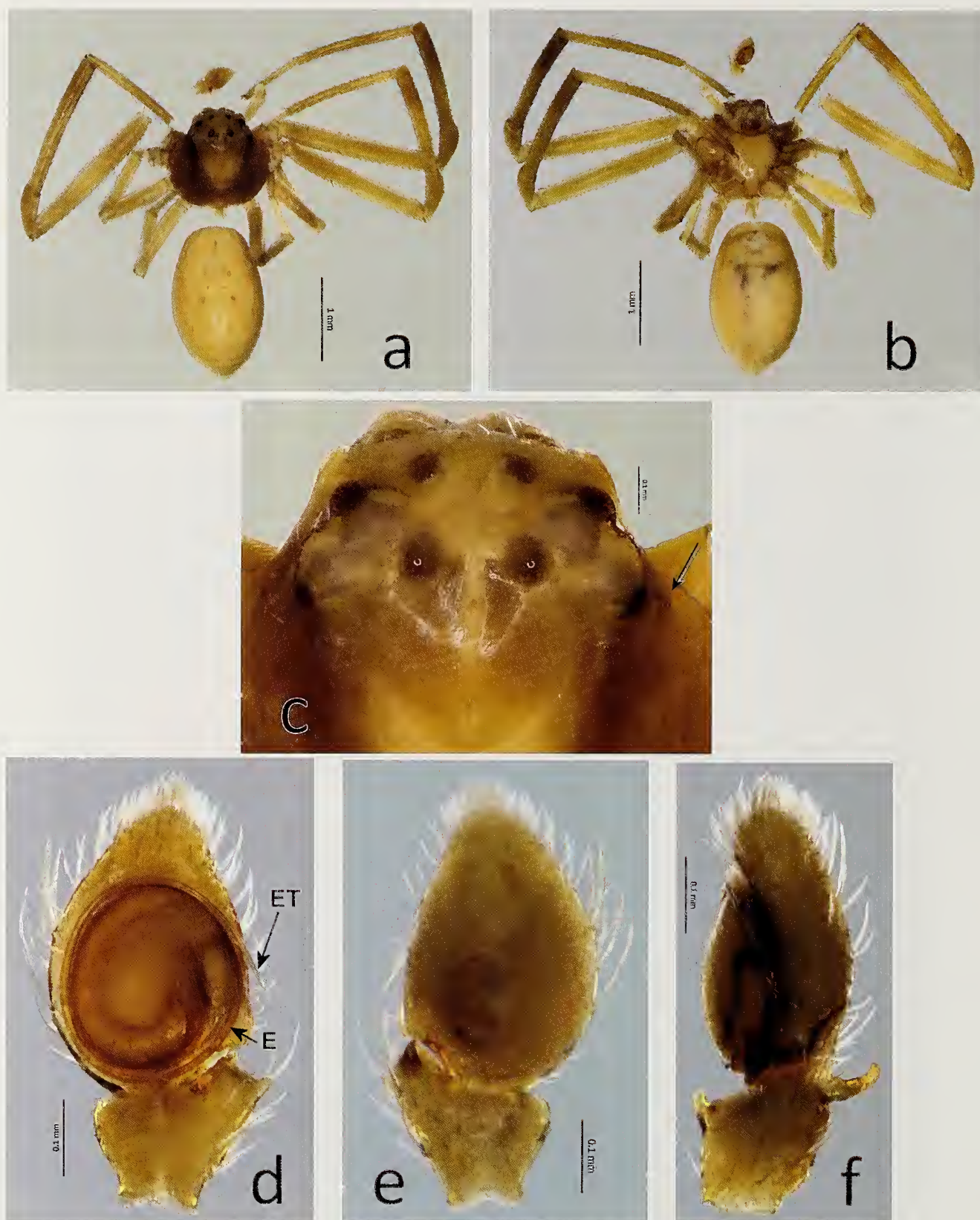


Figure 12.—*Misumessus blackwalli* sp. nov. a–f, Holotype male from Bermuda: a, dorsum; b, venter; c, anterior carapace, arrow to minute tubercle (one each side); d, ventral palp; e, dorsal palp; f, retrolateral palp.



Small tubercle present laterally ventral to eye group on each side (Fig. 12c). RTA with very short base and distally less curled than other species (Fig. 12f). Also, unlike other species, dorsal abdomen has regularly spaced filiform setae rather than spiniform setae, therefore abdominal setae are much less noticeable (Fig. 12a). Embolus base beginning at 2:00, with about 30 degrees more than one revolution around tegulum (Fig. 12d).

**Distribution.**—Bermuda.

**Notes.**—Only the right palp is present, so photos of it are mirror-imaged in the figures. The specimen is partially disarticulated, the left anterior leg is missing, and the abdomen is separated from the cephalothorax (Figs. 12a, b).

*Thomisus pallens* Blackwall, 1868, is the only thomisid species listed from Bermuda (World Spider Catalog 2017). However, the description is of an immature female, gives no characters that would distinguish the species, some previous authors placed it in the quite different genus *Xysticus* (as *X. pallidus*, a lapsus: Simon 1883; Marx 1889), and the type specimen is apparently lost. It is considered a *nomen dubium* by Roewer (1955) and in the World Spider Catalog (2017), and I see no reason to disagree with this assessment. There are at least two characters in the description that suggest it is not a *Misumessus*. Quoting Blackwall (1868: 405), “The eyes, which are dark-coloured, are disposed on the anterior part of the cephalothorax in two transverse curved rows, forming a crescent whose convexity is directed forwards; the four intermediate ones describe a square; and the eyes of each lateral pair are seated obliquely on a conspicuous pale tubercle, the anterior one being the largest of the eight.” The last part of the sentence suggested that the ALEs are the largest eyes, which would be consistent with *Misumessus*, but is also true of some other genera. However, the lateral eyes are indicated as being on discreet pale tubercles, definitely not the situation in *Misumessus*, which has all the eyes enclosed in one contiguous patch of white pigment. Also, the medial eyes in *Misumessus* form a trapezoid, not a square.

Given that Bermuda is near the Gulf Stream and imports a significant portion of its consumables, and potentially any number of species could be introduced there from elsewhere, there is no guarantee that the type specimen of *T. pallens* originated in Bermuda (neither, under the circumstances, is it guaranteed that the present known specimen is native there). Furthermore, the name has not been used since the 19<sup>th</sup> century except in catalogs and in a checklist as *Thomisus* (*Xysticus*) *pallens* Blackwell [sic] by Verrill (1902: 833), who did not examine a specimen and mentioned it only as reported from Bermuda. Apparently he was aware of the earlier citations of the species, and corrected the spelling of the specific epithet.

In addition to lack of use, there is a potential problem with Blackwall's name. *Misumenops* (*sub Misumena*) *pallens* (Keyserling, 1880) is a potential junior homonym if *Thomisus pallens* were to be transferred to *Misumessus*, as *Misumessus* was formerly considered a subgenus of *Misumenops* (Schick 1965). If *Misumessus* were to be subsumed again within *Misumenops*, which would be possible if future molecular data were to indicate *Misumessus* was embedded within and made *Misumenops* paraphyletic, the homonym would be created. Therefore, for all the above reasons, *Thomisus pallens* Black-

wall, 1868 is designated a *nomen oblitum*, and no longer available.

## DISCUSSION

**Comparison of *Misumessus* species.**—Species of *Misumessus* in males differ from each other by the location of the origin of the embolus. Although there is some intraspecific variation in embolus base placement, which typically approaches the variation ranges of the species that are most similar, the range of variation is quite distinct for each species, with no significant overlap with other species, with one exception. This exception is the embolus origin in the western North American *M. dicaprio* and the Bermudan *M. blackwalli*, which in both begins about 2:00; in other respects the two species are quite different.

Since in some species the length and width of the embolus base appear to be variable, a better species indicator may be the position of a small dark area on the tegulum between the embolus base and the adjacent spermophore (e.g., Fig 5b), that appears to be the place where the spermophore folds back on itself and enters the embolus; in retrolateral view, this area appears contorted (e.g., Fig. 4d). It should be pointed out that differences in the width and length of the embolus base in geographically divided populations in otherwise similar specimens may be indicative of cryptic speciation (e.g., *M. bishopae*, *M. quintero*). However, lacking better evidence, this is considered to be intraspecific variation.

The coupling pocket shape and size appear to be more important than the scape shape, and it is best seen in a cleared epigyne, although usually geographic location and somatic face characters will be sufficient to place female specimens. While *M. quintero* has a clearly distinctive scape shape, the scapes of females of other species have subtle details that are present in most specimens of a particular species, so the apparent variability may be more due to outliers than to a normal condition.

Most species of *Misumessus* have few consistent distinctive somatic structures. The midwestern *M. lappi* has a distinctive projecting face structure along with extensive face pigmentation, including the clypeus, that occurs in both sexes (Figs. 8a–c), and the western *M. dicaprio* has distinctive clypeal pigmentation in its more southerly populations (also in both sexes, Fig. 4f). The neotropical *M. quintero* has mostly darker integument color and a distinctive pale cheliceral pattern (Figs. 8d, 9b, f, h). Known females of other species have distinctive differences in the narrow divisions between eyes (Figs. 3j, 4f, 5i).

The midwestern *M. lappi*, with the most distinctive face, occurs conveniently between and divides the ranges of the more widespread eastern and western USA species of *Misumessus* that are less easy to distinguish somatically. Hypothetically, this unusual face structure may be an isolating mechanism where this species comes into contact with other species. However, it appears that the range of this species is limited, and in Mexico and southward, this division does not exist, as *M. lappi* is not known to range that far south. That does not preclude a geographic separation potentially being maintained for the two other species in Mexico due to the existence of longitudinally-oriented mountain ranges such as the Sierra Madre Oriental. However, neither *M. oblongus* nor



*M. dicaprio* have been confirmed as occurring in Mexico, although it seems likely, especially in the case of *M. dicaprio*, that both could be found at least a short distance south of the United States/Mexico border. Gertsch (1939) stated that *M. oblongus* was recorded from Mexico, although he does not give a specific locality that might tell us which species was actually recorded. The localities he gave for individual records of *M. oblongus* appear to represent all four of the species now known to occur in the United States.

Regardless, it is apparent that geographic separation is one of the best ways to distinguish species. Species with variation ranges of the embolus origin that approach or coincide at the extremes of their variation with another species are, in most cases, geographically widely separated. The only two species that approach each other both geographically and in palp morphology are *M. oblongus* and *M. quintero*, which have quite different somatic appearances.

Even though *M. quintero* is the only presently known *Misumessus* species associated with South America, it is possible that there are other misplaced species native to this continent that belong in the genus. For example, South American species with similar-shaped RTAs and approaching the epigynal condition in *Misumessus* do exist (Renato Augusto Teixeira, pers. comm. 2016), such as *Runcinioides litteratus* (Piza, 1933), illustrated by Rinaldi (1988; as *Misumenops litteratus*).

**Comparison of North American Misumenini genera.**—*Misumessus* can be distinguished from other misumenine thomisids (see Gertsch 1939 for comparative illustrations) of North America (NA) in the female by the greatly reduced epigynal coupling pocket that is displaced posteriorly on a scape whose posterior part projects ventrally, and an abdomen that is significantly longer than wide rather than wider than long. Females lack spiniform setae on the carapace, as is typical of *Misumena* and *Misumenoides* (except for a few that may be present near the eyes, but rarely elsewhere), but lack the anterior carapace carina of the latter genus, and lack the anteriorly-placed epigynal coupling pocket of all other NA genera of Misumenini.

In *Misumessus*, body color in life in females is generally pale green to white; in males the body typically is white or yellow, rarely green, although they may have an amber, orange-red (Schick 1965), or brown (*M. quintero*) carapace, and green anterior femora and posterior legs. The predominant color in other NA misumenine females typically is white to yellow, while males are typically white, yellow, or tan in *Mecaphesa* and *Misumenops*, or have a mostly dark (black to dark green) cephalothorax (including appendages) in *Misumena* and *Misumenoides*. However, in life, these are sometimes green or green tinted as well; Lehtinen (2004) considered green on the legs and body to be typical of Misumenini and related tribes. There are no paired dark (usually brown) submarginal stripes (alatal bands; Schick 1965) on the carapace in either sex as occurs in *Mecaphesa* and *Misumenops*, therefore the female usually (except *M. quintero*) lacks dark pigmented areas on the carapace, similar to many *Misumena* females (some *Misumena* have faint submarginal bands, and *Misumenoides* females have dark submarginal bands). Neither sex (other than male *M. lappi*) has the paired dark dorsal abdominal

maculations that typically occur in both sexes of *Mecaphesa* and *Misumenops*.

Purely red pigment (not brownish red or orangish red) is absent in most NA Thomisidae, but shows up sporadically in the Misumenini, occurring as red anterolateral bands in some individuals of *Misumena vatia* (Clerck 1757), and in the same position in some *Mecaphesa asperata* (Hentz, 1847) (Dondale & Redner 1978b). Images of several *Mecaphesa* species and *Misumenoides formosipes* on BugGuide show similar markings. Interestingly, as in *Misumessus*, it appears that the only non-misumenines in NA with red pigment on the abdomen also have a green cephalothorax [J.T. Lapp, pers. comm. 2017; see BugGuide images of *Diaea livens* Simon, 1876, and *Synema viridans* (Banks, 1896)]. Gertsch (1939) reported occasional red lateral margins on the abdomen in *Misumessus oblongus*, and *M. lappi* has paired red dorsal abdominal spots in males. So it is possible that red pigment on what as a group are often referred to as 'flower crab spiders' might be a character indicative of the Misumenini and related crab spiders. Ecologically, however, species of *Misumessus*, as the green color suggests, are not flower dwellers, but normally occur on tree and shrub leaves.

Females somatically are difficult to distinguish from *Misumena*, other than by, usually, integument color and the proportional difference in the shape of the abdomen, so it is no wonder that the type species of *Misumessus* was originally described in *Misumena*. Even the relative size of the ALE to AME can be confusing, as in *Misumena vatia*, these eyes are subequal although either can be slightly larger (J.T. Lapp, pers. comm. 2017), whereas in *Misumessus oblongus* (and all other *Misumessus*), the ALE is noticeably larger than the AME. The small weak setae noted by Lehtinen & Marusik (2008) for females does not alone distinguish *Misumessus* from *Misumena* or *Misumenoides*, and is not the situation for *Misumessus* males (not seen by Lehtinen & Marusik 2008).

Despite previous assertions, a close examination of the female genitalia shows that a coupling pocket is present, and it could be interpreted to be a miniature version of what occurs in *Misumenops*. The *Misumenops* coupling pocket is rather flat and opens entirely posteriorly similar to *Misumessus* and *Misumena*, unlike *Mecaphesa* and *Misumenoides*. The main difference is that the *Misumessus* coupling pocket is no longer anterior. Instead, it has been reduced in size, an extension has pushed it posteriorly, and the extension projects a few degrees toward the venter. Lehtinen & Marusik (2008) described this extension as a scape, but also noted that it had been referred to as a 'wide posteriorly-rounded septum' (Kaston 1981). Unlike a typical septum, the scape does not completely divide the atrium containing the copulatory openings, nor is it entirely attached to the integument. Therefore, calling it a scape is appropriate, as it is separated from the rest of the epigyne except for its anterior attachment, but since apparently no previous authors cleared any specimens, they would not have noticed that the coupling pocket is on the dorsal side of the tip of the scape. When cleared, this miniature coupling pocket has a very similar shape to, but is much smaller than, the type of coupling pocket that occurs in *Misumenops bellulus* (Fig. 13c). This revelation, along with male characters summarized below, appears to contradict the statement by Lehtinen &





Figure 13.—*Misumenops bellulus* (Banks, 1896) from Florida. a–b, Male: a, ventral palp, arrows to arch at distal end of embolus base, separating embolus from tegulum; b, retrolateral palp, arrow to distally pointing RTA. c, Female ventral epigyne, black arrow to copulatory duct, white arrow to coupling pocket. Photo credits: a–c by Joe Lapp.

Marusik (2008) that *Misumessus* is not closely related to *Mecaphesa* or *Misumenops*.

As in *Misumenops* and *Misumena*, the eopulatory openings seem to be consistently near and immediately posterior to the lateral edges of the coupling pocket, or in this case, the scape that contains the coupling pocket. The coupling pockets of *Mecaphesa* and *Misumenoides* are so wide that they generally include the copulatory openings within their periphery, and the copulatory openings are situated along the posterior edge of the pocket opening.

From a somatic viewpoint, males hardly seem to belong with females. Except for the lack of carapace submarginal bands and (usually) abdominal markings, they can easily be mistaken for *Mecaphesa* or *Misumenops* males. Even the lack of submarginal bands can be overlooked, as males are often quite small, and the lateral thoracic part of the carapace is sometimes darker than the ecephalic and median thoracic parts, so a superficial examination might mistake this pigmentation for bands on the carapace. This darker color, when pronounced (e.g., *Misumessus quintero* and to lesser extent *M. dicaprio*), is reminiscent of *Misumena* and *Misumenoides* males.

Males of *Misumessus* (unlike *Misumessus* females) are like both sexes of *Mecaphesa* and *Misumenops* in having many spiniform setae on the carapace, which was noted cursorily by Gertsch (1939), and by usually having regularly spaced spiniforms on the dorsal abdomen. They also have pigmented bands encircling the front two pair of legs like males of these two genera. *Misumessus* males sometimes seem to have a weakly sclerotized median scutum, also reported for species of *Misumenops* by Lehtinen & Marusik (2008). Clavate setae as occur in *Ozyptila* and relatives are lacking.

Males differ from other NA misumenines by having an embolus that exceeds 360 degrees of rotation around the tegulum and lacks the transitional arch at the distal end of the embolus base that occurs in *Misumena*, *Misumenoides*, *Misumenops*, and some *Mecaphesa* (compare, e.g., Figs 12c, h with Fig. 13a). The other NA genera of Misumenini do not have an embolus that exceeds 180 degrees except some *Mecaphesa*, that are no more than 270 degrees but which also lack the transitional arch. *Misumessus* lacks the strongly curled (spiral) embolus tip and corresponding groove on the distal retrolateral side of the cymbium seen in *Mecaphesa*. The embolus tip has a slight curl like *Misumenops*, and emerges in the same area (between 3:00 and 4:30 on a clock face). This similarity was observed by Gertsch (1939) and the lack of a spiral tip was used in his key to *Misumenops* species (when *Mecaphesa* and *Misumessus* were included in *Misumenops*).

Approximately the distal two-thirds of the RTA is directed dorsally rather than entirely distally as in the other genera [e.g., Fig. 13b; but note that NA misumenines in general have the distal end of the RTA shifted to the dorsal edge rather than being a medial continuation of the base, and in some *Mecaphesa*, the distal part of the RTA tilts dorsally (see Gertsch 1939; as *Misumenops*)]. It is hypothesized that the RTA shape of *Misumessus* co-evolved with the scape in order to accommodate the length of the scape. The recurved tip of the RTA could then reach around the tip of the scape to enter the coupling pocket.



According to Lehtinen & Marusik (2008), the ITA and RTA are separate in *Misumessus*, but completely fused in *Misumenops*. Based on the small retrolateral projection of the RTA, the ITA could be considered neither entirely lacking nor fully developed. However, if this projection represents the ITA, there is minimal development in *Misumessus*. In salticids, such a projection would be considered a prong of the RTA (e.g., Edwards 2015).

Relationships with other misumenine genera are obscure, as can be seen from the above discussion, where there is a mix of characters similar to one or another of the other genera. Lehtinen (2004) redefined the Misumenini and noted that even the common genera have not been properly revised. He gave general characteristics for the tribe, but did not cover all the details of the characters discussed here. Polarity of the states of these characters will need to be determined in order to make sense of the overall phylogeny within the tribe. Some of the characters likely will prove to not be distinctive within the Misumenini.

Pickard-Cambridge (1900) was the first to place *M. oblongus* into his genus *Misumenops*, followed by the catalog of Petrunkevitch (1911), who synonymized *Misumessus*. Gertsch (1939) also followed this placement, but it is clear from his description and discussion of the species that he considered it atypical for the genus. Now that the differences he noted have proven to be consistent for several species, it is clear that they form a distinct clade. The set of unique characters that define the group support the elevation of *Misumessus* by Lehtinen & Marusik (2008) to genus status.

#### ACKNOWLEDGMENTS

I am especially grateful to Joe Lapp, who made significant early contributions to developing this revision, and hosted me in his home, but declined to be an author, even though he deserved it; he also provided a pre-submission review. In lieu of authorship, I named the species he discovered after him. I thank the following people for loaning or donating specimens: Lou Sorkin (AMNH), Jan Beealoni (BNHM), Darrell Ubick (CAS), Owen Lonsdale (CNC), Paula Cushing and Jeff Stephenson (DMNS), Petra Sierwald and Crystal Maier (FMNH), Laura Liebensperger and Gonzalo Giribet (MCZ), John Abbot (SEU), Ed Riley and Allen Dean (TAMU), Jon Coddington and Dana DeRoche (USNM), Alex Wild (UTA), and Ingi Agnarsson (UVT); Hank Guarisco loaned specimens from his private collection; Joe Lapp donated specimens from his private collection; and Leslie Bishop donated specimens collected by her and her students in Dominica. Thanks also to the following for various types of assistance: Renato Augusto Texeira provided information about thomisid relationships, and a pre-submission review; Nicole Miller and Clare Wuellner databased specimen collection records, and Joe Lapp converted these records to latitude and longitude coordinates; Matthew Albritton and William Galvis helped develop the distribution map; Mike Rix did a commendable editing job, and two anonymous reviewers provided valuable comments. I also want to gratefully recognize the following photographers for allowing me to reference or use their images: Seth Ausubel, Daniel D. Dye II, Hank Guarisco, Colin Hutton, Ilona Loser, and especially Joe Lapp; the iNaturalist image was submitted by Adam Zorn. In 2010, I

was fortunate to have the opportunity for a pilgrimage to John Blackwall's estate and his grave, for which I thank Dmitri Logunov, David Penney, and Richard Gallon.

#### LITERATURE CITED

- Banks, N. 1904. New genera and species of Nearctic spiders. *Journal of the New York Entomological Society* 12:109–119.
- Blackwall, J. 1868. Notice of several species of spiders supposed to be new or little known to arachnologists. *Annals and Magazine of Natural History* (4)2:403–410.
- Blest, A.D. & D. O'Carroll. 1989. The evolution of the tiered principal retinae of jumping spiders (Araneae: Salticidae). Pp. 155–170. *In* *Neurobiology of Sensory Systems*. (R. Nareish Singh, N.J. Strausfeld (eds.)). Plenum Press, New York.
- Breene, R.G., D.A. Dean, M. Nyffeler & G.B. Edwards. 1993. *Biology, Predation Ecology, and Significance of Spiders in Texas Cotton Ecosystems with a Key to Species*. Texas Agriculture Experiment Station, College Station.
- Chickering, A.M. 1940. The Thomisidae (crab spiders) of Michigan. *Papers of the Michigan Academy of Science, Arts and Letters* 25:189–237.
- Corronca, J.A. & H.R. Terán 1997. Estructura ocular de *Selenops cocheleti* (Araneae, Selenopidae). *Journal of Arachnology* 25:42–48.
- Corronca, J.A. & H.R. Terán. 2000. Optical structure of the crab spider *Misumenops pallens* (Araneae, Thomisidae). *Journal of Arachnology* 28:16–22.
- Dahl, F. 1913. *Vergleichende Physiologie und Morphologie der Spinnentiere unter besonderer Berücksichtigung der Lebensweise*. 1. Die Beziehungen des Körperbaues und der Farben zur Umgebung. Jena:1–113.
- Dondale, C.D. & J.H. Redner. 1978a. Revision of the Nearctic wolf spider genus *Schizocosa* (Araneida: Lycosidae). *Canadian Entomologist* 110:143–181.
- Dondale, C.D. & J.H. Redner. 1978b. The insects and arachnids of Canada, Part 5. The crab spiders of Canada and Alaska. Araneae: Philodromidae and Thomisidae. Research Branch Agriculture Canada Publication 1663:1–255.
- Edwards, G.B. 2004. Eye characters support sister group placement of Salticidae with Thomisidae (Araneae). Poster, American Arachnological Society annual meeting, University of Oklahoma, Norman, OK. Abstract available online at [http://www.americanarachnology.org/meetings/abstracts/AAS\\_2004\\_abstracts.html#D](http://www.americanarachnology.org/meetings/abstracts/AAS_2004_abstracts.html#D)
- Edwards, G.B. 2015. Freyinae, a major new subfamily of Neotropical jumping spiders (Araneae: Salticidae). *Zootaxa* 4036:1–87.
- Emerton, J.H. 1892. New England spiders of the family Thomisidae. *Transactions of the Connecticut Academy of Arts and Sciences* 8:359–381.
- Garrison, N.L., J. Rodriguez, I. Agnarsson, J.A. Coddington, C.E. Griswold, C.A. Hamilton et al. 2016. Spider phylogenomics: untangling the Spider Tree of Life. *PeerJ* 4:e1719; DOI 10.7717/peerj.1719.
- Gertsch, W.J. 1939. A revision of the typical crab spiders (Misumeninae) of America north of Mexico. *Bulletin of the American Museum of Natural History* 76:277–442.
- Homann, H. 1975. Die Stellung der Thomisidae und der Philodromidae im System der Araneae (Chelicerata, Arachnida). *Zeitschrift für Morphologie der Tiere* 80:181–202.
- Huber, B.A. 1995. The retrolateral tibial apophysis in spiders – shaped by sexual selection? *Zoological Journal of the Linnean Society* 113:151–163.
- Jackson, R.R. 1986. Web building, predatory versatility, and the



- evolution of the Salticidae. Pp. 232–268. In *Spiders: Webs, Behavior, and Evolution* (W.A. Shear, ed.). Stanford University Press, Stanford, California.
- Kaston, B.J. 1948. Spiders of Connecticut. *Bulletin of the Connecticut State Geological and Natural History Survey* 70:1–874.
- Kaston, B.J. 1981. *Spiders of Connecticut* (revised edition). *Bulletin of the Connecticut State Geological and Natural History Survey* 70:1–1020.
- Keyserling, E. 1880. Die Spinnen Amerikas, I. Laterigradae. Nürnberg 1:1–283.
- Latreille, P.A. 1804. *Histoire naturelle générale et particulière des Crustacés et des Insectes*. Paris 7:144–305.
- Lehtinen, P.T. 1967. Classification of the cribellate spiders and some allied families, with notes on the evolution of the suborder Araneomorpha. *Annales Zoologici Fennici* 4:199–468.
- Lehtinen, P.T. 2004. Taxonomic notes on the Misumenini (Araneae: Thomisidae: Thomisinae), primarily from the Palaearctic and Oriental regions. Pp. 147–184. In *European Arachnology 2003* (Proceedings of the 21st European Colloquium of Arachnology, St.-Petersburg, 4–9 August 2003). (Logunov, D. V. & D. Penney (eds.)). *Arthropoda Selecta*, Special Issue 1.
- Lehtinen, P.T. & Y.M. Marusik. 2008. A redefinition of *Misumenops* F. O. Pickard-Cambridge, 1900 (Araneae, Thomisidae) and review of the New World species. *Bulletin of the British Arachnological Society* 14:173–198.
- Loerbroeks, A. 1984. Mechanik der Kopulationsorgane von *Misumena vatia* (Clerck, 1757) (Arachnida: Araneae: Thomisidae). *Verhandlungen des Naturwissenschaftlichen Vereins in Hamburg* 27:383–403.
- Maddison, W.P. 2015. A phylogenetic classification of jumping spiders (Araneae: Salticidae). *Journal of Arachnology* 43:231–292.
- Marx, G. 1889. A contribution to the knowledge of the spider fauna of the Bermuda Islands. *Proceedings of the Academy of Natural Sciences of Philadelphia* 1889:98–101.
- Moradmand, M., A.L. Schönhofer & P. Jäger. 2014. Molecular phylogeny of the spider family Sparassidae with focus on the genus *Eusparassus* and notes on the RTA-clade and ‘Laterigradae.’ *Molecular phylogenetics and evolution* 74:48–65.
- Petrunkovitch, A. 1911. A synonymic index-catalogue of spiders of North, Central and South America with all adjacent islands, Greenland, Bermuda, West Indies, Terra del Fuego, Galapagos, etc. *Bulletin of the American Museum of Natural History* 29:1–791.
- Pickard-Cambridge, F.O. 1900. Arachnida - Araneida and Opiliones. In: *Biologia Centrali-Americana, Zoology*. London 2:89–192.
- Polotow, D., A. Carmichael & C.E. Griswold. 2015. Total evidence analysis of the phylogenetic relationships of Lycosoidea spiders (Araneae, Entelegynae). *Invertebrate Systematics* 29: 124–163.
- Ramírez, M.J. 2014. The morphology and phylogeny of dionychan spiders (Araneae: Araneomorphae). *Bulletin of the American Museum of Natural History* 390:1–374.
- Rinaldi, I.M.P. 1988. *Misumenops* Cambridge e *Uraarachne* Keyserling (Araneae, Thomisidae, Thomisinae): Sinonímias, novas combinações e redescrições. *Revista Brasileira de Entomologia* 32:19–30.
- Rocwer, C.F. 1955. Katalog der Araneae von 1758 bis 1940, bzw. 1954. Bruxelles 2:1–1751.
- Schick, R.X. 1965. The crab spiders of California (Araneae, Thomisidae). *Bulletin of the American Museum of Natural History* 129:1–180.
- Simon, E. 1883. Études arachnologiques. 14e Mémoire. XXI. Matériaux pour servir à la faune arachnologique des îles de l’Océan Atlantique (Açores, Madère, Salvages, Canaries, Cap Vert, Sainte-Hélène et Bermudes). *Annales de la Société Entomologique de France* (6) 3:259–314.
- Simon, E. 1897. On the spiders of the island of St. Vincent. III. *Proceedings of the Zoological Society of London* 1897:860–890.
- Simon, E. 1900. Arachnida. Pp. 443–519. In *Fauna Hawaïensis* (2), or the zoology of the Sandwich Isles: being results of the explorations instituted by the Royal Society of London promoting natural knowledge and the British Association for the Advancement of Science. London.
- Sundevall, C.J. 1833. Svenska spindlarnes beskrifning. Fortsättning och slut. Bihang till Kongliga Svenska Vetenskaps-Akademiens Handlingar 1832:172–272.
- Verrill, A.E. 1902. Arancina. Pp. 829–840, Figs. 205–223. In *The Bermuda Islands: their scenery, climate, productions, physiography, natural history and geology; with sketches of their early history and the changes due to man*. *Transactions of the Connecticut Academy of Arts and Sciences* 11:413–956.
- Wallace, H.K. & H. Exline. 1978. Spiders of the genus *Pirata* in North America, Central America and the West Indies (Araneae: Lycosidae). *Journal of Arachnology* 5:1–112.
- Wheeler, W.C., J.C. Coddington, L.M. Crowley, D. Dimitrov, P.A. Goloboff, C.E. Griswold, et al. 2016. The spider tree of life: phylogeny of Araneae based on target-gene analyses from an extensive taxon sampling. *Cladistics* 2016:1–43.
- World Spider Catalog. 2017. World Spider Catalog. Natural History Museum Bern, online at <http://WorldSpiderCatalog.nmbe.ch>, version 18.0.

*Manuscript received 28 March 2017, revised 18 August 2017.*



## A review of Burmese amber arachnids

Paul A. Selden<sup>1,2,3</sup> and Dong Ren<sup>2</sup>: <sup>1</sup>Department of Geology and Paleontological Institute, University of Kansas, 1475 Jayhawk Boulevard, Lawrence, KS 66045, USA; E-mail: selden@ku.edu <sup>2</sup>College of Life Sciences, Capital Normal University, Beijing 100048, People's Republic of China; <sup>3</sup>The Natural History Museum, Cromwell Road, London, SW7 5BD, UK.

**Abstract.** Fossils from the mid-Cretaceous (c. 99 Ma) Myanmar (Burma) amber include all extant orders of Arachnida, including the earliest representatives of Schizomida, Parasitiformes, and Palpigradi. Schizomids are figured from Burmese amber herein for the first time. The most abundant and diverse arachnid order is the Araneae, with 38 families, 93 genera, and 165 species recorded to date. The araneofauna is dominated by haplogynes and palpimanoids, whilst araneoids are rare and members of the RTA clade absent. The arachnofauna is typical of a tropical rainforest habitat, which concurs with evidence from other Burmese amber biota.

**Keywords:** Burmite, Cenomanian, Cretaceous, Mesozoic, Myanmar

Amber from Myanmar (Burma), sometimes known as burmite, has been known for more than 2000 years in Asia. According to Laufer (1907), amber was most probably traded between the *Ai lao*, the many tribes of the present-day Chinese province of Yunnan, and Burma during the first century AD. Later Chinese writings described the amber trade, and it was first mentioned in European literature in the 17th Century by the Portuguese Jesuit Fr Alvarez Semedo (1643, see also 1655). Further details about the history of burmite can be found in Zherikhin & Ross (2000) and Poinar et al. (2008). Burmite is increasingly sold today for its spectacular inclusions of plants, animals, and fungi. Burmese amber hosts an abundant and diverse biota, including: bryophytes, ferns, gymnosperms, angiosperms, fungi, molluscs, onychophorans, vertebrates, nematodes, and arthropods. Burmese is not the oldest amber with arthropod inclusions, but it is one of the most prolific sources today.

The first Burmese amber arachnid inclusions were reported by Cockerell (1917a,b, 1920), from material sent by R.C.J. Swinhoe of Mandalay (Zherikhin & Ross 2000): the pseudoscorpions *Electrobisium acutum* Cockerell, 1917b and *Amblyolpium burmiticum* (Cockerell, 1920), and the acariform mite *Cheyletus burmiticus* Cockerell, 1917. At that time, the age of the amber was unknown; the pieces occur in a clay of Miocene (5–23 Ma) age, but Cockerell (1917a,b) suggested that they may have been reworked from much older deposits, perhaps even Upper Cretaceous. However, interest in Burmese amber waned after the flow of material ceased, and was only re-ignited at the turn of the 21st Century, when material started to become widely available again, and modern dating showed it to be of mid-Cretaceous (99 Ma) age. After 1920, no more arachnids were described from burmite until 2002 (Grimaldi et al. 2002; Lourenço 2002) (Fig. 1). Thereafter, new species have been reported most years, with exceptionally large numbers of arachnids, mainly spiders, described by Jörg Wunderlich in his large tomes on the fauna (Wunderlich 2008b, 2012a,b, 2015a,b, 2017a,b) (Fig. 1).

## GEOLOGY

Burmese amber today comes from a single locality in remote Upper Burma, at Noije Bum hill, Hukawng Valley, northern Myanmar (see location map in Kania et al. 2015). The amber mine and its geological setting was described in detail by Cruickshank & Ko (2003). The amber is dug out by hand, by local Kachin people, in pits along the narrow exposures. Annual production of amber depends on market conditions. It reached 11,000 kg per annum in 1906 (Cruickshank & Ko 2003), but has only reached 500 kg per year more recently (Poinar et al. 2008).

The Indian geologist Noetling (1893) thought its age was Miocene, on account of the similarity of the greenish clays to Miocene rocks nearby. He did record an ammonite in a loose pebble during his visit, but considered it came from further afield. An Eocene (c. 34–56 Ma) age for the strata was proposed by Stuart (1923), based on the presence of the large foraminiferan *Nummulites*, a conclusion supported by Chhibber (1934). Later workers, e.g., Zherikhin & Ross (2000), considered the age of the amber to be Cretaceous, based on its insect content, but thought the pieces were reworked into Eocene-age sediments. Sahni & Sastri (1957) described another foraminiferan, the Cretaceous *Orbitolina*, from the area, but thought that these fossils, too, were derived inclusions in Eocene sediments. It was the detailed study by Cruickshank & Ko (2003) which showed the host clays to be Cretaceous in age. They discovered an *in situ* ammonite during their visit, reported the results of palynological investigations, and re-evaluated the misconceptions of previous workers. More recently, the age of Burmese amber has been dated radiometrically to  $98.79 \pm 0.62$  Ma based on U-Pb zircon dating of the volcanoclastic matrix (Shi et al. 2012).

Burmese amber varies from deep red in color, through orange (the commonest, Fig. 2A), to light, transparent yellow, commonly containing fine bubbles (Grimaldi et al. 2002). Some pieces are flattened and lens-shaped, but rarely contain animal inclusions. Arthropods are most commonly found in pieces shaped like flows or runnels; these comprise no more than 3–4% by mass of all the amber studied by Grimaldi et al.



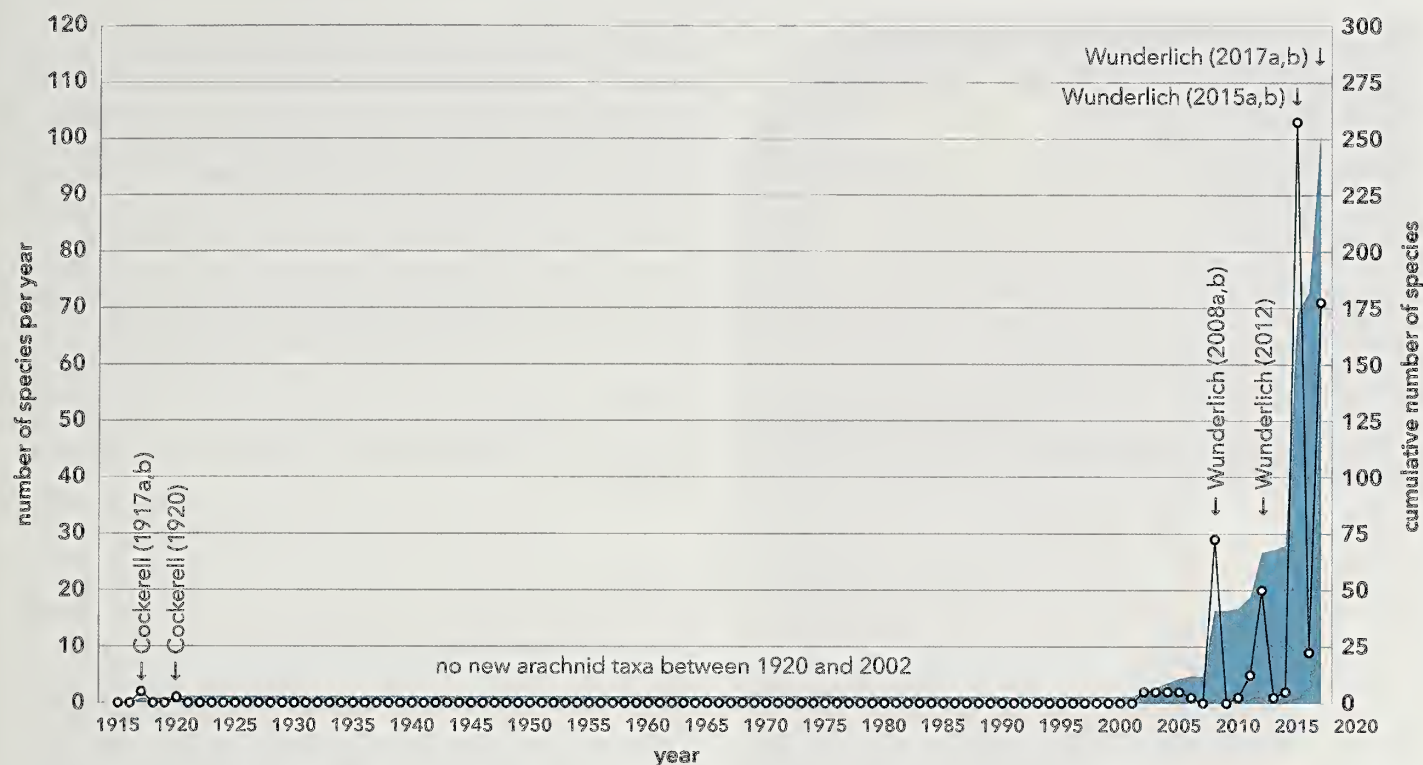


Figure 1.—Graph showing number of fossil arachnid species described from Burmese amber each year from 1917 to the present day (○), and cumulative curve (color). Landmark papers indicated. Data mainly from Dunlop et al. (2017), updated.

(2002) but yielded approximately 85% of the arthropods. In general, arthropod remains occur at the rate of about 46 inclusions per kg of extracted amber. Regarding the source of the resin, spores of both Araucariaceae and Taxodiaceae, both of which contain species which are copious resin producers today, have been found in the amber (Cruickshank & Ko 2003). More recently, nuclear magnetic resonance studies have suggested that the source is most likely an araucariacean tree similar to the modern New Zealand Kauri pine, *Agathis* (Poinar et al. 2007). However, it was pointed out by Grimaldi & Ross (in press) that leafy shoots of *Metasequoia* (Cupressaceae) are common in Burmese amber pieces, so that is a further possibility.

The Myanmar amber locality lies within the West Burma terrane (Broly et al. 2015), which was considered to have rifted off from northwest Australia in the Late Jurassic (156 Ma) and drifted northwards, finally colliding with the Eurasian marginal Sibumasu terrane at around 80 Ma (Heine & Müller 2005; Seton et al. 2012). In this scenario, the amber forest bearing the arachnid fauna was living at the time on an island which had separated from Australia some 75 million years earlier. However, more recent ideas of Metcalfe (2013) suggest that the West Burma terrane formed part of a continent which separated from Australia in the Devonian as the Paleo-Tethys Ocean opened, and then collided with Eurasia (including the North and South China blocks) by Jurassic times. In the latter scenario, the arachnid fauna spread onto the West Burma terrane from Eurasia sometime between Jurassic and mid-Cretaceous times.

## PALEONTOLOGY

The first reviews of Burmese amber arthropods were by Ross & York (2000), who listed the published (type and figured) specimens to that date, and Rasnitsyn & Ross (2000), who listed the families represented in the collections of the Natural History Museum, London (BMNH), including both published and unpublished specimens. The BMNH housed the only scientific collection of Burmese amber at the time, collected early in the 20th Century by R.C.J. Swinhoe (Grimaldi et al. 2002). At the turn of the 21st Century, the arachnid list consisted of one unidentified scorpion (figured in Ross 1998); four specimens of two published pseudoscorpion species (Cockerell 1917a, 1920), and 34 unidentified; 164 mites and ticks, including at least six families, the majority (122) unidentified, and one published (Cockerell 1917b); and 36 spiders in 7 families, but 26 unidentified. The four orders of arachnids known from Burmese amber numbered 239 specimens out of a total of 1198 arthropods in the collection (~20%). Grimaldi et al. (2002) included both BMNH and American Museum of Natural History (AMNH) specimens in their survey, the latter collection having been made in the ensuing two years and amounting to three times as many plant and animal inclusions as those listed for London. These authors added three scorpion fragments, 11 undetermined pseudoscorpions, 207 mites (206 undetermined and one tick), and 128 spiders (10 specimens in eight families, 118 undetermined), making a total of four scorpions, 49 pseudoscorpions, 371 mites and ticks, and 162 spiders: 586 arachnid specimens altogether. A survey by Ross et al. (2010) produced



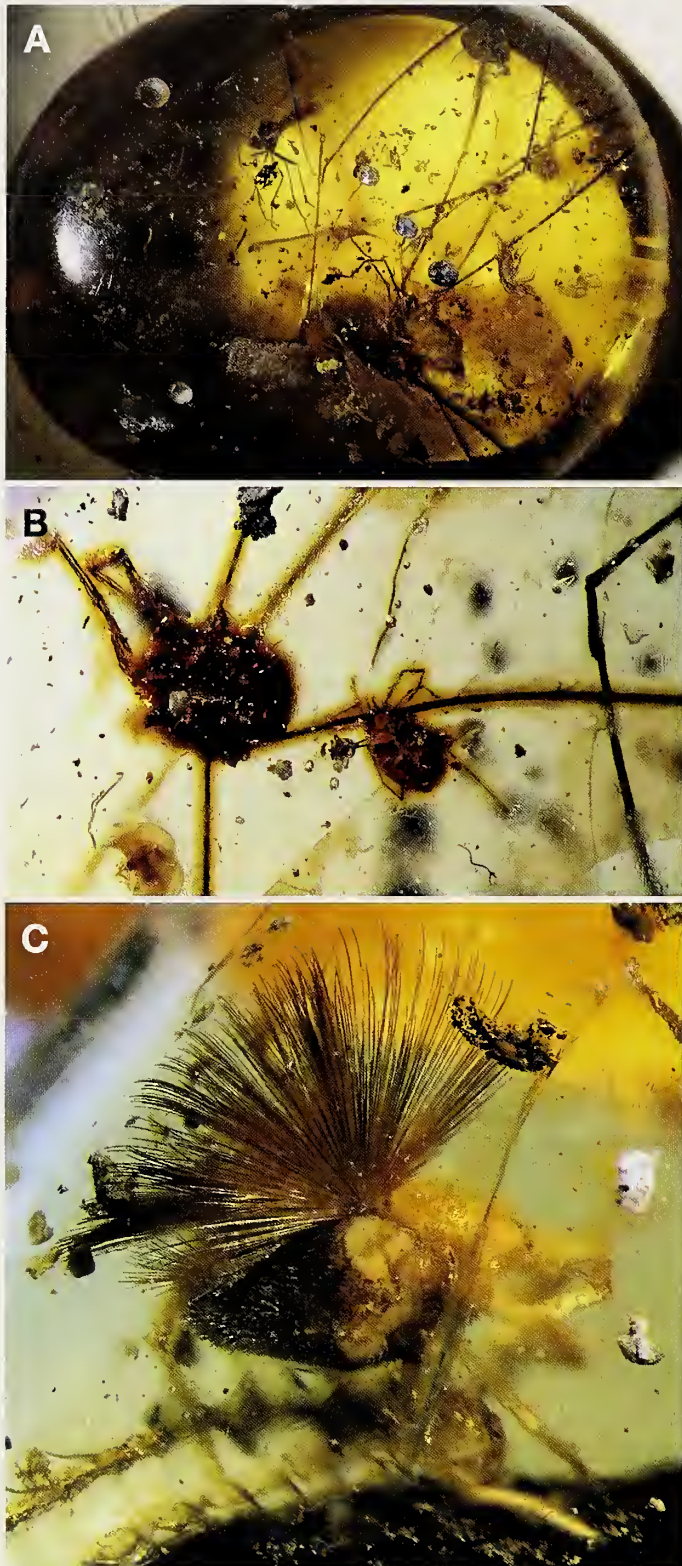


Figure 2.—A. Typical polished cabochon of Burmese amber, containing arthropod inclusions as well as bubbles and debris; B. Acariformes attached (or adjacent?) to the leg of an opilionid; C. Undescribed Acariformes.

the first Opiliones Sundevall, 1833 (two species: Giribet & Dunlop 2005; Poinar 2008), the first described scorpions (two species: Lourenço 2002; Santiago-Blay et al. 2004), two more mites (Poinar & Brown 2003; Poinar & Buckley 2008), and 19 spider species (Penney 2003a, 2004a, 2005; Wunderlich, 2008b). Rasnitsyn et al. (2016) surveyed all Cretaceous ambers, with a supplementary chart listing many recently identified but undescribed arachnids, especially acariform mites. Ross (2017) has published an online list of Burmese amber biota, including arachnids, based on Ross et al. (2010) updated to include the most recent records. Table 1 is a list of families and described species of arachnids recorded from Burmese amber, updated from Ross (2017). Unless otherwise stated, all specimens illustrated here are held in the collections of the College of Life Sciences, Capital Normal University, Beijing.

#### Order Acariformes Zaehvatkin, 1952

While a great many mites are known from Burmese amber (e.g., listed by Kartsev & Makarova in Rasnitsyn & Ross 2000, and Rasnitsyn et al. 2016) (Figs. 2B,C), only two have been described in the literature: *Cheyletus burmiticus* Cockerell, 1917b, and *Protoresinacarus brevipedis* Khaustov & Poinar, 2010. *Cheyletus burmiticus* was placed in the modern family Cheyletidae Leach, 1815, which also contains fossil mites from the Eocene Baltic amber (Koch & Berendt 1854) and Green River (Bradley 1931) deposits. Cheyletidae Leach, 1815 is a large family of mites belonging to the Parasitengona Oudemans, 1909; they are mostly free-living predators but some are permanent ectoparasites of small mammals and birds at the present day. Regarding *C. burmiticus*, Bochkov & Sidorchuk (2016) concluded that it is a heteromorphic male of a free-living cheyletid.

*Protoresinacarus brevipedis* was placed in the extant, previously monotypic family Resinacaridae Mahunka, 1975 (cohort Heterostigmatina Berlese, 1899, superfamily Pyemotoidea Oudemans, 1937) by Khaustov & Poinar (2010). The specimens occur adjacent to a mantispid neuropteran, *Doratomantispa burmanica* Poinar, 2011 (in Poinar & Buckley 2011), from which the authors concluded that the mites were phoretic.

A great many specimens of acariform mites in Burmese amber are undescribed and available for study. A list of identified families was provided by Sidorchuk in the supplementary information of the paper by Rasnitsyn et al. (2016).

#### Order Amblypygi Thorell, 1882

The first Burmese amber amblypygid to be described was *Kronocharon prendinii* Engel & Grimaldi, 2014. Two additional species were described by Wunderlich (2015a): *K. engeli* Wunderlich, 2015 and *K. longicalcaris* Wunderlich, 2015. Interestingly, the holotype of *K. prendinii* is an adult female preserved with three nymphs in the same piece of amber, inferring the possible antiquity of maternal care in these animals. An undescribed specimen of *Kronocharon* is illustrated here (Fig. 3). Fossil amblypygids are known from the Carboniferous of Europe and North America, the Cretaceous (Dunlop & Martill 2002), and Cenozoic ambers (Dunlop et al. 2017). These nocturnal animals inhabit crevices in bark, under



Table 1.—List of families and described species of arachnids recorded from Burmese amber. Data mainly from Ross (2017), updated. Note: some of these determinations are erroneous; see text for details.

---

Arachnida (12 orders, 87 families, 123 genera, 213 species)
Acariformes (15 families, 2 genera, 2 species)
Anystidae
Archaeorhynchidae
Bdellidae
Caceulidae
Cheyletidae
<i>Cheyletus burmiticus</i> Cockerell, 1917b
Enantiopidae?
Eremaeidae
Erythraeidae
Eupodidae
Gymnodameidae
Malaconothridae?
Neoliodidae
Oribatellidae
Oribotritidae?
Resinacaridae
<i>Protoresinacarus brevipedis</i> Khaustov & Poinar, 2010
Tuckerellidae
Amblypygi (1 genus, 3 species)
Family incertae sedis
<i>Kronocharon engeli</i> Wunderlich, 2015a
<i>Kronocharon longicalcaris</i> Wunderlich, 2015a
<i>Kronocharon prendinii</i> Engel & Grimaldi, 2014
Araneae (38 families, 93 genera, 165 species)
Archaeidae
<i>Burmesarchaea alissa</i> Wunderlich, 2017b
<i>Burmesarchaea caudata</i> Wunderlich, 2017b
<i>Burmesarchaea crassicauda</i> Wunderlich, 2017b
<i>Burmesarchaea crassicauda</i> Wunderlich, 2017b
<i>Burmesarchaea gibber</i> Wunderlich, 2017b
<i>Burmesarchaea gibberoides</i> Wunderlich, 2017b
<i>Burmesarchaea grimaldii</i> (Penney, 2003a)
<i>Burmesarchaea longicollum</i> Wunderlich, 2017b
<i>Burmesarchaea longissipes</i> Wunderlich, 2015b
<i>Burmesarchaea pilosus</i> Wunderlich, 2015b
<i>Burmesarchaea propinqua</i> Wunderlich, 2017b
<i>Burmesarchaea pseudogibber</i> Wunderlich, 2017b
<i>Burmesarchaea pustulata</i> Wunderlich, 2017b
<i>Burmesarchaea quadrata</i> Wunderlich, 2017b
<i>Burmesarchaea speciosus</i> Wunderlich, 2008b
<i>Eomysmauchenius dubius</i> Wunderlich, 2017b
<i>Eomysmauchenius septentrionalis</i> Wunderlich, 2008b
<i>Filiauchenius panchentatus</i> Wunderlich, 2008b
<i>Planarchaea kopp</i> Wunderlich, 2015b
<i>Planarchaea oblonga</i> Wunderlich, 2017b
<i>Planarchaea ovata</i> Wunderlich, 2017b
†Burmediatynidae
<i>Burmediatyna clava</i> Wunderlich, 2015b
<i>Burmediatyna excavata</i> Wunderlich, 2015b
<i>Burmediatyna pectin</i> Wunderlich, 2008b
<i>Burmediatyna postcopula</i> Wunderlich, 2017b
<i>Eodeinopsis longipes</i> Wunderlich, 2017b
†Burmascutidae
<i>Burmascutum aenigma</i> Wunderlich, 2008b
†Burmatheleidae
<i>Burmathele biseriata</i> Wunderlich, 2017b
Corinnidae?
†Cretaceothelidae
<i>Cretaceothele lata</i> Wunderlich, 2015b

---

Table 1.—Continued.

---

Deinopidae
<i>Deinopides tranquillus</i> Wunderlich, 2017b
Dipluridae
<i>Cethegoides patricki</i> Wunderlich, 2017b
<i>Phyxioschemoides collembola</i> Wunderlich, 2015b
†Eopsilodercidae
<i>Eopsilodermes loxosceloides</i> Wunderlich, 2008b
<i>Eopsilodermes serenitas</i> Wunderlich, 2015b
<i>Loxodermes curvatus</i> Wunderlich, 2017b
<i>Loxodermes longicymbium</i> Wunderlich, 2017b
<i>Loxodermes rectus</i> Wunderlich, 2017b
<i>Praepholcus hnberi</i> Wunderlich, 2017b
†Fossilcalcaridae
<i>Fossilcalcar praeteritus</i> Wunderlich, 2015b
Hersiliidae
<i>Burmesiola cretacea</i> Wunderlich, 2011
<i>Burmesiola daviesi</i> Wunderlich, 2015b
<i>Spinasilia dissoluta</i> Wunderlich, 2015b
Hexathelidae
<i>Alloatrax incertus</i> Wunderlich, 2017b
†Lagonomegopidae
<i>Albiburmops annulipes</i> Wunderlich, 2017b
<i>Archaelagonops propinquus</i> Wunderlich, 2015b
<i>Archaelagonops salticoides</i> Wunderlich, 2012b
<i>Archaelagonops scorsum</i> Wunderlich, 2015b
<i>Burlagonomegops eskovi</i> Penney, 2005
<i>Cymbiolaganops cymbiolacalcar</i> Wunderlich, 2015b
<i>Lagonoburmops phinosus</i> Wunderlich, 2012b
? <i>Lagonomegops tuber</i> Wunderlich, 2015b
<i>Lineaburmops beigeli</i> Wunderlich, 2015b
<i>Lineaburmops hirsutipes</i> Wunderlich, 2015b
<i>Myanlagonops gracilipes</i> Wunderlich, 2012b
<i>Parviburmops brevipes</i> Wunderlich, 2015b
? <i>Parviburmops bigibber</i> Wunderlich, 2017b
? <i>Paxillomegops brevipes</i> Wunderlich, 2015b
? <i>Paxillomegops comutus</i> Wunderlich, 2017b
<i>Paxillomegops longipes</i> Wunderlich, 2015b
<i>Picturmegops signatus</i> Wunderlich, 2015b
<i>Planinegops parvus</i> Wunderlich, 2017b
Lepetonetidae
<i>Palaeoleptoneta calcar</i> Wunderlich, 2012b
<i>Palaeoleptoneta crns</i> Wunderlich, 2017b
†Micropalpinidae
<i>Micropalpinus poinari</i> Wunderlich, 2008b
†Mongolarachnidae
<i>Longissipalpus cochlea</i> Wunderlich, 2017b
<i>Longissipalpus magnus</i> Wunderlich, 2015b
<i>Longissipalpus maior</i> Wunderlich, 2015b
<i>Longissipalpus minor</i> Wunderlich, 2015b
<i>Pedipalparamus seldeni</i> Wunderlich, 2015b
Mysmenidae?
Nephilidae?
‘ <i>Nephila</i> ’ <i>burmanica</i> (Poinar & Buckley, 2012)
Oecobiidae
<i>Retroecobius chomskyi</i> Wunderlich, 2015b
<i>Retroecobius convexus</i> Wunderlich, 2015b
<i>Zanilia aculeopectens</i> Wunderlich, 2015b
<i>Zanilia antecessor</i> Wunderlich, 2008b
<i>Zanilia quattornammillae</i> Wunderlich, 2015b
Oonopidae
<i>Burmorchestia acuminata</i> Wunderlich, 2017b
<i>Burmorchestia biangulata</i> Wunderlich, 2017b
<i>Burmorchestia plana</i> Wunderlich, 2017b
<i>Burmorchestia pulcher</i> Wunderlich, 2008b

---



Table 1.—Continued.

---

<i>Burmorchestina pulcheroides</i> Wunderlich, 2017b
<i>Burmorchestina tuberosa</i> Wunderlich, 2017b
Palpimanidae
†Parvithelidae
<i>Parvithela muelleri</i> Wunderlich, 2017b
<i>Parvithela spinipes</i> Wunderlich, 2017b
<i>Pulvillothela hanpti</i> Wunderlich, 2017b
†Pholcochyroceridae
<i>Autotomiana hirsutipes</i> Wunderlich, 2015b
<i>Pholcochyrocer altipecten</i> Wunderlich, 2017b
? <i>Pholcochyrocer baculum</i> Wunderlich, 2012b
<i>Pholcochyrocer guttulaeque</i> Wunderlich, 2008b
<i>Pholcochyrocer pecten</i> Wunderlich, 2012b
<i>Spinicreber antiquus</i> Wunderlich, 2015b
<i>Spinipalpus vetus</i> Wunderlich, 2015b
†Plumorsolidae
<i>Burmorsolus nonplumosus</i> Wunderlich, 2015b
<i>Pseudorsolus crassus</i> Wunderlich, 2015b
†Pracarancidae
<i>Praearaneus bruckschi</i> Wunderlich, 2017b
†Praeterleptonetidae
<i>Biapophyses beate</i> Wunderlich, 2015b
<i>Crassitibia longispina</i> Wunderlich, 2015b
<i>Crassitibia tenuimana</i> Wunderlich, 2015b
<i>Curvitibia curima</i> Wunderlich, 2015b
<i>Groehniatus birmanicus</i> Wunderlich, 2015b
<i>Hypotheridiosoma falcata</i> Wunderlich, 2015b
<i>Hypotheridiosoma paracymbium</i> Wunderlich, 2012b
<i>Palaeohydropoda myanmarensis</i> Penney, 2004a
<i>Parvispina tibialis</i> (Wunderlich, 2011)
<i>Praeterleptoneta spinipes</i> Wunderlich, 2008b
<i>Spinipalpitibia maior</i> Wunderlich, 2015b
Psilodercidae
<i>Aculeatosoma pyritmutatio</i> Wunderlich, 2017b
<i>Leclercera ellenbergeri</i> Wunderlich, 2015b
<i>Leclercera longissipes</i> Wunderlich, 2012b
<i>Leclercera sexaculeata</i> Wunderlich, 2015b
<i>Leclercera spicula</i> Wunderlich, 2012b
<i>Priscaleclercera paucispina</i> Wunderlich, 2017b
<i>Priscaleclercera brevispina</i> Wunderlich, 2017b
<i>Proterpsilodermes longisetae</i> Wunderlich, 2015b
? <i>Psilodermes filiformis</i> Wunderlich, 2012b
Segestriidae
<i>Denticulsegestia rigosa</i> Wunderlich, 2015b
<i>Myansegestia caederens</i> Wunderlich, 2015b
<i>Myansegestia engin</i> Wunderlich, 2015b
<i>Parvosegestria longitibialis</i> Wunderlich, 2015b
<i>Parvosegestria obscura</i> Wunderlich, 2015b
<i>Parvosegestria pintgn</i> Wunderlich, 2015b
<i>Parvosegestria triplex</i> Wunderlich, 2015b
Sparassidae?
†Spatiatoridae
<i>Spatiator putescens</i> Wunderlich, 2015b
Telemidae
? <i>Telemoplila crassifemoralis</i> Wunderlich, 2017b
Tetrablemmidae
<i>Bicornoculus levis</i> Wunderlich, 2015b
<i>Brignoliblennum bizarre</i> Wunderlich, 2017b
<i>Brignoliblennum nala</i> Wunderlich, 2017b
<i>Brignoliblennum paranala</i> Wunderlich, 2017b
<i>Cymbioblennum coniger</i> Wunderlich, 2017b
<i>Electroblennium bifida</i> Selden, Zhang & Ren, 2016c
? <i>Eogamasomorpha clara</i> Wunderlich, 2015b
<i>Eogamasomorpha hamata</i> Wunderlich, 2017b

---

Table 1.—Continued.

---

? <i>Eogamasomorpha unicomis</i> Wunderlich, 2017b
<i>Eogamasomorpha mibila</i> Wunderlich, 2008b
<i>Eoscaphiella ohlhoffi</i> Wunderlich, 2011
<i>Furcembolus andersoni</i> Wunderlich, 2008b
<i>Furcembolus crassitibia</i> Wunderlich, 2017b
<i>Furcembolus grossa</i> Wunderlich, 2017b
<i>Furcembolus longior</i> Wunderlich, 2017b
<i>Longissithorax myanmarensis</i> Wunderlich, 2017b
<i>Longithorax furca</i> Wunderlich, 2017b
<i>Palpalpaculla pulcher</i> Wunderlich, 2017b
<i>Praeterpaculla armatura</i> Wunderlich, 2015b
<i>Praeterpaculla biacuta</i> Wunderlich, 2015b
<i>Praeterpaculla dissolata</i> Wunderlich, 2015b
<i>Praeterpaculla equester</i> Wunderlich, 2015b
<i>Praeterpaculla tuberosa</i> Wunderlich, 2015b
<i>Sactosoma filiembolus</i> Wunderlich, 2012b
<i>Uniscutosoma aberrans</i> Wunderlich, 2015b
Tetragnathidae?
Thomisidae?
Theridiosomatidae
<i>Leviunguis bruckschi</i> Wunderlich, 2012b
Theridiidae
<i>Cretotheridion inopinatum</i> Wunderlich, 2015b
Uloboridae
<i>Bicalanistrum mixtum</i> Wunderlich, 2015b
<i>Burmuloborus antefixus</i> Wunderlich, 2015b
<i>Burmuloborus parvus</i> Wunderlich, 2008b
? <i>Burmuloborus prolongatus</i> Wunderlich, 2015b
<i>Furculoborus patellaris</i> Wunderlich, 2017b
<i>Kachin fruticosus</i> Wunderlich, 2017b
<i>Kachin fruticosoides</i> Wunderlich, 2017b
<i>Microuloborus birmanicus</i> Wunderlich, 2015b
<i>Oculloborus curvatus</i> Wunderlich, 2012b
<i>Palaeoniagrammopes vesica</i> Wunderlich, 2008b
<i>Paramiagrammopes cretaceus</i> Wunderlich, 2008b
<i>Paramiagrammopes longichypeus</i> Wunderlich, 2015b
<i>Paramiagrammopes patellidens</i> Wunderlich, 2015b
<i>Propterbachin magnoculus</i> Wunderlich, 2017b
†Vetiatoridae
<i>Pekkachilus vesica</i> Wunderlich, 2017b
<i>Vetiator gracilipes</i> Wunderlich, 2015b
Opiliones (3 families, 3 genera, 3 species)
Epedanidae
<i>Petrobunoides sharmai</i> Selden, Dunlop, Giribet, Zhang & Ren, 2016
†Halithersidae
<i>Halitherses grimaldii</i> Giribet & Dunlop, 2005
Stylocellidae
<i>Palaeosiro burmanicum</i> Poinar, 2008
Palpigradi (1 family, 1 genus, 1 species)
Eukoeneriidae
<i>Electrokoeneria yaksha</i> Engel & Huang, 2016
Parasitiformes (4 families, 4 genera, 4 species)
Argasidae
Ixodidae
<i>Amblyomma</i> sp.
<i>Amblyomma birmitum</i> Chitimia-Dobler et al., 2017
<i>Comphriscutula vetulum</i> Poinar & Buckley, 2008
<i>Cornupalpatum burmanicum</i> Poinar & Brown, 2003
Opilioacaridae
? <i>Opilioacarus groehni</i> Dunlop & Oliviera Bernardi, 2014
Polyaspididae
Pseudoscorpiones (4 families, 3 genera, 3 species)
Cheiridiidae

---



Table 1.—Continued.

<i>Electrobisium acutum</i> Cockerell, 1917a
Chernetidae
Feaellidae
<i>Protofeaella peetersae</i> Henderickx, 2016
Garypinidae
<i>Amblyolpium burmiticum</i> (Cockerell, 1920)
Ricinulei (4 families, 4 genera, 7 species)
†Hirsutisomatidae
<i>Hirsutisoma acutiformis</i> Wunderlich, 2017b
<i>Hirsutisoma bruckschi</i> Wunderlich, 2017b
<i>Hirsutisoma denticulata</i> Wunderlich, 2017b
†Monooculricinuleidae
<i>Monooculricinuleus incisus</i> Wunderlich, 2017b
<i>Monooculricinuleus semiglobulus</i> Wunderlich, 2017b
†Poliocheridae
? <i>Poliochera cretacea</i> Wunderlich, 2012b
†Primoricinuleidae
<i>Primoricinuleus pugio</i> Wunderlich, 2015b
Schizomida
Scorpiones (7 families, 9 genera, 22 species)
Buthidae
<i>Archaeoananteroides maderai</i> Lourenço, 2016 in Lourenço & Velten (2016b)
Chaerilidae
<i>Electrochaerilus buckleyi</i> Santiago-Blay, Fet, Solegrad & Anderson, 2004
†Chaerilobuthidae
<i>Chaerilobuthus birmanicus</i> Lourenço, 2015f
<i>Chaerilobuthus bruckschi</i> Lourenço, 2015f
<i>Chaerilobuthus complexus</i> Lourenço & Beigel, 2011
<i>Chaerilobuthus enigmaticus</i> Lourenço, 2015d
<i>Chaerilobuthus gigantosternum</i> Lourenço, 2016a
<i>Chaerilobuthus longiaculeus</i> Lourenço, 2013
<i>Chaerilobuthus schwarzi</i> Lourenço, 2015 in Lourenço & Velten (2015)
<i>Chaerilobuthus serratus</i> Lourenço, 2016a
†Palaeoburmesebuthidae
<i>Betaburmesebuthus bellus</i> Lourenço, 2016b
<i>Betaburmesebuthus bidentatus</i> Lourenço, 2015c
<i>Betaburmesebuthus fleissneri</i> Lourenço, 2016 in Lourenço & Velten (2016)
<i>Betaburmesebuthus kobberti</i> Lourenço, 2015 Lourenço & Beigel (2015)
<i>Betaburmesebuthus laraflaissnerae</i> Lourenço, 2016 in Lourenço & Velten (2016c)
<i>Betaburmesebuthus muelleri</i> Lourenço, 2015c
<i>Palaeoburmesebuthus grimaldii</i> Lourenço, 2002
<i>Palaeoburmesebuthus ohlhoffi</i> Lourenço, 2015f
†Palaeoescorpiidae
<i>Archaeoscorpis cretacicus</i> Lourenço, 2015e
<i>Burmesescorpiops groehni</i> Lourenço, 2016a
†Palacotrilineatidae
<i>Palaeotrilineatus ellenbergeri</i> Lourenço, 2012
†Sucinolourencoidae
<i>Sucinlourencous adrianae</i> Rossi, 2015
Solifugae (1 genus, 1 species)
Family incertae sedis
<i>Cushingia ellenbergeri</i> Dunlop, Bird, Brookhart & Bechly, 2015
Thelyphonida (1 family, 2 genera, 2 species)
Thelyphonidae
<i>Mesothelyphonus parvus</i> Cai & Huang, 2016
Family incertae sedis
<i>Burmathelyphonia prima</i> Wunderlich, 2015a



Figure 3.—Undescribed specimen of the amblypygid *Kronocharon* Engel & Grimaldi, 2014, scale bar = 1 mm.

stones, and in caves, generally in humid tropical and subtropical regions of the world.

#### Order Araneae Clerck, 1757

By far the largest number of arachnids recorded in Burmese amber belong to this order (some 165 described species in 93 genera), mainly due to the work of Wunderlich (2008a,b, 2011a, 2012b, 2015b, 2017b). The first spiders described from Burmese amber, however, were by Penney (2003a, 2004a, 2005, 2006a). Of the 38 spider families found in the amber, 16 are extinct. The first Mesozoic member of the primitive suborder Mesothelae Pocock, 1892 was described by Wunderlich (2015b) as *Cretaceothele lata* Wunderlich, 2015b (Fig. 4B). Later, Wunderlich (2017b) described three new genera, including the first adult males, and placed the Cretaceous mesotheles in three new extinct families: Burmathelidae Wunderlich, 2017b (Fig. 4A), Cretaceothelidae Wunderlich, 2017b, and Parvithelidae Wunderlich, 2017b. Mesotheles are known today only from south-east Asia, including China and Japan, but are known from the Euramerican region which was tropical in the Carboniferous and Permian periods (Dunlop et al. 2017).

A number of mygalomorphs are known in Burmese amber, including members of Hexathelidae Simon, 1892, Atypidae Thorell, 1870, Dipluridae Simon, 1889 (Fig. 4C), and the extinct Fossilcalcaridae Wunderlich, 2015b. They are repre-





Figure 4.—Mesothele, mygalomorph and haplogyne Araneae in Burmese amber. A. Mesothele spider (possibly *Burmathele* Wunderlich, 2017), dorsal view; B. Mesothele spider (possibly *Cretaceothele* Wunderlich, 2015), dorsal view; C. Mygalomorph spider (Dipluridae?); D. Ochyroceratid spider.

sented predominantly by adult males (no females but some juveniles and exuviae), presumably because adult males leave their retreats to search for females.

Among araneomorph spiders, the haplogynes are well represented in the Burmese amber biota, with some 88 species in 45 genera. Four extinct families of haplogynes erected by Wunderlich are known exclusively from Burmese amber: *Praeterleptonetidae* Wunderlich, 2008b, *Pholcochyroceridae* Wunderlich, 2008b, *Eopsilodercidae* Wunderlich, 2008b, and *Plumorsolidae* Wunderlich, 2008b. As has been mentioned elsewhere (Selden & Penney 2010), Wunderlich's fossil families are generally diagnosed by unclear characters or combinations of characters of related families; they have never been tested cladistically, and the plethora of new names which result from inadequate description serves to muddle rather than elucidate relationships of these fossil spiders. *Mongolarachnidae* Selden, Shi & Ren, 2013 was established for a Jurassic genus of possibly orb weavers from China; Wunderlich (2015b, 2017b)

added two new genera and five species from Burmese amber to this family, which he (Wunderlich 2015b) also moved to the Haplogynae. Among living haplogynes, members of *Ochyroceratidae* Fage, 1912 (including *Psilodercidae* Deeleman-Rheinhold, 1995; Fig. 4D), *Tetrablemmidae* O. Pickard-Cambridge, 1873, *Oonopidae* Simon, 1890, and *Segestriidae* Simon, 1893 are well represented (Figs. 5A,C,D). *Ochyroceratids* and *tetrablemmids* are exclusively tropical/subtropical families, *oonopids* are most diverse in the tropics, while *segestriids* are cosmopolitan in range.

Among the 33 araneomorph families reported in Burmese amber, 13 are extinct. *Micropalpinanidae* Wunderlich, 2008b, *Burmascutidae* Wunderlich, 2008b, *Burmadictynidae* Wunderlich, 2017b, and *Vetiatoridae* Wunderlich, 2017b were erected for a few Cretaceous amber forms. *Lagonomegopidae* Eskov & Wunderlich, 1994 is a large family of spiders only known from Cretaceous ambers. Its name derives from its most characteristic feature: two large eyes on the anterolateral



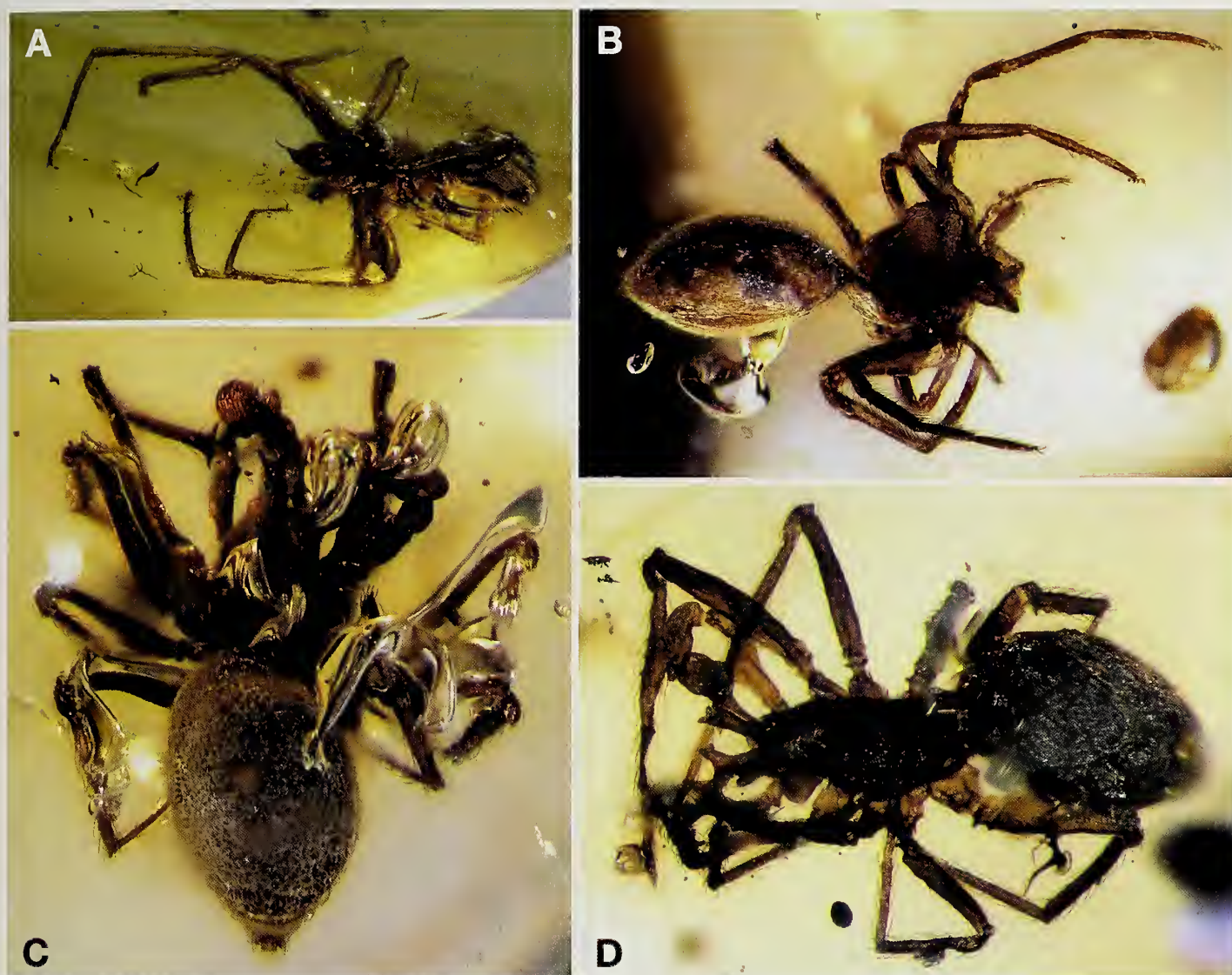


Figure 5.—Haplogye and entelegyne Araneae in Burmese amber. A. Segestriid; B. Lagonomegopid; C. Tetrablemmid *Electroblemma bifida* Selden, Zhang & Ren, 2016c, holotype, dorsal view; D. *Electroblemma bifida*, paratype, dorsolateral view.

flanks of the carapace, a character unknown in any other fossil or extant spider family. Eighteen species in 11 genera are known from Burmese amber (Wunderlich 2015b, 2017b) (Fig. 5B). Spatiatoridae Petrunkevitch, 1942 is a family erected for a Baltic amber genus, to which Wunderlich (2006, 2008a, 2011b) added further Baltic species and two from Burmese amber (Wunderlich 2015b). Wunderlich (2017b) erected a new family, Vetiatoridae, to accommodate *Vetiator* Wunderlich, 2015b, formerly included in Spatiatoridae, and a new genus, *Pekkachilus* Wunderlich, 2017b. A large number of Burmese amber entelegynes belong to the superfamily Palpimanoidea (*sensu* Wood et al. 2012). In addition to species in the Micropalpimanidae, Lagonomegopidae and Spatiatoridae already mentioned, there are 23 species in the extant family Archaeidae C.L. Koch & Berendt, 1854 (which, incidentally, was first described from fossils in Baltic amber). Palpimanoids are relatively common and diverse in the Mesozoic compared to the present day, with species known from the Jurassic and Cretaceous periods, as well as Cenozoic deposits.

Oecobiidae Blackwall, 1862 and Hersiliidae Thorell, 1870 are represented in the Burmese amber by five and three species, respectively. Members of both of these families are ground, rock and bark dwellers. Among cribellate orb weavers in Burmese amber, there are five described species in Wunderlich's (2017b) extinct family Burmadietynidae, 14 in the extant Uloboridae Thorell, 1869, and the possible deinopid *Deinopedes tranquillus* Wunderlich, 2017. Like palpimanoids, cribellate orb weavers are relatively common and diverse among Mesozoic spiders, with species known from the Jurassic as well as the Cretaceous and Cenozoic.

There are a few, mainly doubtful, records of araneoids from Burmese amber. Wunderlich (2008b:644) recorded a juvenile "Araneoidea fam. indet.". Wunderlich (2015b) described a supposed theridiid, *Cretotheridion inopinatum* Wunderlich, 2015, in a new subfamily, Cretotheridiinae Wunderlich, 2015, distinguished from all other theridiids by the lack of a theridioid tarsal comb of serrate bristles (a synapomorphy for Theridiidae Sundevall, 1833 + Nestieidae



Simon, 1894; Griswold et al. 1998) and the lack of a prosomal–opisthosomal stridulatory organ (common in theridiids). One member of the Theridiosomatidae Simon, 1881, *Leviunguis bruckschi* Wunderlich, 2012, has been described from Burmese amber, though many more species await description according to Wunderlich (2017b), and this family is also known from other Cretaceous deposits (Selden 2010; Penney 2014). Finally, *Geratonephila burmanica* Poinar in Poinar & Buckley, 2012 was described by Poinar & Buckley (2012) as a member of the Nephilidae Simon, 1894 (recently returned to Araneidae Simon, 1895 by Dimitrov et al. 2017). Poinar & Buckley (2012) proposed that this was the first evidence of sociality among spiders in the fossil record because there are two specimens which they considered were conspecifics. Penney (2013) considered that, while their description of the holotype as a nephiline was correct, the evidence of sociality was unproven (see also reply by Poinar & Buckley 2013). Wunderlich (2015b) synonymized *Geratonephila* with Recent *Nephila* Leach, 1815, agreed with the comments of Penney (2013) that there was no evidence that the two specimens were conspecific, nor that it showed sociality. From his long experience of working with Burmese amber, during which time he had never seen a nephiline in the deposit, Wunderlich (2015b) considered that the amber was more likely from the Dominican Republic, of Miocene age, in which deposit *Nephila* is quite common, and suggested it might belong to *Nephila tenuis* Wunderlich, 1986.

The RTA clade (Dionycha, Lycosoidea, Amaurobioidea, Dictynoidea: Sierwald 1990; Coddington & Levi 1991), is known from the Mesozoic only from questionable records, including some in Burmese amber, although its roots likely extend back to that era (Dimitrov et al. 2017). For example, the questionable juvenile thomisid listed in Rasnitsyn & Ross (2000) is more likely to be a lagonomegopid. Wunderlich 2008b: 652) described a molted skin as “Araneae indet. (RTA-clade?)” and, in the same article, several questionable Dictynidae O. Pickard-Cambridge, 1871. Wunderlich (2017b) added another doubtful member of the RTA clade from an immature male in Burmese amber. It is likely that this enormous group of spiders did not radiate until late in the Mesozoic, and many of its constituent families (e.g., Thomisidae Sundevall, 1833, Salticidae Blackwall, 1841) did not appear until the Cenozoic.

#### Order Opiliones Sundevall, 1833

Three genera and species of harvestman have been described from Burmese amber, yet many more are now available for study. *Halitherses grimaldii* Giribet & Dunlop, 2005 (Figs. 6A,C,D) was the first Mesozoic harvestman to be accurately described and named (previously recorded examples, not in amber, are either misidentified non-arachnids, or so poorly preserved as to be identifiable only as Opiliones). *Halitherses* was placed by Sharma & Giribet (2014) in Nemastomatidae Simon, 1879 (in the suborder Dyspnoi Hansen & Sørensen, 1904), but was later moved in its own extinct family, Halithersidae Dunlop, Selden & Giribet, 2016 following the discovery of a beautifully preserved penis (Dunlop et al. 2016) (Fig. 6C,D). Shear & Warfel (2016) have suggested that this family may belong within the superfamily Acropsopilionoidea Roewer, 1923.

*Palaeosiro burmanicum* Poinar, 2008 was the first Mesozoic record of the suborder Cyphophthalmi, and also the oldest record of the group; the oldest records prior to this are in Eocene Baltic and Bitterfeld ambers and were placed in the modern genus *Siro* Latreille, 1796 (Dunlop & Giribet 2003; Dunlop & Mitov 2011). *Palaeosiro* was originally placed in the European/North American family Sironidae before being transferred to the Southeast Asian family Stylocellidae by Giribet et al. (2012).

*Petrobunoides sharmai* Selden et al., 2016a (Figs. 6E,F) was described as the oldest member of the suborder Laniatores Thorell, 1876, and its first Mesozoic record; younger laniatoreans are known from Eocene Baltic and Miocene Dominican ambers (Cokendolpher & Poinar 1992; Ubick & Dunlop 2005). Selden et al. (2016a) placed *Petrobunoides* in the extant family Epedanidae Sørensen, 1886, which occurs today exclusively in south-east Asia, with a few species reaching as far north as Nepal and southern China (Kury 2007). Several additional Laniatores species are known from Burmese amber (Fig. 6B), which await formal description.

#### Order Palpigradi Thorell, 1888

Fossil palpigrades are extremely rare. Older references mentioned *Sternarthron zitteli* Haase, 1890 from the Altmühltal Formation (Solnhofen Limestone) of southern Germany, but this has been shown to be an insect nymph (Delclòs et al. 2008). Apart from the Burmese specimen mentioned below, the only other fossil palpigrade is *Paleokoenenia mordax* Rowland & Sissom, 1980, from the Pliocene Onyx Marble Formation (a cave deposit) of Arizona. Hence, the discovery of a fossil palpigrade in Burmese amber extended the fossil record of the group by some 95 million years. *Electrokoenenia yaksha* Engel & Huang in Engel et al. 2016 (Fig. 7A, B) was placed in the family Eukoeneriidae Petrunkevitch, 1955, the larger of the two extant families (4 genera, 85 named species; Giribet et al. 2014).

#### Order Parasitiformes Reuter, 1909

The Parasitiformes is the smaller of the two mite orders, and only 16 fossil species have been described (Dunlop et al. 2017), from strata of Cretaceous to Quaternary age. Of these, four are from the Burmese amber. *Opilioacarus groehni* Dunlop & Bernardi, 2014 is the oldest record of the suborder Opilioacarida Zachvatkin, 1952 (Fig. 7C), one of the most primitive acarine groups, whose members resemble tiny harvestmen. It was the third fossil opilioacarid to be described, others being known from Eocene Baltic amber (Dunlop et al. 2004, 2010).

A larval tick, *Amblyomma* sp., was identified by Klompen (in Grimaldi et al. 2002) and, most recently, a new species of *Amblyomma* has been described (Chitimia-Dobler et al. 2017). Two more larval ticks were described from the amber: *Cornupalpatum burmanicum* Poinar & Brown, 2003 and *Compluriscutata vetulum* Poinar & Buckley, 2008. All of these specimens belong to the modern family of hard ticks Ixodidae Koch, 1844 (suborder Ixodida Leach, 1815). Poinar (2015) has described patches of *Rickettsia*-like cells from the body cavity of the larval tick *Cornupalpatum burmanicum*.



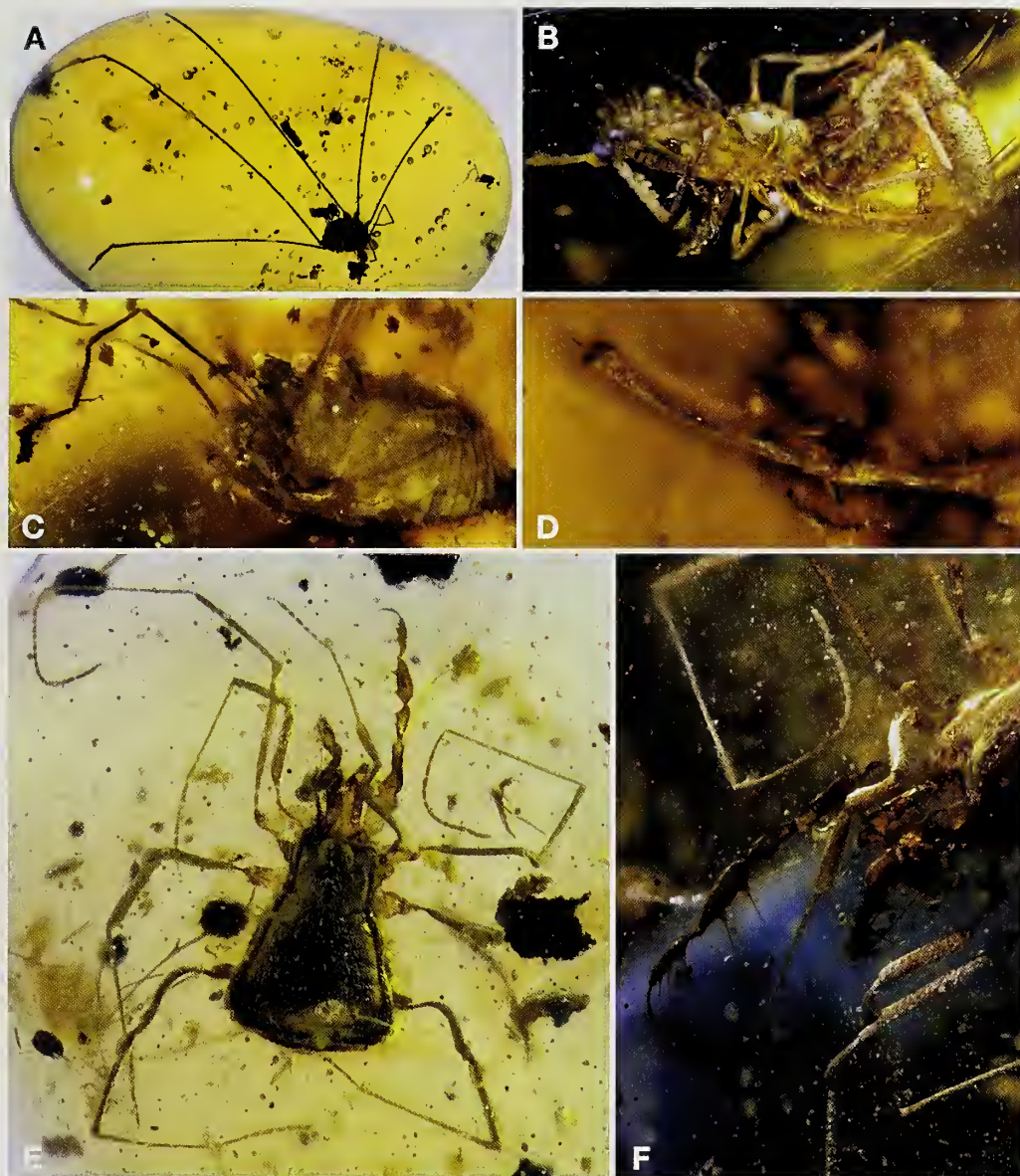


Figure 6.—Opiliones in Burmese amber. A. *Halitherses grimaldii* Giribet & Dunlop, 2005 in an amber cabochon; B. Undescribed Laniatores; C. *Halitherses grimaldii* side view of body; D. *Halitherses grimaldii* detail of extended penis (see Dunlop et al. 2016); E. The oldest described Laniatores, *Petrobunoides sharmai* Selden et al., 2016a, holotype, dorsal view; F. *Petrobunoides sharmai*, left frontal view, showing chelicerae, pedipalps, and parts of legs I and II.

#### Order Pseudoscorpiones Latreille, 1817

Two pseudoscorpions from Burmese amber were described early in the twentieth century by Cockerell (1917a, 1920): *Electrobisium acutum* Cockerell, 1917a and *Amblyolpium burmiticum* (Cockerell, 1920). *Electrobisium* was placed in the extant Neobisiidae Chamberlin, 1930 by Cockerell (1917a), but Judson (1997, 2000) moved it to another extant family, Cheiridiidae Hansen, 1894. *Amblyolpium burmiticum*, originally placed in the extant genus *Garypus* L. Koch, 1873, was placed in another extant genus, *Amblyolpium* Simon, 1898, in the extant family Garypinidae Daday, 1889.

More recently, a third species was described: *Protofeabella peetersae* Henderickx in Henderickx & Boone, 2016. Henderickx & Boone (2016) placed this species in Feaellidae Ellingsen,

1906, pointing out that the superfamily Feaelloidea Ellingsen, 1906 constitutes the most primitive group within the pseudoscorpions, according to the study of Muriénne et al. (2008). Judson (2017) studied an additional adult male of *Protofeabella* and considered it to be most likely a stem-group feaellid.

Judson (2000) mentioned the presence of fragmentary specimens of Chthonioidea and Cheliferoidea in the material housed in the BMNH. Many more pseudoscorpion specimens from Burmese amber (Fig. 8) are undergoing study at present, so a much greater diversity of this order is to be expected in the near future.

#### Order Ricinulei Thorell, 1876

Ricinulei is a small order of arachnids with extremely thick cuticle which live in tropical forests and caves. The first



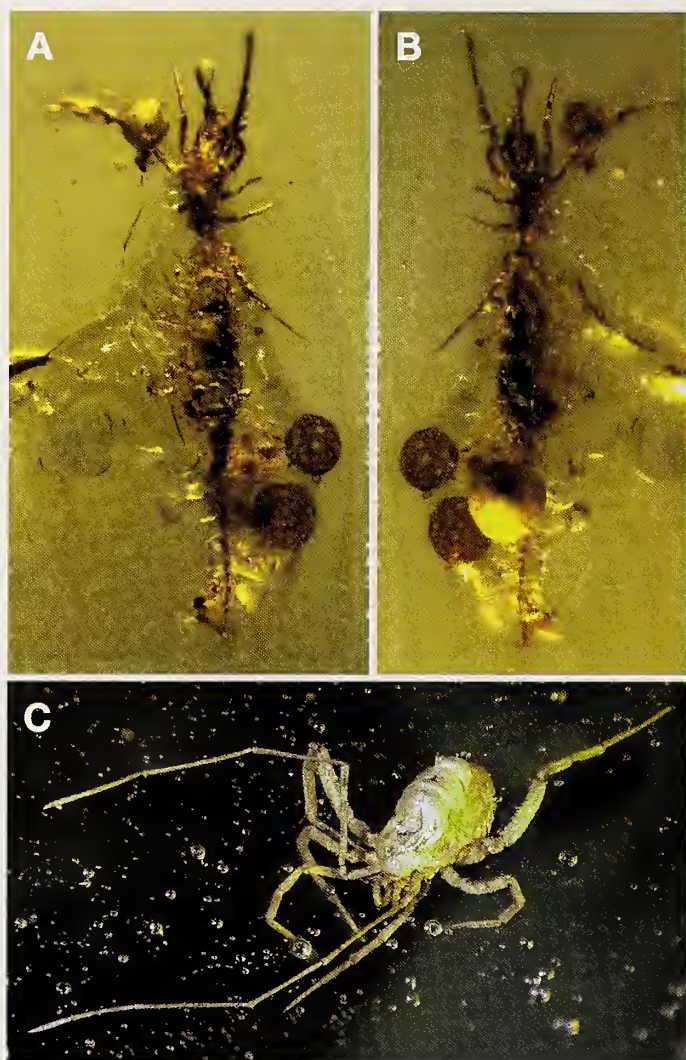


Figure 7.—Palpigradi and Parasitiformes in Burmese amber. A. Oldest known palpigrade, *Electrokoenia yaksha* Engel & Huang, 2016, holotype, dorsal view; B. Same, ventral view. Specimen in the collection of the Nanjing Institute of Geology and Palaeontology, Chinese Academy of Sciences, Nanjing, China. C. Parasitiformes: Opilioacarida.

species ever described was a fossil, mistaken for a beetle: *Curculioides ansticii* Buckland, 1837. Ricinulei occur today only in Central America and the Caribbean region (including Texas caves), and in West Africa. Until recently, fossil Ricinulei were known only from the Carboniferous. Wunderlich (2012a) described the first Mesozoic ricinuleid specimens as Ricinulei indet. and *?Poliochera cretacea* Wunderlich, 2012a (Fig. 9C). Later, Wunderlich (2015a) described another new genus and species as *Primorycinuleus pugio* Wunderlich, 2015a (Figs. 9A, B). Both of these Burmese amber species were known only from nymphs. Wunderlich (2015a) rearranged the higher classification of Ricinulei to accommodate unusual aspects of *Primorycinuleus*, which lacks visible opisthosomal segmentation and bears a reduced or absent fixed finger on the pedipalp. In Wunderlich's (2015a) scheme, all ricinuleids, living and extinct, would be in one suborder: Posteriorricinulei Wunderlich, 2015a, except for *Primorycinuleus*, for which the new

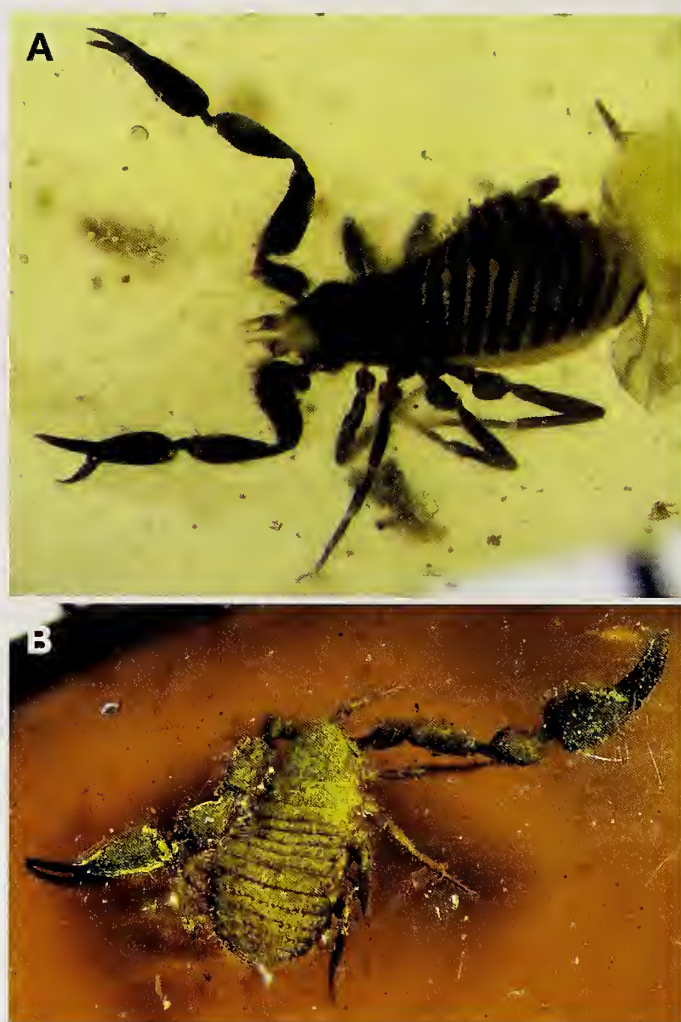


Figure 8.—Pseudoscorpiones in Burmese amber. A. Undescribed pseudoscorpion (Withiidae?); B. Undescribed pseudoscorpion (Chernetidae?).

suborder Primorycinulei Wunderlich, 2015a was erected. However, examination of the specimen (Wunderlich coll. F2635/BU/CJW) indicates that the pedipalp fixed finger is present on the right side. Nevertheless, the pedipalp morphology is unlike that seen in other ricinuleids, and the lack of obvious segmentation (although there are paired spots on the ventral surface where sulci would occur in other ricinuleids) is unusual, but probably not sufficient to place the nymphal specimen in its own suborder.

Wunderlich (2017a) described five more Burmese amber ricinuleids, in two new genera: *Hirsutisoma* Wunderlich, 2017a and *Monooculricinuleus* Wunderlich, 2017a, for which he also created monotypic families. He placed the new families in the suborder Primorycinulei on account of the wide sternum, the large eyes, absence of a median tarsal claw, and the presence of single, long finger on the pedipalp. *Hirsutisoma bruckschi* Wunderlich, 2017b is a complete adult male, showing the characteristic sperm transfer modifications of leg 3, and is the smallest known adult ricinuleid. *Hirsutisoma* shows extreme hairiness for a ricinuleid, particularly on the dorsal opisthosoma. *Monooculricinuleus* is named for the single pair of eyes on a median carapace eye tubercle: an extremely unusual



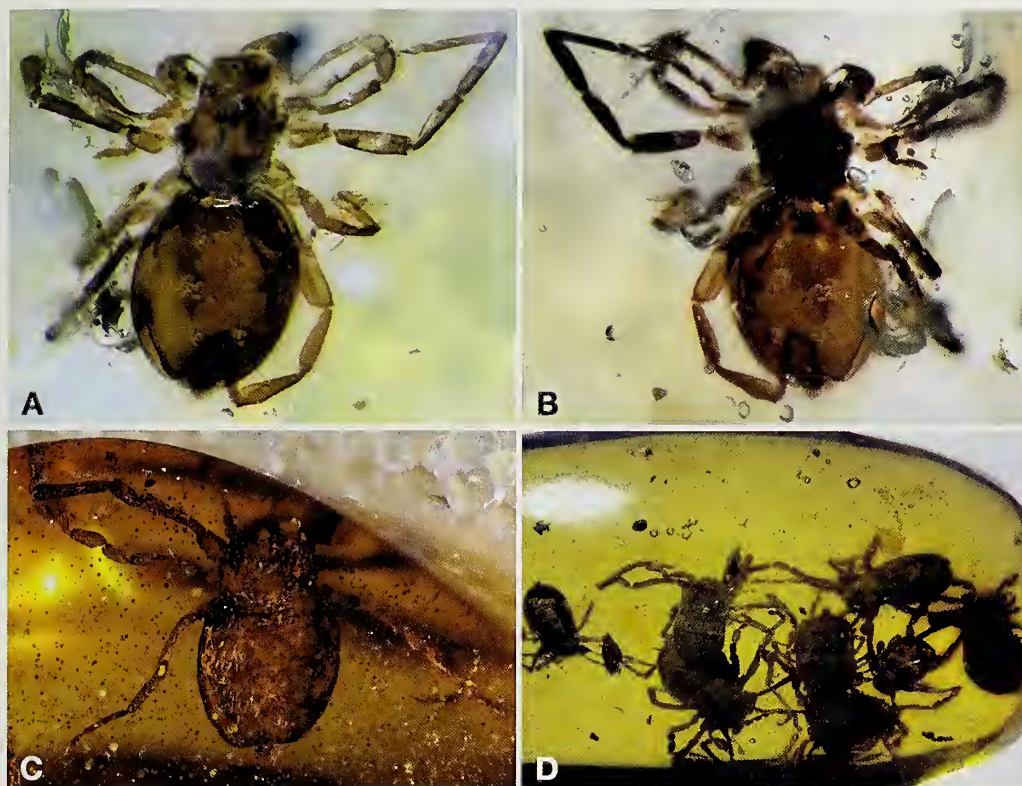


Figure 9.—Ricinulei in Burmese amber. A. *Primoricinuleus pugio* Wunderlich, 2015, dorsal view; B. Same, ventral view; C. *?Poliochera cretacea* Wunderlich, 2012, dorsal view; D. Aggregation of juvenile ricinuleids in a single amber cabochon.

feature compared to other ricinuleids. However, in a recent communication (Jörg Wunderlich *in litt.*, September 19, 2017), it appears that *Monooculricinuleus* is really an opilionid, and so requires redescription.

Ricinuleids are unknown today in Asia, so the presence of high diversity of this order in Burmese amber is evidence for a different, perhaps wider, distribution in the mid-Cretaceous than today, and that the present-day ricinuleid fauna is relict and impoverished compared to that of the past. Some specimens in Burmese amber show aggregations of juveniles (Fig. 9D), a phenomenon which has only recently been described for extant ricinuleids (García et al. 2015).

#### Order Schizomida Petrunkevitch, 1945

The fossil record of this small group of arachnids is sparse. They have been described only from the so-called Onyx Marble of Arizona, a cave deposit dated at probably Pliocene (c. 2.58–5.33 Ma) (Petrunkevitch 1945; Pierce, 1951), and Dominican amber, which is probably Miocene (c. 5–23 Ma) in age (Krüger & Dunlop 2010). Wunderlich (2015a) mentioned specimens of this order in Burmese amber, and a few dozen specimens have been examined in Burmese amber by the present authors, but none has yet been formally described. The Burmese example figured here (Fig. 10A) is the oldest record of the order, the first record of schizomids from the Mesozoic, and it at least doubles the fossil record of the group. Schizomids inhabit soils, litter and caves mostly in tropical regions.

#### Order Scorpiones C.L. Koch, 1851

To date, 22 species of scorpion in nine genera have been described from Burmese amber, mainly by Lourenço and colleagues (Lourenço 2002, 2003, 2012, 2013, 2015a,b,c,d,e, 2016a,b; Lourenço & Beigel 2011, 2015; Lourenço & Velten 2015, 2016a,b,c) and most have been placed in extinct buthoid families: Palaeoburmesebuthidae Lourenço, 2015e (7 spp.), Chaerilobuthidae Lourenço & Beigel, 2011 (8 spp.), Palaeotrilineatidae Lourenço, 2012 (1 sp.), Sucinlourencoidae Rossi, 2015 (1 sp.), and one (*Archaeoananteroides maderai* Lourenço, 2016 in Lourenço & Velten 2016b) has been assigned tentatively to the extant Buthidae C.L. Koch, 1837. The other two specimens have been referred to the Chactioidea Pocock, 1893: *Electrochaerilus buckleyi* Santiago-Blay et al., 2004, placed by its describers in a new subfamily of the extant Chaerilidae Pocock, 1893; and *Burmesescorpiops groehni* Lourenço, 2016a, placed in the extinct family Palaeoescorpiidae Lourenço, 2003. Fig. 10B shows the holotype specimen of *Betaburmesebuthus bellus* Lourenço, 2016b. It was pointed out by Dunlop & Penney (2012) that the relationships of the Cretaceous fossil scorpions are in need of testing with cladistic methods.

#### Order Solifugae Sundevall, 1833

The fossil record of Solifugae is very poor. In the Paleozoic, a single, very poorly preserved specimen, *Protosolpuga carbonaria* Petrunkevitch, 1913, from the Carboniferous of Illinois, is referable to this order. Two species are known from



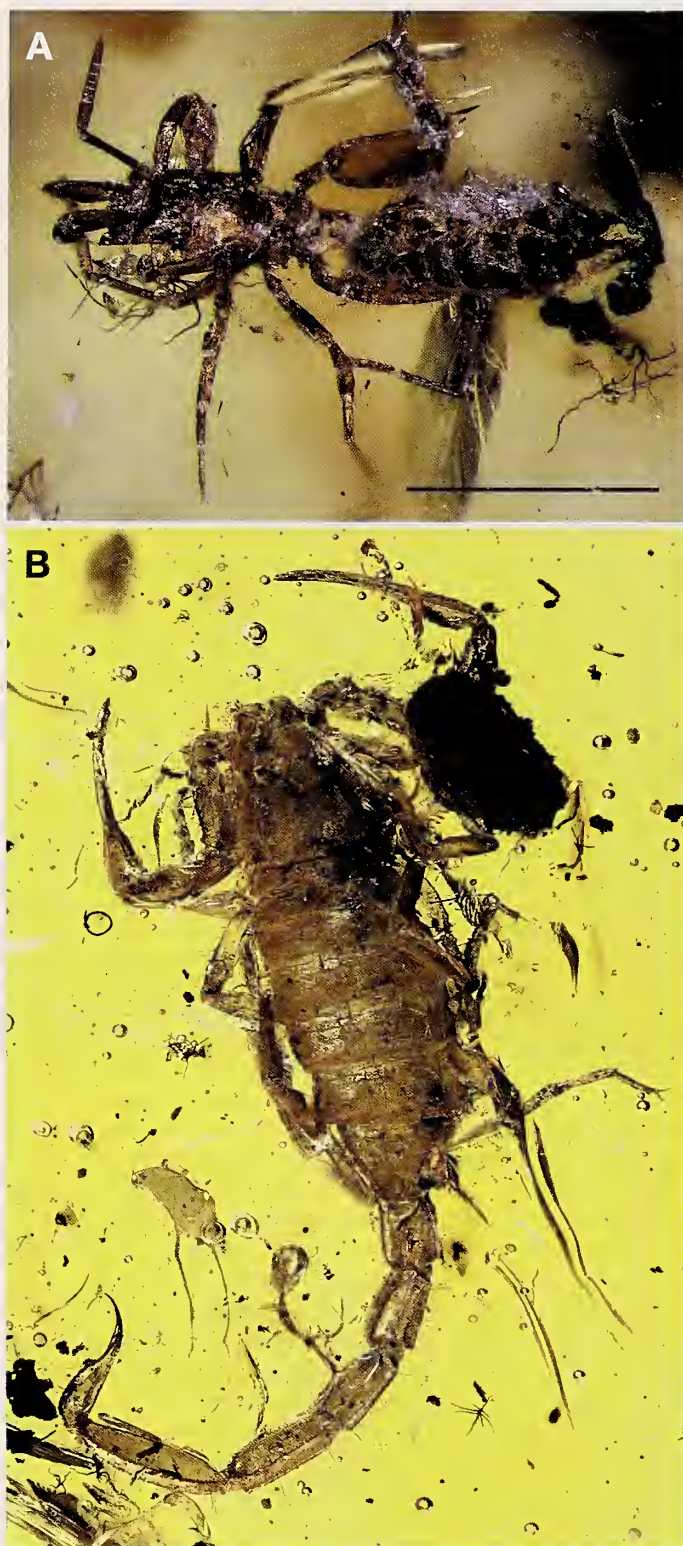


Figure 10.—Schizomida and Scorpiones in Burmese amber. A. Undescribed schizomid specimen, scale bar = 1 mm; B. Scorpion *Betaburmesebuthus bellus* Lourenço, 2016; specimen in the collection of the Museum of the Geological-Palaeontological Institut, University of Hamburg.

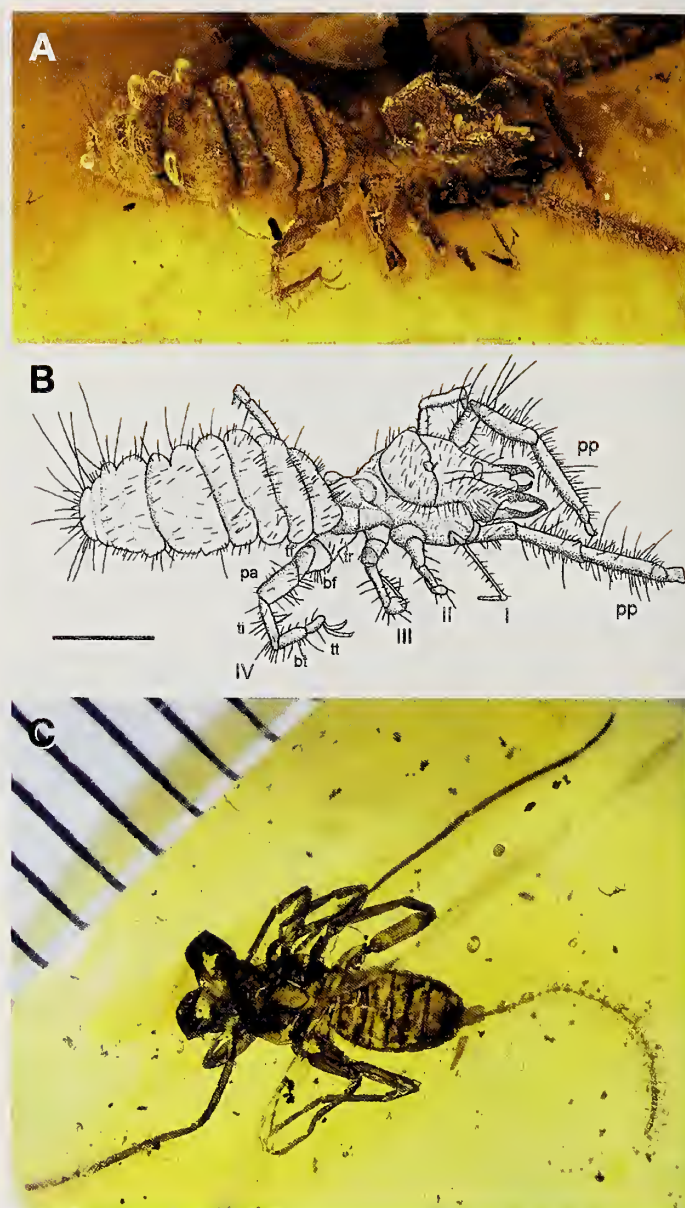


Figure 11.—Solifugae and Thelyphonida in Burmese amber. A. Solifuge *Cushingia* cf. *ellenbergeri* Dunlop et al., 2015, dorsolateral view; B. Same, explanatory drawing; bf basifemur, bt basitarsus, pa patella, pp pedipalp, tf telofemur, tt telotarsus, ti tibia, tr trochanter, legs numbered I–IV, scale bar = 1 mm (from Bartel et al. 2016); C. Undescribed specimen of thelyphonid *Mesothelyphonus parvus* Cai & Huang, 2017, with mm scale.

the Mesozoic: the Burmese amber one mentioned here, and one from the Cretaceous Crato Formation of Brazil (Selden & Shear 1996). Two species are known from Cenozoic ambers, from the Dominican Republic and the Baltic (Poinar & Santiago-Blay 1989; Dunlop et al. 2004, respectively). The single genus and species described from Burmese amber, *Cushingia ellenbergeri* Dunlop et al. 2015 (Fig. 11A, B) was not placed in a family, but it appears to have most characters in common with the living genus *Dinorhax*, which is the only extant species found in south-east Asia, and one of the few solifuges not associated with an arid environment (Dunlop et al. 2015; Bartel et al. 2016). Modern solifuges are associated



Table 2.—Numbers of described species of arachnid orders recorded in Burmese amber compared to other major Cretaceous ambers with arachnids. \* Schizomida are recorded herein but as yet undescribed. Data mainly from Dunlop et al. (2017), updated.

ORDER	MYANMAR	LEBANON	NEW JERSEY	SPAIN	CANADA	FRANCE	JORDAN
Acariformes	2			10	2	1	
Amblypygi	3						
Araneae	196	5	3	5	3	2	6
Opiliones	3						
Palpigradi	1						
Parasitiformes	4		1				
Pseudoscorpiones	3					1	
Ricinulei	8						
Schizomida	*						
Scorpiones	22	1				1	
Solifugae	1						
Thelyphonida	2						
TOTAL	244	6	4	15	5	5	6

with arid environments, so their occurrence in ambers derived from humid forests in the Mesozoic and Cenozoic hints at broader habitat tolerances in the past.

#### Order Thelyphonida Latreille, 1804

Fossil thelyphonids preserved in rock are known from seven species in the Carboniferous of Europe and North America, and one from the Cretaceous of Brazil (Tetlie & Dunlop 2008; Selden et al. 2016b; Dunlop et al. 2017). Two genera and species of thelyphonid (Fig. 11C) are known from Burmese amber: *Burmathelyphonia prima* Wunderlich, 2015a and *Mesothelyphonus parvus* Cai & Huang, 2017. These are the only amber-preserved fossil thelyphonids known, and only the second and third species recorded from the Mesozoic. Thelyphonids are nocturnal hunters which inhabit tropical and subtropical areas of the world today; they are mainly found in forests but are also known from arid regions of the southern states of the USA. The order is absent from Europe and Australia, a single species occurs in Africa, but thelyphonids are common in south-east Asia and the Americas.

#### DISCUSSION

The first significant point emerging from this survey is that all living arachnid orders are found in Burmese amber. All arachnid orders in burmite have been formally described with exception of the Schizomida, for which this publication is the first to be figured. For Schizomida, Parasitiformes and Palpigradi, the Burmese amber records are the oldest for the group. The most abundant and diverse order recorded from Burmese amber is the Araneae, because there is a bias towards this group in the works of Wunderlich (2008a,b, 2011a, 2012b, 2015b, 2017b). However, it is likely that data for the acarine orders will surpass those of spiders when more work has been done. The diversity of Ricinulei seems extraordinary in comparison with the lack of records from other ambers, but some of this is erroneous (see above), and it is likely that these rarely collected arachnids will turn up elsewhere when more material comes to light (see Table 2). Burmese is also the only amber to have produced Palpigradi; this, too, can be

explained by the sheer numbers of arachnid inclusions discovered in the burmite compared with other ambers.

Second, advancement in our knowledge of mid-Cretaceous arachnofaunas is greatly increased by the sheer numbers of specimens available, compared with Mesozoic occurrences known just a decade ago (Table 2). The abundance of recently described arachnid fossils in Burmese amber will provide a great deal of data to aid phylogenetic studies. The rapid growth in data from the Burmese amber, however, should not allow specimens from other Mesozoic ambers, such as New Jersey and Canadian, to be forgotten. Other Cretaceous ambers with arachnid inclusions exist, although the amber from Ethiopia, originally thought to be Cretaceous in age (Schmidt et al. 2010) has now been shown to be Cenozoic (Coty et al. 2016). Older ambers bearing arachnids come from the Lebanon (c. 130 Ma; Penney & Selden 2002; Penney 2003b; Wunderlich 2008b), Isle of Wight (c. 127 Ma; Selden 2002), Jordan (c. 125–140 Ma; Kaddumi 2007; Wunderlich 2008b, 2012b), sites in Burgos, Cantabria and Teruel, Spain (c. 110 Ma; Alonso et al. 2000; Arillo & Subías 2000, 2002; Penney 2006b; Peñalver et al. 2007; Nájjarro et al. 2009; Arillo et al. 2009, 2010, 2012, 2016; Saupe et al. 2012), and Charente-Maritime, France (c. 101 Ma; Néraudeau et al. 2002, 2008; Perrichot et al. 2007; Judson 2009; Judson & Mäkol 2009). Younger are: New Jersey (c. 92 Ma; Klompen & Grimaldi 2001; Penney 2002, 2004b; Wunderlich 2011a), Vendée, France (c. 90 Ma; Perrichot & Néraudeau 2014; Sidorchuk et al. 2015; Néraudeau et al. 2017), Taimyr, Russia (c. 85 Ma; Eskov & Wunderlich 1994), Alabama (c. 82 Ma; Bingham et al. 2008), and Canada (c. 78 Ma; McAlpine & Martin 1969; Schawaller 1991; Poinar et al. 1997; Penney 2004c, 2006a; Penney & Selden 2006; McKellar & Wolfe 2010). Stratigraphical charts of these arachnid-bearing amber deposits are provided in Peris et al. (2016, fig. 3) and Rasnitsyn et al. (2016, fig. 1).

Looking at the species present in the Burmese amber, and comparing them with their modern counterparts, it is clear that the amber represents a tropical forest environment. For example, ricinuleids are unknown outside the tropics, with the exception of Texas cavernicole habitats (Gertsch & Mulaik 1939). Among the spider families represented in Burmese amber, Tetrablemmidae and Ochyroceratidae are tropical in distribution and typically forest dwellers. Rasnitsyn (1996)



considered that the Burmese amber habit could not be tropical rainforest because of its lack of social insects (termites, bees, and ants). However, termites are known (e.g., Poinar 2009), as are eusocial insects (Yamamoto et al. 2016), and many insects and other biota found in Burmese amber are today restricted to tropical rainforests; e.g., 'passaloid' Coleoptera (Boucher et al. 2016). Grimaldi & Ross (in press) discussed other biota which suggest a tropical rainforest ecosystem, including: abundant liverworts, slime molds, ferns, angiosperms with tropical characteristics (e.g., leaves with drip tips), and onychophorans (Grimaldi et al. 2002; de Sena Oliveira et al. 2016). Burmese amber represents a unique window onto life in a tropical rainforest in the middle of the Cretaceous period, within which its abundant and diverse arachnofauna played a prominent ecological role.

### ACKNOWLEDGMENTS

PAS thanks Zhipeng Zhao, Xiaodan Lin, and Chongchuang Deng (CNU, Beijing) for accompanying him to Shanghai and Chongqing to visit collections of Burmese amber. Dying Huang and Wilson Lourenço kindly gave their permission to use the pictures in Figs. 7A,B and 10B, respectively; Fig. 11A,B is reproduced from Bartel et al. (2016); all other photographs are by PAS. PAS thanks Jason Dunlop, Mark Harvey, Joanna Mąkol, Andrew Ross, and Jörg Wunderlich for discussions. This research is supported by the National Natural Science Foundation of China (No. 31672323, 41688103, 31230065), and Program for Changjiang Scholars and Innovative Research Team in University (17R75).

### LITERATURE CITED

- Alonso, J., A. Arillo, E. Barrón, J.C. Corral, J.O. Grimalt, J.F. López, et al. 2000. A new fossil resin with biological inclusions in Lower Cretaceous deposits from Álava (northern Spain, Basque-Cantabrian Basin). *Journal of Paleontology* 74:158–178.
- Arillo, A. & L.S. Subías. 2000. A new fossil oribatid mite, *Arachaeorcheses munguezae* n. gen. n. sp. from Spanish Lower Cretaceous amber. *Mitteilungen aus dem Geologisch-Paläontologischen Institut der Universität Hamburg* 84:231–236.
- Arillo, A. & L.S. Subías. 2002. Second fossil oribatid mite from the Spanish Lower Cretaceous amber. *Eupterotegans bitranslamellatus* n. sp. (Acariformes, Oribatida, Cephcidae). *Acarologia* 42:403–406.
- Arillo, A., L.S. Subías & A. Sánchez-García. 2016. New species of fossil oribatid mites (Acariformes, Oribatida), from the Lower Cretaceous amber of Spain. *Cretaceous Research* 63:68–76.
- Arillo, A., L.S. Subías & U. Shtanchaeva. 2009. A new fossil species of oribatid mite, *Ametropoctus valeriae* sp. nov. (Acariformes, Oribatida, Ametropoctidae), from the Lower Cretaceous amber of San Just, Teruel Province, Spain. *Cretaceous Research* 30:322–324.
- Arillo, A., L.S. Subías & U. Shtanchaeva. 2010. A new genus and species of oribatid mite, *Cretaceobodes martinezae* gen. et sp. nov. from the Lower Cretaceous amber of San Just (Teruel Province, Spain) (Acariformes, Oribatida, Otocephidae). *Paleontological Journal* 44:287–290.
- Arillo, A., L.S. Subías & U. Shtanchaeva. 2012. A new species of fossil oribatid mite (Acariformes, Oribatida, Trhypochthoniidae) from the Lower Cretaceous amber of San Just (Teruel Province, Spain). *Systematic & Applied Acarology* 17:106–112.
- Bartel, C., J.A. Dunlop & T.L. Bird. 2016. The second camel spider (Arachnida, Solifugae) from Burmese amber. *Arachnology* 17:161–164.
- Berlese, A. 1899. Gli acari agrarii. Puntat II. *Rivista di Patologia Vegetale*, Padova 7:312–344.
- Bingham, P.S., C.E. Savrda, T.K. Knight & R.D. Lewis. 2008. Character and genesis of the Ingersoll Shale, a compact continental Fossil-Lagerstätte, Upper Cretaceous Eutaw Formation, eastern Alabama. *PALAIOS* 23:391–401.
- Blackwall, J. 1841. The difference in the number of eyes with which spiders are provided proposed as the basis of their distribution into tribes; with descriptions of newly discovered species and the characters of a new family and three new genera of spiders. *Transactions of the Linnean Society of London* 18:601–670.
- Blackwall, J. 1862. Descriptions of newly-discovered spiders from the island of Madeira. *Annals and Magazine of Natural History* (series 3) 9:370–382.
- Bochkov, A. & E. Sidorchuk. 2016. A new Eocene free-living cheyletid mite from Baltic amber. *Acta Palaeontologica Polonica* 61:1–6.
- Boucher, S., M. Bai, B. Wang, W. Zhang & X. Yang. 2016. †Passalopalpidae, a new family from the Cretaceous Burmese amber, as the possible sister group of Passalidae Leach (Coleoptera: Scarabaeoidea). *Cretaceous Research* 64:67–78.
- Bradley, W.H. 1931. Origin and microfossils of the oil shale of the Green River formation of Colorado and Utah. *US Geological Survey Professional Paper* 168:i–v & 1–58.
- Broly, P., S. Maillet & A.J. Ross. 2015. The first terrestrial isopod (Crustacea: Isopoda: Oniscidea) from Cretaceous Burmese amber of Myanmar. *Cretaceous Research* 55:220–228.
- Buckland, W. 1837. The Bridgewater treatises on the power, wisdom and goodness of God as manifested in the creation. Treatise VI. *Geology and mineralogy with reference to natural theology*, second edition. London, W. Pickering.
- Cai, C. & D. Huang. 2017. A new genus of whip-scorpions in Upper Cretaceous Burmese amber: Earliest fossil record of the extant subfamily Thelyphoninae (Arachnida: Thelyphonida: Thelyphonidae). *Cretaceous Research* 69:100–105.
- Chamberlin, J.C. 1930. A synoptic classification of the false scorpions or chela-spinners, with a report on a cosmopolitan collection of the same. Part II. The Diplophryonida (Arachnida-Chelonethida). *Annals and Magazine of Natural History* (series 10) 5:1–48, 585–620.
- Chhibber, H.L. 1934. *The Mineral Resources of Burma*. MacMillan, New York.
- Chitima-Dobler, L., B.C. de Araujo, B. Ruthensteiner, T. Pfeffer & J. A. Dunlop. 2017. *Aniblyomma birmanum* a new species of hard tick in Burmese amber. *Parasitology* 113:1–8.
- Clerck, C. 1757. Svenska spindlar, uti sina hufvud-slågter indelte samt under några och sextio särskildte arter beskrefne och med illuminerade gurer uplyste. L. Salvii, Stockholm.
- Cockerell, T.D.A. 1917a. Arthropods in Burmese amber. *American Journal of Science* (series 4) 44:360–368.
- Cockerell, T.D.A. 1917b. Arthropods in Burmese amber. *Psyche* 24:40–45.
- Cockerell, T.D.A. 1920. Fossil arthropods in the British Museum.—I. *Annals and Magazine of Natural History* (series 9) 5:273–279.
- Coddington, J.A. & H.W. Levi. 1991. Systematics and evolution of spiders (Araneae). *Annual Review of Ecology and Systematics* 22:565–592.
- Cokendolpher, J.C. & G.O. Poinar. 1992. Tertiary harvestmen from Dominican Republic amber (Arachnida: Opiliones: Phalangodidae). *Bulletin of the British Arachnological Society* 9:53–56.
- Coty, D., M. Lebon & A. Nel. 2016. When phylogeny meets geology and chemistry: doubts on the dating of Ethiopian amber. *Annales de la Société Entomologique de France* 52:161–166.



- Cruikshank, R.D. & K. Ko. 2003. Geology of an amber locality in the Hukawng Valley, northern Myanmar. *Journal of Asian Earth Sciences* 21:441–455.
- Daday, E. 1889. A Magyar nemzeti Múzeum álskorpiónak áttekintése. *Természettudományi Füzetek* 11:111–136, 165–192.
- Deeleman-Reinhold, C.L. 1995. The Ochyroceratidae of the Indo-Pacific region (Araneae). *Raffles Bulletin of Zoology Supplement* 2:1–103.
- Declòs, X., A. Nel, D. Azar, G. Bechly, J.A. Dunlop, M.S. Engel et al. 2008. The enigmatic Mesozoic insect taxon Chresmodidae (Polyneoptera): New palaeobiological and phylogenetic data, with the description of a new species from the Lower Cretaceous of Brazil. *Neues Jahrbuch für Geologie und Paläontologie Abhandlungen* 247:353–381.
- Dimitrov, D., L.R. Benavides, M.A. Arnedo, G. Giribet, C.E. Griswold, N. Scharff et al. 2017. Rounding up the usual suspects: a standard target-gene approach for resolving the interfamilial phylogenetic relationships of cribellate orb-weaving spiders with a new family-rank classification (Araneae, Araneoidea). *Cladistics* 33:221–250.
- Dunlop, J.A. & L.F. de Oliveira Bernardi. 2014. An opilioacarid mite in Cretaceous Burmese amber. *Naturwissenschaften* 101:759–763.
- Dunlop, J.A. & G. Giribet. 2003. The first fossil cyphophthalmid (Arachnida, Opiliones) from Bitterfeld amber, Germany. *Journal of Arachnology* 31:371–378.
- Dunlop, J.A. & D.M. Martill. 2002. The first whipspider (Arachnida: Amblypygi) and three new whipscorpions (Arachnida: Thelyphoridae) from the Lower Cretaceous Crato Formation of Brazil. *Transactions of the Royal Society of Edinburgh, Earth Sciences* 92:325–334.
- Dunlop, J.A. & P.G. Mitov. 2011. The first fossil cyphophthalmid harvestman from Baltic amber. *Arachnologische Mitteilungen* 40:47–54.
- Dunlop, J.A. & D. Penney. 2012. *Fossil Arachnids*. Siri Scientific Press, Manchester, UK.
- Dunlop, J.A., T.L. Bird, J.O. Brookhart & G. Bechly. 2015. A camel spider from Cretaceous Burmese amber. *Cretaceous Research* 56:265–273.
- Dunlop, J.A., D. Penney & D. Jekel. 2017. A summary list of fossil spiders and their relatives. In: *World Spider Catalog*, version 18.0. Natural History Museum Bern, online at <http://wsc.nmbe.ch>
- Dunlop, J.A., P.A. Selden & G. Giribet. 2016. Penis morphology in a Burmese amber harvestman. *The Science of Nature* 103(11):1–5.
- Dunlop, J.A., C. Sempf & J. Wunderlich. 2010. A new opilioacarid mite in Baltic amber. Pp. 59–70. In *European Arachnology 2008*. (W. Nentwig, M. Schmidt-Entling, C. Kropf, eds.). Natural History Museum, Bern.
- Dunlop, J.A., J. Wunderlich & G.O. Poinar. 2004. The first fossil opilioacariform mite (Acari: Opilioacariformes) and the first Baltic amber camel spider (Solifugae). *Transactions of the Royal Society of Edinburgh: Earth Sciences* 94:261–273.
- Ellingsen, E. 1906. Report on the pseudoscorpions of the Guinea Coast (Africa) collected by Leonardo Fae. *Annali del Museo Civico de Storia Naturale di Genova (serie 3)* 2:243–265.
- Engel, M.S. & D.A. Grimaldi. 2014. Whipspiders (Arachnida: Amblypygi) in amber from the Early Eocene and mid-Cretaceous, including maternal care. *Novitates Paleontologicae* 9:1–17.
- Engel, M.S., L.C.V. Breitkreuz, C. Cai, M. Alvarado, D. Azar & D. Huang. 2016. The first Mesozoic microwhip scorpion (Palpigradi): a new genus and species in mid-Cretaceous amber from Myanmar. *The Science of Nature* 103(19):1–7.
- Eskov, K.Y. & J. Wunderlich. 1994. On the spiders from Taimyr ambers, Siberia, with the description of a new family and with general notes on the spiders from the Cretaceous resins. *Beiträge zur Araneologie* 4:95–107.
- Fage, L. 1912. Études sur les araignées cavernicoles. I. Revision des Ochyroceratidae (n. fam.). *Biospélogica*, XXV. Archives de Zoologie expérimentale et générale 10:97–162.
- García, L.F., E. Torrado-León, G. Talarico & A.V. Peretti. 2015. First characterization of the behavioral repertory in a ricinuleid: *Cryptocellus narino* Platnick & Paz 1979 (Arachnida, Ricinulei, Ricinoididae). *Journal of Insect Behavior* 28:447–459.
- Gertsch, W.J. & S. Mulaik. 1939. Report on a new ricinuleid from Texas. *American Museum Novitates* 1037:1–5.
- Giribet, G. & J.A. Dunlop. 2005. First identifiable Mesozoic harvestman (Opiliones: Dyspnoi) from Cretaceous Burmese amber. *Proceedings of the Royal Society of London B* 272:1007–1013.
- Giribet, G., E. McIntyre, E. Christian & L. Espinosa. 2014. The first phylogenetic analysis of Palpigradi (Arachnida) the most enigmatic arthropod order. *Invertebrate Systematics* 28:350–360.
- Giribet, G., P.P. Sharma, L.R. Benavides, S.L. Boyer, R.M. Clouse, B.L. de Bivort et al. 2012. Evolutionary and biogeographical history of an ancient and global group of arachnids (Arachnida: Opiliones: Cyphophthalmi) with a new taxonomic arrangement. *Biological Journal of the Linnean Society* 105:92–130.
- Grimaldi, D.A. & A.J. Ross. In press. Extraordinary Lagerstätten in amber, with particular reference to the Cretaceous of Myanmar. In *Major Lagerstätten of the world*. (N. Fraser & H.-D. Sues, eds.). Dunedin Press, Edinburgh.
- Grimaldi, D.A., M.S. Engel & P.C. Nascimbene. 2002. Fossiliferous Cretaceous amber from Myanmar (Burma): its rediscovery, biotic diversity, and palaeontological significance. *American Museum Novitates* 3361:1–71.
- Griswold, C.E., J.A. Coddington, G. Hormiga & N. Scharff. 1998. Phylogeny of the orb-weaving spiders (Araneae, Orbiculariae: Deinopoidea, Araneoidea). *Zoological Journal of the Linnean Society* 123:1–99.
- Haase, E. 1890. Beitrag zur Kenntniss der fossilen Arachniden. *Zeitschrift der Deutsche Geologische Gesellschaft* 1890:629–657.
- Hansen, H.J. 1894. *Arthrogastra Danica: en monographisk fremstilling af de i Danmark levende Meirer og Mosskorpioner med bidrag til sidstnævnte underordens systematik*. *Naturhistorisk Tidsskrift (series 3)* 14:491–554.
- Hansen, H.J. & W. Sørensen. 1904. *On Two Orders of Arachnida*. Cambridge University Press, Cambridge.
- Heine, C. & R. Müller. 2005. Late Jurassic rifting along the Australian North West Shelf: margin geometry and spreading ridge configuration. *Australian Journal of Earth Sciences* 52:27–39.
- Henderickx, H. & M. Boon. 2016. The basal pseudoscorpion family Feaellidae Ellingsen, 1906 walks the Earth for 98,000,000 years: a new fossil genus has been found in Cretaceous Burmese amber (Pseudoscorpiones: Feaellidae). *Entomo-Info* 27:7–12.
- Judson, M.L.I. 1997. Catalogue of the pseudoscorpion types (Arachnida: Chelonethi) in the Natural History Museum, London. *Occasional Papers on Systematic Entomology* 11:1–54.
- Judson, M.L.I. 2000. *Electrobisium acutum* Coekreell, a cheiridiid pseudoscorpion from Burmese amber, with remarks on the validity of the Cheiridioidea (Arachnida, Chelonethi). *Bulletin of the Natural History Museum London (Geology)* 56:79–83.
- Judson, M.L.I. 2009. Cheliferoid pseudoscorpions (Arachnida, Chelonethi) from the Lower Cretaceous of France. *Geodiversitas* 31:61–71.
- Judson M.L.I. 2017. A new subfamily of Feaellidae (Arachnida, Chelonethi, Feaelloidea) from Southeast Asia. *Zootaxa* 4258:1–33.
- Judson, M.L.I. & J. Mąkol. 2009. A mite of the family Tanaupodidae (Arachnida, Acari, Parasitengona) from the Lower Cretaceous of France. *Geodiversitas* 31:41–47.
- Kaddumi, H.F. 2007. *Amber of Jordan: the oldest prehistoric insects in fossilized resin*. Second edition. Eternal River Museum of Natural History, Amman, Jordan.
- Kania, I., B. Wang & J. Szewdo. 2015. *Dicranoptycha* Osten Sacken,



- 1860 (Diptera, Limoniidae) from the earliest Cenomanian Burmese amber. *Cretaceous Research* 52:522–530.
- Khaustov, A.A. & G.O. Poinar. 2010. *Protoresinacarus brevipedis* gen. n., sp. n. from Early Cretaceous Burmese amber: the first fossil record of mites of the family Resinacaridae (Acari: Heterostigmata: Pyemotoidea). *Historical Biology* 23:219–222.
- Klompén, H. & D.A. Grimaldi. 2001. First Mesozoic record of a parasitiform mite: a larval argasid tick in Cretaceous amber (Acari: Ixodida: Argasidae). *Annals of the Entomological Society of America* 94:10–15.
- Koch, C.L. 1837. Uebersicht des Arachnidensystems I. C. H. Zeh'sche Buchhandlung, Nürnberg.
- Koch, C.L. 1844. Systematische Uebersicht über die Ordnung der Zecken. *Archiv für Naturgeschichte* 10:217–239.
- Koch, C.L. 1851. Uebersicht des Arachnidensystems 5. C. H. Zeh'sche Buchhandlung, Nürnberg.
- Koch, C.L. & G.C. Berendt. 1854. Die im Bernstein befindlichen Myriapoden, Arachniden und Apteren der Vorwelt. In *Die in Bernstein befindlichen organischen Reste der Vorwelt gesammelt in Verbindung mit mehreren bearbeitet und herausgegeben* I. (Berendt, G.C., ed.). Nicolai, Berlin.
- Koch, L. 1873. Übersichtliche Darstellung der europäischen Chernetiden (Pseudoscorpiones). Bauer und Raspe, Nürnberg.
- Krüger, J. & J.A. Dunlop. 2010. Schizomids (Arachnida: Schizomida) from Dominican Republic amber. *Alavesia* 3:43–53.
- Kury, A.B. 2007. Epeiridae Sørensen, 1886. Pp. 188–191. In *Harvestmen: The Biology of Opiliones*. (R. Pinto-da-Rocha, G. Machado & G. Giribet, eds.). Harvard University Press, Cambridge, MA.
- Latreille, P.A. 1796. Précis de caractères génériques des insectes, disposés dans un ordre naturel. Prévot, Paris.
- Latreille, P.A. 1804. Histoire naturelle, générale et particulière, des crustacés et des insectes, volume 7. F. Dufart, Paris:144–305.
- Latreille, P.A. 1817. Les Crustacés, les Arachnides et les Insectes. In *Le Règne Animal distribué d'après son organisation, pour servir de base à l'histoire naturelle des animaux et d'introduction à l'anatomie comparée*, 1st edition, volume III. Deterville, Paris.
- Laufer B. 1907. Historical jottings on amber in Asia. *Memoirs of the American Anthropological Association* 1:211–244.
- Leach, W.E. 1815. A tabular view of the external characters of four classes of animals which Linné arranged under Insecta; with the distribution of the genera composing three of these classes into orders, and descriptions of several new genera and species. *Transactions of the Linnean Society of London* 11:306–400.
- Lourenço, W.R. 2002. The first scorpion fossil from the Cretaceous amber of Myanmar (Burma). New implications for the phylogeny of Buthoidea. *Comptes Rendus Palevol* 1:97–101.
- Lourenço, W.R. 2003. The first scorpion fossil from the Cretaceous amber of France. New implications for the phylogeny of Chactoida. *Comptes Rendus Palevol* 2:213–219.
- Lourenço, W.R. 2012. About the scorpion fossils from the Cretaceous amber of Myanmar (Burma) with the descriptions of a new family, genus and species. *Acta Biológica Paranaense* 41:75–87.
- Lourenço, W.R. 2013. A new species of *Chaerilobuthus* Lourenço & Beigcl, 2011 from Cretaceous Burmese amber (Scorpiones: Chaerilobuthidae). *Acta Biológica Paranaense* 42:1–5.
- Lourenço, W.R. 2015a. New contribution to the knowledge of Cretaceous amber scorpions: descriptions of two new species of *Betaburmesebuthus* Lourenço, 2015 (Scorpiones: Archaeobuthidae: Palaeoburmesebuthinae). *Rivista Aracnologica Italiana* 3:27–36.
- Lourenço, W.R. 2015b. An unusual new species of *Chaerilobuthus* Lourenço & Beigcl, 2011 (Scorpiones: Chaerilobuthidae) from the Cretaceous amber of Myanmar (Burma). *Rivista Aracnologica Italiana* 5:44–48.
- Lourenço, W.R. 2015c. New contribution to the knowledge of Cretaceous Burmese amber scorpions: descriptions of two new species of *Betaburmesebuthus* Lourenço, 2015 (Scorpiones: Archaeobuthidae: Palaeoburmesebuthinae). *Rivista Aracnologica Italiana* 1:27–36.
- Lourenço, W. 2015d. A new subfamily, genus and species of fossil scorpions from Cretaceous Burmese amber (Scorpiones: Palaeo-oescorpiidae). *Beiträge zur Araneologie* 9:457–464.
- Lourenço, W. 2015e. Clarification of the familial status of the genus *Palaeoburmesebuthus* Lourenço, 2002 from Cretaceous Burmese amber (Scorpiones: Archaeobuthidae: Palaeoburmesebuthinae). *Beiträge zur Araneologie* 9:465–475.
- Lourenço, W.R. 2016a. A new genus and three new species of scorpions from Cretaceous Burmese amber (Scorpiones: Chaerilobuthidae: Palaeo-oescorpiidae). *Arthropoda Selecta* 25:67–74.
- Lourenço, W.R. 2016b. A preliminary synopsis on amber scorpions with special reference to Burmite species: an extraordinary development of our knowledge in only 20 years. *ZooKeys* 600:75–87.
- Lourenço, W.R. & A. Beigcl. 2011. A new scorpion fossil from the Cretaceous amber of Myanmar (Burma). New phylogenetic implications. *Comptes Rendus Palevol* 10:635–639.
- Lourenço, W.R. & A. Beigcl. 2015. A new genus and species of Palaeoburmesebuthinae Lourenço, 2015 (Scorpiones: Archaeobuthidae) from Cretaceous amber of Myanmar. *Beiträge zur Araneologie* 9:476–480.
- Lourenço, W.R. & J. Velten. 2015. Another new species of *Chaerilobuthus* Lourenço & Beigcl, 2011 (Scorpiones: Chaerilobuthidae) from the Cretaceous amber of Myanmar (Burma). *Rivista Aracnologica Italiana* 5:2–8.
- Lourenço, W. R. & J. Velten. 2016a. One more new species of *Betaburmesebuthus* Lourenço, 2015 (Scorpiones: Palaeoburmesebuthinae) from Cretaceous burmite. *Arachnida. Rivista Aracnologica Italiana* 6:4–11.
- Lourenço, W.R. & J. Velten. 2016b. A new genus and species of fossil scorpion from Burmese Cretaceous amber (Scorpiones: Buthoidea: Buthidae). *Rivista Aracnologica Italiana* 10:2–9.
- Lourenço, W.R. & J. Velten. 2016c. A sixth new species of Cretaceous Burmese amber scorpion of the genus *Betaburmesebuthus* Lourenço, 2015 (Scorpiones: Palaeoburmesebuthidae). *Rivista Aracnologica Italiana* 10:10–17.
- Mahunka, S. 1975. Neue und auf Insekten lebende Milben aus Australien und Neu-Guinea (Acari: Acarida, Tarsonemida). *Annales Historico-Naturales Musei Nationalis Hungarici* 67:317–325.
- McAlpine, J.F. & J.E.H. Martin. 1969. Canadian amber – a paleontological treasure chest. *Canadian Entomologist* 101:819–838.
- McKellar, R.C. & A.P. Wolfe. 2010. Canadian amber. Pp. 96–113. In *Biodiversity of Fossils in Amber from the Major World Deposits*. (D. Penney, ed.). Siri Scientific Press, Manchester, UK.
- Metcalf, I. 2013. Gondwana dispersion and Asian accretion: tectonic and palaeogeographic evolution of eastern Tethys. *Journal of Asian Earth Sciences* 66:1–33.
- Murienn, J., M.S. Harvey & G. Giribet. 2008. First molecular phylogeny of the major clades of Pseudoscorpiones (Arthropoda: Chelicerata). *Molecular Phylogenetics and Evolution* 49:170–184.
- Najarro, M., E. Peñalver, I. Rosales, R. Pérez-de la Fuente, V. Daviero-Gomez, B. Gomez et al. 2009. Unusual concentration of Early Albian arthropod-bearing amber in the Basque-Cantabrian Basin (El Sopla, Cantabria, Northern Spain): Palaeoenvironmental and palaeobiological implications. *Geologica Acta* 7:363–387.
- Néraudeau, D., V. Perrichot, D.J. Batten, A. Boura, V. Girard, L. Jeanneau et al. 2017. Upper Cretaceous amber from Vendée, north-western France: Age dating and geological, chemical, and palaeontological characteristics. *Cretaceous Research* 70:77–95.
- Néraudeau, D., V. Perrichot, J-P. Colin, V. Girard, B. Gomez, F. Guillocheau et al. 2008. A new amber deposit from the Cretaceous



- (uppermost Albian-lowermost Cenomanian) of southwestern France. *Cretaceous Research* 29:925–929.
- Néraudeau, D., V. Perrichot, J. Dejax, E. Masure, A. Nél, M. Philippe et al. 2002. A new fossil locality with insects in amber and plants (likely Uppermost Albian): Archingeay (Charente-Maritime, France). *Geobios* 35:233–240.
- Noetling, F. 1893. On the occurrence of Burmite, a new fossil resin from Upper Burma. Records of the Geological Survey of India 26:31–40.
- Oudemans, A.C. 1909. Über die bis jetzt genauer bekannten Thrombidium-larven und über eine neue Klassifikation der Prostigmata. *Tijdschrift voor Entomologie* 52:19–61.
- Oudemans, A.C. 1937. Kritisch historisch overzicht der aarologie door Dr. A. C. Oudemans. Pp. 2737–3379. *In* Derde Gedeelte 1805–1850, Band G, Algemeen register. E.J. Brill, Leiden.
- Peñalver, E., X. Delclòs & C. Soriano. 2007. A new rich amber outcrop with palaeobiological inclusions in the Lower Cretaceous of Spain. *Cretaceous Research* 28:791–802.
- Penney, D. 2002. Spiders in Upper Cretaceous amber from New Jersey (Arthropoda: Araneae). *Palaentology* 45:709–724.
- Penney, D. 2003a. *Afrarchaea grimaldii*, a new species of Archaeidae (Araneae) in Cretaceous Burmese amber. *Journal of Arachnology* 31:122–130.
- Penney, D. 2003b. A new deinopoid spider from Cretaceous Lebanese amber. *Acta Palaentologica Polonica* 48:569–574.
- Penney, D. 2004a. A new genus and species of Pisauridae (Araneae) in Cretaceous Burmese amber. *Journal of Systematic Palaentology* 2:141–145.
- Penney, D. 2004b. New spiders in Upper Cretaceous amber from New Jersey in the American Museum of Natural History (Arthropoda: Araneae). *Palaentology* 47:367–375.
- Penney, D. 2004c. Cretaceous Canadian amber spider and the palpmannoidean nature of lagonomegopids. *Acta Palaentologica Polonica* 49:579–584.
- Penney, D. 2005. The fossil spider family Lagonomegopidae in Cretaceous ambers with descriptions of a new genus and species from Myanmar. *Journal of Arachnology* 33:439–444.
- Penney, D. 2006a. Fossil oonopid spiders in Cretaceous ambers from Canada and Myanmar. *Palaentology* 49:229–235.
- Penney, D. 2006b. The oldest lagonomegopid spider, a new species in Lower Cretaceous amber from Álava, Spain. *Geologica Acta* 4:377.
- Penney, D. 2013. Predatory behaviour of Cretaceous social orb-weaving spiders: comment. *Historical Biology* 26:132–134.
- Penney, D. 2014. A fossil ray spider (Araneae: Theridiosomatidae) in Cretaceous amber from Vendée, France. *Paleontological Contributions* 10:5–8.
- Penney, D. & P.A. Selden. 2002. The oldest linyphiid spider, in Lower Cretaceous Lebanese amber (Araneae, Linyphiidae, Linyphiinae). *Journal of Arachnology* 30:487–493.
- Penney, D. & P.A. Selden. 2006. First fossil Huttoniidae (Arthropoda: Chelicerata: Araneae) in late Cretaceous Canadian amber. *Cretaceous Research* 27:442–446.
- Peris, D., E. Ruzzier, V. Perrichot & X. Delclòs. 2016. Evolutionary and paleobiological implications of Colcoptera (Insecta) from Tethyan-influenced Cretaceous ambers. *Geoscience Frontiers* 7:695–706.
- Perrichot, V., D. Néraudeau, A. Nél & G. de Ploeg. 2007. A reassessment of the Cretaceous amber deposits from France and their palaeontological significance. *African Invertebrates* 48:213–227.
- Perrichot, V. & D. Néraudeau. 2014. Introduction to thematic volume 'Fossil arthropods in Late Cretaceous Vendean amber (North-western France)'. *Paleontological Contributions* 10:1–4.
- Petrunkévitch, A.I. 1913. A monograph of the terrestrial Palaeozoic Arachnida of North America. Transactions of the Connecticut Academy of Arts and Sciences 18:1–137.
- Petrunkévitch, A.I. 1942. A study of amber spiders. Transactions of the Connecticut Academy of Arts and Sciences 34:119–464.
- Petrunkévitch, A.I. 1945. *Calcitro fisheri*. A new fossil arachnid. *American Journal of Science* 243:320–329.
- Petrunkévitch, A.I. 1955. Arachnida. Pp. 42–162. *In* Treatise on Invertebrate Paleontology, Part P, Arthropoda 2. (R.C. Moore, ed.). Geological Society of America, Boulder, and University of Kansas Press, Lawrence, KS.
- Pickard-Cambridge, O. 1871. Arachnida. *The Zoological Record* 7:207–224.
- Pickard-Cambridge, O. 1873. On some new genera and species of Araneida. *Proceedings of the Zoological Society of London* 41:112–129, pls. XII–XIV.
- Pierce, W.D. 1951. Fossil arthropods from onyx-marble. *Bulletin of the Southern Californian Academy of Sciences* 50:34–49.
- Pocock, R.I. 1892. *Liphistius* and its bearing upon the classification of spiders. *Annals and Magazine of Natural History (series 6)* 10:306–314.
- Pocock, R. I. 1893. Notes on the classification of scorpions, followed by some observations on synonymy, with descriptions of new genera and species. *Annals and Magazine of Natural History (series 6)* 12:303–330.
- Poinar, G.O. 2008. *Palaeosiro burmanicum* n. gen., n. sp., a fossil Cyphophthalmi (Arachnida: Opiliones: Sironidae) in Early Cretaceous Burmese amber. *Advances in Arachnology and Developmental Biology. Papers Dedicated to Prof. Dr. Božidar Čurčić*. Institute of Zoology, Belgrade, Monographs 12:267–274.
- Poinar, G.O. 2009. Description of an early Cretaceous termite (Isoptera: Kalotermitidae) and its associated intestinal protozoa, with comments on their co-evolution. *Parasites and Vectors* 2:12–17.
- Poinar, G.O. 2015. Rickettsial-like cells in the Cretaceous tick, *Cornipalpatum burmanicum* (Ixodida: Ixodidae). *Cretaceous Research* 52:623–627.
- Poinar, G.O. & A.E. Brown. 2003. A new genus of hard ticks in Cretaceous Burmese amber (Acari: Ixodida: Ixodidae). *Systematic Parasitology* 54:199–205.
- Poinar, G.O. & R. Buckley. 2008. *Comphuriscutula vetuhuu* (Acari : Ixodida : Ixodidae), a new genus and new species of hard tick from lower Cretaceous Burmese amber. *Proceedings of the Entomological Society of Washington* 110:445–450.
- Poinar, G.O. & R. Buckley. 2011. *Doratomantispa burmanica* n. gen., n. sp. (Neuroptera: Mantispidae), a new genus of mantidflies in Burmese amber. *Historical Biology* 23:169–176.
- Poinar, G.O. & R. Buckley. 2012. Predatory behaviour of the social orb-weaver spider, *Geratonephila burmanica* n. gen., n. sp. (Araneae: Nephilidae) with its wasp prey, *Casoscelio incassus* n. gen., n. sp. (Hymenoptera: Platygasteridae) in Early Cretaceous Burmese amber. *Historical Biology* 24:519–525.
- Poinar, G.O. & R. Buckley. 2013. Predatory behaviour of Cretaceous social orb-weaving spiders: response to Penney. *Historical Biology* 26:135–136.
- Poinar, G.O. & J.A. Santiago-Blay. 1989. A fossil solpugid, *Haplodontus proterus*, new genus, new species (Arachnida: Solpugida) from Dominican amber. *Journal of the New York Entomological Society* 97:125–132.
- Poinar, G.O., R. Buckley & A.E. Brown. 2008. The secrets of burmite amber. *Mid-America Palaeontological Society Digest* 20:21–29.
- Poinar, G., G.W. Krantz, A.J. Boucot & T.M. Pike. 1997. A unique Mesozoic parasitic association. *Naturwissenschaften* 84:321–322.
- Poinar, G., J.B. Lambert & Y. Wu. 2007. Araucarian source of fossiliferous Burmese amber: spectroscopic and anatomical evidence. *Journal of the Botanical Research Institute of Texas* 1:449–455.



- Rasnitsyn, A. P. 1996. Conceptual issues in phylogeny, taxonomy, and nomenclature. *Contributions in Zoology* 66:3–41.
- Rasnitsyn, A.P. & A.J. Ross. 2000. A preliminary list of arthropod families present in the Burmese amber collection at The Natural History Museum, London. *Bulletin of the Natural History Museum London (Geology)* 56:21–24.
- Rasnitsyn, A.P., A.S. Bashkuev, D.S. Kopylov, E.D. Lukashevich, A.G. Ponomarenko, Y.A. Popov et al. 2016. Sequence and scale of changes in the terrestrial biota during the Cretaceous (based on materials from fossil resins). *Cretaceous Research* 61:234–255.
- Reuter, E. 1909. Zur Morphologie und Ontogenie der Acariden mit besonderen Berücksichtigung von *Pediculopsis graninum* (E. Reut.). *Acta Societatis Scientiarum Fennicae* 36:1–288, pls. I–VI.
- Roewer, C-F. 1923. Die Weberknechte der Erde. Systematische Bearbeitung der bisher bekannten Opiliones. Gustav Fischer, Jena.
- Ross, A.J. 1998. Amber: the Natural Time Capsule. The Natural History Museum, London.
- Ross, A.J. 2017. Burmese (Myanmar) amber taxa, on-line checklist v.2017.2, online at [www.nms.ac.uk/explore/stories/natural-world/burmese-amber/](http://www.nms.ac.uk/explore/stories/natural-world/burmese-amber/)
- Ross, A.J., C. Mellish, P.V. York & B. Crighton. 2010. Burmese amber. Pp. 208–235. *In* Biodiversity of Fossils in Amber from the Major World Deposits. Siri Scientific Press, Manchester, UK.
- Ross, A.J. & P.V. York. 2000. A list of type and figured specimens of insects and other inclusions in Burmese amber. *Bulletin of the Natural History Museum London (Geology)* 56:11–20.
- Rossi, A. 2015. A new family, genus and species of scorpion from burmite of Myanmar (Scorpiones: Sucinlourencoidae). *Rivista Aracnologica Italiana* 1:3–21.
- Rowland, J.M. & W.D. Sissom. 1980. Report on a fossil paligrade from the Tertiary of Arizona, and a review of the morphology and systematics of the order (Arachnida: Paligradida). *Journal of Arachnology* 8:69–86.
- Saube, E.E., R. Pérez de la Fuente, P.A. Selden, X. Delclòs, P. Tafforeau & C. Soriano. 2012. New *Orchestina* Simon, 1882 (Araneae: Oonopidae) from Cretaceous ambers of Spain and France: first spiders imaged using phase-contrast X-ray synchrotron microtomography. *Palaentology* 55:127–143.
- Sahni, M.R. & V.V. Sastri. 1957. A monograph of the orbitolines found in the Indian continent (Chitral, Gilgit, Kashmir), Tibet and Burma, with observations on the age of the associated volcanic series. *Palaentologia Indica* 33(3):1–50; pls. 1–6.
- Santiago-Blay, J.A., V. Fct, M.E. Soleglad & S.R. Anderson. 2004. A new genus and subfamily of scorpions from Lower Cretaceous Burmese amber (Scorpiones: Chacrididae). *Revista Ibérica de Aracnología* 9:3–14.
- Schawaller, W. 1991. The first Mesozoic pseudoscorpion, from Cretaceous Canadian amber. *Palaentology* 34:971–976.
- Schmidt, A. R., V. Perrichot, M. Svojtká, K.B. Anderson, K.H. Belete, R. Bussert et al. 2010. Cretaceous African life captured in amber. *Proceedings of the National Academy of Sciences of the USA* 107:7329–7334.
- Selden, P.A. 2002. First British Mesozoic spider, from Cretaceous amber of the Isle of Wight, southern England. *Palaentology* 45:973–983.
- Selden, P.A. 2010. A theridiosomatid spider from the Early Cretaceous of Russia. *Bulletin of the British Arachnological Society* 15:69–78.
- Selden, P.A. & D. Penney. 2010. Fossil spiders. *Biological Reviews* 85:171–206.
- Selden, P.A. & W.A. Shear. 1996. The first Mesozoic Solifugae (Arachnida), from the Cretaceous of Brazil, and a redescription of the Palaeozoic solifuge. *Palaentology* 39:583–604.
- Selden, P.A., J.A. Dunlop, G. Giribet, W. Zhang & D. Ren. 2016a. The oldest armoured harvestman (Arachnida: Opiliones: Lania-  
tores), from Upper Cretaceous Myanmar amber. *Cretaceous Research* 65:206–212.
- Selden P.A., J.A. Dunlop & L. Simonetto. 2016b. A fossil whip-scorpion (Arachnida: Thelyphonida) from the Upper Carboniferous of the Carnic Alps (Friuli, NE Italy). *Rivista Italiana di Paleontologia e Stratigrafia* 122:7–12.
- Selden, P.A., C. Shih & D. Ren. 2013. A giant spider from the Jurassic of China reveals greater diversity of the orbicularian stem group. *Naturwissenschaften* 100:1171–1181.
- Selden, P. A., W. Zhang & D. Ren. 2016c. A bizarre armoured spider (Araneae: Tetrablemmidae) from Upper Cretaceous Myanmar amber. *Cretaceous Research* 66:129–135.
- Smedo, A. 1643. *Relatione della grande monarchia della Cina*. Hermann Schus, Rome.
- Smedo, A. 1655. *The History of that Great and Renowned Monarchy of China*. John Crook, London. [English version of Smedo 1643].
- de Sena Oliveira, I., M. Bai, H. Jahn, V. Gross, C. Martin, J.U. Hammel et al. 2016. Earliest onychophoran in amber reveals Gondwanan migration patterns. *Current Biology* 26:2594–2601.
- Seton, M., R.D. Müller, S. Zahirovic, C. Gaina, T. Torsvik, G. Shephard et al. 2012. Global continental and ocean basin reconstructions since 200 Ma. *Earth Science Reviews* 113:212–270.
- Sharma, P.P. & G. Giribet. 2014. A revised dated phylogeny of the arachnid order Opiliones. *Frontiers in Genetics* 5(255):1–13.
- Shear, W.A. & J.G. Warfel. 2016. The harvestman genus *Taracus* Simon 1879, and the new genus *Oskoron* (Opiliones: Ischyropsalidoidea: Taracidae). *Zootaxa* 4180:1–71.
- Shi, G.H., D.A. Grimaldi, G.E. Harlow, J. Wang, J. Wang, M.C. Yang et al. 2012. Age constraint on Burmese amber based on U-Pb dating of zircons. *Cretaceous Research* 37:155–163.
- Sidorchuk, E.A., V. Perrichot & E.E. Lindquist. 2015. A new fossil mite from French Cretaceous amber (Acari: Heterostigmata: Nasutiacaridae superfam. nov.), testing evolutionary concepts within the Eleutherengona (Acariformes). *Journal of Systematic Palaentology* 14:297–317.
- Sierwald, P. 1990. Morphology and homologous features in the male palpal organ in Pisauridae and other spider families, with notes on the taxonomy of Pisauridae (Arachnida: Araneae). *Nemouria* 35:1–59.
- Simon, E. 1879. *Les Arachnides de France*. Volume 7. Roret, Paris: 1–332.
- Simon, E. 1881. *Les arachnides de France*. Volume 5, part 1. Roret, Paris:1–180.
- Simon, E. 1889. Voyage de M. E. Simon au Venezuela (décembre 1887 – avril 1888). 4c Mémoire. *Annales de la Société Entomologique de France (série 6)* 9:169–220.
- Simon, E. 1890. Études arachnologiques. 22c Mémoire. XXXIV. *Annales de la Société Entomologique de France (série 6)* 10:77–124.
- Simon, E. 1892. *Histoire naturelle des araignées*. Volume 1, part 1. Roret, Paris:1–254.
- Simon, E. 1893. *Histoire naturelle des araignées*, volume 1, part 2. Roret, Paris:257–488.
- Simon, E. 1894. *Histoire naturelle des araignées*, volume 1, part 3. Roret, Paris:489–760.
- Simon, E. 1895. *Histoire naturelle des araignées*, volume 1, part 4. Roret, Paris:761–1084.
- Simon, E. 1898. Étude sur les arachnides de la région des Maures (Var). *Feuille des Jeunes Naturalistes (série 3)* 29:2–4.
- Sørensen, W. 1886. Opiliones. Pp. 53–86. *In* *Die Arachniden Australiens nach der Natur Beschrieben und Abgebildet*. (L. Koch & E. Keyserling, eds.). Bauer und Raspe, Nürnberg.
- Stuart, M. 1923. Geological traverses from Assam to Myitkyina through the Hukong Valley; Myitkyina to northern Putao;



- Myitkyina to the Chinese frontier. Records of the Geological Survey of India 54:398–411; pl. 29.
- Sundevall, J.C. 1833. Conspectus Arachnidum. C.F. Berling, Londini Gothorum.
- Tettie O.E. & J.A. Dunlop. 2008. *Geralimura carbonaria* (Arachnida: Uropygi) from Mazon Creek, Illinois, USA, and the origin of subchelate pedipalps in whip scorpions. Journal of Paleontology 82:299–312.
- Thorell, T. 1869. On European spiders. Part I. Review of the European genera of spiders, preceded by some observations on zoological nomenclature. Nova Acta Regiae Societatis Scientiarum Upsaliensis (3)7:1–108.
- Thorell, T. 1870. On European spiders. Part 2. Nova Acta Societas Scientiae Uppsaliensis (3)7:109–242.
- Thorell, T. 1876. Sopra alcuni Opilioni (Phalangidea) d'Europa e dell'Asia occidentale, con un quadro dei generi europei di quest'Ordine. Annali del Museo Civico di Storia Naturale di Genova (serie 1) 8:452–508.
- Thorell, T. 1882. Descrizione di Alcuni Araenidi Inferiori dell'Arcipelago Malese. Annali del Museo Civico di Storia Naturale di Genova 18:21–69.
- Thorell, T. 1888. Pedipalpi e Scorpioni dell'Arcipelago Malese conservati nel Museo Civico di Storia Naturale di Genova. Annali del Museo Civico di Storia Naturale di Genova, 26:327–428.
- Ubick, D. & J.A. Dunlop. 2005. On the placement of the Baltic amber harvestman *Gonyleptes nemastomoides* Koch & Berendt, 1854, with notes on the phylogeny of Cladonychiidae (Opiliones, Laniatores, Travunioidea). Mitteilungen aus dem Museum für Naturkunde Berlin, Geowissenschaftliche Reihe 8:75–82.
- Wood, H.M., C.E. Griswold & R.G. Gillespie. 2012. Phylogenetic placement of pelican spiders (Archaeidae, Araneae), with insight into evolution of the 'neck' and predatory behaviours of the superfamily Palpimanoidea. Cladistics 28:598–626.
- Wunderlich, J. 1986. Spinnenfauna Gestern und Heute. Fossile Spinnen in Bernstein und ihre heute lebenden Verwandten. Erich Bauer Verlag bei Quelle und Meyer, Wiesbaden.
- Wunderlich, J. 2006. *Spatiator martensi* n. sp., a second species of the extinct spider species Spatiatoridae in Eocene Baltic amber. Zootaxa 1325:313–318.
- Wunderlich, J. 2008a. Descriptions of fossil spider (Araneae) taxa mainly in Baltic amber, as well as certain related extant taxa. Beiträge zur Araneologie 5:44–139.
- Wunderlich, J. 2008b. The dominance of ancient spider families of the Araneae: Haplogyne in the Cretaceous, and the late diversification of advanced ecribellate spiders of the Entelegynae after the Cretaceous–Tertiary boundary extinction events, with descriptions of new families. Beiträge zur Araneologie 5:524–675.
- Wunderlich, J. 2011a. Some fossil spiders (Araneae) in Cretaceous ambers. Beiträge zur Araneologie 6:539–557.
- Wunderlich, J. 2011b. Some fossil spiders (Araneae) in Eocene European ambers. Beiträge zur Araneologie 6:472–538.
- Wunderlich, J. 2012a. Description of the first fossil Ricinulei in amber from Burma (Burmese), the first report of this arachnid order from the Mesozoic and from Asia, with notes on the related extinct order Trigonotarbita. Beiträge zur Araneologie 7:233–244.
- Wunderlich, J. 2012b. On the fossil spider (Araneae) fauna in Cretaceous ambers, with descriptions of new taxa from Myanmar (Burma) and Jordan, and on the relationships of the superfamily Leptonetoidea. Beiträge zur Araneologie 7:157–232.
- Wunderlich, J. 2015a. New and rare fossil Arachnida in Cretaceous Burmese Amber (Amblypygi, Ricinulei and Uropygi: Thelephoniida). Beiträge zur Araneologie 9:409–436.
- Wunderlich, J. 2015b. On the evolution and the classification of spiders, the Mesozoic spider faunas, and descriptions of new Cretaceous taxa mainly in amber from Myanmar (Burma)(Arachnida: Araneae). Beiträge zur Araneologie 9:21–408.
- Wunderlich, J. 2017a. New extinct taxa of the arachnid order Ricinulei, based on new fossils preserved in mid Cretaceous Burmese amber. Beiträge zur Araneologie 10:48–71.
- Wunderlich, J. 2017b. New and rare fossil spiders (Araneae) in mid Cretaceous amber from Myanmar (Burma), including the description of new extinct families of the suborders Mesothelae and Opisthothelae, as well as notes on the taxonomy, the evolution and the biogeography of the Mesothelae. Beiträge zur Araneologie 10:72–279.
- Yamamoto, S., M. Maruyama & J. Parker. 2016. Evidence for social parasitism of early insect societies by Cretaceous rove beetles. Nature Communications 7:1–9.
- Zachvatkin, A.A. 1952. [The division of the Acarina into orders and their position in the system of the Chelicerata.] Parazitologicheskii Sbornik Zoologicheskii Institut Akademii Nauk SSSR, 14:5–46. [in Russian].
- Zherikhin, V.V. & A.J. Ross. 2000. A review of the history, geology and age of Burmese amber (Burmite). Bulletin of the Natural History Museum London (Geology) 56:3–10.

Manuscript received 15 April 2017, revised 12 June 2017.



## An unusual new wolf spider species from the Erg Chebbi Desert in Morocco (Araneae: Lycosidae: Evippinae)

Steffen Bayer<sup>1</sup>, Rainer Foelix<sup>2</sup> and Mark Alderweireldt<sup>3</sup>: <sup>1</sup>Staatliches Museum für Naturkunde Karlsruhe, Erbprinzenstrasse 13, 76133 Karlsruhe, Germany. E-mail: steffen.bayer@smnk.de; <sup>2</sup>Schanzmättelstrasse 15, 5000 Aarau, Switzerland; <sup>3</sup>University of Ghent, Terrestrial Ecology Unit, K.L. Ledeganckstraat 35, 9000 Ghent, Belgium

**Abstract.** A new species of the lycosid subfamily Evippinae is introduced and preliminarily assigned to the genus *Evippomma* Roewer, 1959. It was found in the Erg Chebbi Desert in Morocco. *Evippomma rechenbergi* sp. nov. is a wolf spider with unusual morphological and behavioural features, e.g., having exceptional scales on most of its body and carrying sand by interconnecting sand grains with silk threads. A detailed description and delimitation of this species is given. Its genus-affiliation is found uncertain. We conclude that a comprehensive revision and phylogenetic study of all African genera of the subfamily Evippinae are needed to enable unambiguous identification (including unambiguous genus identification) and for a better understanding of phylogenetic relationships among these genera.

**Keywords:** Diagnostic characters; taxonomy; scales; *Evippa*; *Evippomma*

ZooBank publication: <http://zoobank.org/?lsid=urn:lsid:zoobank.org:pub:A7A0A1CA-B430-4987-9218-41333E8815DD>

In 2007, Ingo Rechenberg from the Technical University in Berlin observed two unusual tube-dwelling spider species in the Erg Chebbi dunes, a north-eastern outcrop of the Sahara Desert in Morocco. One was a sparassid (*Cebrennus rechenbergi* Jäger, 2014) that carries sand with specialized pedipalps when digging its burrow. Even more remarkable was a peculiar rolling movement that this spider performs when disturbed (Rast et al. 2015). The other spider living in the same habitat was a wolf spider (Fig. 1) that could not be identified at that time. Although this spider also builds vertical tubes like *C. rechenbergi*, it uses a different technique when carrying sand: with the aid of its spinnerets it connects sand grains and then carries off small sand/silk bundles (Foelix et al. 2015, 2017). One morphological peculiarity of this wolf spider is that its body is covered by numerous lanceolate scale hairs (Foelix et al. 2015) (Fig. 4A, B). Scales are well known in Salticidae (Hill 1979; Metzner 1999) and also in a few other families like Gnaphosidae (Platnick & Shadab 1988) and Oxyopidae (Deeleman-Reinhold 2009) but not in Lycosidae, except for the few species of the genus *Evippomma* from central and southern Africa (Alderweireldt 1992). Furthermore, the spigots on the spinnerets of this unusual wolf spider are remarkably long (Fig. 4C, D). They are pushed between the sand grains while building the wall of the spider's burrow in order to achieve a stable tube. Neighbouring sand grains are tightly connected and arranged like stones in a vault (Foelix et al. 2016, 2017). Due to these interesting morphological and behavioural features, it seemed desirable to identify the specimens from Erg Chebbi to species level and to determine the taxonomic position of this species. After initial assessments it could be assigned to the subfamily Evippinae Zyuzin, 1985 following the definition of Zyuzin (1985). Subsequently, the third author was consulted and after re-examination of several representatives of Evippinae, it became obvious that our specimens belonged to a new species. However, its genus affiliation within the subfamily Evippinae was puzzling. The two genera *Evippa* Simon, 1882 and *Evippomma* Roewer, 1959 were the best candidates to include the new species, but the

diagnostic characters of both genera did not unambiguously match the new species. The North African species of the genera *Evippa* and *Evippomma* were first revised by Roewer (1959, 1960). His diagnoses for many genera and also for many species were not coherent. Roewer (1959, 1960) only gave minor consideration to common structural patterns of the copulatory organs, many of which nowadays are considered extremely important for taxonomic research (Alderweireldt 1992, 1996, 1999; Bayer 2012, 2014; Bayer & Schönhofner 2013; Jäger 2014; Dupérré 2015). Furthermore, Roewer (1959, 1960) included highly variable somatic characters in his diagnoses. *Evippa* and *Evippomma* were revised by Alderweireldt (1991, 1992), who concluded that the two genera are closely related. The present study, therefore, provides the first description of the specimens from Erg Chebbi, comments on the possible relationships of this taxon and introduces some unusual morphological features.

### METHODS

The spiders examined in the present study were collected by Prof. I. Rechenberg in the Erg Chebbi Desert in Morocco. Rechenberg also took several photos of living spiders in their natural desert habitat. Specimens were examined and drawn under a Leica M165C stereomicroscope with a camera lucida. Images of preserved spiders and copulatory organs were taken with a Sony DSC W70 compact camera using an ocular of the stereomicroscope. The material was preserved in 75% ethanol. Before dissection and preparation, the female copulatory organs were cleared of surrounding hairs. The opaque tissue around the vulva was removed using minute pins in order to have a better view on the various vulval structures. Generally, vulvae were cleared in 96% DL-lactic acid (C<sub>3</sub>H<sub>6</sub>O<sub>3</sub>). In males, the cymbial hairs of areas close to the bulb were removed so that all crucial structures could be seen. Scanning electron micrographs were taken with a Zeiss DSM-950, following gold sputter-coating.





Figure 1A–D.—*Evippomma rechenbergi* sp. nov., habitus: A, living female in natural habitat, dorsal view; B, male prosoma, frontal view, showing the eye arrangement and the dense cover of white scale hairs; C, female paratype (EC04), ventral view; D, male holotype (EC01), lateral view. Images (A–B) by I. Rechenberg.

All measurements and all numbers listed next to the scale bars are in millimeters (mm). For males, measurements of holotype are provided first, followed by those of paratypes as ranges in parentheses. For female paratypes, measurements are provided as ranges in parentheses. For the present study, the “opisthosoma length” excludes the spinnerets and the petiole. The leg formula (from longest to shortest leg) and leg spination pattern follows Bayer (2012). For leg/palp spination the segments are listed in the following sequence: femur, patella, tibia and metatarsus (metatarsus absent in palp, however, here palpal tarsus mostly with spines). All spines on the prolateral surface of the respective limb segment were counted and listed, followed by the dorsal, retrolateral and ventral surfaces. Thus the resulting number is generally 4-digits. If a spination pattern of a certain limb article differs between the left and right sides, the pattern for the right side is

listed in curly brackets, without a blank. Palp and leg lengths are listed as: total (femur, patella, tibia, metatarsus, tarsus).

Regular solid lines on illustrations indicate edges/margins/rims of structures as recognised in the respective view; weak solid lines indicate edges of fine structures, e.g. membranous structures or fine grooves in the area of the epigyne; dashed lines indicate inner walls of ducts and/or slits; dotted lines (rough) indicate structures visible through the cuticle (e.g., parts of vulva visible through the epigynal cuticula); dotted lines (fine) indicate color differences (e.g., border of epigynal field). A schematic illustration of the course of the internal duct system of the vulva is included in the present study (Fig. 3C). Therein the areas of the spermathecae or lateral vesicles including spermathecal heads are indicated with “T”-symbols, the copulatory opening with a circle, and the end of the



fertilisation duct in the direction of the uterus externus with an arrow.

The following abbreviations are used throughout the text: ALE, anterior lateral eye; AME, anterior median eye; C, conductor; CB, base of conductor; CT, tip of conductor; CD, copulatory duct; CL, carapace length; CO, copulatory opening; CW, carapace width; CY, cymbium; CYA, eymbium alveolus; DSV, duct connecting spermatheca and lateral vesicle; E, embolus; EA, epigynal atrium/a; EB, embolic base; EF, epigynal field; FD, fertilisation duct; IV/CL, ratio of total length of leg IV versus carapace length; LL, lateral lobe (of epigyne); MA, median apophysis (of bulbus genitalis); MAH, hook of MA; MAL, rounded lobe of MA; MAT, tip of MA; MS, median septum of epigyne; OL, opisthosoma length; OW, opisthosoma width; PLE, posterior lateral eye; PME, posterior median eye; S, spermatheca; s.a., subadult; SD, spermathecal duct (in male bulb); SH, spermathecal head/s; T, tegulum; TE, tegulum extension; TF, tegulum fold; TL, total body length; V, lateral vesicle.

Specimens are deposited in the following collections: MAC, Private Collection of Mark Alderweireldt, Ghent, Belgium; MNHN, Muséum National de Histoire Naturelle, Paris, France (C. Rollard); SMF, Senckenberg Museum, Frankfurt am Main, Germany (P. Jäger; technical curator: J. Altmann); SMNK, Staatliches Museum für Naturkunde Karlsruhe, Germany (H. Höfer; technical curator: F. Meyer).

## TAXONOMY

**Family Lycosidae** Sundevall, 1833

**Subfamily Evippinae** Zyuzin, 1985

**Genus *Evippomma*** Roewer, 1959

Roewer 1959: 198 (Description and diagnosis of the genus).

Type species *Evippa cristata* Simon, 1910 (= *Evippa squamulata* Simon, 1898) by subsequent designation of the author.

***Evippomma rechenbergi*** sp. nov.

<http://zoobank.org/?lsid=urn:lsid:zoobank.org:act:F4444D8D-9D37-4ADF-8298-93B0B0D03C4C>

(Figs. 1–8)

**Type material.**—*Holotype male*. MOROCCO: *Meknès-Tafilalet*: Erg Chebbi Desert, near Tisserdmine, ca. 760 m, sample no. EC01, 31°17'29"N, 03°58'51"W, sand dunes in the desert, 18 April 2016, I. Rechenberg (SMNK).

**Paratypes.** MOROCCO: *Meknès-Tafilalet*: 1 ♂, same data as holotype except sample no. EC02 (MAC 2004); 2 ♀, same data as holotype except sample nos. EC03–04 (one of which [EC04] collected as juvenile, raised in lab [Berlin] by I. Rechenberg, adult at ca. 25 May 2016, died ca. 30 May 2016), 01–17 April 2016 (SMNK); 1 ♀, same data except sample no. EC05 (collected as juvenile, raised in lab [Berlin] by I. Rechenberg; adult ca. 30 September 2016, died ca. 05 October 2016) (SMF); 1 ♀, same data as holotype except ca. 750 m, sample no. EC06, 31°16'08.5"N, 03°59'27.6"W, 30 November 2011 (SMF); 1 ♀, same data except sample no. EC07, 13 September 2015 (MAC 2005); 1 ♂, same data except sample no. EC08, 12 August 2016 (SMNK); 1 ♀, same data except sample no. EC09, 28 August 2016 (SMNK); 1 ♂, same data

except sample no. EC10, 02 September 2016 (SMNK); 1 ♂, same data except sample no. EC11 (SMF).

**Other material examined.**—MOROCCO: *Meknès-Tafilalet*: 1 ♂, 1 sub-adult juvenile ♀, Erg Chebbi Desert, near Tisserdmine, ca. 750m, sample nos. EC12 [♂; only both palps left, gold-sputtered]/EC13 [juv.], 31°16'08.5"N, 03°59'27.6"W, sand dunes in the desert, 11 September 2015, I. Rechenberg (SMNK); 4 juveniles, same data except sample nos. EC14–17, 28 November – 06 December 2011 (SMF); 1 juvenile, same data except sample no. EC18, November 2016 (SMNK); 5 sub-adult juvenile ♂, 5 sub-adult juvenile ♀, 1 juvenile, same data except ca. 760 m, 31°17'29"N, 03°58'51"W, sample nos. EC19–23 [s.a. ♂]/EC24–28 [s.a. ♀]/EC29 [juv.], 01–17 April 2016 (SMNK).

**Etymology.**—The specific epithet is a patronym in honor of Ingo Rechenberg, who collected all of the material examined herein and who provided many new insights into the biology of spiders living in the Erg Chebbi Desert.

**Diagnosis.**—This species can be distinguished from all other *Evippomma* (and *Evippa*) species except *E. simoni* Alderweireldt, 1992 by the absence of a transverse depression behind the ocular area of the carapace; by the presence of a mainly uniform light yellowish-beige color with barely any markings (Fig. 1A–D); by the slender and pointed morphology of the male conductor tip (visible at least in prolateral or ventral view; Fig. 2A, B, F); and by the shape of the female epigyne, which has clearly recognizable atria (Fig. 3A, D) and an absence of twists in the duct connecting the spermathecae and lateral vesicles (Fig. 3B–C, E). Males can be distinguished from *E. simoni* by the shape of the median apophysis, which has a rounded lobe retrolaterally and a converging, elongated distal part with a pointed tip (Fig. 2B, F). Females of *E. rechenbergi* sp. nov. cannot currently be delimited from *E. simoni*, as females of the latter species are still unknown.

**Description (male).**—Total length 9.7 (9.0–12.5), carapace length 4.5 (4.3–5.3), maximal carapace width 3.3 (3.3–3.8), width of eye rectangle 1.4 (1.4–1.7), opisthosoma length 5.1 (4.6–6.3), opisthosoma width 2.7 (2.7–3.5).

**Coloration.** General appearance pale yellow to beige with hardly any dark markings or patterns (Fig. 1B, D). Sternum and carapace pale yellow to beige, minimally darker than legs, palps, chelicerae and opisthosoma; carapace with few slightly darker striae running radially from fovea to lateral margin. Legs, palps and sternum uniformly pale yellowish beige. Opisthosoma and spinnerets dorsally slightly lighter pale yellowish beige, ventrally even lighter beige; opisthosoma dorsally in proximal half with minimally darker lanceolate cardiac mark.

**General morphology.** Cheliceral furrow with 3 promarginal (central one larger than others) and 2 retromarginal teeth (proximal one slightly larger than distal one). Fovea dash-like, in narrow dimple, located almost centrally on carapace (slightly shifted posteriorly), fovea length 0.98 (0.95–1.05). Body (especially carapace) covered with conspicuous flat, leaf-shaped hairs (scale-hairs, scales) (Fig. 4A, B). Spinnerets, especially anterior ones, with very long spigots (Fig. 4C); each spigot consisting of a conical bulb proximally and a long, flexible shaft distally (Fig. 4D).

**Eyes:** AME 0.23 (0.21–0.26), ALE 0.12 (0.11–0.13), PME 0.43 (0.41–0.45), PLE 0.38 (0.37–0.43), AME–AME 0.13 (0.14).



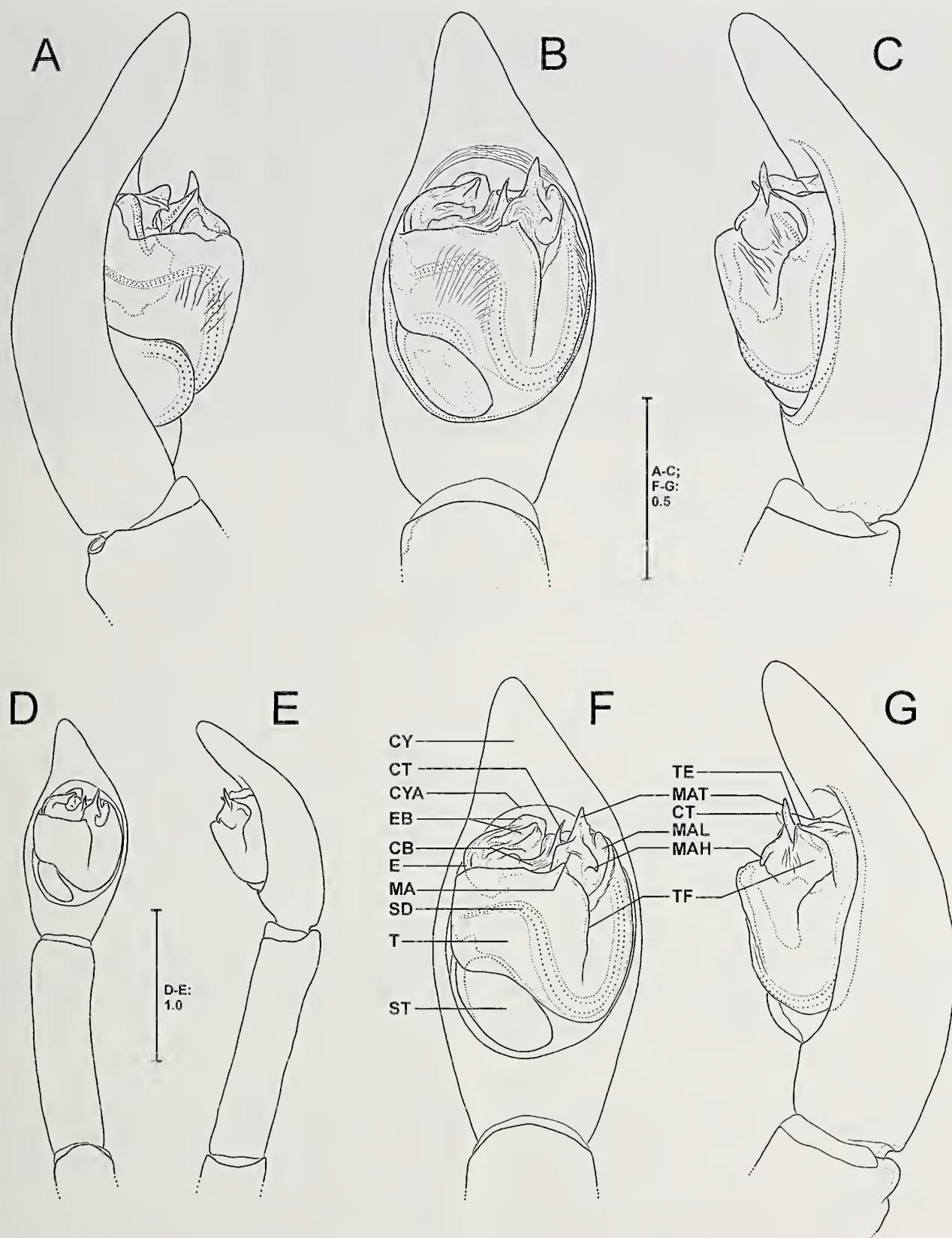


Figure 2A-G.—*Evipponma rechenbergi* sp. nov., illustrations of male copulatory organ. A-E, Holotype (EC01): A, prolateral view, B, D, ventral view; C, E, retrolateral view. F-G, Paratype (EC02): F, ventral view, G, retrolateral view. Abbreviations: CB, conductor base; CT, conductor tip; CY, cymbium; CYA, cymbium alveolus; E, embolus; EB, embolus base; MA, median apophysis; MAH, hook of MA; MAL, rounded lobe of MA; MAT, tip of MA; SD, spermatheca; ST, subtegulum; T, tegulum; TE, tegulum extension; TF, tegulum fold.



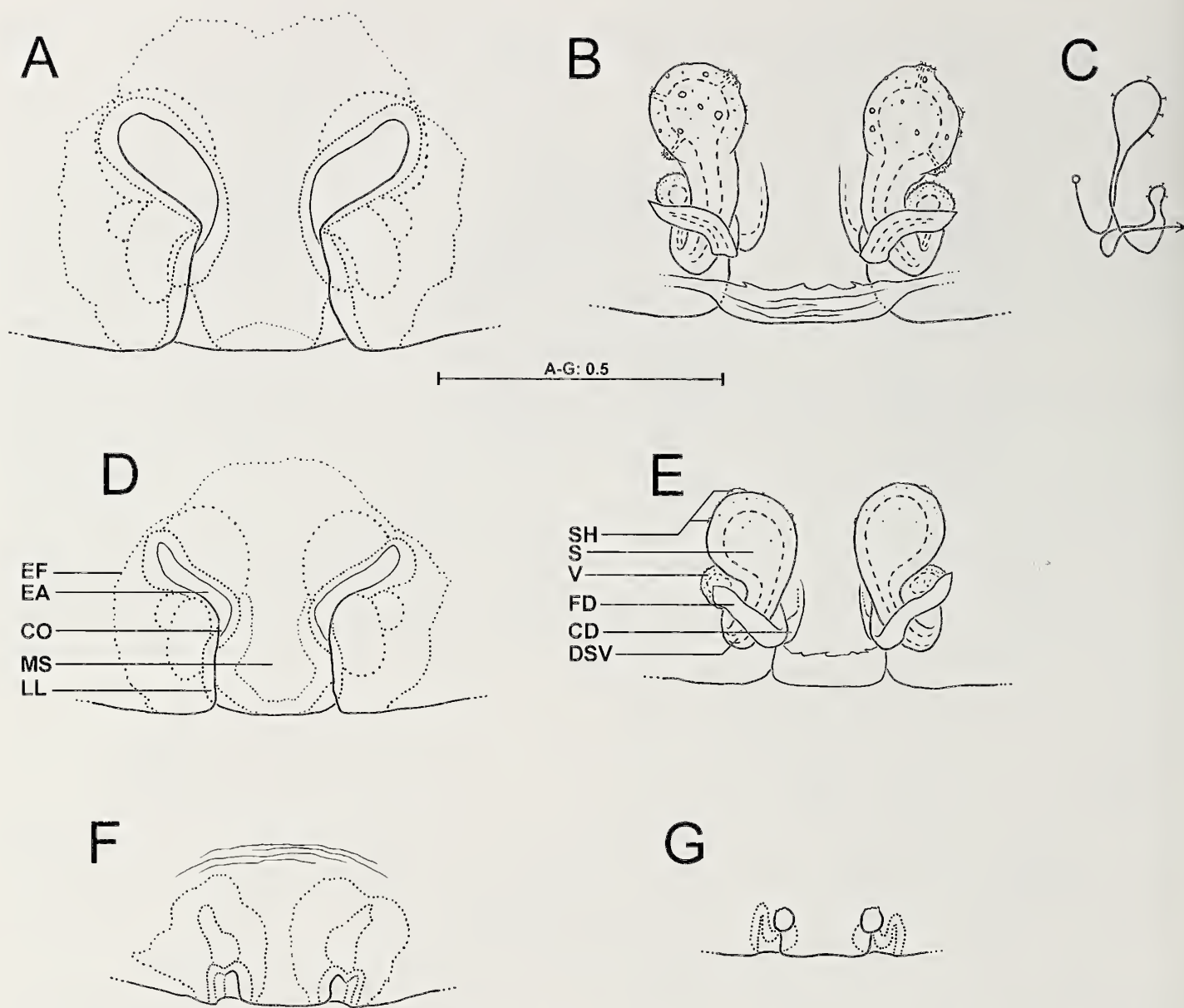


Figure 3A–G.—*Evippomma rechenbergi* sp. nov., illustrations of female copulatory organ. A–C, Paratype (EC03): A, epigyne, ventral view; B, vulva, dorsal view; C, schematic course of internal duct system. D–E, Paratype (EC07): D, epigyne, ventral view; E, vulva, dorsal view. F–G, Subadult female (EC13): F, pre-epigyne, ventral view; G, pre-vulva, dorsal view. Abbreviations: CD, copulatory duct; CO, copulatory opening; DSV, duct connecting spermatheca and lateral vesicle; EA, epigynal atrium; EF, epigynal field; FD, fertilisation duct; LL, lateral lobe; MS, median septum (of epigyne); S, spermatheca; SH, spermathecal head(s); V, lateral vesicle.

AME–ALE 0.06 (0.05–0.06), PME–PME 0.47 (0.46–0.58), PME–PLE 0.45 (0.45–0.55), AME–PME 0.09 (0.09–0.11), PLE–PLE 0.97 (0.96–1.13), clypeus height at AME 0.15 (0.15–0.31), clypeus height at ALE 0.15 (0.15–0.25).

**Legs:** Tarsi of legs without pseudo-articulation (Fig. 5A; in contrast to most *Evippa* species, where it is present; see Alderweireldt 1991, fig. 9); distally with very long and stiff hairs (Fig. 5C) being slightly broadened at distal end, present on all legs, however, clearly longest on leg IV; tarsi of legs I and II with conspicuous and peculiarly-curved long spines situated slightly ventral of the tarsal claws, these converging dorsally in between two superior tarsal claws (Fig. 5A, B).

Tarsi of legs I & II also with conspicuous broad short spines (setae) ventro-distally (Fig. 5A, B). Superior tarsal claws very long (longest at leg IV; Fig. 5C). Inferior tarsal claw very small (20–30  $\mu$ m; seemingly atrophied) and without teeth (Fig. 5A).

**Spination:** Spination of paratypes in parentheses; the order represents the frequency of occurrence. Palp: femur 1410 (1410, 1420), patella 1200 (1200), tibia 0100 (0100), tarsus —. Legs: femur I 3340{3350} (3340, 3350, 3360, 3370), II 3350{3440} (4340, 3340, 3350, 3380), III 4340 (4340, 3340, 4330), IV 5350{4330} (4340, 4350, 5340); patella I–IV 1210 (1210); tibia I 32210{32310} (32310, 32210, 33310), II 32310{32210} (33310, 32310, 22310), III 3326 (3226, 3326,



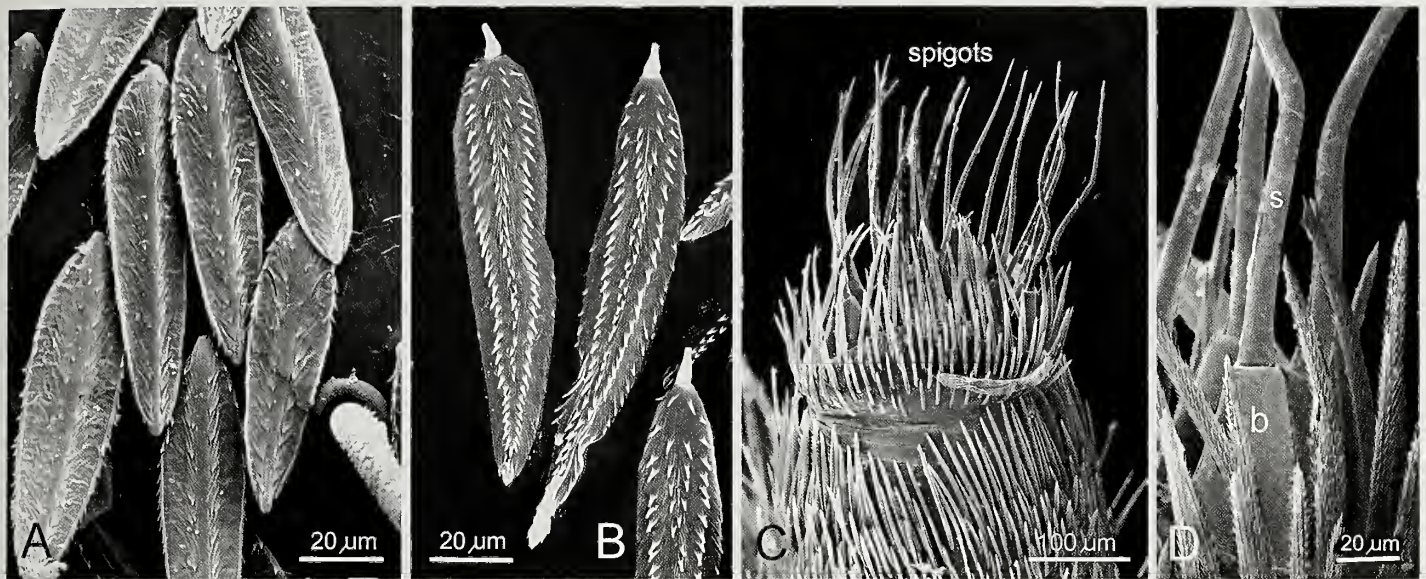


Figure 4A–D.—*Evippomma rechenbergi* sp. nov., scanning electron micrographs: A, leaf-shaped scale hairs with many small protrusions arranged in rows, dorsal view; B, same, ventral view, showing several longitudinal rows of denticles; C, lateral view of anterior spinneret of male covered with many hairs and exceptionally long spigots; D, detail of spigot showing conical bulb (b) at the base and a long, flexible shaft (s) extending distally.

4226, 5326, 4326), IV 4235{5236} (5336, 5236, 4226, 3326), distal-most pair of ventral spines on all tibiae clearly smaller than others, pre-distal pair shifted laterally (could also be counted as one additional prolateral and one additional retrolateral spine instead of a ventral pair); metatarsus I 4045 (4045), II 4045 (4045, 4035) III 4045 (4045), IV 5046 (5046), distal-most section with no pair of spines ventrally but with one spine centrally, forming part of a ring of five spines around distal-most part of metatarsus. Palpal cymbium apically and pre-apically with 5–10 relatively broad spines of moderate length (5–6 x longer than wide).

**Measurements of palp and legs:** Palp 6.7 (6.6–7.3) [2.6 (2.6–2.8), 1.0 (1.0–1.1), 1.5 (1.5–1.7), 1.6 (1.5–1.7)], I 19.9 (19.5–21.3) [5.3 (5.2–5.7), 2.0 (2.0–2.2), 4.9 (4.7–5.2), 5.3 (5.2–5.6), 2.4 (2.4–2.6)], II 19.1 (18.9–20.6) [5.0 (5.0–5.1), 1.9 (1.9–2.2), 4.4 (4.3–4.7), 5.3 (5.2–5.8), 2.4 (2.4–2.8)], III 19.3 (18.9–20.1) [4.8 (4.7–5.1), 1.8 (1.8–2.0), 3.8 (3.7–4.1), 5.9 (5.7–5.9), 3.0 (3.0–3.1)], IV 22.9 (22.4–24.4) [5.7 (5.6–5.8), 2.0 (2.0–2.4), 5.2 (5.0–5.6), 6.7 (6.6–7.3), 3.3 (3.2–3.4)]. Leg formula: 4132 (4123, 4132); legs quite long: IV/CL = 5.09 (4.60–5.22).

**Copulatory organ:** See also respective aspects in diagnosis above. Embolic base broad and prominent, with many ridges and some lobes, especially a protruding sharp edge pointing retrolatero-apically (Figs. 2B & 6B); embolic base located mesially to prolaterally at distal section of tegulum, embolus long and flagelliform and in ventral view not visible, except for its very proximal section. Most part of conductor membranous, distal section sclerotized, slender and apically pointed (Fig. 2B, F). Median apophysis complex, with hook-shaped extension centrally, rounded lobe retrolaterally and relatively slender and pointed tip (Fig. 2F). Central part of tegulum broad, sperm duct U-shaped in retrolateral to central section of tegulum and running more or less transversally in prolateral section (Fig. 2F). Subtegulum in ventral view clearly visible prolatero-proximally in cymbium alveolus (Figs. 2B, F & 6B,

D–F). Cymbium at alveolus-section broad, becoming slender distally, at distal section with 5–10 short, relatively broad setae (Fig. 6B). Palpal tibia longer than cymbium (Figs. 2D, E & 6A).

**Description (female).**—Total length 12.4–16.1, carapace length 5.0–6.2, maximal carapace width 3.6–4.4, width of eye rectangle 1.8–2.1, opisthosoma length 6.3–8.3, opisthosoma width 4.1–5.4.

**Coloration:** As in male, but carapace as pale as legs and without (or indistinct) striae running radially from fovea to lateral margin; sternum minimally darker than legs, with light brown to brown extremely narrow margin (Fig. 1C); lanceolate cardiac mark dorsally on opisthosoma hardly darker than rest of opisthosoma and thus sometimes not recognizable as such.

**General morphology:** Cheliceral furrow with 3 promarginal (central one larger than others) and 2 retromarginal teeth (proximal tooth slightly larger than distal one). Fovea dash-like, in narrow dimple, located centrally on carapace (slightly shifted posteriorly), fovea-length 0.93–1.15. Body (especially carapace) covered with conspicuous flat, leaf-shaped hairs (scale-hairs, scales) (Fig. 4A, B). Spinnerets generally as in male, but broader, having very long spigots (Fig. 4C). Each spigot consists of a conical bulb proximally and a long, flexible shaft distally (Fig. 4D).

**Eyes:** AME 0.25–0.31, ALE 0.15–0.18, PME 0.51–0.54, PLE 0.47–0.54, AME–AME 0.14–0.16, AME–ALE 0.05–0.06, PME–PME 0.68–0.71, PME–PLE 0.58–0.68, AME–PME 0.10–0.14, PLE–PLE 1.22–1.38, clypeus height at AME 0.16–0.17, clypeus height at ALE 0.14–0.16.

**Legs:** The leg tarsi of females look like those of males (see description section above referring to Fig. 5A–C). However, in females, the long and stiff hairs are only present on legs III and IV (on leg III clearly shorter).





Figure 5A–C.—*Evippomma rechenbergi* sp. nov., tips of female (paratype, EC03) tarsi (including claws and other micro-structures) of right leg I (A–B) and left leg IV (C). A, Prolateral view, showing several stout and broad setae ventro-distally and a pair of conspicuously curved, long spines converging between the two superior claws. Both of these structures are only present on the tarsi of legs I and II. B, ventral view, showing spines converging between the claws and further ventrally a small (20–30  $\mu$ m) third claw without teeth. C, Prolateral view, showing the tarsal claws of leg IV and many long and stiff hairs around the distal part of the tarsi (except ventrally).

**Spination:** Standard pattern or most frequent pattern first; lesser frequent patterns [if existing] in parentheses; if more than one, listed in the sequence of their frequency. Palp: femur 0300 (0200), patella 1000 (1200), tibia 2121 (1201), tarsus 3004. Legs: femur I 2200, II 2200 (3200), III 3210 (2210, 4210, 4200), IV 0200; patella I 1010 (1000), II 1000 (1010), III 1100 (1200), IV 0000; tibia I 30110 (30210, 20210, 20110, 40210), II 30010 (30110, 20110, 20010, 4009), III 3025 (3026, 3226, 3225, 3036), IV 0034 (1034, 1024, 0024, 1134), distal-most pair of five ventral pairs of spines on tibiae I & II clearly smaller than others, pre-distal pair shifted laterally (could also be counted as one additional prolateral and one additional retrolateral spine instead of a ventral pair); metatarsus I 4035 (4025, 3027), II 4025 (4035, 3017) III 4045 (4035, 3037), IV 4045 (4046, 4035, 4036, 4026, 3028), distal-most section of metatarsus without a pair of spines ventrally but with one single spine centrally, forming part of a ring of five spines around distal-

most part of metatarsus. Spines of palpal segments thinner than those on legs, sometimes difficult to distinguish from regular hairs.

**Measurements of palp and legs:** Palp 5.7–7.2 [2.2–2.6, 0.9–1.2, 1.0–1.5, 1.6–1.9], I 13.7–16.7 [4.1–5.2, 2.0–2.4, 3.3–4.0, 2.7–3.2, 1.6–1.9], II 12.9–15.5 [3.9–4.8, 1.9–2.2, 2.8–3.5, 2.6–3.2, 1.7–1.9], III 12.5–15.1 [3.6–4.6, 1.8–2.1, 2.2–2.9, 3.1–3.6, 1.8–2.1], IV 15.4–19.5 [4.3–5.6, 2.1–2.3, 3.4–4.5, 3.6–4.5, 2.0–2.6]. Leg formula: 4123; legs moderately long: IV/CL = 3.05–3.21.

**Copulatory organ:** See also respective aspects in diagnosis above. Epigyne with septum slightly converging anteriorly, epigynal atria at least twice as long as broad and oriented diagonally (Figs. 3A, D & 7A–D). Epigynal field not distinctly developed but recognisable as such, especially posterior half (Figs. 3A, D & 7A–D). Proximal sections of copulatory ducts located medial to spermatheca (and other vulval structures)



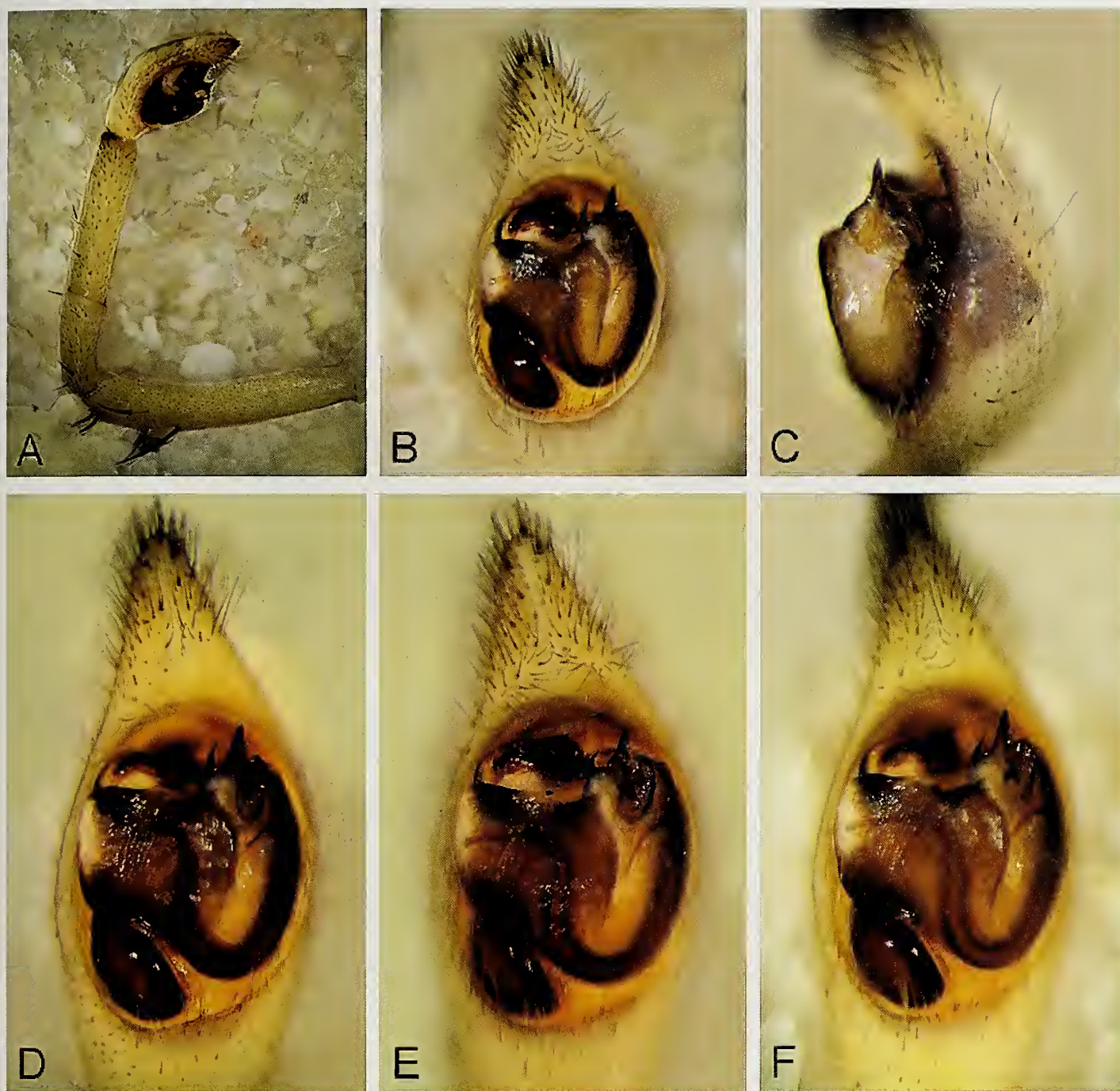


Figure 6A–F.—*Evippomma rechenbergi* sp. nov., photos of male copulatory organ. A–C, Holotype (EC01): A, pedipalp, prolateral view; B, bulbus genitalis, ventral view, showing tip of cymbium with several short, broad setae; C, same, retrolateral view. D, Paratype (EC11), bulbus genitalis, ventral view. E, Paratype (EC08), bulbus genitalis, ventral view. F, Paratype (EC10), bulbus genitalis, ventral view.

(Figs. 3E & 8A–D). Spermatheca large and voluminous and with several, small and flat spermathecal heads distributed over its surface. Duct connecting spermatheca and lateral vesicle regularly curved, without twisted sections. Lateral vesicles with many small tubercles. Fertilization ducts running diagonally from mesio-posteriorly to antero-laterally (Figs. 3B, E & 8A–D).

**Primordial copulatory organ:** Pre-epigynes and pre-vulvae of subadult females – though by far not completely developed as

copulatory organ – have been investigated in some families (e.g., Pisauridae, Psecridae) belonging to the Lycosoidea (Sierwald 1989; Bayer 2011). In the genus *Fecenia* Simon, 1887 (Psecridae) characters of pre-epigynes and pre-vulvae were even of diagnostic interest and could be included in an identification key to the species (Bayer 2011). Therefore, primordial copulatory organs of subadult females were here also investigated. In Figure 3F, the pre-epigyne is shown, exhibiting already a short and broad pre-septum. Epigynal



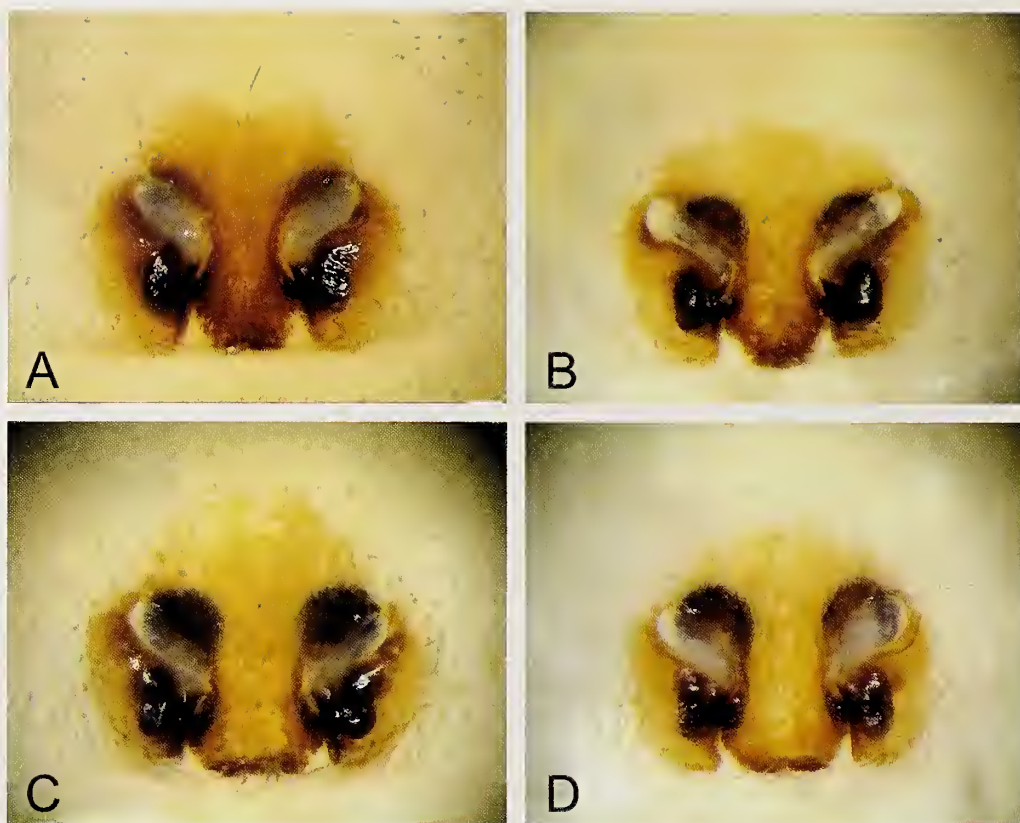


Figure 7A-D.—*Evippomma rechenbergi* sp. nov., photos of female epigynes, ventral view: A, paratype (EC03); B, paratype (EC04); C, paratype (EC09); D, paratype (EC06).

field still divided in two halves. Epigynal atria not recognizable. In pre-vulva approximately round structures visible (Fig. 3G), apparently becoming spermathecae later on. Lateral to each pre-spermatheca, there exists a flimsy structure exhibiting a very narrow arc orientated anteriorly.

**Intraspecific variation of copulatory organs.**—*Males:* Slight differences in some bulbal structures. In one specimen, the conductor tip (ventral view) slightly shorter (Fig. 6E) than in others (Figs. 2B, F & 6B, D, F). Retrolateral margin of ventral-most part of tegulum (means tegulum-part ventral of the tegulum gap holding the approximately transversal section of spermatheca) in some specimens (Fig. 6B, F) reaching further proximally than in others (Fig. 6D, E). U-shaped loop of sperm duct, in ventral view visible in retrolateral section of tegulum, in one specimen (Fig. 6E) slightly shorter than in remaining specimens. Central hook of median apophysis in one specimen (Fig. 2F, G) minimally larger than in others (Figs. 2B, C & 6B–F).

*Females:* Epigynes in some specimens with clearly narrower atria (Figs. 3D & 7C) than in others (Figs. 3A & 7A, D). Epigynal septum in some individuals wider (Figs. 7C, D) than in others (Figs. 3A, D & 7A, B). Vulva: in some females spermathecae minimally broader (Figs. 3E & 8B, C) than in others (Figs. 3B & 8A, D). In specimens shown in Figures 8B and 8C, the lateral vesicles and final sections of connecting duct (between spermathecae and lateral vesicles) reaching slightly further laterally in comparison to others (Figs. 3B, E & 8A, 8D).

**Distribution.**—To date, *E. rechenbergi* is known only from the type locality in Morocco (Erg Chebbi Desert).

## DISCUSSION

The results of our morphological investigations do not allow an unambiguous assignment of *E. rechenbergi* to any of the already described genera of the subfamily Evippinae. To date, five evippine genera are known from Africa: *Zenonina* Simon, 1898, which has not been studied since the lycosid revision by Roewer (1959); *Proevippa* Purcell, 1903, which was revised by Russell-Smith (1981) sub *Chaleposa* Simon, 1910 (its junior synonym) and later also studied by Alderweireldt and Jocqué (1995); *Pseudevippa* Simon, 1910 includes only one species that is only known from females and considered closely related to the similar genus *Evippa* (see Alderweireldt 1991); and finally the two genera *Evippa* and *Evippomma*, that include the most similar species compared with our specimens from Erg Chebbi. These two genera are difficult to distinguish as they share many characters. Their high similarity indicates that both these genera are most likely closely related (Alderweireldt 1992). Representatives of both genera have a distinct depression on the carapace behind the ocular area (Alderweireldt 1991, fig. 1.2), a long, filiform embolus, a complex median apophysis, very large spermathecae connected with conspicuously twisted internal ducts and similar dimensions and arrangement of the eyes.



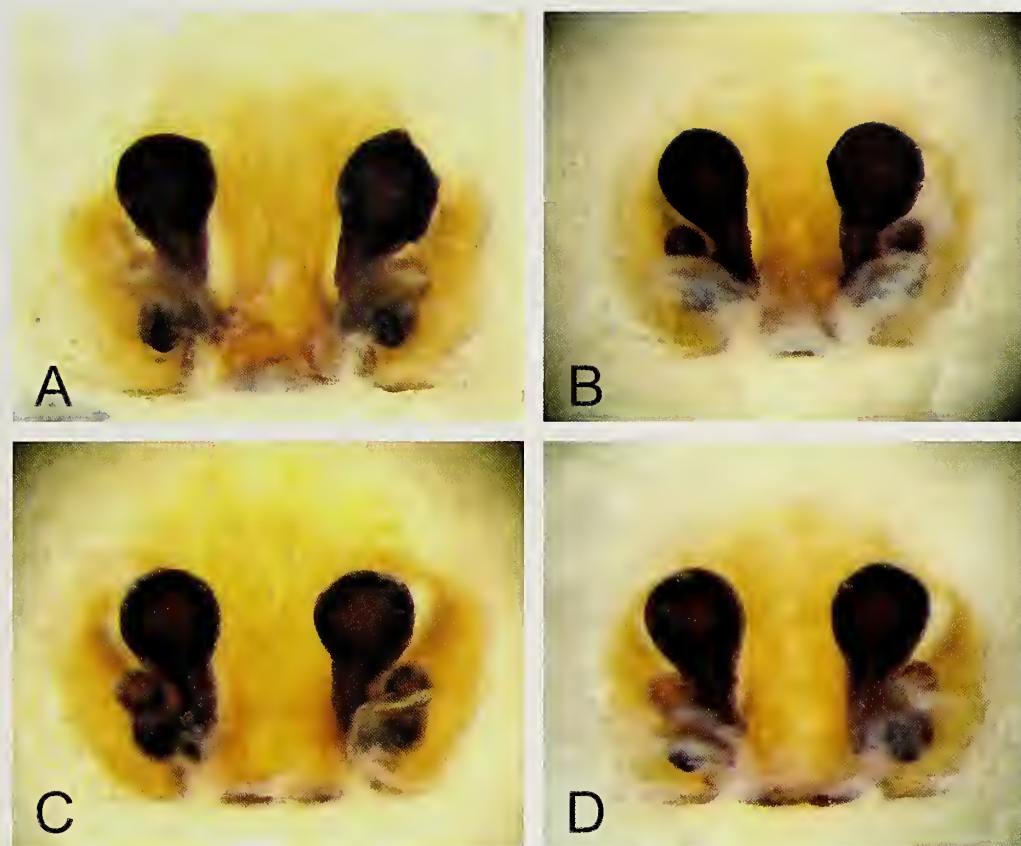


Figure 8A–D.—*Evippomma rechenbergi* sp. nov., photos of female vulvae, dorsal view: A, paratype (EC03); B, paratype (EC05); C, paratype (EC09); D, paratype (EC06).

According to Alderweireldt (1991), the main diagnostic characters for *Evippa* are: pseudo-articulation of the tarsi (Alderweireldt 1991, fig. 9); at least six pairs (and usually seven pairs) of ventral spines (including a small distal pair) on tibia I (and mostly also on tibia II); epigyne generally with shallow atria (Fig. 3D); and median septum of epigyne longer than broad.

For the genus *Evippomma*, Alderweireldt (1992) suggested the following as the main diagnostic characters: five or six pairs of ventral spines (including a small distal pair) on tibia I (and mostly also on tibia II); body densely covered with conspicuous flat, leaf-shaped hairs (scales); a striking fringe of black hairs ventrally and dorsally on tibiae I (Alderweireldt 1992, fig. 1d); median apophysis of male palp generally with a hook-shaped part (Alderweireldt 1992, fig. 1c); epigynal septum generally as long as broad (at most indistinctly longer than broad); vulva additionally with a lateral vesicle on each side (Alderweireldt 1992, fig. 1f).

Given these diagnoses, the focal species from Erg Chebbi would neither fit within *Evippa* nor in *Evippomma*. Since the species from Erg Chebbi exhibits four of six of the important characters diagnostic for *Evippomma* (five pairs of ventral tibial spines; scale hairs; median apophysis with hook-shaped part; lateral vesicles present) but only two of four characters diagnostic for *Evippa* (epigynal septum longer than broad; atria clearly recognisable), we preliminarily assign it to *Evippomma*. Our decision should be regarded as an assignment *incertae sedis*. The species *E. simoni* also lacks the fringe of

black hairs on tibia I, the transversal depression on the carapace, and is also of pale coloration (however to date only one male [holotype] known; preserved for a very long time in alcohol; may have bleached) and shows general structures of the palpal bulb that are similar to those of *E. rechenbergi*. Alderweireldt (1992) included *E. simoni* in the genus *Evippomma* with some reservations. Due to the somatic similarity and especially the similarity of the complex bulbal structures of the male palp, we consider these two species closely related. Unfortunately, the female of *E. simoni* is still unknown, and, as such, it is not clear if female characters would corroborate the hypothesis of a close relationship. In our opinion, it would be justified to establish a new genus to which both these species could be assigned to. On the other hand, it is also conceivable that these species belong to either an expanded *Evippa* which is synonymized with *Evippomma* (with a revised and more inclusive diagnosis for the former), or to *Evippomma* with a revised diagnosis. However, clarifying these issues in the genus-group taxonomy would require two main approaches. First, a comprehensive revision of the Evippinae of Africa that would need to include a re-examination of the type specimens of many species, especially those of the type species of allied genera (e.g., *Proevippa*, *Pseudevippa* and *Zenonina*). However, this is outside of the scope of the present study. Secondly, phylogenetic studies would be informative, using either morphological, molecular (several genetic markers) or ideally combined approaches. This is also out of the scope of the present study. Another reason for not establishing a new genus



at this time is the missing female of *E. simoni*, which would at least complicate the definition of a new genus.

Several *Evippa* species were placed as *nomina dubia* in the course of the revision of this genus by Alderweireldt (1991). Some of them were only characterized by descriptions from more than one hundred years ago which are today only partly of significance. For some of them illustrations exist, e.g., for *E. unguolata* (O. Pickard-Cambridge, 1876) by Strand (1908, pl. VIII, fig. 13), by Denis (1947, pl. I, fig. 14), by Roewer (1959, fig. 95), and by Denis (1966, pl. VIII, figs. 42–43). The illustration of the epigyne in Denis (1947) is somewhat reminiscent of the epigyne of *E. rechenbergi*. The female specimen examined by Denis was unfortunately not available at the MNHN (C. Rollard, pers. comm.). Denis (1947), however, mentioned a distinct marking on the carapace, which would argue against conspecificity with *E. rechenbergi*. As the syntypes of *E. unguolata* examined and described by Pickard-Cambridge (1876) are all juvenile, a clear definition of this species is not possible. Alderweireldt (1991), therefore, justifiably regarded it as a *nomen dubium*, together with some other species, that are also indefinable. It therefore remains puzzling as to which species may have been examined and identified as *E. unguolata* by Strand (1908), Denis (1947, 1966) and Roewer (1959).

*Evippomma rechenbergi* has several conspicuous morphological features. Most of the body is covered with lanceolate, leaf-shaped scale hairs (Fig. 4A, B). Their function is not yet understood, although it is possible that they generate special reflection effects (in sun or moon light). The scales have a typical microstructure (Fig. 4A, B) that differs on the ventral and dorsal surfaces. Some scales are covered by small pores which may play a role in pheromone secretion. The conspicuous broad short spines (setae) ventro-distally on the tarsi of legs I & II (Fig. 5A, B) are strong and resistant and might facilitate digging in dry sand. Moreover, it was observed (I. Rechenberg, pers. comm.) that only the first two leg pairs are used for digging, and these setae are only found on the tarsi of legs I & II. This is also corroborated by the blunt tips of the superior tarsal claws of legs I and II (Fig. 5A). Around the distal-most section of the tarsi (except ventrally) there are long stiff hairs, and on the tarsi of leg IV (Fig. 5C) these are conspicuously long and stiff and exhibit a slightly broadened distal end. These hairs might facilitate walking on the dry and loose sand. In females, these long and stiff hairs are only present on the tarsi of legs III and IV. At leg pair IV, which provides the shear force while walking, they are clearly longer.

#### ACKNOWLEDGMENTS

Many thanks to Ingo Rechenberg (Berlin, Germany), who collected all of the spider material examined herein, provided photos of living spiders in the desert, and raised spiders in his laboratory in Berlin. We are also grateful to Luis Piacentini (Buenos Aires, Argentina), Anton Nadolny (Sevastopol, Crimea), Dimitri Logunov (Manchester, UK) and Robert Bosmans (Ghent, Belgium) who kindly commented on the taxonomy of Evippinae. Thanks to Peter Jäger, Julia Altmann (SMF) and Hubert Höfer (SMNK) for the loan of spider specimens and for the integration of type material into the scientific collections of their respective institutes. Christine Rollard (MNHN) kindly provided information on the

arachnid collection of the MNHN. Many thanks to Michael Rix and to the two reviewers of our manuscript, Volker Framenau and Cor Vink, for their helpful comments and reviews.

#### LITERATURE CITED

- Alderweireldt, M. 1991. A revision of the African representatives of the wolf spider genus *Evippa* Simon, 1882 (Araneae, Lycosidae) with notes on allied species and genera. *Journal of Natural History* 25:359–381.
- Alderweireldt, M. 1992. A taxonomic revision of the African wolf spider genus *Evippomma* Roewer, 1959 (Araneae, Lycosidae). *Journal of African Zoology* 106:153–167.
- Alderweireldt, M. 1996. A taxonomic revision of the genus *Ocyale* Audouin, 1826 in Africa (Araneae: Lycosidae). *Journal of Natural History* 30:1349–1365.
- Alderweireldt, M. 1999. A revision of Central African *Trabea* (Araneae, Lycosidae) with the description of two new species from Malawi and a redescription of *T. purcelli*. *Journal of Arachnology* 27:449–457.
- Alderweireldt, M. & R. Jocqué. 1995. A description of the female of *Proevippa lightfooti* Purcell, 1903 (Araneae, Lycosidae) together with a redescription of the male. *Biologisch Jaarboek Dodona* 62:109–113.
- Bayer, S. 2011. Revision of the pseudo-orbweavers of the genus *Fecenia* Simon, 1887 (Araneae, Psecchridae), with emphasis on their pre-epigyne. *Zokeys* 153:1–56.
- Bayer, S. 2012. The lace-sheet-weavers – a long story (Araneae: Psecchridae: *Psecchrus*). *Zootaxa* 3379:1–170.
- Bayer, S. 2014. Seven new species of *Psecchrus* and additional taxonomical contributions to the knowledge of the spider family Psecchridae (Araneae). *Zootaxa* 3826:1–54.
- Bayer, S. & A. Schönhofer. 2013. Phylogenetic relationships of the spider family Psecchridae inferred from molecular data, with comments on the Lycosoidea (Arachnida: Araneae). *Invertebrate Systematics* 27:53–80.
- Deeleman-Reinhold, C.L. 2009. Description of the lynx spiders of a canopy fogging project in northern Borneo (Araneae: Oxyopidae), with description of a new genus and six new species of *Haniataliwa*. *Zoologische Mededelingen* 83:673–700.
- Denis, J. 1947. Spiders. In: Results of the Armstrong College expedition to Siwa Oasis (Libyan desert), 1935. *Bulletin de la Société Fouad Ier d'Entomologie* 31:17–103.
- Denis, J. 1966. Les araignées du Fezzân. *Bulletin de la Société d'Histoire Naturelle d'Afrique du Nord* 55:103–144.
- Dupérré, N. 2015. Description of a new genus and thirteen new species of Ctenidae (Araneae, Ctenidae) from the Chocó region of Ecuador. *Zootaxa* 4028:451–484.
- Foelix, R., I. Rechenberg, B. Erb & A.-C. Joel. 2015. Zum Sandtransport der "Radlerspinne" *Cebrennus rechenbergi* Jäger, 2014. *Arachne* 20(6):14–21.
- Foelix, R., I. Rechenberg, B. Erb, & A.-C. Joel. 2016. Über den Bau der Wohnröhren bei wüstenlebenden Spinnen. *Arachne* 21(1):1–17.
- Foelix, R., I. Rechenberg, B. Erb, A. Albin, & A. Aisenberg. 2017. Sand transport and burrow construction in sparassid and lycosid spiders. *Journal of Arachnology* 45:255–264.
- Hill, D.E. 1979. The scales of salticid spiders. *Zoological Journal of the Linnean Society (London)* 65:193–218.
- Jäger, P. 2014. *Cebrennus* Simon, 1880 (Araneae: Sparassidae): a revisionary up-date with the description of four new species and an updated identification key for all species. *Zootaxa* 3790:319–356.
- Metzner, H. 1999. Die Springspinnen (Araneae, Salticidae) Griechenlands. *Andrias* 14:1–279.
- Pickard-Cambridge, O. 1876. Catalogue of a collection of spiders made in Egypt, with descriptions of new species and characters of a



- new genus. Proceedings of the Zoological Society of London 44:541–630.
- Platnick, N.I. & M.U. Shadab. 1988. A revision of the American spiders of the genus *Micaria* (Araneae, Gnaphosidae). American Museum Novitates 2916:1–64.
- Rast, B., I. Wendt, G. Ackermann & M. Hüsser. 2015. *Cebrennus rechenbergi* – Akrobatik in der Wüste. Arachne 20(6):4–13.
- Roewer, C.F. 1959. Araneae Lycosaeformia II (Lycosidae). Exploration du Parc National de l'Upemba, Mission G. F. de Witte 55:1–518.
- Roewer, C.F. 1960. Araneae Lycosaeformia II (Lycosidae) (Fortsetzung und Schluss). Exploration du Parc National de l'Upemba, Mission G. F. de Witte 55:519–1040.
- Russell-Smith, A. 1981. A revision of the genus *Chaleposa* Simon (Araneae: Lycosidae). Journal of Natural History 15:223–244.
- Sierwald, P. 1989. Morphology and ontogeny of female copulatory organs in American Pisauridae, with special reference to homologous features (Arachnida: Araneae). Smithsonian Contributions to Zoology 484:1–24.
- Strand, E. 1908. Nordafrikanische, hauptsächlich von Carlo Freiherr von Erlanger gesammelte Lycosiden. Archiv für Naturgeschichte 73:291–376.
- Zyuzin, A.A. 1985. Generic and subfamilial criteria in the systematics of the spider family Lycosidae (Aranei), with the description of a new genus and two new subfamilies. Trudy Zoologicheskogo Instituta Akademija Nauk SSSR 139:40–51.

*Manuscript received 15 December 2016, revised 2 March 2017.*



## Effects of nectar feeding on cannibalism in striped lynx spiderlings *Oxyopes salticus* (Araneae: Oxyopidae)

Laurel B. Lietzenmayer<sup>1,2</sup> and James D. Wagner<sup>1</sup>: <sup>1</sup>Department of Biology, Transylvania University, Brown Science Building, 300 North Broadway, Lexington, Kentucky 40508-1797 USA; <sup>2</sup>Present address: Department of Entomology and Nematology, University of Florida, Steinmetz Hall, 1881 Natural Area Drive, Gainesville, FL 32608-1902 USA; E-mail: lblietzenmayer@gmail.com

**Abstract.** The timing and nutritional value of a first meal is important for spiderlings, but little is known about what spiderlings specifically consume. For wandering spiders, nectar feeding is a common occurrence thought to be directly beneficial in providing nutrients and serving to fuel energy costly for foraging. Cannibalism is also prevalent among many spiders. We suspect in spiderlings of the cursorial species, *Oxyopes salticus* Hentz, 1845, nectar feeding could decrease cannibalism by causing satiation, or increase cannibalism by enhancing energy levels and rates of interaction. We conducted laboratory experiments to test the longevity of newly hatched *O. salticus* in the presence of different nutrient resources and the effect these resources had on cannibalism rates. Spiderlings were housed solitarily or in pairs and given access to different nutrient resources that reflect those available in the wild, including nectar and insect prey items (fructose, protein, and water). In a 14-day period, we recorded the number of days each spiderling was alive to determine survivorship. By the end of the experiment, 60% of spiderlings housed with fructose were still alive and 10% survived when housed with protein or water. Based on survivorship models, the predicted mean age at death differed between treatments (15.9 days for fructose, 11.2 days for protein, and 9.5 days for water). Spiderlings housed in pairs declined more rapidly in survivorship compared to solitary spiderlings, suggesting cannibalism occurred across all treatments. Fructose significantly increased longevity of spiderlings regardless of their housing and reduced cannibalism.

**Keywords:** Lynx spider, nectivory, predation, survivorship

For spiderlings, finding nutrient resources in the early life stages is critical to their survival. Body size positively correlates with the supply of nutrient reserves in the body (Hvam et al. 2005), and newly hatched wolf spiderlings cannot survive more than a few weeks without a meal before their nutrient reserves fully depreciate (Toft & Wise 1999). Early stages molt more frequently than later instars (Foelix 2011), making the timing and nutritional value of that first meal essential. Highly nutritional meals that are quick and easy to obtain will result in more frequent molts earlier in life, allowing spiderlings to surpass competitors in size and expand the range of potential prey items (Oelbermann & Scheu 2002; Mayntz et al. 2003). However, it may be difficult for spiders like the striped lynx spider, *Oxyopes salticus* Hentz, 1845, to find appropriate sized prey compared to spiderlings of other species. Striped lynx spiderlings are relatively small; by carapace width, *O. salticus* spiderlings are  $0.58 \pm 0.04$  mm (mean  $\pm$  SE) (Young & Lockley 1986) whereas wolf spiderlings, like *Tigrosa helluo* (Walckenaer, 1837) (given as *Hogna helluo* in Walker et al. 2003), are  $0.88 \pm 0.05$  mm (Walker et al. 2003). Considering their smaller body size, amount of nutrient reserves, and range of potential prey items, striped lynx spider hatchlings may be attaining their first meal in alternative ways, including cannibalism or nectar feeding.

Nectar feeding has been observed in many wandering spiders (Taylor & Foster 1996; Jackson et al. 2001; Nyffeler et al. 2016). It is thought that wandering spiders are likely to nectar feed due to low success rates of hunting and the direct benefit they receive from feeding on the plant's extrafloral nectaries and flowers which are predictable and sessile food resources that could help fuel their cursorial lifestyle (Taylor & Bradley 2009). For two wandering spiders, *Hibana velox*

(Becker, 1879) (Anyphaenidae) and *Cheiracanthium mildei* L. Koch, 1864 (Eutichuridae), nectar has been shown to increase molting, foraging activity, and survival in spiderlings (Taylor & Bradley 2009). A ghost spider, *Hibana futilis* (Banks, 1898), can respond to and track chemical cues associated with nectar, allowing it to forage for nectar as it moves among particular plants (Patt & Pfannenstiel 2008). Overall, the high metabolic costs of the foraging strategy of wandering spiders can be supplemented by nectar as an energy rich food source.

Cannibalism provides another readily available nutrient source for spiderlings and is prevalent in many spider species during early life stages (Hvam et al. 2005; Wise 2006). However, the nutritional benefits of cannibalism are contested. Cannibalism has been argued to provide more optimal nutrients for conspecifics than heterospecific diets (Mayntz & Toft 2006), but it has also been shown that conspecifics provide a low-quality diet resulting in slow growth (Oelbermann & Scheu 2002; Mayntz & Toft 2006).

There are several costs to cannibalism that may reduce its prevalence among spiderlings, including the risk of injury from prey with similar predatory abilities, the possible reduction of inclusive fitness, and the potential of contracting pathogens from conspecifics (Pfennig et al. 1998; Jackson et al. 2001; Hvam et al. 2005; Mayntz & Toft 2006; Petersen et al. 2010). In two species of wolf spider, *Pardosa prativaga* (L. Koch, 1870) and *P. amentata* (Clerck, 1757), individuals were usually reluctant to cannibalize and only did so as a last resort to avoid starvation, suggesting that hunger level was the main motivator for cannibalistic behavior (Hvam et al. 2005; Petersen et al. 2010). For spiderlings, if an alternative food source like nectar is available and readily consumed, cannibalism may be less likely to occur. However, it is also



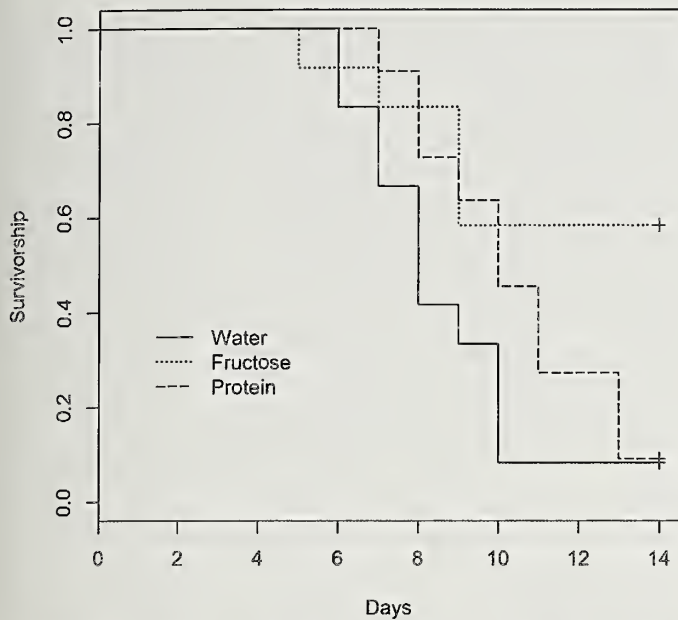


Figure 1.—Survivorship curves of solitary *O. salticus* spiderlings when housed with different food resources (Water, Fructose, Protein). Survivorship refers to the percentage of spiderlings alive each day for a 14-day period.

possible that higher energy levels associated with sugar intake from nectar could increase cannibalism rates, as spiderlings are more active and more likely to interact with conspecifics and partake in risky behaviors (Jackson et al. 2001; Taylor & Pfannenstiel 2009). For the wolf spider *T. helluo*, early instars were more cannibalistic when alternative food was available and exhibit high levels of aggression that can be directed toward conspecifics when contained in high densities (Roberts et al. 2003). Spiderlings may be using nectar as a preliminary energy source to fuel future hunting. Therefore, nectar feeding may be used by striped lynx spiderlings in different ways; nectar may satiate spiders and reduce their tendency to cannibalize or nectar may increase energy levels that drive cannibalistic events.

In this experiment, we tested cannibalism rates within pairs of unrelated lynx spider hatchlings in the presence of different nutrient sources: water, protein, or nectar. Through this laboratory study, we expected to gain information regarding (1) how different resources affect the longevity of newly hatched spiderlings and (2) how cannibalistic behavior varies in the presence of different resources. Our main goal was to detect the presence of nectar feeding in spiderlings and determine how this behavior ultimately affects the tendency to cannibalize.

## METHODS

Mature female striped lynx spiders, *Oxyopes salticus*, were collected in grassy fields at the University of Kentucky Agricultural Farm (GPS: 38° 06' 30.7"N, 84° 29' 53.2"W). In the lab, females were kept in separate containers (8.5 cm x 8.5 cm x 16 cm) and were fed daily with field captured insects until they laid egg cases ( $6.33 \pm 0.92$  days [mean  $\pm$  SE]). This allowed for standardization of age and hunger level of new

hatchlings. Adult females tended to their egg cases until they hatched ( $19.67 \pm 0.92$  days [mean  $\pm$  SE]), and testing began after spiderlings dispersed throughout the container (24 hours). Three broods from three individual females were included in each treatment, with spiderling age varying only by one day.

Control survival treatments had a solitary housed spiderling while the cannibalism treatments housed a pair of unrelated spiderlings. Spiderlings were placed in plastic cylindrical vials ( $7 \times 2.5$  cm) with two 0.5 mL microcentrifuge tubes opened to the inside and secured in holes drilled into the lids. For both solitary and paired spiderlings, one microcentrifuge tube always contained water while the other tube was stocked with either water, artificial nectar, or protein solution. Artificial nectar was created using a 20% fructose solution (Nicolson & Thornburg 2007). Protein solution was created using EAS Soy Protein powder diluted to a 12.6% solution. Using the 20% fructose solution as a reference, both nectar and protein solutions were created with sterilized water at concentrations that yielded the same caloric value (1.8 cal/mL). Each treatment had 12 replicates and all broods were equally represented in each treatment.

To reduce mold and bacteria, tubes and vials were rinsed in ethanol prior to set up and sterile gauze was used to plug the microcentrifuge tubes. The duration of the experiment was 14 days and vials were checked daily for deaths. We could distinguish natural deaths from cannibalism when cannibalism was observed directly. Water, fructose, and protein solutions were replenished every three days.

**Statistical analysis.**—Statistical analyses were conducted using R (build version 3.2.3 (2015-12-10) and R Studio (version 0.99.491) installed with the Survival (2.39-5) and Survminer (0.2.1) libraries (Crawley 2013). The best fit model for the survivorship curve utilized an underlying Weibull distribution where hazards were non-constant with age (can increase or decrease) typified by Type I and Type III survivorship curves. This model fit the data significantly better than the alternative model where hazards remained constant over age which is typified by the Type II survivorship curve. Because some treatments resulted in spiders surviving the entire length of the experiment, we used a survivorship model with censored data. Censored data biases the estimates of lifespan since those individuals did not die within the time frame of the experiment so our response variable is not lifespan per se. To acknowledge this, we use the term longevity instead because the data only represents how long the spiders endured within the time frame of the experiment. In Fig. 2 a post-hoc pairwise comparison of the survivorship curves was made using the Benjamini & Hochberg (1995) method to adjust p-values for multiple comparisons.

## RESULTS

**Survivorship curves.**—Daily census data allowed us to generate survivorship curves for each of the food treatments. To examine how food influenced the shape of the survivorship curve, we restricted our analysis to solitary spiderlings to avoid any confounding influence a cannibalism event can have on survivorship. The type of food resources available significantly influenced the shape of the mortality curves and mean age at death for the solitary spiderlings (Fig. 1). By the end of the 14-day experiment, 60% of the spiderlings housed



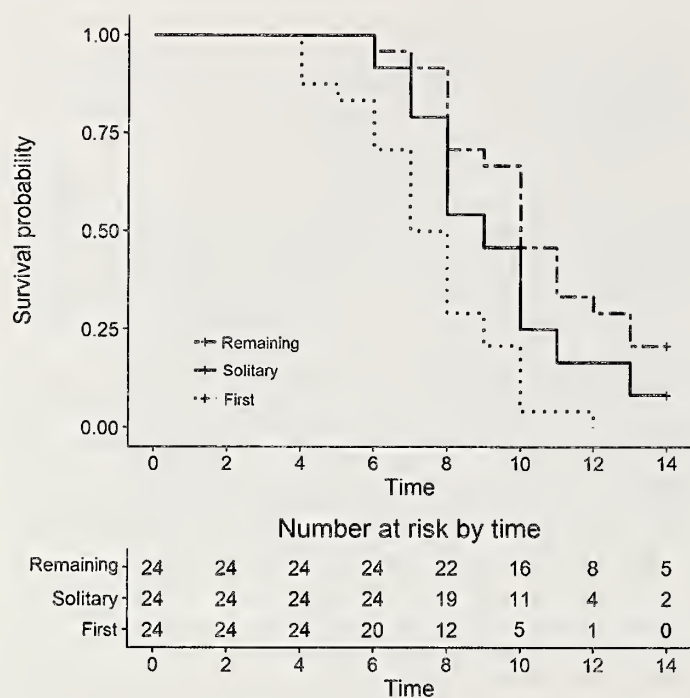


Figure 2.—Survivorship curves of solitary *O. salticus* spiderlings compared to both the first dead and remaining *O. salticus* spiderlings in pairs across water and protein treatments over the 14-day period. Fructose treatments are excluded. The table below the graph includes a summary of number of surviving individuals (at risk) at each time point.

with fructose were still alive, which was in sharp contrast to the protein and water treatment where only 10% survived. Analysis of the survivorship curves revealed that the fructose treatment was significantly different from the water treatment (Fig. 1; Survreg, Fructose: Water  $z = 3.22$ ,  $n = 36$ ,  $P = 0.0013$ ). The protein treatment was intermediate between the water and fructose treatment but not significantly different from the water treatment (Survreg, Protein: Water  $z = 1.20$ ,  $n = 36$ ,  $P = 0.229$ ). Based on the survivorship model for each treatment the predicted mean age at death for water was 9.5 days, fructose 15.9 days, and protein was 11.2 days. The predicted mean age of death for the fructose model exceeded that length of the experiment (14 days) because many of the spiderlings lived to the end of the experiment which increased the amount of censored data in the model.

**Did cannibalism occur?**—During the daily inspections of the paired vials, we observed five instances of spiderlings actively feeding on another individual although no direct attacks or captures were observed. To evaluate if housing with another spider increased rate of mortality, we compared the survivorship curves of the solitary spiders with that of the spider that died first and the remaining spider in the paired vial for the water and protein treatments. We excluded the fructose treatments in this analysis because fructose increased survival above expected and nearly eliminated cannibalism with 16 of the 24 spiderlings in paired treatment surviving the entire 14-day experiment. Spiderlings who died first in paired vials showed a more rapid decline in survivorship compared to solitary spiderlings (Fig. 2;  $P = 0.011$ ) and the remaining paired spiderlings (Fig. 2;  $P = 0.0001$ ). Solitary spiderlings

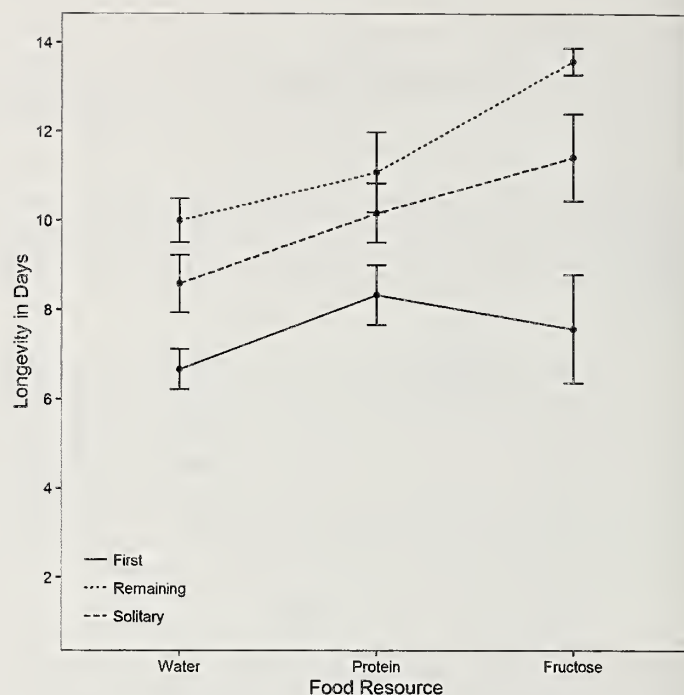


Figure 3.—Interactions between food resource and status (solitary, 1st dead spiderling, 2nd remaining spiderling) on *O. salticus* longevity. Spiderlings in a pair that survived to the end of the experiment were excluded. Points represent mean longevity for spiderlings in each treatment (mean  $\pm$  SE).

showed no difference in survival compared to the remaining paired spiderlings (Fig. 2;  $P = 0.103$ ).

**Cannibalism and longevity.**—To examine how food resource may interact with cannibalism to influence longevity, we ran an ANOVA to see how status (solitary, 1<sup>st</sup> dead spiderling, 2<sup>nd</sup> remaining spiderling) and food resource (fructose, protein, water) influenced longevity. We excluded from the analysis pairs where both spiders survived to the end of the experiment since this analysis is designed to examine factors influencing cannibalism and cannibalism did not occur in those vials. A Bartlett's test for the homogeneity of variances determined that our data is normally distributed (status:  $\chi^2(2) = 0.177$ ; food:  $\chi^2(2) = 0.046$ ). The ANOVA indicated both main effects significantly predicted longevity (status:  $F_{2,87} = 20.94$ ,  $P < 0.001$ ; food:  $F_{2,87} = 7.47$ ,  $P < 0.0001$ ) with no significant interaction between status and the food available (Fig. 3;  $F_{4,87} = 1.995$ ,  $P = 0.102$ ).

## DISCUSSION

Our data shows that different resources affect the longevity of newly hatched spiderlings (Fig. 1). Spiderlings readily fed on the fructose resource and it significantly increased their survival. In all the treatments, spiders were given access to two vials – all food types were paired with a vial of water. We interpret that spiders recognized the fructose as a food source different from water and took advantage of that resource to improve their survival. However, further studies are necessary to confirm spiderling recognition of artificial nectar over water. It is not clear that the spiders recognized the protein vials as readily. The protein food source was derived from a



vanilla flavored powder, which may have affected how the spiderlings reacted to it. This may explain why the survivorship of spiderlings from the protein treatment was not significantly different from the water treatment, as the spiderlings may have not recognized the protein solution as a resource superior to water alone. In future studies, soybean liquid may be a more beneficial alternative to protein powder as it has been shown as a successful protein source in artificial spider diets (Amalin et al. 1999, 2001). It is also important to note that in nature, nectar could also be providing spiderlings with some proteins (Nicolson & Thornburg 2007). Using mixtures that are more reflective of the protein compositions found in natural nectar that lynx spiderlings have access to in the wild may further reduce cannibalistic behavior, including various nectarins and phosphatases that are common in many plant nectars (Nicolson & Thornburg 2007).

This study has provided new insight on the nutritional ecology of *O. salticus*, a species of considerable interest from an agroecological point of view. As one of the most abundant spiders in field crops in the United States, *O. salticus* has been known to consume a number of common crop pests, including the tarnished plant bug, *Lygus lineolaris*, and the bollworm, *Helicoverpa zea* (Young & Lockley 1985; Young & Edwards 1990). Striped lynx spiders are also more tolerant of hot and dry crop situations than other common predators, making them an important species to consider for biocontrol efforts (Young & Edwards 1990; Nyffeler & Sunderland 2003). Our findings may be useful for supporting and rearing *O. salticus* populations for use in agroecosystems.

Creating artificial nectar of nectar proteins and accurate sugar compositions could help to more accurately reflect spiderling behavior after its consumption. Most plant nectar consists primarily of sucrose, but high variability among species requires more knowledge on the particular plant species within lynx spider habitats (Handel et al. 1972). If spiderlings do recognize and respond to fructose solutions in the lab, this may connect to the presence of nectar feeding in the wild by *O. salticus* spiderlings due to their small size and cursorial lifestyle among the vertical space of plants. Spending most of their juvenile life in close proximity to nectar resources, we suspect that these spiderlings are taking advantage of nectar as an energy source to increase their longevity. Nectar feeding has already been observed in wandering spiders (Taylor & Foster 1996; Jackson et al. 2001; Taylor & Bradley 2009), including two individual lynx spiders (Taylor & Pfannenstiel 2008).

The results of this experiment suggest that *O. salticus* spiderlings do exhibit cannibalistic behavior. Although we cannot explicitly conclude that all first deaths in paired spiderlings were a result of cannibalism, our data and direct observations provide strong evidence that cannibalism was occurring. In addition to directly observing five instances of spiderlings feeding on a conspecific, we explain cannibalism in terms of paired spiderling longevity compared to solitary spiderling longevity. Spiderlings that died first among pairs had a more rapid decline in longevity than solitary spiderlings and the second remaining spiderling (Fig. 2), suggesting that these spiderlings were dying earlier than we would expect given their nutritional resources. However, the remaining spiderlings in pairs did not show any overall benefit to

cannibalizing because the longevity of solitary and remaining spiderlings did not differ (Fig. 2).

We found that nectar as an alternative food source greatly reduced cannibalism in the early instars, with only 33% mortality for paired spiderlings with nectar available (and 50% of pairs exhibiting no cannibalism) compared to 90% mortality for paired spiderlings without an alternative food source. Food limitation is considered the single most important factor promoting cannibalism because hunger increases foraging activity and risk taking during foraging (Wise 2006). It may be that nectar feeding resulted in lower hunger levels, deterring spiderlings from cannibalizing. Because both water and fructose were available to spiderlings, our data suggests that nectar is actively being chosen as an alternative, less risky food source to conspecifics, resulting in a drastic decrease in cannibalism. An alternative explanation for the lower rates of cannibalism in the presence of fructose may be that spiderlings are using this resource to increase their energy levels and avoid being cannibalized by evading the potential cannibal. However, this hypothesis seems unlikely because hungry spiders display increased aggression and risk taking behavior (Petersen et al. 2010); both spiderlings in a pair were likely to consume nectar and reduce their hunger and aggression levels.

Our findings are congruent with other studies that have shown cannibalism is less likely to occur when spiders are satiated and similar in size (Vanacker et al. 2004; Rickers & Scheu 2005; Wise 2006; Peterson et al. 2010). In a natural setting, spiderlings that take advantage of nectar sources may be able to reduce the frequency of cannibalistic events, creating an opportunity for spiderlings to grow at varying rates depending on their access to nectar. If body size ratios increased after several instars, the potential for cannibalism may increase. Studies have shown with increasing size variation, there is an increased propensity for cannibalism (Hvam et al. 2005; Petersen et al. 2010).

A longer observation period might show interactions we fail to see in only two weeks, particularly in the fructose treatments because of the high percentage of survival at the end of the experiment. Other experiments related to food sources and survival of spiderlings have used 6 to 27 weeks of observation, showing longer term effects that we are unable to see in 14 days (Toft & Wise 1999; Mayntz & Toft 2001; Oelbermann & Scheu 2002). However, these experiments were performed with wolf spiders, *Pardosa amentata* and *Pardosa lugubris* (Walckenaer, 1802), which can survive longer (12–21 days) than *O. salticus* (9.5 days) when being starved with access to water. Lynx spiders may hatch with less fat reserves than wolf spiders, making them unable to survive for comparable periods of time to wolf spiders. This makes our shorter period of time more appropriate to the specific study species used.

Cannibalism rates among different species of spiderlings are comparable to the 90% mortality after 14 days we observed in water treatments. In *P. palustris* (Linnaeus, 1758), there was 95% mortality among juveniles with no alternative food source besides conspecifics (Rickers & Scheu 2005). A rate of cannibalism of 70% after 14 days of starvation was seen in *P. agrestis* (Samu et al. 1999). Dwarf spiders, *Oedothorax gibbosus* (Blackwall, 1841) (Linyphiidae), showed 61–90% mortality after 20 days (Vanacker et al. 2004). Variation



occurs from inconsistent methods in experimental design, but all studies resulted in over 60% mortality. When given access to nectar, lynx spiderling mortality reduced to 33% after 14 days, considerably less than other groups without the addition of an alternative food source.

Ultimately, this study adds to the growing body of evidence of spider nectivory (Nyffeler et al. 2016), particularly in spiderlings when nutrient resources in the early life stages is crucial to survival. In the lynx spider, and species with similar lifestyles, nectar feeding may play an essential role in the first meal of many spiderlings. Nectar feeding provides the essential nutrients to increase the longevity of spiderlings while also reducing costly cannibalistic behaviors.

## ACKNOWLEDGMENTS

We would like to thank the two anonymous reviewers for their helpful and constructive comments that improved our manuscript. We would also like to thank the Transylvania University Biology Department for their valuable comments regarding experimental design and statistical analyses and the University of Kentucky Entomology Department for access to the Spindletop Research Farm to collect the spiders. This work was supported by Kenan Fund for Student Research (awarded to L. Lietzenmayer).

## LITERATURE CITED

- Amalin, D.M., J. Peña, J. Reiskind & R. McSorley. 2001. Comparison of the survival of three species of sac spiders on natural and artificial diets. *Journal of Arachnology* 29:253–262.
- Amalin, D.M., J. Reiskind, R. McSorley & J. Peña. 1999. Survival of the hunting spider, *Hibana velox* (Araneae, Anyphaenidae), raised on different artificial diets. *Journal of Arachnology* 27:692–696.
- Benjamini, Y. & Hochberg, Y. 1995. Controlling the false discovery rate: A practical and powerful approach to multiple testing. *Journal of the Royal Statistical Society, Series B (Methodological)* 57:289–300.
- Crawley, M.J. 2013. *The R Book: Second Edition*. Wiley, West Sussex.
- Foelix, R. 2011. *The Biology of Spiders*. 3rd ed. Oxford University Press, Oxford, United Kingdom.
- Handel, E.V., J.S. Haeger & C.W. Hansen. 1972. The sugars of some Florida nectars. *American Journal of Botany* 59:1030–1032.
- Hvam, A., D. Mayntz & R.K. Nielsen. 2005. Factors affecting cannibalism among newly hatched wolf spiders (Lycosidae, *Pardosa amentata*). *Journal of Arachnology* 33:377–383.
- Jackson, R.R., S.D. Pollard, X.J. Nelson, G.B. Edwards & A.T. Barrion. 2001. Jumping spiders (Araneae: Salticidae) that feed on nectar. *Journal of Zoology* 255:25–29.
- Mayntz, D. & S. Toft. 2001. Nutrient composition of the prey's diet affects growth and survivorship of a generalist predator. *Oecologia* 127:207–213.
- Mayntz, D. & S. Toft. 2006. Nutritional value of cannibalism and the role of starvation and nutrient imbalance for cannibalistic tendencies in a generalist predator. *Journal of Animal Ecology* 75:288–297.
- Mayntz, D., S. Toft & F. Vollrath. 2003. Effects of prey quality and availability on the life history of a trap-building predator. *Oikos* 101:631–638.
- Nicolson, S.W. & R.W. Thornburg. 2007. Nectar chemistry. Pp. 215–264. *In* *Nectaries and Nectar*. (S. W. Nicolson, M. Nepi & E. Pacini, eds.). Springer, Berlin-Heidelberg.
- Nyffeler, M. & K.D. Sunderland. 2003. Composition, abundance and pest control potential of spider communities in agroecosystems: a comparison of European and US studies. *Agriculture, Ecosystems & Environment* 95:579–612.
- Nyffeler, M.N., E.J. Olson & W.O.C. Symondson. 2016. Plant-eating by spiders. *Journal of Arachnology* 44:15–27.
- Oelbermann, K. & S. Scheu. 2002. Effects of prey type and mixed diets on survival, growth and development of a generalist predator, *Pardosa lugubris* (Araneae: Lycosidae). *Basic and Applied Ecology* 3:285–291.
- Patt, J.M. & R.S. Pfannenstiel. 2008. Odor-based recognition of nectar in cursorial spiders. *Entomologia Experimentalis et Applicata* 127:64–71.
- Petersen, A., K.T. Nielsen, C.B. Christensen & S. Toft. 2010. The advantage of starving: success in cannibalistic encounters among wolf spiders. *Behavioral Ecology* 21:1112–1117.
- Pfennig, D.W., S.G. Ho & E.A. Hoffman. 1998. Pathogen transmission as a selective force against cannibalism. *Animal Behavior* 55:1255–1261.
- Rickers, S. & S. Scheu. 2005. Cannibalism in *Pardosa palustris* (Araneae, Lycosidae): effects of alternative prey, habitat structure, and density. *Basic and Applied Ecology* 6:471–478.
- Roberts, J.A., P.W. Taylor & G.W. Uetz. 2003. Kinship and food availability influence cannibalism tendency in early-instar wolf spiders (Araneae: Lycosidae). *Behavioral Ecology and Sociobiology* 54:416–422.
- Samu, F., S. Toft & B. Kiss. 1999. Factors influencing cannibalism in the wolf spider *Pardosa agrestis* (Araneae, Lycosidae). *Behavioral Ecology and Sociobiology* 45:349–354.
- Taylor, R.M. & R.A. Bradley. 2009. Plant nectar increases survival, molting, and foraging in two foliage wandering spiders. *Journal of Arachnology* 37:232–237.
- Taylor, R.M. & A.W. Foster. 1996. Spider nectarivory. *American Entomologist* 42:82–86.
- Taylor, R.M., & R.S. Pfannenstiel. 2008. Nectar feeding by wandering spiders on cotton plants. *Environmental Entomology* 37:996–1002.
- Taylor, R.M. & R.S. Pfannenstiel. 2009. How dietary plant nectar affects the survival, growth, and fecundity of a cursorial spider *Cheiracanthium inclusum* (Araneae: Miturgidae). *Environmental Entomology* 38:1379–1386.
- Toft, S. & D.H. Wise. 1999. Growth, development, and survival of a generalist predator fed single- and mixed-species diets of different quality. *Oecologia* 119:191–197.
- Vanacker, D., K. Deroose, S. Pardo, D. Bonte & J. Maelfait. 2004. Cannibalism and prey sharing among juveniles of the spider *Oedothorax gibbosus* (Blackwall, 1841) (Erigoninae, Linyphiidae, Araneae). *Belgian Journal of Zoology* 134:23–28.
- Walker, S.E., A.L. Rypstra & S.D. Marshall. 2003. The relationship between offspring size and performance in the wolf spider *Hogna helluo* (Araneae: Lycosidae). *Evolutionary Ecology Research* 5:19–28.
- Wise, D.H. 2006. Cannibalism, food limitation, intraspecific competition, and the regulation of spider populations. *Annual Review of Entomology* 51:441–465.
- Young, O.P. & G.B. Edwards. 1990. Spiders in United States field crops and their potential effect on crop pests. *Journal of Arachnology* 18:1–27.
- Young, O.P. & T.C. Lockley. 1985. The striped lynx spider, *Oxyopes salticus* (Araneae: Oxyopidae), in agroecosystems. *Entomophaga* 30:329–346.
- Young, O.P. & T.C. Lockley. 1986. Predation of striped lynx spider, *Oxyopes salticus* (Araneae: Oxyopidae), on tarnished plant bug, *Lygus lineolaris* (Heteroptera: Miridae): A laboratory evaluation. *Annals of the Entomological Society of America* 79:879–883.



## Population structure of the expansive wasp spider (*Argiope bruennichi*) at the edge of its range

Wioletta Wawer<sup>1</sup>, Robert Rutkowski<sup>1</sup>, Henrik Krehenwinkel<sup>2,3</sup>, Dorota Lutyk<sup>4</sup>, Karolina Pusz-Bocheńska<sup>1</sup> and Wiesław Bogdanowicz<sup>1</sup>: <sup>1</sup>Museum and Institute of Zoology, Polish Academy of Sciences, Wilcza 64, 00-679 Warszawa, Poland. E-mail: wawer@miiz.waw.pl; <sup>2</sup>Department of Evolutionary Genetics, Max Planck Institute for Evolutionary Biology, 24306 Plön, Germany; <sup>3</sup>Department for Environmental Sciences, Policy and Management, University of California, Berkeley, CA, USA; <sup>4</sup>Institute of Environmental Sciences, Jagiellonian University, Gronostajowa 7, 30-387 Kraków, Poland.

**Abstract.** The wasp spider *Argiope bruennichi* (Scopoli, 1772) is of Mediterranean-Pontian origin, but for decades it has been expanding northwards, including into the territory of Poland. Based on well-documented expansion records, we can distinguish “old” (south-eastern and south-western) and “new” populations (north-eastern), respectively, from the 1930s to the 2000s. In Poland, some populations of *A. bruennichi* were expected to be more genetically isolated from others, due to distance effects or differential times of arrival. We evaluated whether the oldest populations were in a state of Hardy-Weinberg equilibrium (*HWE*), and whether recently founded populations were in an expansion phase. Specimens of *A. bruennichi* ( $n = 184$ ) were collected at six localities in Poland and single sampling sites in Italy and Japan. Nine microsatellite loci were amplified although only five were useful in the final analyses. Based on the genotypes obtained, we estimated basic measures of genetic diversity and tested for deviation from *HWE*. The results showed a low level of polymorphism amongst the investigated markers, and accordingly, we found a low genetic diversity in populations. Only populations from Italy and Japan, and one population from Poland, were in *HWE*. The level of genetic differentiation among sampling sites from Poland was also very low. The high dispersal ability of the wasp spider appears to have facilitated high gene flow among populations. The peripheral and recently settled populations were characterized by the highest heterozygosity and the lowest inbreeding coefficient ( $F_{IS}$ ). The remaining Polish populations are therefore still in the expansion phase, as indicated by deviations from *HWE*.

**Keywords:** Gene flow, dispersal, population structure, Araneae

The current distributions of species in Central Europe reflect the continent's glacial and post-glacial history, as well as the impacts of human activity on the environment. Habitat changes, such as a reversion to early successional stages and an increase in fallow areas, favor the migration and development of terrestrial arthropod populations. Habitat changes may inhibit range expansion, especially if the distances between patches are too large (Greze et al. 2004). However, in the case of organisms with high dispersal abilities, movement is still possible over long distances (Nee & May 1992; Kareiva & Wennergren 1995).

Spiderlings or even some adult spiders can spread through the air over large distances (sometimes even several thousand kilometers) by ballooning on lengths of silk (Gressitt 1965). This allows an unstable or newly accessible environment to be inhabited (Meijer 1977). Species with a high potential for dispersal generally display a homogeneous population structure, even over considerable distances (Slatkin 1993). In the case of orb-weaving spiders, whose dispersal capabilities are usually very high, a similarly high level of gene flow can often be observed among populations (Ramirez & Fandino 1996; Ramirez & Haakonsen 1999; Lee et al. 2004; Jung et al. 2006). Many studies have investigated genetic differentiation among populations of spiders (e.g., Ramirez & Fandino 1996; Ramirez & Haakonsen 1999; Lee et al. 2004; Jung et al. 2006; Croucher et al. 2011; Krehenwinkel et al. 2016b), but the balance between genetic drift and migration at the margins of a species' range is still poorly understood. Krehenwinkel & Tautz (2013) and Krehenwinkel et al. (2015) examined the genetic variability in native and invasive populations of the “wasp spider” *Argiope bruennichi* (Scopoli, 1772), revealing

marked distinctions between them. They also pointed to a significant role for genetic admixture, as reflected in a high genetic diversity in populations at the edges of the range.

*Argiope bruennichi* is of Mediterranean-Pontian origin, and its current range extends over the Palearctic region (Jäger 2012). During the past decades, populations of the wasp spider have been expanding northwards. In Poland, the first localities appeared in the west (1930s) and in the south-east (1960s), but this species was still rare until the 1990s (Urbański 1948; Barabasz & Górz 1998). In the late 1990s, the number of localities at which the wasp spider increased considerably, and the species was soon present across the whole territory of Poland, except in the north-east where the climate is particularly harsh. Low temperature seems to matter most where the expansion of thermophilous species is concerned, and is considered as a limiting factor (Guttmann 1979; Kumschick et al. 2011) that probably explains the later arrival of *A. bruennichi* in the northern part of Europe (Jonsson 2004; Terhivuo et al. 2011). The rapid expansion in range may be the result of climatic warming, or else the local adaptation of the species to lower temperatures (Kumschick et al. 2011). Some studies have shown that an invasive population can exhibit increased cold tolerance, e.g., through the generation of an admixture of European and Asian lineages, the latter probably being pre-adapted for lower temperatures (Krehenwinkel & Tautz 2013; Krehenwinkel et al. 2015, 2016a). It is nevertheless likely that, in such newly-colonized areas as the mountains of southern Poland or the north-east of Poland, populations of *A. bruennichi* will be vulnerable to severe temperature fluctuations to the point at which effective long-term colonization may be hindered. On the other hand, stable



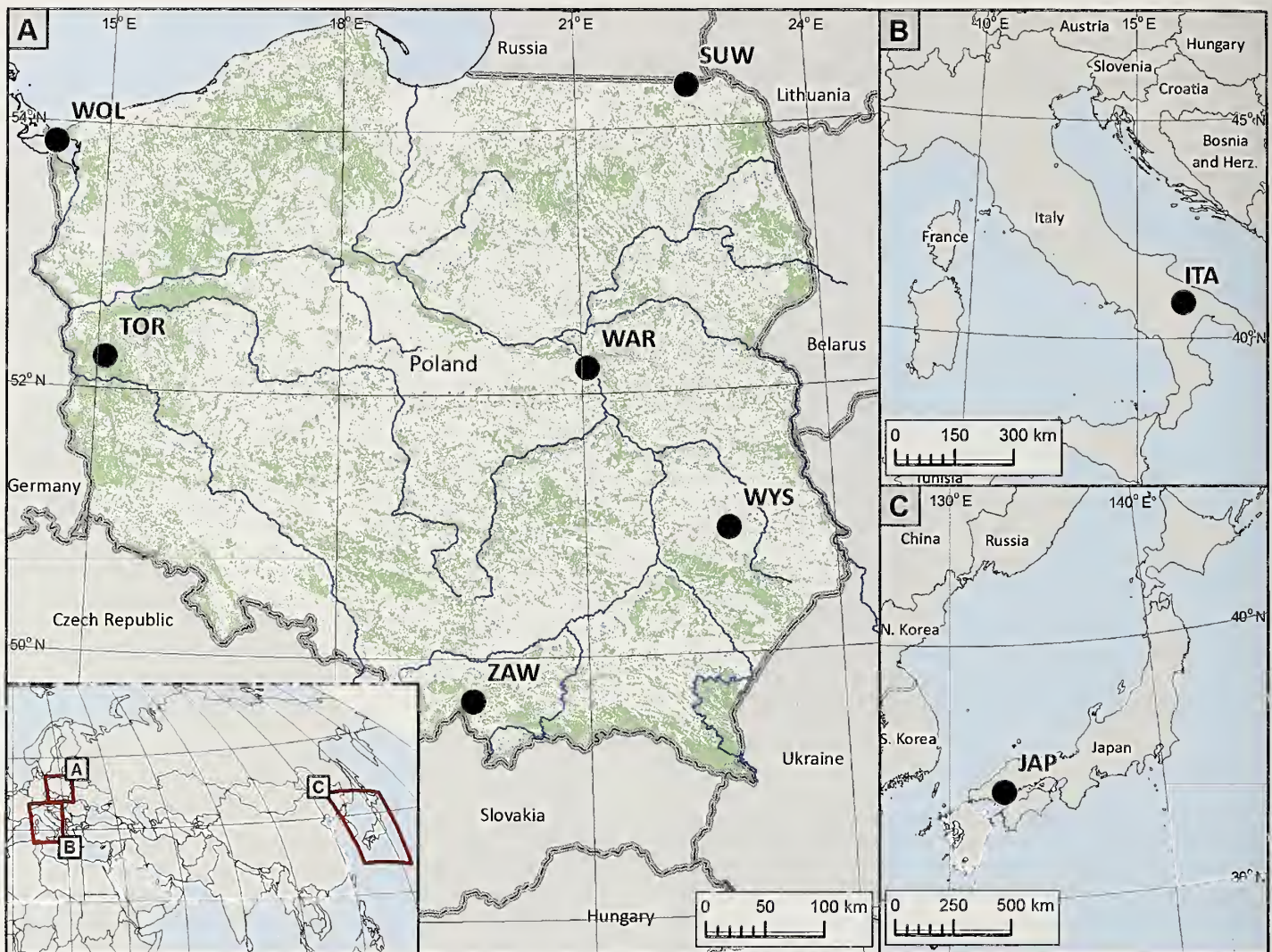


Figure 1.—Map showing the sampling locations.

populations can be expected to persist in the areas that were occupied first.

It is now recognized that genetic diversity decreases with increasing distance from the source population, and this is also true of invasive species (Ciosi et al. 2011; Kim & Sappington 2013; Kononov et al. 2016). Populations at the limits of a species' range differ from those at the source in manifesting reduced levels of polymorphisms that reflect the overall loss of genetic variation. Likewise, at a finer geographic scale, the further from the center of the habitat, the lower the heterozygosity (Peter & Slatkin 2013). Hardy-Weinberg disequilibrium has been observed in distinct locations for certain invasive species, across several generations (Zima et al. 2016). Moreover, edge populations can show low genetic variation when an investigated generation derives from just a few founder migrants (Bunn & Hughes 1997). We therefore hypothesized that due to the small sizes and potentially ephemeral nature of founding populations, the genetic diversity of *A. bruennichi* would be lowest in north-eastern Poland, where the climate is harsh and the species only appeared recently. We in turn expect that the oldest populations – from the west and south-east of Poland – are

in a state of Hardy-Weinberg equilibrium and present higher genetic diversity, while populations from the north-east of Poland remain in the expansion phase and are thus more likely to deviate from Hardy-Weinberg equilibrium.

## METHODS

**Study sites.**—Specimens of *A. bruennichi* were collected from six localities in Poland (Fig. 1), taking into account the time of colonization and the presence of dispersal barriers (e.g., forests, rivers, mountains and human structures). These localities were: SUW (harsh climate conditions, youngest population, arrival ca. 2005, at 54°18'50"N, 22°27'18"E); TOR (mid-forest meadow habitat, oldest population, arrival ea. 1930s, at 52°14'18"N, 15°06'16"E); WAR (city habitat, at 52°11'30"N, 21°04'07"E); WOL (island habitat, at 53°50'56"N, 14°19'43"E); WYS (open area habitat without barriers, at 50°56'54"N, 22°43'36"E); ZAW (mountain valley habitat, at 49°40'20"N, 19°37'43"E). Additional samples came from "old" populations in Italy (1 locality, at 40°49'N, 16°25'E) and Japan (1 locality, at 34°15'N, 132°34'E). We



Table 1.—Characterization of microsatellite polymorphisms in eight populations ( $n = 184$ ) of *A. bruenichii*.  $n$  — sample size within population with successful amplification;  $A$  — number of alleles;  $R_A$  — allelic richness;  $R_P$  — private allelic richness;  $E_A$  — effective number of alleles;  $H_O$  — heterozygosity observed;  $H_E$  — heterozygosity expected;  $HWE$  —  $P$ -values for HWE exact test for heterozygote deficiency/excess (those statistically significant are in bold);  $F_{IS}$  — fixation index; \* — statistically significant values of  $F_{IS}$  and  $P$ -values for  $HWE$  after Bonferroni correction (800 randomizations, adjusted  $P$ -value at  $\alpha = 0.05$  was 0.0013).

Locus	$A$	$R_A$	$R_P$	$E_A$	$H_O$	$H_E$	$HWE$	$F_{IS}$
WAR ( $n = 25$ )								
MA3	10	7.31	0.11	2.84	0.480	0.648	< <b>0.05</b>	0.278
MA5	7	5.64	0.02	2.80	0.680	0.642	0.616	-0.038
MA7	2	2.00	0.00	1.77	0.400	0.435	0.663	0.101
MA33	6	5.34	0.71	3.58	0.320	0.721	< <b>0.001</b> *	0.570*
MA35	3	2.81	0.03	1.44	0.360	0.306	1.000	-0.155
TOR ( $n = 25$ )								
MA3	8	7.00	0.13	4.48	0.320	0.777	< <b>0.001</b> *	0.601*
MA5	5	4.78	0.08	3.25	0.720	0.692	0.751	-0.020
MA7	3	2.56	0.26	1.71	0.320	0.414	0.484	0.246
MA33	4	3.97	0.00	2.69	0.360	0.628	< <b>0.01</b>	0.443
MA35	2	2.00	0.00	1.32	0.200	0.241	0.386	0.189
WOL ( $n = 25$ )								
MA3	6	5.37	0.00	2.28	0.423	0.561	< <b>0.05</b>	0.265
MA5	6	5.36	0.00	2.73	0.654	0.634	0.757	-0.012
MA7	3	2.54	0.24	1.36	0.308	0.266	1.000	-0.140
MA33	3	3.00	0.00	2.75	0.154	0.636	< <b>0.001</b> *	0.766*
MA35	2	2.00	0.00	1.30	0.269	0.233	1.000	-0.136
WYS ( $n = 25$ )								
MA3	10	7.76	0.57	4.58	0.640	0.782	0.126	0.201
MA5	8	6.87	0.07	4.11	0.600	0.757	< <b>0.01</b>	0.227
MA7	3	2.56	0.56	1.76	0.520	0.431	0.730	-0.186
MA33	5	4.78	0.15	2.98	0.240	0.665	< <b>0.001</b>	0.651*
MA35	4	3.12	0.81	1.56	0.440	0.358	0.710	-0.208
SUW ( $n = 25$ )								
MA3	11	8.66	1.04	4.39	0.640	0.772	< <b>0.05</b>	0.191
MA5	8	6.88	0.59	4.22	0.640	0.763	0.176	0.181
MA7	2	2.00	0.00	1.85	0.640	0.461	0.091	-0.371
MA33	4	3.37	0.00	2.09	0.520	0.522	0.525	0.025
MA35	4	3.37	0.28	2.09	0.560	0.522	0.899	-0.052
ZAW ( $n = 25$ )								
MA3	9	7.52	0.42	4.03	0.800	0.752	0.978	-0.043
MA5	6	5.10	0.05	2.58	0.600	0.613	0.230	0.041
MA7	2	2.00	0.00	1.27	0.160	0.211	0.287	0.262
MA33	3	3.00	0.00	2.68	0.200	0.626	< <b>0.001</b> *	0.692*
MA35	3	2.81	0.03	1.56	0.200	0.358	< <b>0.05</b>	0.457
ITA ( $n = 20$ )								
MA3	8	6.71	0.00	2.52	0.700	0.604	0.341	-0.134
MA5	4	3.70	0.00	2.69	0.550	0.629	0.668	0.150
MA7	3	2.62	0.70	1.16	0.050	0.141	< <b>0.05</b>	0.661*
MA33	2	2.00	0.00	2.00	0.550	0.499	1.000	-0.077
MA35	2	2.00	0.00	1.92	0.300	0.480	0.153	0.397
JAP ( $n = 14$ )								
MA3	4	4.00	0.15	2.97	0.357	0.663	< <b>0.05</b>	0.490
MA5	4	4.00	0.09	2.35	0.357	0.574	0.066	0.409
MA7	3	3.00	1.00	1.81	0.357	0.446	0.316	0.235
MA33	4	4.00	1.00	1.46	0.357	0.314	1.000	-0.102
MA35	6	6.00	4.00	3.73	0.643	0.732	0.125	0.158



Table 2.—Mean allelic diversity and heterozygosity indices for five microsatellite loci in eight populations ( $n = 184$ ) of *A. bruennichi*.  $A$  — mean number of alleles;  $R$  — allelic richness;  $P_A$  — private alleles;  $R_P$  — private allelic richness;  $E_A$  — effective number of alleles;  $H_O$  — heterozygosity observed;  $H_E$  — heterozygosity expected;  $HWE$  —  $P$ -values for  $HWE$  exact test for heterozygote deficiency/excess;  $F_{IS}$  — fixation index; \* — statistically significant values of  $F_{IS}$  and  $P$ -values for  $HWE$  after Bonferroni correction (800 randomizations, adjusted  $P$ -value at  $\alpha = 0.05$  was 0.0013).

Population	$A$	$R$	$P_A$	$R_P$	$E_A$	$H_O$	$H_E$	$HWE$	$F_{IS}$
WAR	5.60	4.62	0.20	0.17	2.49	0.448	0.551	<0.001	0.206
TOR	4.40	4.06	0.00	0.09	2.69	0.384	0.550	<0.001*	0.321*
WOL	4.00	3.65	0.00	0.05	2.08	0.362	0.466	<0.001*	0.243*
WYS	6.00	5.02	0.24	0.43	3.00	0.488	0.599	<0.001	0.204*
SUW	5.80	4.86	0.20	0.38	2.93	0.600	0.608	0.083	0.034
ZAW	4.60	4.09	0.00	0.10	2.42	0.392	0.512	<0.001*	0.254*
ITA	3.80	3.41	0.20	0.14	2.06	0.430	0.471	0.172	0.111
JAP	4.20	4.20	0.73	1.25	2.46	0.414	0.546	0.050	0.276

collected the specimens in wastelands or meadows, as is typical for the species.

**Sample collection.**—We collected 184 specimens of *A. bruennichi* in July and August. In Poland, approximately 25 specimens were collected from each location, resulting in 150 specimens collected in 2012. Additionally, in 2013, we received specimens from Italy ( $n = 20$ ) and Japan ( $n = 14$ ). The collected material was stored in 95% ethanol at the Museum and Institute of Zoology (Polish Academy of Sciences), in Warsaw, Poland.

**DNA extraction and amplification.**—DNA extractions using a single leg from each spider were performed using the NucleoSpin® Tissue kit (Macherey-Nagel) according to the manufacturer's protocol. We aimed to amplify the following nine microsatellite loci in two multiplex reactions, as described by Krehenwinkel & Tautz (2013): MA3, MA5, MA7, MA11, MA13, MA27, MA33, MA35 and MA57. Each forward primer was labelled with one of the following fluorescent dyes (WellRED Dyes): Dye2, Dye3 or Dye4. The reaction mixture contained: 1.5  $\mu$ l of the mixture of primers ("forward" and "reverse" for each locus, each primer at 2 pmol/ $\mu$ l); 7.5  $\mu$ l PCR Master Mix (QIAGEN); and 1  $\mu$ l of DNA extract. The reaction mix was then filled to 15  $\mu$ l with water for PCR (Sigma-Aldrich). The reactions were performed under the following conditions: 15 min at 95°C; followed by 40 cycles of: 30 s at 94°C, 90 s at 57°C, 90 s at 72°C; with a final 30 s at 94°C, 90 s at 57°C, and 10 min at 72°C. The genotyping analyses were performed using a CEQ™ 8000 sequencer (Beckman Coulter).

Table 3.—Genetic differentiation among populations of *A. bruennichi*, estimated as  $F_{ST}$ . (\* — statistically significant values after Bonferroni correction, 560 randomizations, adjusted  $P$ -value at  $\alpha = 0.05$  was 0.002). The overall  $F_{ST} = 0.058$  (95% CI 0.023–0.118).

Population	TOR	WOL	WYS	SUW	ZAW	ITA	JAP
WAR	0.010	0.005	-0.003	0.022	0.007	0.041	0.182*
TOR		0.024	-0.010	0.020	0.008	0.063*	0.239*
WOL			0.024	0.049	0.002	0.033	0.252*
WYS				0.002	0.004	0.042*	0.206*
SUW					0.030	0.031*	0.163*
ZAW						0.023*	0.243*
ITA							0.238*

**Data analyses.**—For each locus within each population, deviation from Hardy-Weinberg equilibrium (hereafter  $HWE$ ) and linkage disequilibrium ( $LD$ ) was assessed using Fisher's exact test in Genepop version 4 (Raymond & Rousset 1995; Rousset 2008), with the following settings: 10,000 dememorization steps, followed by 1,000 batches and 10,000 iterations. Basic genetic indices were calculated for each locus within each population as follows: (i) the number of alleles ( $A$ ); (ii) the allelic richness, or the number of alleles corrected for sample size using the rarefaction method with a sample of 14 individuals ( $R_A$ ; Petit et al. 1998); (iii) the effective number of alleles ( $E_A$ ); (iv) the number of private alleles ( $R_P$ ); (v) the observed ( $H_O$ ) and expected heterozygosity ( $H_E$ ) (Nei & Roychoudhury 1974); and (vi) the inbreeding coefficient ( $F_{IS}$ ). These analyses were performed using the programs GenA1Ex (Paekall & Smouse 2001), FSTAT version 2.9.3.2 (Goudet 2001), and HP-RARE (Kalinowski 2005). Moreover, for each population we estimated mean values of  $A$ ,  $R_A$ ,  $R_P$ ,  $H_O$ ,  $H_E$  and  $F_{IS}$ .

Genetic differentiation among populations was assessed as  $F_{ST}$  (Weir & Cockerham 1984). Pairwise  $F_{ST}$  values and their significance, as well as overall  $F_{ST}$  with corresponding 95% confidence intervals were calculated in FSTAT.

The Bayesian-clustering method STRUCTURE version 2.3.4 (Pritchard et al. 2000) was used to examine how well the predefined "populations" corresponded to genetic groups ( $K$ ). STRUCTURE was run 10 times for each user-defined  $K$ , with an initial burn-in of 500,000, and 1,000,000 iterations of the total data set. The admixture model of ancestry and the correlated model of allele frequencies were used. Sampling location was not used as prior information. Next, we examined  $\Delta K$  statistics to identify the largest change in the estimates of  $K$  produced by STRUCTURE, as  $\Delta K$  may provide a more realistic estimation of  $K$  than those based on likelihood (Evanno et al. 2005). STRUCTURE was run for user defined values of  $K = 1-8$ .

To obtain the  $\Delta K$ , we used STRUCTURE HARVESTER version 0.6.94 (Earl & von Holdt 2011). We then applied CLUMPP version 1.1.2 (Jakobsson & Rosenberg 2007) to average the multiple runs given by STRUCTURE and correct for label switching. The output from CLUMPP was visualized with DISTRUCT version 1.1 (Rosenberg 2004).

As the identification of genetic structure in STRUCTURE relies on  $HWE$  optimization, and the majority of the sampling



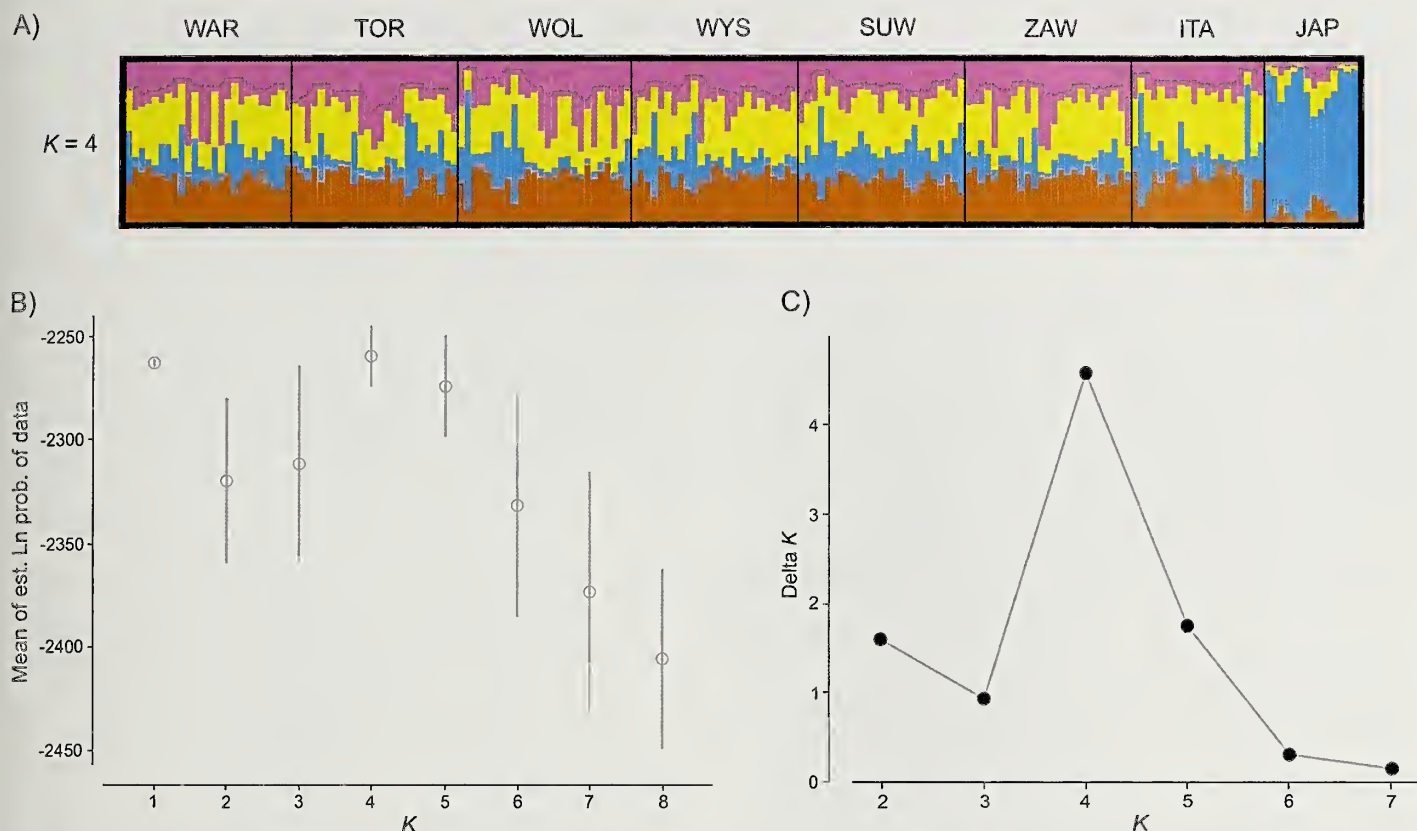


Figure 2.—Genetic structure in eight studied populations of *A. bruennichi*, inferred using STRUCTURE: A. bar plots for four genetic clusters; B. estimated mean (and SD) likelihoods; C.  $\Delta K$  curves as a function of  $K$ . In bar plots each individual is represented by a vertical bar partitioned into segments. The length of each segment describes the estimated membership proportions to each of the genetic clusters.  $\Delta K$  suggested the presence of four genetic clusters, however the mean likelihood was the highest and had the smallest variance for  $K = 1$ .

sites in our study were not in *HWE*, we also obtained an additional representation of the genetic structure using principal component analysis (PCA). This multivariate descriptive method is not dependent on any model assumption and can thus provide a useful validation of the Bayesian clustering output (Patterson et al. 2006; McVean 2009; François & Durand 2010). We used the R package ADEGENET version 1.3.4 (Jombart 2008) to carry out standard PCA. The results of the analysis were presented graphically along the first and second axes according to the highest Eigen values.

## RESULTS

We failed to amplify the loci MA11 and MA13 in the majority of samples from Poland. Locus MA27 was monomorphic, while MA57 failed to amplify in samples from Italy. Hence, final analyses were performed for five microsatellite loci, i.e., MA3, MA5, MA7, MA33 and MA35.

The most polymorphic locus at the population level was MA3 ( $A$  ranging from 6 to 11 alleles,  $R$  from 5.4–8.7), except for the JAP population, where MA35 had the highest number of alleles ( $A = 6$ ). In the remaining loci, we observed rather low levels of polymorphism, usually from 2 to 5 alleles (Table 1). There was no significant linkage disequilibrium (*LD*) among loci within populations (1,600 permutations, adjusted  $P$ -value after Bonferroni correction: 0.006). In the majority of populations, two out of five loci were not in *HWE* (Table

1). Exceptions were populations SUW and ITA, for which only one locus exhibited a deviation from *HWE*. In all cases, significant deviation from *HWE* was due to heterozygote deficiency. The inbreeding coefficient ( $F_{IS}$ ) was significant for locus MA33 in five of the eight investigated populations. Other than MA33, a significant  $F_{IS}$  was also found at locus MA3 in TOR, and MA7 in ITA (Table 1). In general, the observed heterozygosity was greatest at loci MA3 and MA5 in populations from Poland and ITA, while in JAP the highest  $H_O$  was found at locus MA35 (Table 1).

For mean indicators of genetic diversity (Table 2), populations could be divided into a first group with  $A$  around 6.0 and  $R > 4.60$  (WAR, WYS, SUW), and a second group consisting of all remaining populations ( $A < 4.60$ ;  $R < 4.09$ ). In general, allelic diversity and allelic richness were greater in populations from Poland, as opposed to Italy or Japan (Table 2). A similar pattern was observed for  $H_O$ . However, the highest mean number of private alleles ( $P_A$ ) and the greatest value for private allelic richness ( $R_P$ ) were observed in the case of JAP.

Five out of eight investigated populations were not in *HWE*; in four of these  $F_{IS}$  was found to be significantly higher than zero (Table 2). Only one population from Poland (SUW), seemed to be in *HWE*, along with ITA and JAP.

Genetic differentiation ( $F_{ST}$ ) was very limited and non-significant among the populations from Poland (Table 3). We found small but significant  $F_{ST}$  values in pairwise comparisons



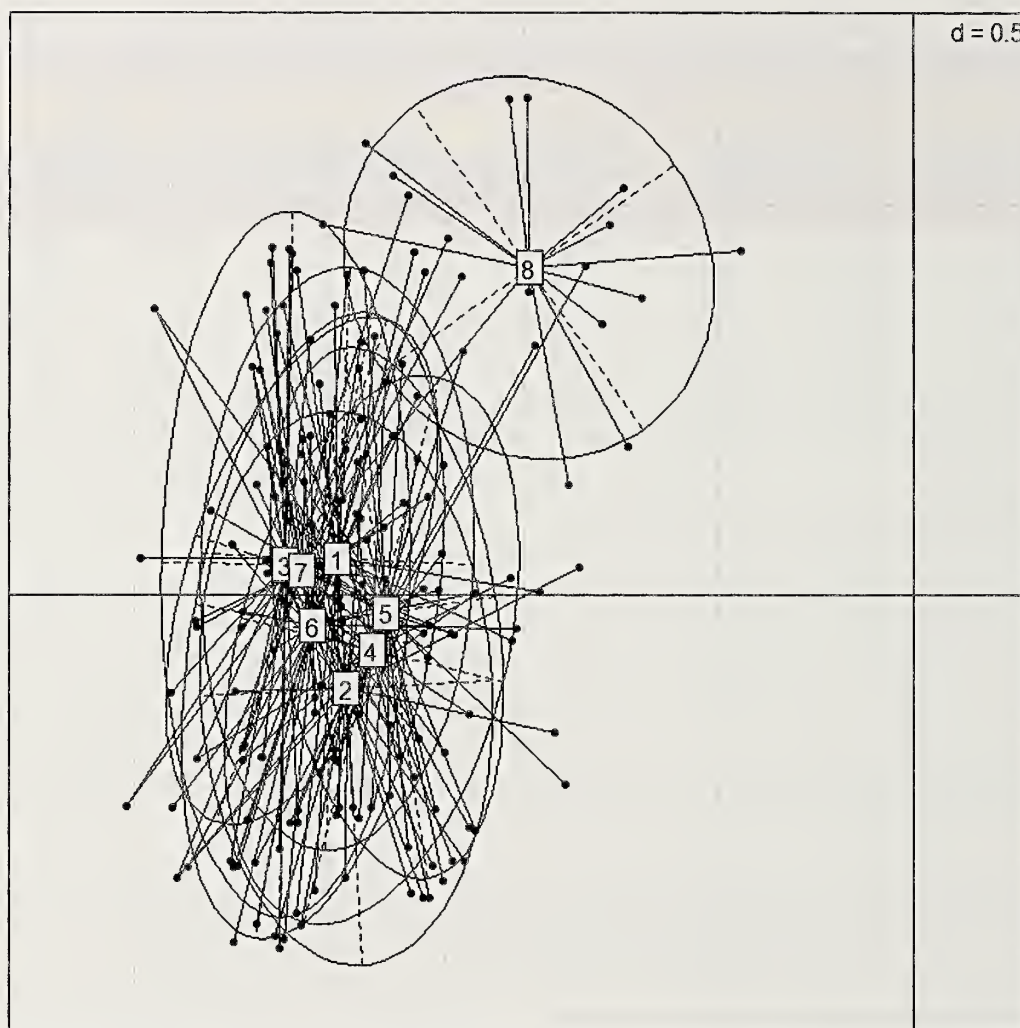


Figure 3.—Principal Component Analysis of *A. bruennichi* genotypes in eight examined populations. The results are presented along the first and second axes according to the highest eigenvalues. 1 – WAR; 2 – TOR; 3 – WOL; 4 – WYS; 5 – SUW; 6 – ZAW; 7 – ITA; 8 – JAP.

between populations from Poland and Italy. Genetic differentiation between JAP and the remaining populations was high and significant (Table 3).

Results from STRUCTURE analyses indicated the highest mean likelihood for  $K=1$  and low variance among iterations, however a high likelihood was also found for  $K=4$  (Fig. 2A, B). Individuals from Poland and Italy were not assigned to a particular cluster, but rather had a mixed probability of ancestry from four genetic groups. The population from Japan consisted of individuals from a single cluster. The  $\Delta K$  supported division of the observed genetic variability into four genetic clusters (Fig. 2C), and PCA analysis in turn suggested a division of populations into two genetic groups (Fig. 3), of which the first consisted of the populations from Poland and Italy and the second (mainly) of samples from Japan.

## DISCUSSION

Our study indicated that genetic differentiation among populations of *A. bruennichi* in Poland was very low. Counter to our expectations, we infer that the strong dispersal abilities

of this species ensure intensive gene flow, resulting in homogeneity of all the Polish populations, which are probably still undergoing range expansion. Similar results have been obtained for other populations of orb-weaving spiders (Ramirez & Fandino 1996; Ramirez & Haakonsen 1999; Lee et al. 2004; Jung et al. 2006), and indeed strong gene flow is frequently observed between populations of species with high dispersal abilities (Waples 1987; Bohonak 1999). However, significant genetic differences for species with high dispersal abilities have also been recorded (Sielezniew & Rutkowski 2012; Lemic et al. 2013; Pentek-Zakar 2015).

According to Vucetich & Waite (2003), populations at the edge of a species' range are generally smaller than those at the core, and observations for *A. bruennichi* suggest that the north-eastern (SUW) population is indeed smaller than others (e.g., 0.2 ind. /m<sup>2</sup> in SUW and 1.75 ind. /m<sup>2</sup> in HOR) (W. Wawer, unpubl. data). However, neither the new (SUW) nor the old (e.g., WYS and WOL) populations are in *HWE* (Table 1). In fact, due to a heterozygote deficiency, many populations of expansive species are not found to indicate *HWE*, e.g., among Lepidoptera (Wei et al. 2013), Coleoptera (Wu et al. 2016) and Diptera (Yan et al. 2015). In the case of spiders,



*HWE* has usually been noted in stable-range populations (Ramirez & Chi 2004; Ramirez et al. 2007, 2013).

Allelic richness was found to be higher in Poland than in Italy. This observation supported previous results, indicating high genetic diversity in expanding populations of the species (Krehenwinkel & Tautz 2013). It is possible that there is still ongoing gene flow among populations in Poland, eliminating founder effects and isolation in newly colonized areas (Greenbaum et al. 2014). Higher genetic diversity in Poland as compared to Italy has also been recorded in other invertebrates (Sielezniew et al. 2015), and was explained by “the rear edge hypothesis”, whereby rear edge populations are usually small in size and are thus characterized by low genetic diversity and high inter-population genetic differentiation (Hampe & Petit 2005). Furthermore, marked genetic differentiation between Asian and European populations was also revealed in our study. Similar results were obtained by Krehenwinkel & Tautz (2013), who confirmed genetic distinctness when East Asian and Western Palearctic populations were compared. As the peripheral and recently settled (SUW) population was characterized by the highest value for heterozygosity ( $H_O = 0.600$ ) and the lowest inbreeding coefficient ( $F_{IS} = 0.034$ ), it is possible to conclude that a small population of *A. bruennichi* at the edge of its range is connected with others by gene flow. Moreover, despite their relatively long-term persistence (of ca. 80 years), the remaining Polish populations appear to still be in the expansion phase, given the lack of *HWE*. Similar results were obtained by Wellenreuther et al. (2011) for populations of the highly vagile blue-tailed damselfly, *Ischnura elegans* (Vander Linden, 1820). Generally, populations displaying a high expansion rate are associated by gene flow, such that even long distances or geographical barriers do not inhibit the process (Wellenreuther et al. 2011). And although genetic diversity is greater far from the center, in most cases distant populations are seen to be similar genetically (Eckert et al. 2008).

At this stage of the research, we cannot confirm the hypothesis of a colonization of Polish territory from both the east and west (Urbański 1948; Barabasz & Górz 1998). Analyses of genetic structure indicated similarity between the Polish and Italian populations, and while the Alps are known to have acted as an initial barrier to the possible northward expansion of Mediterranean genetic pools (Bilton et al. 1998; Hewitt 1999), the Appenine Peninsula might be a possible source area of invertebrate populations in Central and Northern Europe (Patricelli et al. 2013). This observation supports previous results obtained by Krehenwinkel & Tautz (2013), suggesting that northern territories of Europe were colonized from southern localities rather than from eastern areas.

#### ACKNOWLEDGMENTS

We are grateful to our colleagues, Dr. Pamela Loverre (University of Bari Aldo Moro, Italy) and Dr. Yoshiko Honda (Fumakilla Limited, Japan) for collection the specimens of the wasp spider. We also thank two anonymous reviewers for their valuable comments and suggestions. The study was supported by the Polish National Science Centre (NCN), grant no. 2012/05/N/NZ8/02105.

#### LITERATURE CITED

- Barabasz, B. & A. Górz. 1998. *Argiope bruennichi* (Scopoli, 1772) – rzadki i słabo zbadany gatunek pająka w Polsce. *Fragmenta Faunistica* 41:255–267.
- Bilton, D.T., P.M. Mirol, S. Mascheretti, K. Fredga, J. Zima & J.B. Searle. 1998. Mediterranean Europe as an area of endemism for small mammals rather than a source for northwards postglacial colonization. *Proceedings of the Royal Society of London Series B* 265:1219–1226.
- Bohonak, A.J. 1999. Dispersal, gene flow and population structure. *Quarterly Review of Biology* 74:21–45.
- Bunn, S.E. & J.M. Hughes. 1997. Dispersal and recruitment in streams: evidence from genetic studies. *Journal of the North American Benthological Society* 16:338–346.
- Ciosi, M., N.J. Miller, S. Toepfer, A. Estoup & T. Guillemaud. 2011. Stratified dispersal and increasing genetic variation during the invasion of Central Europe by the western corn rootworm, *Diabrotica virgifera virgifera*. *Evolutionary Applications* 4:54–70.
- Croucher, P.J.P., G.S. Oxford & R.G. Gillespie. 2011. Population structure and dispersal in a patchy landscape: nuclear and mitochondrial markers reveal area effects in the spider *Theridion californicum* (Araneae: Theridiidae). *Biological Journal of the Linnean Society* 104:600–620.
- Earl, D.A. & B.M. von Holdt. 2011. STRUCTURE HARVESTER: a website and program for visualizing STRUCTURE output and implementing the Evanno method. *Conservation Genetics Resources* 4:359–361.
- Eckert, C.G., K.E. Samis & S.C. Loughheed. 2008. Genetic variation across species' geographical ranges: the central-marginal hypothesis and beyond. *Molecular Ecology* 17:1170–1188.
- Evanno, G., S. Regnaut & J. Goudet. 2005. Detecting the number of clusters of individuals using the software STRUCTURE: a simulation study. *Molecular Ecology* 14:2611–2620.
- François, O. & E. Durand. 2010. Spatially explicit Bayesian clustering models in population genetics. *Molecular Ecology Resources* 10:773–784.
- Goudet, J. 2001. FSTAT V2.9.3, a program to estimate and test gene diversities and fixation indices. (Updated from: Goudet, J. 1995. FSTAT V1.2: a computer program to calculate F-statistics. *Journal of Heredity* 86: 485–486.) Online at <https://www2.unil.ch/popgen/softwares/fstat.htm>
- Greenbaum, G., A.R. Templeton, Y. Zarmi & S. Bar-David. 2014. Allelic richness following population founding events – a stochastic modeling framework incorporating gene flow and genetic drift. *PLoS ONE* 9(12):e115203. doi:10.1371/journal.pone.0115203.
- Gressitt, J.L. 1965. Biogeography and ecology of land arthropods of Antarctica. Pp. 431–490. *In* *Biology and Ecology of Antarctica*. (J. van Mieghem, P. van Oye, eds). *Monographiae Biologicae* 15.
- Greze, A., T. Zaviero, L. Tischendorf & L. Fahrig. 2004. A transient, positive effect of habitat fragmentation on insect population densities. *Oecologia* 141:444–451.
- Guttmann, R. 1979. Zur Arealentwicklung und Ökologie der Wespenspinne (*Argiope bruennichi*) in der Bundesrepublik Deutschland und den angrenzenden Ländern. *Bonner zoologische Beiträge* 30:454–486.
- Hampe, A. & R.J. Petit. 2005. Conserving biodiversity under climate change: The rear edge matters. *Ecology Letters* 8:461–467.
- Hewitt, G.M. 1999. Post-glacial re-colonization of European biota. *Biological Journal of the Linnean Society* 68:87–112.
- Jakobsson, M. & N.A. Rosenberg. 2007. CLUMPP: a cluster matching and permutation program for dealing with label switching and multimodality in analysis of population structure. *Bioinformatics* 23:1801–1806.
- Jäger, P. 2012. A review on the spider genus *Argiope* Audouin, 1826 with special emphasis on broken emboli in female epigynes



- (Araneae: Araneidae: Argiopinae). Beiträge zur Araneologie 7:272–331.
- Jombart, T. 2008. ADEGENET: a R package for the multivariate analysis of genetic markers. *Bioinformatics* 24:1403–1405.
- Jonsson, L.J. 2004. Getingspindeln. *Argiope bruennichi*, etablerad och sprider sig norrut i Sverige. *Entomologisk Tidskrift* 125:117–120.
- Jung, J., J.-W. Lee, J.-P. Kim & W. Kim. 2006. Genetic variations of the golden orb-web spider *Nephila clavata* (Araneae: Tetragnathidae) in Korea, using AFLP markers. *Korean Journal of Genetics* 28:325–332.
- Kalinowski, S.T. 2005. A computer program for performing rarefaction on measures of allelic diversity. *Molecular Ecology Notes* 5:187–189.
- Kareiva, P. & U. Wennergren. 1995. Connecting landscape patterns and population processes. *Nature* 373:299–302.
- Kim, K.S. & T.W. Sappington. 2013. Population genetics strategies to characterize long-distance dispersal of insects. *Journal of Asia-Pacific Entomology* 16:87–97.
- Kononov, A., K. Ustyantsev, B. Wang, V.C. Mastro, V. Fet, A. Blinov et al. 2016. Genetic diversity among eight *Dendrolimus* species in Eurasia (Lepidoptera: Lasiocampidae) inferred from mitochondrial COI and COII, and nuclear ITS2 markers. *BMC Genetics* 17 (Suppl. 3):157.
- Krehenwinkel, H. & D. Tautz. 2013. Northern range expansion of European populations of the wasp spider *Argiope bruennichi* is associated with global warming-correlated genetic admixture and population-specific temperature adaptations. *Molecular Ecology* 22:2232–2248.
- Krehenwinkel, H., M. Graze, D. Rodder, K. Tanaka, Y.G. Baba, C. Muster et al. 2016a. A phylogeographical survey of a highly dispersive spider reveals eastern Asia as a major glacial refugium for Palaearctic fauna. *Journal of Biogeography* 43:1583–1594.
- Krehenwinkel, H., D. Rödder, M. Năpăruș-Aljančič & M. Kuntner. 2016b. Rapid genetic and ecological differentiation during the northern range expansion of the venomous yellow sac spider *Cheiracanthium punctatum* in Europe. *Evolutionary Applications*. doi:10.1111/eva.12392
- Krehenwinkel, H., D. Rödder & D. Tautz. 2015. Eco-genomic analysis of the poleward range expansion of the wasp spider *Argiope bruennichi* shows rapid adaptation and genomic admixture. *Global Change Biology* 21:4320–4332.
- Kumschick, S., S. Fronzek, M.H. Entling & W. Nentwig. 2011. Rapid spread of the wasp spider *Argiope bruennichi* across Europe: a consequence of climate change? *Climatic Change* 109:319–329.
- Lee, J.-W., L. Jiang, Y.-C. Su & I. Tso. 2004. Is central mountain range a barrier to giant wood spider *Nephila pilipes*? A population genetic approach. *Zoological Studies* 43:112–122.
- Lemie, D., K.M. Mikac & R. Bazok. 2013. Historical and contemporary population genetics of the invasive western corn rootworm (Coleoptera: Chrysomelidae) in Croatia. *Environmental Entomology* 42:811–819.
- McVean, G. 2009. A genealogical interpretation of principal components analysis. *PLoS Genetics* 5:e1000686.
- Meijer, J. 1977. The immigration of spiders (Araneida) into a new polder. *Ecological Entomology* 2:81–90.
- Nee, S. & R.M. May. 1992. Dynamics of metapopulations – habitat destruction and competitive coexistence. *Journal of Animal Ecology* 61:37–40.
- Nei, M. & A.K. Roychoudhury. 1974. Sampling variances of heterozygosity and genetic distance. *Genetics* 76:379–390.
- Peakall, R. & P.E. Smouse. 2001. GENALEX 6: Genetic Analysis in Excel. Population genetic software for teaching and research. *Molecular Ecology Resources* 6: 288–295. Online at <http://onlinelibrary.wiley.com/doi/10.1111/j.1471-8286.2005.01155.x/full>
- Patterson, N., A.L. Price & D. Reich. 2006. Population structure and eigenanalysis. *PLoS Genetics* 2:e190.
- Patricelli, D., M. Sielezniew, D. Ponikwiecka-Tyszko, M. Ratkiewicz, S. Bonelli, F. Barbero et al. 2013. Contrasting genetic structure of rear edge and continuous range populations of a parasitic butterfly infected by *Wolbachia*. *BMC Evolutionary Biology* 13:14. Online at <http://www.biomedcentral.com/1471-2148/13/14>
- Pentek-Zakar, E., A. Oleksa, T. Borowik & S. Kusza. 2015. Population structure of honey bees in the Carpathian Basin (Hungary) confirms introgression from surrounding subspecies. *Ecology and Evolution* 5:5456–5467.
- Peter, B.M. & M. Slatkin. 2013. Detecting range expansions from genetic data. *Evolution* 67:3274–3289.
- Petit, R.J., A. El Mousadik & O. Pons. 1998. Identifying populations for conservation on the basis of genetic markers. *Conservation Biology* 12:844–855.
- Pritchard, J.K., M. Stephens & P. Donnelly. 2000. Inference of population structure using multilocus genotype data. *Genetics* 155:945–959.
- Ramirez, M.G. & B. Chi. 2004. Cryptic speciation, genetic diversity and gene flow in the California turret spider *Atypoides riversi* (Araneae: Araneidae). *Biological Journal of the Linnean Society* 82:27–37.
- Ramirez, M.G. & L.B. Fandino. 1996. Genetic variability and gene flow in *Metepeira ventura* (Araneae, Araneidae). *Journal of Arachnology* 24:1–8.
- Ramirez, M.G. & K.E. Haakonsen. 1999. Gene flow among habitat patches on a fragmented landscape in the spider *Argiope trifasciata* (Araneae: Araneidae). *Heredity* 83:580–585.
- Ramirez, M.G., S.S. Eiman, M.M. Wetkowski, M.K. Mooers, M.H. Alvarez, K.G. Mitchell et al. 2007. Heterozygosity and fitness in a California population of the labyrinth spider *Metepeira ventura* (Araneae, Araneidae). *Invertebrate Biology* 126:67–73.
- Ramirez, M.J., A.M. Ravelo & L. Lopardo. 2013. A simple device to collect, store and study samples of two-dimensional spider webs. *Zootaxa* 3750:189–192.
- Raymond, M. & F. Rousset. 1995. GENEPOP (version 1.2): population genetics software for exact tests and ecumenicism. *Journal of Heredity* 86:248–249.
- Rosenberg, N.A. 2004. DISTRUCT, a program for the graphical display of population structure. *Molecular Ecology Notes* 4:137–138.
- Rousset, F. 2008. Genepop'007: a complete reimplementation of the Genepop software for Windows and Linux. *Molecular Ecology Resources* 8:103–106.
- Sielezniew, M. & R. Rutkowski. 2012. Population isolation rather than ecological variation explains the genetic structure of endangered myrmecophilous butterfly *Phengaris* (= *Maculinea*) *arion*. *Journal of Insect Conservation* 16:39–50.
- Sielezniew, M., D. Patricelli, R. Rutkowski, M. Witek, S. Bonelli & M.M. Buś. 2015. Population genetics of the endangered obligatorily myrmecophilous butterfly *Phengaris* (= *Maculinea*) *arion* in two areas of its European range. *Insect Conservation and Diversity* 8:505–516.
- Slatkin, M. 1993. Isolation by distance in equilibrium and non-equilibrium populations. *Evolution* 47:264–279.
- Terhivuo, J., N.R. Fritzén, S. Koponen & T. Pajunen. 2011. Increased number of observations and notes of offspring production in the invasive orb-web spider *Argiope bruennichi* (Scopoli, 1772) (Araneae: Araneidae) in Finland. *Memoranda Societatis pro Fauna et Flora Fennica* 87:95–101.
- Urbański, J. 1948. *Argiope bruennichi* (SCOPOLI) 1772 na wyspie Wolin oraz rozmieszczenie tego gatunku na ziemiach polskich (Arachn., Aran. Argiopidae). *Badania Fizjograficzne nad Polską Zachodnią* 1:160–169.
- Vucetich, J.A. & T.A. Waite. 2003. Spatial patterns of demography and genetic processes across the species' range: Null hypotheses for landscape conservation genetics. *Conservation Genetics* 4:639–645.



- Waples, R.S. 1987. A multispecies approach to the analysis of gene flow in marine shore fishes. *Evolution* 41:385–400.
- Wei, S.-J., B.-C. Shi, Y.-J. Gong, G.-H. Jin, X.-X. Chen & X.-F. Meng. 2013. Genetic structure and demographic history reveal migration of the diamondback moth *Plutella xylostella* (Lepidoptera: Plutellidae) from the southern to northern regions of China. *PLoS ONE* 8: e59654.
- Weir, B.S. & C.C. Cockerham. 1984. Estimating *F*-statistics for the analysis of population structure. *Evolution* 38:1358–1370.
- Wellenreuther, M., R.A. Sánchez-Guillén, A. Cordero-Rivera, E.I. Svensson & B. Hansson. 2011. Environmental and climatic determinants of molecular diversity and genetic population structure in a coenagrionid damselfly. *PLoS ONE* 6(6):e20440. doi:10.1371/journal.pone.0020440.
- Wu, Y., F. Li, Z. Li, V. Stejskal, Z. Kučerová, G. Opit et al. 2016. Microsatellite markers for *Cryptolestes ferrugineus* (Coleoptera: Laemophloeidae) and other *Cryptolestes* species. *Bulletin of Entomological Research* 106:154–160.
- Yan, W., L. Liu, S. Huang, C. Li, Z. Ma & W. Qin. 2015. Development and characterization of microsatellite markers for the fruit fly, *Bactrocera tau* (Diptera: Tephritidae). *Applied Entomology and Zoology* 50:545–548.
- Zima, J., O. Lebrasseur, M. Borovanská & M. Janda. 2016. Identification of microsatellite markers for a worldwide distributed, highly invasive ant species *Tapinoma melanocephalum* (Hymenoptera: Formicidae). *European Journal of Entomology* 113:409–414.

*Manuscript received 31 August 2016, revised 1 June 2017.*



## **Pseudoscorpions of the family Cheiridiidae (Arachnida: Pseudoscorpiones) recovered from burial sediments at Pachacamac (500–1,500CE), Perú**

**Johnica J. Morrow<sup>1</sup>, Livia Taylor<sup>2</sup>, Lauren Peck<sup>1</sup>, Christian Elowsky<sup>3</sup>, Lawrence Stewart Owens<sup>4</sup>, Peter Eeckhout<sup>5</sup>, and Karl J. Reinhard<sup>1</sup>:** <sup>1</sup>Pathoecology Laboratory, School of Natural Resources, University of Nebraska-Lincoln, Lincoln, Nebraska, USA. E-mail: johnica.morrow@unl.edu; <sup>2</sup>Department of Anthropology, University of Nebraska-Lincoln, Lincoln, Nebraska, USA; <sup>3</sup>Department of Agronomy and Horticulture, University of Nebraska-Lincoln, Lincoln, Nebraska, USA; <sup>4</sup>History, Classics and Archaeology, Birkbeck College, University of London, 27-28 Russell Square, London WC1B 5DQ, Great Britain; <sup>5</sup>Département Histoire, Art et Archéologie, Orientation Amérique Précolombienne, Université Libre de Bruxelles, Av. F. Roosevelt 50 (CP133/01), 1050 Brussels, Belgium

**Abstract.** Fragmented remains of pseudoscorpions belonging to the family Cheiridiidae (Arachnida, Pseudoscorpiones) were recovered from Ychsma polity (c. AD 1000–1475) burial sediments from Pachacamac, Perú. Sediments from 21 burials were examined following rehydration in 0.5% trisodium phosphate for 48 h and subsequent screening through a 250  $\mu$ m mesh. Materials larger than 250  $\mu$ m were surveyed for the presence of arthropods. A total of two samples contained pseudoscorpion fragments, which were collected and quantified to determine the minimal number of pseudoscorpions present per gram of each sample. Following quantification, pseudoscorpion specimens were imaged utilizing confocal laser scanning microscopy (CLSM) to assist with identification efforts. Specimens have morphological characteristics consistent with those found in members of the pseudoscorpion family Cheiridiidae. Members of this family have not been previously described from archaeological materials recovered from Perú, and the implications of pseudoscorpions as members of the archaeological corpocenos have not been fully interpreted. Herein, we report the first recovery of pseudoscorpions from archaeological materials at Pachacamac, and discuss the significance of their roles in the archaeological corpocenos.

**Keywords:** Archaeoarchaeology, burial sediments, corpocenos, macrofossil analysis, confocal laser scanning microscopy

The corpocenos, as defined by Morrow et al. (2016), is the community of organisms associated with corpses. In the present study, an analysis of burial sediments was conducted in order to further our understanding of the archaeological corpocenos at Pachacamac. These sediments represented a series of Ychsma burials from Pachacamac, a large multi-period site on the Peruvian Central Coast. Populated by a series of cultural groups including the Lima and the Inca, Pachacamac has been extensively excavated for over a century. Material used in the present study came from a current excavation project focusing upon the comparatively unknown Ychsma polity (c. AD 1000–1475). This is the first time that Ychsma interments – or any individual from the Central Coast – have been analyzed in this manner. Herein, we present the systematic sampling of 21 burials from Pachacamac. During these analyses, fragments of mites, insects, and pseudoscorpions were recovered from the burial sediments.

**Archaeological background and field sampling.**—The site of Pachacamac covers approximately 600 ha at the mouth of the Lurin River, near modern Lima on the Central Coast of Peru. GPS coordinates for Pachacamac are as follows: 12.25983°S, 76.899478°W. The settlement was occupied for over a thousand years, to include the Early Intermediate Period/EIP (ca. 200 BC–AD 600 [Lima culture]); the Middle Horizon/MH (ca. AD 600–1000 [Wari culture]); the Late Intermediate Period/LIP (ca. AD 1000–1475 [Ychsma culture]); and the Late Horizon/LH (ca. AD 1475–1533 [Inca culture]). Each of these cultures built monumental structures and augmented the site's size and popularity, which reached Pan-Andean importance as a paramount pilgrimage center in the LH (Fleming 1983; Eeckhout 2003, 2013). The Ychsma Project was designed

to investigate the function, development and influence of Pachacamac from the MH to the LH, with special focus on monumental architecture and related material culture (Eeckhout 2000, 2003, 2013). Another important aspect of the site is its special relationship with the sphere of death, because several cemeteries are to be found within its boundaries, as well as burials within some of its buildings. Pachacamac is famous in Peruvian archaeology for being the first site to have been excavated using modern archaeological approaches. The stratigraphic sequence generated by Uhle (1903) was the first of its type in South America, and is still widely used today. This relative chronology considered not only architectural remains but also funerary data, with particular reliance upon superimposed burials of different periods in Cemetery I, at the foot of the temple of the eponymous god.

Several seasons of excavation and observation at the site indicate that the 'typical' grave is a basic pit, containing a few stones or used adobes to prop up or secure the body. There is no evidence of thatching, although there are some indications of mud plastering over light reed roofs. The most common variant, however, is collective burial, which follow a fairly consistent pattern. The basic foundation comprises an irregularly shaped, depressed chamber surrounded by several rough-cut poles that support a reed roof. The chamber was filled with bodies, usually in the seated or recumbent flexed "fetal" position and wrapped in textiles and/or reeds and rushes. Where original position could be determined, approximately 40% of burials were tightly flexed on their sides, with their arms wrapped around (or between) their legs. Most of the remainder showed signs of having originally been interred in a seated, crouched position, with their heads either upright



Table 1.—Collection data and subsample weights for Pachacamac burial sediments containing pseudoscorpion fragments. Weight is expressed in grams (g).

Lab ID	Burial Number	Collection Region	Corpse Age (years)	Corpse Sex	Subsample Weight
P7	E81	Pelvis	40–50	Female	4.23
P17	E118	Pelvis	3.5	Unknown	0.58

or resting on their knees, and their arms wrapped around their legs (Eeckhout & Owens 2015a, b). Young children were often found in a supine, extended position, especially when associated with adults. Other burial styles include those previously described as ‘deviant’ by Eeckhout & Owens (2008) – including cist burials, extended burials, and possible live burials – in that they flouted all the standards known for the period and the site.

Unfortunately, most potential information about burial customs has been lost because of severe and almost uninterrupted looting since the Spanish conquest. Nevertheless, during the 2004 field season, we found an intact MH to LIP sector of Cemetery I, which had been protected by rubble and collapsed LH structures. The funerary remains were from sealed contexts c. 2m below the modern ground surface, which was bare of any vegetation cover. This precludes the possibility that the invertebrate remains recovered reflect modern infestation of the mummy bundles. This area proved to be extremely rich in burial remains, many of which truncated earlier layers and individuals. It seems that the desire to be buried in this location, just in front of the Temple of Ychsma (renamed Pachacamac by the Incas), was so great that people did not hesitate to disturb older graves in order to create new ones. This behavior has been provisionally attributed to Ychsma-Pachacamac’s reputation as a curative deity, and receives some support from the unusually high number of individuals affected by serious diseases, especially in the upper levels of the sequence (Eeckhout & Owens 2008; Owens & Eeckhout 2015).

**Arthropod analyses.**—The discovery of pseudoscorpion fragments was serendipitous. Our sampling strategy was designed for the recovery of parasite eggs and dietary residues following the methods of Berg (2002) and Reinhard et al. (1986). However, the most informative remains recovered were arthropods. It appears that the proliferation of these organisms in the burial environment had reduced the preservation potential of parasite eggs and dietary residues.

Previous studies of archaeological materials have reported fragments of pseudoscorpions from archaeological contexts (Huchet 2010; Palla et al. 2011). These studies reported exuvia belonging to the superfamily Chthonioidea (Huchet 2010) and a single chela from a member of family Cheliferidae (Palla et al. 2011). Pseudoscorpions are often found in context with decomposing material because of their roles as predators of other arthropods associated with decomposition, such as the larvae of clothes moths, flies, earwig beetles, ants, small adult flies, and mites. These organisms may arrive at the bodies of dead animals via phoresy on a wide range of insects attracted to corpses and carrion. Herein, we report the first instance of nearly-complete specimens being recovered from Peruvian mummies and provide a quantitative analysis of organismal

presence. These data are valuable for elucidating the role that pseudoscorpions play in the archaeological coprocenosis.

## METHODS

Permission for analysis was granted to Professor Peter Eeckhout (ULB) by “Resolución Directorial Nacional n°259/INC”, February 20, 2008, previously the Instituto Nacional de Cultura and now the Ministerio de Cultura. The remains assessed in the current publication are archaeologically derived but non-anthropogenic, being samples of organic food remains. Permits for analysis and study are covered under the terms of the original permission “Resolución Directorial Nacional n°259/INC”.

For this study, 41 soil samples were taken from 21 stratigraphically secure and intact burials (Table 1). Control samples from adjacent to the cranium and “coprolite” samples from the pelvic girdles were analyzed from 20 burials. One burial was represented by a pelvic sample only. In the laboratory, numbers were assigned to the samples with “A” designations referring to pelvic samples and “B” designations referring to cranial samples. The plan was for the analysis of paired samples to provide a comparative basis to evaluate the dietary content of the “coprolite” samples. It was anticipated that the content of the control samples would allow us to distinguish which items reflected contaminants from the site that had filtered into the burials.

Samples were sorted, photographed and weighed. A subsample from each original sample was removed and placed in a contamination-free beaker for rehydration in 0.5% trisodium phosphate. The weights of the rehydration samples ranged from 5 to 15 g. All samples were rehydrated for 48 h. One *Lycopodium* spore tablet (batch 124961, containing approximately 12,540 *Lycopodium* spores) was dissolved in dilute hydrochloric acid for every 5 g of sample. These were added after rehydration had been achieved. Importantly, 11 of the “coprolite” samples produced copious black, opaque, viscous residues that would have prevented further analysis. To eliminate these residues, 4.0% KOH was added to the beakers of rehydrating material. The rehydration colors for each sample were recorded. Each sample was subsequently disaggregated via a magnetic stirring apparatus. Disaggregated samples were then screened through a 250 µm mesh screen while rinsing with distilled water. The material smaller than 250 µm (microremains) was collected and concentrated via repeated centrifugation. The microremains were scanned for dietary residues and parasite eggs. The macroscopic remains (those materials larger than 250 µm) were dried on 12.5 cm diameter filter paper circles and examined stereoscopically for dietary and environmental fossils.

Macroremains were examined, sorted based on the type of material recovered, and fragments of arthropods were counted. Invertebrate fragments were stored in clean, appropriately-labeled ½ dram vials with black, screwcap lids containing pulp-based seals. Pseudoscorpion fragment recovered were counted based on type (i.e., cephalothorax/abdomen fragment or appendage fragment). These counts were then used to determine the minimal number of individuals (MNI) present in each sample (Table 2). Given the MNI, the number of pseudoscorpions per gram of sediment was estimated using the original weight of the sample (Table 2). This determination



Table 2.—Pseudoscorpion fragment counts, minimal number of individuals (MNI), and arachnid concentrations for Pachacamac burial sediments containing pseudoscorpion fragments. "Bodies" refers to the cephalothorax/abdomens of specimens recovered. "Appendages" refers to the individual disarticulated pedipalps of specimens recovered.

Lab ID	Bodies	Appendages (Pedipalps)	MNI	Arachnid Concentration
P7	0	15	8	2 pseudoscorpions/gram
P17	31	5	31	53 pseudoscorpions/gram

of pseudoscorpion concentration is important for future comparative studies of the archaeological corpocenosis.

Images of select pseudoscorpion specimens were taken using a PC-mount JVC digital camera (KY-F75U) under a Leica stereoscope (10447177). The computer software Auto-Montage by Syncrosopy was used to create images of a few specimens (Fig. 1). Subsequently, other specimens were examined via confocal laser scanning microscopy (CLSM) (Figs. 2–4). A Nikon Eclipse 90i compound microscope equipped with a Nikon A1 confocal and associated NIS-Elements 4.40 acquisition software was used to obtain images of both dorsal and ventral sides of pseudoscorpion specimens. Additionally, CLSM was used to capture images of a disarticulated pedipalp (Fig. 4). Channel 1 used an excitation of 404.7 nm with an emission range of 425–475 nm and is pseudocolored blue. Channel 2 features an excitation of 488 nm with an emission range of 425–475 nm and is pseudocolored green. Channel 3 features an excitation of 640.5 nm with an emission range of 425–475 nm and is pseudocolored red. The CLSM resulted in a red coloration of chitinous structures

and a blue/green coloration of cuticular waxes. These images were used to highlight diagnostic morphological characteristics useful for specimen identification.

Identifications of the specimens were made based on morphological features using Legg & Jones (1988), and Harvey (1992, 2013) as references. Identifications were later confirmed by Dr. Mark Harvey (Western Australian Museum, Perth).

## RESULTS

A total of two samples examined from Pachacamac burials yielded fragments of pseudoscorpions (Tables 1, 2; Figs. 1–4). The majority of the remains were comprised of cephalothorax/abdomens missing most of the appendages; however, partial pedipalps were also recovered. One of the pedipalp fragments retained the movable chelal finger, while the others displayed only the hand and fixed chelal finger (Fig. 4).

The MNI and pseudoscorpion concentration was calculated for each of the samples. Sample P17 contained the highest concentration of pseudoscorpions based on MNI counts (Table 2). Pseudoscorpion fragments were not found in the sample from the head region (P16) of the individual in Burial E-113 (Lab ID = P16 & P17), but were abundant within the sample from the pelvic region (P17) (Table 2). The individual within this burial was a child of unknown sex who died around the age of 3.5 years (Table 1). Samples from the pelvic (P7) region of the individual in Burial 81 contained pseudoscorpion fragments. These fragments represented eight individual pseudoscorpions within the samples. The pseudoscorpion concentration for this sample was 53 pseudoscorpions/gram



Figure 1.—Auto-Montage images of pseudoscorpions recovered from Pachacamac samples. Left to Right: dorsal view of specimen, ventral view of specimen. Scale bar = 500  $\mu$ m.





Figure 2.—Confocal laser scanning microscopy image of the dorsal view of a pseudoscorpion recovered from Pachacamac sample P17. Scale bar = 500  $\mu$ m.



Figure 3.—Confocal laser scanning microscopy image of the ventral view of a pseudoscorpion recovered from Pachacamac sample P17. Scale bar = 500  $\mu$ m.

of burial sediment (Table 2). The individual in Burial 81 was a female who died between the ages of 40 and 50 years (Table 1).

Careful examinations of the morphological features of the specimens revealed that these pseudoscorpions belong in the family Cheiridiidae Hansen, 1894. These specimens possessed strongly granulate integuments, ten visible abdominal segments divided into separate halves, a subtriangular carapace, and a single pair of eyes on the cephalothorax. The specimens did not appear to possess V-shaped tergites or posterior expansions on coxa IV. Following this tentative designation, photographs of the specimens were sent to Dr. Mark Harvey of the Western Australian Museum, who concurred that these specimens belong within the family Cheiridiidae.

## DISCUSSION

Previously, two studies examining material from mummies reported pseudoscorpion fragments (Huchet 2010; Palla et al. 2011). These studies reported exuvia belonging to the superfamily Chthonioidea from the abdominal cavity of *Namenkhet Amun*, an Egyptian mummy (Huchet 2010) and a single chela from an unknown species of pseudoscorpion collected during an analysis of mummified material (Palla et al. 2011). The present study therefore documents the first occurrence of pseudoscorpions belonging the family Cheiridiidae to be reported from ancient Peruvian burials.

Members of the family Cheiridiidae were first recognized as a group known as the Cheiridiinae by Hansen in 1894 for the genus *Cheiridium* Menge, 1855 and was treated as belonging to the family Cheliferidae. In 1931, Chamberlin elevated this group to the family level, calling them the Cheiridiidae, which



Figure 4.—Confocal laser scanning microscopy image of a disarticulated pseudoscorpion pedipalp recovered from Pachacamac sample P17. Scale bar = 500  $\mu$ m.



now includes two subfamilies: the Cheiridiinae (five genera) and the Pycnocheiridiinae (two genera). Additionally, the genus *Electrobisium* Cockerell, 1917, which is known only from Burma amber deposits dating to the Upper Cretaceous, belongs within the subfamily Cheiridiinae. Members of the Cheiridiidae are widely distributed, though a few are restricted to South Africa (*Pycnocheiridium* Beier, 1957), tropical South America (*Leptocheiridium* Mahnert & Schmidt, 2011), and the western Pacific (*Nesocheiridium* Beier, 1957). The genera *Apocheiridium* Chamberlin, 1924, *Cheiridium*, *Cryptocheiridium* Chamberlin, 1931, and *Neocheiridium* Beier, 1932 are reported from multiple continents. The pseudoscorpions from Pachacamac are not morphologically consistent with *Apocheiridium* (Beier, 1964; Benedict 1978), but could potentially belong to *Cheiridium* or *Neocheiridium*, both of which are known to occur in the Americas.

Members of the family Cheiridiidae have not been previously reported from Perú (Harvey 2013); however, Cheiridids have been found in other South American countries, including Argentina, Brazil, Chile, Colombia, Ecuador, and Paraguay (Harvey 2013; Quirós-Rodríguez et al. 2015). The incomplete nature of the invertebrate record in Perú makes it unclear whether pseudoscorpions recovered in the present study are unreported although native to this region, or if these specimens represent transported non-native species. Pachacamac was a site of religious significance, housing the human remains of individuals who are likely to have lived in geographic locations far from the site. Historic sources describe pilgrimages of the living to Pachacamac made by ancient people residing some 1,600 kilometers away (Bauer & Stanish 2001). If these pseudoscorpions did not come to the burials after corpses were interred, then it is possible that they were transported either by humans or other animals, such as scavengers.

Pseudoscorpions are voracious predators of mites and small insects that may be attracted to human corpses. There would be no shortage of prey items for these predators at Pachacamac as corpses were quickly infested by a wide range of flies and beetles that produce larvae within decomposing flesh. A variety of mites are also encountered in forensic analyses of corpses. The specific roles of mites as members of the coprocenosis are still under investigation in modern contexts. These investigations will be helpful in elucidating the roles of these arthropods as members of the archaeological coprocenosis. A few studies have begun characterizing mites recovered from archaeological contexts to further elucidate the nature of their presence within coprolites, mummies, and archaeological sediments (Morrow et al. 2013, 2016). These mites could be brought to the corpses via phoresy utilizing flies, beetles, or other necrophagous insects or predators of necrophagous insects. Mites are themselves excellent prey items for pseudoscorpions present at corpses. Subsequent analyses of the burial sediments from Pachacamac (unpublished data) have revealed some samples to have mites that remain unidentified at the present time; however, no mites were recovered from samples P7 or P17, which did contain fragments of pseudoscorpions. Like these prey, pseudoscorpions are able to be dispersed via phoresy utilizing a wide range of insects for transportation (Perotti et al. 2010, Poinar et al. 1998). Some pseudoscorpions are even known to use

vertebrates, such as birds (Turienzo et al. 2010), as transport hosts arriving at corpses.

The present study reports the first members of the pseudoscorpion family Cheiridiidae to be recovered from archaeological contexts. Specimens from this study were quantified using a novel technique for reporting pseudoscorpion concentrations and the MNI among the samples analyzed. Additionally, the employment of Auto-Montage stereomicroscopy and confocal laser scanning microscopy has demonstrated the practicality of using these techniques to assist with the taxonomic identification of arthropods recovered from archaeological contexts. As future archaeological studies examine pseudoscorpion and other arachnid remains from coprolites, mummies, and burial sediments, it is advisable for these studies to employ similar methods for quantification and identification. Such studies would provide comparative data vital for the characterization of the archaeological coprocenosis.

## ACKNOWLEDGMENTS

Auto-Montage images in this research were taken in the Biodiversity Synthesis Laboratory of the University of Nebraska State Museum (NSF/BS&I Multi-user Equipment grant DBI 0500767 to M. L. Jameson and F. C. Ocampo). The authors thank Shawn Shumaker for his advice on the project and the Forensic Science Program at UN-L for providing stereomicroscopes used for counting and sorting specimens. The authors also thank Dr. Mark Harvey for his valuable assistance with specimen identification.

## LITERATURE CITED

- Bauer, B.S. & C. Stanish. 2001. *Ritual and Pilgrimage in the Ancient Andes*. Austin: University of Texas Press.
- Beier, M. 1964. Die Pseudoscorpioniden-Fauna Chiles. *Annalen des Naturhistorischen Museums in Wien* 307–375.
- Benedict, E.M. 1978. False scorpions of the genus *Apocheiridium* Chamberlin from western North America (Pseudoscorpionida, Cheiridiidae). *Journal of Arachnology* 5:231–241.
- Berg, G.E. 2002. Last meals: recovering abdominal contents from skeletonized remains. *Journal of Archaeological Science* 29:1349–1365.
- Eeckhout, P. 2000. The palaces of the Lords of Ychsma. An archaeological reappraisal of the function of pyramids with ramps at Pachacamac, central coast of Peru. *Journal of American Archaeology* 17-18-19:217–254.
- Eeckhout, P. 2003. Ancient monuments and patterns of power at Pachacamac, central coast of Peru. *Beiträge zur Allgemeine und Vergleichenden Archäologie* 23:139–182.
- Eeckhout, P. 2013. Change and permanency on the coast of ancient Peru: the religious site of Pachacamac. *World Archaeology* 45:119–142.
- Eeckhout, P. & L.S. Owens. 2008. Human sacrifice at Pachacamac. *Latin American Antiquity* 19:375–398.
- Eeckhout, P. & L.S. Owens. 2015a. The impossibility of death: introduction. Pp. 1–11. *In* *Funerary Patterns and Models in the Ancient Andes: The Return of the Living Dead*. (Eeckhout, P. & L.S. Owens (eds.)). Cambridge University Press.
- Eeckhout, P. & L.S. Owens. 2015b. *Funerary Practices and Models in the Ancient Andes*. Cambridge: Cambridge University Press.
- Fleming, S. 1983. The mummies of Pachacamac. *Expedition* 28:39–45.
- Harvey, M.S. 1992. The phylogeny and classification of the



- Pseudoscorpionida (Chelicerata: Arachnida). *Invertebrate Taxonomy* 6:1373–1435.
- Harvey, M.S. 2013. Pseudoscorpions of the World, version 3.0. Western Australian Museum, Perth. Online at <http://www.museum.wa.gov.au/catalogues/pseudoscorpions>
- Huchet, J.B. 2010. Archaeoentomological study of the insect remains found within the mummy of Namenkhet Amon, San Lazzaro Armenian Monastery, Venice/Italy. *Advances in Egyptology* 1:59–80.
- Legg, G. & R.E. Jones. 1988. Synopses of the British Fauna (New Series). 40. Pseudoscorpions (Arthropoda). Brill/Backhuys, Leiden
- Morrow, J.J., J. Newby, D. Piombino-Mascali & K.J. Reinhard. 2016. Taphonomic considerations for the analysis of parasites in archaeological materials. *International Journal of Paleopathology* 13:56–64.
- Morrow, J.J., D. Piombino-Mascali, D. Lippi & K.J. Reinhard. 2013. Archaeoparasitological analysis of viscera from the Medici family (Saint Lorenzo Basilica, Florence, Italy). *Medicea*.
- Owens, L.S. & P. Eeckhout. 2015. To the god of death, disease and healing: social bioarchaeology of cemetery I at Pachacamac. Pp. 158–185. *In* *Funerary Patterns and Models in the Ancient Andes: the Return of the Living Dead*. (P. Eeckhout, L.S. Owens (eds.)). Cambridge University Press, Cambridge.
- Palla, F., L. Sineo & B. Manachini. 2011. Bacteria, fungi and arthropod pests collected on modern human mummies. *Journal of Entomological and Acarological Research* 43:69–76.
- Perotti, M.A., H.R. Braig & M.L. Goff. 2010. Phoretic mites and carcasses: Acari transported by organisms associated with animal and human decomposition. Pp. 69–91. *In* *Current Concepts in Forensic Entomology* (J. Amendt, M.L. Goff, C.P. Campobasso, M. Grassberger (eds)). New York: Springer Science & Business Media.
- Poinar, G.O., Jr, B.P.M. Čurčić & J.C. Cokendolpher. 1998. Arthropod phoresy involving pseudoscorpions in the past and present. *Acta Arachnologica* 47:79–96.
- Quirós-Rodríguez, J.A., E. Bedoya Roqueme & R. Bedoya Cochet. 2015. Primer reporte de la familia Cheiridiidae en Colombia. *Acta Biologica Colombiana* 20:217–220.
- Reinhard, K.J., U.E. Confalonieri, B. Hermann, L.F. Ferreira & A.J. Araújo. 1986. Recovery of parasite remains from coprolites and latrines: aspects of paleoparasitological technique. *Homo* 37:217–239.
- Turienzo, P., O. di Iorio & V. Manhnert. 2010. Global checklist of pseudoscorpions (Arachnida) found in birds' nests. *Revue Suisse de Zoologie* 117:557–598.
- Uhle, M. 1903. Pachacamac. Report of The William Pepper, M.D., LL.D. Peruvian Expedition of 1896. The Department of Archaeology of the University of Pennsylvania, Philadelphia.

*Manuscript received 22 January 2017, revised 17 April 2017.*



## Three new species of comb-tailed spiders (Araneae: Hahniidae) from a Mexican oak forest with comments on their natural history and sexual behavior

M. Antonio Galán-Sánchez<sup>1</sup> and Fernando Alvarez-Padilla<sup>1,2</sup>: <sup>1</sup>Laboratorio de Aracnología, Facultad de Ciencias, Universidad Nacional Autónoma de México s/n Ciudad Universitaria, México D. F. Del. Coyoacán, Código postal 04510, México; <sup>2</sup>Research Associate, Department of Entomology, California Academy of Sciences, San Francisco, California, USA. E-mail: [fap@ciencias.unam.mx](mailto:fap@ciencias.unam.mx)

**Abstract.** Three new hahniid species, *Hahnina quadriseta* sp. nov., *Neoantistea multidentata* sp. nov. and *N. aspeubira* sp. nov., are described from a total of 1,131 individuals collected during spider inventories in Veraeruz, Mexico. All specimens were collected inside four plots of *Quercus* forest, from leaf litter using active searching, sifted litter processed with Berlese funnels and pitfall traps. Sexual behavior and the natural history of *N. aspeubira* sp. nov. are analyzed. In addition, the stridulatory organ morphology of both *Neoantistea* species is described. Stridulatory organs are absent in *Hahnina quadriseta* sp. nov., although present in other species of this genus. More information regarding this inventory and additional views of specimens can be found online at <http://www.unamfcaracnolab.com>

**Keywords:** Taxonomy, RTA clade, Nearctic, Mexico, stridulatory organ.

**ZooBank publication:** <http://zoobank.org/?lsid=urn:lsid:zoobank.org:pub:C2D143C3-BA0A-4CF8-8CFF-E4117529328D>

The family Hahniidae includes small, entelegyne ecribellate spiders, some of which are characterized by a distinctive transverse arrangement of the spinnerets. Hahniidae have a wide distribution and comprise 249 species included in 28 genera, with a high diversity in the Holarctic and Paleotropical regions (World Spider Catalog 2017). The most important taxonomic synopses of this group were made by Opell & Beatty (1976) for all Nearctic species and Forster (1970) for the New Zealand fauna; since then, no revisions have been made for these or any other regions, including Mexico. Recent, smaller taxonomic studies on this family have focused on the Palearctic and Paleotropical faunas, describing a considerable number of species for *Hahnina* C. L. Koch, 1841, *Alistra* Thorell, 1894 and the new genus *Pacifantistea* Marusik, 2011 from eastern Russia (Chen et al. 2003; Zhang & Zhang 2003; Chen et al. 2009; Marusik 2011; Zhang et al. 2011, 2013; Zhang & Zhang 2013; Liu et al. 2015; Suguro 2015).

The taxonomy and systematics of the family Hahniidae have proven to be a challenge that remains unresolved. All phylogenetic studies place Hahniidae inside the RTA clade (Coddington & Levi 1991; Wheeler et al. 2016); however, its rank as a family (Bertkau 1878) has been debated throughout its taxonomic history. Some authors have considered it a subfamily of Agelenidae (Emerton 1890; Simon 1892; Britton 1938; Gertsch 1949; Bonnet 1959; Kaestner 1968); while other researchers considered it a separate family (Petrunkevitch 1933; Gerhardt & Kaestner 1938; Kaston 1948).

The position of Hahniidae at more inclusive taxonomic levels has also presented several challenges. Based upon the number of cardiac ostia and extension of trachea into the cephalothorax, this family was first considered a member of the Lycosoidea (Gerhardt & Kaestner 1938; Kaston 1948). Later, Hahniidae was included inside Amaurobioidea based upon the male pedipalp anatomy and the presence of unbranched trachea (Lehtinen 1967). Finally, this family was included in Dictynoidea (Forster 1970; Coddington & Levi

1991) based upon a detailed analysis of the tracheal system morphology (Forster 1970). However, the inclusion of Hahniidae within these superfamilies, although based in each instance on a thorough examination of their anatomy, only considered separate character systems in isolation, without phylogenetic analysis.

Molecular phylogenetic analyses (Spagna & Gillespie 2008; Miller et al. 2010; Spagna et al. 2010) questioned Forster's Dictynoidea. A recent, comprehensive, multi-gene analysis (Wheeler et al. 2016) has radically rearranged the RTA clade, including Forster's Dictynoidea. Cryphoecinae, formerly Hahniidae, have been transferred to Cybaeidae, leaving only Hahniinae and Cybaeolinae confirmed as hahniids. Hahniidae appear related to a relimited Dictynidae and a resurrected Toxopidae, and these, in turn, to an enlarged Cybaeidae (Wheeler et al. 2016, fig. 5).

Currently Hahniidae (*sensu* Wheeler et al. 2016) includes two subfamilies: Hahniinae and Cybaeolinae, which can be differentiated by the arrangement of their spinnerets. Of these subfamilies, Hahniinae is well represented in the Nearctic region with 27 species and a distribution extending from Canada to southwest Mexico. Twelve species are known to inhabit the Mexican territory. Seven species are described from both sexes, four only by females and one by two male specimens. The distribution of these species within Mexico and information indicating if they are represented by one or both sexes is presented in Table 1.

Web construction, sexual behavior and other aspects of the biology in hahniids have been understudied. For Nearctic Hahniidae, Opell & Beatty (1976) reviewed the natural history of *Neoantistea* Gertsch, 1934 species and described their microhabitats, web-building behavior, egg sac morphology and phenology. Likewise, morphological analysis of stridulatory structures and their implications for behavior have been poorly analyzed. Stridulatory organs have been reported for several genera such as *Antistea* Simon, 1898, *Neoantistea*, *Hahnina* and *Pacifantistea*; however, most of the studies only



Table 1.—Diversity of Hahniidae in Mexico. Abbreviations: B. C. N. = Baja California Norte.

Genus	Species	Distribution	Description		
			♂ ♀	♀	♂
<i>Neoantistea</i>	<i>N. pueblensis</i> Opell & Beatty, 1976	Puebla	X		
	<i>N. mulaiki</i> Gertsch, 1946	Tamaulipas	X		
	<i>N. lyrica</i> Opell & Beatty, 1976	Hidalgo	X		
	<i>N. inaffecta</i> Opell & Beatty, 1976	Colima	X		
	<i>N. jacalana</i> Gertsch, 1946	Hidalgo		X	
	<i>N. hidalgoensis</i> Opell & Beatty, 1976	Hidalgo		X	
	<i>N. spica</i> Opell & Beatty, 1976	Distrito Federal		X	
	<i>N. inifistula</i> Opell & Beatty, 1976	Veracruz		X	
<i>Hahnia</i>	<i>H. cinerea</i> Emerton, 1890	Puebla	X		
	<i>H. sanjuanensis</i> Exline, 1938	B. C. N.	X		
	<i>H. nobilis</i> Opell & Beatty, 1976	Hidalgo	X		
	<i>H. veracruzana</i> Gertsch & Davis, 1940	Veracruz			X

mentioned the presence of these organs (Harm 1966; Forster 1970; Brignoli 1976, 1977, 1978; Opell & Beatty 1976; Benoit 1978; Bosmans & Thijs 1980; Marusik 2011; Zhang et al. 2011, 2013; Zhang & Zhang, 2013). Only one study documented the stridulatory organs with scanning electron microscope (SEM) images (Joequé & Bosmans 1982). The latter paper described and discussed the differences between these organs in *H. eburneensis* Joequé & Bosmans, 1982 and 16 other species of *Hahnia*, identifying five stridulatory organ types on the chelicerae retrolateral surface, concluding that the presence of several types of stridulatory organs in this genus could offer characters to separate closely related species. It is important to mention that *H. quadriseta* sp. nov. did not present any kind of stridulatory structure.

The three species described here were collected as part of a spider inventory done in Mexican *Quercus* forests, and are described from a total of 1,131 individuals. In addition, the natural history, sexual behavior and stridulatory organs of *N. aspembira* sp. nov. and the detailed anatomy of the stridulatory organ of *N. multidentata* sp. nov. are described and discussed.

## METHODS

**Sampling and spider collection.**—The specimens were collected as part of a spider inventory following standardized protocols (Coddington et al. 1991) inside two *Quercus* oak forests: one near the boundary of the Pico de Orizaba National Park, ca. two km southwest from Atotonilco de Calcahualco, Veracruz, Mexico, from May 2012 to February 2013; and another at Xamatiepac de Calcahualco, ca. 23 km east from Pico de Orizaba National Park, Veracruz, Mexico, from April 2013 to February 2014. All specimens were collected inside four plots of one hectare each. Atotonilco: Plot I with central coordinates 19°8'17.4" N, 97°12'16.2" W and an elevation of 2,300 m; Plot II 19°8'30.2" N, 97°12'21.5" W and 2,388 m. Xamatiepac: Plot I 19°7'34.1" N, 97°4'1.5" W and 1,710 m; Plot II 19°7'32.5" N, 97°4'3.2" W and 1,700 m. All species were collected from leaf litter with active searching, and from sifted leaf litter processed with Berlese funnels and pitfall traps.

**Morphological methods and material examined.**—All specimens were collected and stored in 96% ethanol. Photographs of external anatomy were taken with a Nikon DS-Fi2 camera connected to a Nikon SMZ1000 dissecting microscope and a Nikon E200 Microscope under LED illumination. Multi-focal images were captured using Nikon (NIS Elements 4.0) software and montage processing done with Helicon Focus (5.3.14). Female genitalia were dissected and digested following the protocol of Alvarez-Padilla & Hormiga (2007 (2008)), cleared with clove oil and mounted in temporary preparations (Coddington 1983). Cleared genitalia were analyzed and photographed using the Nikon E200 Microscope. Illustrations were done with Nikon Y-IDT drawing tube. SEM samples were coated with gold and images taken with a JEOL JSM-5310LV SEM. All measurements were done using a metric ocular graticule and are given in millimeters. Left male pedipalps were illustrated and photographed. Leg measurements are shown as: total length (femur, patella and tibia, metatarsus, tarsus).

Additional information regarding these inventory methods and high-resolution versions of the images are available online at <http://www.unamfcaracnolab.com> (Alvarez-Padilla Laboratory 2014). Type material is deposited in the Colección Nacional de Arácnidos (CNAN), Instituto de Biología, Universidad Nacional Autónoma de México. Additional examined material is deposited in the Laboratorio de Aracnología Collection, Facultad de Ciencias, (CAFC-UNAM).

**Behavioral observations.**—Live spiders were collected from the study plots and kept individually inside plastic cages (width x length x height: 5 × 8 × 5 cm; 6 × 9 × 6 cm) with leaf litter from the same place. The spiders were fed with *Drosophila melanogaster* (nubbin strain) once a week. The description of behavior was based on the direct observation of 10 specimens (2 ♂, 7 ♀, 1 immature) and took place from 27 October to 30 November 2015. All sexual behaviors were observed at room temperature that averaged 19.8 ± 1.8°C. The courtship was observed during dark conditions (01:32 AM) under red light.

The following abbreviations are used in the text and figures: ALE, anterior lateral eyes; ALS, anterior lateral



spinnerets; AME, anterior median eyes; B, bursae; Bg, Bennett's glands; Bh, basal hematodochae; Cd, copulatory ducts; Co, copulatory openings; E, embolus; Eb, embolus base; Fd, fertilization ducts; LS, lower sheet; ML, middle layer; Pa, patellar apophysis; PLE, posterior lateral eyes; PLS, posterior lateral spinnerets; PME, posterior median eyes; PMS, posterior median spinnerets; O, refuge opening; RTA, retrolateral tibial apophysis; RTM, retrolateral tibial macroseta; S, spermathecae; SEM, scanning electron microscope; Sd, spermathecae; Ss, secondary spermathecae; T, tegulum; US, upper sheet.

## TAXONOMY

Family *Hahniidae* Bertkau, 1878

Subfamily *Hahniinae* Bertkau, 1878

Genus *Hahnia* C. L. Koch, 1841

*Hahnia quadriseta* sp. nov.

<http://zoobank.org/?lsid=urn:lsid:zoobank.org:act:D3E256B0-F181-4894-8B16-11D8E738C991>

Figs. 1–17, 55

**Type material.**—*Holotype male*. MEXICO: *Veracruz*: Atonileo de Calcahualco, ca. 15 km from Pico de Orizaba Volcano, Plot II, 19°8'30.2" N, 97°12'21.5" W, elev. 2,388 m, oak forest, leaf litter, collected with pitfall traps, 4–14 October 2012 (CNAN-T1138).

**Paratypes.** MEXICO: *Veracruz*: 1 ♀ allotype, same data as holotype (CNAN-T1139); 2 ♂, 1 ♀, same data except 21–30 May 2012, pitfall trap (CAFC-UNAM); 1 ♀, same locality data except Plot I, 19°8'17.4" N, 97°12'16.2" W, elev. 2,300 m, 21–30 May 2012, F.A. Rivera-Quiroz (CACF-UNAM); 3 ♂, same data except 4–14 October 2012, Berlese funnel (CNAN).

**Other material examined.**—MEXICO: *Veracruz*: 1 ♂, Atonileo de Calcahualco, 15 km from Pico de Orizaba Volcano, Plot I, 19°8'17.4" N, 97°12'16.2" W 2,300 m, 21–30 May 2012, U. Garcilazo-Cruz (CAFC-UNAM); 2 ♂, 1 ♀, same data except 4–14 October 2012, U. Garcilazo-Cruz (CAFC-UNAM); 2 ♂, 3 ♀, same data except 15–24 February 2013, F. Alvarez-Padilla (CAFC-UNAM); 2 ♂, 5 ♀, same locality data except Plot II, 19°8'30.2" N, 97°12'21.5" W, 2,388 m, 21–30 May 2012, Berlese funnel (CAFC-UNAM); 1 ♂, 1 ♀, same data except 4–14 October 2012, pitfall trap (CAFC-UNAM); 2 ♂, 3 ♀, same data except 15–24 February 2013, Berlese funnel (CAFC-UNAM); 1 ♀, Xamactipac de Calcahualco, Plot I, 19°7'34.1" N, 97°4'1.5" W, 1,710 m, 19–27 April 2013, F. J. Salgueiro-Sepúlveda (CAFC-UNAM); 2 ♂, 1 ♀, same data except 2–11 October 2013, D. Piedra-Jimenez (CAFC-UNAM); 1 ♂, same data except 4–17 February 2014, M. Servín-Pastor (CAFC-UNAM); 2 ♀, same locality data except Plot II, 19°7'32.5" N, 97°4'3.2" W, 1,700 m, 4–17 February 2014, Berlese funnel (CAFC-UNAM).

**Etymology.**—The specific epithet is a noun in apposition from the Latin *quadrus* (four) and *seta* (hair or bristle), referring to the presence of four macrosetae on the retrolateral surface of the male palpal tibia.

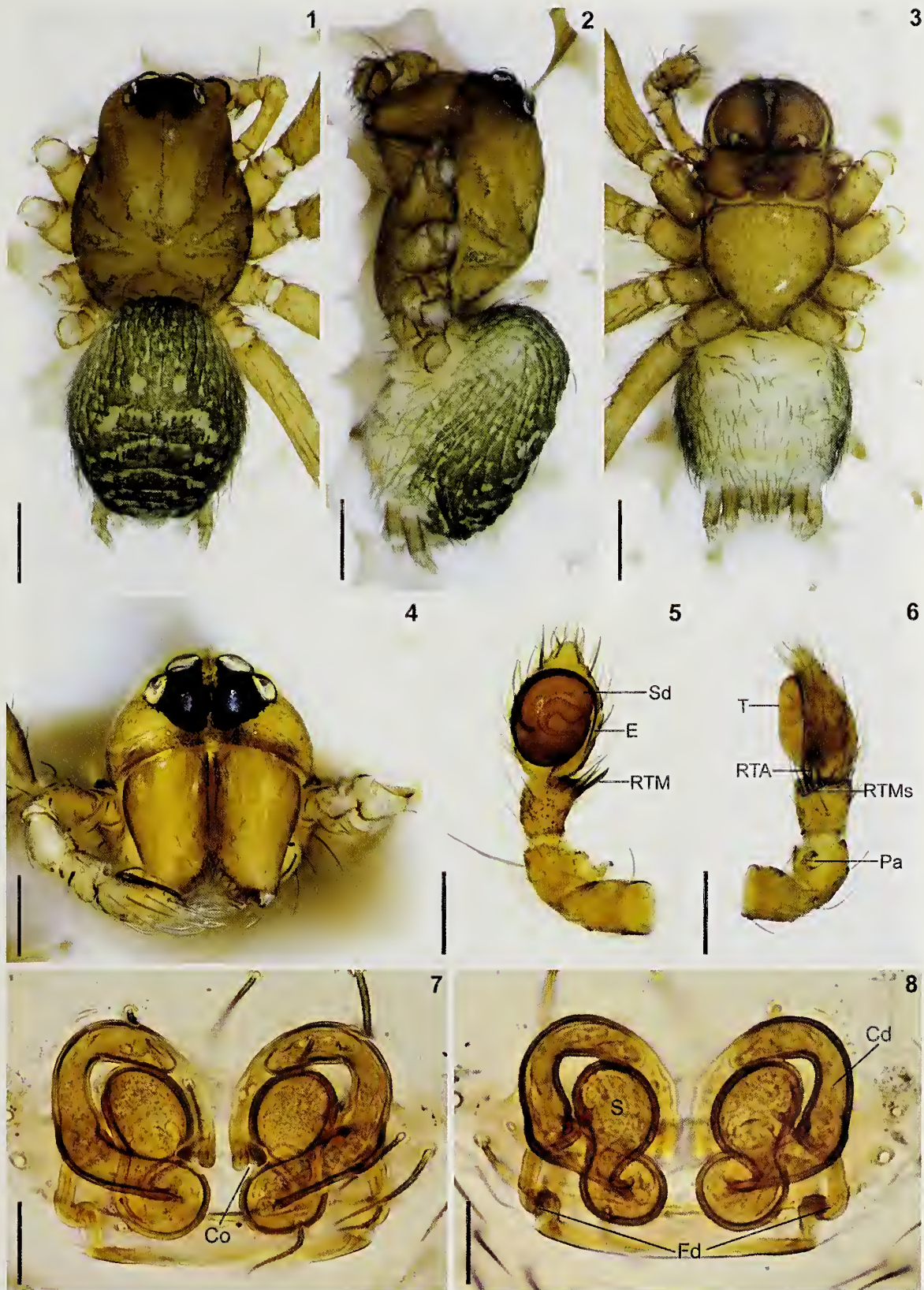
**Diagnosis.**—*Hahnia quadriseta* sp. nov. is similar to *H. senaria* Zhang, Li & Zheng, 2011 in having only six eyes and by having the same somatic appearance (Figs. 1, 4; see also Zhang et al. 2011: figs. 22, 23). Both sexes differ from *H.*

*senaria* by the position of the tracheal spiracle closer to the base of the median spinnerets (Fig. 3). Females of this species differ by the presence of two conspicuous copulatory openings located medially, and by the long copulatory ducts and long fertilization ducts originating laterally on the spermathecae (Figs. 7, 8, 16, 17). Males of this species differ by the presence of four macrosetae slightly curved apically on the retrolateral surface of the palpal tibia (RTMs) (Figs. 10, 11), and by the short and slightly serrated RTA (Figs. 10, 12).

**Description.**—*Male* (Holotype). Total length 1.4. Cephalothorax 0.57 long, 0.42 wide. Carapace dorsal surface light brown, slightly darker in pars cephalica; pars thoracica with a reticulated dark pattern concentrated behind the pars cephalica and over the radial furrows (Fig. 1); pear-shaped, narrowed anteriorly, highest point of carapace located between ocular region and fovea. Fovea indistinct; stridulatory organs absent. Ocular region 0.12 long, 0.20 wide, dark color, with setae located between PLE-PME and PME-PME. Six eyes with an arrangement of two triads, posterior eye row procurved in frontal view (Fig. 4). Eye sizes and interdistances: ALE, PLE and PME equal in size (0.05); ALE-ALE equal to PME-PME (0.03), ALE-PLE equal to PLE-PME (0.01). Clypeus less than a diameter of ALE, 0.04. Chelicerae 0.22 long, 0.12 wide, yellow-brown, retrolateral edges slightly concave apically, two promarginal and two retromarginal teeth. Endites 0.13 long, 0.14 wide, same color and pattern as the chelicerae, convergent apically, retrolateral edges concave, serrula darker in coloration. Labium 0.05 long, 0.09 wide, same color pattern as the endites, with strong basal notches. Sternum 0.30 long, 0.30 wide, same color pattern as carapace, margin darker. Shield-shaped, truncated anteriorly, narrowed posteriorly, margins undulated and slightly elevated between coxae (Fig. 3). Abdomen oval, covered with setae, raised anteriorly above posterior region of carapace (Fig. 2), stridulatory organs absent. Dorsal pattern greyish, with five chevron-like markings that extend towards the posterior edge and two semicircular spots located in anterior region (Fig. 1). Ventral surface white. Colulus indistinct. Spinnerets light brown; PMS 0.07, ALS proximal segment 0.09, distal segment 0.03, PLS proximal segment 0.10, distal segment 0.08. Legs: I 1.33 (0.40) (0.45) (0.25) (0.23); II 1.19 (0.36) (0.39) (0.24) (0.20); III 1.09 (0.31) (0.34) (0.24) (0.20); IV 1.36 (0.40) (0.44) (0.28) (0.24); leg formula: 4123; light brown; all femora with ventral row of five to six macrosetae; patella and tibia I to IV dorsal surface with macroseta; tarsi without macrosetae. Pedipalp: Patella larger than tibia. Patella with a short retro-basal apophysis, wider at base, bifurcated and hook-shaped (Figs. 11, 13, 15). Tibia wider anteriorly. Cymbium oval, longer than wide, tip slightly elongated. Embolus originating pro-basally, extending around the tegulum and ending near at the base of cymbium (Fig. 15). Tegulum disk-shaped, spermathe duct following the regular margin and with three turns before entering the embolus (Figs. 5, 15).

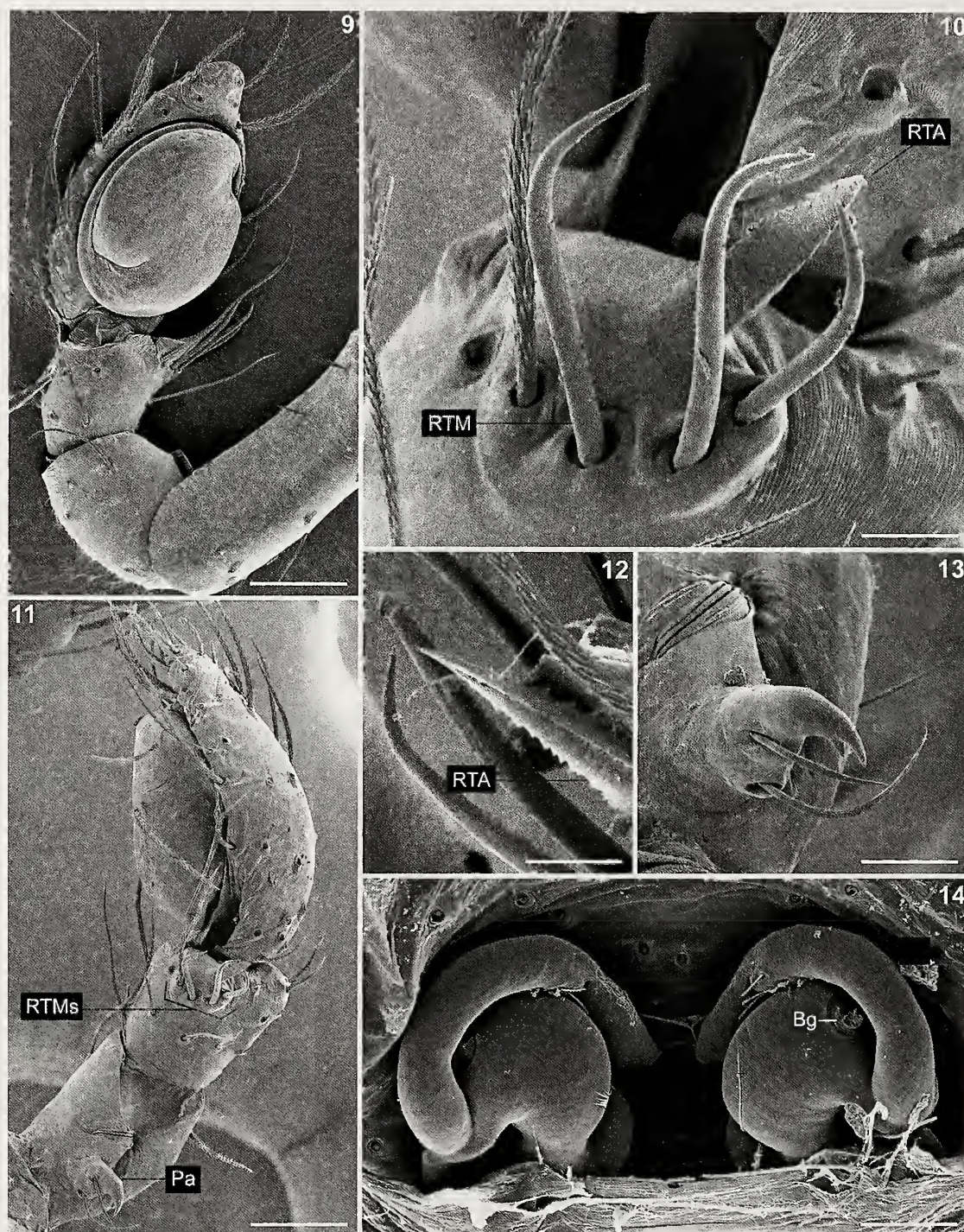
**Female** (Allotype). Total length 1.3. As in male except as noted: Cephalothorax: Carapace 0.48 long, 0.37 wide. Ocular region 0.10 long, 0.15 wide. Clypeus low 0.03. Endites 0.11 long, 0.13 wide. Sternum 0.27 long, 0.27 wide. Abdomen: Tracheal system with a broad spiracle, closer to spinnerets than to epigastric furrow, internally composed of two short





Figures 1–8.—*Hahnia quadriseta* sp. nov.: 1–6, male; 7–8, female. 1, Habitus dorsal view; 2, same lateral view; 3, same ventral view; 4, prosoma anterior view; 5, left pedipalp ventral view; 6, same retrolateral view; 7, epigynum ventral view (cleared); 8, epigynum dorsal view (cleared). Scale bars = 0.5 mm except cleared epigyna = 0.05 mm. Cd, copulatory duct; Co, copulatory opening; E, embolus; Fd, fertilization duct; Pa, patellar apophysis; RTA, retrolateral tibial apophysis; RTMs, retrolateral tibial macrosetae; Sd, spermatic duct; S, spermathecae; T, tegulum.



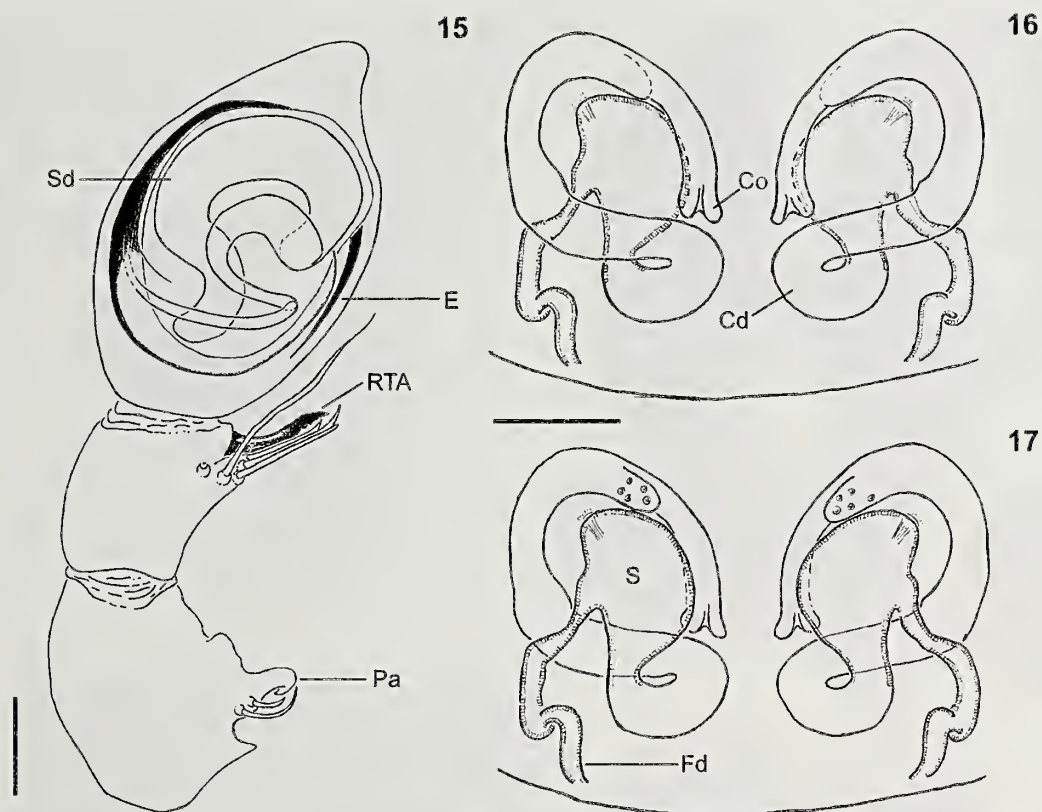


Figures 9–14.—*Hahnia quadriseta* sp. nov.: 9–13, male; 14, female. 9, Pedipalp ventral view; 10, retrolateral surface of pedipalp; 11, pedipalp retrolateral view; 12, RTA dorsal view; 13, patellar apophysis retrolateral view; 14, epigynum dorsal view. Scale bars = 0.01 mm. Bg, Bennett's glands; Pa, patellar apophysis; RTA, retrolateral tibial apophysis; RTMs, retrolateral tibial macrosetae.

tubular tracheae branching in tracheoles that extend towards the cephalothorax (Fig. 55). Distal segment of PLS 0.06. Legs: I 1.10 (0.35) (0.36) (0.20) (0.19); II 0.99 (0.30) (0.32) (0.19) (0.18); III 0.93 (0.29) (0.29) (0.19) (0.16); IV 1.16 (0.35) (0.38) (0.24) (0.19). Epigynum flat, copulatory ducts long, approximately half as wide as spermathecae and surrounding them

completely and forming a posterior coil (Figs. 7, 16). Spermathecae oval, fertilization ducts nearly straight, longer than spermathecae and less than half the spermathecae width and crossing over the copulatory ducts in dorsal view (Figs. 8, 17). The Bennett's glands are located in the anterior region of the spermathecae (Fig. 14). The presence of the glandular





Figures 15–17.—*Hahnia quadriseta* sp. nov., illustrations: 15, male left pedipalp ventral view; 16, cleared epigynum ventral view; 17, cleared epigynum dorsal view. Scale bars = 0.05 mm. Cd, copulatory duct; Co, copulatory opening; E, embolus; Fd, fertilization duct; Pa, patellar apophysis; RTA, retrolateral tibial apophysis; Sd, spermatic duct; S, spermathecae.

pores and ducts forming a “lump” over the copulatory ducts could indicate that this region is the secondary spermathecae (Figs. 14, 17).

**Variation** ( $n = 30$ ).—Males total length 1.2–1.4. Females total length 1.2–1.5. Copulatory openings vary in position from the medial region to the anterior region. Spermathecae vary in orientation from vertical to slightly inclined relative to the epigastric furrow. Specimen coloration varies in its pigmentation from light brown to dark brown. Five specimens presented a dorsal surface of the abdomen without chevron-like markings. Several specimens presented damaged eyes due to physical trauma.

**Distribution**.—Oak forest in the Atotonilco and Xamatipac de Calchahualco regions, Veracruz, Mexico (Figs. 72–74).

**Biology**.—This species was the most abundant of the family Hahniidae in our inventory. Male and female individuals were collected all year long; however, females were more abundant from May to February, while males were more abundant in February. The presence of a larger number of adult specimens in February could indicate that the breeding season is during winter, gradually decreasing towards spring and again increasing approaching autumn. Juveniles are mainly found in early spring and late summer. Most specimens were caught by cryptic searching (610 individuals), followed by sifting leaf litter processed with Berlese funnels (298 individuals) and pitfall traps (58 individuals). Ten

specimens were found upon vegetation either by direct collecting or beating.

#### Genus *Neoantistea* Gertsch, 1934

##### *Neoantistea multidentata* sp. nov.

<http://zoobank.org/?lsid=urn:lsid:zoobank.org:act:3555CCA7-5301-463D-BAAA-DB9010A80162>

org:act:3555CCA7-5301-463D-BAAA-DB9010A80162

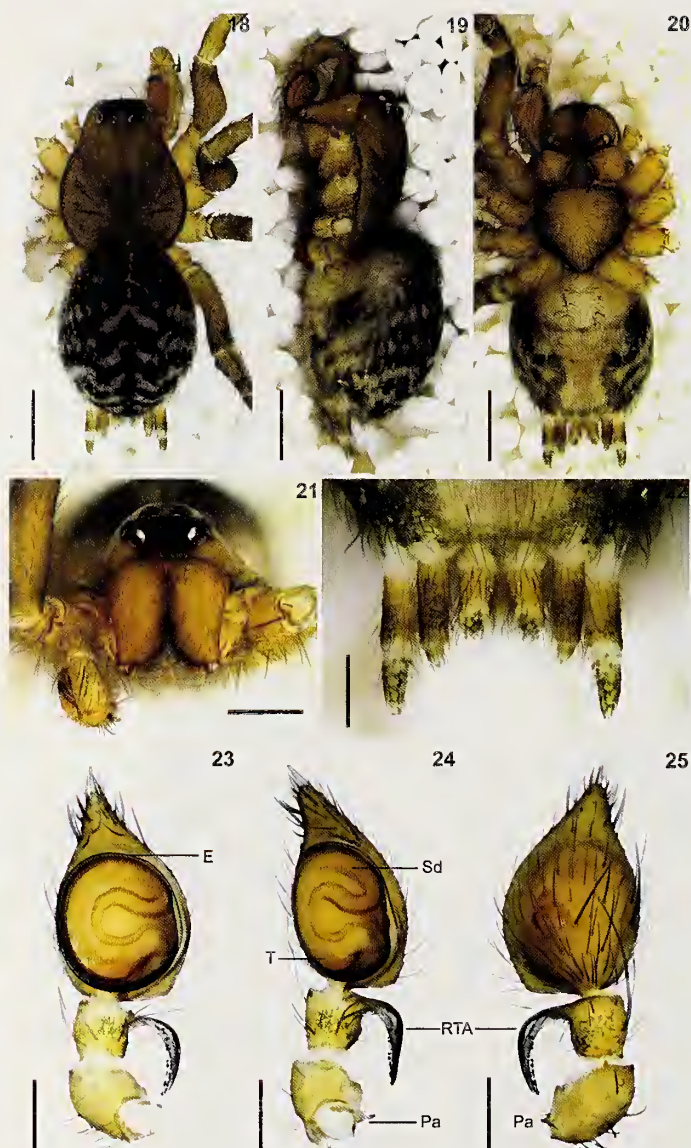
Figs. 18–32, 50, 51, 56, 63, 67–70

**Type material**.—*Holotype male*. MEXICO: Veracruz: Atotonilco de Calchahualco, ca. 15 km from the Pico de Orizaba Volcano, Plot I, 19°8'17.4" N, 97°12'16.2" W, elev. 2,300 m, oak forest, leaf litter, collected with cryptic searching, 4–14 October 2012, F.M. Labarque (CNAN-T1140).

**Paratypes**. MEXICO: Veracruz: 1 ♀ allotype, same data as holotype, U.G. Cruz (CNAN-T1141); 1 ♂, 1 ♀, Atotonilco de Calchahualco, Plot I, 19°8'17.4" N, 97°12'16.2" W, elev. 2,300 m, 4–14 October 2012, M.A. Hernández-Patricio (CAFC-UNAM); 1 ♂, 1 ♀, same data except 15–24 February 2013, F.M. Labarque (CAFC-UNAM).

**Other material examined**.—MEXICO: Veracruz: 3 ♂, 10 ♀, Atotonilco de Calchahualco, 15 km away from the Pico de Orizaba Volcano, Plot I, 19°8'17.4" N, 97°12'16.2" W, 2,300 m, 4–14 October 2012, U. Garcilazo-Cruz, T. Silva, D. Polotow, F.M. Labarque (CAFC-UNAM); 1 ♂, 1 ♀, same





Figures 18–25.—*Neoantistea multidentata* sp. nov., male: 18, habitus dorsal view; 19, same lateral view; 20, same ventral view; 21, prosoma anterior view; 22, spinnerets ventral view; 23, left pedipalp ventral view; 24, same retrolateral view; 25, same dorsal view. Scale bars = 0.2 mm except habitus = 0.5 mm. E, embolus; Pa, patellar apophysis; RTA, retrolateral tibial apophysis; Sd, spermathecal duct; T, tegulum.

data except 15–24 February 2013, Berlese funnel, U. Garcilazo-Cruz (CAFC-UNAM).

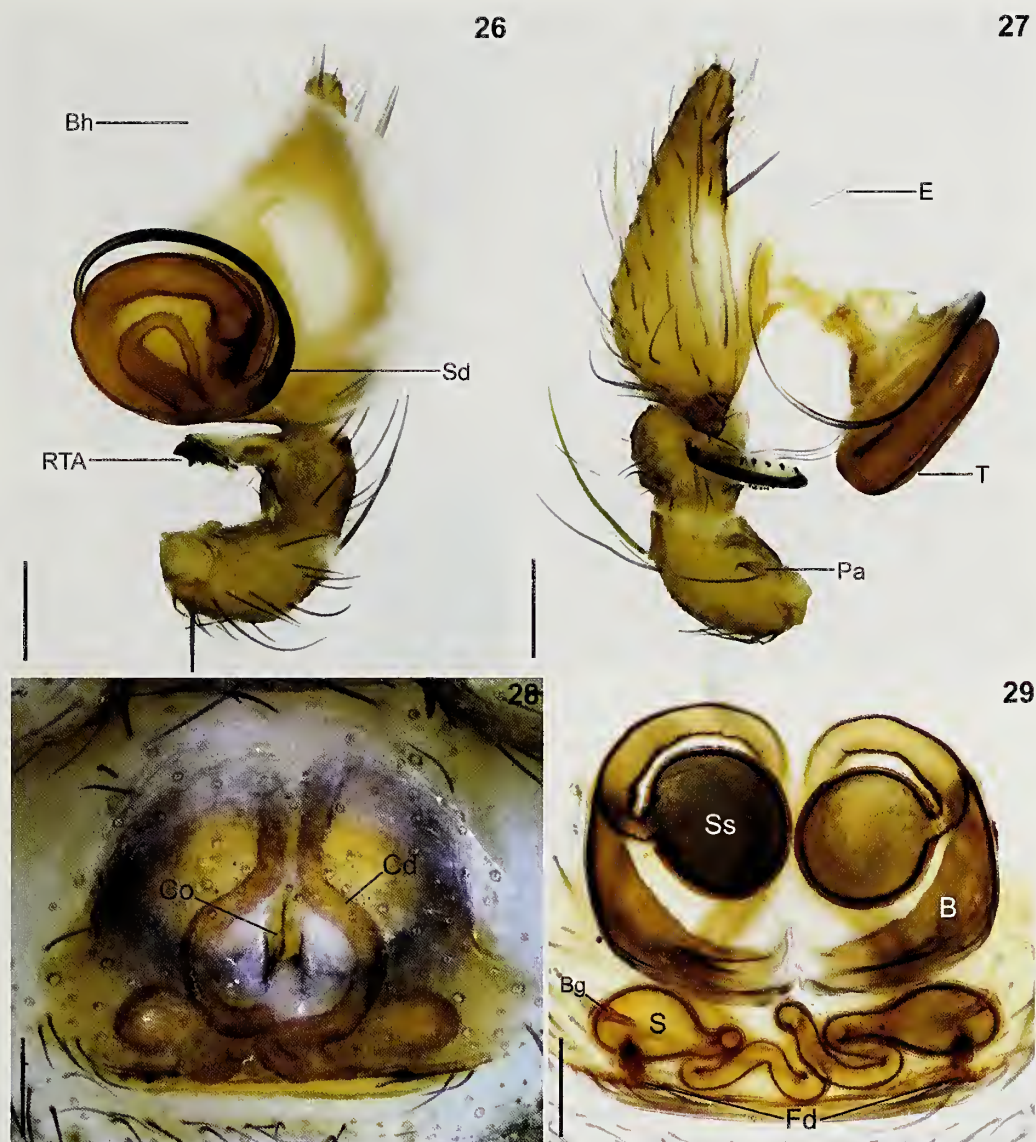
**Etymology.**—The specific epithet is a combination of adjectives from the Latin *multi* (many) and *dentatus* (toothed), referring to the presence of lines of numerous teeth on the RTA.

**Diagnosis.**—*Neoantistea multidentata* sp. nov. is similar to *N. riparia* (Keyserling, 1887), *N. procteri* Gertsch, 1946, *N. coconino* Chamberlin & Ivie, 1942, *N. gosiuta* Gertsch, 1934, *N. mulaiki* Gertsch, 1946, *N. crandalli* Gertsch, 1946 and *N. santana* Chamberlin & Ivie, 1942 in having the RTA strongly curved proximally (Figs. 24, 26; Opell & Beatty 1976: figs. 24,

26, 30, 40, 46, 56, 62), but differs from these species by having two discontinuous lines of teeth on the inner margins of the RTA (Figs. 25, 30), a long and filiform embolus originating retro-basally, and the distal segment of the PLS shorter than the proximal segment (Figs. 22, 23, 27). The epigynum of *N. multidentata* sp. nov. has a unique anatomy characterized by wide and strongly sclerotized bursae, originating laterally from the secondary spermathecae and oriented towards the medial region (Fig. 29), and semicircular secondary spermathecae, almost as wide as the bursae and located near the anterior margin of the epigynum (Fig. 29).

**Description.**—*Male* (Holotype). Total length 2.8. Cephalothorax 1.6 long, 1.1 wide. Carapace dorsal surface brown; pars thoracica with a reticulated dark pattern concentrated behind the pars cephalica and over the radial furrows (Fig. 18); pear-shaped, narrowed anteriorly, fovea longitudinal and brown; inconspicuous stridulatory organ on posterior margin composed of rough area with tiny flattened hooks (Fig. 63). Ocular region 0.20 long, 0.37 wide, slightly dark. Eight eyes, both eye rows slightly procurved in frontal view (Fig. 21). Eye sizes and interdistances: AME, PLE and PME equal in size (0.08), ALE (0.1); AME-AME, AME-ALE, ALE-PLE equal in distance (0.01), PLE-PME (0.03), PME-PME (0.06). Clypeus greater than a diameter of AME, 0.12. Chelicerae 0.48 long, 0.24 wide, reddish brown; retrolateral edges slightly concave apically, three promarginal and four retromarginal teeth. Endites 0.26 long, 0.30 wide, light brown, convergent apically, slightly elongated posteriorly, serrula darker in coloration. Labium 0.13 long, 0.20 wide, same color pattern as the carapace, with strong basal notches. Sternum 0.56 long, 0.62 wide, light brown in medial region, margin darker, shield-shaped, truncated anteriorly, narrowed posteriorly, lateral margins with narrow lobes opposite coxae (Fig. 20). Abdomen oval, covered with setae, raised anteriorly above posterior region of carapace, with stridulatory organ dorsolateral to the pedicel composed of two groups of numerous slender and flat macrosetae (Fig. 65). Dorsal pattern greyish-black, with five chevron-like markings that extend towards the postero-lateral region (Fig. 18). Ventral surface white. Colulus indistinct. Spinnerets light brown, ALS and PLS dark distally; PMS (0.15), ALS proximal segment (0.15), distal segment (0.04), PLS proximal segment (0.20), distal segment (0.10). Legs: I 3.05 (0.85) (0.95) (0.75) (0.50); II 2.99 (0.88) (0.99) (0.64) (0.48); III 2.72 (0.75) (0.83) (0.66) (0.48); IV 3.51 (0.91) (1.30) (0.80) (0.50); leg formula: 4123; dark brown, all femora, tibiae and metatarsi with proximal and distal dark rings; patella and tibia I to IV dorsal surface with macroseta; tarsi without dark rings or macrosetae. Pedipalp: Patella larger than tibia. Patella with retro-basal apophysis, wider at its base, tapering distally and curved apically (Fig. 51). Retro-basal apophysis flanked by two macrosetae; one smaller than this apophysis, the other considerably longer (Fig. 51). RTA strongly curved, tip bent dorsally and five straight setae at its base (Figs. 25, 50). Cymbium oval, longer than wide, tip elongated. Embolus originating retro-basally and extending around the tegulum making a full turn (Fig. 30). Tegulum disk-shaped, spermathecal duct following the tegular margin and with three turns before entering the embolus (Figs. 23, 26, 30).





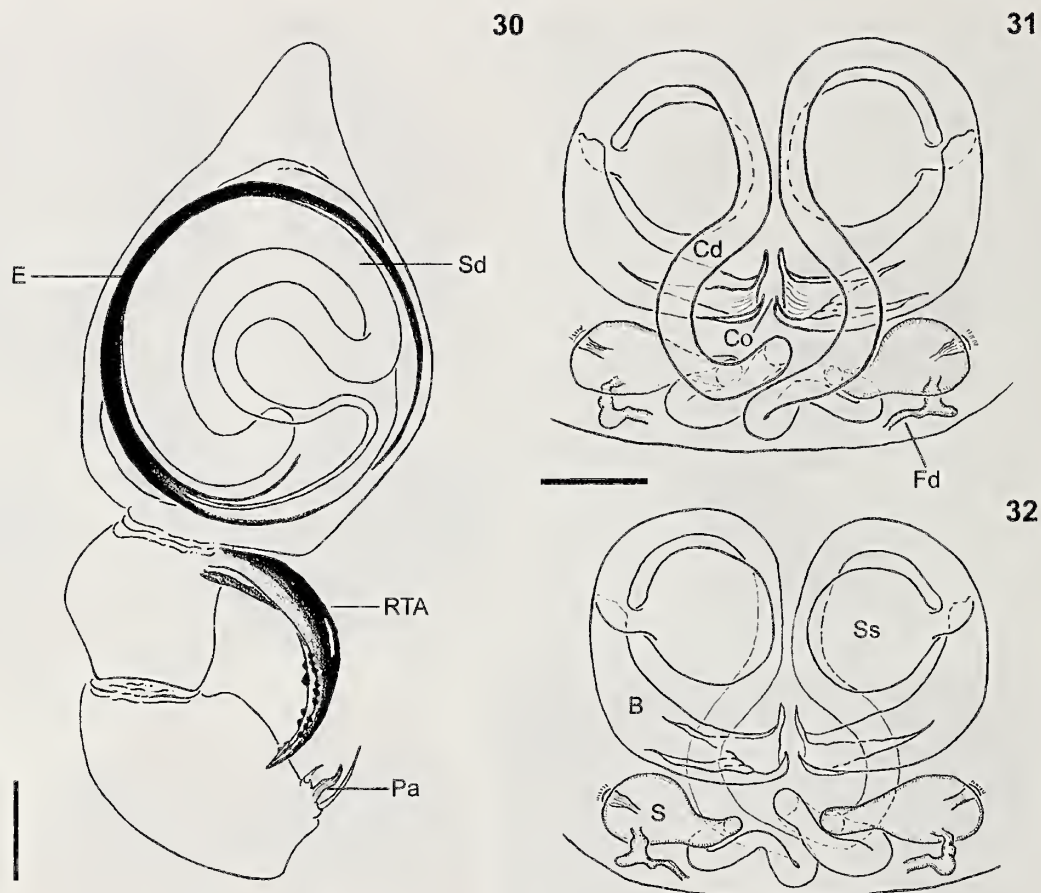
Figures 26-29.—*Neoantistea multidentata* sp. nov. 26, Expanded right male pedipalp, ventral view; 27, same retrolateral view; 28, female epigynum ventral view; 29, same dorsal view (cleared). Scale bars = 0.2 mm (Figs. 26-28), 0.1 mm (Fig. 29). B, bursae; Bg, Bennett's glands; Bh, basal hematodochae; Cd, copulatory duct; Co, copulatory opening; Fd, fertilization duct; Pa, patellar apophysis; RTA, retrolateral tibial apophysis; Sd, spermatic duct; S, spermathecae; Ss, secondary spermathecae; T, tegulum.

**Female** (Allotype). Total length 3.4. As in male except as noted: Cephalothorax: Carapace 2.0 long, 1.3 wide. Ocular region 0.20 long, 0.38 wide. Eyes and interdistances: ALE (0.09), AME-AME (0.02), PME-PME (0.07). Chelicerae 0.59 long, 0.28 wide. Endites 0.30 long, 0.28 wide. Sternum 0.60 long, 0.70 wide. Abdomen: Tracheal system with distinctive spiracle closer to epigastric furrow than to spinnerets, internally composed of four short tubular tracheae branching in tracheoles that extend towards the posterior and anterior region of the body (Fig. 56). PMS 0.20, ALS proximal segment 0.20, distal segment 0.03. Legs: I 3.13 (0.75) (1.3) (0.60) (0.48); II 2.88 (0.80) (1.0) (0.63) (0.45); III 2.79 (0.83) (0.90) (0.63) (0.43); IV 3.6 (1.0) (1.2) (0.85) (0.55). Epigynum flat, copulatory ducts opening inside a central atrium located between the primary and secondary spermathecae (Fig. 28).

Copulatory ducts visible in ventral view, path surrounding the secondary spermathecae and with several coils before entering the primary spermathecae (Figs. 28, 29). Primary spermathecae oval, located posterior to the secondary spermathecae and smaller than these (Fig. 29). Fertilization ducts short and thick, originating posteriorly from the primary spermathecae. The Bennett's glands are located in the lateral region of the primary spermathecae. (Figs. 29, 32).

**Variation** ( $n = 15$ ).—Males total length 2.5–2.8. Females total length 3.1–3.4. Coils of ducts vary considerably in orientation. Spermathecae vary in orientation from horizontal to slightly inclined relative to the epigastric furrow. Specimen coloration varies in pigmentation from reddish brown to dark-brown. One specimen presented seven eyes.





Figures 30–32.—*Neoantistea multidentata* sp. nov., illustrations: 30, male left pedipalp ventral view; 31, cleared female epigynum ventral view; 32, same dorsal view. Scale bars = 0.1 mm. B, bursae; Cd, copulatory duct; Co, copulatory opening; E, embolus; Fd, fertilization duct; Pa, patellar apophysis; RTA, retrolateral tibial apophysis; Sd, spermatic duct; S, spermathecae; Ss, secondary spermathecae.

**Distribution.**—Oak forest in the Atotonilco de Calcahualco region, Veracruz, Mexico (Figs. 72–74).

**Biology.**—Male and female individuals were collected in October (11 females and four males) and February (only two individuals collected). The presence of adult specimens in October could indicate that the breeding season is during autumn, declining rapidly toward winter (where the time of egg laying and hatching could occur) and rising again toward the autumn. It is likely that juvenile populations are found in early spring and late summer because adult specimens are not found during May and there is a remarkably low number of adults in February. Most specimens were caught in leaf litter with cryptic searching (16 individuals) and only one specimen was found by Berlese funnel.

*Neoantistea aspembira* sp. nov.

<http://zoobank.org/?lsid=urn:lsid:zoobank.org:act:43E98FC4-99A7-4483-B45B-876917321272>

org:act:43E98FC4-99A7-4483-B45B-876917321272

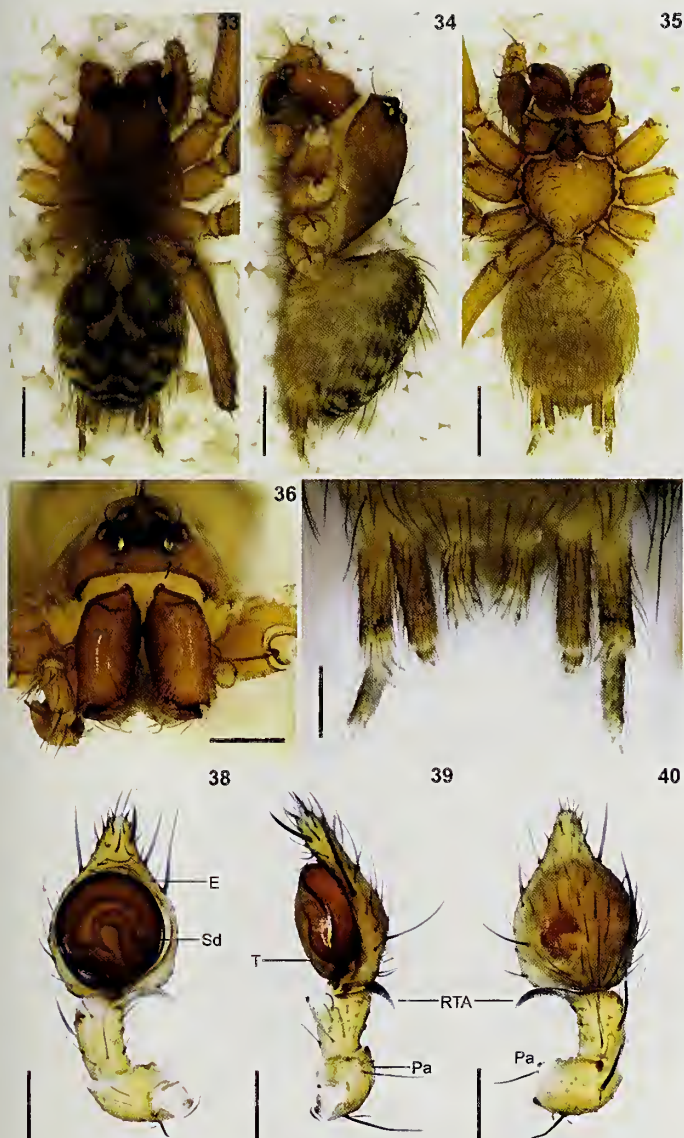
Figs. 33–49, 52–54, 57–62, 64, 66, 71

**Type material.**—*Holotype male*. MEXICO: Veracruz: Atotonilco de Calcahualco, ca. 15 km from the Pico de Orizaba Volcano, Plot I, 19°8'17.4" N, 97°12'16.2" W, elev. 2,300 m, oak forest, leaf litter, collected with pitfall traps, 21–30 May 2012 (CNAN-T1142).

**Paratypes.** MEXICO: Veracruz: 1 ♀ allotype, same data as holotype except Plot II, 19°8'30.2" N, 97°12'21.5" W, elev. 2,388 m (CNAN-T1143); 1 ♀, same data as holotype except F. Alvarez-Padilla (CAFC-UNAM); 1 ♂, same data except 4–14 October 2012 (CAFC-UNAM); 1 ♀, same data except Plot II, 19°8'30.2" N, 97°12'21.5" W, elev. 2,388 m, 21–30 May 2012, F.A. Rivera-Quiroz (CAFC-UNAM); 1 ♂, same data except 15–24 February 2013 (CAFC-UNAM).

**Other material examined.**—MEXICO: Veracruz: 2 ♀, Atotonilco de Calcahualco, 15 km away from the Pico de Orizaba Volcano, Plot I, 19°8'17.4" N, 97°12'16.2" W, 2,300 m, 21–30 May 2012, pitfall trap (CAFC-UNAM); 2 ♂, same data except 4–14 October 2012 (CAFC-UNAM); 1 ♂, 1 ♀, same data except 15–24 February 2013, F.A. Rivera-Quiroz (CAFC-UNAM); 2 ♂, 3 ♀, same data except Plot II, 19°8'30.2" N, 97°12'21.5" W, 2,388 m, 21–30 May 2012, pitfall trap (CAFC-UNAM); 3 ♀, same data except 4–14 October 2012, T. Silva (CAFC-UNAM); 1 ♂, 1 ♀, same data except 15–24 February 2013, U. Garcilazo-Cruz (CAFC-UNAM); 1 ♂, Xamaetipac de Calcahualco, Plot I, 19°7'34.1" N, 97°4'1.5" W, 1,710 m, 19–27 April 2013, pitfall trap (CAFC-UNAM); 1 ♂, same data except 2–11 October 2013, F.A. Rivera-Quiroz (CAFC-UNAM); 1 ♂, same data except 4–17 February 2014, pitfall trap, (CAFC-UNAM); 1 ♂, Plot





Figures 33–40.—*Neoantistea aspeimbira* sp. nov., male: 35, habitus dorsal view; 36, same lateral view; 37, same ventral view; 38, prosoma anterior view; 39, spinnerets ventral view; 40, left pedipalp ventral view; 41, same retrolateral view; 42, same dorsal view. Scale bars = 0.2 mm except habitus = 1 mm. E, embolus; Pa, patellar apophysis; RTA, retrolateral tibial apophysis; Sd, spermathecal duct; T, tegulum.

II, 19°7'32.5" N, 97°4'3.2" W, 1,700 m, 19–27 April 2013, Berlese funnel (CAFC-UNAM); 1 ♂, 2 ♀, same data except 2–11 October 2013, U. Garcilazo-Cruz, (CAFC-UNAM); 1 ♀, same data except 4–17 February 2014 (CAFC-UNAM).

**Etymology.**—The specific epithet is a combination of the Latin adjective *asper* (rough) and the English noun *mbira* (African musical instrument), referring to the rough texture of the cephalothorax cuticle around the pedicel and the corresponding shape of the stridulatory organ over the anterior surface of the abdomen.

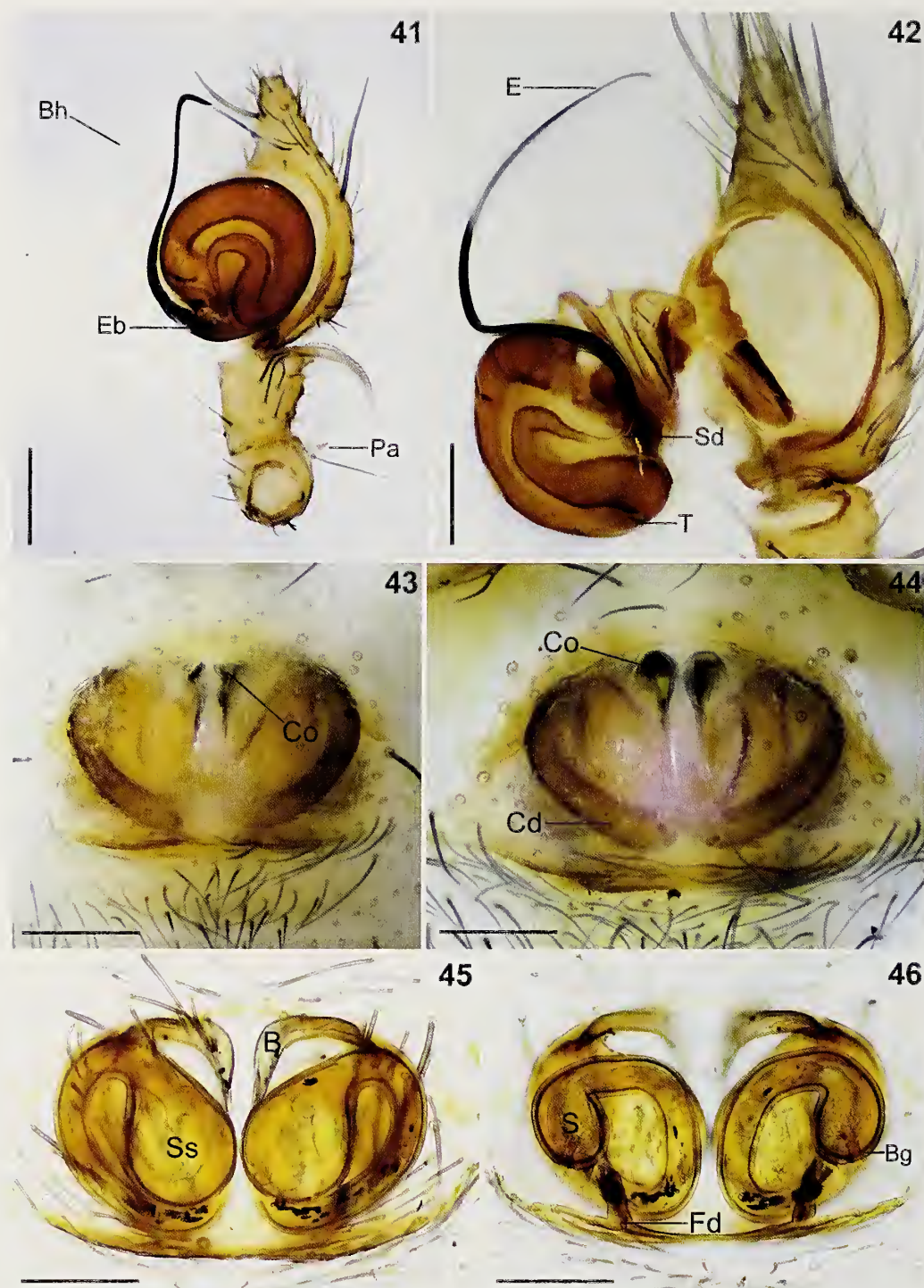
**Diagnosis.**—*Neoantistea aspeimbira* sp. nov. is similar to *N. pueblensis* Opell & Beatty, 1976, *N. inaffecta* Opell & Beatty, 1976, and *N. magna* (Keyserling, 1887) by the perpendicular

position of the RTA relative to the tibia longitudinal axis (Opell & Beatty 1976: figs. 36, 37, 68, 69, 74, 75). It differs from these species by having a distally curved RTA with serrated pattern along inner margin, and by having a short patellar apophysis which is projected dorsally with a cone-shaped tip (Figs. 47, 52, 53). The epigynum of *N. aspeimbira* sp. nov. has a unique anatomy characterized by an epigynum with secondary spermathecae located ventrally and larger in size than the primary spermathecae (Figs. 45, 48). Primary spermathecae oval, with almost the same width as the copulatory ducts, located laterally and posterior to the secondary spermathecae (Figs. 46, 49).

**Description.**—*Male* (Holotype). Total length 2.9. Cephalothorax 1.6 long, 0.95 wide. Carapace dorsal surface light brown, darker in pars cephalica; pars thoracica with radial furrows extending towards the carapace edges (Fig. 33); pear-shaped, narrowed anteriorly, fovea longitudinal and brown; inconspicuous stridulatory organ on posterior margin composed of rough area with tiny flattened hooks. Ocular region 0.24 long, 0.42 wide. Eight eyes, both eye rows slightly procurved in frontal view (Fig. 36). Eye sizes and interdistances: AME (0.07), ALE (0.12), PLE and PME equal in size (0.1); AME-AME (0.03), AME-ALE (0.01), ALE-PLE contiguous, PLE-PME (0.03), PME-PME (0.08). Clypeus greater than a diameter of AME, 0.15. Chelicerae 0.62 long, 0.30 wide, reddish; retrolateral edges slightly concave apically, three promarginal and four retromarginal teeth. Endites 0.24 long, 0.28 wide, light brown, convergent apically, slightly elongated posteriorly, serrula darker in color. Labium 0.13 long, 0.25 wide, same color pattern as the endites, with strong basal notches. Sternum 0.55 long, 0.72 wide, light brown, margin darker. Shield-shaped, truncated anteriorly, narrowed posteriorly, anterior margin undulated, lateral margins with narrow lobes opposite coxae (Fig. 35). Abdomen oval, covered with setae, raised anteriorly above posterior region of carapace, with stridulatory organ dorsolateral to the pedicel composed of two groups of wide and flat macrosetae (Figs. 34, 64, 66). Dorsal pattern greyish, with five chevron-like markings that extend towards the postero-lateral region and two semicircular spots located in anterior region (Figs. 33, 60). Ventral surface white. Colulus indistinct. Spinnerets light brown, PLS dark distally; PMS (0.2), ALS proximal segment (0.25), distal segment (0.24). Legs: I 3.85 (1.1) (1.3) (0.85) (0.60); II 3.81 (1.1) (1.3) (0.81) (0.60); III 3.52 (1.1) (1.1) (0.82) (0.50); IV 4.0 (1.1) (1.3) (1.0) (0.60); leg formula: 4123; light brown, precoxal triangles present, all femora and tibiae with proximal and distal dark rings. Patella I to IV dorsal surface with two macrosetae. Tibia I to IV with four macrosetae; two dorsal, one prolateral and one retrolateral. Metatarsus III–IV with four macrosetae, same distribution as tibia; tarsi without macrosetae. Pedipalp: Patella almost same length as the tibia. Retro-basal apophysis flanked by two macrosetae (Fig. 53). Tibia longer than wide. Cymbium oval, slightly longer than wide, tip slightly elongated; embolus originating pro-basally, extending around the tegulum making nearly a full turn (Fig. 38). Tegulum disk-shaped, spermathecal duct following the tegular margin and with three turns before entering the embolus (Figs. 41, 47).

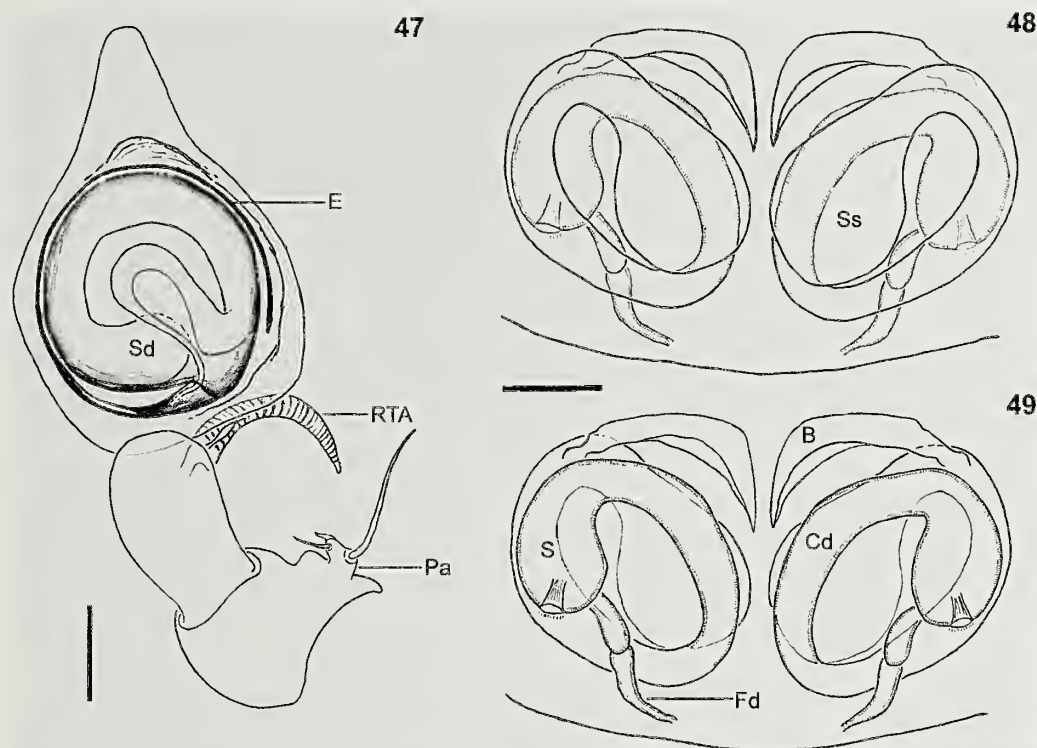
*Female* (Allotype). Total length 2.5. As in male except as noted: Cephalothorax: Carapace 1.0 long, 0.60 wide. Dorsal





Figures 41–46.—*Neoantistea aspembira* sp. nov. 41, Expanded male left pedipalp, ventral view; 42, expanded male right pedipalp, prolateral view; 43, female epigynum ventral view; 44, same ventral view with mating plug; 45, female epigynum ventral view (cleared); 46, same dorsal view. Scale bars = 0.2 mm (Figs. 41–44), 0.1 mm (Figs. 45, 46). B, bursae; Bg, Bennett's glands; Bh, basal hematodochae; Cd, copulatory duct; Co, copulatory opening; E, embolus; Eb, embolus base; Fd, fertilization duct; Pa, patellar apophysis; Sd, spermathecae; S, spermathecae; Ss, secondary spermathecae; T, tegulum.





Figures 47–49.—*Neoantistea aspembira* sp. nov., illustrations: 47, male left pedipalp, ventral view; 48, cleared female epigynum ventral view; 49, same dorsal view. Scale bars = 0.1 mm. B, bursae; Cd, copulatory duct; E, embolus; Fd, fertilization duct; Pa, patellar apophysis; RTA, retrolateral tibial apophysis; Sd, spermatic duct; S, spermathecae; Ss, secondary spermathecae.

surface light brown. Pars thoracica with a reticulated dark pattern concentrated behind the pars cephalica and over the radial furrows. Ocular region 0.15 long, 0.34 wide. Eyes and interdistances: AME (0.05), ALE (0.09), PLE (0.08), PME (0.06); PME-PME (0.07). Clypeus 0.09. Chelicerae 0.45 long, 0.20 wide; light brown. Endites 0.20 long, 0.22 wide. Labium 0.15 wide. Sternum 0.35 long, 0.52 wide. Abdomen: Tracheal system with distinctive spiracle closer to epigastric furrow than to spinnerets, internally composed of four short tubular tracheae branching in tracheoles that extend towards the posterior and anterior region of body (Fig. 54). PMS (0.15), ALS proximal segment (0.20), PLS proximal segment (0.15), distal segment (0.15). Legs: I 2.4 (0.70) (0.80) (0.50) (0.40); II 2.36 (0.70) (0.76) (0.50) (0.40); III 2.3 (0.65) (0.70) (0.55) (0.40); IV 2.77 (0.77) (0.90) (0.65) (0.45). Epigynum: flat, two copulatory openings located anterior to the spermathecae (Figs. 43, 44). Bursae separate, curved, originating dorsally from the secondary spermathecae (Figs. 45, 49). Copulatory ducts long, visible in ventral view, path partially surrounding the secondary spermathecae (Fig. 45). Fertilization ducts short and thin, originating posteriorly from the primary spermathecae (Fig. 49). The Bennett's glands are located in the posterior region of the primary spermathecae (Figs. 46, 49).

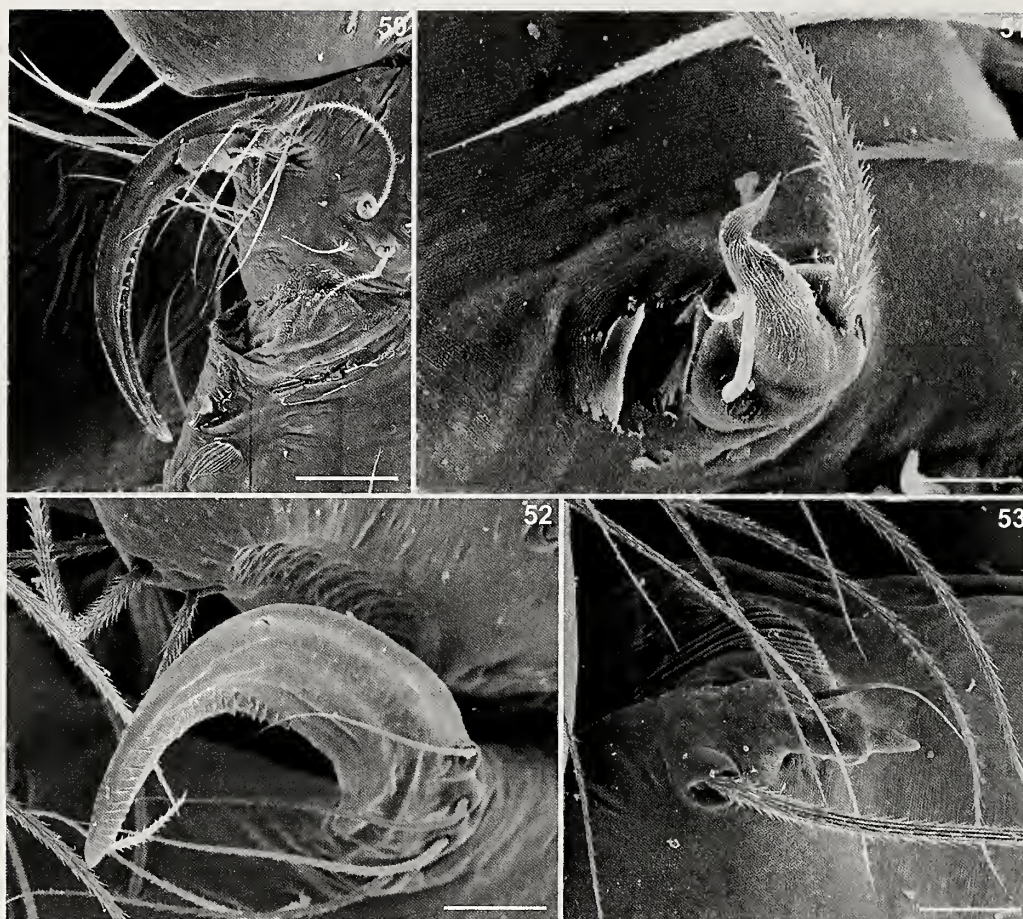
**Variation** ( $n = 24$ ).—Males total length 2.1–2.9. Females total length 2.3–2.7. Coils of ducts vary slightly in orientation. Specimen coloration varies in pigmentation from whitish to reddish brown. Patterns on the dorsal surface of the carapace also vary in pigmentation from greyish to dark. Several specimens presented damaged legs.

**Distribution.**—Oak forest in the Atotonilco and Xamaticpac de Calcahualco region, Veracruz, Mexico (Figs. 72–74).

**Biology.**—Male and female individuals were collected during all three expeditions. The presence of a low number of male specimens but a high number of females in October could indicate that the breeding season is during winter and spring, when more specimens were collected (23 females and 19 males in February; 31 females and 20 males in May). Juveniles are probably present in late spring to early autumn. Most specimens were caught in soil and leaf litter with pitfall traps (60 individuals), by cryptic searching (51 individuals) and with Berlese funnels (23 individuals); only four specimens were found by looking up in vegetation from the ground.

**Natural history.**—*Neoantistea aspembira* sp. nov. inhabits oak forest mainly in leaf litter (under the surface layer) near the bases of trees where more organic matter accumulates. Under laboratory conditions all specimens built webs over the substrate, where they spent most of their time. Structurally the webs consisted of two sheets separated by tangled middle threads (Fig. 62). The upper sheet functioned as a primary trap and was formed by unevenly spaced parallel lines crossed perpendicularly by dispersed lines that do not have any sticky property. The middle layer of threads was formed by a few lines slightly inclined connecting both sheets at one extreme of the web. The lower sheet had the same weaving as the upper sheet, but was considerably denser and had one to three openings used by the spider to either take refuge, escape or catch prey (Fig. 61). When a prey item (*Drosophila*) was caught on the upper sheet, the spider ran through one of these





Figures 50–53.—Pedipalps of *Neoantistea* species: 50, RTA of *N. multidentata* sp. nov. dorsal view; 51, patellar apophysis of *N. multidentata* sp. nov. retrolateral view; 52, RTA of *N. aspembira* sp. nov. dorsal view; 53, patellar apophysis of *N. aspembira* retrolateral view. Scale bars = 0.01 mm.

holes, climbed the middle layer of threads and bit the fly through the upper sheet. In some cases, the lower sheet had a “shelter” formed by a small ellipsoidal web approximately the same length as the spider (2–3 mm). The total size of the web depended on the support structures and the size of the plastic cages.

**Sexual behavior and reproduction.**—Eight attempts at courtship between two males and seven females of *N. aspembira* sp. nov. were performed, however, only one was successful. The male courtship consisted of three basic displays: (A) chemo-exploration; (B) acoustic signaling; and (C) tactile stimulation following mating, conforming to “level two” in Foelix (2011). Chemo-exploration during the pre-courtship display (searching phase) started when the male walked around the substrate and came into contact with the female silk threads. In this phase, the male contacted the web by vertical movements of the pedipalps for approximately 10 seconds. This display is presumably used for detecting pheromones as evidenced in lycosids (Stratton & Uetz 1983; Hebets et al. 1996). During acoustic signaling, the male approached the female with vibrations and stridulations, touching the web with the pedipalps and legs in the following sequence: (1) the male produced vibrations in the web with

legs I (left) and II (right) flexed near the body; (2) leg vibrations were followed by a constant and vertical movement of the abdomen and pedicel, presumably to produce sounds with the stridulatory organ; and (3) stridulation was followed by continuous vibration of the pedipalps. These periods of activity were intercalated with periods of approximately 10 seconds of rest, after which the sequence of movements 1 to 3 were performed again, but exchanging legs I (right) and II (left) during the first phase. The male continued this behavior for approximately 35 minutes accompanied by a circular motion around the female while producing a layer of very thin threads. During tactile stimulation the male approached the female with the first pair of legs lifted, accompanied by palpal drumming (1–2 drums/sec) and stridulation by vertical and lateral movements of the abdomen. The female responded by lifting the first pair of legs and stridulating by moving the abdomen vertically while establishing contact with the male for approximately five seconds. Mating lasted approximately 48 minutes. The female remained motionless while the male, located under her abdomen, held her with the first two pairs of legs and inserted his palps: twice on the left side and twice on the right side with the left palp, and twice on the left side and twice on the right side with the right palp.





Figures 54–56.—Respiratory system of Hahniidae species: 54, Tracheae and book lungs of *N. aspembira* sp. nov., dorsal view; 55, tracheae of *H. quadriseta* sp. nov., dorsal view; 56, cleared tracheal spiracle of *N. multidentata* sp. nov., dorsal view. Scale bars = 0.1 mm (Figs. 54, 56), 0.01 mm (Fig. 55).

**Morphology of stridulatory organs.**—The new species *N. multidentata* and *N. aspembira* present simple stridulatory organs (Jocqué 2005), most likely used for intraspecific communication during species mate recognition and as defense against predators (Uhl & Elias 2011). All specimens including immatures have these structures.

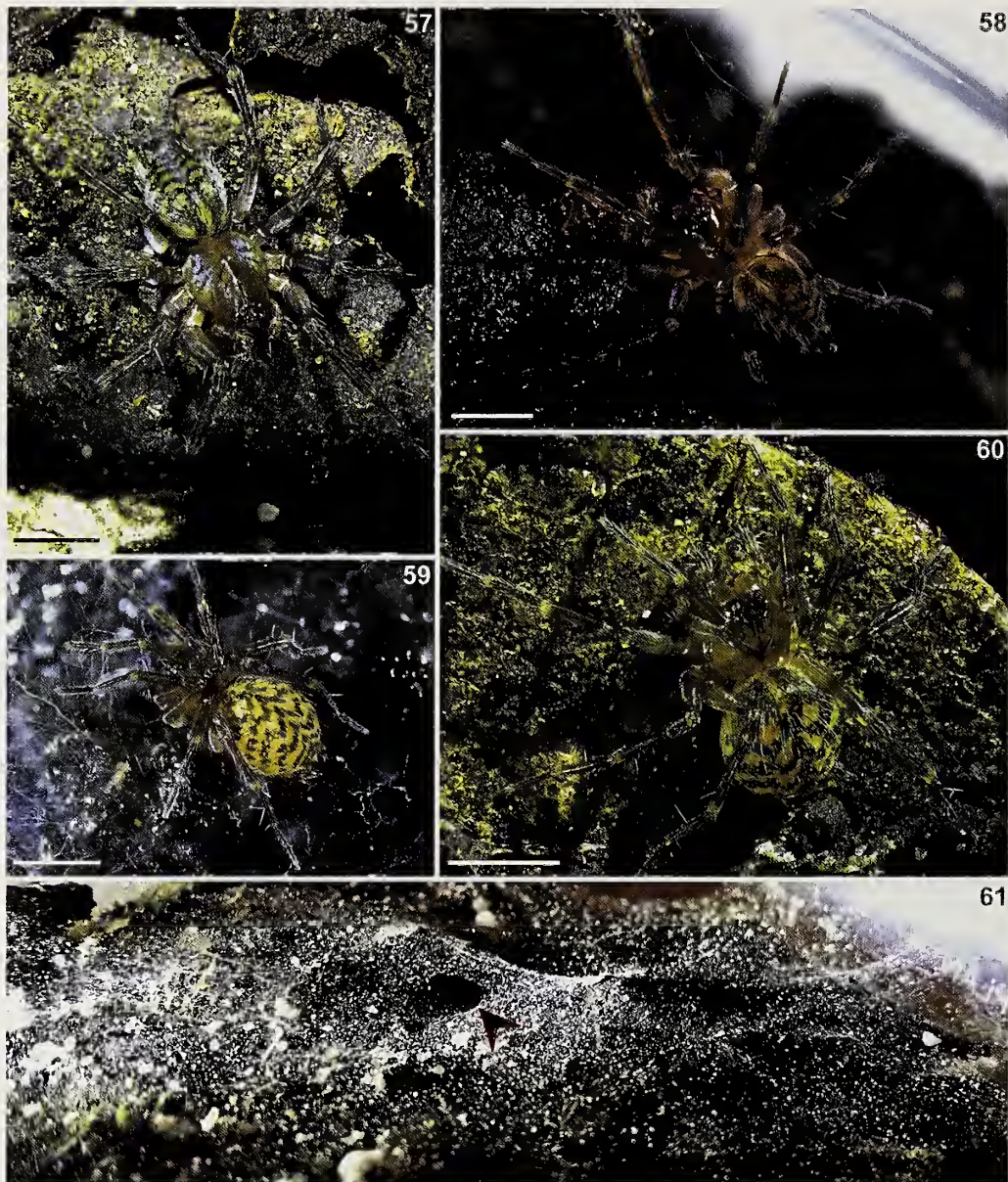
The stridulatory organs are formed by antagonistic structures on the cephalothorax (*plectron*) and the abdomen (*file*) following the nomenclature of Jocqué (2005). The *plectron* structures are located on the posterior region as an elevation of the cuticle and are formed by a rough area of cuticular modifications resembling tiny flattened hooks, which are only observable with SEM microscopy (Figs. 63, 69). These hooks form discontinuous lines extending from one end to the other of this area concentrating towards the posterior edge of the carapace (Fig. 68). The *file* is located at the anterior region of the abdomen and is formed by two clusters of modified macrosetae parallel to each other and slightly oriented towards the ventral surface (Figs. 64–66); the surface of each *file* macroseta is covered by longitudinal grooves (Figs. 70, 71). The *file* clusters are separated by a space of unmodified cuticle

(ca. 0.5 x the width of the *file*) that bears two long and filiform macrosetae possibly used for receiving and decoding the vibratory signals (Figs. 65, 66).

The spatial arrangement of the *file* and *plectron* combined with the observations during courtship indicate that stridulatory sounds are produced by vertical movements of the abdomen promoting the rubbing of both structures (Fig. 67). The *N. multidentata* *file* was composed of two groups of 22 to 27 flattened macrosetae with three to four longitudinal grooves covering their total length (Fig. 70). For *N. aspembira*, the number of macrosetae is reduced to 14 to 16 per group; they are 0.3 x as long as the ones present in *N. multidentata* and provided with four to five longitudinal grooves (Fig. 71). The size differences of the *file* macrosetae between the two species suggest different frequencies of sound for species mate recognition.

The stridulatory behavior of *N. aspembira* was documented by the following five combinations: female vs. juvenile, female vs. female, male vs. female, male vs. juvenile and male vs. male. In all cases the individuals were kept in the same web, separating themselves by a distance of ea. 2 cm apart and for a





Figures 57- 61.—Natural history of *N. aspebira* sp. nov.: 57, male habitus dorsal view; 58, male on the upper sheet of web; 59, female on the lower sheet of web; 60, female habitus dorsal view; 61, general aspect of *N. aspebira* sp. nov. web (lower sheet), arrow to refuge openings. Scale bars = 1 mm.

time of ca. 20 minutes. Subsequently, the individual which had been introduced moved away and built its own web. Juvenile and adult interactions ranged between one and three minutes ( $2:31 \pm 0:23$ ) except in male-female interactions where continuous communication by the male during courtship was observed (described in the previous section). Neither aggressive behavior nor cooperation was observed among individuals; however, disputes over the same prey (*D. melanogaster*) were observed between adults vs. juveniles and females vs. males. Finally, male vs. male territorial behavior was observed, characterized by the elevation and drumming on the web by the first pair of legs.

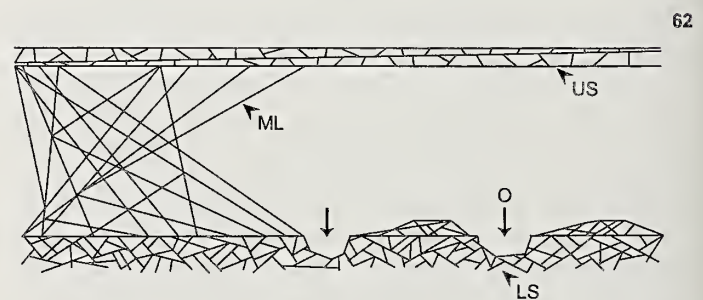


Figure 62.—Schematic representation of *N. aspebira* sp. nov. web. LS, lower sheet; ML, middle layer; O, refuge opening; US, upper sheet.





Figures 63–66.—Stridulatory organs morphology: 63, *N. multidentata* sp. nov., prosoma dorsal view, arrow to *plectron* structures; 64, *N. aspebira* sp. nov., living male individual, arrow to *file* structures; 65, *file* clusters of *N. multidentata* sp. nov.; 66, same but *N. aspebira* sp. nov. Scale bars = 0.5 mm (Fig. 63); 1 mm (Fig. 64); 0.2 mm (Figs. 65, 66).

## DISCUSSION

**Communication in *Neoantistea*.**—The presence of stridulatory organs in both sexes and juvenile stages of *N. aspebira* suggests that communication in these spiders is not restricted to courtship and male agonistic encounters. Communication through these organs possibly plays several roles such as: avoiding other predators, during parent-offspring recognition, species recognition and social dominance interactions. Individuals of *N. aspebira* exhibited three mechanisms of acoustic signaling: stridulation, tremulation and percussion. These mechanisms have different properties that can be propagated either via airborne vibrations or through the substrate, depending on the different frequencies and amplitudes produced. Thus, the combination of different mechanisms can produce a multicomponent signal that could elicit the behaviors mentioned above (Uhl & Elias 2011).

Observation of live *N. aspebira* specimens suggests that signals produced by these structures have the potential for species recognition as observed in courtship between males and females. It is important to mention that both of the newly described *Neoantistea* species are sympatric in both reproductive seasons, with more adults collected in autumn, and sharing the same microhabitat. However, differences in the size of *file* macrosetae from stridulatory organs, observation of male courtship and other somatic features differentiate them.

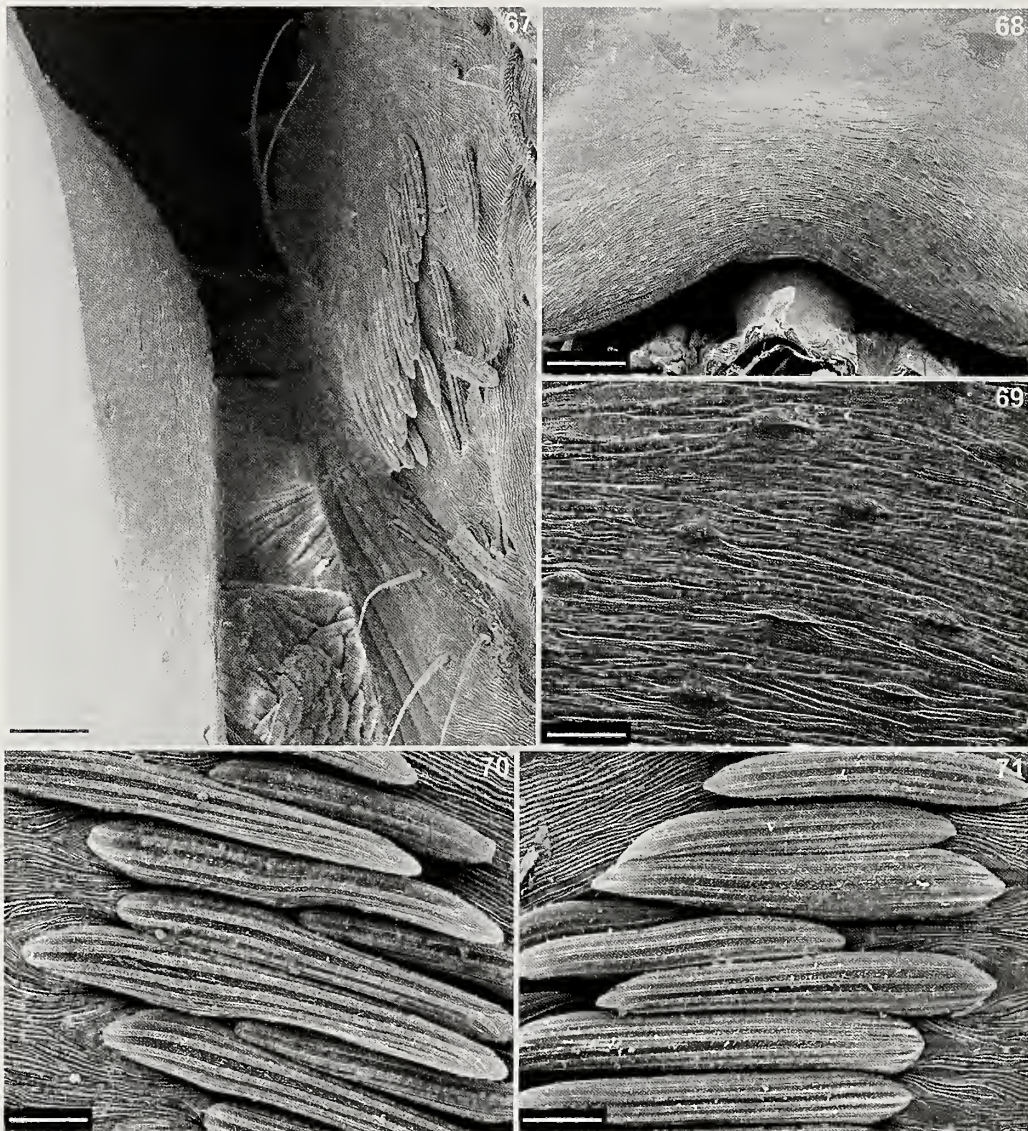
**Importance of Mexican oak forest ecosystems.**—Temperate forests in Mexico represent one of the most important

vegetation types covering approximately 24% of the country's area (CONAFOR 2009). The dominant species in Mexican temperate forest ecosystems are *Pinus* spp. and *Quercus* spp., mixed with other taxa such as: *Abies*, *Pseudotsuga*, *Picea*, *Cupressus* and *Juniperus* with a more restricted distribution (Galicia et al. 2015). Moreover, these ecosystems harbor many other species of several animal groups such as amphibians, birds, reptiles and mammals (Challenger 1998; Ceballos et al. 2002; Galieia et al. 2015).

Oak forests are mainly distributed throughout the Northern Hemisphere, and Mexico is recognized as the major diversity centre for *Quercus* with 170 native species of a total of 450 worldwide. Most Mexican oak species occur in the central and southern regions and the Sierra Madre Oriental with an estimated 109 endemic species (Rzedowski 1978; Zavala Chávez 2007; Galicia et al. 2015). The current distribution and richness of this genus in Mexico can be explained by paleoclimatic evidence and geological activity that produced numerous extinction and diversification events (Espinosa Organista et al. 2008; Galicia et al. 2015; Rodríguez Correa et al. 2015).

The diversity of Hahniiidae in Mexico is represented by twelve species, most of them distributed in temperate zones, particularly in the central and southern parts of the country where up to ten species occur (Opell & Beatty 1976). The three species described here were collected as part of the first spider inventory of Mexican oak forests. This inventory and the





Figures 67–71.—Stridulatory organs morphology: 67, relative position of *plectron* and *file*; 68, *plectron* of *N. multidentata* sp. nov., posterior view; 69, detail of *plectron* structures; 70, *file* macrosetae of *N. multidentata* sp. nov.; 71, same but *N. aspembira* sp. nov. Scale bars = 0.01 mm.

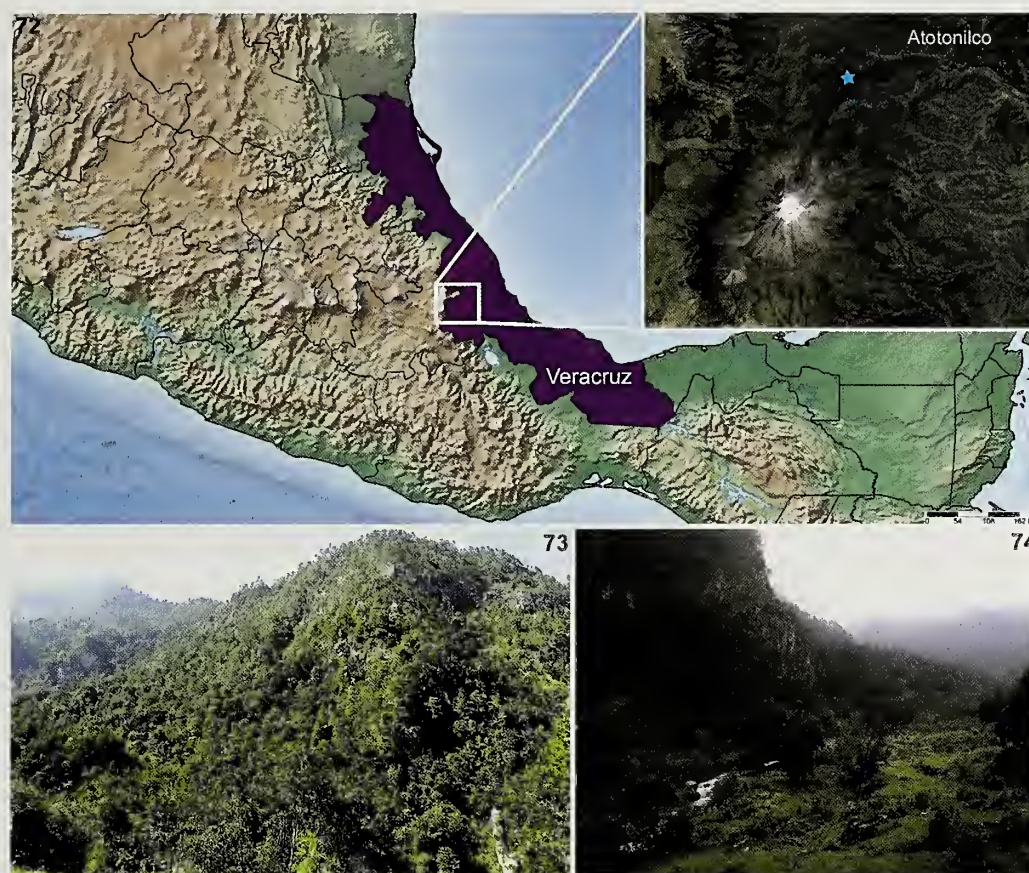
species distributions provided by Opell & Beatty (1976) suggest that Mexican hahniids may be more diverse in oak forests, however, this conclusion is preliminary given that knowledge on hahniid diversity still is far from complete. Finally, this result predicts a potentially high spider diversity and endemism for these ecosystems, and provides data that may help to include oak forests among the protected areas of Mexico.

#### ACKNOWLEDGEMENTS

We would like to thank Francisco J. Salgueiro-Sepúlveda, Dulce F. Piedra-Jiménez, Mariana Servín-Pastor, Leonel Perez-Miguel, Maira S. Montejo-Cruz, Miguel Hernández-Patricio, Uriel Garcilazo-Cruz and F. Andrés Rivera-Quiroz for collecting most of the specimens during two spider inventories. Thanks to international collaborators Facundo

Labarque, Danielle Polotow and Thiago Silva for their participation in one of the 2012 expeditions. Participation by Labarque and Polotow was facilitated by Exline-Frizzell, Bill and Maria Peck, and Schlinger Arachnology fellowships from the California Academy of Sciences. Thanks also to Ali Zeltzin Lira-Olguin and Josue Lopez-Granados for helping us during the collection of live specimens, and Silvia Espinosa Matias for assisting with the SEM images. Thanks to all people from Pico de Orizaba National Park for all of their support and collaboration during expeditions, and thanks to Charles Griswold, Martín Ramírez, Cor Vink, Uriel Garcilazo-Cruz, F. Andrés Rivera-Quiroz and two anonymous referees for comments that helped to improve the manuscript. Funding was provided by UNAM-DGAPA-PAPIIT project IN213612. All species described were collected under permit SGPA/DGVS/02403/12 issued by SEMARNAT.





Figures 72–74.—Distribution map and habitat of Hahniidae species: 72, type locality; 73, *Quercus* forest at Atotonilco de Calchahualeo; 74, mountain landscape near to Pico de Orizaba Volcano. Photos: Ali Zeltzin Lira Olguin.

#### LITERATURE CITED

- Alvarez-Padilla, F. 2014. Cyberdiversity of Araneomorphae from Mexico. Facultad de Ciencias, UNAM. Online at <http://www.unamfearcenolab.com/>
- Alvarez-Padilla, F. & G. Hormiga. 2007 (2008). A protocol for digesting internal soft tissues and mounting spiders for scanning electron microscopy. *Journal of Arachnology* 35:538–542.
- Benoit, P.L.G. 1978. Hahniidae du Mont Kenya (Araneae). *Revue de Zoologie Africaine* 92:609–621.
- Bertkau, P. 1878. Versuch einer natürlichen Anordnung der Spinnen, nebst Bemerkungen zu einzelnen Gattungen. *Archiv für Naturgeschichte* 44:351–410.
- Bonnet, P. 1959. *Bibliographia Araneorum*. Toulouse, France.
- Bosmans, R. & E. Thijs. 1980. Spiders of the family Hahniidae from Mount Kenya. *Revue de Zoologie Africaine* 94:559–569.
- Brignoli, P.M. 1976. Ragni d'Italia XXVII. Nuovi dati su Agelenidae, Argynonidae, Hahniidae, Oxyopidae e Pisauridae, eavernicoli ed epigei (Araneae). *Quaderni del Museo di Speleologia "V. Rivera"* 4:3–117.
- Brignoli, P.M. 1977. Sur quelques Agelenidae et Hahniidae (Araneae) d'Afrique du Nord. *Revue Arachnologique* 1:13–22.
- Brignoli, P.M. 1978. Quelques notes sur les Agelenidae, Hahniidae, Oxyopidae et Pisauridae de France et d'Espagne (Araneae). *Revue Suisse de Zoologie* 85:265–294.
- Bristowe, W.S. 1938. The classification of spiders. *Proceedings of the Zoological Society of London (B)* 108:285–322.
- Ceballos, G., J. Arroyo-Cabales & R. Medellín. 2002. The Mammals of Mexico: composition, distribution, and conservation status. *Occasional Papers of the Museum, Texas Tech University* 218:1–27.
- Challenger, A. 1998. Utilización y Conservación de los Ecosistemas Terrestres de México. Pasado, Presente y Futuro, Comisión Nacional para el Conocimiento y Uso de la Biodiversidad, México, Mexico City.
- Chamberlin, R.V. & W. Ivie. 1942. A hundred new species of American spiders. *Bulletin of the University of Utah* 32(13):1–117.
- Chen, S.H., Y. Wang & S.C. Chen. 2003. A newly recorded spider of the family Hahniidae (Arachnida, Araneae) from Taiwan. *Journal of Taiwan normal University: Mathematics, Science & Technology* 48:25–30.
- Chen, X., H.M. Yan & C.M. Yin. 2009. Two new species of the genus *Hahnia* from China (Araneae: Hahniidae). *Acta Arachnologica Sinica* 18:66–70.
- Coddington, J.A. 1983. A temporary slide-mount allowing precise manipulation of small structures. Pp. 291–292. *In* *Taxonomy, Biology and Ecology of the Araneae*. (J.A. Coddington, ed.). *Verhandlungen des Naturwissenschaftlichen Vereins in Hamburg NP*.
- Coddington, J.A. & H.W. Levi. 1991. Systematics and evolution of spiders (Araneae). *Annual Review of Ecology and Systematics* 22:565–592.
- Coddington, J.A., C.E. Griswold, D.S. Davila, E. Penaranda & S.F. Larcher. 1991. Designing and testing sampling protocols to estimate biodiversity in tropical Ecosystems. Pp. 44–60. *In* *The Unity of Evolutionary Biology: Proceedings of the Fourth International Congress of Systematic and Evolutionary Biology*. Vol. 2. (E.C. Dudley, ed.). Dioscorides Press, Portland OR.
- Comisión Nacional Forestal (CONAFOR). 2009. El Inventario Nacional Forestal y de Suelos de México 2004–2009. Una



- herramienta que da certeza a la planeación, evaluación y el desarrollo forestal de México. Guadalajara, México.
- Emerton, J.H. 1890. New England spiders of the families Drassidae, Agelenidae and Dysderidae. Transactions of the Connecticut Academy of Arts and Sciences 8:166–206.
- Espinosa-Organista, D., S. Ocegueda-Cruz, C. Aguilar-Zúñiga, O. Flores-Villela & J. Llorente-Bousquets. 2008. El conocimiento biogeográfico de las especies y su regionalización natural. Pp. 33–65. In Capital Natural de México. Vol. I Conocimiento Actual de la Biodiversidad. (J. Sarukhan, ed.). CONABIO, Mexico City.
- Exline, H. 1938. The Arancida of Washington: Agelenidae and Hahniidae. University of Washington Publications in Biology 9:1–44.
- Foelix, R.F. 2011. Biology of Spiders. 3rd edition. Oxford University Press, New York.
- Forster, R.R. 1970. The spiders of New Zealand. Part III. Otago Museum Bulletin 3:1–184.
- Galicia, L., C. Potvin & C. Messier. 2015. Maintaining the high diversity of pine and oak species in Mexican temperate forests: a new management approach combining functional zoning and ecosystem adaptability. Canadian Journal of Forest Research 45:1358–1368.
- Gerhardt, U. & A. Kaestner. 1938. Araneae. Pp. 497–656. In Handbuch der Zoologie. (W. Kükenthal, & T. Krumbach (eds.). De Gruyter, Berlin.
- Gertsch, W.J. 1934. Some American spiders of the family Hahniidae. American Museum Novitates 712:1–32.
- Gertsch, W.J. 1946. Five new spiders of the genus *Neoantistea*. Journal of the New York Entomological Society 54:31–36.
- Gertsch, W.J. 1949. American Spiders. Princeton, Van Nostrand.
- Gertsch, W.J. & L.I. Davis. 1940. Report on a collection of spiders from Mexico. II. American Museum Novitates 1059:1–18.
- Harm, M. 1966. Die Deutsche Hahniidae (Arachn. Araneae). Senckenbergiana Biologica 47:345–370.
- Hebets, E.A., G.L. Stratton & G.L. Miller. 1996. Habitat and courtship behavior of the wolf spider *Schizocosa retrorsa* (Banks) (Araneae, Lycosidae). Journal of Arachnology 24:141–147.
- Jocqué, R. 2005. Six stridulating organs on one spider (Araneae, Zodariidae): is this the limit? Journal of Arachnology 33:597–603.
- Jocqué, R. & R. Bosmans. 1982. A new *Hahnina* from Ivory Coast with a note on stridulating organs in the Hahniidae (Arancida). Bulletin of the British Arachnological Society 5:319–323.
- Kaestner, A. 1968. Invertebrate Zoology, Vol. 2. Wiley Interscience, New York.
- Kaston, B.J. 1948. Spiders of Connecticut. Bulletin Connecticut Geological and Natural History Survey 70:48–54, 291–294.
- Keyserling, E. 1887. Neue Spinnen aus America. VII. Verhandlungen der Kaiserlich-Königlichen Zoologisch-Botanischen Gesellschaft in Wien 37:421–490.
- Koch, C.L. 1841. Die Arachniden. Neunter Band, Nürnberg.
- Lehtinen, P.T. 1967. Classification of the cribellate spiders and some allied families, with notes on the evolution of the suborder Araneomorpha. Annales Zoologici Fennici 4:199–468.
- Liu, N., G.Q. Huang & Z.S. Zhang. 2015. A new species of genus *Hahnina* (Araneae: Hahniidae) from South China. Zootaxa 3994:295–300.
- Marusik, Y.M. 2011. A new genus of hahniid spiders from Far East Asia (Araneae: Hahniidae). Zootaxa 2788:57–68.
- Miller, J.A., A. Carmichael, M.J. Ramírez, J.C. Spagna, C.R. Haddad, M. Řezáč, et al. 2010. Phylogeny of entelegyne spiders: affinities of the family Penestomidae (NEW RANK), generic phylogeny of Eresidae, and asymmetric rates of change in spinning organ evolution (Araneae, Araneioidea, Entelegynae). Molecular Phylogenetics and Evolution 55:786–804.
- Opell, B.D. & J.A. Beatty. 1976. The Nearctic Hahniidae (Arachnida: Araneae). Bulletin of the Museum of Comparative Zoology 147:393–433.
- Petrunkovitch, A. 1933. An inquiry into the natural classification of spiders, based on a study of their internal anatomy. Transactions of the Connecticut Academy of Arts and Sciences 31:299–389.
- Rodríguez-Correa, H., K. Oyama, I. MacGregor-Fors & A. González-Rodríguez. 2015. How are oaks distributed in the neotropics? A perspective from species turnover, areas of endemism, and climatic niches. International Journal of Plant Sciences 176:222–231.
- Rzedowski, J. 1978. Vegetación de México. Limusa, México.
- Simon, E. 1892. Histoire naturelle des araignées. Paris.
- Simon, E. 1898. Histoire naturelle des araignées. Paris 2.
- Spagna, J. & R.G. Gillespie. 2008. More data, fewer shifts: molecular insights into the evolution of the spinning apparatus in non-orb-weaving spiders. Molecular Phylogenetics and Evolution 46:347–368.
- Spagna, J.C., S.C. Crews & R.G. Gillespie. 2010. Patterns of habitat affinity and Austral/Holarctic parallelism in diutynoid spiders (Araneae: Entelegynae). Invertebrate Systematics 24:238–257.
- Stratton, G.E. & G.W. Uetz. 1983. Communication via substratum-coupled stridulation and reproductive isolation in wolf spiders (Araneae: Lycosidae). Animal Behavior 31:164–172.
- Suguro, T. 2015. New data of *Hahnina* (Araneae: Hahniidae) in Japan, with a description of a new species. Acta Arachnologica 64:11–15.
- Thorell, T. 1894. Förteckning öfver arachnider från Java och närgränsande öar, insamlade af Carl Aurivillius; jemte beskrifningar å några sydasiatiska och sydamerikanska spindlar. Bihang till Kungliga Svenska Vetenskaps-Akademiens Handlingar 20:1–63.
- Uhl, G. & D.O. Elias. 2011. Communication. Pp. 127–188. In Spider Behaviour: Flexibility and Versatility. (M. E. Herberstein, ed.). Cambridge University Press, Cambridge.
- Wheeler, W.C., J.A. Coddington, L.M. Crowley, D. Dimitrov, P.A. Goloboff, C.E. Griswold, et al. 2016. The spider tree of life: Phylogeny of Araneae based on target-gene analyses from an extensive taxon sampling. Cladistics doi: 10.1111/cla.12182.
- World Spider Catalog. 2017. World Spider Catalog. Version 17. Natural History Museum, Bern. Online at <http://wsc.nmbe.ch/>
- Zavala-Chávez, F. 2007. Guía de los encinos de la Sierra de Tepotzotlán, México. Universidad Autónoma de Chapingo, Chapingo, México.
- Zhang, F. & C. Zhang. 2003. On two newly recorded species of the spider from China (Araneae: Salticidae, Hahniidae). Journal of Hebei University (Natural Science Edition) 23:51–54.
- Zhang, Z.S., S.Q. Li & G. Zheng. 2011. Comb-tailed spiders from Xishuangbanna, Yunnan Province, China (Araneae, Hahniidae). Zootaxa 2912:1–27.
- Zhang, Z.S. & Y.G. Zhang. 2013. Synonymy and misidentification of three *Hahnina* species (Araneae: Hahniidae) from China. Zootaxa 3682:521–533.
- Zhang, Z.S., S. Li & D.S. Pham. 2013. First description of comb-tailed spiders (Araneae: Hahniidae) from Vietnam. Zootaxa 3613:343–356.

Manuscript received 2 December 2016, revised 12 March 2017.



# Systematics of the spiny trapdoor spiders of the genus *Cataxia* (Mygalomorphae: Idiopidae) from south-western Australia: documenting a threatened fauna in a sky-island landscape

Michael G. Rix<sup>1,2,3</sup>, Karlene Bain<sup>4</sup>, Barbara Y. Main<sup>4</sup>, Robert J. Raven<sup>1</sup>, Andrew D. Austin<sup>2</sup>, Steven J. B. Cooper<sup>5,2</sup> and Mark S. Harvey<sup>3,4,6</sup>: <sup>1</sup>Biodiversity and Geosciences Program, Queensland Museum, South Brisbane, Queensland 4101, Australia. E-mail: michael.rix@qm.qld.gov.au; <sup>2</sup>Australian Centre for Evolutionary Biology and Biodiversity, School of Biological Sciences, The University of Adelaide, Adelaide, South Australia 5005, Australia; <sup>3</sup>Department of Terrestrial Zoology, Western Australian Museum, Welshpool, Western Australia 6106, Australia; <sup>4</sup>School of Animal Biology, The University of Western Australia, Crawley, Western Australia 6009, Australia; <sup>5</sup>Evolutionary Biology Unit, South Australian Museum, Adelaide, South Australia 5005, Australia; <sup>6</sup>School of Natural Sciences, Edith Cowan University, Joondalup, Western Australia 6027, Australia

**Abstract.** The spiny trapdoor spiders (Idiopidae) of the *Cataxia bolganupensis*-group from south-western Australia are revised, and six species are re-recognized: *C. barrettae* sp. nov., *C. bolganupensis* (Main, 1985), *C. colesi* sp. nov., *C. melindae* sp. nov., *C. sandorum* sp. nov. and *C. stirlingi* (Main, 1985). All species exhibit extreme short-range endemism, with allopatric sky-island distributions in mesic montane habitats of the Stirling Range, Porongurup Range and Mount Manypeaks. A molecular phylogenetic analysis of mitochondrial cytochrome *c* oxidase subunit I (*COI*) and cytochrome *b* (*CYB*) sequences complements the morphological taxonomy, along with a key to species and detailed information on their distributions and habitat preferences. All six species are assessed as ‘endangered’ using IUCN criteria, with the major threatening processes being the spread of the plant pathogenic fungus *Phytophthora* (causing dieback), climate change and inappropriate fire regimes.

**Keywords:** Taxonomy, new species, mesic zone, biodiversity hotspot, biogeography

ZooBank publication: <http://zoobank.org/?lsid=urn:lsid:zoobank.org:pub:0F9FBAE7-841C-4758-BBF8-6F447E375219>

The spiny trapdoor spiders of the *Cataxia bolganupensis*-group (Figs. 1–9) are an iconic component of south-western Australia’s mygalomorph spider fauna, recognized for their unusual ‘sky-island’ biogeography (see Hedin et al. 2015), habitat specificity and highly restricted distributions, i.e., short-range endemism (Main 1993b; Barrett & Yates 2015; Rix et al. 2015). Found only in temperate montane habitats of the Stirling Range, Porongurup Range and Mount Manypeaks, in Western Australia’s Great Southern Region north and east of Albany (Figs. 10, 14–17), these spiders have been the subject of ongoing ecological study and taxonomic comparison since Main (1985) described the first two species. Detailed survey work in the intervening years has clarified the discrete, highly localized and markedly allopatric distributions of each of these described species, and revealed populations of four additional undescribed species in surrounding mountainous areas (Figs. 10–16). Together, these six species form a monophyletic (Rix et al. 2017a; Fig. 17) and morphologically distinctive assemblage, now restricted to just a handful of mesic upland habitats in the south-western Australian biodiversity hotspot (Rix et al. 2015, 2017c).

The first and only previously described species in the *bolganupensis*-group of *Cataxia* Rainbow, 1914 – *C. bolganupensis* (Main, 1985) and *C. stirlingi* (Main, 1985) (Figs. 1, 4) – were both originally placed in the genus *Neohomogona* Main, 1985, the identity of which vacillated for a number of years. Raven (1985), in an addendum following the publication of Main (1985), first synonymized *Neohomogona* with *Cataxia*, noting what were interpreted as diagnostic autapomorphies in the former, such as the reduction or absence of posterior

median spinnerets. Main (1993a) then re-erected *Neohomogona*, although Raven’s (1985) synonymy was later upheld by Rix et al. (2017c), following a detailed molecular phylogenetic analysis of Australian Idiopidae (Rix et al. 2017a). While the *bolganupensis*-group of *Cataxia*, synonymous with Main’s (1985, 1993a) concept of *Neohomogona* (= *Cataxia*), is almost certainly reciprocally monophyletic relative to other Cataxiini, the genus *Cataxia* (*sensu* Rix et al. 2017c) is overall a relatively homogeneous assemblage of species, most of which occur in the mesic zone of eastern Australia, and all of which are united in a single crown-group lineage (Rix et al. 2017a). Western Australian taxa in the *bolganupensis*-group are, however, unusual in having lost the posterior median spinnerets (Figs. 45, 67), and in having lost any semblance of burrow door-building behavior. Indeed, all Western Australian species build ornate, open-holed palisade burrows, which they usually adorn with a radial skirt of leaves, twigs and other debris (Figs. 7–9). To the trained eye these distinctive burrows are useful markers for detecting the presence or otherwise of spiders in suitable habitats.

The aims of this revision are thus two-fold. Firstly, we describe the known species of *Cataxia* from Western Australia using morphological and complementary molecular criteria, thus adding another fully revised lineage to a growing list of well-documented arachnid and myriapod taxa with short-range endemic sky-island distributions in the same montane areas (e.g., see Rix et al. 2009; Edward & Harvey 2010; Cooper et al. 2011; Rix & Harvey 2012a, b; Harvey et al. 2015; Rix et al. 2015). Secondly, we assess the conservation status of this potentially threatened fauna using IUCN criteria, as per





Figures 1–9.—Images of live specimens and burrows of *Cataxia* of the *bolganupensis*-group from south-western Australia: 1, female *C. bolganupensis* (Main) from Porongurup National Park; 2, female *C. colesi* sp. nov. from Toolbrunup Peak, Stirling Range National Park; 3, female *C. sandsorum* sp. nov. from south face of Pyungoorup Peak, Stirling Range National Park (missing left pedipalp); 4, *C. stirlingi* (Main) from Bluff Knoll, Stirling Range National Park; 5, female *C. barrettiae* sp. nov. from Mondurup Peak, Stirling Range National Park; 6, male *C. barrettiae* sp. nov. from Talyuberlup Peak, Stirling Range National Park; 7, burrow of *C. stirlingi* (Main) from Bluff Knoll, Stirling Range National Park; 8, burrow of *C. sandsorum* sp. nov. from south face of Pyungoorup Peak, Stirling Range National Park; 9, burrow of *C. barrettiae* sp. nov. from Talyuberlup Peak, Stirling Range National Park. Images by M. Harvey.

Harvey et al. (2015). South-western Western Australia is a highly diverse yet threatened biodiversity hotspot (Myers et al. 2000; Rix et al. 2015), and conservation considerations are necessarily central to any synopsis of the region's remarkable biota, including trapdoor spiders (Rix et al. 2017b). Six species of south-western Australian *Cataxia* are recognized in this study, taking the total number of described species in the genus to 15.

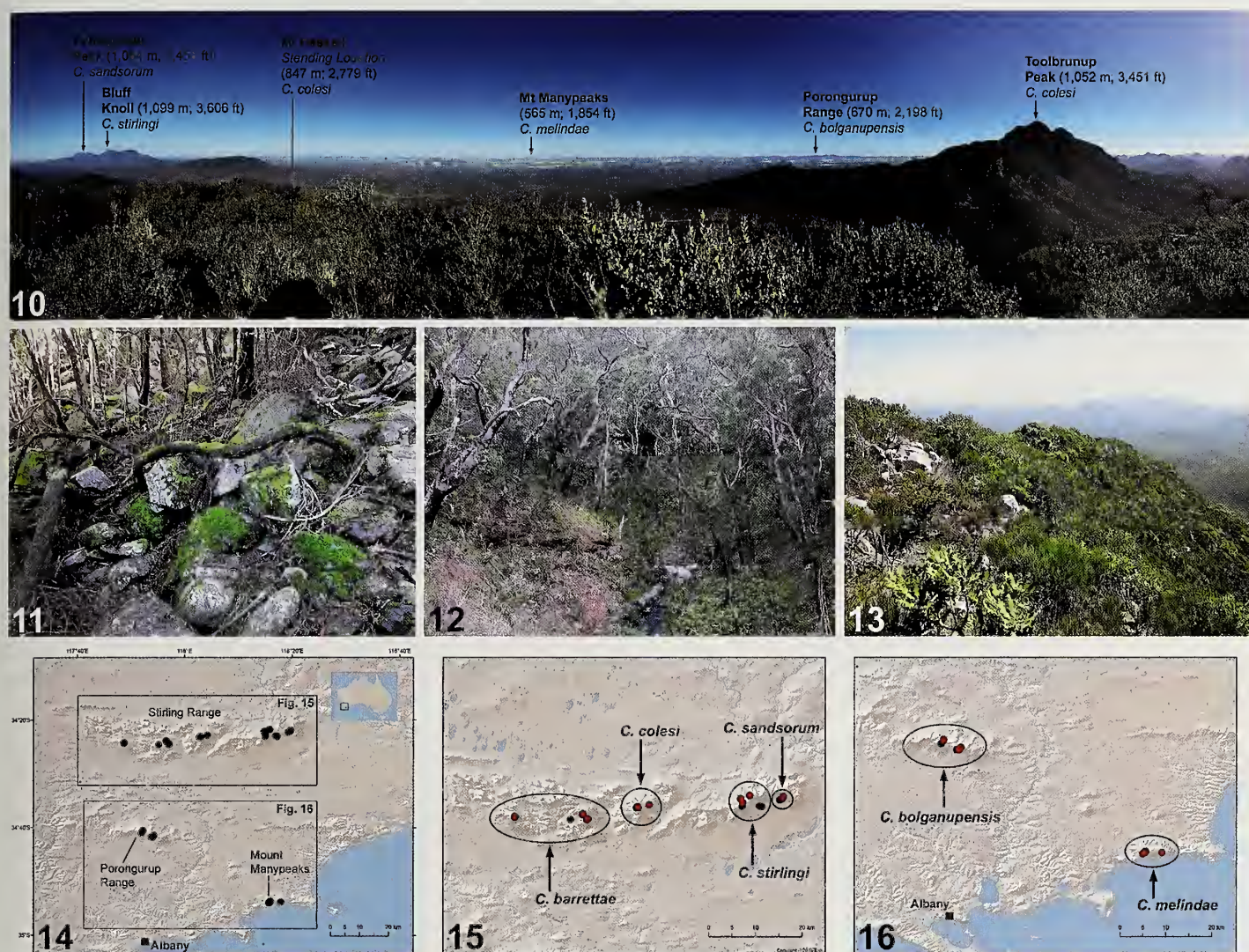
## METHODS

**Species concepts.**—The species concepts applied in this paper are unified (de Queiroz 2007) and integrative, combining morphological autapomorphy with molecular monophyly as assessed using a mitochondrial barcoding approach. These molecular data thus complement the morphological synopsis,

and are included: (1) to test the congruence between morphological data and mitochondrial genetic signal; and (2) to provide diagnostic molecular autapomorphies, numbered according to standard sequences. The data are not intended to explore the phylogenetic relationships among species, or the phylogeography of included lineages; these analyses will be conducted in a forthcoming multi-locus treatment. Cytochrome *c* oxidase subunit I (*COI*) and cytochrome *b* (*CYB*) reference sequences for the numbering of nucleotides in diagnoses are derived from a specimen of *C. bolganupensis* (WAM T131631), as follows: *COI* (658 bp, GenBank accession number KY295345); *CYB* (686 bp, GenBank accession number KY295466).

**Morphological methods.**—Morphological methods, including the format of species descriptions, follow Rix et al. (2017c). Specimens were examined using a Zeiss Stemi SV11 stereomicroscope.





Figures 10–16.—Habitats and distributions of *Cataxia* of the *bolganupensis*-group: 10, panoramic image showing almost the entire distribution of *Cataxia* in south-western Australia (excluding only the range of *C. barrettiae* sp. nov. on Talyuberlup Peak, Mount Magog and Mondurup Peak), taken in an easterly (left) to south-westerly (right) arc from the summit of Mount Hassell, Stirling Range National Park (SRNP); 11, mesic closed woodland habitat of *C. colesi* sp. nov. on the southern slope of Toolbrunup Peak (SRNP); 12, riparian habitat of *C. sandsorum* sp. nov. on the south face of Pyungoorup Peak (SRNP); 13, montane heathland habitat of *C. barrettiae* sp. nov. on the summit of Mondurup Peak (SRNP); 14–16, maps showing collection records of *Cataxia* from south-western Australia; red dots denote specimens sequenced for the molecular analyses. See inset map in Fig. 14 for the location of the mapped area relative to the rest of Australia. Images (10, 13) by M. Harvey; images (11–12) by M. Rix.

croscopie, and female genitalia were cleared in 100% lactic acid at room temperature. Measurements (in millimetres, to one decimal place) and digital automontage images were taken using a Leica M165C stereomicroscope with mounted DFC425 digital camera, and processed using Leica Application Suite Version 3.7 software. Species are presented in this paper in alphabetical order. Leg segments were measured along the dorsal prolateral edge, in prolateral view. Total body length measurements include the chelicerae, in dorsal view. Eleven (of 12) available male specimens of *Cataxia* from south-western Australia were illustrated for this study, either within the primary numbered plates or, for additional specimens, as an ‘Atlas’ series of more rapidly assembled single-shot images in four standard views (see Supplementary File 1, online at <http://dx.doi.org/10.1636/JoA-S-17-012.S1>).

The latter are included for ease of comparison to the type specimens, to directly illustrate the subtle morphological variation in key characters typical of Mygalomorphae, and to provide a digital record of the specimens available in collections.

Specimens are lodged at the Western Australian Museum, Perth (WAM), either in the primary registered collection, or in the former personal collection of one of us (WAM BYM Collection). The following abbreviations are used throughout the text: ALE, anterior lateral eye/s; AME, anterior median eye/s; *COI*, cytochrome *c* oxidase subunit I; *CYB*, cytochrome *b*; IBRA, Interim Biogeographic Regionalisation of Australia Version 7 (online at <https://www.environment.gov.au/land/nrs/science/ibra>; accessed May 2017); PLE, posterior lateral eye/s; PME, posterior median eye/s; PMS, posterior median



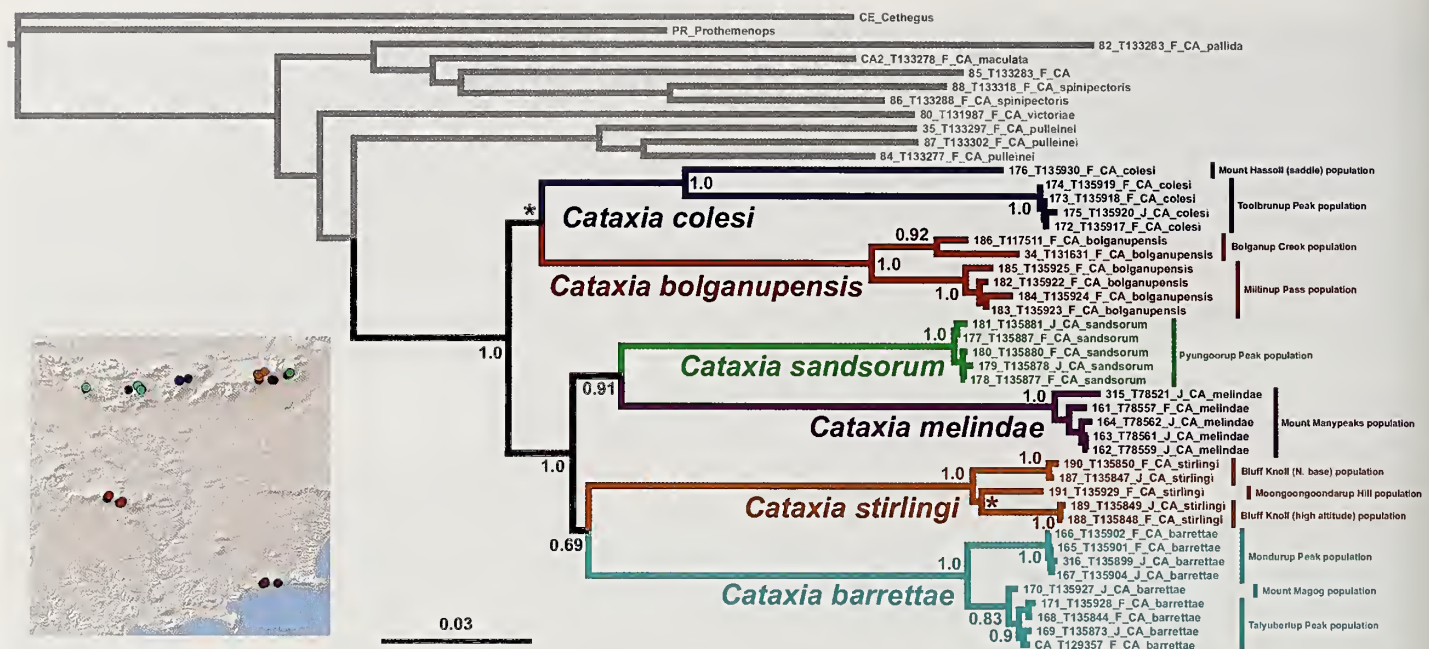


Figure 17.—Tamura-Nei neighbour-joining tree of concatenated *COI* (658 bp) and *CYB* (686 bp) data for 35 specimens of *Cataxia* in the *bolganupensis*-group, color-coded and annotated according to species designation and distribution (see inset map). Posterior probabilities resulting from a partitioned Bayesian analysis of the same dataset are shown at each major node; two highlighted (\*) clades were not recovered in the Bayesian 50% majority-rule consensus tree. See inset map in Figure 14 for the location of the mapped area relative to the rest of Australia.

spinnerets; RTA, retrolateral tibial apophysis (of male pedipalp).

**Molecular methods.**—Mitochondrial *COI* and *CYB* sequences were generated for 35 specimens of *Cataxia* in the *bolganupensis*-group, using a next-generation parallel tagged amplicon sequencing (TAS) approach, described in detail by Rix et al. (2017a). For each specimen sequenced, DNA voucher codes and GenBank accession numbers are provided next to repository registration numbers in the material examined section for each species (below), in the form: [DNA\_Voucher\_Code; GB\_COI\_No.; GB\_CYB\_No.]. Outgroup sequences were obtained from data previously published by Rix et al. (2017a). The ultimate outgroup for the molecular analyses was the diplurid spider *Cethegus fugax* (Simon, 1908). Other outgroups included several species of Idiopidae, including an undescribed species of *Prothemenops* Schwendinger, 1991, and nine of the 10 non-*bolganupensis*-group *Cataxiini* sequenced by Rix et al. (2017a). In total, mitochondrial sequences were analyzed for 46 specimens (Supplementary File 2, online at <http://dx.doi.org/10.1636/JoA-S-17-012.S2>).

Alignments for both the *COI* (658 bp) and *CYB* (686 bp) datasets were conducted in Geneious R6 (Biomatters Ltd.; online at <http://www.geneious.com/>; accessed May 2017), using the MAFFT v7.017 plugin with default parameters. For the resulting concatenated (1,344 bp; no indels) dataset (see Supplementary File 2, online at <http://dx.doi.org/10.1636/JoA-S-17-012.S2>), Geneious R6 was used to generate a neighbor-joining tree using a Tamura-Nei genetic distance model, and uncorrected pairwise distance comparisons were calculated in MEGA v6.06 (Tamura et al. 2013). Prior to Bayesian analysis, PartitionFinder Version 1.1.1 (Lanfear et

al. 2012) was used to simultaneously choose an optimal partitioning scheme and appropriate models of nucleotide substitution, favoring a four-partition model (i.e., TVM+G for *COI*+*CYB* codon position one [cp1]; TrN+I+G for *COI*+*CYB* cp3; TVM+G for *COI* cp2; and HKY+G for *CYB* cp2). These partitions were then analyzed in MrBayes Version 3.1.2 (Huelsenbeck & Ronquist 2001; Ronquist & Huelsenbeck 2003), with substitution model parameters estimated independently for each partition ([Unlink tratio = (all) pinvar=(all) shape=(all) statefreq=(all) revmat=(all)]) and rates allowed to vary across partitions ([Prset applyto=(all) ratepr=variable]). Four Markov Chain Monte Carlo (MCMC) chains were run for 10 million generations, sampling every 1000 generations, with the first 10% of sampled trees discarded as 'burnin' ([burnin = 1000]). Summary statistics of estimated parameters, including ESS values, were assessed using Tracer Version 1.6 (Rambaut et al. 2014), and FigTree Version 1.4.2 (online at <http://tree.bio.ed.ac.uk/software/figtree/>; accessed May 2017) was used to visualise a 50% majority-rule consensus tree of the post-burnin sample.

**Conservation assessments.**—The conservation of Australian trapdoor spiders may be an issue of national significance (Rix et al. 2017b), and the conservation status of each species of *Cataxia* from south-western Australia was assessed using a standard International Union for the Conservation of Nature (IUCN) approach, similar to that applied by Harvey et al. (2015) for migid trapdoor spiders of the genus *Bertmainius* Harvey, Main, Rix & Cooper, 2015. As long-term data on population reductions (Criterion A), population sizes or declines (Criterion C) or the number of mature individuals in any one population (Criterion D) were not available, we assessed all taxa using information on their



geographic range (Criterion B). These assessments therefore focused on the extent of occurrence of each species, the area of occupancy within that range, and the health or otherwise of occupied habitats. Individual assessments are listed for each species under their relevant entry in the Taxonomy section (below).

## RESULTS AND DISCUSSION

**Molecular analyses.**—Bayesian analysis of the concatenated *COI* and *CYB* data recovered six major clades, each concordant with the morphological species hypotheses presented below; these results are presented on a single neighbor-joining tree (Fig. 17) for ease of pairwise distance comparison. Mean intra-specific pairwise divergence distances for the concatenated dataset ranged from 4.8% in *C. colesi* sp. nov., to between 0.3% and 3.0% in *C. sandsorum* sp. nov. and *C. bolganupensis*, respectively. Mean inter-specific pairwise distances varied from 14.2% between *C. melindae* sp. nov. and *C. sandsorum* sp. nov., to 18.3% between *C. bolganupensis* and *C. stirlingi*. Pairwise divergences for *COI* and *CYB* were each largely proportional to the concatenated dataset, with *CYB* contributing a slightly higher rate relative to *COI*, as follows: *COI* (mean intra-specific = 0% – 4.2%; mean inter-specific = 10.6% – 16.3%); *CYB* (mean intra-specific = 0.6% – 5.5%; mean inter-specific = 16.2% – 22.8%). Summary pairwise distance matrices for all three datasets are presented in Supplementary File 3 (online at <http://dx.doi.org/10.1636/JoA-S-17-012.S3>).

Mitochondrial genetic structure was evident between all major populations (Fig. 17), including within seemingly homogeneous habitats (e.g., in *C. bolganupensis* in the Porongurup National Park). Similarly, in the Toolbrunup-Hassell uplands, populations of *C. colesi* sp. nov. on Toolbrunup Peak and the Mount Hassell saddle showed deep mitochondrial genetic divergence. These data, while clearly preliminary in the absence of nuclear markers, are consistent with the disjunct nature of individual populations in the field, and highlight potential barriers to effective dispersal (at least of females) in these complex montane environments.

**Conservation assessments.**—All six species of western Australian *Cataxia* were assessed as threatened using IUCN criteria, even conservatively applying Criteria B1 and B2. The total of area of occupancy (Criterion B2) of each species is not more than 10 km<sup>2</sup>, and usually significantly less. For example, on Mondurup Peak in the western Stirling Range National Park, surveys have revealed that the single local population of *C. barrettae* sp. nov. is restricted to just a 50 m zone of altitude on the summit of the mountain, above ca. 770 m (M. Rix, M. Harvey, pers. obs.). This represents a total area of occupancy at this site of no more than 10 hectares. Together, these geographic occurrence data reveal just how localized populations of *Cataxia* are in the sky-island landscapes of the Great Southern Region, and we consider our current knowledge to be accurate given the decades of dedicated survey work that has been undertaken by various workers throughout the area.

The final conservation consideration in each case, in addition to criteria B1 and B2a, was therefore related to assessing any decline in the area, extent and/or quality of habitat (Criterion B2b[iii]). Severe habitat declines due to

*Phytophthora* – a pathogenic fungus causing plant dieback (Shearer et al. 2004) – are a major concern in the Great Southern Region of south-western Australia, as are inappropriate fire regimes in sensitive montane habitats, and a potential increase in the frequency and/or intensity of wildfires due to climate change (see Barrett & Yates 2015 for a detailed summary of these issues in the Stirling Range National Park; and Laurance et al. 2011 for a summary of risks to the Mediterranean-climate ecosystems of south-western Australia more generally). *Cataxia* are susceptible to wildfires in the short term (Main 1993b), and entirely dependent upon mesic, sheltered microhabitats in the long term; these documented habitat changes and future risks clearly qualify for listing under Criterion B2b[iii]. As a result, all six species were assessed as: B1, B2a, b[iii] ('endangered'). Some species, such as *C. sandsorum* sp. nov., may be realistically assessed as 'critically endangered' in the near future, if habitat degradation in the eastern Stirling Range continues (see Barrett & Yates 2015).

## TAXONOMY

**Family Idiopidae** Simon, 1889  
**Subfamily Arbanitinae** Simon, 1903  
**Tribe Cataxiini** Rainbow, 1914  
**Genus *Cataxia*** Rainbow, 1914

*Cataxia* Rainbow, 1914: 222.

*Homogona* Rainbow, 1914: 189. Type species *H. pulleinei* Rainbow, 1914, by monotypy (synonymized by Raven, 1985: 154 *contra* Main, 1993a: 600).

*Neohomogona* Main, 1985: 42. Type species *N. bolganupensis* Main, 1985, by original designation (synonymized by Raven, 1985: 175 *contra* Main, 1993a: 600)

**Type species.**—*Cataxia maculata* Rainbow, 1914, by monotypy.

**Diagnosis.**—Species of *Cataxia* can be distinguished from other Arbanitinae by the presence of a non-hirsute, glabrous carapace, combined with the absence of leg scopulae on females, and the absence of scopulae on the anterior leg metatarsi of males (Rix et al. 2017c).

**Distribution.**—The genus *Cataxia* has been recorded from extreme south-western Australia and eastern mainland Australia, from the Wet Tropics (Queensland) south to western Victoria. *Cataxia* are absent from Tasmania, South Australia and the central arid zone (Rix et al. 2017c).

**Composition and remarks.**—The genus *Cataxia* includes 15 described species: *C. babindaensis* Main, 1969, *C. barrettae* sp. nov., *C. bolganupensis* (Main, 1985), *C. colesi* sp. nov., *C. cunicularis* (Main, 1983), *C. dietrichae* Main, 1985, *C. eungellaensis* Main, 1969, *C. maculata* Rainbow, 1914, *C. melindae* sp. nov., *C. pallida* (Rainbow & Pulleine, 1918), *C. pulleinei* (Rainbow, 1914), *C. sandsorum* sp. nov., *C. spinipectoris* Main, 1969, *C. stirlingi* (Main, 1985) and *C. victoriae* (Main, 1985). Numerous undescribed species are also known from mesic habitats in eastern Australia, especially the rainforests of eastern Queensland (Rix et al. 2017c).



THE *BOLGANUPENSIS*-GROUP

The *bolganupensis*-group comprises six species of *Cataxia*, all endemic to the Great Southern Region of south-western Western Australia (Fig. 14). Together they form a reciprocally monophyletic assemblage, relative to the *maculata*-group and the

*pulleinei*-group (previously *Homogona* Rainbow, 1914 = *Cataxia*) (Rix et al. 2017a, c). They can be distinguished from other species of *Cataxia* by the reduction or absence of posterior median spinnerets (Figs. 45, 67), and by the unique morphology of their ornate, open-holed, palisade burrows (Figs. 7–9).

KEY TO THE SPECIES OF *CATAXIA* FROM SOUTH-WESTERN WESTERN AUSTRALIA

NB. Distributions are included, as follows: PNP, Porongurup National Park; SRNP, Stirling Range National Park; MMNR, Mount Manypeaks Nature Reserve (Fig. 14).

1. Males ..... 2
- Females ..... 7
2. Tibia of leg I with pair of opposing prolateral clasping spurs (Figs. 48, 70, 92, 114) ..... 3
- Tibia of leg I without pair of prolateral clasping spurs (Figs. 26, 135) ..... 6
3. Lateral margins of carapace sharply indented between level of coxae II and III (Fig. 105); cheliceral paturons each with pair of deep concave depressions (Fig. 107) ..... *C. sandsorum* sp. nov. (SRNP)
- Carapace without lateral indentations; chelicerae unmodified. .... 4
4. Pedipalpal tibia relatively long, ~2.0 x longer than wide (Figs. 49, 71) ..... 5
- Pedipalpal tibia relatively stout, ~1.7 x longer than wide (Fig. 93) ..... *C. melindae* sp. nov. (MMNR)
5. RTA with relatively dense field of spinules, largely restricted to antero-dorsal surface of RTA (Figs. 49, 50); spinules on curved retro-ventral margin of palpal tibia small and irregularly-arranged (Figs. 49, 50) ..... *C. bolganupensis* (Main, 1985) (PNP)
- RTA with relatively sparse field of spinules, extending onto retrolateral surface of RTA (Figs. 71, 72); spinules on curved retro-ventral margin of palpal tibia larger and more uniformly arranged between RTA and distal retrolateral tibial apophysis (Figs. 71, 72) ..... *C. colesi* sp. nov. (SRNP)
6. RTA short, stout and broadly rounded distally in retrolateral view (Fig. 136); pair of macrosetae on distal margin of prolateral tibia I relatively long and thin, not markedly differentiated from other spine-like setae on tibia (Fig. 135).... *C. stirlingi* (Main, 1985) (SRNP)
- RTA proportionally longer and more pointed distally in retrolateral view (Fig. 27); pair of macrosetae on distal margin of prolateral tibia I shorter, more strongly developed and clearly differentiated from other spine-like setae on tibia (Fig. 26)..... *C. barrettiae* sp. nov. (SRNP)
7. Sternum short, sub-circular or subquadrate in ventral view, almost as wide as long (Fig. 101)... *C. melindae* sp. nov. (MMNR)
- Sternum clearly longer than wide, rectangular or oval in ventral view (Figs. 35, 57, 79, 123, 144) ..... 8
8. Ventral tibia I with row of at least 5 porrect, spine-like macrosetae (Figs. 58, 59)... *C. bolganupensis* (Main, 1985) (PNP)
- Ventral tibia I with no more than 4 porrect spine-like macrosetae (Figs. 36, 37, 80, 81, 124, 125, 145, 146)..... 9
9. Labium with sparse field of spinules posteriorly (Figs. 34, 143)..... *C. barrettiae* sp. nov. (SRNP) and *C. stirlingi* (Main, 1985) (SRNP)\*
- Labium without field of spinules (Figs. 78, 122)..... 10
10. Posterior eye row as wide as or wider than anterior eye row (Fig. 77); pars cephalica with relatively low profile in lateral view (Fig. 76) ..... *C. colesi* sp. nov. (SRNP)
- Anterior eye row marginally broader than posterior eye row (Fig. 121); pars cephalica with relatively high profile in lateral view (Fig. 120) ..... *C. sandsorum* sp. nov. (SRNP)

\*By our assessment, females of *C. barrettiae* and *C. stirlingi* appear to be indistinguishable morphologically; males or molecular data are required for accurate identification.

*Cataxia barrettiae* Rix, Bain, Main & Harvey, sp. nov.

<http://zoobank.org/?lsid=urn:lsid:zoobank.org:act:7E916DCC-1C89-465A-86E9-90132B1EE881>

org:act:7E916DCC-1C89-465A-86E9-90132B1EE881  
(Figs. 5–6, 9, 15, 18–38)

*Neohomogona stirlingi* Main, 1985: 47 (in part; male specimens likely mislabeled as from “Mount Hassell”).

*Cataxia* sp. ‘T129357’ Rix et al., 2017a: 304 (molecular exemplar specimen with taxon code ‘CA’); Rix et al., 2017c: 622, fig. 266.

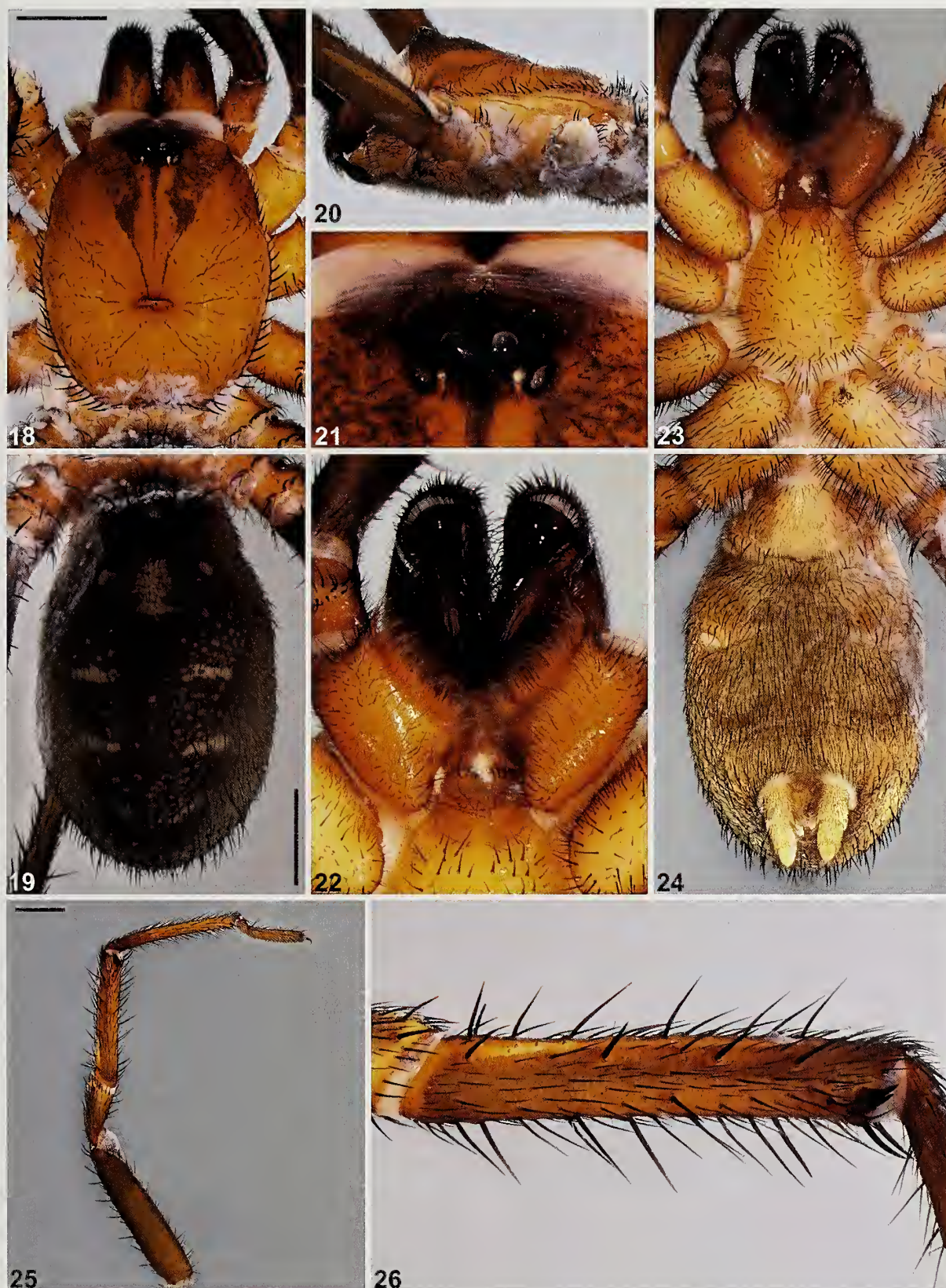
**Type material.**—*Holotype male*. AUSTRALIA: *Western Australia*: Stirling Range National Park, Talyuberlup Peak, track to summit (IBRA\_ESP), 34°24'28"S, 117°57'10"E, 15

April 2015, dug from burrow [and molted to maturity November 2015], 589 m, M.G. Rix, M.S. Harvey (WAM T135872).

**Paratype.** AUSTRALIA: *Western Australia*: 1 ♀, same data as holotype except 34°24'28"S, 117°57'11"E, 14 April 2015, dug from burrow, 555 m, M.G. Rix, M.S. Harvey, N.J. Tarnatic, A. Coles (WAM T135844, DNA\_Voucher\_168, GB\_COI\_KY485321, GB\_CYB\_KY485354).

**Other material examined.**—AUSTRALIA: *Western Australia*: 1 ♀, Stirling Range National Park, Talyuberlup Peak (IBRA\_ESP), 34°24'34"S, 117°57'05"E, 13 December 2014, dug from burrow, K. Bain (WAM T135928, DNA\_Voucher\_171, GB\_COI\_KY485320, GB\_CYB\_KY485353); 1 juve-





Figures 18–26.—*Cataxia barrettiae* sp. nov., male holotype (WAM T135872), somatic morphology: 18–19, carapace and abdomen, dorsal view; 20, cephalothorax, lateral view; 21, eyes, dorsal view; 22, mouthparts, ventral view; 23–24, cephalothorax and abdomen, ventral view; 25, leg I, prolateral view; 26, leg I tibia, prolateral view. Scale bars = 2.0.





Figures 27–29.—*Cataxia barrettiae* sp. nov., male holotype (WAM T135872), pedipalp: 27, retrolateral view; 28, retro-ventral view; 29, prolateral view. Scale bar = 2.0.

nile, same data except track to summit, 34°24'28"S, 117°57'10"E, 15 April 2015, 589 m, M.G. Rix, M.S. Harvey (WAM T135873, DNA\_Voucher\_169, GB\_CO1\_KY485322, GB\_CYB\_KY485355); 1 ♀ [in fragments following RNA preservation], same data except 34°24'29"S, 117°57'11"E, 14 February 2013, hand collected in montane heathland, 567 m, M.G. Rix, S.E. Harrison (WAM T129357, DNA\_Voucher\_CA, GB\_CO1\_KY295229, GB\_CYB\_KY295356); 1 juvenile, same data (WAM T129358); 1 juvenile, same data (WAM T135352); 1 juvenile [in fragments following RNA preservation], same data (WAM T135353); 1 juvenile, same data except walking track near summit, 34°24'27"S, 117°57'10"E, dug from burrow, 583 m, M.S. Harvey, M.E. Blofelds, F. Harvey, E. Harvey (WAM T136803); 1 juvenile, Stirling Range National Park, Mount Magog (IBRA\_ESP), 34°23'52"S, 117°56'36"E, 14 December 2014, dug from burrow, K. Bain (WAM T135927, DNA\_Voucher\_170, GB\_CO1\_KY485323, GB\_CYB\_KY485356); 1 juvenile, same data except 34°23'59"S, 117°56'35"E, 24 April – 3 September 1996, wet pitfall, J.M. Waldock, B.Y. Main (WAM T42314); 2 ♀, Stirling Range National Park, Mt Magog picnic site (IBRA\_ESP), 34°24'32"S, 117°55'12"E, 24 April 1996, M.S. Harvey, J.M. Waldock, B.Y. Main (WAM T132546); 1 ♂, Stirling Range National Park, Mondurup Peak, Site 217 (IBRA\_ESP), 34°24'18"S, 117°48'44"E, 16 June 1996, wet pitfall trap, 775 m, S. Barrett (WAM T130329); 1 ♂, same data except Site 218, 34°24'18"S, 117°48'45"E, 770 m (WAM T130331); 1 ♂, same data (WAM T130332); 5 juveniles, same data (WAM T130330); 1 ♀, 1 juvenile, same data (WAM T130333); 1 juvenile, same data except 34°24'11"S, 117°48'47"E, dug from burrow in heathland on summit, 769 m, M.G. Rix, M.S. Harvey, N.J. Tatarnic (WAM T135899, DNA\_Voucher\_316, GB\_CO1\_KY485324, GB\_CYB\_KY485357); 1 juvenile,

same data except 34°24'11"S, 117°48'46"E, 770 m (WAM T135904, DNA\_Voucher\_167, GB\_CO1\_KY485327, GB\_CYB\_KY485360); 1 ♀, same data except 34°24'10"S, 117°48'45"E, 779 m (WAM T135902, DNA\_Voucher\_166, GB\_CO1\_KY485325, GB\_CYB\_KY485358); 1 ♀, same data (WAM T135901, DNA\_Voucher\_165, GB\_CO1\_KY485326, GB\_CYB\_KY485359); 1 juvenile, same data (WAM T135903); 1 ♂, "Mount Hassell" (but likely mislabeled; see below), 4 April 1957, A.R. Main (WAM T143031); 1 ♂, same data (WAM T143032).

**Etymology.**—The specific epithet is named in honor of Sarah Barrett, whose pioneering survey work in high altitude habitats of the Great Southern Region resulted in the collection of many important specimens of *Cataxia*, including the only males of this species known from Mondurup Peak.

**Diagnosis.**—Males of *Cataxia barrettiae* can be distinguished from those of *C. bolganupensis*, *C. colesi*, *C. melindae* and *C. sandsorum* by the absence of prolateral clasp spurs on the leg I tibia (Fig. 26; cf. Figs. 47, 48); and from *C. stirlingi* by the longer, more distally pointed RTA (Fig. 27; cf. Fig. 136), and by the more strongly developed macrosetae on the distal prolateral tibia I (Fig. 26; cf. Fig. 135). Females of this species can be distinguished from those of *C. melindae* by the shape of the sternum, which is proportionally longer (Fig. 35; cf. Fig. 101); from *C. bolganupensis* by the less spinose morphology of the leg I tibia (which has no more than 4 porrect, ventral spine-like macrosetae) (Figs. 36, 37; cf. Figs. 58, 59); and from *C. colesi* and *C. sandsorum* by the presence of a sparse field of spinules on the posterior labium (Fig. 34; cf. Figs. 78, 122). By our assessment, females of this species appear to be morphologically indistinguishable from those of *C. stirlingi*.

Males, females and juveniles of this species can also be distinguished from all other species in the *bolganupensis*-group





Figures 30–38.—*Cataxia barrettiae* sp. nov., female paratype (WAM T135844): 30–31, carapace and abdomen, dorsal view; 32, cephalothorax, lateral view; 33, eyes, dorsal view; 34, mouthparts, ventral view; 35, cephalothorax, ventral view; 36, leg I, prolateral view; 37, leg I, retrolateral view; 38, spermathecae, dorsal view. Scale bars = 2.0 (30–31, 36–37), 0.5 (38).

by the following 39 unique mitochondrial nucleotide substitutions (based on nine specimens; Fig. 17): **COI**: G(11), C(49), G(121), G(175), G(181), G(208), C(212), C(238), A(244), C(266), A(316), T(373), C(385), G(458), C(459), G(460), G(481), A(514), C(574), A(619). **CYB**: C(45), C(120), C(156), G(360), A(363), G(379), G(384), G(399), G(402), T(405), C(453), A(457), G(462), C(552), A(566), C(599), A(600), A(607), C(617).

**Description (male holotype).**—Total length 16.7. Carapace 6.4 long, 5.2 wide. Abdomen 8.1 long, 5.2 wide. Carapace (Fig. 18) tan (rich red-brown in life; Fig. 6), with black ocular region

and darker brown lyra-like pattern on pars cephalica; lateral margins with uniformly-spaced fringe of porrect black setae; fovea straight. Eye group (Fig. 21) rectangular, 0.5 x as long as wide; PLE–PLE/ALE–ALE ratio 0.9; AME separated by their own diameter; PME separated by 2.6 x diameter of AME; PME and PLE separated by less than half diameter of AME, PME positioned in line with level of PLE. Maxillae and labium without cuspules (Fig. 22). Abdomen (Fig. 19) oval, dark grey-brown in dorsal view, with beige-grey mottling and prominent beige-grey sigilla spots, the latter forming four paired bands posteriorly (in dorsal view). Dorsal surface of abdomen (Fig.



19) covered with stiff, porrect black setae, each with slightly raised, dark brown sclerotic base; sclerotized sigilla absent. Legs (Figs. 25, 26) variable shades of tan (darker red-brown in life, with contrasting slate-grey femora; Fig. 6), with light scopulae on tarsi I–II; tibia I without clasping spurs but with paired prolateral macrosetae on raised distal protuberance, and adjacent proventral macroseta. Leg I: femur 6.4; patella 2.8; tibia 5.1; metatarsus 5.7; tarsus (slightly damaged) 2.7; total 22.7. Leg I femur–tarsus/carapace length ratio 3.6. Pedipalpal tibia (Figs. 27–29) 1.9 x longer than wide; RTA relatively short, rounded but somewhat conical distally, with dense field of retrolateral spinules; tibia also with long field of smaller spinules extending along curved retroventral edge (distal to base of RTA), these spinules enlarged into a row of eight macrosetae on short distal retrolateral tibial apophysis. Cymbium (Figs. 27–29) setose but without field of spinules. Embolus (Figs. 27–29) approximately 1.5 x length of bulb, gradually tapering distally without additional adornment.

**Description (female paratype, WAM T135844).**—Total length 22.7. Carapace 7.2 long, 5.5 wide. Abdomen 11.5 long, 6.7 wide. Carapace (Fig. 30) tan, with darker brown pars cephalica and mostly black ocular region; fovea straight. Eye group (Fig. 33) rectangular, 0.5 x as long as wide; PLE–PLE/ALE–ALE ratio 0.9; AME separated by slightly more than their own diameter; PME separated by 2.7 x diameter of AME; PME and PLE separated by less than half diameter of AME. PME positioned slightly anterior to level of PLE. Maxillae with field of cuspules confined to inner corner (Fig. 34); labium without cuspules but with sparse field of posterior spinules (Fig. 34). Abdomen (Fig. 31) oval, light grey-brown in dorsal view, with beige-grey mottling and prominent beige-grey sigilla spots, the latter forming four paired bands posteriorly (in dorsal view); sclerotized sigilla absent. Legs (Figs. 36, 37) variable shades of tan (darker red-brown in life, with contrasting slate-grey femora; Fig. 5); scopulae absent; tibia I with 4 porrect, ventral spine-like macrosetae; metatarsus I and tarsus I with additional rows of prolateral and ventral spine-like macrosetae. Leg I: femur 5.6; patella 3.2; tibia 3.7; metatarsus 3.1; tarsus 2.2; total 17.8. Leg I femur–tarsus/carapace length ratio 2.5. Pedipalp tan, heavily spinose on tibia and tarsus, without tarsal scopula. Genitalia (Fig. 38) with pair of anteriorly curved sac-like spermathecae, each composed of internal, sclerotized glandular chamber and membranous outer wall.

**Distribution and remarks.**—*Cataxia barrettiae* has a highly restricted distribution in the Stirling Range National Park, where it is known only from the summit of Mondurup Peak and from the adjacent Talyuberlup–Magog uplands, on Talyuberlup Peak, Mount Magog and their associated southern slopes and drainage channels (Figs. 14, 15). Two male specimens collected in 1957 and represented only by disarticulated fragments, cited in Main (1985: 47) as being from “Mount Hassell”, are likely mislabeled, as this species has never been recorded from the Toolbrunup–Hassell uplands in the intervening 60 years. The habitat is montane heathland (Fig. 13), usually above 500 m (above 770 m on Mondurup Peak), where the spiders are relatively common and locally abundant. This species builds a palisade burrow with a fully open hole and no door, which is usually adorned with a radial skirt of leaves

and twigs (Fig. 9). Based on the few specimens that have been collected, males may wander and mate in winter.

**Conservation status.**—This species has a total (maximum) extent of occurrence of less than 50 km<sup>2</sup>, and an actual area of occupancy of significantly less than 10 km<sup>2</sup>. Given that the number of well-defined locations at which the species has been found is less than five, and that there is continuing decline in the quality of habitat in the Stirling Range National Park due to *Phytophthora* dieback (Barrett & Yates 2015), climate change in south-western Australia (Indian Ocean Climate Initiative 2002; Barrett & Yates 2015), and a potential increase in the severity and/or frequency of wildfires, this species is considered to be ‘endangered’ (IUCN B1, B2a, b[iii]).

*Cataxia bolganupensis* (Main, 1985)

(Figs. 1, 16, 39–60)

*Neohomogona bolganupensis* Main, 1985: 43, figs. 158–164, 169–177, 181–186, 205, 220–222; Main, 1993a: 600.

*Cataxia bolganupensis* (Main): Raven, 1985: 175; Rix et al., 2017c: 625, figs. 259–260, 264, 270.

**Type material.**—*Holotype male*. AUSTRALIA: *Western Australia*: Porongurup National Park, track on Nancy Peak, above Bolganup Dam (IBRA\_JAF), [34°41'S, 117°52'E], 19 December 1955, hand collected [and molted into maturity April 1956], B.Y. Main (WAM T16395; examined).

**Paratypes.** AUSTRALIA: *Western Australia*: 1 ♀ (allotype), same data as holotype (WAM T16396); 1 ♀, same data (WAM T16397); 1 ♀, same data (WAM T16398); 1 ♀, same data (WAM T16399); 28 ♀ and/or juveniles, same data (WAM BYM Collection; not recently examined); 1 ♀, same data as holotype except 24 March 1956 (WAM T16401); 11 ♀ and/or juveniles, same data (WAM BYM Collection; not recently examined); 1 ♀, same data as holotype except 6 April 1957 (WAM T16402); 11 ♀ and/or juveniles, same data (WAM BYM Collection; not recently examined); 1 ♀, same data as holotype except 1 July 1957, A.R. Main (WAM T16403); 1 ♀, same data (WAM T16404); 1 ♀, same data (WAM T16405); 1 ♀, same data (WAM T16406); 11 ♀ and/or juveniles, same data (WAM BYM Collection; not recently examined).

**Other material examined.**—AUSTRALIA: *Western Australia*: 1 ♂, Porongurup National Park, S. end of Millinup Pass (IBRA\_JAF), 34°41'43"S, 117°53'51"E, 28 April – 2 September 1996, wet pitfall trap, M.S. Harvey, J.M. Waldock, B.Y. Main (WAM T95754); 1 ♀, same data except 30 March 1993, dug from burrow in karri forest, M.S. Harvey, J.M. Waldock (WAM T29940); 1 ♀, Porongurup National Park, Millinup Pass (IBRA\_JAF), 34°41'44"S, 117°54'03"E, 21 April 2015, dug from burrow in karri forest, 286 m, M.G. Rix, M.S. Harvey, N.J. Tataranic (WAM T135924, DNA\_Voucher\_184, GB\_CO1\_KY485335, GB\_CYB\_KY485368); 1 ♀, same data except 34°41'28"S, 117°54'18"E, 411 m (WAM T135923, DNA\_Voucher\_183, GB\_CO1\_KY485336, GB\_CYB\_KY485369); 1 ♀, same data except 34°41'25"S, 117°54'20"E, 407 m (WAM T135922, DNA\_Voucher\_182, GB\_CO1\_KY485337, GB\_CYB\_KY485370); 1 ♀, same data except 34°41'43"S, 117°54'07"E, 308 m (WAM T135925, DNA\_Voucher\_185, GB\_CO1\_KY485334,



GB\_CYB\_KY485367); 1 juvenile, same data (WAM T135926); 1 ♀, Porongurup National Park, track just E. of Tree-in-the-Rock Day Use Area (IBRA\_JAF), 34°40'34"S, 117°52'19"E, 9 October 2013, hand collected in karri forest, M.G. Rix, M.S. Harvey (WAM T131631, DNA\_Voucher\_34, GB\_CO1\_KY295345, GB\_CYB\_KY295466); 1 juvenile, Porongurup National Park, Tree-in-the-Rock Day Use Area, Bolganup Road, 34°40'33"S, 117°52'18"E, dug from burrow, 377 m, M.S. Harvey (WAM T117511, DNA\_Voucher\_186, GB\_CO1\_KY485333, GB\_CYB\_KY485366).

**Diagnosis.**—Males of *Cataxia bolganupensis* can be distinguished from those of *C. barrettiae* and *C. stirlingi* by the presence of prolateral clasp spurs on the leg I tibia (Figs. 47, 48; cf. Figs. 26, 135); from *C. sandsorum* by the presence of smoothly rounded carapace margins between the level of coxae II and III (Fig. 39; cf. Fig. 105); from *C. melindae* by the shape of the pedipalpal tibia, which is proportionally longer (Fig. 49; cf. Fig. 93); and from *C. colesi* by the presence of a relatively dense field of spinules on the RTA (with these spinules largely restricted to the antero-dorsal surface of the RTA) (Figs. 49, 50; cf. Figs. 71, 72), and by the presence of small and irregularly-arranged spinules on the curved retroventral margin of the palpal tibia (Figs. 49, 50; cf. Figs. 71, 72). Females of this species can be distinguished from those of all other species in the *bolganupensis*-group by the more heavily spinose morphology of tibia I, which has a ventral row of at least 5 porrect, spine-like macrosetae (Figs. 58, 59; cf. Figs. 36, 37, 80, 81, 102, 103, 124, 125, 145, 146).

Males, females and juveniles of this species can also be distinguished from all other species in the *bolganupensis*-group by the following 39 unique mitochondrial nucleotide substitutions (based on six specimens; Fig. 17): **COI**: C(13), A(40), T(271), G(469), A(526), T(610). **CYB**: A(36), G(37), G(48), C(49), A(141), T(169), A(171), C(174), A(196), C(208), C(225), G(231), T(268), G(339), G(363), T(379), A(423), G(426), T(442), G(466), T(502), G(504), C(507), A(511), G(519), A(531), A(558), C(579), G(601), C(616), T(625), T(626), C(663).

**Description (male holotype).**—Total length 16.4. Carapace 7.4 long, 6.1 wide. Abdomen 6.8 long, 4.4 wide. Carapace (Fig. 39) tan, with mostly black ocular region; lateral margins with uniformly-spaced fringe of porrect black setae; fovea straight, with pronounced posterior pit. Eye group (Fig. 42) rectangular, 0.6 x as long as wide; PLE–PLE/ALE–ALE ratio 1.0; AME separated by slightly less than their own diameter; PME separated by 2.7 x diameter of AME; PME and PLE separated by less than half diameter of AME, PME positioned slightly anterior to level of PLE. Maxillae with field of cuspules confined to inner corner (Fig. 43); labium without cuspules. Abdomen (Fig. 40) oval, light grey-brown in dorsal view, with beige-grey mottling and beige-grey sigilla spots, the latter forming four faint paired bands posteriorly (in dorsal view). Dorsal surface of abdomen (Fig. 40) covered with stiff, porrect black setae, each with slightly raised, dark brown sclerotic base; sclerotized sigilla absent. Legs (Figs. 46–48) variable shades of tan, with light scopulae on tarsi I–II; tibia I bearing prolateral clasp spurs. Leg I: femur 7.7; patella 3.5; tibia 6.1; metatarsus 6.7; tarsus 3.8; total 27.8. Leg I femur–tarsus/carapace length ratio 3.7. Pedipalpal tibia (Figs. 49–51) 2.0 x longer than wide; RTA short, rounded, with dense field of spinules largely restricted to

antero-dorsal surface; tibia also with irregularly-arranged field of small spinules extending along curved retroventral edge (distal to base of RTA), these spinules enlarged into a cluster of 10 macrosetae on short distal retrolateral tibial apophysis. Cymbium (Figs. 49–51) setose but without field of spinules. Embolus (Figs. 49–51) approximately 1.5 x length of bulb, gradually tapering distally without additional adornment.

**Description (female, WAM T135925).**—Total length 25.8. Carapace 8.4 long, 6.7 wide. Abdomen 13.9 long, 8.4 wide. Carapace (Fig. 52) tan, with darker ocular region; fovea straight. Eye group (Fig. 55) rectangular, 0.5 x as long as wide; PLE–PLE/ALE–ALE ratio 1.0; AME separated by their own diameter; PME separated by 3.0 x diameter of AME; PME and PLE separated by less than half diameter of AME, PME positioned anterior to level of PLE. Maxillae with field of cuspules confined to inner corner (Fig. 56); labium without cuspules. Abdomen (Fig. 53) oval, dark grey-brown in dorsal view, with beige-grey mottling and prominent beige-grey sigilla spots, the latter forming four paired bands posteriorly (in dorsal view); sclerotized sigilla absent. Legs (Figs. 58–59) variable shades of tan (darker red-brown in life, with contrasting darker femora; Fig. 1); scopulae absent; tibia I with 6 porrect, ventral spine-like macrosetae; metatarsus I and tarsus I with additional rows of prolateral and ventral spine-like macrosetae. Leg I: femur 6.3; patella 3.7; tibia 3.9; metatarsus 3.6; tarsus 2.3; total 19.9. Leg I femur–tarsus/carapace length ratio 2.4. Pedipalpal tan, heavily spinose on tibia and tarsus, without tarsal scopula. Genitalia (Fig. 60) with pair of anteriorly curved sac-like spermathecae, each composed of internal, sclerotized glandular chamber and membranous outer wall.

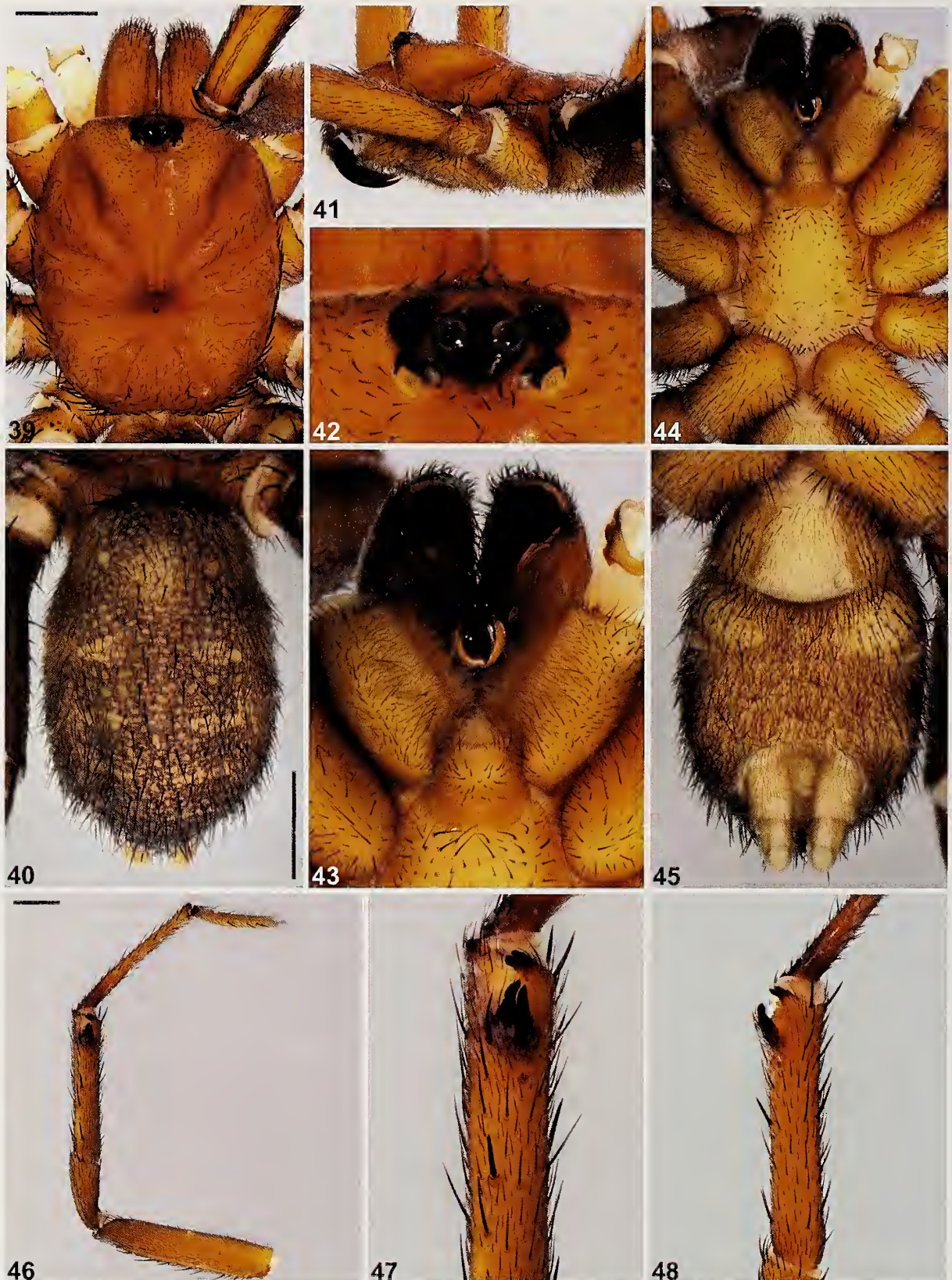
**Distribution and remarks.**—*Cataxia bolganupensis* has a highly restricted distribution in the Porongurup National Park, north of Albany (Figs. 10, 14, 16), where it can be found in wet karri forest on the southern side of the range. It is currently known only from the Millinup Pass and Bolganup Creek areas, but is usually locally abundant and may be found in other small pockets of the park. This species builds a palisade burrow with a fully open hole and no door, which is usually adorned with a radial skirt of leaves and twigs. Based on the few specimens that have been collected, males probably wander and mate in late autumn or winter.

**Conservation status.**—This species has a total (maximum) extent of occurrence of less than 50 km<sup>2</sup>, and an actual area of occupancy of less than 10 km<sup>2</sup>. Given that the number of well-defined locations at which the species has been found is less than five, and that there is continuing decline in the quality of habitat in the Porongurup National Park due to climate change in south-western Australia (Indian Ocean Climate Initiative 2002; Barrett & Yates 2015), and a potential increase in the severity and/or frequency of wildfires (e.g. as in 2007), this species is considered to be 'endangered' (IUCN B1, B2a, b[iii]).

*Cataxia colesi* Rix, Bain, Main & Harvey, sp. nov.  
http://zoobank.org/?lsid=urn:lsid:zoobank.org:act:0101F8D7-2E72-4803-A354-267BB85D20A2  
(Figs. 2, 15, 61–82)

**Type material.**—*Holotype male*. AUSTRALIA: Western Australia: Stirling Range National Park, Toolbrunup Peak, Site 228 (IBRA\_ESP), 34°23'11"S, 118°02'48"E, 2 September 1995, pitfall trap, 800 m, S. Barrett (WAM T32557).





Figures 39–48.—*Cataxia bolganupensis* (Main, 1985), male holotype (WAM T16395), somatic morphology: 39–40, carapace and abdomen, dorsal view; 41, cephalothorax, lateral view; 42, eyes, dorsal view; 43, mouthparts, ventral view; 44–45, cephalothorax and abdomen, ventral view; 46, leg I, prolateral view; 47, leg I tibia, clasp spurs, prolateral view; 48, leg I tibia, pro-ventral view. Scale bars = 2.0.





Figures 49–51.—*Cataxia bolganupensis* (Main, 1985), male holotype (WAM T16395), pedipalp: 49, retrolateral view; 50, retro-ventral view; 51, prolateral view. Scale bar = 2.0.

**Paratype.** AUSTRALIA: *Western Australia*: 1 ♀, Stirling Range National Park, Toolbrunup Peak, track to summit (IBRA\_ESP), 34°23'11"S, 118°03'00"E, 19 April 2015, dug from burrow in mesic gully, 751 m, A. Coles, M.G. Rix, M.S. Harvey, N.J. Tataric (WAM T135917, DNA\_Voucher\_172, GB\_CO1\_KY485345, GB\_CYB\_KY485378).

**Other material examined.**—AUSTRALIA: *Western Australia*: 1 ♀, Stirling Range National Park, Toolbrunup Peak, track to summit (IBRA\_ESP), 34°23'11"S, 118°03'00"E, 19 April 2015, dug from burrow in mesic gully, 751 m, A. Coles, M.G. Rix, M.S. Harvey, N.J. Tataric (WAM T135919, DNA\_Voucher\_174, GB\_CO1\_KY485346, GB\_CYB\_KY485379); 1 juvenile, same data (WAM T135920, DNA\_Voucher\_175, GB\_CO1\_KY485344, GB\_CYB\_KY485377); 1 ♀, same data (WAM T135918, DNA\_Voucher\_173, GB\_CO1\_KY485347, GB\_CYB\_KY485380); 1 ♀, Stirling Range National Park, Toolbrunup Peak, near summit (IBRA\_ESP), 34°23'02"S, 118°02'55"E, hand collected, 964 m, M.G. Rix (WAM T131646); 1 ♀, Stirling Range National Park, saddle between Mount Hassell and Toolbrunup Peak (IBRA\_ESP), 34°22'50"S, 118°04'15"E, 14 December 2014, dug from burrow, K. Bain (WAM T135930, DNA\_Voucher\_176, GB\_CO1\_KY485343, GB\_CYB\_KY485376).

**Etymology.**—The specific epithet is named in honor of Alec Coles, currently CEO of the Western Australian Museum, whose collecting prowess helped secure some of the specimens used in this study.

**Diagnosis.**—Males of *Cataxia colesi* can be distinguished from those of *C. barrettiae* and *C. stirlingi* by the presence of prolateral clasp spurs on the leg I tibia (Figs. 69, 70; cf. Figs. 26, 135); from *C. sandsorum* by the presence of smoothly rounded carapace margins between the level of coxae II and

III (Fig. 61; cf. Fig. 105); from *C. melindae* by the shape of the pedipalpal tibia, which is proportionally longer (Fig. 71; cf. Fig. 93); and from *C. bolganupensis* by the presence of a relatively sparse field of spinules on the RTA (with these spinules extending onto the retrolateral surface of the RTA) (Figs. 71, 72; cf. Figs. 49, 50), and by the presence of larger and more uniformly-arranged spinules on the curved retro-ventral margin of the palpal tibia (Figs. 71, 72; cf. Figs. 49, 50). Females of this species can be distinguished from those of *C. melindae* by the shape of the sternum, which is proportionally longer (Fig. 79; cf. Fig. 101); from *C. bolganupensis* by the less spinose morphology of the leg I tibia (which has no more than 4 porrect, ventral spine-like macrosetae) (Figs. 80, 81; cf. Figs. 58, 59); from *C. barrettiae* and *C. stirlingi* by the absence of a field of spinules on the posterior labium (Fig. 78; cf. Figs. 34, 143); and from *C. sandsorum* by the lower profile of the pars cephalica (Fig. 76; cf. Fig. 120), and by the shape of the posterior eye row, which is as wide as or wider than the anterior eye row (Fig. 77; cf. Fig. 121).

Males, females and juveniles of this species can also be distinguished from all other species in the *bolganupensis*-group by the following 20 unique mitochondrial nucleotide substitutions (based on five specimens; Fig. 17): **COI**: T(40), T(100), A(148), C(172), G(271), A(289), T(316), T(412), T(482), C(628). **CYB**: T(111), C(254), A(291), G(468), T(522), C(546), G(555), G(580), G(598), T(624).

**Description (male holotype).**—Total length 14.9. Carapace 6.3 long, 5.2 wide. Abdomen 6.7 long, 5.2 wide. Carapace (Fig. 61) dark tan, with black ocular region and darker brown lyra-like pattern on pars cephalica; lateral margins with uniformly-spaced fringe of porrect black setae; fovea straight. Eye group (Fig. 64) rectangular, 0.6 x as long as wide; PLE–





Figures 52–60.—*Cataxia bolganupensis* (Main, 1985), female (WAM T135925): 52–53, cephalothorax and abdomen, dorsal view; 54, cephalothorax, lateral view; 55, eyes, dorsal view; 56, mouthparts, ventral view; 57, cephalothorax, ventral view; 58, leg I, prolateral view; 59, leg I, retrolateral view; 60, spermathecae, dorsal view. Scale bars = 2.0 (52–53, 58–59), 0.5 (60).

PLE/ALE–ALE ratio 1.0; AME separated by their own diameter; PME separated by 2.6 x diameter of AME; PME and PLE separated by less than half diameter of AME, PME positioned slightly anterior to level of PLE. Maxillae with field of cuspules confined to inner corner (Fig. 65); labium without cuspules. Abdomen (Fig. 62) oval, grey in dorsal view, with beige-brown mottling and beige-brown sigilla spots, the latter forming very faint paired bands posteriorly (in dorsal view). Dorsal surface of abdomen (Fig. 62) covered with stiff, porrect black setae, each with slightly raised, dark brown sclerotic base; sclerotized sigilla absent. Legs (Figs. 68–

70) variable shades of tan, with light scopulae on tarsi I–II; tibia I bearing prolateral clasp spurs. Leg I: femur 6.9; patella 3.1; tibia 5.4; metatarsus 6.8; tarsus 3.7; total 25.8. Leg I femur–tarsus/carapace length ratio 4.1. Pedipalpal tibia (Figs. 71–73) 2.0 x longer than wide; RTA short, rounded, with relatively sparse field of large retrolateral spinules; tibia also with long field of large, uniformly-arranged spinules extending along curved retroventral edge (distal to base of RTA), these spinules slightly enlarged into a cluster of three macrosetae on short distal retrolateral tibial apophysis. Cymbium (Figs. 71–73) setose but without field of spinules.





Figures 61–70.—*Cataxia colesi* sp. nov., male holotype (WAM T32557), somatic morphology: 61–62, cephalothorax and abdomen, dorsal view; 63, cephalothorax, lateral view; 64, eyes, dorsal view; 65, mouthparts, ventral view; 66–67, cephalothorax and abdomen, ventral view; 68, leg I, prolateral view; 69, leg I tibia, elapsing spurs, prolateral view; 70, leg I tibia, pro-ventral view. Scale bars = 2.0.





Figures 71–73.—*Cataxia colesi* sp. nov., male holotype (WAM T32557), pedipalp: 71, retrolateral view; 72, retro-ventral view; 73, prolateral view. Scale bar = 2.0.

Embolus (Figs. 71–73) approximately 1.5 x length of bulb, gradually tapering distally without additional adornment.

**Description (female paratype, WAM T135917).**—Total length 28.2. Carapace 9.4 long, 7.2 wide. Abdomen 14.5 long, 8.7 wide. Carapace (Fig. 74) dark tan-brown, with darker pars cephalica and mostly black ocular region; fovea straight. Eye group (Fig. 77) rectangular, 0.6 x as long as wide; PLE–PLE/ALE–ALE ratio 1.0; AME separated by their own diameter; PME separated by 3.0 x diameter of AME; PME and PLE separated by slightly more than half diameter of AME, PME positioned slightly anterior to level of PLE. Maxillae with field of cuspules confined to inner corner (Fig. 78); labium without cuspules. Abdomen (Fig. 75) oval, dark grey in dorsal view, with beige-grey mottling and prominent beige-grey sigilla spots, the latter forming four paired bands posteriorly (in dorsal view); sclerotized sigilla absent. Legs (Figs. 80–81) variable shades of tan (darker red-brown in life, with contrasting darker femora; Fig. 2); scopulae absent; tibia I with 3 porrect, ventral spine-like macrosetae; metatarsus I and tarsus I with additional rows of prolateral and ventral spine-like macrosetae. Leg I: femur 7.0; patella 4.0; tibia 4.3; metatarsus 3.7; tarsus 2.3; total 21.3. Leg I femur–tarsus/carapace length ratio 2.3. Pedipalp tan, heavily spinose on tibia and tarsus, without tarsal scopula. Genitalia (Fig. 82) with pair of obliquely directed bulbous spermathecae, each composed of internal, sclerotized glandular chamber and membranous outer wall.

**Distribution and remarks.**—*Cataxia colesi* is the largest species in the *bolganupensis*-group, and has a highly restricted distribution in the Stirling Range National Park, where it is known only from the Toolbrunup-Hassell uplands, on Toolbrunup Peak, Mount Hassell, and the saddle between the two peaks (Figs. 10, 14, 15). It is usually found in heavily

shaded, mesic habitats above 500 m altitude (Fig. 11), and while patchily distributed can be locally abundant. This species builds a short palisade burrow with a fully open hole and no door, which is usually adorned with leaves and twigs. Based on the single male specimen that has been collected, males may wander in spring.

**Conservation status.**—This species has a total (maximum) extent of occurrence and area of occupancy each of significantly less than 10 km<sup>2</sup>. Given that the number of well-defined locations at which the species has been found is less than five, and that there is continuing decline in the quality of habitat in the Stirling Range National Park due to *Phytophthora diebaek* (Barrett & Yates 2015), climate change in south-western Australia (Indian Ocean Climate Initiative 2002; Barrett & Yates 2015), and a potential increase in the severity and/or frequency of wildfires, this species is considered to be 'endangered' (IUCN B1, B2a, b[iii]).

*Cataxia melindae* Rix, Bain, Main & Harvey, sp. nov.

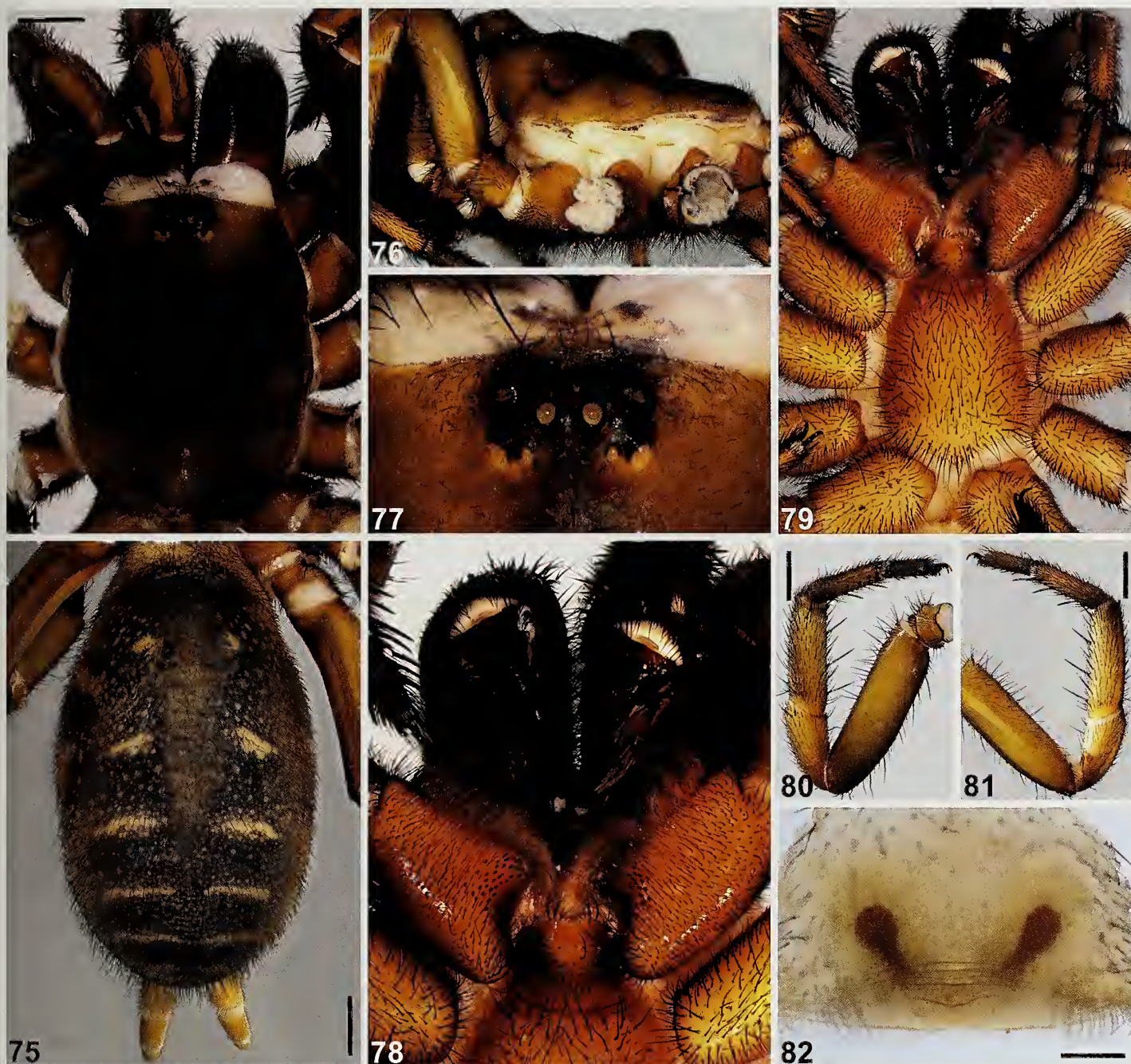
<http://zoobank.org/?lsid=urn:lsid:zoobank.org:act:A69A716F-C769-4343-9411-8E4F4E25C345>

(Figs. 16, 83–104)

**Type material.**—*Holotype male*. AUSTRALIA: *Western Australia*: Mount Manypeaks Nature Reserve, Mount Manypeaks, Site 202 (IBRA\_ESP), 34°53'40"S, 118°16'02"E, 3 May 1996, wet pitfall, S. Barrett (WAM T132544).

*Paratypes*. AUSTRALIA: *Western Australia*: 1 ♂, Mount Manypeaks Nature Reserve, Mount Manypeaks, Site 201 (IBRA\_ESP), 34°53'40"S, 118°16'01"E, 3 May 1996, wet pitfall, S. Barrett (WAM T132545); 1 ♀, Mount Manypeaks Nature Reserve, Mount Manypeaks, Site 3 (IBRA\_ESP), 34°53'48"S, 118°17'58"E, 26 October 2006, hand collected from burrow in





Figures 74–82.—*Cataxia colesi* sp. nov., female paratype (WAM T135917): 74–75, carapace and abdomen, dorsal view; 76, cephalothorax, lateral view; 77, eyes, dorsal view; 78, mouthparts, ventral view; 79, cephalothorax, ventral view; 80, leg I, prolateral view; 81, leg I, retrolateral view; 82, spermathecae, dorsal view. Scale bars = 2.0 (74–75, 80–81), 0.5 (82).

gully, M.L. Moir, A. Sampey (WAM T78521, DNA\_Voucher\_315, GB\_COI\_KY485348, GB\_CYB\_KY485381).

**Other material examined.**—AUSTRALIA: *Western Australia*: 1 juvenile, Mount Manypeaks Nature Reserve, Mount Manypeaks, near summit, Site 5, 34°53'49"S, 118°15'57"E, 1 December 2006, hand collected from burrow in gully, M.L. Moir, K.E.C. Brennan, B. Atkinson (WAM T78561, DNA\_Voucher\_163, GB\_COI\_KY485350, GB\_CYB\_KY485383); 1 ♀, same data (WAM T78559, DNA\_Voucher\_162, GB\_COI\_KY485351, GB\_CYB\_KY485384); 1 juvenile, same data (WAM T78562, DNA\_Voucher\_164,

GB\_COI\_KY485349, GB\_CYB\_KY485382); 1 juvenile, same data (WAM T78560); 1 juvenile, same data (WAM T78563); 1 juvenile, same data (WAM T78784); 1 ♀, same data except Site 6, 34°53'57"S, 118°15'43"E, hand collected from burrow (WAM T78557, DNA\_Voucher\_161, GB\_COI\_KY485352, GB\_CYB\_KY485385).

**Etymology.**—The specific epithet is named in honor of Melinda Moir, whose dedicated survey work in the Mount Manypeaks Nature Reserve resulted in the collection of many important specimens of *Cataxia*, including the molecular exemplar specimens analyzed in this study.





Figures 83–92.—*Cataxia melindae* sp. nov., male holotype (WAM T132544), somatic morphology: 83–84, carapace and abdomen, dorsal view; 85, cephalothorax, lateral view; 86, eyes, dorsal view; 87, mouthparts, ventral view; 88–89, cephalothorax and abdomen, ventral view; 90, leg I, prolateral view; 91, leg I tibia, clasp spurs, prolateral view; 92, leg I tibia, pro-ventral view. Scale bars = 2.0.





Figures 93–95.—*Cataxia melindae* sp. nov., male holotype (WAM T132544), pedipalp: 93, retrolateral view; 94, retro-ventral view; 95, prolateral view. Scale bar = 2.0.

**Diagnosis.**—Males of *Cataxia melindae* can be distinguished from those of *C. barrettiae* and *C. stirlingi* by the presence of prolateral claspingspurs on the leg I tibia (Figs. 91, 92; cf. Figs. 26, 135); from *C. sandsorum* by the presence of smoothly rounded carapace margins between the level of coxae II and III (Fig. 83; cf. Fig. 105); and from *C. bolganupensis* and *C. colesi* by the shape of the pedipalpal tibia, which is proportionally shorter and stouter (Fig. 93; cf. Figs. 49, 71). Females of this species can be distinguished from those of all other species in the *bolganupensis*-group by the shape of the sternum, which is short, sub-circular or subquadrate and almost as wide as long (Fig. 101; cf. Figs. 35, 57, 79, 123, 144).

Males, females and juveniles of this species can also be distinguished from all other species in the *bolganupensis*-group by the following 37 unique mitochondrial nucleotide substitutions (based on five specimens; Fig. 17): **COI**: C(31), C(85), A(94), G(133), C(178), A(184), T(364), A(391), G(415), C(445), G(474), G(483), A(496), T(631). **CYB**: T(37), C(48), A(60), C(69), C(83), A(132), C(177), G(204), C(270), C(348), G(372), A(387), G(393), T(435), C(450), C(486), A(489), A(498), T(520), C(522), G(573), G(582), T(594).

**Description (male holotype).**—Total length 14.2. Carapace 5.9 long, 4.7 wide. Abdomen 6.0 long, 3.8 wide. Carapace (Fig. 83) tan, with mostly black ocular region and darker brown lyra-like pattern on pars cephalica; lateral margins with uniformly-spaced fringe of porrect black setae; fovea straight. Eye group (Fig. 86) rectangular, 0.5 x as long as wide; PLE–PLE/ALE–ALE ratio 0.9; AME separated by slightly less than their own diameter; PME separated by 2.3 x diameter of AME; PME and PLE separated by less than half diameter of AME, PME positioned in line with level of PLE. Maxillae and labium without cuspules (Fig. 87). Abdomen (Fig. 84) oval, dark grey-brown in dorsal view, with dark beige-brown

mottling and dark beige-brown sigilla spots, the latter forming four paired bands posteriorly. Dorsal surface of abdomen (Fig. 84) covered with stiff, porrect black setae, each with slightly raised, dark brown sclerotic base; sclerotized sigilla absent. Legs (Figs. 90–92) variable shades of tan, with light scopulae on tarsi I–II; tibia I bearing prolateral claspingspurs. Leg I: femur 6.2; patella 2.6; tibia 4.8; metatarsus 5.5; tarsus 3.0; total 22.0. Leg I femur–tarsus/carapace length ratio 3.8. Pedipalpal tibia (Figs. 93–95) stout, 1.7 x longer than wide; RTA short, rounded, with relatively sparse field of retrolateral spinules; tibia also with irregularly-arranged field of small spinules extending along curved retroventral edge (distal to base of RTA), these spinules enlarged into a row of 10 macrosetae on short distal retrolateral tibial apophysis. Cymbium (Figs. 93–95) setose but without field of spinules. Embolus (Figs. 93–95) approximately 1.5 x length of bulb, gradually tapering distally without additional adornment.

**Description (female paratype, WAM T78521).**—Total length 19.1. Carapace 6.6 long, 5.0 wide. Abdomen 9.8 long, 5.8 wide. Carapace (Fig. 96) dark tan-brown, with darker pars cephalica and mostly black ocular region; fovea straight. Eye group (Fig. 99) rectangular, 0.5 x as long as wide; PLE–PLE/ALE–ALE ratio 0.9; AME separated by their own diameter; PME separated by 3.0 x diameter of AME; PME and PLE separated by less than half diameter of AME, PME positioned slightly anterior to level of PLE. Maxillae with field of cuspules confined to inner corner (Fig. 100); labium without cuspules. Abdomen (Fig. 97) oval, dark grey-brown in dorsal view, darker posteriorly, with beige-brown mottling and prominent beige-grey sigilla spots, the latter forming three paired bands posteriorly (in dorsal view); sclerotized sigilla absent. Legs (Figs. 102–103) variable shades of tan; scopulae absent; tibia I with 3 porrect, ventral spine-like macrosetae; metatarsus I and





Figures 96–104.—*Cataxia melindae* sp. nov., female paratype (WAM T78521): 96–97, carapace and abdomen, dorsal view; 98, cephalothorax, lateral view; 99, eyes, dorsal view; 100, mouthparts, ventral view; 101, cephalothorax, ventral view; 102, leg I, prolateral view; 103, leg I, retrolateral view; 104, spermathecae, dorsal view. Scale bars = 2.0 (96–97, 102–103), 0.5 (104).

tarsus I with additional rows of prolateral and ventral spine-like macrosetae. Leg I: femur 4.6; patella 2.7; tibia 3.2; metatarsus 2.6; tarsus 1.7; total 14.8. Leg I femur–tarsus/carapace length ratio 2.2. Pedipalp tan, heavily spinose on tibia and tarsus, without tarsal scopula. Genitalia (Fig. 104) with pair of short, anteriorly curved and slightly bulbous spermathecae, each composed of internal, sclerotized glandular chamber and membranous outer wall.

**Distribution and remarks.**—*Cataxia melindae* has a highly restricted distribution in the Mount Manypeaks Nature Reserve, east of Albany, where it is known only from near the

summit and south-eastern slopes of Mount Manypeaks (Figs. 10, 14, 16). The preferred habitat seems to be mesic gullies in dense heathland. Little else is known of the biology of this species, although based on the few specimens that have been collected, males probably wander and mate in late autumn.

**Conservation status.**—This species has a total (maximum) extent of occurrence and area of occupancy each of less than 10 km<sup>2</sup>. Given that the number of well-defined locations at which the species has been found is less than five, and that there is continuing decline in the quality of habitat in the Mount Manypeaks Nature Reserve due to *Phytophthora* dieback,



climate change in south-western Australia (Indian Ocean Climate Initiative 2002; Barrett & Yates 2015), and a potential increase in the severity and/or frequency of wildfires, this species is considered to be ‘endangered’ (IUCN B1, B2a, b[iii]).

***Cataxia sandsorum*** Rix, Bain, Main & Harvey, sp. nov.  
<http://zoobank.org/?lsid=urn:lsid:zoobank.org:act:C24909E5-1B79-487D-AD34-357C69660DCA>  
 (Figs. 3, 8, 15, 105–126)

**Type material.**—*Holotype male*. AUSTRALIA: *Western Australia*: Stirling Range National Park, S. face of Pyungoorup Peak (IBRA\_ESP), 34°22′17″S, 118°19′20″E, 4 September – 18 December 1996, wet pitfall trap, M.S. Harvey, J.M. Waldoock, B.Y. Main (WAM T42313).

*Paratype*. AUSTRALIA: *Western Australia*: 1 ♀, same data as holotype except 18 December 1996, hand collected, B.Y. Main (WAM T38922).

**Other material examined.**—AUSTRALIA: *Western Australia*: 2 ♀, Stirling Range National Park, S. face of Pyungoorup Peak (IBRA\_ESP), 34°22′17″S, 118°19′20″E, 27 April 1996, 330 m, M.S. Harvey, J.M. Waldoock, B.Y. Main (WAM T132547); 1 ♀, Stirling Range National Park, gully at S. face of Pyungoorup Peak (IBRA\_ESP), 34°21′54″S, 118°19′43″E, 16 April 2015, dug from burrow in mesic gully, 425 m, M.G. Rix, M.S. Harvey (WAM T135887, DNA\_Voucher\_177, GB\_COI\_KY485342, GB\_CYB\_KY485375); 1 juvenile, same data (WAM T135880, DNA\_Voucher\_180, GB\_COI\_KY485339, GB\_CYB\_KY485372); 1 juvenile, same data (WAM T135881, DNA\_Voucher\_181, GB\_COI\_KY485338, GB\_CYB\_KY485371); 1 juvenile, same data (WAM T135879); 1 ♀, same data except 34°22′00″S, 118°19′43″E, 371 m (WAM T135877, DNA\_Voucher\_178, GB\_COI\_KY485341, GB\_CYB\_KY485374); 1 juvenile, same data except 34°21′57″S, 118°19′43″E, 380 m (WAM T135878, DNA\_Voucher\_179, GB\_COI\_KY485340, GB\_CYB\_KY485373); 1 ♀, Stirling Range National Park, base of Pyungoorup Peak (IBRA\_ESP), 34°22′11″S, 118°19′34″E, 5 August 2008, hand collected, M.G. Rix, M.S. Harvey (WAM T131647); 1 juvenile, same data (WAM T131649); 1 ♀, same data except 34°21′54″S, 118°19′44″E (WAM T131648).

**Etymology.**—The specific epithet is named in honor of Ayleen and Tony Sands, for their wonderful hospitality and for their dedication to preserving and promoting the biodiversity of the Stirling Range National Park.

**Diagnosis.**—Males of *Cataxia sandsorum* can be distinguished from those of all other species in the *bolganupensis*-group by the presence of a sharp indentation on each side of the carapace, between the level of coxae II and III (Fig. 105; cf. Figs. 18, 39, 61, 83, 127), and by the presence of a pair of deep concave depressions on each cheliceral paturon (Fig. 107; cf. Figs. 63, 129). Females of this species can be distinguished from those of *C. melindae* by the shape of the sternum, which is proportionally longer (Fig. 123; cf. Fig. 101); from *C. bolganupensis* by the less spinose morphology of the leg I tibia (which has no more than 4 porrect, ventral spine-like macrosetae) (Figs. 124, 125; cf. Figs. 58, 59); from *C. barrettae* and *C. stirlingi* by the absence of a field of spinules on the posterior labium (Fig. 122; cf. Figs. 34, 143); and from *C. colesi* by the higher profile of the pars cephalica (Fig. 120; cf. Fig. 76), and by

the shape of the anterior eye row, which is marginally wider than the posterior eye row (Fig. 121; cf. Fig. 77).

Males, females and juveniles of this species can also be distinguished from all other species in the *bolganupensis*-group by the following 28 unique mitochondrial nucleotide substitutions (based on five specimens; Fig. 17): **COI**: A(46), G(49), C(202), T(217), C(232), A(295), G(424), A(451), C(508), A(517), C(533), G(574), A(628). **CYB**: C(82), T(83), C(162), A(186), T(234), C(244), A(300), C(345), C(354), T(376), T(377), A(402), T(426), C(493), C(519).

**Description (male holotype).**—Total length 15.6. Carapace 6.4 long, 4.8 wide. Abdomen 6.4 long, 3.9 wide. Carapace (Fig. 105) tan, with darker ocular region and darker brown lyra-like pattern on pars cephalica; lateral margins sharply indented between level of coxae II and III, with uniformly-spaced fringe of porrect black setae; fovea straight. Eye group (Fig. 108) rectangular, 0.5 x as long as wide; PLE–PLE/ALE–ALE ratio 0.9; AME separated by slightly less than their own diameter; PME separated by 2.4 x diameter of AME; PME and PLE separated by less than half diameter of AME, PME positioned in line with level of PLE. Maxillae and labium without cuspules (Fig. 109). Abdomen (Fig. 106) oval, light grey in dorsal view, with beige-grey mottling and beige-grey sigilla spots, the latter forming four paired bands posteriorly. Dorsal surface of abdomen (Fig. 106) covered with stiff, porrect black setae, each with slightly raised, dark brown sclerotie base; sclerotized sigilla absent. Legs (Figs. 112–114) variable shades of tan, with light scopulae on tarsi I–II; tibia I bearing prolateral claspings spurs. Leg I: femur 6.8; patella 3.0; tibia 5.3; metatarsus 5.9; tarsus 3.0; total 24.1. Leg I femur–tarsus/carapace length ratio 3.8. Pedipalpal tibia (Figs. 115–117) 2.0 x longer than wide; RTA short, rounded, with dense field of retrolateral spinules; tibia also with long field of spinules of varying sizes extending along curved retroventral edge (distal to base of RTA), these spinules enlarged into a divided cluster of nine macrosetae on short distal retrolateral tibial apophysis. Cymbium (Figs. 115–117) setose but without field of spinules. Embolus (Figs. 115–117) approximately 1.5 x length of bulb, gradually tapering distally without additional adornment.

**Description (female paratype, WAM T38922).**—Total length 21.3. Carapace 7.0 long, 5.4 wide. Abdomen 10.6 long, 6.4 wide. Carapace (Fig. 118) dark tan, with darker pars cephalica and mostly black ocular region; fovea straight. Eye group (Fig. 121) rectangular, 0.5 x as long as wide; PLE–PLE/ALE–ALE ratio 0.9; AME separated by their own diameter; PME separated by 3.0 x diameter of AME; PME and PLE separated by less than half diameter of AME, PME positioned slightly anterior to level of PLE. Maxillae with field of cuspules confined to inner corner (Fig. 122); labium without cuspules. Abdomen (Fig. 119) oval, grey in dorsal view, with beige-grey mottling and prominent beige-grey sigilla spots, the latter forming four paired bands posteriorly (in dorsal view); sclerotized sigilla absent. Legs (Figs. 124, 125) variable shades of tan (darker red-brown in life, with contrasting darker femora; Fig. 3); scopulae absent; tibia I with 3 porrect, ventral spine-like macrosetae; metatarsus I and tarsus I with additional rows of prolateral and ventral spine-like macrosetae. Leg I: femur 5.5; patella 3.4; tibia 3.7; metatarsus 3.3; tarsus 2.2; total 18.1. Leg I femur–tarsus/carapace length ratio 2.6. Pedipalp tan, heavily spinose on tibia and tarsus, without tarsal scopula. Genitalia (Fig. 126) with pair of anteriorly





Figures 105–114.—*Cataxia sandsorum* sp. nov., male holotype (WAM T42313), somatic morphology: 105–106, carapace and abdomen, dorsal view; 107, cephalothorax, lateral view; 108, eyes, dorsal view; 109, mouthparts, ventral view; 110–111, cephalothorax and abdomen, ventral view; 112, leg I, prolateral view; 113, leg I tibia, clasp spurs, prolateral view; 114, leg I tibia, pro-ventral view. Scale bars = 2.0.





Figures 115–117.—*Cataxia sandsorum* sp. nov., male holotype (WAM T42313), pedipalp: 115, retrolateral view; 116, retro-ventral view; 117, prolateral view. Scale bar = 2.0.

curved sac-like spermathecae, each composed of internal, sclerotized glandular chamber and membranous outer wall.

**Distribution and remarks.**—*Cataxia sandsorum* has a highly restricted distribution in the Stirling Range National Park, where it is known only from the eastern side of the eastern massif, in the vicinity of Pyungoorup Peak and adjacent Ellen Peak (Figs. 10, 14–15). The habitat at the type locality is upland riparian (mesic) eucalypt forest on the heavily shaded southern side of the range (Fig. 12), where the spiders are locally abundant. Its distribution closely abuts that of *C. stirlingi* (Fig. 15), although the two species have never been found in direct sympatry. *Cataxia sandsorum* builds a palisade burrow with a fully open hole and no door, which is usually adorned with a radial skirt of leaves and twigs (Fig. 8). Based on the single male specimen that has been collected, males may wander and mate in spring.

**Conservation status.**—This species has a total (maximum) extent of occurrence and area of occupancy each of significantly less than 10 km<sup>2</sup>. Given that this species has only been found at just a single well-defined location, and that there is continuing decline in the quality of habitat in the eastern Stirling Range National Park due to severe *Phytophthora* dieback (Barrett & Yates 2015), climate change in south-western Australia (Indian Ocean Climate Initiative 2002; Barrett & Yates 2015), and a potential increase in the severity and/or frequency of wildfires, this species is considered to be ‘endangered’ (IUCN B1, B2a, b[iii]).

*Cataxia stirlingi* (Main, 1985)  
(Figs. 4, 7, 15, 127–147)

*Neohomogona stirlingi* Main, 1985: 43, figs. 165–168, 178–180, 206–207, 219; Main, 1993a: 600.

*Cataxia stirlingi* (Main): Raven, 1985: 175.

**Type material.**—*Holotype male*. AUSTRALIA: *Western Australia*: Stirling Range National Park, south base of Bluff Knoll (IBRA\_ESP), [34°23'S, 118°15'E], 5 April 1957, hand collected, A.R. Main (WAM T16407; examined).

**Paratypes.** AUSTRALIA: *Western Australia*: 1 ♀ (allotype), same data as holotype except 10 June 1954, B.Y. Main (WAM T16408); 1 ♀, same data (WAM T16410); 1 ♀, same data as holotype (WAM T16400); 1 ♀, same data (WAM T16411); 14 ♀ and/or juveniles, same data (WAM BYM Collection; not recently examined); 1 ♂, same data (molted to maturity before 14 May 1958) (WAM BYM Collection; not recently examined); 1 ♀, same data as holotype except 8 June 1954, B.Y. Main (WAM T16409); 21 ♀, 26 juveniles, same data (WAM BYM Collection; not recently examined).

**Other material examined.**—AUSTRALIA: *Western Australia*: 1 ♀, Stirling Range National Park, Bluff Knoll, track to summit (IBRA\_ESP), 34°22'09"S, 118°14'52"E, 15 April 2015, dug from burrow, 494 m, M.G. Rix, M.S. Harvey, N.J. Tatarnic, A. Coles (WAM T135850, DNA\_Voucher\_190, GB\_CO1\_KY485331, GB\_CYB\_KY485364); 1 juvenile, same data except 34°22'09"S, 118°14'48"E, 492 m (WAM T135847, DNA\_Voucher\_187, GB\_CO1\_KY485332, GB\_CYB\_KY485365); 1 ♀, same data except 34°22'35"S, 118°15'02"E, 758 m (WAM T135848, DNA\_Voucher\_188, GB\_CO1\_KY485330, GB\_CYB\_KY485363); 1 juvenile, same data (WAM T135849, DNA\_Voucher\_189, GB\_CO1\_KY485329, GB\_CYB\_KY485362); 1 ♀, Stirling Range National Park, gully on Ellen Track near Moongoongoonderup Creek (IBRA\_ESP), [34°23'S, 118°17'E], 27 April 1996, hand collected, B.Y. Main, M.S. Harvey, J.M. Waddock (WAM T44291); 1 ♀, Stirling Range National Park, Moongoongoonderup Hill (IBRA\_ESP), 34°21'46"S, 118°15'52"E, 15 December 2014, dug from burrow, K. Bain





Figures 118–126.—*Cataxia sandsorum* sp. nov., female paratype (WAM T38922): 118–119, carapace and abdomen, dorsal view; 120, cephalothorax, lateral view; 121, eyes, dorsal view; 122, mouthparts, ventral view; 123, cephalothorax, ventral view; 124, leg I, prolateral view; 125, leg I, retrolateral view; 126, spermathecae, dorsal view. Scale bars = 2.0 (118–119, 124–125), 0.5 (126).

(WAM T135929, DNA\_Voucher\_191, GB\_CO1\_KY485328, GB\_CYB\_KY485361); 1 juvenile (tenuously identified; see below), Stirling Range National Park, near W. end of Ellen Track (IBRA\_ESP), 34°23'04"S, 118°17'17"E, 30 April – 4 September 1996, wet pitfall, M.S. Harvey et al. (WAM T42330).

**Diagnosis.**—Males of *Cataxia stirlingi* can be distinguished from those of *C. bolganupensis*, *C. colesi*, *C. melindae* and *C. sandsorum* by the absence of prolateral clasp spurs on the leg I tibia (Fig. 135; cf. Figs. 47, 48); and from *C. barrettae* by the shorter, more distally rounded shape of the RTA (Fig. 136;

cf. Fig. 27), and by the less strongly developed macrosetae on the distal prolateral tibia I (Fig. 135; cf. Fig. 26). Females of this species can be distinguished from those of *C. melindae* by the shape of the sternum, which is proportionally longer (Fig. 144; cf. Fig. 101); from *C. bolganupensis* by the less spinose leg I tibia (with no more than 4 porrect, ventral spine-like macrosetae) (Figs. 145, 146; cf. Figs. 58, 59); and from *C. colesi* and *C. sandsorum* by the presence of a sparse field of spinules on the posterior labium (Fig. 143; cf. Figs. 78, 122). By our assessment, females of this species appear to be morphologically indistinguishable from those of *C. barrettae*.





Figures 127–135.—*Cataxia stirlingi* (Main, 1985), male holotype (WAM T16407), somatic morphology: 127–128, carapace and abdomen, dorsal view; 129, cephalothorax, lateral view; 130, chela, dorsal view; 131, mouthparts, ventral view; 132–133, cephalothorax and abdomen, ventral view; 134, leg I, prolateral view; 135, leg I tibia, prolateral view. Scale bars = 2.0.





Figures 136–138.—*Cataxia stirlingi* (Main, 1985), male holotype (WAM T16407), pedipalp: 136, retrolateral view; 137, retro-ventral view; 138, prolateral view. Scale bar = 2.0.

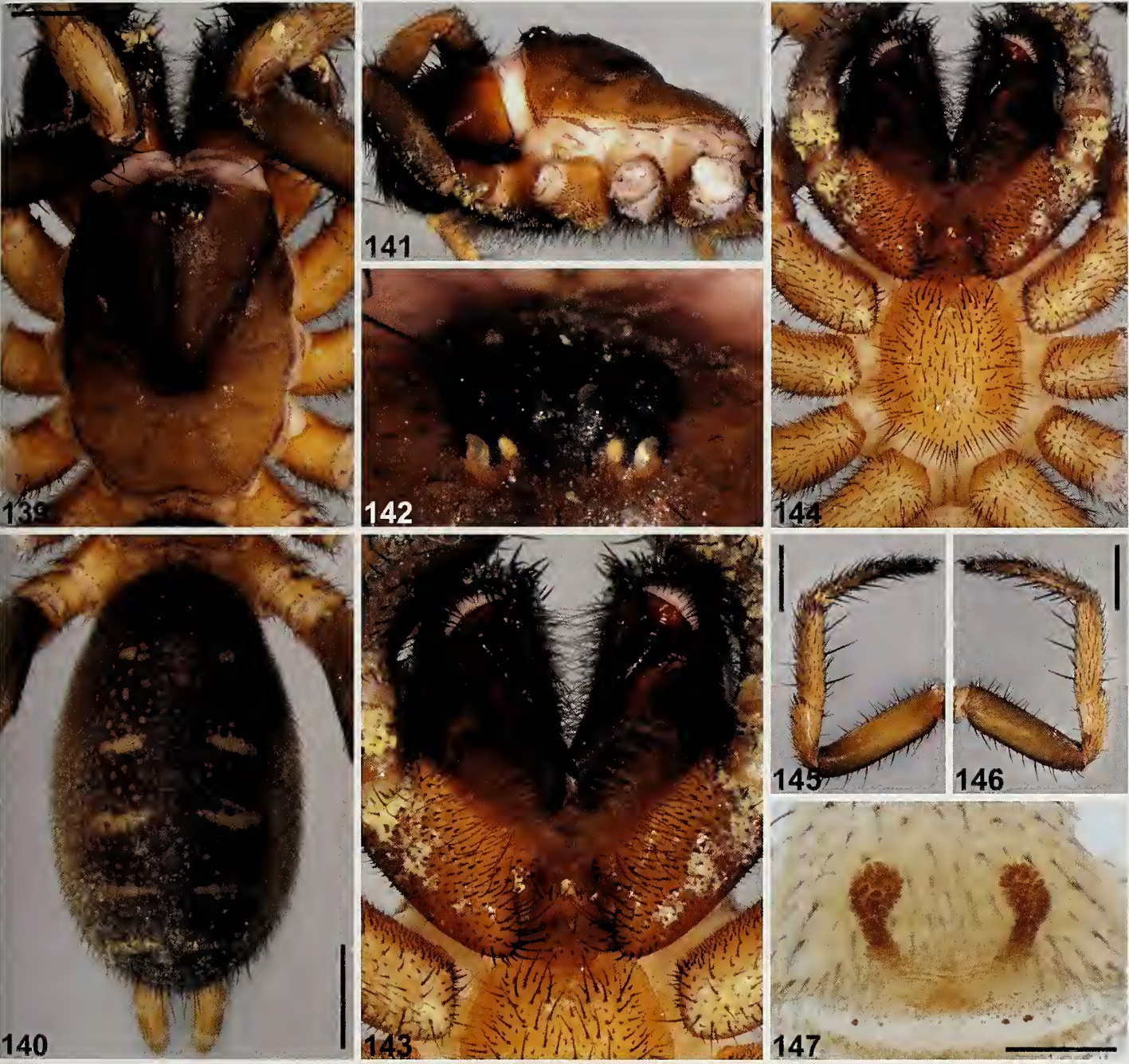
Males, females and juveniles of this species can also be distinguished from all other species in the *bolganupensis*-group by the following 32 unique mitochondrial nucleotide substitutions (based on five specimens; Fig. 17): **COI**: A(73), G(160), A(163), A(253), C(271), C(274), A(412), A(460), C(484), A(487), G(496), G(592), T(619). **CYB**: A(23), A(114), G(125), T(129), T(132), C(149), A(180), C(230), G(318), T(321), G(415), C(417), T(466), A(477), A(501), T(607), T(634), G(637), A(639).

**Description (male holotype).**—Total length 13.4. Carapace 5.6 long, 4.5 wide. Abdomen 5.9 long, 4.0 wide. Carapace (Fig. 127) tan, with black ocular region and slightly darker lyra-like pattern on pars cephalica; lateral margins with uniformly-spaced fringe of porrect black setae; fovea straight. Eye group (Fig. 130) rectangular, 0.5 x as long as wide; PLE–PLE/ALE–ALE ratio 0.8; AME separated by slightly more than their own diameter; PME separated by 2.4 x diameter of AME; PME and PLE separated by less than half diameter of AME, PME positioned in line with level of PLE. Maxillae with field of cuspules confined to inner corner (Fig. 131); labium without cuspules. Abdomen (Fig. 128) oval, dark grey-brown in dorsal view, with faint beige-brown mottling and prominent beige-brown sigilla spots, the latter forming four paired bands posteriorly. Dorsal surface of abdomen (Fig. 128) covered with stiff, porrect black setae, each with slightly raised, dark brown sclerotic base; sclerotized sigilla absent. Legs (Figs. 134–135) variable shades of tan, with light scopulae on tarsi I–II; tibia I without clasping spurs but with paired prolateral macrosetae on slightly raised distal protuberance, and adjacent proventral macroseta. Leg I: femur 5.7; patella 2.6; tibia 4.6; metatarsus 5.1; tarsus 3.0; total 21.0. Leg I femur–tarsus/carapace length ratio 3.8. Pedipalpal tibia (Figs. 136–138) 1.9 x longer than wide; RTA relatively short, rounded,

with dense field of retrolateral spinules; tibia also with long field of smaller spinules extending along curved retroventral edge (distal to base of RTA), these spinules enlarged into a row of nine macrosetae on short distal retrolateral tibial apophysis. Cymbium (Figs. 136–138) setose but without field of spinules. Embolus (Figs. 136–138) approximately 1.5 x length of bulb, gradually tapering distally without additional adornment.

**Description (female, WAM T135848).**—Total length 16.6. Carapace 5.7 long, 4.2 wide. Abdomen 8.2 long, 4.8 wide. Carapace (Fig. 139) light tan, with darker brown pars cephalica and mostly black ocular region; fovea straight. Eye group (Fig. 142) rectangular, 0.5 x as long as wide; PLE–PLE/ALE–ALE ratio 0.9; AME separated by their own diameter; PME separated by 2.6 x diameter of AME; PME and PLE separated by less than half diameter of AME, PME positioned slightly anterior to level of PLE. Maxillae with field of cuspules confined to inner corner (Fig. 143); labium without cuspules but with sparse field of posterior spinules (Fig. 143). Abdomen (Fig. 140) oval, dark grey-brown in dorsal view, with beige-grey mottling and prominent beige-grey sigilla spots, the latter forming four paired bands posteriorly (in dorsal view); sclerotized sigilla absent. Legs (Figs. 145, 146) variable shades of tan (darker red-brown in life, with contrasting slate-grey femora; Fig. 4); scopulae absent; tibia I with 3 porrect, ventral spine-like macrosetae; metatarsus I and tarsus I with additional rows of prolateral and ventral spine-like macrosetae. Leg I: femur 4.2; patella 2.4; tibia 2.9; metatarsus 2.5; tarsus 1.7; total 13.5. Leg I femur–tarsus/carapace length ratio 2.4. Pedipalp tan, heavily spinose on tibia and tarsus, without tarsal scopula. Genitalia (Fig. 147) with pair of anteriorly curved, slightly bulbous spermathecae,





Figures 139–147.—*Cataxia stirlingi* (Main, 1985), female (WAM T135848): 139–140, carapace and abdomen, dorsal view; 141, cephalothorax, lateral view; 142, eyes, dorsal view; 143, mouthparts, ventral view; 144, cephalothorax, ventral view; 145, leg 1, prolateral view; 146, leg 1, retrolateral view; 147, spermathecae, dorsal view. Scale bars = 2.0 (139–140, 145–146), 0.5 (147).

each composed of internal, sclerotized glandular chamber and membranous outer wall.

**Distribution and remarks.**—*Cataxia stirlingi* is the smallest species in the *bolganupensis*-group, and has a highly restricted distribution in the Stirling Range National Park, where it is known only from the western side of the eastern massif, from Bluff Knoll to Moongoongoonderup Hill, with an isolated record (tenuously linked here based on geography) from near Ellen Track, south-east of Bluff Knoll (Figs. 10, 14, 15). The habitat is generally montane heathland and adjacent eucalypt forest above 400 m altitude, where the spiders are patchily

distributed and generally rare, although sometimes locally abundant. Its distribution closely abuts that of *C. sandsorum* (Fig. 15), although the two species have never found in direct sympatry. *Cataxia stirlingi* builds a small palisade burrow with a fully open hole and no door, which is usually adorned with a radial skirt of leaves and twigs (Fig. 7). Based on the two male specimens that have been collected/reared, males may wander and mate in mid-late autumn.

**Conservation status.**—This species has a total (maximum) extent of occurrence of less than 20 km<sup>2</sup>, and an actual area of occupancy of significantly less than 10 km<sup>2</sup>. Given that the



number of well-defined locations at which the species has been found is less than five, and that there is continuing decline in the quality of habitat in the eastern Stirling Range National Park due to severe *Phytophthora* dieback (Barrett & Yates 2015), climate change in south-western Australia (Indian Ocean Climate Initiative 2002; Barrett & Yates 2015), and a potential increase in the severity and/or frequency of wildfires (e.g. as in 1991, 2000), this species is considered to be 'endangered' (IUCN B1, B2a, b[iii]).

## ACKNOWLEDGMENTS

This study is the culmination of over 25 years of field work in the Great Southern Region of south-western Australia, during which time numerous individuals have helped to survey for *Cataxia*, to collect material for molecular analysis, to collect the all-important male specimens required for morphological analysis, and to fund this field work. We would like to especially thank Sarah Barrett and Melinda Moir for their efforts in systematically sampling the montane invertebrate fauna of the Stirling Range National Park and Mount Manypeaks, often going to great lengths to access difficult terrain at high altitude. Many other collectors have also contributed specimens or assisted with field work over the years, including Ben Atkinson, Māra Blossfelds, Karl Brennan, Alec Coles, Sarah Comer, Alan Danks, Sophie Harrison, the late Bert Main, Nik Tatarnic, Alison Sampey, Deon Utber and Julianne Waldock. The 'South Coast Threatened Invertebrates Recovery Team' and the staff of the Western Australian (W.A.) Department of Parks and Wildlife's Albany Regional Office have supported this project over many years, and we would especially like to acknowledge the assistance of Sarah Comer, Alan Danks and Deon Utber. This work was funded by an Australian Biological Resources Study (ABRS) Taxonomy Research Grant (No. RF21506) to MGR, RJR and MSH, an Australian Research Council (ARC) Linkage Grant (No. LP120200092) to ADA, MGR, SJBC and MSH, and a Bioplatforms Australia (BPA) Grant to ADA and SJBC. The W.A. Department of Parks and Wildlife (formerly Department of Conservation and Land Management) and the Western Australian Museum's Butler Bequest Fieldwork Grants Fund provided additional financial assistance with field work.

## LITERATURE CITED

- Barrett, S. & C.J. Yates. 2015. Risks to a mountain summit ecosystem with endemic biota in southwestern Australia. *Austral Ecology* 40:423–432.
- Cooper, S.J.B., M.S. Harvey, K.M. Saint & B.Y. Main. 2011. Deep phylogeographic structuring of populations of the trapdoor spider *Moggridgea tingle* (Migidae) from southwestern Australia: evidence for long-term refugia within refugia. *Molecular Ecology* 20:3219–3236.
- de Queiroz, K. 2007. Species concepts and species delimitation. *Systematic Biology* 56:879–886.
- Edward, K.L. & M.S. Harvey. 2010. A review of the Australian millipede genus *Atelomastix* (Diplopoda: Spirostreptida: Iulomorphidae). *Zootaxa* 2371:1–63.
- Harvey, M.S., B.Y. Main, M.G. Rix & S.J.B. Cooper. 2015. Refugia within refugia: *in situ* speciation and conservation of threatened *Bertmainius* (Araneae: Migidae), a new genus of relictual trapdoor spiders endemic to the mesic zone of south-western Australia. *Invertebrate Systematics* 29:511–553.
- Hedin, M., D. Carlson & F. Coyle. 2015. Sky island diversification meets the multispecies coalescent – divergence in the spruce-fir moss spider (*Microhexura montivaga*, Araneae, Mygalomorphae) on the highest peaks of southern Appalachia. *Molecular Ecology* 24:3467–3484.
- Huelsenbeck, J.P. & F. Ronquist. 2001. MRBAYES: Bayesian inference of phylogenetic trees. *Bioinformatics* 17:754–755.
- Indian Ocean Climate Initiative. 2002. Climate Variability and Change in South West Western Australia. Indian Ocean Climate Initiative, Perth.
- Lanfear, R., B. Calcott, S.Y.W. Ho & S. Guindon. 2012. Partition-Finder: combined selection of partitioning schemes and substitution models for phylogenetic analyses. *Molecular Biology and Evolution* 29:1695–1701.
- Laurance, W.F., B. Dell, S.M. Turton, M.J. Lawes, L.B. Hutley, H. McCallum, et al. 2011. The ten Australian ecosystems most vulnerable to tipping points. *Biological Conservation* 144:1472–1480.
- Main, B.Y. 1985. Further studies on the systematics of ctenizid trapdoor spiders: a review of the Australian genera (Araneae: Mygalomorphae: Ctenizidae). *Australian Journal of Zoology Supplementary Series* 108:1–84.
- Main, B.Y. 1993a. From flood avoidance to foraging: adaptive shifts in trapdoor spider behaviour. *Memoirs of the Queensland Museum* 33:599–606.
- Main, B.Y. 1993b. Spiders of the Stirling Range. *Landscape* 8(3):28–34.
- Myers, N., R.A. Mittermeier, C.G. Mittermeier, G.A.B. da Fonseca & J. Kent. 2000. Biodiversity hotspots for conservation priorities. *Nature* 403:853–858.
- Rainbow, W.J. 1914. Studies in Australian Araneidae – No. 6. The Terretelariae. *Records of the Australian Museum* 10:187–270.
- Rambaut, A., M.A. Suchard, D. Xie & A.J. Drummond. 2014. Tracer v1.6. Available online at <http://beast.community/index.html> (accessed May 2017).
- Raven, R.J. 1985. The spider infraorder Mygalomorphae (Araneae): cladistics and systematics. *Bulletin of the American Museum of Natural History* 182:1–180.
- Rix, M.G. and M.S. Harvey. 2012a. Australian Assassins, Part II: A review of the new assassin spider genus *Zephyrarchaea* (Araneae, Archaeidae) from southern Australia. *ZooKeys* 191:1–62.
- Rix, M.G. and M.S. Harvey. 2012b. Phylogeny and historical biogeography of ancient assassin spiders (Araneae: Archaeidae) in the Australian mesic zone: evidence for Miocene speciation within Tertiary refugia. *Molecular Phylogenetics and Evolution* 62:375–396.
- Rix, M.G., S.J.B. Cooper, K. Meusemann, S. Klopstein, S.E. Harrison, M.S. Harvey et al. 2017a. Post-Eocene climate change across continental Australia and the diversification of Australasian spiny trapdoor spiders (Idiopidae). *Molecular Phylogenetics and Evolution* 109:302–320.
- Rix, M.G., D.L. Edwards, M. Byrne, M.S. Harvey, L. Joseph & J.D. Roberts. 2015. Biogeography and speciation of terrestrial fauna in the south-western Australian biodiversity hotspot. *Biological Reviews* 90:762–793.
- Rix, M.G., J. Huey, B.Y. Main, J.M. Waldock, S.E. Harrison, S. Comer, et al. 2017b. Where have all the spiders gone? The decline of a poorly known invertebrate fauna in the agricultural and arid zones of southern Australia. *Austral Entomology* 56:14–22.
- Rix, M.G., R.J. Raven, B.Y. Main, S.E. Harrison, A.D. Austin, S.J.B. Cooper et al. 2017c. The Australasian spiny trapdoor spiders of the family Idiopidae (Mygalomorphae: Arbanitinae): a relimitation and revision at the generic level. *Invertebrate Systematics* 31: 566–634.



- Rix, M.G., J.D. Roberts & M.S. Harvey. 2009. The spider families Synotaxidae and Malkaridae (Arachnida: Araneae: Araneoidea) in Western Australia. *Records of the Western Australian Museum* 25:295–304.
- Ronquist, F. & J.P. Huelsenbeck. 2003. MrBayes 3: Bayesian phylogenetic inference under mixed models. *Bioinformatics* 19:1572–1574.
- Shearer, B.L., C.E. Crane and A. Cochrane. 2004. Quantification of the susceptibility of the native flora of the South-West Botanical Province, Western Australia, to *Phytophthora cinnamomi*. *Australian Journal of Botany* 52:435–443.
- Tamura, K., G. Stecher, D. Peterson, A. Filipski & S. Kumar. 2013. MEGA6: Molecular evolutionary genetics analysis version 6.0. *Molecular Biology and Evolution* 30:2725–2729.

*Manuscript received 5 February 2017, revised 15 May 2017.*



# Redescription of *Geogarypus minor*, type species of the genus *Geogarypus*, and description of a new species from Italy (Pseudoscorpiones: Geogarypidae)

Giulio Gardini<sup>1</sup>, Loris Galli<sup>2</sup> and Matteo Zinni<sup>2</sup>: <sup>1</sup>Via Monte Corno 12/1, 16166 Genoa, Italy. E-mail: giuliogardini@libero.it <sup>2</sup>DISTAV, Università degli Studi di Genova, Corso Europa 26, 16132 Genoa, Italy

**Abstract.** The type species of the pseudoscorpion genus *Geogarypus* Chamberlin, 1930, *Geogarypus minor* (L. Koch, 1873), is redescribed from the newly designated female lectotype and numerous specimens from southern France, Corsica and Italy. *Geogarypus nigritarsis* (Simon, 1879) is newly designated as a junior subjective synonym of *G. minor*, and a new species, *G. italicus* sp. nov. (type locality Bergeggi, Western Liguria, Italy), is described from specimens from mainland Italy, Sicily and Sardinia. A key to the Mediterranean-Macaronesian species of the genus is proposed.

**Keywords:** New species, new synonymy, type species, lectotype, Mediterranean-Macaronesian area, *Geogarypus*

ZooBank publication: <http://zoobank.org/references/urn:lsid:zoobank.org:pub:B6C60C51-5C0B-4481-8B77-13BA7F44B1CC>

The pseudoscorpion family Geogarypidae is widely distributed around the world and currently contains three genera: *Geogarypus* Chamberlin, 1930, *Afrogarypus* Beier, 1931 and *Indogarypus* Beier, 1957 (Harvey 1986, 1992). Diagnostic characters of these genera, reported in Harvey (1986), are the absence of a sulcus on pedipalpal chela and the presence of accessory teeth on fixed chelal finger in *Geogarypus* (however *G. mirei* Heurtault, 1970 lacks accessory teeth), the presence of a dorsal sulcus and the absence of accessory teeth in *Afrogarypus*, and the presence of both an interno-lateral sulcus and accessory teeth in *Indogarypus*. The relationships among Geogarypidae and other families of Garypoidea are subsequently discussed in Harvey (1992).

The pseudoscorpion genus *Geogarypus* was established by Chamberlin (1930), and includes 45 extant and three fossil nominal species. The genus is widely distributed in most temperate and tropical regions of the world, and is only noticeably absent from the Nearctic Region (Harvey 2013; Batuwita & Benjamin 2014; Nassirikhani 2014). The fossil species are known only from Baltic and Rovno amber (Henderickx & Perkovsky 2012; Harvey 2013). Eight species are known from the Mediterranean-Macaronesian area, of which only *Geogarypus minor* (L. Koch, 1873) and *G. nigritarsis* (Simon, 1879) are widely distributed in this area, with the others more localised (Harvey 2013).

The present work presents a modern redescription of *G. minor*, the type species of the genus, and the description of a new species of *Geogarypus* from Italy. A key to Mediterranean-Macaronesian species of *Geogarypus* is also presented.

## METHODS

This study is based on the examination of 2,025 adult specimens and 466 nymphs of *Geogarypus*, lodged chiefly in the collection of the first author (GG, those without acronym in the text) and in the following institutions: Muséum d'Histoire naturelle, Geneva (MHNG), Muséum National d'Histoire Naturelle, Paris (MNHN), Museo Civico di Storia Naturale "G. Doria", Genoa (MSNG), Museo Civico di Storia Naturale, Verona (MSNV), Departamento de Biología Animal (Zoología), Universidad de La Laguna, Tenerife

(MZUL), Museo di Zoologia dell'Università degli Studi, Padua (MZUP), and Natural History Museum, London (NHM).

The specimens here referred to *G. minor* and *G. italicus* were compared with the following material:

**Material examined of *Geogarypus shulovi*.**—GREECE: *Dodecanese*: *Kōs*: 1 ♂, 2 ♀ with embryos, Lambi, garden and beach of Hotel Atlantis, 21–27 June 1993, F. Gasparo. **TURKEY**: *Mersin*: 1 ♀, 1 tritonymph, near Tönük, 380 m a.s.l., 8 July 1988, G. Gardini, R. Rizzerio & S. Zoia. *Isparta*: 1 ♀, Bademli, 16 July 1988, G. Gardini, R. Rizzerio & S. Zoia.

**Material examined of *Geogarypus mirei*.**—SPAIN: *Canary Islands*: *Gran Canaria*: 1 ♂, 1 ♀ (*G. mirei*, V. Mahnert det.), Maspalomas Dunas, aus trockenen Stengel, 9 December 2002, H.-P. Reike (MHNG).

**Material examined of *Geogarypus canariensis*.**—SPAIN: *Canary Islands*: *Tenerife*: 1 ♂, 1 ♀ (*G. canariensis*, V. Mahnert det.), Icod de los Vinos, 500 m a.s.l., 10 March 1974, T. Palm, *Laurus* (MHNG); 1 ♂, 1 ♀ (*G. canariensis*, V. Mahnert det.), Tenerife, 30 November 1977, Heiss (MHNG); 1 ♀ (*G. canariensis*, V. Mahnert det.), Cueva del Viento, 7 February 1981, J.L. Martin (MZUL); 1 ♂ (remains), 4 ♀ (*G. canariensis*, V. Mahnert det.), Aguamansa, 1100–1400 m a.s.l., 13–17 February 1982, K. Thaler (MHNG); 1 ♀ (*G. canariensis*, V. Mahnert det.), Monte del Agua, 22 December 1987, P. Oromí (MZUL); 1 ♀, Aguamansa, 7 May 1995, C. Canepari; 1 ♀ (*G. canariensis*, V. Mahnert det.), Cañadas, Risco Verde, 8 June 1995, N. Arechavaleta (MZUL); 1 ♀ (*G. canariensis*, P. Oromí det.), Cañadas, San Antonio, 25 May 1996, P. Oromí (MZUL); 1 ♂, 3 ♀ (*G. minor*, V. Mahnert det.), La Victoria, pine forest, 7 April 2001, G.B. Delgrado (MHNG).

**Material examined of *Geogarypus cf. canariensis*.**—SPAIN: *Canary Islands*: *Gran Canaria*: 1 ♂, 1 ♀ (*G. minor*, V. Mahnert det.), Buco Oscuro, 8 January 1988, P. Oromí (MHNG). *Lanzarote*: 1 ♂, 1 ♀ (*G. minor*, V. Mahnert det.), Mta. Clara, Caldera, termizado, 25–28 February 2002, Giet (MHNG); 1 ♂, 1 ♀ (*G. canariensis*, V. Mahnert det.), Valle do Temisa, MSS, 13 January 2007, M. Egoz (MZUL).

Specimens were cleared in 10% KOH solution at 40°C for several hours, washed in distilled water and temporarily mounted—after dissection of right palp, chelicera, legs I and





Figures 1–2.—1, *Geogarypus minor* (L. Koch, 1873), female lectotype from Corsica (NHM); 2, *Geogarypus italicus* sp. nov., male holotype from Bergeggi, Liguria (MHNG) (Phot. C. Giusto). Scale line : 1 mm.

IV—in cavity slides with 60% lactic acid. Each specimen was rinsed, after study, in distilled water and returned to a vial of 70% ethanol together with the dissected portions in glass capillary tubes. All specimens were studied using an Olympus BHB compound microscope; drawings were made with the aid of a Nachet drawing tube. Measurements (expressed in mm) and proportions are given as length/breadth for carapace, chelicerae and pedipalps and as length/depth for legs; depth was also measured for the palpal chela. Terminology and reference points for measurements largely follow Chamberlin (1931), and the terminology of trichobothria and cheliceral setae also follow Harvey (1986, 1992); the use of the terms antiaxial and paraxial follows Judson (2007).

Synonymies are supplied in the case of changes relative to the catalogue of Harvey (2013), as a consequence of revised identifications. The Italian regions are listed in the order from N to S, followed by Sicily and Sardinia. As regards Sardinia,

its administrative division into four Provinces (Sassari, Nuoro, Oristano, Cagliari) is followed, as used formally before 2005.

## SYSTEMATICS

Family Geogarypidae Chamberlin, 1930

Genus *Geogarypus* Chamberlin, 1930

*Geogarypus* Chamberlin 1930:609.

**Type species.**—*Garypus minor* L. Koch, 1873, by original designation.

*Geogarypus minor* (L. Koch, 1873)

<http://zoobank.org/NomenclaturalActs/urn:lsid:zoobank.org:aet:0954EDF3-4758-4A78-9793-9A4B1A49A655>

Figs 1, 3–24, 46–47, 54

*Garypus minor* L. Koch 1873:38; Ellingsen 1908:670 (Giglio Is., in part: see *G. italicus*).

*Garypus nigrimanus* Simon 1879:47, 312. **Syn. nov.**

*Garypus meridionalis* Canestrini 1885:n.7.

*Garypus nigrimanus* Simon: Simon 1898:21; Simon 1900:592; Gestro 1904:14 (Cagliari; Golfo Aranci, in part: see *G. italicus*).

*Geogarypus nigrimanus* (Simon): Beier 1963a:259; Lazzeroni 1969:335 (Ginosa Marina; Ciminà, Antonimina, in part: see *G. italicus*); Callaini 1983:151; Callaini 1989:145 (Levanzo Is.); Gardini et al. 1997:223.

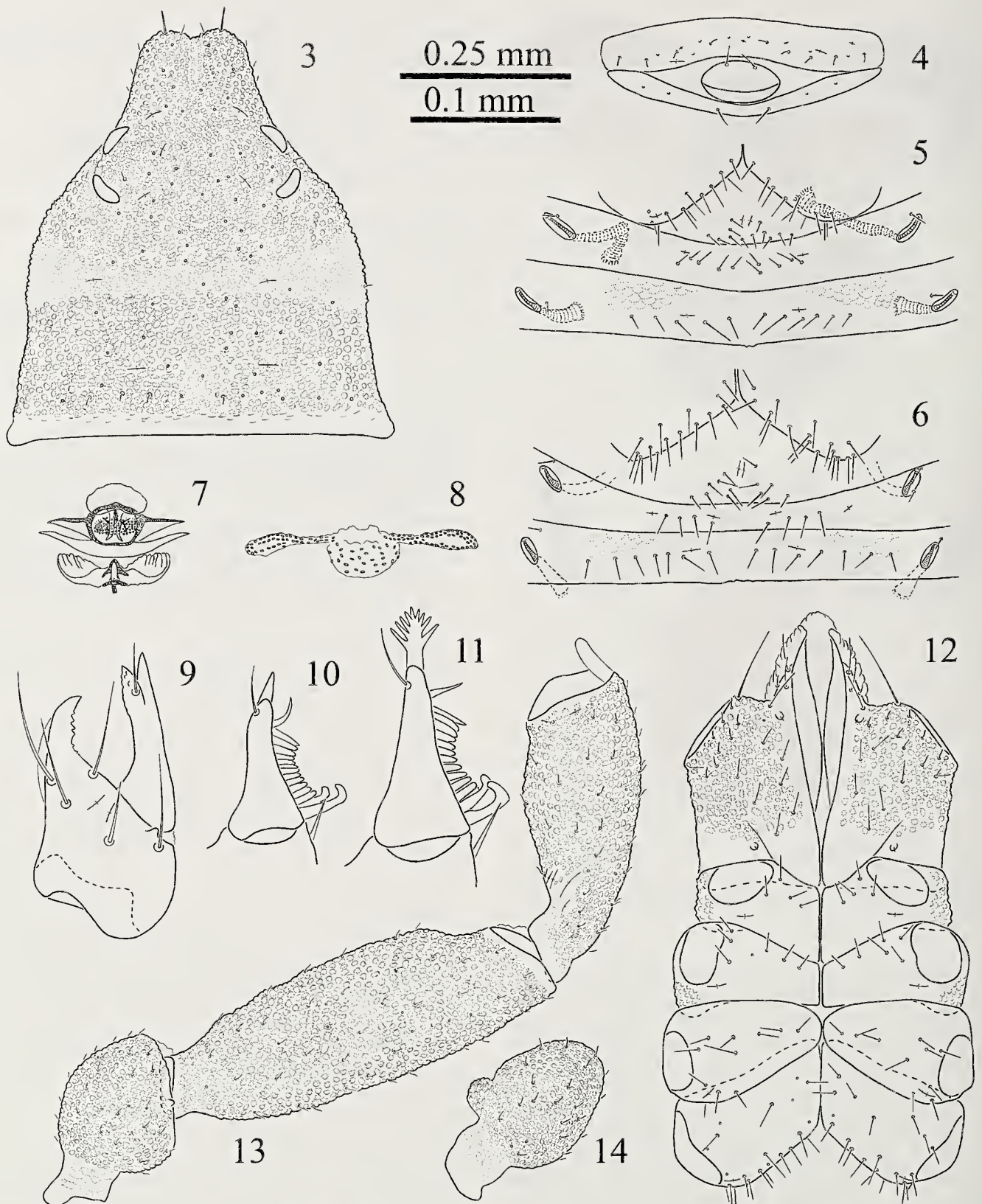
**Material examined.**—*Lectotype* of *Garypus minor*: FRANCE: ♀ (here designated), “Corsica / E. Simon” “BMNH 1913.9.1.449” “*Garypus minor* L. Koch / Syntype (?) ♀ / M. Judson det. 1992” (NHM).

*Paralectotypes* (probable) of *Garypus minor*: FRANCE and ALGERIA: 5 ♂, 21 ♀ (mixture of probable paralectotypes and non-types, together with 1 ♀ of *Geogarypus* sp.), “2376, *G. minor* L.K., Corsica, Alg.” (MNHN).

*Syntypes* of *Garypus nigrimanus*: FRANCE: 5 ♂, 15 ♀ (syntypes mixed with non-type specimens), “2362, *G. nigrimanus* E.S., Gallia <sup>m</sup> Corsica”, “St Martin Vesubie, A. Gr[ouville]. 1911” (MNHN).

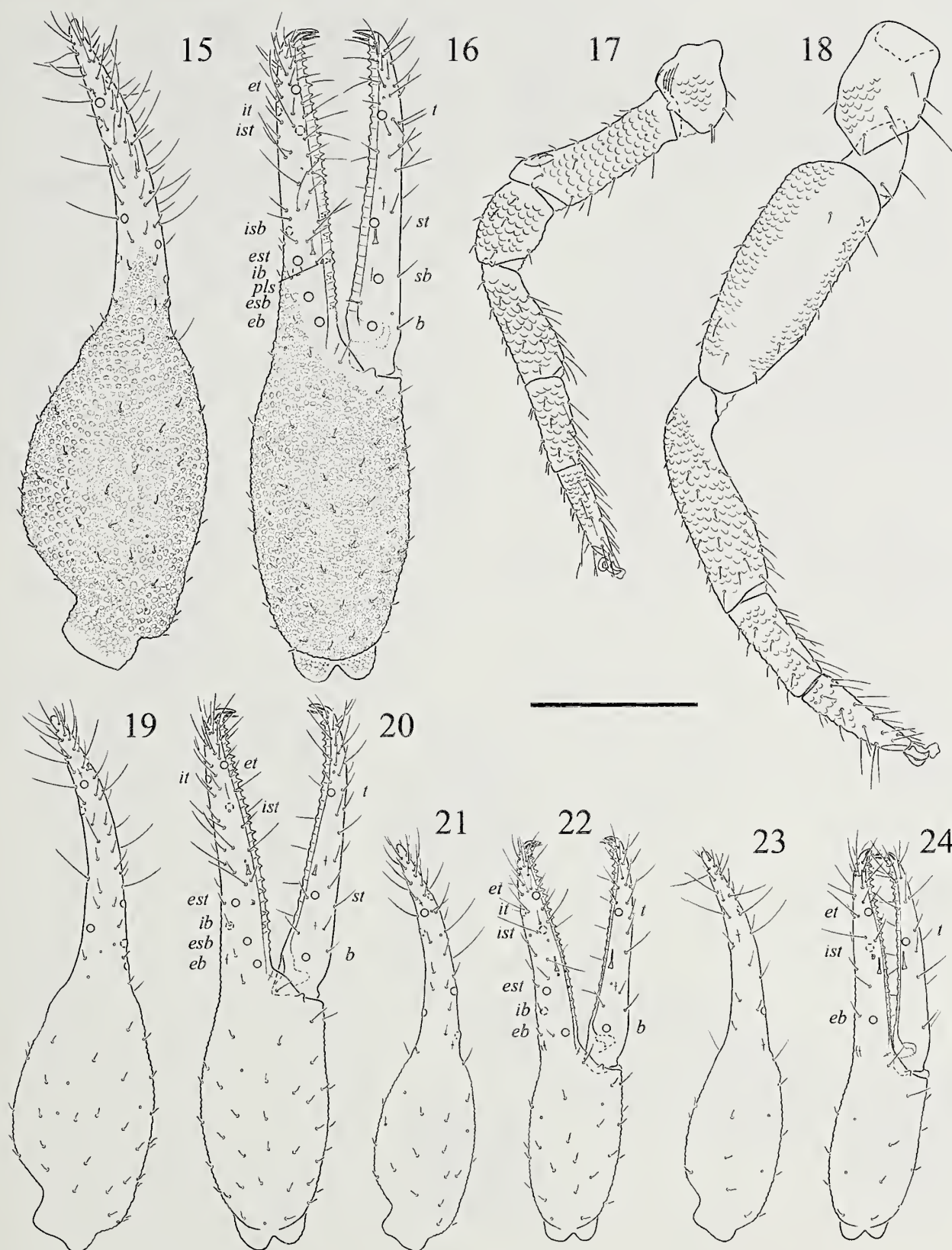
*Other material*: FRANCE: *Pyrénées Orientales*: 1 ♂, 1 ♀, Perpignan, Salses, 30 April 1967, G. Osella (MSNV). *Hérault*: 1 tritonymph, Montpellier, Clapiers, 80 m a.s.l., 30 April 2015, G. Gardini, leaf litter garigue; 1 tritonymph (*G. nigrimanus*, V. Mahnert det.), Frontignan, Montagne de la Gardiole, 24 July 1977, P. Haymoz (MHNG). *Gard*: 1 deutonymph (*G. nigrimanus*, V. Mahnert det.), Ussel, 26 July 1980, F. Baud, wood (MHNG). *Bouches du Rhône*: 1 ♀ (*G. minor*, V. Mahnert det.), Martigue, 16 September 1978, V. Mahnert, leaf litter in town (MHNG). *Vauchuse*: 1 ♀ (*G. minor*, V. Mahnert det.), Montagne du Luberon, Cucuron, 2 August 1975, P. Haymoz (MHNG); 1 ♂ (*G. minor*, V. Mahnert det.), Montagne du Luberon, Vitrolles, 2 August 1975, P. Haymoz (MHNG). *Var*: 1 ♂, 1 ♀, Hyères, Villa Noailles, 116 m a.s.l., 5 April 2015, G. Gardini, under *Pistacia lentiscus*; 4 ♂, 1 tritonymph, Hyères, Île de Porquerolles, 10–50 m a.s.l., 19 May 2013, G. Gardini, C. Giusto & S. Zoia; 16 ♂, 19 ♀, 1 tritonymph, Hyères, Île de Bagaud, 9 December 2011, P. Ponel, *Quercus ilex* wood; 14 ♂, 24 ♀, Hyères, Île de Bagaud, 9 December 2011, P. Ponel, under *Pistacia lentiscus*; 8 ♂, 11 ♀,





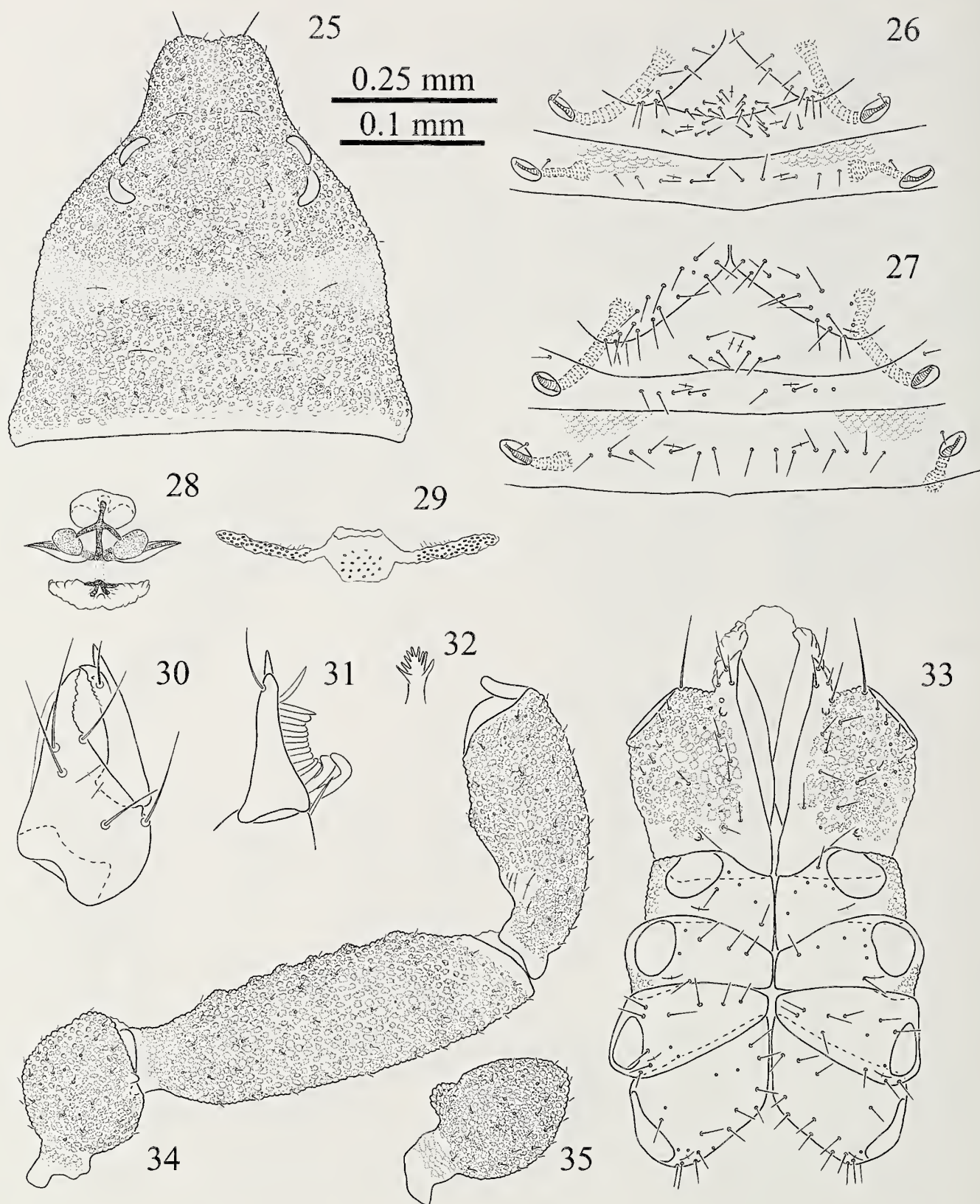
Figures 3-14.—*Geogarypus minor* (L. Koch, 1873), male from Finale Ligure, Caprazoppa (7 October 1975), unless stated otherwise. 3, Carapace, dorsal; 4, Tergites and sternites XI-XII, posterior; 5, Sternites II-IV; 6, Sternites II-IV, female; 7, Genitalia, ventral; 8, Genitalia, ventral, female; 9, Chelicera, dorsal; 10, Movable finger with galea, rallum and serrula exterior, lateral; 11, Movable finger with galea, rallum and serrula exterior, lateral, female; 12, Coxal area, ventral; 13, Right trochanter, femur and patella, dorsal; 14, Right trochanter, lateral. Scale lines: 0.25 mm (Figs. 3-8, 12-14), 0.1 mm (Figs. 9-11).





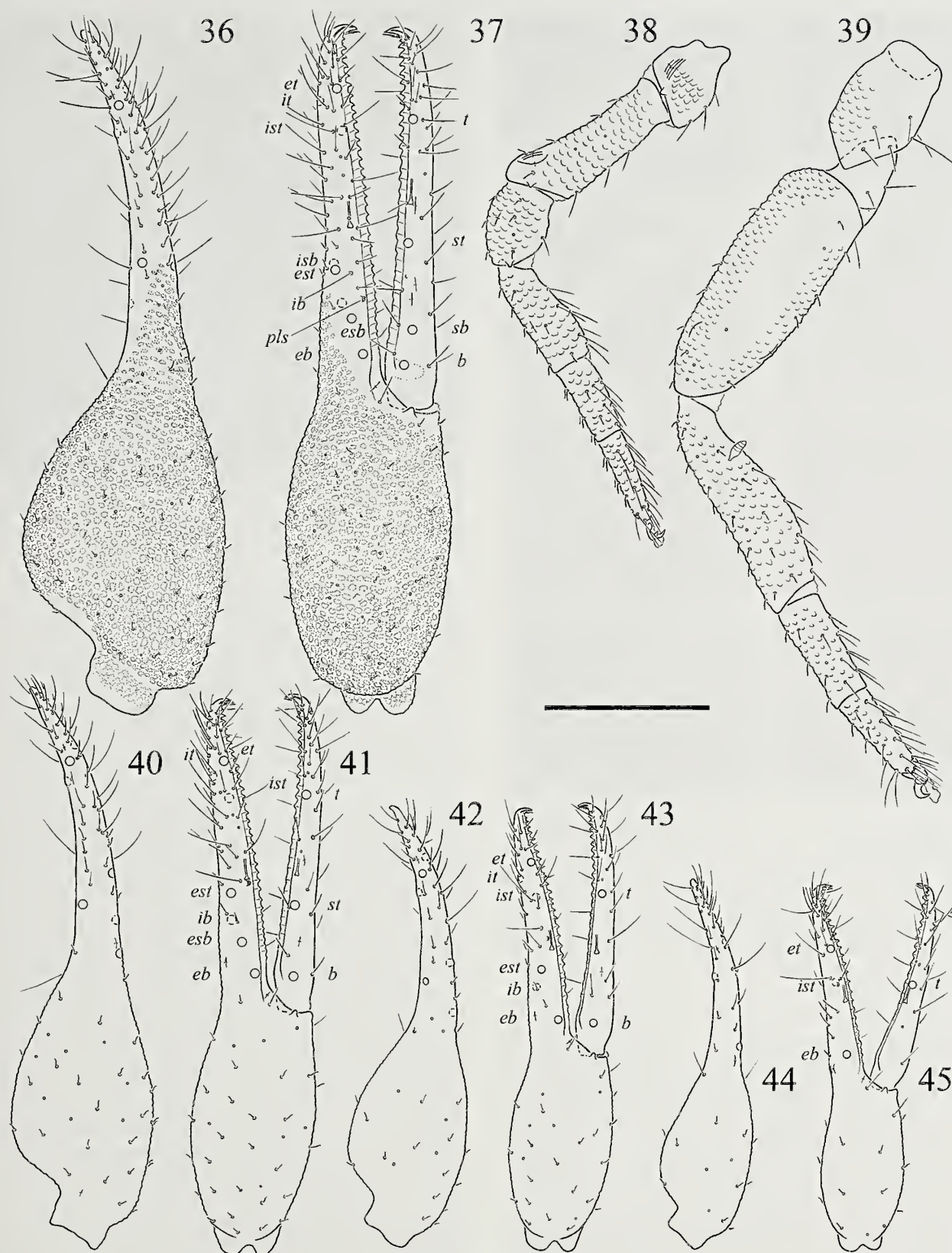
Figures 15–24.—*Geogarypus minor* (L. Koch, 1873), male from Finale Ligure, Caprazoppa (7 October 1975), unless stated otherwise. 15, Right chela, dorsal; 16, Right chela, lateral; 17, Right leg I, lateral; 18, Right leg IV, lateral. 19, Right chela, dorsal (granulation omitted), tritonymph; 20, Right chela, lateral (granulation omitted), tritonymph; 21, Right chela, dorsal (granulation omitted), deutonymph; 22, Right chela, lateral (granulation omitted), deutonymph; 23, Right chela, dorsal, protonymph from Caronia, Mt. Pagano (granulation omitted); 24, Right chela, lateral, protonymph from Caronia, Mt. Pagano (granulation omitted). Scale line: 0.25 mm.





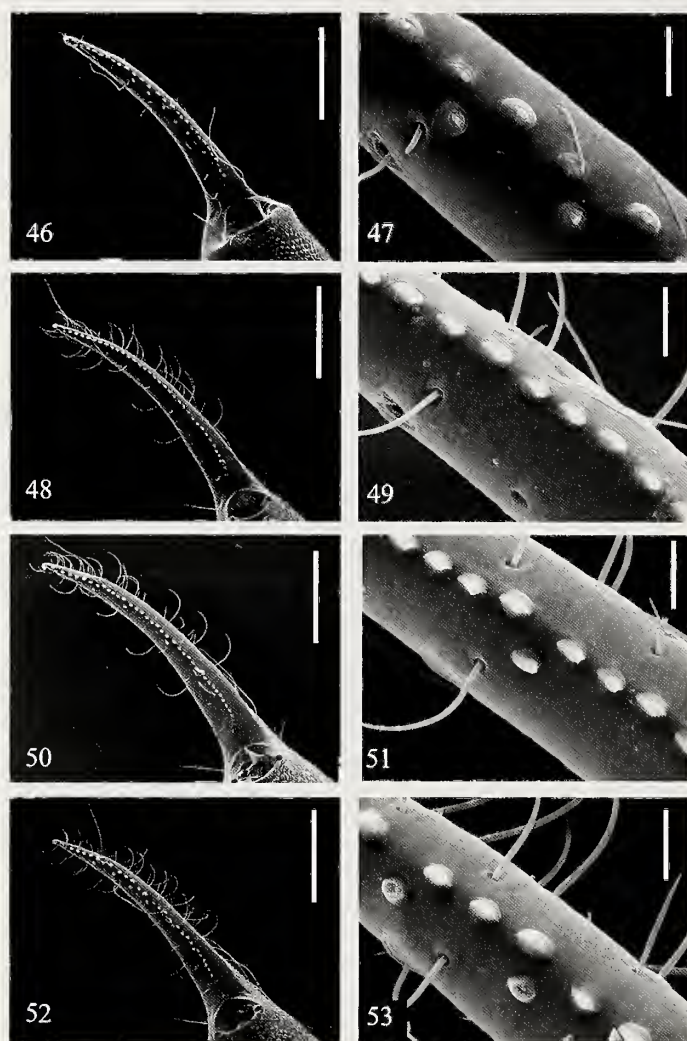
Figures 25–35.—*Geogarypus italicus* sp. nov., male paratype from Bergeggi (30 July 2007), unless stated otherwise. 25, Carapace, dorsal; 26, Sternites II–IV; 27, Sternites II–IV, female paratype from Bergeggi (30 July 2007); 28, Genitalia, ventral; 29, Genitalia, ventral, female paratype from Bergeggi (30 July 2007); 30, Chelicera, dorsal; 31, Movable finger with galea, rallum and serrula exterior, lateral; 32, Galea, female paratype from Bergeggi (30 July 2007); 33, Coxal area, ventral; 34, Right trochanter, femur and patella, dorsal; 35, Right trochanter, lateral. Scale lines: 0.25 mm (Figs. 25–29, 33–35), 0.1 mm (Figs. 30–32).





Figures 36–45.—*Geogarypus italicus* sp. nov., male paratype from Bergeggi (30 July 2007), unless state otherwise. 36, Right chela, dorsal; 37, Right chela, lateral; 38, Right leg I, lateral; 39, Right leg IV, lateral [with *Amphoromorpha* sp. (Zygomycota) on tibia]; 40, Right chela, dorsal (granulation omitted), tritonymph paratype from Bergeggi (30 July 2007); 41, Right chela, lateral (granulation omitted), tritonymph paratype from Bergeggi (30 July 2007); 42, Right chela, dorsal (granulation omitted), deutonymph paratype from Bergeggi (30 July 2007); 43, Right chela, lateral (granulation omitted), deutonymph paratype from Bergeggi (30 July 2007); 44, Right chela, dorsal (granulation omitted), protonymph paratype from Bergeggi (30 July 2007); 45, Right chela, lateral (granulation omitted), protonymph paratype from Bergeggi (30 July 2007). Scale line: 0.25 mm.





Figures 46–53.—Dentition of left chelal finger (♀) and detail at level of trichobothrium *ist*, ventral view. 46, 47, *Geogarypus minor* (L. Koch, 1873) from Finale Ligure, Caprazoppa (7 October 1975); 48, 49, *G. italicus* sp. nov., paratype from Bergoglio (15 October 2007); 50, 51, *G. italicus* sp. nov. from Popoli, Capo Pescara (20 November 1991); 52, 53, *G. canariensis* (Tullgren, 1900) from Tenerife, Orotava, Aguamansa (13/17 February 1982). Scale line 200µm and 20µm for full vision and detail, respectively.

1 tritonymph, Hyères, Île de Bagaud, 13 December 2012, P. Ponel, under *Myrtus communis*; 7 ♂, 3 ♀, Hyères, Île de Bagaud, 13 December 2012, P. Ponel, under *Pistacia lentiscus*; 1 ♂, 1 ♀, Ramatuelle, Plage de l'Escalet, 20 May 2013, G. Gardini, C. Giusto & S. Zoia; 1 ♀, Signes, Plateau de Siou Blanc, 640 m a.s.l., 20 May 2013, G. Gardini, C. Giusto & S. Zoia. *Alpes Maritimes*: 3 ♂, 7 ♀ (*G. nigrimanus*, E. Simon det.), near Nice, February 1901, A. Dodero (MSNG). *Corse*: 1 ♀, Aleria, near Frassicia, 27 April 2001, R. Poggi (MSNG); 3 ♂, 3 ♀, Lugo di Nazza, near Pinzalone, 150 m a.s.l., 20 May 2002, R. Poggi (MSNG); 1 ♀ (*G. nigrimanus*, G. Callaini det.), Bastia, Pineto, 2 August 1978, A. Sette (MSNV); 1 deutonymph, St-Florent, Quercialba, 21 April 1992, M. Bodon; 1 ♂ (*G. nigrimanus*, G. Callaini det.), Desert Agriates, Baccialu, 29 May 1979, R. Poggi, leaf litter *Erica* sp. (MSNG); 1 ♀ (*G. nigrimanus*, V. Mahnert det.), Cauria, Dolmen (Bosquet), 24

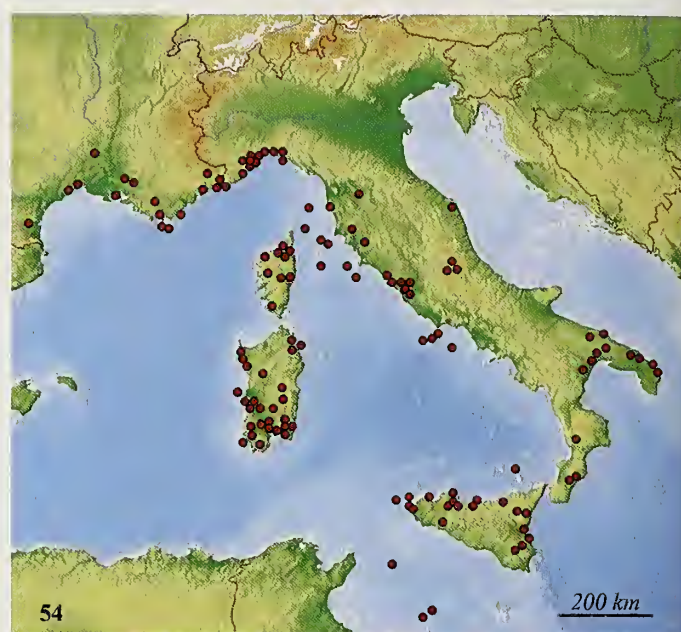


Figure 54.—Map depicting known distribution of *Geogarypus minor* (L. Koch, 1873) from southern France, Corse and Italy.

April 1973, S. Vit (MHNG); 1 ♀ (*G. minor*, V. Mahnert det.), Oletta, St-François, 6 July 1974, I. Löbl (MHNG); 1 ♂, 1 ♀ (*G. minor*, V. Mahnert det.), Guagno-Les-Bain, 17 July 1974, I. Löbl (MHNG); 1 ♂, Calvi, Forêt de Bofinatu, 800 m a.s.l., 30 April 2001, B. Knoflach & K. Thaler (MHNG).

**ITALY:** *Liguria: Imperia Prov.*: 1 ♂, Ventimiglia, Grimaldi, 10 January 1975, G. Gardini, under stone near the sea; 1 ♂, 1 ♀, 1 tritonymph, Ventimiglia, Mortola Inferiore, 9 January 1975, G. Gardini, soil near the sea; 1 ♂, Ventimiglia, Mortola Inferiore, Villa Hanbury, 9 January 1975, G. Gardini, under bark of *Pinus halepensis*; 1 ♂, 1 tritonymph, Ventimiglia, Mortola Superiore, 150 m a.s.l., 16 May 1976, R. Poggi, under *Pistacia lentiscus*; 8 ♂, 5 ♀, 1 tritonymph, Ventimiglia, Mortola Superiore, 30 March 1976, G. Gardini, under *Pistacia lentiscus*; 1 ♀ (together with 1 ♂ of *G. italicus*), Ventimiglia, Torri, Val Bevera, 60 m a.s.l., 31 March 2008, R. Poggi (MSNG). *Liguria: Savona Prov.*: 1 ♀, Laigueglia, Capo Mele, 6 March 1973, G. Gardini, under *Pistacia lentiscus*; 1 ♀, Laigueglia, Capo Mele, 24 February 1974, G. Gardini, cliff; 1 ♂ (*G. nigrimanus*, G. Callaini det.), Laigueglia, Capo Mele, 230 m a.s.l., 10 July 1977, R. Poggi (MSNG); 2 tritonymphs, 1 deutonymph, Laigueglia, Capo Mele, 230 m a.s.l., 16 June 1984, R. Poggi, under *Cistus* (MSNG); 1 tritonymph (*G. nigrimanus*, G. Gardini det.), Laigueglia, Capo Mele, 11 May 1990, R. Poggi (MSNG); 2 ♂, 2 ♀ (*G. nigrimanus*, G. Gardini det.), Laigueglia, Capo Mele, 22 June 1990, R. Poggi, under *Pistacia lentiscus* (MSNG); 1 ♀ (*G. nigrimanus*, G. Gardini det.), Laigueglia, Capo Mele, 19 October 1990, R. Poggi (MSNG); 1 ♀ (*Garypus minor*, E. Simon det.), Albenga, 29 May 1900, A. Dodero (MSNG); 1 ♂, 1 ♀, 1 tritonymph, Toirano, Salto del Lupo, 183 m a.s.l., 5 July 2009, R. Poggi (MSNG); 1 ♀, Ceriale, Peagna, 10 November 1988, G. Gardini; 3 ♂, 3 ♀ (*Garypus nigrimanus*, E. Simon det.), Finale Ligure, Caprazoppa, 22 May 1899, A. Dodero (MSNG); 7 ♂, 11 ♀, Finale Ligure, Caprazoppa, 11 November 1973, G.



Bartoli, G. Gardini & R. Poggi, under *Euphorbia*; 2 ♂, 4 ♀, Finale Ligure, Caprazoppa, 10 December 1973, G. Bartoli, under *Cistus*; 3 ♂, 2 ♀, Finale Ligure, Caprazoppa, 10 March 1974, G. Gardini, sieved in garigue; 11 ♂, 12 ♀, 2 tritonymphs, 2 deutonymphs, Finale Ligure, Caprazoppa, 7 October 1975, R. Poggi, sieved under *Cistus* and *Euphorbia*; 1 ♂, 3 ♀, Finale Ligure, Caprazoppa, 21 November 1975, G. Bartoli; 2 ♂, 1 ♀, 1 tritonymph (*G. nigrimanus*, G. Callaini det.), Finale Ligure, Caprazoppa, 26 December 1977, G. Bartoli, sieved under *Cistus* and *Pistacia* (MSNG); 1 ♂, Finale Ligure, Caprazoppa, 29 October 1982, G. Gardini, under *Euphorbia*; 1 tritonymph, 1 deutonymph, Finale Ligure, Caprazoppa, 7 March 1985, C. Giusto; 4 ♂, 4 ♀, Finale Ligure, Caprazoppa, 220 m a.s.l., 14 November 1998, C. Giusto; 5 ♀, Finale Ligure, Caprazoppa, 190 m a.s.l., 44°09'50"N, 8°19'17"E, 18 December 2015, G. Gardini & A. Trotta, garigue; 1 ♂, 1 ♀, Finale Ligure, Caprazoppa, Cava di Rio Fine, 80 m a.s.l., 44°09'42.71"N, 8°19'29.81"E, 21 November 2015, G. Gardini, C. Giusto & A. Trotta, Mediterranean scrub; 1 deutonymph, Finale Ligure, Caprazoppa, Torre Colombara, 10 m a.s.l., 44°09'47.15"N, 8°20'13.36"E, 21 November 2015, G. Gardini, C. Giusto & A. Trotta, cliff, under *Limonium*; 2 ♀, Noli, Semaforo di Capo Noli, 4 April 1976, R. Poggi, under *Cistus*; 1 ♂, 1 ♀ (together with 2 ♀, 3 tritonymphs of *G. italicus*), Spotorno, 16 January 1977, G. Gardini, under *Pistacia*; 3 ♂, 1 tritonymph (together with 5 ♂, 5 ♀, 2 tritonymphs of *G. italicus*), Spotorno, Isola di Bergeggi, 7 May 2007, R. Poggi (MSNG). *Liguria: Genoa Prov.*: 1 ♀, Arenzano, Rio Cantarena, 500 m a.s.l., 20 November 1994, G. Gardini, sieved under *Quercus ilex*; 1 ♀, Genova, Sestri Ponente, Monte Gazzo, 410 m a.s.l., 23 November 2010, M. Capurro & S. Ferretti, *Quercus ilex* wood; 3 ♀ (*Garypus minor*, E. Simon det.), Sestri Ponente, Borzoli, Villa Doria, 1883, G. Doria (MSNG); 1 ♀, Genova, Santa Tecla, May 1901, G. Mantero (MSNG); 1 ♂, 2 ♀, 1 tritonymph (*G. minor*, M. Beier det.), Genova, San Rocco, September 1929, F. Capra (MSNG); 2 ♂, Genova, Forte Richelieu, 16 April 2001, S. Zoia; 2 ♂, Genova, Quinto al Mare, 25 January 1976, S. Riese, under bark of *Pinus*; 1 ♂, Genova, Quinto al Mare, Rio San Pietro, 70 m a.s.l., 18 October 2009, G. Gardini, hollow *Olea europaea*; 1 ♂, Genova, Quinto al Mare, Rio San Pietro, 50 m a.s.l., 29 March 2011, C. Giusto; 11 ♀, Genova, Quinto al Mare, slope S Monte Fasce, 520 m a.s.l., 20 May 2005, G. Gardini & A. Trotta, in brood nests; 1 ♀, Genova, Quinto al Mare, slope SE Monte Fasce, 200 m a.s.l., 14 March 2006, G. Gardini; 1 ♀, Genova, Quinto al Mare, 500 m a.s.l., 5 November 2006, G. Gardini & S. Zoia; 2 ♀, Genova, Quinto al Mare, slope W Monte Fasce, 500 m a.s.l., 7 April 2010, G. Gardini; 1 ♀, 1 deutonymph, Genova, Quinto al Mare, slope S Monte Fasce, 480 m a.s.l., 44°23'46"N, 9°01'46"E, 1 December 2015, G. Gardini, garigue; 1 ♂, 1 ♀, Genova, Quinto al Mare, slope Monte Moro, 150 m a.s.l., 24 September 2003, G. Gardini, *Quercus pubescens* wood; 1 ♀, Genova, Quinto al Mare, 100 m a.s.l., 15 February 2008, G. Gardini; 6 ♂, 1 tritonymph, Genova, Quinto al Mare, slope SW Monte Moro, 150 m a.s.l., 14 January 2007, G. Gardini, under *Arbutus unedo*; 5 ♀, Genova, Quinto al Mare, slope W Monte Moro, 150 m a.s.l., 5 March 2010, G. Gardini, in brood nests; 1 ♂ (together with 3 ♂ of *G. italicus*), Genova, Quinto al Mare, 240 m a.s.l.,

44°23'44"N, 9°01'24"E, 26 November 2015, G. Gardini, under *Arbutus unedo*; 1 ♂, Genova, Quinto al Mare, slope S Monte Moro, 110 m a.s.l., 44°23'24"N, 9°01'01"E, 4 December 2015, G. Gardini, sub *Arbutus* and *Myrtus*; 2 ♂, 1 tritonymph, Camogli, slope E Monte Toceo, 440 m a.s.l., 5 November 1998, G. Gardini, under *Calicotome* and *Euphorbia*; 4 ♂, 3 ♀, 7 tritonymphs, 1 deutonymph, Portofino, Punta Chiappa, 2 m a.s.l., 4 January 1984, C. Giusto, under *Limonium*. *Tuscany: Florence Prov.*: 1 ♀, Fiesole, 9 April 1984, G. Gardini & S. Zoia. *Tuscany: Livorno Prov.*: 1 ♀ (*Garypus minor*, E. Ellingsen det.), near Livorno, June 1908, A. Andreini (MSNG); 1 tritonymph (*Garypus minor*, E. Ellingsen det.), Isola di Gorgona, [no date], A. Andreini (MSNG); 1 ♂, Isola di Gorgona, settore settentrionale, 4 October 2016, R. Poggi (MSNG); 1 ♀, Isola di Capraia, 7 October 1974, G. Gardini, under *Pistacia*; 3 ♂, 1 ♀, Isola di Capraia, 12 September 1992, C. Bellò; 1 ♂, 1 ♀, Isola di Capraia, Capraia Isola, 1 October 1974, G. Gardini, under *Pistacia*; 1 ♂, 1 ♀, Isola di Capraia, Le Cote, Semaforo, 3 October 1974, G. Gardini under *Pistacia*; 1 ♂, Isola di Capraia, near Capraia Isola, 7 June 1993, S. Zoia; 1 ♂, 3 ♀, Isola d'Elba, Portoferraio, San Giovanni, 22 December 1975, G. Gardini, under bark of *Eucalyptus*; 1 tritonymph, Isola d'Elba, Rio nell'Elba, Nisporto, 23 August 1993, C. Giusto, under *Juniperus phoenicea*; 1 ♂, 1 ♀, Isola d'Elba, San Martino, Villa di Napoleone, 2 November 2007, G. Gardini; 3 ♀, Isola d'Elba, Capoliveri, Punta Buzzancone, 1 m a.s.l., 3 November 2007, G. Gardini, under *Phragmites*; 4 ♂, 5 ♀, Isola d'Elba, Capo d'Enfola, 100 m a.s.l., 3 October 2016, R. Poggi, sieved in Mediterranean shrub (MSNG); 1 ♀, Isola di Montecristo, Cala Maestra, 5 May 1976, R. Poggi, under *Cistus*; 1 ♀ (*G. nigrimanus*, G. Callaini det.), Isola di Montecristo, 10 June 1977, R. Poggi, under *Cistus monspeliensis* (MSNG); 1 ♀, Isola di Montecristo, 7 June 1989, R. Poggi (MSNG); 1 ♀, 1 tritonymph (*G. nigrimanus*, G. Callaini det.), Isola di Montecristo, Convento, 300 m a.s.l., 24 July 1980, R. Poggi, under *Cistus* (MSNG); 1 ♂, 2 ♀, 1 tritonymph (*G. nigrimanus*, G. Callaini det.), Isola di Montecristo, Belvedere, 12 May 1981, G. Osella, under *Cistus* (MSNV). *Tuscany: Grosseto Prov.*: 1 ♂ (*G. minor*, M. Beier det.), near Grosseto, Poggio Cavallo, March 1918, A. Andreini (MSNG); 1 ♂, near Massa Marittima, 7 April 1994, G. Gardini, *Quercus suber* wood; 9 ♂, 21 ♀ (*Garypus minor*, E. Ellingsen det.) (together with 9 ♂, 10 ♀, 2 tritonymphs of *G. italicus*), Isola del Giglio, [no date], G. Doria (MSNG); 1 ♂, 2 ♀ (*Garypus minor*, E. Ellingsen det.) (together with 2 ♀ of *G. italicus*), Isola del Giglio, November 1902, G. Doria (MSNG); 3 ♂, 3 ♀ (*Garypus minor*, E. Ellingsen det.), Isola del Giglio, February 1904, G. Doria (MSNG); 1 ♀, Isola del Giglio, il Franco, 18 July 2009, G. Caoduro; 2 ♂, 2 ♀, Isola di Giannutri, 20 May 1978, G. Gardini, *Quercus ilex* wood and garigue. *Marche: Ancona Prov.*: 1 ♂, 1 ♀, 2 tritonymphs, 2 deutonymphs, near Massignano, Pian di Raggetti, 350 m a.s.l., 16 June 2009, R. Poggi, *Quercus ilex* wood (MSNG). *Latium: Rome Prov.*: 56 ♂, 48 ♀, 2 tritonymphs and 146 further specimens (*Garypus minor*, E. Ellingsen det.), [Rome Province, 1907 or 1908, A. Rossi] (MSNG); 75 ♂, 45 ♀ (*Garypus minor*, E. Ellingsen det.), [Roma], Tre Fontane, 26 January 1908, [A. Rossi] (MSNG); 25 ♂, 22 ♀ (*Garypus minor*, E. Ellingsen det.), Roma, Viale Parioli, 2 February 1908, [A. Rossi] (MSNG); 1



♀ (*Garypus minor*, E. Ellingsen det.), [Tivoli], 4 October 1908, [A. Rossi] (MSNG); 12 ♂, 20 ♀ (*Garypus minor*, E. Ellingsen det.), [Sacrofano], Monte Musino, 12 April 1908, [A. Rossi] (MSNG); 4 ♀ (*Garypus minor*, E. Ellingsen det.), [Roma], Acquacetosa [Acqua Acetosa], 27 September 1908, [A. Rossi] (MSNG); 1 ♂, 1 ♀ (*Garypus minor*, G. Canestrini det.), "Roma-Emilia" [sic!], 1883 (MZUP); 1 ♂, 1 ♀ (*Garypus minor*, G. Canestrini det.), Roma, 1885 (MZUP); 1 ♂, 1 ♀ (remains) (*Garypus*, G. Canestrini det.), Roma, 1885 (MZUP); 1 ♀, Sasso di Furbara, 19 March 1969, P. Brignoli; 1 ♂, 2 ♀, Allumiere, Monte Tolfaccia, 25 April 1979, G. Gardini & S. Zoia; 2 ♂, 1 ♀, Allumiere, slope N Monte Tolfaccia, 300 m a.s.l., 22 September 1999, C. Giusto, on *Ononis* sp.; 1 ♂, 4 ♀, Castel di Guido, Oasi L.I.P.U., 3 October/4 November 2009, F. Baini, *Quercus cerris* and *Q. frainetto* wood; 1 ♀, Castel di Guido, Oasi L.I.P.U., 9 April 2010, F. Baini, *Quercus cerris* and *Q. frainetto* wood. *Latium*: *Latina* Prov.: 2 ♂, 4 ♀, Ponza, Isola di Ponza, 3 October 1990, G. Osella; 1 ♂, 1 ♀, 2 tritonymphs, Ponza, Isola di Ponza, Piana dell'Incenso, 4 October 1990, R. Poggi, under *Arbutus* (MSNG); 1 ♀, Ponza, Isola di Ponza, La Forna, 100 m a.s.l., 9 April 2010, G. Ruzzante; 1 ♂, 1 ♀, Ponza, Isola di Zannone, 100 m a.s.l., 20 May 1987, R. Poggi (MSNG); 1 ♀, Ponza, Isola di Zannone, 9 October 1990, G. Osella; 1 ♂, 1 ♀, Ponza, Isola di Zannone, Capo Negro, 3 October 1990, R. Poggi (MSNG); 1 ♀, Ponza, Isola Palmarola, Porto, 2 October 1990, R. Poggi (MSNG); 3 ♀, Ponza, Isola Palmarola, valico per Vrieci, 2 October 1990, R. Poggi, under *Pistacia lentiscus* (MSNG); 3 ♂, 1 ♀, Ventotene, Isola Ventotene, Monte dell'Arco, 5 October 1990, R. Poggi (MSNG); 1 ♂, Ventotene, Isola Ventotene, Cala Rossano, 5 October 1990, R. Poggi (MSNG); 4 ♂, 6 ♀, Ventotene, Isola Ventotene, Punta degli Olivi, 50 m a.s.l., October 2010, G. Ruzzante. *Abruzzo*: *L'Aquila* Prov.: 1 ♀, Capo d'Aequa, 6 January 1994, G. Osella; 1 ♂, Rocca di Cambio, Altopiano delle Rocche, 1350 m a.s.l., 22 May 1994, G. Osella; 1 ♂, 4 ♀, Ofena, 550 m a.s.l., 20 November 1994, G. Osella. *Basilicata*: *Matera* Prov.: 2 ♂, 1 ♀, Policoro, 27 March 1988, F. Angelini; 4 ♂, 4 ♀, Policoro, 13 August 1989, F. Angelini. *Apulia*: *Bari* Prov.: 5 ♂, 3 ♀, 2 tritonymphs, Adelfia, 1.IV.1988, F. Angelini; 1 ♀, Monopoli, Impalata, 26 January 1997, G. Osella, *Quercus ilex* wood; 1 ♀, San Pietro Vernotico, Cerano, 7 September 1973, G. Gardini, *Quercus ilex* wood; 1 ♀, Mesagne, Bosco Preti, 2 December 1989, F. Angelini, *Quercus ilex* wood. *Apulia*: *Taranto* Prov.: 2 ♂, 1 ♀ (*G. minor*, M. Beier det.), Mottola, San Basilio, 1 November 1908, A. Andreini (MSNG); 1 ♀ (*G. minor*, M. Beier det.), id., 1 June 1909, A. Andreini (MSNG); 1 ♀ (*G. nigrimanus*, G. Lazzeroni det.), Taranto, Ginosa Marina, 24 September 1967, C. Baroni Urbani (MSNV); 1 ♂, Martina Franca, San Paolo, 300 m a.s.l., 2 May 2002, S. Zoia & F. Polese, hollow in *Olea europaea*. *Apulia*: *Lecce* Prov.: 3 ♂, 2 ♀, 1 tritonymph, 8 deutonymphs, San Cataldo, Frigole, 6 September 1973, G. Gardini; 1 ♀, San Cataldo, 15 October 1996, D. Ferreri; 1 ♀, Otranto, shore NW of Alimini Grande, 30 April 2002, S. Zoia & F. Polese. *Calabria*: *Catanzaro* Prov.: 1 ♀, Terme di Caronte, 3 December 1994, G. Osella. *Calabria*: *Reggio di Calabria* Prov.: 2 ♀ (*G. nigrimanus*, G. Lazzeroni det.) (together with 1 ♂, 1 ♀, 2 tritonymphs of *G. italicus*), Ciminà, 320 m a.s.l., 25 October 1966, G. Osella (MSNV); 2 ♂, 3 ♀ (*G. nigrimanus*, G. Lazzeroni det.) (together with 2 ♀ of *G.*

*italicus*), Antonimina, 350 m a.s.l., 26 October 1966, G. Osella (MSNV). *Sicily*: *Messina* Prov.: 2 tritonymphs (*G. nigrimanus*, G. Gardini det.), Caronia, slope Monte Pagano, 500 m a.s.l., September/November 1987, G. Sabella, mixed thermophilous wood; 1 ♀, 1 tritonymph, 1 protonymph (*G. nigrimanus*, G. Gardini det.), Caronia, slope Monte Pagano, 500 m a.s.l., July/August 1988, G. Sabella, mixed thermophilous wood; 1 ♂, 1 ♀, 1 tritonymph, 10 deutonymphs (*G. nigrimanus*, G. Gardini det.), Caronia, slope Monte Pagano, 350 m a.s.l., August/October 1987, G. Sabella, *Quercus suber* wood; 1 ♀, 4 tritonymphs, 4 deutonymphs (*G. nigrimanus*, G. Gardini det.), Caronia, slope Monte Pagano, 350 m a.s.l., July/October 1988, G. Sabella, *Quercus suber* wood; 1 ♀, Isola di Lipari, Quattropani, 370 m a.s.l., 10 September 1996, R. Poggi (MSNG). *Sicily*: *Palermo* Prov.: 1 ♂, 7 ♀, 1 tritonymph, Palermo, Orto Botanico, 4 October 1979, G. Gardini; 1 ♀, Palermo, Madonna dei Boschi, 14 June 1981, G. Gardini; 5 ♀ (together with 2 ♂, 2 ♀ of *G. italicus*), Palermo, slope Monte Busambra, 15 June 1981, G. Gardini; 11 ♂, 25 ♀, 2 tritonymphs, Godrano, 5 October 1979, G. Gardini, under bark *Eucalyptus*; 1 ♂, 1 ♀, 1 tritonymph, Godrano, Bosco della Ficuzza, 23 November 1974, Romano, under bark *Eucalyptus*; 1 ♀, Godrano, Bosco della Ficuzza, 26 November 1978, Romano, under bark *Eucalyptus*; 2 ♀, Godrano, Bosco della Ficuzza, 15 June 1981, G. Gardini; 1 ♀, Piana degli Albanesi, Maganoce, 19 November 1972, Romano; 25 ♂, 15 ♀, Cefalù, Castel di Tusa, 19 October 1976, G. Parodi, under stones; 1 deutonymph, Collesano, Piano Zucchi, 1050 m a.s.l., 31 May 1985, R. Rizzierio & S. Zoia, *Quercus ilex* wood. *Sicily*: *Trapani* Prov.: 1 ♀ (together with 1 ♂ of *G. italicus*), Scopello, Riserva Naturale dello Zingaro, 17 November 2001, B. Massa; 1 ♀, Scopello, Riserva Naturale dello Zingaro, 31 October 2001, B. Massa; 1 ♀, 2 tritonymphs (together with 1 ♀ of *G. italicus*), Scopello, Riserva Naturale dello Zingaro, 26 May 2002, B. Massa; 1 ♀ (together with 1 ♀ of *G. italicus*), Scopello, Riserva Naturale dello Zingaro, 30 June 2002, B. Massa; 1 ♀ (*G. nigrimanus*, G. Lazzeroni det.), Isola di Levanzo, October 1967, Riggio, Osella & Krapp (MSNV); 1 ♀, Isola di Levanzo, 15 September 1996, R. Poggi, with ants (MSNG); 3 ♂, 1 ♀, Isola di Levanzo, 15 September 1996, R. Poggi, under *Pistacia* (MSNG); 1 ♂, Isola di Favignana, 2 May 1981, G. Osella; 3 ♀, Isola di Favignana, 3 April 1990, S. Zoia; 4 ♀, Isola di Favignana, 27 April 1991, R. Poggi (MSNG); 1 ♀ (*G. Lazzeroni* det.), Isola di Favignana, Montagna Grossa, 19 March 1969, G. Osella (MSNV); 1 ♂, 1 ♀, Isola di Marettimo, il Passo, 4 May 1991, G. Osella; 1 ♀, Isola Grande dello Stagnone, 6 May 1991, G. Osella; 1 ♀, Isola di Pantelleria, Specchio di Venere, 8 December 1992, R. Poggi (MSNG). *Sicily*: *Catania* Prov.: 1 ♀ (*G. nigrimanus*, M. Beier det.), Catania, between Fiume Simeto and San Leonardo, 18 November 1961, M. La Greca (MSNV); 2 ♀, Randazzo, Piana di Randazzo, 29 April 1982, G. Gardini & R. Rizzierio; 1 ♀, Fiumefreddo, 14 November 1994, F. Di Franco, under *Arundo donax*. *Sicily*: *Agrigento* Prov.: 1 ♀ (*G. nigrimanus*, M. Beier det.), Sciacca, Monte Cronio, 26 November 1961, La Greca, Sichel & Alicata (MSNV); 1 ♂, Isola di Linosa, 29 April 1991, R. Poggi (MSNG); 1 ♀, Isola di Linosa, 1 December 1992, R. Poggi (MSNG); 3 ♂, 2 ♀, Isola di Lampione, 24 September 1996, R. Poggi, under *Atriplex* sp. (MSNG). *Sicily*: *Siracusa* Prov.: 3 ♀ (*G.*



*nigrimanus*, M. Beier det.), Ferla, 20/22 July 1969, L. Magnano (MSNV); 1 ♀ (*G. nigrimanus*, M. Beier det.), Bucecheri, 23 July 1969, L. Magnano (MSNV); 2 ♂, 1 ♀ (*G. nigrimanus*, M. Beier det.), near Melilli, 20/26 July 1969, L. Magnano (MSNV). *Sardinia: Sassari Prov.*: 1 ♂ (*Garypus nigrimanus*, E. Simon det.), Golfo Aranci, April 1902, A. Dodero (MSNG); 2 ♂, 2 ♀ (*Garypus nigrimanus*, E. Simon det.) (together with 1 ♂ of *G. italicus*), Golfo Aranci, April 1902, A. Dodero (MSNG); 1 ♀ (*Garypus nigrimanus*, E. Simon det.), Golfo Aranci, March 1903, A. Dodero (MSNG); 1 ♀ (*Garypus minor*, E. Ellingsen det.), Golfo Aranci, 1907, T. Derosas (MSNG); 1 ♂ (together with 1 ♀ of *G. italicus*), Golfo Aranci, 11 May 2000, R. Poggi; 1 deutonymph, Alghero, Punta La Speranza, 26 July 1975, S. Zoia; 1 ♀, Alghero, 10 km S from Alghero, 20 m a.s.l., 16 May 2003, R. Poggi (MSNG); 1 ♂, near Palmadula, 23 November 1991, R. Poggi, *Quercus ilex* wood (MSNG); 1 ♂, Loiri, Porto San Paolo, Vaccileddi, 100 m a.s.l., 17 April 2012, C. Torti, *Quercus ilex* wood; 2 ♂, 2 ♀, Isola Tavolara, 8 June 1989, G. Osella; 1 ♂, Isola Tavolara, 18 May 1994, G. Osella & M. Zuppa. *Sardinia: Oristano Prov.*: 4 ♂, 1 ♀, Isola Mal di Ventre, 15 June 1989, G. Osella; 6 ♂, 2 ♀, Cabras, Is Aruttas, 1 February 1995, C. Meloni, under *Pistacia lentiscus*; 1 ♀, Tharros, 22 March 1997, P. Leo; 1 ♂, 2 ♀, near Uras, October 1999, L. Fancello (MSNG); 2 ♂, 1 ♀, near Mogoro, October 1999, L. Fancello (MSNG); 1 ♂, 1 ♀, Arborea, 4 May 2000, R. Poggi, under algae and *Posidonia oceanica* (MSNG). *Sardinia: Nuoro Prov.*: 1 ♂ (*G. minor*, M. Beier det.), Macomer, April 1909, A. Dodero (MSNG); 2 ad. 2 juv., Seui, December 1999, L. Fancello (MSNG); 1 ♀, Gennargentu, Bruncu Spina, 1700–1800 m a.s.l., 4 May 1992, K. Thaler (MHNG). *Sardinia: Cagliari Prov.*: 5 ♂, 2 ♀, 1 tritonymph (*Garypus nigrimanus*, E. Simon det.), Cagliari, [no date], A. Dodero (MSNG); 1 ♂, 3 ♀, 1 tritonymph (*Garypus nigrimanus*, E. Simon det.), Cagliari, May 1902, A. Dodero (MSNG); 5 ♂, 3 ♀, Cagliari, Stagno di Molentargius, 20 September 1995, C. Meloni; 1 ♀, Quartu Sant'Elena, Capitanica, September 1999, L. Fancello (MSNG); 2 ♂, 1 ♀, Elmas, 7 March 1979, P. Leo; 1 ♂, near Elmas, 26 February 1978, C. Meloni, under bark *Eucalyptus*; 1 ♀, Carbonia, Monte Sirai, 150 m a.s.l., 5 May 2000, R. Poggi (MSNG); 1 ♂, Chia, Porto Campana, January 2000, L. Fancello (MSNG); 1 ♂, 1 ♀, Costa Rei, Stagno Santa Giusta, October 1999, L. Fancello (MSNG); 5 ♂, 1 ♀, Decimomannu, 28 April 1995, C. Meloni, under *Olea europaea*; 5 ♂, 7 ♀, 7 tritonymphs, Gergei, December 1999, L. Fancello (MSNG); 2 ♀, Iglesias, Masua, January 2000, L. Fancello (MSNG); 1 ♀, Isola di Sant'Antioco, 11 May 1988, R. Argano; 1 ♂, 2 ♀, Isola di Sant'Antioco, Cala Lunga, 13 June 1989, G. Osella; 1 ♂, Isola di Sant'Antioco, Fonte Cannai, 30 m a.s.l., 5 May 2000, R. Poggi (MSNG); 4 ♂, 5 ♀, Siliqua, Argiolas, October 1999, L. Fancello (MSNG); 1 ♀, 1 tritonymph, Sinnai, San Basilio, Rio Longu, September 1999, L. Fancello (MSNG); 1 ♀, Villasalto, Foresta Riu Tolu, 250 m a.s.l., October 1999, L. Fancello (MSNG); 2 ♂, 2 ♀, Monte Sette Fratelli, San Pietro, 200–400 m a.s.l., October 1999, L. Fancello (MSNG).

**Diagnosis.**—A *Geogarypus* that differs from other extant and fossil species of the genus in the following combination of characters: carapace red-brown, uniformly coloured, legs not banded; tergites individed, most sternites divided by a median

thin suture, pseudotactile setae absent; vestitural setae not clavate; legs diplotarsate; galea of male simple, acuminate, of female with 9 distal rami; pedipalpal hand, chiefly in males, often darker than other chelal segments; paraxial surface of pedipalpal hand with a weak rounded hump at the base of fixed finger; pedipalpal femur and patella rarely weakly wrinkled; fixed and movable chelal fingers respectively with 8 and 4 trichobothria; trichobothrium *it* mostly closer to *et* than *ist*, *est* mostly halfway between *isb* and *ib*, trichobothrium *st* closer to *sb* than *t*; fixed chelal finger weakly heterodentate, with 4 to 9 paraxial additional teeth on the proximal half; 1 (rarely 2) pit-like structure (*pls*) at level of trichobothrium *est*; venom ducts long, nodus ramosus respectively at level of *est* and between *st-sb*; length of pedipalpal femur 0.45–0.60 (♂), 0.55–0.82 (♀) mm, length of chela with pedicel 0.75–0.94 (♂), 0.89–1.33 (♀) mm.

**Description (adults).**—Integument pigmented, carapace and pedipalps (fingers excepted) with star-like hispid granulation and small investing setae apically slightly sygmoid; carapace uniformly red-brown; tergites red-brown, I–II with a darker area on each extremity and one in the middle, III–VIII with a thin white area in the middle; sternites IV–VIII uncoloured in the middle; pedipalps red-brown, hand (chiefly in males) often darker than other palpal segments; legs uniformly pale; pleural membrane longitudinally wrinkled-plicate, with transverse series of investing microsetae. Carapace (Fig. 3) 1.0–1.2 times as long as broad, subtriangular, with notch on anterior margin; anterior margin with 4 setae, the lateral longer and thicker than the medial ones; posterior margin with 10–16 setae; anterior furrow nearer the posterior eyes than the posterior margin of carapace, posterior basal furrow nearly indistinct; ocular area as in Fig. 3, diameter of eyes 0.05–0.065 mm; ratio of cucullus/carapace length 0.23–0.30. Chaetotaxy and lyrifissures (in brackets) of tergites I–XII: 10–15(6–8): 12–15(8–10): 12–16(8–10): 14–18(8–10): 14–17(8–10): 13–20(8–10): 13–16(8–10): 12–18(8–10): 10–14(8–10): 9–12(10): 8–9(6): 2(0). Chaetotaxy of sternites II–XII: ♂, 11–14: (1)8–13(1–2): (1)10–14(1): 14–18: 14–20: 14–19: 14–18: 11–14: 6–10: 2:0; ♀, 10–14: (1–2)6–10(1–2): (1–2)11–16(1–2): 15–18: 15–19: 14–19: 13–18: 9–13: 7–8: 2:0; tergites and sternites XI–XII as in Fig. 4; sternites II–IV with setae, spiracles and tracheae of ♂ and ♀ respectively in Figs. 5 and 6; genitalia of ♂ and ♀ respectively in Figs. 7 and 8; genital atrium of ♂ with 2+2 (rarely 2+4) setae. Chelicerae (Figs. 9–11) 1.7–2.0 times as long as broad, palm with 5 setae, *bs* shorter and thicker than others; fixed finger with 4–6 teeth; movable finger with 3–5 subapical reduced teeth with rounded tips, *gs* subapical; galea simple, acuminate in ♂, with 9 apical rami in ♀ (Fig. 11); rallum with one aspinose blade; serrula exterior with 15 blades, the two proximal blades sickle-shaped, the distal one acuminate and stretched forwards (Figs. 10–11). Coxal area (Fig. 12): manducatory process with 3 setae, the lateral one shorter; pedipalpal coxa with 14–19 setae (the antero-lateral one, on maxillary shoulder, very long) and two circular lyrifissures (*mml* and *pml*); chaetotaxy of eoxae I–IV: I 3–5 (mostly 4), II 4–7 (mostly 6, rarely 4), III 8–14 (mostly 11–12), IV 17–21 (♂) 22–30 (♀); coxae III–IV without granulation, lyrifissures as in Fig. 13. Pedipalp: trochanter (Figs. 13–14) 1.45–1.65 times as long as broad, with a ventral rounded apophysis; femur (Fig. 13) 3.05–3.55 times as long as broad, with short pedicel;



patella (Fig. 13) 2.6–2.8 times as long as broad; chela with pedicel (Figs. 15–16) 3.45–4.25 ( $\delta$ ), 3.3–3.8 ( $\varphi$ ) times as long as broad, 3.9–4.25 ( $\delta$ ), 3.7–4.1 ( $\varphi$ ) times as long as deep; hand of chela with pedicel 1.55–1.95 ( $\delta$ ), 1.55–1.75 ( $\varphi$ ) times as long as broad, 1.8–2.05 ( $\delta$ ), 1.7–1.95 ( $\varphi$ ) times as long as deep; paraxial surface of pedipalpal hand, in dorsal view, with a weak rounded hump at the base of fixed finger; fixed and movable fingers respectively with 8 and 4 trichobothria (Fig. 16), *it* mostly closer to *et* than *ist* (rarely *it* halfway between *et-ist*; Fig. 16), *est* mostly halfway between *isb* and *ib* (rarely *est* nearer *ib* than *isb*; Fig. 16); dorsal surface of fixed chelal finger granulated as far as trichobothrium *est*; fixed chelal finger with 30–36 teeth with dental canals and 3–5 basal microtubercles; distal half of fixed chelal finger slightly heterodentate (one long tooth alternate with two shorter teeth; Fig. 16), with acuminate, anteriorly slightly curved teeth; proximal half of fixed chelal finger with triangular teeth gradually rounded and reduced in size towards the finger base and with 4 to 9 paraxial additional teeth—with dental canals—on the proximal half (rarely 1–2 additional teeth distad of the mid-finger) (Figs. 46–47); 1 (rarely 2) pit-like structure (*pls*; Fig. 16) at level of trichobothrium *est*; venom ducts long, nodus ramosus respectively at level of *est* and between *st-sb*; movable chelal finger with 27–38 teeth with dental canals, distal quarter of movable finger with 6–12 triangular, acuminate teeth (the distal one small) and, proximad of trichobothrium *t*, with flat teeth gradually reduced in size, reaching back to *b*; trichobothrium *st* closer to *sb* than *t*; ratio of movable finger/hand of chela with pedicel 1.1–1.4 ( $\delta$ ), 1.0–1.3 ( $\varphi$ ); ratio of pedipalpal femur/movable finger 1.0–1.25 ( $\delta$ ), 1.0–1.1 ( $\varphi$ ); ratio of pedipalpal femur/carapace 0.9–1.0 ( $\delta$ ), 0.9–1.1 ( $\varphi$ ). Leg I (Fig. 17): trochanter 1.2–1.4, femur 2.3–2.8, patella 1.4–1.65, tibia 2.5–3.2, metatarsus 2.3–2.8, tarsus 3.0–4.0 times as long as deep; claws smooth and shorter than arolium. Leg IV (Fig. 18): trochanter 1.3–1.8, femur 1.2–1.45, patella 2.4–2.9, tibia 3.2–4.2, metatarsus 2.5–3.1, tarsus 3.1–3.75 times as long as deep; claws smooth and shorter than arolium.

Measurements (in mm). Body length 1.4–1.8 ( $\delta$ ), 1.6–2.2 ( $\varphi$ ). Carapace 0.48–0.60  $\times$  0.47–0.56 ( $\delta$ ), 0.60–0.74  $\times$  0.53–0.74 ( $\varphi$ ), cucullus length (from anterior eyes) 0.12–0.16 ( $\delta$ ), 0.15–0.20 ( $\varphi$ ). Chelicerae 0.15–0.17  $\times$  0.075–0.10 ( $\delta$ ), 0.18–0.25  $\times$  0.095–0.135 ( $\varphi$ ), movable finger length 0.08–0.12 ( $\delta$ ), 0.11–0.155 ( $\varphi$ ). Pedipalp: trochanter 0.22–0.26  $\times$  0.15–0.17 ( $\delta$ ), 0.25–0.345  $\times$  0.17–0.225 ( $\varphi$ ); femur 0.45–0.60  $\times$  0.14–0.18 ( $\delta$ ), 0.55–0.82  $\times$  0.17–0.25 ( $\varphi$ ); patella 0.35–0.45  $\times$  0.13–0.17 ( $\delta$ ), 0.44–0.62  $\times$  0.16–0.22 ( $\varphi$ ); chela (with pedicel) 0.75–0.94  $\times$  0.20–0.26 ( $\delta$ ), 0.89–1.33  $\times$  0.25–0.38; chela (without pedicel) length 0.72–0.90 ( $\delta$ ), 0.85–1.29 ( $\varphi$ ); chela depth 0.18–0.23 ( $\delta$ ), 0.23–0.35 ( $\varphi$ ); hand length (with pedicel) 0.32–0.44 ( $\delta$ ), 0.40–0.60 ( $\varphi$ ); hand length (without pedicel) 0.29–0.395 ( $\delta$ ), 0.36–0.56 ( $\varphi$ ); movable finger length 0.44–0.52 ( $\delta$ ), 0.50–0.76 ( $\varphi$ ). Leg I: trochanter 0.11–0.135  $\times$  0.08–0.105 ( $\delta$ ), 0.135–0.16  $\times$  0.10–0.12 ( $\varphi$ ); femur 0.18–0.245  $\times$  0.08–0.09 ( $\delta$ ), 0.23–0.30  $\times$  0.085–0.11 ( $\varphi$ ); patella 0.11–0.13  $\times$  0.075–0.09 ( $\delta$ ), 0.125–0.17  $\times$  0.08–0.11 ( $\varphi$ ); tibia 0.15–0.19  $\times$  0.06–0.07 ( $\delta$ ), 0.18–0.26  $\times$  0.06–0.08 ( $\varphi$ ); metatarsus 0.095–0.13  $\times$  0.04–0.055 ( $\delta$ ), 0.12–0.17  $\times$  0.05–0.06 ( $\varphi$ ); tarsus 0.10–0.14  $\times$  0.035–0.04 ( $\delta$ ), 0.12–0.16  $\times$  0.04–0.045 ( $\varphi$ ). Leg IV: trochanter 0.16–0.20  $\times$  0.10–0.13 ( $\delta$ ), 0.18–0.24  $\times$  0.115–0.15 ( $\varphi$ ); femur 0.095–0.13  $\times$  0.075–0.09 ( $\delta$ ), 0.11–0.15  $\times$  0.075–0.105 ( $\varphi$ ); patella 0.28–0.38

$\times$  0.115–0.16 ( $\delta$ ), 0.34–0.50  $\times$  0.125–0.20 ( $\varphi$ ); tibia 0.265–0.33  $\times$  0.07–0.10 ( $\delta$ ), 0.30–0.46  $\times$  0.08–0.11 ( $\varphi$ ); metatarsus 0.13–0.16  $\times$  0.05–0.06 ( $\delta$ ), 0.16–0.21  $\times$  0.06–0.07 ( $\varphi$ ); tarsus 0.14–0.16  $\times$  0.04–0.05 ( $\delta$ ), 0.15–0.19  $\times$  0.045–0.06 ( $\varphi$ ).

**Description (tritonymph).**—Carapace and pedipalps with weak pigmentation and granulation. Carapace 0.9–1.05 times as long as broad, furrows, anterior setae and ocular area as in adults; posterior margin with 10–13 setae; diameter of anterior eyes 0.045–0.055 mm, posterior eyes 0.040–0.050 mm; ratio of cucullus/carapace length 0.20–0.24. Chaetotaxy and lyrifissures (in brackets) of tergites I–XII: 10–11(8); 8–12(6–8); 10–12(6–8); 10–11(6–8); 10–11(7–8); 10–12(8); 10–11(8); 9–11(6–8); 9–10(8–9); 10(8); 8(8); 2(0). Chaetotaxy of sternites II–XII: 2–4; (1)4–6(1); (1)7–10(1); 12; 12–14; 12–14; 10–13; 7–9; 6; 2; 0. Chelicerae 1.75–1.9 times as long as broad, palm with 5 setae; fixed finger with 4–5 teeth; movable finger with 3–4 subapical reduced teeth with rounded tips, *gs* subapical; galea with 7 apical rami; rallum with one aspinose blade; serrula exterior with 13 blades, shape of proximal and distal blades as in adult. Coxal area: manducatory process with 3 setae, the lateral one shorter; pedipalpal coxa with 13–14 setae (the antero-lateral one very long) and two circular lyrifissures (*mml* and *pml*); chaetotaxy of eoxae I–IV: I 3–4, II 4–5, III 6–8, IV 12–13. Pedipalp: trochanter 1.4–1.5 times as long as broad, with a ventral rounded apophysis; femur 3.2–3.6 times as long as broad, with short pedicel; patella 2.55–2.8 times as long as broad; chela with pedicel (Figs. 19–20) 3.8–3.9 times as long as broad, 4.05–4.35 times as long as deep; hand of chela with pedicel 1.65–1.8 times as long as broad, 1.85–1.95 times as long as deep; fixed and movable fingers respectively with 7 and 3 trichobothria (Fig. 20), *isb* and *sb* absent; dorsal surface of fixed chelal finger granulated as far as trichobothrium *est*; fixed chelal finger with 27–35 teeth with dental canals and 2–3 basal microtubercles; distal half of fixed chelal finger slightly heterodentate (one long tooth alternate with two shorter teeth; Fig. 20), with acuminate, anteriorly slightly curved teeth; proximal half of fixed chelal finger with triangular teeth gradually reduced in size towards the finger base and with 2 to 7 paraxial additional teeth—with dental canals—on the proximal half (rarely 2 additional teeth distad of the mid-finger); 1 pit-like structure (*pls*) at level of trichobothrium *est* (Fig. 20); venom ducts long, nodus ramosus respectively distad of *est* and *st*; movable chelal finger with 22–32 teeth with dental canals, distal third of movable finger with 7–10 triangular, acuminate teeth and, proximad of trichobothrium *t*, with flat teeth gradually reduced in size, reaching back halfway between *st-b*; ratio of movable finger/hand of chela with pedicel 1.15–1.25; ratio of pedipalpal femur/movable finger 1.05–1.15; ratio of pedipalpal femur/carapace 0.9–1.0. Leg I: trochanter 1.2–1.4, femur 2.1–2.8, patella 1.5–1.7, tibia 2.5–2.8, metatarsus 2.2, tarsus 2.5, metatarsus+tarsus 4.3–5.0 times as long as deep; claws smooth and shorter than arolium. Leg IV: trochanter 1.5–2.1, femur 1.2–1.4, patella 2.4–2.7, tibia 3.4–3.85, metatarsus 2.3–2.8, tarsus 2.7–3.5 times as long as deep; claws smooth and shorter than arolium.

Measurements (in mm). Body length 1.3–1.6. Carapace 0.47–0.55  $\times$  0.455–0.54, cucullus length (from anterior eyes) 0.095–0.125. Chelicerae 0.135–0.17  $\times$  0.07–0.09, movable finger length 0.09–0.10. Pedipalp: trochanter 0.18–0.225  $\times$  0.13–0.145; femur 0.43–0.50  $\times$  0.12–0.155; patella 0.305–0.365



$\times 0.115$ – $0.135$ ; chela (with pedicel)  $0.70$ – $0.85 \times 0.18$ – $0.225$ ; chela (without pedicel) length  $0.67$ – $0.82$ ; chela depth  $0.16$ – $0.205$ ; hand length (with pedicel)  $0.30$ – $0.38$ ; hand length (without pedicel)  $0.27$ – $0.35$ ; movable finger length  $0.38$ – $0.47$ . Leg I: trochanter  $0.11$ – $0.115 \times 0.08$ – $0.09$ ; femur  $0.17$ – $0.22 \times 0.07$ – $0.085$ ; patella  $0.105$ – $0.115 \times 0.065$ – $0.075$ ; tibia  $0.125$ – $0.17 \times 0.05$ – $0.06$ ; metatarsus  $0.10 \times 0.045$ – $0.05$ ; tarsus  $0.10$ – $0.12 \times 0.04$ ; metatarsus + tarsus  $0.20$ – $0.22 \times 0.045$ – $0.05$ . Leg IV: trochanter  $0.15$ – $0.17 \times 0.08$ – $0.10$ ; femur  $0.08$ – $0.105 \times 0.07$ – $0.085$ ; patella  $0.255$ – $0.31 \times 0.105$ – $0.12$ ; tibia  $0.24$ – $0.28 \times 0.065$ – $0.075$ ; metatarsus  $0.115$ – $0.15 \times 0.05$ – $0.06$ ; tarsus  $0.12$ – $0.14 \times 0.04$ – $0.045$ .

**Description (deutonymph).**—Carapace and pedipalps with weak pigmentation and granulation. Carapace  $0.95$ – $1.0$  times as long as broad, anterior setae and ocular area as in adults, furrows nearly indistinct; posterior margin with 8 setae; diameter of anterior eyes  $0.035$ – $0.050$  mm, posterior eyes  $0.035$ – $0.045$  mm; ratio of cucullus/carapace length  $0.22$ – $0.235$ . Chaetotaxy and lyrifissures (in brackets) of tergites I–XII: 7–8(4): 6–8(4): 6(6): 6(6): 6–7(6): 6(6): 6(6): 6–7(6): 6(6): 4(?): 2(0). Chaetotaxy of sternites II–XII: 0: (1)4(1): (1)4(1): 6–7: 6: 6: 4–5: 4: 2: 0. Chelieerae  $1.6$ – $1.7$  times as long as broad, palm with 5 setae; fixed finger with 4 teeth; movable finger with 3 subapical reduced teeth with rounded tips, *gs* subapical; galea with 5 apical rami; rallum with one aspinose blade; serrula exterior with 11 blades, shape of proximal and distal blades as in adult. Coxal area: manducatory process with 3 setae, the lateral one shorter; pedipalpal coxa with 7–8 setae (the antero-lateral one very long) and two circular lyrifissures (*mml* and *pml*); chaetotaxy of coxae I–IV: I 2, II 3, III 3–5, IV 4–7. Pedipalp: trochanter  $1.4$ – $1.55$  times as long as broad, with a ventral rounded apophysis; femur  $3.2$ – $3.75$  times as long as broad, with a short pedicel; patella  $2.45$ – $2.65$  times as long as broad; chela with pedicel (Figs. 21–22)  $3.9$ – $4.35$  times as long as broad,  $4.2$ – $4.65$  times as long as deep; hand of chela with pedicel  $1.7$ – $1.9$  times as long as broad,  $1.9$ – $2.05$  times as long as deep; fixed and movable fingers respectively with 6 and 2 trichobothria (Fig. 22), *isb*, *esb* and *st*, *sb* absent; dorsal surface of fixed chelal finger granulated as far as trichobothrium *est*; fixed chelal finger with 22–33 teeth with dental canals and 2–3 basal microtubercles; distal third of fixed chelal finger slightly heterodentate (one long tooth alternate with two shorter teeth: Fig. 22), with acuminate teeth; proximal two thirds of fixed chelal finger with triangular teeth gradually reduced in size towards the finger base and with 2–4 paraxial additional teeth—with dental canals—on the proximal half; 1 pit-like structure (*pls*) distad of trichobothrium *est* (Fig. 22); venom ducts long, nodus ramosus respectively distad of *est* and halfway between *b*–*t*; movable chelal finger with 19–27 teeth with dental canals, distal third of movable finger with 7–10 triangular, acuminate teeth and, proximad of trichobothrium *t*, with flat teeth gradually reduced in size, reaching back to *b*; ratio of movable finger/hand of chela with pedicel  $1.1$ – $1.25$ ; ratio of pedipalpal femur/movable finger  $1.0$ – $1.1$ ; ratio of pedipalpal femur/carapace  $0.8$ – $0.9$ . Leg I: trochanter  $1.2$ – $1.4$ , femur  $2.2$ – $2.8$ , patella  $1.3$ – $1.65$ , tibia  $2.0$ – $2.5$ , metatarsus+tarsus  $4.25$ – $4.5$  times as long as deep; claws smooth and shorter than arolium. Leg IV: trochanter  $1.4$ – $1.6$ , femur  $1.05$ – $1.35$ , patella  $2.35$ – $2.45$ , tibia  $3.2$ – $3.65$ , metatarsus  $1.95$ – $2.5$ ,

tarsus  $2.5$ – $3.2$  times as long as deep; claws smooth and shorter than arolium.

Measurements (in mm). Body length  $1.0$ – $1.3$ . Carapace  $0.38$ – $0.45 \times 0.39$ – $0.44$ , cucullus length (from anterior eyes)  $0.09$ – $0.10$ . Chelieerae  $0.11$ – $0.13 \times 0.065$ – $0.07$ , movable finger length  $0.07$ – $0.09$ . Pedipalp: trochanter  $0.14$ – $0.155 \times 0.09$ – $0.11$ ; femur  $0.32$ – $0.40 \times 0.09$ – $0.115$ ; patella  $0.23$ – $0.29 \times 0.09$ – $0.11$ ; chela (with pedicel)  $0.55$ – $0.70 \times 0.14$ – $0.16$ ; chela (without pedicel) length  $0.52$ – $0.68$ ; chela depth  $0.13$ – $0.15$ ; hand length (with pedicel)  $0.25$ – $0.31$ ; hand length (without pedicel)  $0.23$ – $0.29$ ; movable finger length  $0.30$ – $0.39$ . Leg I: trochanter  $0.075$ – $0.09 \times 0.06$ – $0.065$ ; femur  $0.13$ – $0.17 \times 0.055$ – $0.06$ ; patella  $0.07$ – $0.10 \times 0.055$ – $0.06$ ; tibia  $0.10$ – $0.125 \times 0.045$ – $0.05$ ; metatarsus + tarsus  $0.15$ – $0.18 \times 0.035$ – $0.04$ . Leg IV: trochanter  $0.095$ – $0.14 \times 0.065$ – $0.085$ ; femur  $0.07$ – $0.095 \times 0.06$ – $0.075$ ; patella  $0.19$ – $0.24 \times 0.075$ – $0.10$ ; tibia  $0.16$ – $0.22 \times 0.05$ – $0.06$ ; metatarsus  $0.08$ – $0.10 \times 0.04$ – $0.05$ ; tarsus  $0.10$ – $0.11 \times 0.03$ – $0.04$ .

**Description (protonymph).**—Carapace and pedipalps whitish, with weak granulation. Carapace  $0.9$  times as long as broad, anterior setae and ocular area as in adults, furrows indistinct; posterior margin with 4 setae; diameter of anterior eyes  $0.037$  mm, posterior eyes  $0.034$  mm; ratio of cucullus/carapace length  $0.23$ . Tergites I–XI with 4 setae, tergite XII 2. Chaetotaxy of sternites II–XII: 0: (0)2(0): (1)2(1): 4: 4: 4: 4: 4: 4: 0. Chelicerae  $1.7$  times as long as broad, palm with 4 setae, *sbs* absent; fixed finger with 4 teeth; movable finger with 2–3 subapical reduced teeth with rounded tips, *gs* absent; galea with 3 apical rami; rallum with one aspinose blade; serrula exterior with 10 blades, shape of proximal and distal blades as in adult. Coxal area: manducatory process with 2 setae (lateral seta absent); pedipalpal coxa with 3 setae (the anterior very long) and one circular lyrifissure (*mml*); chaetotaxy of coxae I–IV: 1. Pedipalp: trochanter  $1.5$  times as long as broad, with a ventral rounded apophysis; femur  $3.3$  times as long as broad, with a distinct pedicel; patella  $2.6$  times as long as broad; chela with pedicel (Figs. 23–24)  $4.14$  times as long as broad,  $4.3$  times as long as deep; hand of chela with pedicel  $1.9$  times as long as broad,  $2.0$  times as long as deep; fixed and movable fingers respectively with 3 and 1 trichobothria (Fig. 24), *it*, *est*, *isb*, *ib*, *esb* and *st*, *sb*, *b* absent; dorsal surface of fixed chelal finger slightly granulated as far as trichobothrium *eb*; fixed chelal finger with 23 teeth with dental canals and 5 basal microtubercles; distal third of fixed chelal finger slightly heterodentate, with acuminate teeth; proximal two third of fixed chelal finger with triangular teeth gradually rounded and reduced in size towards the finger base; additional teeth absent; 1 pit-like structure (*pls*) at level of trichobothrium *ist* (Fig. 24); venom ducts long, nodus ramosus respectively proximad of *ist* and *t*; movable chelal finger with 19 teeth with dental canals, distal third of movable finger with 7 triangular, acuminate teeth, proximally with flat teeth gradually reduced in size; ratio of movable finger/hand of chela with pedicel  $1.15$ ; ratio of pedipalpal femur/movable finger  $1.1$ ; ratio of pedipalpal femur/carapace  $0.9$ . Leg I: trochanter  $1.05$ , femur  $2.35$ , patella  $1.35$ , tibia  $2.0$ , metatarsus+tarsus  $3.5$  times as long as deep; claws smooth and shorter than arolium. Leg IV: trochanter  $1.65$ , femur  $1.3$ , patella  $2.4$ , tibia  $3.0$ , metatarsus  $2.1$ , tarsus  $2.85$  times as long as deep; claws smooth and shorter than arolium.



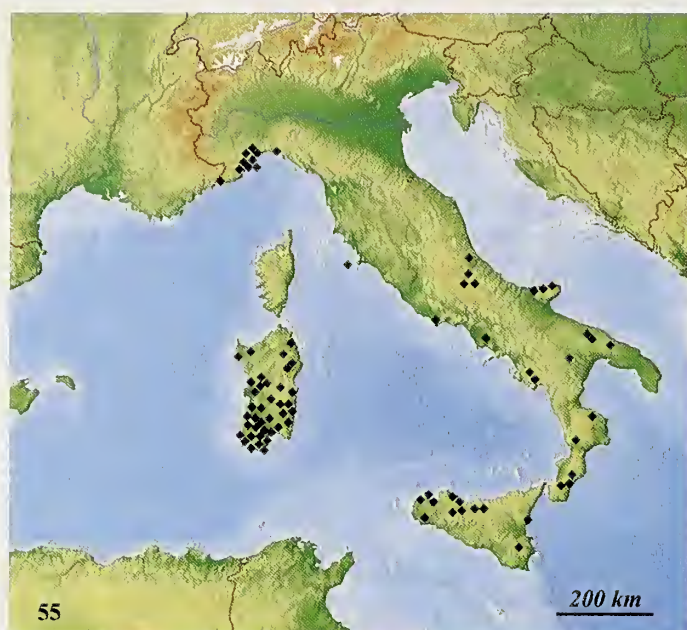


Figure 55.—Map depicting distribution of *Geogarypus italicus* sp. nov.

Measurements (in mm). Body length 0.8. Carapace  $0.34 \times 0.39$ , cucullus length (from anterior eyes) 0.08. Chelicerae  $0.11 \times 0.065$ , movable finger length 0.07. Pedipalp: trochanter  $0.135 \times 0.09$ ; femur  $0.30 \times 0.09$ ; patella  $0.22 \times 0.085$ ; chela (with pedicel)  $0.52 \times 0.125$ ; chela (without pedicel) length 0.50; chela depth 0.12; hand length (with pedicel) 0.24; hand length (without pedicel) 0.22; movable finger length 0.28. Leg I: trochanter  $0.07 \times 0.065$ ; femur  $0.13 \times 0.055$ ; patella  $0.075 \times 0.055$ ; tibia  $0.10 \times 0.055$ ; metatarsus + tarsus  $0.14 \times 0.04$ . Leg IV: trochanter  $0.10 \times 0.06$ ; femur  $0.07 \times 0.055$ ; patella  $0.17 \times 0.07$ ; tibia  $0.15 \times 0.05$ ; metatarsus  $0.085 \times 0.04$ ; tarsus  $0.10 \times 0.035$ .

**Distribution.**—*Geogarypus minor* has been recorded from Algeria, Morocco, Portugal, Spain, France, Italy, Malta, Croatia, Albania, Greece, Turkey, and possibly Sudan.

**Remarks.**—*Geogarypus minor* was described by L. Koch (1873)—as *Garypus minor*—on an uncertain number of Corsican specimens received from Eugène Simon. The original text does not reveal if Koch's description is based on one or more specimens, and even the indication of the type locality ("Auf Corsica von Herrn E. Simon entdeckt") does not give any information on this subject; the sentence (p. 39) "das bewegliche Zangenglied in ein feines Stielchen endend" certainly deals with the shape of the female galea, but it is uncertain if this character was observed in one or more specimens. The female deposited in Ludwig Koch's Collection (NHM) was regarded as a syntype by Judson (1997), as there is no evidence that it is the holotype, whereas specimens of *G. minor* in Simon's Collection (MNHN) are a mixture of probable type and non-type material (see above: Type material examined). Therefore, the female of NHM is here designated as the lectotype of *G. minor*.

A redescription of *Garypus minor*, likely based on the examination of specimens (including males) from Corsica and Algeria, was published by Simon (1879), and was followed by

the description of a new species, *Garypus nigrimanus*, based on specimens collected in southern France (Montpellier and Hyères) and Corsica. The key to species proposed by Simon provides only a single character to distinguish *G. minor* from *G. nigrimanus*, i.e., the different granulation of the palpal segments: clearly wrinkled and gnarled in *G. minor*, smooth in *G. nigrimanus*. This is in evident contrast to the original description of *G. minor* ("Das Femoralglied...fein granuliert") (Koch 1873) and also with respect to the full description of palpal granulation of both species given by Simon (1879). All subsequent authors have distinguished *G. minor* from *G. nigrimanus* based chiefly on the characters proposed by Simon (1879), except for Ellingsen (1908) (see Remarks under *Geogarypus italicus*).

After Chamberlin (1930), who established the genus *Geogarypus* with *Garypus minor* as the type species and proposed a key to species including *G. nigrimanus*, very little morphological data on these species are presented in subsequent literature. Apart from a dorso-ventral illustration of *G. nigrimanus* (Chamberlin 1931), both *G. minor* and *G. nigrimanus* were redescribed, with illustration of respective pedipalps, by Beier (1932, reproduced in Beier 1963b) based upon specimens of unknown provenance. Some basic morphometric data of an insular population of *G. minor* were reported by Gardini (1975) and an illustration of the pedipalp of a male of the above species is provided by Harvey (1986).

The female lectotype of *G. minor* (Fig. 1) corresponds well to the original description of the species, chiefly in palpal granulation, with the femur lacking in wrinkles. Comparison of the lectotype and the probable type and non-type specimens of both *G. minor* and *G. nigrimanus*, together with the examination of the above listed material (Fig. 54, including specimens from Montpellier, Hyères and Corsica), reveals that the palpal granulation is mostly fine, rarely with the femur weakly wrinkled; besides, all of the specimens examined share the shape of the chelal hand with a weak rounded hump on the paraxial surface at the base of fixed finger (see Figs. 1, 15 and Chamberlin 1931:227, fig. 62; Harvey 1986:759, fig. 4). The following synonymy is therefore proposed: *Geogarypus nigrimanus* (Simon, 1879) is a new junior subjective synonym of *Geogarypus minor* (L. Koch, 1873).

The synonymy of *Geogarypus meridionalis* (Canestrini, 1885) with *G. minor*—first proposed by Beier (1963b)—is confirmed in spite of the types collected from Rome being untraceable, since all specimens examined from the type locality belong to *G. minor*.

Many Mediterranean records of *G. minor* (Harvey 2011, 2013) remain to be verified (see Remarks under *G. italicus*).

*Geogarypus minor* is most similar to *G. canariensis* (Tullgren, 1900) from Tenerife, Canary Islands. The key presented below compares *G. minor* and the other Mediterranean-Macaronesian species of *Geogarypus*.

***Geogarypus italicus* sp. nov.**

<http://zoobank.org/NomenclaturalActs/urn:lsid:zoobank.org:act:7546836B-334E-4B02-AA7A-BA7BF2DCE8FA>

Figs. 2, 25–45, 48–51, 55

*Garypus minor*: Simon 1898:21 (Uras, Cagliari, Flumentorgiu); Gestro 1904:14 (Uras, Cagliari, Flumentorgiu, Capo Caccia; Golfo Aranci, in part: see *G. minor*); Ellingsen



1908:670 (in part: see *G. minor*); Ellingsen 1909:207, 209 (Camaldoli, Vallo di Lucania; Golfo Aranci, in part: see *G. minor*).

*Geogarypus minor*: Beier 1962:285 (Rodi Garganico); Lazzeroni 1969:335 (Rodi Garganico; Ciminà, Antonimina, in part: see *G. minor*).

**Material examined.**—*Holotype male*: ITALY: *Liguria*: *Savona Prov.*: Bergeggi, soil on cork oak wood (44°15'27"N, 8°26'35"E), 100 m a.s.l., 30 July 2007, M. Capurro, D. Duradoni & L. Galli (deposited in MHNG).

*Paratypes*: *Liguria*: *Imperia Prov.*: 1 ♂ (together with 1 ♀ of *G. minor*), Ventimiglia, Val Bevera, Torri, 60 m a.s.l., 31 March 2008, R. Poggi (MSNG). *Liguria*: *Savona Prov.*: 3 ♂, 1 ♀, 1 tritonymph, 1 deutonymph, Villanova di Albenga, Coasco, 44°03'18"N, 8°07'37"E, 54 m a.s.l., 21 September 2015, G. Gardini, C. Giusto & A. Trotta, Mediterranean scrub; 2 ♂, near Toirano, 16 February 1985, G. Gardini, under *Olea europaea*; 2 ♂, 2 ♀, Boissano, 11 March 1979, G. Gardini, under *Pistacia lentiscus*; 1 ♀, Boissano, slope Monte Ravinet, 6 May 1990, G. Gardini & R. Benelli, under *Pistacia lentiscus*; 2 ♂, Boissano, slope SW Monte Ravinet, 900 m a.s.l., 10 April 1977, S. Zoia; 1 ♂, Finale Ligure, Perti, 145 m a.s.l., 19 November 2016, R. Poggi (MSNG); 1 deutonymph, Noli, Capo Noli, 7 January 1973, G. Gardini; 1 ♀, Noli, Capo Noli, 14 January 1973, G. Gardini; 1 ♀, Noli, Capo Noli, 3 April 1977, G. Gardini & S. Zoia, sieved in garigue; 2 ♀, 3 tritonymphs (together with 1 ♂, 1 ♀ of *G. minor*), Spotorno, 16 January 1977, G. Gardini, under *Pistacia lentiscus*; 1 ♂, 1 ♀, Bergeggi, 44°15'27"N, 8°26'35"E, 100 m a.s.l., 1 January 2007, M. Capurro, D. Duradoni & L. Galli, soil on cork oak wood; 17 ♂, 3 ♀, 3 tritonymphs, Bergeggi, 6 March 2007, M. Capurro, D. Duradoni & L. Galli, soil on cork oak wood; 13 ♂, 8 ♀, 4 tritonymphs, 1 deutonymph, 5 protonymphs, Bergeggi, 9 May 2007, M. Capurro, D. Duradoni & L. Galli, soil on cork oak wood; 20 ♂, 11 ♀, 24 tritonymphs, 19 protonymphs, Bergeggi, 5 July 2007, M. Capurro, D. Duradoni & L. Galli, soil on cork oak wood; 1 ♂, 1 tritonymph, 28 deutonymphs, 35 protonymphs, Bergeggi, 30 July 2007, M. Capurro, D. Duradoni & L. Galli, soil on cork oak wood; 26 ♂, 1 ♀, 15 tritonymphs, 11 deutonymphs, Bergeggi, 17 September 2007, M. Capurro, D. Duradoni & L. Galli, soil on cork oak wood; 8 ♂, 7 ♀, 18 tritonymphs, 5 deutonymphs, Bergeggi, 15 October 2007, M. Capurro, D. Duradoni & L. Galli, soil on cork oak wood; 9 ♂, 8 ♀, 19 tritonymphs, 7 deutonymphs, 2 protonymphs, Bergeggi, 20 November 2007, M. Capurro, D. Duradoni & L. Galli, soil on cork oak wood; 4 ♂, 2 ♀, 4 tritonymphs, 2 deutonymphs, Bergeggi, 28 December 2007, M. Capurro, D. Duradoni & L. Galli, soil on cork oak wood; 6 ♂, 3 ♀, 6 tritonymphs, 2 deutonymphs, Bergeggi, 31 January 2008, M. Capurro, D. Duradoni & L. Galli, soil on cork oak wood; 1 ♂, 2 ♀, Bergeggi, 16 March 2008, R. Poggi (MSNG); 4 ♀, 2 deutonymphs, Bergeggi, Isola di Bergeggi, 13 May 2003, G. Gardini & A. Trotta; 5 ♂, 5 ♀, 2 tritonymphs (together with 3 ♂, 1 tritonymph of *G. minor*), Bergeggi, Isola di Bergeggi, 7 May 2007, R. Poggi (MSNG); 1 ♀, 1 tritonymph, Bergeggi, Isola di Bergeggi, 21 May 2007, E. Borgo (MSNG); 1 tritonymph, Segno, Rocca dei Corvi, 1 March 1983, S. Zoia; 1 ♀, 1 deutonymph, Quiliano, Tre Ponti, 80 m a.s.l., 29 October 1980, G. Gardini & S. Zoia. *Liguria*: *Genoa Prov.*: 3 ♂

(together with 1 ♂ of *G. minor*), Genova, Quinto al Mare, slope W Monte Moro, 44°23'44"N, 9°01'24"E, 240 m a.s.l., 26 November 2015, G. Gardini, under *Arbutus unedo*.

*Other material examined*: ITALY: *Tuscany*: *Grosseto Prov.*: 9 ♂, 10 ♀, 2 tritonymphs (*Garypus minor*, E. Ellingsen det.) (together with 9 ♂, 21 ♀ of *G. minor*), Isola del Giglio, [no date], G. Doria (MSNG); 2 ♀ (*Garypus minor*, E. Ellingsen det.) (together with 1 ♂, 2 ♀ of *G. minor*), Isola del Giglio, November 1902, G. Doria (MSNG); 2 ♂, 2 ♀, 1 tritonymph 1 deutonymph, Isola del Giglio, Promontorio del Franco, 17 April 1974, G. Gardini, *Quercus ilex* wood and under *Cistus*; 4 ♀, 1 tritonymph, Isola del Giglio, Promontorio del Franco, April 1985, A. Focarile, under *Cistus*. *Latium*: *Latina Prov.*: 2 ♂, 1 tritonymph, Circeo, Quarto Caldo, Faro, 5 m a.s.l., 15 June 2014, G. Gardini, under *Juniperus*. *Abruzzo*: *L'Aquila Prov.*: 2 ♀, 2 tritonymph, Fucino, Castelnuovo, 15 March 1992, G. Osella, under *Salix*; 3 ♂, 1 ♀, 1 tritonymph, Valle Peligna, 27 February 1992, M. Riti & G. Osella; 1 ♂, 2 ♀, 1 tritonymph, Valle Peligna, 19 March 1992, G. Osella; 3 ♀, 2 tritonymphs, 2 deutonymphs, Valle Peligna, 9 May 1992, M. Riti & G. Osella; 1 ♀, Valle Peligna, 16 May 1992, G. Osella; 3 ♀, 3 deutonymphs, Valle Peligna, 6 June 1992, Di Marco & Osella, under *Cistus*; 1 ♀, 1 tritonymph, Valle Peligna, 28 August 1992, G. Osella; 3 ♀, 1 tritonymph, 3 deutonymphs, Valle Peligna, 3 October 1992, G. Osella; 1 ♀, Valle Peligna, Sorgenti Fiume Pescara, 3 October 1992, G. Osella. *Abruzzo*: *Chieti Prov.*: 7 ♂, 3 tritonymphs (*Geogarypus minor*, M. Beier det.), near Chieti, 1912, A. Andreini (MSNG); 6 ♂, 8 ♀, 8 tritonymphs, 2 deutonymphs (*Geogarypus minor*, M. Beier det.), near Chieti, February 1912, A. Andreini, leaf litter (MSNG); 10 ♂, 7 ♀ (*Geogarypus minor*, M. Beier det.), near Chieti, March 1912, A. Andreini, leaf litter (MSNG). *Abruzzo*: *Pescara Prov.*: 3 ♀, 1 tritonymph, Popoli, 25 April 1999, G. Osella; 1 ♀, Popoli, Colle Capo Pescara, 42°09'57"N, 13°49'05"E, 350 m a.s.l., 18 June 1991, M. Riti; 1 ♀, 1 deutonymph, Popoli, Colle Capo Pescara, 19 August 1991, M. Riti; 2 ♂, 2 ♀, Popoli, Colle Capo Pescara, 29 August 1991, M. Riti, under *Thymus* and *Artemisia*; 1 ♂, 1 ♀, 1 tritonymph, Popoli, Colle Capo Pescara, 14 September 1991, G. Osella; 6 ♂, 10 ♀, 8 tritonymphs, 3 deutonymphs, Popoli, Colle Capo Pescara, 17 October 1991, G. Osella & M. Riti; 6 ♂, 8 ♀, 14 tritonymphs, Popoli, Colle Capo Pescara, 20 November 1991, G. Osella & M. Riti; 3 ♀, 1 tritonymph, Popoli, Colle Capo Pescara, 3 October 1992, G. Osella; 1 ♂, 1 ♀, Popoli, Colle Capo Pescara, 26 February 1994, G. Osella. *Campania*: *Naples Prov.*: 1 ♀ (*Garypus minor*, E. Ellingsen det.), Napoli, Camaldoli, 18 May 1904, F. Solari (MSNG). *Campania*: *Salerno Prov.*: 1 ♂, Vallo della Lucania, [no date], F. Solari (MSNG); 1 ♀, 1 tritonymph (*Garypus minor*, E. Ellingsen det.), Vallo della Lucania, May 1902, F. Solari (MSNG); 11 ♂, 5 ♀ (*Garypus minor*, E. Ellingsen det.), Vallo della Lucania, June 1904, F. Solari (MSNG); 1 ♂, 1 ♀, 1 deutonymph, San Giovanni a Piro, Monte Bulgheria, 800 m a.s.l., 20 April 1992, G. Gardini, *Quercus ilex* wood. *Basilicata*: *Matera Prov.*: 2 ♂, 2 ♀, Accettura, Bosco Gallipoli-Cognato, 1000 m a.s.l., 28 August 1989, F. Angelini, oak wood. *Apulia*: *Foggia Prov.*: 1 ♀ (*G. minor*, M. Beier det.), Rodi Garganico, 1 October 1961 (MSNV); 3 ♀, between Sannicandro and San Marco in Lamis, 600 m a.s.l., 8 April 1996, G. Osella, oak wood; 1 ♀, Peschici, Manacore del Gargano, Torre Usmai, 20 m a.s.l., 20 July



1996, C. Giusto. *Apulia: Bari Prov.*: 1 ♀ (*G. minor*, M. Beier det.), near Cassano Murge, November 1908, A. Andreini (MSNG); 2 ♀ (*G. minor*, M. Beier det.), Grumo Appula, December 1909, A. Andreini (MSNG). *Apulia: Taranto Prov.*: 1 ♀, near Martina Franca, 13 August 1995, S. Vit. *Calabria: Cosenza Prov.*: 1 ♂, Bocchigliero, Monte Basilicò, 1600 m a.s.l., 12 June 1992, G. Osella, oak wood; 2 ♂, 5 ♀, 5 tritonymphs, 1 deutonymph, Bocchigliero, Monte Basilicò, 900 m a.s.l., 9 October 1993, G. Osella, under *Quercus frainetto*; 1 ♂, 1 tritonymph, Bocchigliero, Monte Basilicò, 1 December 1994, G. Osella, under *Quercus* sp. *Calabria: Catanzaro Prov.*: 1 ♂, 1 ♀, Sambiasse, near Terme Caronte, 28 May 1985, S. Zoia & R. Rizzerio, *Quercus ilex* wood. *Calabria: Reggio di Calabria Prov.*: 1 ♂, 1 ♀, 2 tritonymphs (*G. minor*, G. Lazzeroni det.) (together with 2 ♀ of *G. minor*), Ciminà, 320 m a.s.l., 25 October 1966, G. Osella (MSNV); 2 tritonymphs (*Geogarypus* sp., G. Lazzeroni det.), Ciminà, 320 m a.s.l., 25 October 1966, G. Osella (MSNV); 2 ♀ (*G. minor*, G. Lazzeroni det.) (together with 2 ♂, 3 ♀ of *G. minor*), Antonimina, 350 m a.s.l., 26 October 1966, G. Osella (MSNV); 1 ♀, Delianuova, 8 April 1989, Gentile & Luchetti, pitfall trap; 1 ♂, 2 ♀, Delianuova, 14 June 1989, Gentile & Luchetti, pitfall traps. *Sicily: Palermo Prov.*: 1 ♂, Palermo, Monte Pellegrino, 3 October 1979, G. Gardini; 2 tritonymphs, Palermo, Monte Pellegrino, 400 m a.s.l., 16 March 2015, P. Magrini; 2 ♂, 2 ♀ (together with 5 ♀ of *G. minor*), Corleone, slope Rocca Busambra, 15 June 1981, G. Gardini; 1 deutonymph, Corleone, slope NE Rocca Busambra, 650 m a.s.l., 30 May 1985, R. Rizzerio & S. Zoia; 1 ♀, Corleone, Bosco della Ficuzza, near Case Cucco, 1000 m a.s.l., 29 May 1985, S. Zoia & R. Rizzerio; 1 ♂, 1 tritonymph, Corleone, Bosco della Ficuzza, 800 m a.s.l., 2 May 2000, S. Zoia & F. Polese, oak wood; 1 ♂, Corleone, Ficuzza, 6 January 1994, P. Magrini; 1 deutonymph, Caltavuturo, 450 m a.s.l., 30 May 1985, R. Rizzerio & S. Zoia, *Quercus ilex* wood; 1 deutonymph, Marineo, Bosco del Cappellero, 29 May 1985, R. Rizzerio & S. Zoia; 1 ♀, Scillato, Collesano, 2 January 1994, P. Magrini. *Sicily: Trapani Prov.*: 1 tritonymph, Castellammare, Monte Inici, 1000 m a.s.l., 30 December 1994, G. Gardini, under *Quercus ilex*; 2 ♂, 10 ♀, 1 tritonymph, Mazara del Vallo, Gorgi Tondi, 30 April 2000, S. Zoia & F. Polese, *Quercus ilex* wood; 1 ♀, Custonaci, Monte Sparagio, 455 m a.s.l., 16 March 2015, P. Magrini; 9 ♂, 10 ♀, 7 tritonymphs, Scopello, Riserva Naturale dello Zingaro, 31 December 1994, G. Gardini & S. Zoia, *Quercus ilex* wood; 1 ♂, Scopello, Riserva Naturale dello Zingaro, 17 October 2001, B. Massa; 1 ♂ (together with 1 ♀ of *G. minor*), Scopello, Riserva Naturale dello Zingaro, 17 November 2001, B. Massa; 1 ♂, Scopello, Riserva Naturale dello Zingaro, 16 March 2002, B. Massa; 1 ♀ (together with 1 ♀, 2 tritonymphs of *G. minor*), Scopello, Riserva Naturale dello Zingaro, 26 May 2002, B. Massa; 1 ♀ (together with 1 ♀ of *G. minor*), Scopello, Riserva Naturale dello Zingaro, 30 June 2002, B. Massa; 1 ♀, 1 protonymph, Scopello, Riserva Naturale dello Zingaro, 14.VII.2002, B. Massa. *Sicily: Catania Prov.*: 1 ♀, 1 tritonymph, Aci Trezza, Isola Lachea, 28 April 2000, S. Zoia & F. Polese, under *Opuntia*. *Sicily: Siracusa Prov.*: 1 ♀, 1 tritonymph, Palazzolo Acreide, Bosco Bauli, 380 m a.s.l., 7 April 2011, P. Magrini. *Sardinia: Sassari Prov.*: 1 ♀ (*Garypus minor*, E. Simon det.), Capo Caccia, April 1902, A. Dodero

(MSNG); 1 ♂ (*Garypus minor*, E. Simon det.) (together with 2 ♂, 2 ♀ of *G. minor*), Golfo Aranci, April 1902, A. Dodero (MSNG); 2 ♀ (*Garypus minor*, E. Simon det.), Golfo Aranci, April 1903, A. Dodero (MSNG); 1 ♀ (together with 1 ♂ of *G. minor*), Golfo Aranci, 11 May 2000, R. Poggi; 1 ♂, 2 ♀, Monti, 23 May 1976, R. Poggi, under *Quercus* and *Cistus*; 1 ♂, Sassari, Caniga, 17 March 1984, G. Gardini. *Sardinia: Oristano Prov.*: 1 ♀ (*Garypus minor*, E. Simon det.), Santu Lussurgiu, February 1901, Lostia (MSNG); 1 ♀ (*Garypus minor*, E. Simon det.), Uras, 25 April 1902, A. Dodero (MSNG); 1 ♂, 2 ♀, Abbasanta, 5 February 1985, C. Meloni; 2 ♀, id., Losa, 300 m a.s.l., 14 December 1994, C. Meloni; 1 ♀, Bauladu, 1 March 1989, L. Fancello & P. Leo; 1 ♀, Asuni, 23 February 1990, P. Leo. *Sardinia: Nuoro Prov.*: 1 ♂, Baunei, near Perda Longa, 20 m a.s.l., [no date], C. Torti; 1 ♀, Borore, 400 m a.s.l., 24 March 1985, C. Meloni, under bark *Eucalyptus*; 1 ♀, Desulo, 1120 m a.s.l., 28 May 1974, L. Briganti, under *Quercus ilex*; 1 ♀, Gairo Marina, 16 May 1980, G. Gardini, near the sea; 3 ♂, 1 deutonymph, Gairo Marina, 14 June 1983, C. Torti, under *Pistacia lentiscus*; 2 ♂, Gairo Marina, 14 April 2009, C. Torti, under *Myrtus* near the sea; 1 ♂, Gairo Taquisara, Ussassai, 23 June 1983, C. Torti, *Quercus ilex* wood; 1 ♂, 1 ♀, Gairo Cardedu, 26 June 1984, C. Torti, *Quercus ilex* wood; 1 ♀, Ierzu, Sant'Antonio, 27 June 1984, C. Torti, *Quercus ilex* wood on limestone; 1 ♀, Siniseola, slope S Monte Albo, 4 April 1997, S. Vit, *Quercus ilex* wood; 1 ♂, Lula, Foresta Demaniale Monte Aludè, 270 m a.s.l., 12 April 2012, C. Torti; 1 ♂, 1 ♀, Perdasdefogu, 18 June 1983, C. Torti, *Quercus ilex* wood; 1 ♂, 3 ♀, Santa Caterina di Pittinuri, Cuglieri, 24 May 1980, I. Marcellino; 2 ♀, Tertenia, Barisoni, 6 November 1992, C. Meloni, under *Pistacia lentiscus*. *Sardinia: Cagliari Prov.*: 2 ♂, 7 ♀ (*Garypus minor*, E. Simon det.), Cagliari, [no date], A. Dodero (MSNG); 1 ♂, Cagliari, Cala Regina, 15 March 1989, L. Fancello & P. Leo; 2 ♀, Cagliari, Cala Regina, 19 March 1995, L. Fancello; 3 ♂, 1 ♀ (*Garypus minor*, E. Simon det.), Carloforte, 20 May 1901, A. Dodero (MSNG); 1 ♂, Isola Sant'Antioco, Cala Lunga, 11 February 1984, L. Fancello & P. Leo; 1 ♀ (*Garypus minor*, E. Simon det.), Flumentorgiu, [no date], F. Solari (MSNG); 1 ♂, 1 ♀ (*Garypus minor*, E. Simon det.), Flumentorgiu, May 1897, F. Solari (MSNG); 1 ♂, 1 tritonymph, Arbus, Marina di Arbus, 14 April 1980, I. Marcellino; 7 ♂, 7 ♀, Arbus, Marina di Arbus, 2 November 1980, I. Marcellino; 1 ♂, Capoterra, 27 February 2003, L. Fancello; 3 ♀, Carbonia, Perdaxius, 6 May 2009, L. Fancello; 1 ♂, 2 ♀, Chia, 21 May 1994, C. Meloni; 1 ♂, 1 ♀, Chia, 14 May 1995, C. Meloni, under *Pistacia lentiscus*; 4 ♂, 15 ♀, Decimomannu, 19.IV.1995, C. Meloni, under *Olea europaea*; 1 ♂, 1 ♀, Domus de Maria, Cala de sa Musica, 45 m a.s.l., December 2008, G. Ruzzante; 2 ♂, 1 ♀, 1 tritonymph, Domus de Maria, Punta su Pisu, 19 m a.s.l., December 2006, G. Ruzzante; 15 ♂, 7 ♀, 4 tritonymphs, 1 deutonymph, Domus de Maria, Punta su Pisu, 19 m a.s.l., 15,30 September 2007, G. Ruzzante; 1 ♂, 1 ♀, Domus de Maria, Punta su Pisu, 19 m a.s.l., December 2007, G. Ruzzante; 11 ♂, 12 ♀, 13 tritonymphs, Domus de Maria, Punta su Pisu, 19 m a.s.l., September/November 2008, G. Ruzzante, dried faggot; 15 ♂, 7 ♀, 2 tritonymphs, 1 deutonymph, Domus de Maria, Punta su Pisu, 19 m a.s.l., September/November 2009, G. Ruzzante, dried faggot; 1 ♀, 2 tritonymphs, Domus de Maria, Punta su Pisu, 19 m a.s.l., 13



August 2011, G. Ruzzante; 1 tritonymph, Fluminimaggiore, Is Arenas, 29 March 1991, G. Gardini, *Quercus ilex* wood; 2 ♀, Fluminimaggiore, Perd'e Fogu, 2 April 1995, C. Meloni, under *Olea europaea*; 5 ♂, 5 ♀, 7 tritonymphs, near Fluminimaggiore, 2 April 1997, S. Vit; 1 ♀, Guspini, Sedda Orbadas, 200 m a.s.l., 9 April 1995, C. Meloni; 1 ♂, 2 ♀, 2 tritonymphs, Iglesias, Tempio di Antas, 29 March 1991, G. Gardini, *Quercus ilex* wood; 1 tritonymph, Muravera, Monte Narba, 600 m a.s.l., 30 March 1997, S. Vit; 1 ♀, Nuxis, Tattinu, 825 m a.s.l., 13 April 2014, C. Torti, under *Pistacia lentiscus*; 5 ♂, 12 ♀, Pabillonis, October 1983, P. Leo; 4 ♂, 3 ♀, Pula, 16 April 2012, L. Fancello; 1 ♂, 3 ♀, Sarroch, 6 April 1995, C. Meloni, under *Olea europaea*; 2 ♂, 5 ♀, Sarroch, Bacch'e Linna, 4 April 2010, L. Fancello; 9 ♂, 13 ♀, 4 tritonymphs, Serrenti, Gutturu Marongiu, 14 February 1995, C. Meloni; 3 ♂, 3 ♀, Siliqua, Monte Vannena, 60 m a.s.l., 9 October 1994, C. Meloni, under *Olea europaea*; 1 ♀, Sinnai, Corongiu, 4 January 1996, P. Leo; 1 ♂, near Teulada, 200 m a.s.l., 13 April 1980, I. Marcellino; 1 ♂, Villa San Pietro, 6 April 1995, C. Meloni, under *Olea europaea*; 3 ♀, Villamas-sargia, 31 March 1995, C. Meloni, under *Olea europaea*; 3 ♂, 3 ♀, Sant'Antioco, Isola il Toro, 14 June 1989, R. Poggi, under *Ecballium*; 1 ♂, 1 ♀, Sant'Antioco, 14 June 1989, G. Osella; 1 ♂, Sant'Antioco, Isola la Vacca, 14 June 1989, G. Osella.

**Diagnosis.**—A species of *Geogarypus* that differs from other extant and fossil species of the genus in the following combination of characters: carapace brown, uniformly coloured, legs not banded; tergites undivided, most sternites divided by a median thin suture, pseudotactile setae absent; vestitural setae not clavate; legs diplotarsate; galea of male simple and acuminate, of female with 9 distal rami; pedipalps often grey-dark; paraxial margin of pedipalpal hand noticeably swollen; pedipalpal femur and patella strongly wrinkled; fixed and movable chelal fingers respectively with 8 and 4 trichobothria; trichobothrium *it* mostly halfway between *et* and *ist*, *est* mostly closer to *isb* than *ib*, trichobothrium *st* closer to *sb* than *t*; fixed chelal finger homodentate, without or with 1 to 9 paraxial additional teeth on the distal half; 1 pit-like structure (*pls*) at level of trichobothria *est-esb*; venom ducts long, nodus ramosus respectively distad of *est* and *st*; length of pedipalpal femur 0.48–0.61 (♂), 0.56–0.74 (♀) mm, length of chela with pedicel 0.78–1.0 (♂), 0.94–1.20 (♀) mm.

**Description (adults).**—Integument strongly pigmented, carapace and pedipalps (fingers excepted) with star-like hispid granulation and small investing setae apically slightly sigmoid; carapace uniformly dark-brown, sometimes blackish; tergites dark-brown, I–II with a darker area on each extremity and one in the middle, III with a wide lighter medial area, IV–VIII with a thin whitish area in the middle; sternites II–III mostly whitish, IV–VIII uncoloured in the middle; pedipalps dark-brown or blackish; legs uniformly brown pale; pleural membrane longitudinally wrinkled-plicate, with transverse series of investing microsetae. Carapace (Fig. 25) 0.85–1.1 times as long as broad, subtriangular, with notch on anterior margin; anterior margin with 4 setae, the lateral longer and thicker than the medial ones; posterior margin with 12–16 setae; anterior furrow nearer the posterior eyes than the posterior margin of carapace, posterior basal furrow nearly indistinct; ocular area as in Fig. 25, diameter of eyes 0.04–0.055 mm; ratio of cucullus/carapace length 0.27–0.34.

Chaetotaxy of tergites I–XII: 12–15: 11–14: 12–14: 10–14: 12–15: 12–16: 13–16: 12–15: 13–15: 10–13: 10–13: 2. Chaetotaxy of sternites II–XII: ♂, 7–9: (1)14–15(1): (1)14–16(1): 17–21: 15–17: 14–15: 12–14: 8–9: 6–7: 2: 0; ♀, 8–9: (1)8–9(1): (1)14–15(1): 18–21: 15–18: 13–14: 11–14: 9–10: 7–9: 2: 0; sternites II–IV with setae, spiracles and tracheae of ♂ and ♀ respectively in Figs. 26 and 27; genitalia of ♂ and ♀ respectively in Figs. 28 and 29; genital atrium of ♂ with 2+2 setae. Chelicerae (Figs. 30–32) 2.0–2.4 (♂), 1.9–2.1 (♀) times as long as broad, palm with 5 setae, *bs* shorter and thicker than others; fixed finger with 4–6 teeth; movable finger with 3–5 subapical reduced teeth with rounded tips, *gs* subapical; galea simple, acuminate in ♂ (Fig. 31), with 9 apical rami in ♀ (Fig. 32); rallum with one aspinose blade; serrula interior with 12, exterior with 15 blades, the two proximal blades sickle-shaped, the distal one acuminate and stretched forward (Fig. 31). Coxal area (Fig. 33): manducatory process with 3 setae, the lateral one shorter; pedipalpal coxa with 11–19 setae (the antero-lateral one, on maxillary shoulder, very long) and two circular lyrifissures (*mml* and *pml*); chaetotaxy of coxae I–IV: I 5–7, II 6–9, III 10–16 (mostly 12–13), IV 18–23; coxae III–IV without granulation, lyrifissures as in Fig. 33. Pedipalp: trochanter (Figs. 34–35) 1.25–1.45 times as long as broad, with a ventral rounded apophysis; femur (Fig. 34) 3.1–3.45 times as long as broad, with short pedicel; patella (Fig. 34) 2.3–2.6 times as long as broad; chela with pedicel (Figs. 36–37) 3.3–3.85 (♂), 3.1–3.7 (♀) times as long as broad, 3.85–4.55 (♂), 3.5–4.2 (♀) times as long as deep; hand of chela with pedicel 1.4–2.0 (♂), 1.45–1.9 (♀) times as long as broad, 1.6–2.35 (♂), 1.65–2.1 (♀) times as long as deep; paraxial profile of pedipalpal hand, in dorsal view, noticeably swollen; fixed and movable fingers respectively with 8 and 4 trichobothria (Fig. 37), trichobothrium *it* mostly halfway between *et* and *ist* (rarely *it* closer to *et* than *ist*; Fig. 37), *est* mostly closer to *isb* than *ib*; dorsal surface of fixed chelal finger granulated as far as trichobothria *isb-est*; fixed chelal finger with 32–39 teeth with dental canals, homodentate, acuminate and anteriorly curved in the distal half of the finger, gradually reduced in size towards the finger base (Fig. 37); fixed finger without paraxial additional teeth in Ligurian specimens (Figs. 48–49) and in few specimens from Latium (Circeo), Calabria (Delianuova) and from many Sicilian localities (rarely with additional teeth on the other palpal chela or, a few, together with specimens bearing additional teeth); specimens from central and southern Italy, Sicily and Sardinia mostly with 1–3 (rarely 4–5) paraxial additional teeth—with dental canals—on the distal half of fixed chelal finger, mostly at level respectively of 9<sup>th</sup>, 12<sup>th</sup> and 15<sup>th</sup> distal serial teeth (Figs. 50–51); 1 pit-like structure (*pls*) between trichobothria *est-esb* (Fig. 37); venom ducts long, nodus ramosus respectively distad of *est* and *st*; movable chelal finger with 21–28 teeth with dental canals, distal half of movable finger with 10–12 triangular, acuminate teeth, proximal half with flat teeth gradually reduced in size, reaching back to *b*; trichobothrium *st* closer to *sb* than *t*; ratio of movable finger/hand of chela with pedicel 1.0–1.4 (♂), 1.0–1.2 (♀); ratio of pedipalpal femur/movable finger 1.05–1.2 (♂ ♀); ratio of pedipalpal femur/carapace 0.9–1.1 (♂), 0.9–1.0 (♀). Leg I (Fig. 38): trochanter 1.1–1.35, femur 2.4–3.15, patella 1.2–1.7, tibia 2.15–2.9, metatarsus 1.8–2.5, tarsus 3.1–4.0 times as long as deep; claws smooth and shorter than



arolium. Leg IV (Fig. 39): trochanter 1.4–1.7, femur 1.1–1.55, patella 2.35–2.9, tibia 3.4–4.25, metatarsus 2.5–3.2, tarsus 2.65–4.3 times as long as deep; claws smooth and shorter than arolium.

Measurements (in mm). Body length 1.45–1.9 (♂), 1.65–2.3 (♀). Carapace  $0.53\text{--}0.65 \times 0.52\text{--}0.67$  (♂),  $0.58\text{--}0.75 \times 0.63\text{--}0.78$  (♀), cucullus length (from anterior eyes) 0.15–0.19 (♂), 0.16–0.23 (♀). Chelicerae  $0.15\text{--}0.18 \times 0.07\text{--}0.11$  (♂),  $0.16\text{--}0.21 \times 0.08\text{--}0.12$  (♀), movable finger length 0.10–0.115 (♂), 0.10–0.14 (♀). Pedipalp: trochanter  $0.22\text{--}0.28 \times 0.16\text{--}0.20$  (♂),  $0.24\text{--}0.34 \times 0.17\text{--}0.24$  (♀); femur  $0.48\text{--}0.61 \times 0.15\text{--}0.195$  (♂),  $0.56\text{--}0.74 \times 0.17\text{--}0.225$  (♀); patella  $0.345\text{--}0.42 \times 0.135\text{--}0.18$  (♂),  $0.39\text{--}0.51 \times 0.15\text{--}0.21$  (♀); chela (with pedicel)  $0.78\text{--}1.0 \times 0.23\text{--}0.30$  (♂),  $0.94\text{--}1.20 \times 0.27\text{--}0.39$  (♀); chela (without pedicel) length 0.76–0.97 (♂), 0.91–1.16 (♀); chela depth 0.20–0.26 (♂), 0.25–0.34 (♀); hand length (with pedicel) 0.35–0.50 (♂), 0.42–0.57 (♀); hand length (without pedicel) 0.33–0.46 (♂), 0.39–0.53 (♀); movable finger length 0.44–0.58 (♂), 0.51–0.68 (♀). Leg I: trochanter  $0.10\text{--}0.13 \times 0.08\text{--}0.10$  (♂),  $0.11\text{--}0.16 \times 0.08\text{--}0.13$  (♀); femur  $0.19\text{--}0.255 \times 0.06\text{--}0.095$  (♂),  $0.18\text{--}0.29 \times 0.07\text{--}0.11$  (♀); patella  $0.10\text{--}0.125 \times 0.07\text{--}0.085$  (♂),  $0.11\text{--}0.145 \times 0.08\text{--}0.11$  (♀); tibia  $0.13\text{--}0.19 \times 0.05\text{--}0.065$  (♂),  $0.15\text{--}0.23 \times 0.06\text{--}0.08$  (♀); metatarsus  $0.09\text{--}0.125 \times 0.04\text{--}0.05$  (♂),  $0.09\text{--}0.135 \times 0.05\text{--}0.06$  (♀); tarsus  $0.11\text{--}0.13 \times 0.03\text{--}0.04$  (♂),  $0.10\text{--}0.17 \times 0.03\text{--}0.045$  (♀). Leg IV: trochanter  $0.16\text{--}0.20 \times 0.095\text{--}0.13$  (♂),  $0.18\text{--}0.25 \times 0.115\text{--}0.155$  (♀); femur  $0.09\text{--}0.13 \times 0.07\text{--}0.10$  (♂),  $0.11\text{--}0.16 \times 0.08\text{--}0.12$  (♀); patella  $0.30\text{--}0.39 \times 0.11\text{--}0.165$  (♂),  $0.31\text{--}0.455 \times 0.11\text{--}0.18$  (♀); tibia  $0.25\text{--}0.34 \times 0.07\text{--}0.095$  (♂),  $0.26\text{--}0.41 \times 0.07\text{--}0.11$  (♀); metatarsus  $0.14\text{--}0.17 \times 0.05\text{--}0.065$  (♂),  $0.14\text{--}0.20 \times 0.05\text{--}0.08$  (♀); tarsus  $0.12\text{--}0.16 \times 0.04\text{--}0.05$  (♂),  $0.13\text{--}0.17 \times 0.04\text{--}0.06$  (♀).

**Description (tritonymph).**—Carapace and pedipalps with weak pigmentation and granulation. Carapace 0.9–1.0 times as long as broad, furrows, anterior setae and ocular area as in adults; posterior margin with 9–11 (mostly 10) setae; diameter of anterior and posterior eyes 0.03–0.04 mm; ratio of cucullus/carapace length 0.28–0.32. Chaetotaxy of tergites I–XII: 9–11: 9–10: 9–10: 9–10: 9–10: 9–11: 9–11: 9–10: 10: 7–9: 6–8: 2. Chaetotaxy of sternites II–XII: 2: (1)4–6(1): (1)6–11(1): 10–15: 9–12: 9–11: 8–10: 6–7: 6–7: 2: 0. Chelicerae 1.85–2.0 times as long as broad, palm with 5 setae; fixed finger with 5–6 teeth; movable finger with 3–4 subapical reduced teeth with rounded tips, *gs* subapical; galea with 7 apical rami; rallum with one aspinose blade; serrula exterior with 12–13 blades, shape of proximal and distal blades as in adult. Coxal area: manducatory process with 3 setae, the lateral one shorter; pedipalpal coxa with 10–16 setae (the antero-lateral one very long) and two circular lyrifissures (*mml* and *pml*); chaetotaxy of coxae I–IV: I 3–4, II 3–5, III 7–9, IV 12–15. Pedipalp: trochanter 1.3–1.4 times as long as broad, with a ventral rounded apophysis; femur 3.05–3.55 times as long as broad, with a short pedicel; patella 2.15–2.6 times as long as broad; chela with pedicel (Figs. 40–41) 3.5–3.95 times as long as broad, 4.05–4.1 times as long as deep; hand of chela with pedicel 1.7–1.95 times as long as broad, 2.0–2.1 times as long as deep; fixed and movable fingers respectively with 7 and 3 trichobothria (Fig. 41), *isb* and *sb* absent; dorsal surface of fixed chelal finger granulated as far as trichobothrium *est*; fixed chelal finger with 28–34 teeth

with dental canals and 1–2 basal microtubercles; distal half of fixed chelal finger with acuminate, anteriorly slightly curved teeth; proximal half of fixed chelal finger with triangular teeth gradually rounded and reduced in size towards the finger base (Fig. 41), mostly with 2 paraxial additional teeth—with dental canals—on the distal half, rarely without additional teeth (Ligurian specimens); 1 pit-like structure (*pls*) at level of trichobothrium *est* (Fig. 41); venom ducts long, nodus ramosus respectively at level of *est* and distad of *st*; movable chelal finger with 22–28 teeth with dental canals, distal third of movable finger with 7–10 triangular, acuminate teeth and, proximad of trichobothrium *t*, with flat teeth gradually reduced in size, reaching back to *st-b*; ratio of movable finger/hand of chela with pedicel 1.1–1.2; ratio of pedipalpal femur/movable finger 1.0–1.1; ratio of pedipalpal femur/carapace 0.9–0.95. Leg I: trochanter 1.1–1.5, femur 2.5–3.0, patella 1.3–1.65, tibia 2.0–2.4, metatarsus+tarsus 3.6–4.5 times as long as deep; claws smooth and shorter than arolium. Leg IV: trochanter 1.3–1.6, femur 1.3–1.5, patella 2.6–3.1, tibia 3.3–3.65, metatarsus 2.2–2.6, tarsus 2.75–3.6 times as long as deep; claws smooth and shorter than arolium.

Measurements (in mm). Body length 1.4–1.8. Carapace  $0.46\text{--}0.53 \times 0.46\text{--}0.54$ , cucullus length (from anterior eyes) 0.13–0.15. Chelicerae  $0.13\text{--}0.15 \times 0.07\text{--}0.08$ , movable finger length 0.07–0.09. Pedipalp: trochanter  $0.17\text{--}0.21 \times 0.12\text{--}0.15$ ; femur  $0.43\text{--}0.50 \times 0.13\text{--}0.15$ ; patella  $0.29\text{--}0.34 \times 0.12\text{--}0.14$ ; chela (with pedicel)  $0.74\text{--}0.85 \times 0.19\text{--}0.22$ ; chela (without pedicel) length 0.71–0.82; chela depth 0.18–0.21; hand length (with pedicel) 0.37–0.42; hand length (without pedicel) 0.34–0.39; movable finger length 0.40–0.46. Leg I: trochanter  $0.09\text{--}0.11 \times 0.06\text{--}0.08$ ; femur  $0.15\text{--}0.16 \times 0.05\text{--}0.06$ ; patella  $0.09\text{--}0.10 \times 0.06\text{--}0.07$ ; tibia  $0.12\text{--}0.14 \times 0.05\text{--}0.06$ ; metatarsus + tarsus  $0.16\text{--}0.18 \times 0.04\text{--}0.05$ . Leg IV: trochanter  $0.13\text{--}0.16 \times 0.08\text{--}0.10$ ; femur  $0.10\text{--}0.11 \times 0.07\text{--}0.075$ ; patella  $0.25\text{--}0.27 \times 0.08\text{--}0.10$ ; tibia  $0.20\text{--}0.23 \times 0.06\text{--}0.07$ ; metatarsus  $0.10\text{--}0.13 \times 0.04\text{--}0.05$ ; tarsus  $0.10\text{--}0.12 \times 0.03\text{--}0.04$ .

**Description (deutonymph).**—Carapace and pedipalps with weak pigmentation and granulation. Carapace 1.0 time as long as broad, anterior setae and ocular area as in adults, furrows nearly indistinct; posterior margin with 6–8 setae; diameter of anterior eyes 0.03 mm, posterior eyes 0.03–0.04 mm; ratio of cucullus/carapace length 0.25–0.30. Chaetotaxy of tergites I–XII: 6–7: 6–7: 5–7: 6–7: 6–7: 5–7: 6–7: 6: 6: 4–5: 2. Chaetotaxy of sternites II–XII: 0: (1)3–5(1): (1)5–6(1): 5–7: 6–7: 6–7: 6–7: 4–5: 4: 20. Chelicerae 1.7–2.15 times as long as broad, palm with 5 setae; fixed finger with 4–5 teeth; movable finger with 3–4 subapical reduced teeth with rounded tips, *gs* subapical; galea with 5 apical rami; rallum with one aspinose blade; serrula exterior with 11 blades, shape of proximal and distal blades as in adult. Coxal area: manducatory process with 3 setae, the lateral one shorter; pedipalpal coxa with 7–10 setae (the antero-lateral one very long) and two circular lyrifissures (*mml* and *pml*); chaetotaxy of coxae I–IV: I 2, II 3, III 4, IV 7. Pedipalp: trochanter 1.35–1.55 times as long as broad, with a ventral rounded apophysis; femur 3.1–3.5 times as long as broad, with a short pedicel; patella 2.2–2.55 times as long as broad; chela with pedicel (Figs. 42–43) 3.8–4.2 times as long as broad, 4.3–4.35 times as long as deep; hand of chela with pedicel 1.9–2.0



times as long as broad, 2.05–2.2 times as long as deep; fixed and movable fingers respectively with 6 and 2 trichobothria (Fig. 43), *isb*, *esb* and *st*, *sb* absent; dorsal surface of fixed chelal finger granulated as far as trichobothrium *est*; fixed chelal finger with 26–28 teeth with dental canals and 1–2 basal microtubercles; distal half of fixed chelal finger with acuminate teeth; proximal half with triangular teeth gradually rounded and reduced in size towards the finger base (Fig. 43), mostly with 1 paraxial additional tooth—with dental canal—on the distal half, rarely without additional tooth (Ligurian specimens); 1 pit-like structure (*pls*) distad of trichobothrium *est* (Fig. 43); venom ducts long, nodus ramosus respectively distad of *est* and halfway between *t*–*b*; movable chelal finger with 22–24 teeth with dental canals, distal third of movable finger with 7–11 triangular, acuminate teeth and, proximad of trichobothrium *t*, with flat teeth gradually reduced in size, reaching back to *b*; ratio of movable finger/hand of chela with pedicel 1.0–1.2; ratio of pedipalpal femur/movable finger 0.9–1.05, ratio of pedipalpal femur/carapace 0.8–0.9. Leg I: trochanter 1.3–1.5, femur 2.2–2.6, patella 1.3–1.6, tibia 1.8–2.5, metatarsus+tarsus 3.75–5.0 times as long as deep; claws smooth and shorter than arolium. Leg IV: trochanter 1.55, femur 1.3–1.8, patella 2.5–2.85, tibia 2.8–3.4, metatarsus 1.8–2.25, tarsus 2.5–3.3 times as long as deep; claws smooth and shorter than arolium.

**Measurements (in mm).** Body length 1.1–1.2. Carapace  $0.39\text{--}0.43 \times 0.38\text{--}0.43$ , cucullus length (from anterior eyes) 0.10–0.12. Chelicerae  $0.12\text{--}0.13 \times 0.06\text{--}0.07$ , movable finger length 0.07. Pedipalp: trochanter  $0.15\text{--}0.17 \times 0.10\text{--}0.11$ ; femur  $0.33\text{--}0.35 \times 0.10\text{--}0.11$ ; patella  $0.22\text{--}0.24 \times 0.09\text{--}0.10$ ; chela (with pedicel)  $0.61\text{--}0.65 \times 0.15\text{--}0.17$ ; chela (without pedicel) length 0.59–0.63; chela depth 0.14–0.15; hand length (with pedicel) 0.29–0.33; hand length (without pedicel) 0.27–0.31; movable finger length 0.32–0.38. Leg I: trochanter  $0.08\text{--}0.09 \times 0.06$ ; femur  $0.11\text{--}0.13 \times 0.05$ ; patella  $0.07\text{--}0.08 \times 0.05\text{--}0.06$ ; tibia  $0.09\text{--}0.10 \times 0.04\text{--}0.05$ ; metatarsus + tarsus  $0.14\text{--}0.15 \times 0.03\text{--}0.04$ . Leg IV: trochanter  $0.11 \times 0.07$ ; femur  $0.08\text{--}0.09 \times 0.05\text{--}0.06$ ; patella  $0.18\text{--}0.20 \times 0.07\text{--}0.08$ ; tibia  $0.15\text{--}0.17 \times 0.05\text{--}0.06$ ; metatarsus  $0.08\text{--}0.09 \times 0.04\text{--}0.05$ ; tarsus  $0.09\text{--}0.10 \times 0.03\text{--}0.04$ .

**Description (protonymph).**—Carapace and pedipalps withish, with weak granulation. Carapace 0.85–1.0 times as long as broad, anterior setae and ocular area as in adults, furrows indistinct; posterior margin with 4 setae; diameter of anterior and posterior eyes 0.03 mm; ratio of cucullus/carapace length 0.22–0.28. Tergites I–XI with 4 (rarely 3) setae, tergite XII 2. Chaetotaxy of sternites II–XII: 0: (0)2(0): (1)2(1): 4: 4: 4: 4: 4: 2: 0; Chelicerae 1.75–2.0 times as long as broad, palm with 4 setae, *sbs* absent; fixed finger with 4–5 teeth; movable finger with 3–4 subapical reduced teeth with rounded tips, *gs* absent; galea with 3 apical rami; rallum with one aspinose blade; serrula exterior with 10–11 blades, proximal and distal blades as in adult. Coxal area: manducatory process with 2 setae (lateral seta absent); pedipalpal coxa with 3 setae (the anterior very long) and one circular lyrifissure (*mmf*); chaetotaxy of coxae I–IV: 1. Pedipalp: trochanter 1.2–1.5 times as long as broad, with a ventral rounded apophysis; femur 2.7–3.5 times as long as broad, with a short pedicel; patella 2.0–2.7 times as long as broad; chela with pedicel (Figs. 44–45) 3.8–4.2 times as long as broad, 4.3 times as long as deep; hand of chela with pedicel 1.9–2.1 times as long as

broad, 2.2 times as long as deep; fixed and movable fingers respectively with 3 and 1 trichobothria (Fig. 45), *it*, *est*, *isb*, *ib*, *esb* and *st*, *sb*, *b* absent; dorsal surface of fixed chelal finger slightly granulated as far as trichobothrium *eb*; fixed chelal finger with 19–24 teeth with dental canals and 3–5 basal microtubercles; distal half of fixed chelal finger with acuminate teeth; proximal half with triangular and rounded teeth gradually reduced in size towards trichobothrium *eb* (Fig. 45); additional teeth absent; 1 pit-like structure (*pls*) at level of trichobothrium *ist* (Fig. 45); venom ducts long, nodus ramosus respectively proximad of *ist* and proximad of *t*; movable chelal finger with 15–20 teeth with dental canals, distal third of movable finger with 6–8 triangular, acuminate teeth, proximally with flat teeth gradually reduced in size; ratio of movable finger/hand of chela with pedicel 1.0–1.15; ratio of pedipalpal femur/movable finger 0.95–1.05, ratio of pedipalpal femur/carapace 0.8–1.0. Leg I: trochanter 1.2–1.4, femur 2.4–3.3, patella 1.2–1.5, tibia 2.0–2.25, metatarsus+tarsus 3.3–4.0 times as long as deep; claws smooth and shorter than arolium. Leg IV: trochanter 1.3–1.65, femur 1.4–1.75, patella 2.0–2.8, tibia 2.4–3.2, metatarsus 1.5–1.75, tarsus 2.3–3.0 times as long as deep; claws smooth and shorter than arolium.

**Measurements (in mm).** Body length 0.85–1.0. Carapace  $0.27\text{--}0.34 \times 0.32\text{--}0.38$ , cucullus length (from anterior eyes) 0.07–0.09. Chelicerae  $0.10\text{--}0.11 \times 0.05\text{--}0.06$ , movable finger length 0.05–0.06. Pedipalp: trochanter  $0.11\text{--}0.13 \times 0.08\text{--}0.09$ ; femur  $0.27\text{--}0.28 \times 0.08\text{--}0.11$ ; patella  $0.16\text{--}0.20 \times 0.07\text{--}0.08$ ; chela (with pedicel)  $0.49\text{--}0.55 \times 0.12\text{--}0.14$ ; chela (without pedicel) length 0.47–0.53; chela depth 0.125; hand length (with pedicel) 0.23–0.27; hand length (without pedicel) 0.21–0.25; movable finger length 0.26–0.29. Leg I: trochanter  $0.06\text{--}0.07 \times 0.05$ ; femur  $0.10\text{--}0.12 \times 0.03\text{--}0.05$ ; patella  $0.05\text{--}0.06 \times 0.04\text{--}0.05$ ; tibia  $0.08\text{--}0.09 \times 0.04$ ; metatarsus + tarsus  $0.10\text{--}0.12 \times 0.03$ . Leg IV: trochanter  $0.08\text{--}0.10 \times 0.05\text{--}0.06$ ; femur  $0.07 \times 0.04\text{--}0.05$ ; patella  $0.14\text{--}0.17 \times 0.06\text{--}0.07$ ; tibia  $0.12\text{--}0.14 \times 0.04\text{--}0.05$ ; metatarsus  $0.06\text{--}0.07 \times 0.04$ ; tarsus  $0.07\text{--}0.09 \times 0.03$ .

**Distribution.**—*Geogarypus italicus* has been recorded from the following regions of Italy (Fig. 55): Liguria, Tuscany, Latium, Abruzzo, Campania, Basilicata, Apulia, Calabria, Sicily, and Sardinia.

**Remarks.**—*Geogarypus italicus* shares with *G. minor*, a widespread species in the Mediterranean-Macaronesian area, the same distribution in mainland Italy, Sicily and Sardinia, often with syntopic populations (Figs. 54–55). The presence of *G. italicus*, a species with a palpal femur with evident wrinkles, together with *G. minor* probably contributed to perpetuate the error of Simon (1879) in interpreting both *G. minor* and *G. nigrimanus* (see Remarks under *G. minor*).

The high variability of *G. minor* from Giglio Island (Tuscany) emphasized by Ellingsen (1908) is due to the presence on that island of both *G. minor* and *G. italicus*, in MSNG mixed in the same vials (see above under Other material examined). Consequently, many Italian records of *G. minor* (Gardini 2000) remain to be verified.

The relationships of *G. italicus* within the Mediterranean-Macaronesian *Geogarypus* fauna are uncertain, but morphological comparisons are outlined in the proposed key.

**Etymology.**—The name refers to the geographical provenance of the examined specimens.



KEY TO ADULTS OF THE MEDITERRANEO-MACARONESIAN SPECIES OF *GEOGARYPUS*

1. Galea conical, acuminate in male, apically indented or slightly bifurcate in female; distal half of fixed chelal finger with 1–3 antiaxial additional (“accessory”) teeth; pedipalpal femur and patella always without wrinkles; carapace two-coloured, uniformly brown or red-brown distad the anterior furrow, with a median dark area and two lateral pale ones proximad the anterior furrow ..... 2
  - Galea conical, acuminate in male, with 9 (rarely 8) apical rami in female; fixed chelal finger without or with 1–15 paraxial additional (“accessory”) teeth; pedipalpal femur and patella without or with wrinkles; carapace uniformly brown or red-brown ..... 4
2. Trichobothrium *st* closer to *t* than *sb*; different coloured areas of carapace less contrasted, gradually faded each others; pedipalps (♀) more slender: femur 4.0–4.8, patella 3.2–3.7, chela with pedicel 3.9–4.7 times as long as broad ..... 3
  - Trichobothrium *st* closer to *sb* than *t*; different coloured areas of carapace more contrasted, clearly separated each others; pedipalps (♀) less slender: femur 3.9, patella 3.0, chela 3.6 times as long as broad (Israel) ..... *G. pulcher* Beier, 1963
3. Smaller: length of pedipalpal femur 0.76 (♂), 0.75–0.85 (♀), patella 0.55 (♂), 0.56–0.62 (♀), chela with pedicel 1.24 (♂), 1.22–1.34 (♀), hand with pedicel 0.56 (♂), 0.52–0.63 (♀), finger 0.70 (♂), 0.69–0.75 (♀) mm [Chad; introduced to Gran Canaria Isl (Mahnert 2011)] ..... *G. mirei* Heurtault, 1970
  - Larger: length of pedipalpal femur 0.85–0.92 (♂), 0.85–1.0 (♀), patella 0.60–0.68 (♂), 0.62–0.78 (♀), chela with pedicel 1.32 (♂), 1.40–1.41 (♀), hand with pedicel 0.62–0.71 (♂) 0.68–0.78 (♀), finger 0.72–0.81 (♂), 0.74–0.90 (♀) mm (Greece, Turkey, Israel, Iran, Turkmenistan) ..... *G. shulovi* Beier, 1963
4. Pedipalpal femur mostly without wrinkles (Fig. 13), rarely weakly wrinkled; fixed chelal finger heterodentate (teeth irregularly aligned, distal half of finger with one long tooth alternate with two-three shorter teeth: Figs. 16, 20), with 3–15 paraxial additional teeth ..... 5
  - Pedipalpal femur strongly wrinkled (Fig. 34); fixed chelal finger homodentate (teeth regularly aligned and decreasing in size proximally: Fig. 37, 41), without or with 1–9 paraxial additional teeth on the distal half (Figs. 48–51) (Italy) ..... *G. italicus* sp. nov.
5. Pedipalpal hand, in dorsal view, with irregular outline at the base of fingers; fixed chelal finger with 30–36 teeth with dental canals; smaller: length of pedipalpal femur 0.45–0.62 (♂) 0.53–0.82 (♀), patella 0.35–0.45 (♂), 0.38–0.62 (♀), chela with pedicel 0.75–0.94 (♂), 0.80–1.33 (♀), hand with pedicel 0.32–0.44 (♂), 0.39–0.60 (♀), finger 0.44–0.53 (♂) 0.47–0.76 (♀) mm ..... 6
  - Pedipalpal hand, in dorsal view, oval, with regular outline at the base of fingers; fixed chelal finger with 38–45 teeth with dental canals; larger: length of pedipalpal femur 0.69–0.72 (♂), 0.80–0.84 (♀), patella 0.51–0.54 (♂), 0.545–0.64 (♀), chela with pedicel 1.14–1.15 (♂) 1.25–1.40 (♀), hand with pedicel 0.53–0.54 (♂) 0.58–0.68 (♀), finger 0.65–0.66 (♂), 0.71–0.75 (♀) mm (Morocco) ..... *G. maroccanus* Beier, 1961
6. Paraxial surface of pedipalpal hand with a weak rounded hump at the base of fixed finger (Fig. 15); fixed chelal finger with 4–9 paraxial additional (“accessory”) teeth mostly on its proximal half (Figs. 16, 46–47) (Algeria, Morocco, Portugal, Spain, France, Italy, Malta, Croatia, Albania, Greece, Turkey, Sudan (?)) ..... *G. minor* (L. Koch, 1873)
  - Paraxial-ventral surface of pedipalpal hand with a hollow at the base of movable finger; fixed chelal finger with 3–7 paraxial additional (“accessory”) teeth mostly on its distal half (Figs. 52–53) [Canary Islands (Tenerife)] ..... *G. canariensis* (Tullgren, 1900)

## DISCUSSION

Seven species of the genus *Geogarypus* are known from Mediterraneo-Macaronesian area. The above key is based on data from the original description of *G. pulcher* Beier, 1963—integrated with those from Mahnert (1974)—and from the redescription of *G. maroccanus* Beier, 1961 by Callaini (1988). Descriptions of *G. shulovi* Beier, 1963 are integrated with data from Beier (1965) and those of both *G. shulovi* and *G. mirei* Heurtault, 1970 are integrated with examination of specimens listed above (see Methods).

*Geogarypus canariensis* was described (as *Garypus canariensis*) from Tenerife, Barranco de Ruiz (Tullgren 1900). The female holotype of *G. canariensis* is untraceable and the redescrptions presented by Beier (1956) and Callaini (1988) on specimens from Morocco most likely represent other species. Since all of the studied specimens from Tenerife are morphologically homogeneous, they all are referred to *G. canariensis*, whereas the specimens from other Canarian islands—morphologically differentiated and to be reviewed

when more material is available—are provisionally referred to *G. cf. canariensis* and excluded from the above key.

## ACKNOWLEDGMENTS

We are grateful to Janet Beccaloni (NHM), Mark L.I. Judson (MNHN), Leonardo Latella (MSNV), Paola Niccolosi (MZUP), Pedro Oromí (DZUL) Peter Schwendinger (MHNG) and Maria Tavano (MSNG) for the loan of *Geogarypus* specimens; Henri-Pierre Aberlenc (Montferrier-sur-Lez, France) for his hospitality during field researches near Montpellier; Pierre Oger (Waret l'Évêque, Belgium) provided important material from southern France; Carlo Giusto (Genoa), Mark S. Harvey (Perth), Mark L.I. Judson (Paris), Volker Mahnert (Geneva) and Juan A. Zaragoza (Alicante) kindly made suggestions and improvements to this study. We are grateful to Laura Negretti (DISTAV, Genoa University) for her help in the acquisition of SEM images.



## LITERATURE CITED

- Batuwita, S. & S.P. Benjamin. 2014. An annotated checklist and a family key to the pseudoscorpion fauna (Arachnida: Pseudoscorpiones) of Sri Lanka. *Zootaxa* 3814(1):37–67.
- Beier, M. 1932. Pseudoscorpionidea I. Subord. Chthoniinea et Neobisiinea. *Das Tierreich*, 57. W. De Gruyter, Berlin & Leipzig.
- Beier, M. 1956. Ueber Pseudoscorpione aus Spanische-Marocco. *Eos*, Madrid 31:303–310.
- Beier, M. 1962. Appenninische Pseudoscorpione. *Memorie del Museo Civico di Storia Naturale di Verona* 10:283–286.
- Beier, M. 1963a. Sizilianische Pseudoscorpione. *Bollettino delle sedute della Accademia Gioenia di Scienze Naturali in Catania* (4)(7):253–263.
- Beier, M. 1963b. Ordnung Pseudoscorpionidea (Afterscorpione). *Bestimmungsbücher zur Bodenfauna Europas*, vol. 1. Akademie-Verlag, Berlin.
- Beier, M. 1965. Anadolu'nun Pseudoscorpion faunası. *Die Pseudoscorpioniden-Fauna Anatoliens*. Istanbul Üniversitesi Fen Fakültesi Mevzuatı 29B:81–105.
- Callaini, G. 1983. Pseudoscorpioni dell'Isola di Montecristo (Arachnida). *Notulae Chernetologicae* IX. *Redia*, Firenze 66:147–165.
- Callaini, G. 1988. Gli Pseudoscorpioni del Marocco. (Notulae Chernetologicae, XXVII). *Annali del Museo Civico di Storia Naturale "G. Doria"*, Genova 87:31–66.
- Callaini, G. 1989. Il popolamento delle Isole Egadi. Un esempio dell'interesse biogeografico degli Pseudoscorpioni (Arachnida) (Notulae Chernetologicae XXIX). *Annali del Museo Civico di Storia Naturale "G. Doria"*, Genova 87:137–148.
- Canestrini, J. 1885. Chernetides Italici. In: A. Berlese, Aeri, Myriapoda et Scorpiones hucusque in Italia reperta, fascicolo XIX. A. Berlese: Padova.
- Chamberlin, J.C. 1930. A synoptic classification of the false scorpions or chela-spinners, with a report on a cosmopolitan collection of the same. Part II. The Diplosphyronida (Arachnida – Chelonethida). *Annals and Magazine of Natural History* (10)5:1–48, 585–620.
- Chamberlin, J.C. 1931. The Arachnid order Chelonethida. Stanford University Publications, University Series, (Biol. Sci.) 7:1–284.
- Ellingsen, E. 1908. Materiali per una fauna dell'Arcipelago Toscano. VIII. Isola del Giglio. Notes on Pseudoscorpions. *Annali del Museo Civico di Storia Naturale*, Genova 43:668–670.
- Ellingsen, E. 1909. Contribution to the knowledge of the Pseudoscorpions from the materials belonging to the Museo Civico in Genova. *Annali del Museo Civico di Storia Naturale*, Genova 44:205–220.
- Gardini, G. 1975. Pseudoscorpioni dell'Isola di Capraia (Arcipelago Toscano). *Lavori della Società italiana di Biogeografia* (n.s.)5[1974]:385–396.
- Gardini, G. 2000. Catalogo degli Pseudoscorpioni d'Italia (Arachnida). *Fragmenta Entomologica*, Roma 32(suppl.):1–181.
- Gardini, G., G. Sabella & L. Saccione. 1997. Studi sulle comunità di Pseudoscorpioni dei sistemi forestali dei Nebrodi (Sicilia nordorientale) (Pseudoscorpionida). *Fragmenta Entomologica*, Roma 29(2):213–237.
- Gestro, R. 1904. Una gita in Sardegna. Divagazioni biogeografiche. *Bollettino della Società Geografica Italiana*, Roma (4)5(4):1–39.
- Harvey, M.S. 1986. The Australian Geogarypidae, new status, with a review of the generic classification (Arachnida: Pseudoscorpionida). *Australian Journal of Zoology* 34:753–778.
- Harvey, M.S. 1992. The phylogeny and classification of the Pseudoscorpionida (Chelicerata: Arachnida). *Invertebrate Taxonomy* 6:1373–1435.
- Harvey, M.S. 2011. *Cheiridium tetraphthalmum* Daday, a new synonym of *Larca lata* (Hansen) (Pseudoscorpiones, Larcidae). *Arachnologische Mitteilungen* 41:31–33.
- Harvey, M.S. 2013. Pseudoscorpions of the World, version 3.0. Western Australian Museum, Perth. Online at <http://www.museum.wa.gov.au/catalogues-beta/pseudoscorpions> [accessed 25 Dec. 2016].
- Henderickx, H. & E.E. Perkovsky. 2012. The first geogarypid (Pseudoscorpiones, Geogarypidae) in Rovno Amber (Ukraine). *Vestnik Zoologii* 46(3):33–36.
- Judson, M.L.I. 1997. Catalogue of the pseudoscorpion types (Arachnida: Chelonethi) in the Natural History Museum, London. *Occasional Papers on Systematic Entomology* 11:1–54.
- Judson, M.L.I. 2007. A new and endangered species of the pseudoscorpion genus *Lagynochthonius* from a cave in Vietnam, with notes on chelal morphology and the composition of the Tyrannoethonini (Arachnida, Chelonethi, Chthoniidae). *Zootaxa* 1627:53–68.
- Koch, L. 1873. Uebersichtliche Darstellung der Europäischen Chernetiden (Pseudoscorpione). Bauer & Raspe, Nürnberg.
- Lazzeroni, G. 1969. Sur la faune de Pseudoscorpions de la région apenninique méridionale. (Recherches sur les Pseudoscorpions. III). *Memorie del Museo Civico di Storia Naturale di Verona* 16(1968):321–344.
- Mahnert, V. 1974. Einige Pseudoscorpione aus Israel. *Revue Suisse de Zoologie* 81:377–386.
- Mahnert, V. 2011. A nature's treasury: Pseudoscorpion diversity of the Canary Islands, with the description of nine new species (Pseudoscorpiones, Chthoniidae, Cheiridiidae) and new records. *Revista ibérica de Aracnología* 19:27–45.
- Nassirkhani, M. 2014. A new pseudoscorpion species of the genus *Geogarypus* (Arachnida: Pseudoscorpiones) from Iran. *Acta Arachnologica* 63:99–103.
- Simon, E. 1879. Les Arachnides de France, vol. 7, les Ordres des Chernetes, Scorpiones et Opiliones. Librairie Encyclopédique de Roret, Paris: [1–78].
- Simon, E. 1898. Studio sui Chernetes italiani conservati nel Museo Civico di Genova, con descrizione di una nuova specie. *Annali del Museo Civico di Storia Naturale*, Genova 39:20–24.
- Simon, E. 1900. Studio sui Chernetes italiani conservati nel Museo Civico di Genova. II. *Annali del Museo Civico di Storia Naturale*, Genova 40:593–595.
- Tullgren, A. 1900. Chelonethi (Pseudoscorpiones) from the Canary and the Balearic Islands. *Entomologisk Tidskrift* 21:153–157.

*Manuscript received 13 March 2017, revised 17 April 2017.*



## SHORT COMMUNICATION

### Effect of weather conditions on cohort splitting in a wolf spider species

Zoltán Rádai<sup>1\*</sup>, Balázs Kiss<sup>2</sup> and Ferenc Samu<sup>2</sup>: <sup>1</sup>MTA-DE Lendület Behavioural Ecology Research Group, Department of Evolutionary Zoology and Human Biology, University of Debrecen, Debrecen, Hungary; E-mail: zradai.sci@gmail.com  
<sup>2</sup>Plant Protection Institute, Centre for Agricultural Research, Hungarian Academy of Sciences, Budapest, Hungary

**Abstract.** Cohort splitting has been described as differences in time until maturation and / or life span in the same age group. Cohort splitting generally occurs when individuals of a cohort originating from the same season experience different environmental conditions, such as in early and late progenies. However, in the wolf spider *Pardosa agrestis* (Westring, 1861) spiderlings of the same clutch may follow either slow or rapid development, leading to a second adult peak within a year comprised of the rapidly developing individuals. We hypothesized that weather conditions experienced by the spiderlings in their early ontogeny may contribute to a life history decision between slow and rapid development. To test this hypothesis, we have used long term collection data and non-parametric habitat modeling. We found that highest abundance of the rapidly developing phenotype was correlated with a narrow range of early weather conditions. This result is in accordance with our early choice hypothesis, although the possibility remains that differential survival of the developmental morphs also contributes to the observed pattern.

**Keywords:** Lycosidae, habitat modeling, long term sampling, development, ontogeny

Cohort splitting can be defined as a life history scenario in which individuals within a cohort exhibit variation in developmental rates, maturation time and / or life span, leading to a divergence of individual ontogenies within an age group (Danks 1992; Watts & Thompson 2012; Crowley & Hopper 2015). This phenomenon is well described in several arthropod groups (Sunderland et al. 1976; David et al. 1993; Moreira & Peckarsky 1994; Townsend & Pritchard 1998; David et al. 1999; Bonte & Macfai 2001; Johansson et al. 2001; Gonçalves et al. 2005; Kozáčeková et al. 2009), as well as in some vertebrates (Newman 1989, 1992; Post et al. 1997; Callihan et al. 2008).

Different factors may play a role in orchestrating cohort splitting, such as genetic polymorphism, maternal effects and environmental cues (reviewed in Crowley & Hopper 2015). Cases of environmentally induced differences in developmental trajectories are well described in animals, for example in relation to population density (Post et al. 1997), prey availability (Pickup & Thompson 1990), ambient temperature (Callihan et al. 2008) or photoperiod (Kozáčeková et al. 2009). Such changes in developmental trajectories due to environmental factors are often regarded as bet-hedging strategies in unpredictable environments (Stearns & Crandall 1981; Tuljapurkar 1994; Watts & Thompson 2012), and can have considerable impact on the fitness of the individuals (Hopper 1999).

An interesting case of cohort splitting was described in populations of the wolf spider *Pardosa agrestis* (Westring, 1861), an epigeic spider species, dominant in agricultural habitats of Central Europe (Samu & Szinetár 2002). Unlike the typical univoltine *Pardosa* life cycles in the temperate regions—where generally one sexually mature cohort exists in each year (see Schaefer 1977)—this semelparous species exhibits a phenology with two adult peaks, and hence two reproductive periods in a year (Samu et al. 1998). As Kiss and Samu (2002, 2005) have shown, this phenological pattern arises from developmental asynchrony in the early summer progeny. Some of the spiderlings, hatching from the first adult generation, between May and June, are only able to reach maturity in the next spring or summer, after overwintering. Others, even from the same brood, are capable of reaching adulthood and reproduce in about three months, thus comprise a second generation within a year (Fig. 1).

The background of this case of cohort splitting is largely unknown, although previous studies suggested that photoperiod and ambient temperature might be key factors, as spiderlings experiencing long day-length and high (but not stressful) temperatures matured sooner and in higher proportions compared to spiderlings reared in short day-length and lower temperatures (Kiss & Samu 2002; Rádai, unpublished results). In artificial rearing experiments, the ratio of slowly and rapidly developing spiderlings varies among clutches (i.e., among mothers) which might indicate genetic involvement in the rapid development (Kiss 2003; Rádai et al., unpublished data). Still, the strong influence of ambient conditions suggests that cohort splitting may be the result of a decision on the part of the offspring, in an early time window of their ontogeny.

In this study we propose an early choice hypothesis, stating that weather conditions experienced by the early summer progeny of *P. agrestis* contribute to a decision between slow and rapid developmental life histories. Based on the results presented by Kiss and Samu (2002) and Kiss (2003), in an early choice scenario we predict to see that under a narrow range of favourable early weather conditions more spiderlings will choose rapid development. Hence, in years when early weather conditions fall in this narrow range, we would expect to see higher abundances of second generation adults during late summer in natural *P. agrestis* populations. To test this hypothesis, we have used long term collection data from the natural habitats of this spider species in Hungary (Samu 1999), and long term weather data provided by the CarpatClim project (Szalai et al. 2012).

Our working data table consisted of 535 samples (with a total of 5284 collected adult *P. agrestis* specimens), recorded between 1993 and 2002 in the months from August to November, from the vicinity of 13 settlements across Hungary. For each sample we defined sampling success as the number of adult spiders collected with a given sampling method, at the sampling site and date. Sampling method was either suction sampling or using pitfall traps. Because suction sampling and pitfall traps might differ in how they relate sampling success to density and activity of the animals, our records of sampling successes reflected a combination of both abundance and activity during sampling. In all cases, sampling effort was specified as the number of pitfall traps used, or number of sampling transects of identical lengths (10 meters) for suction sampling. For early weather



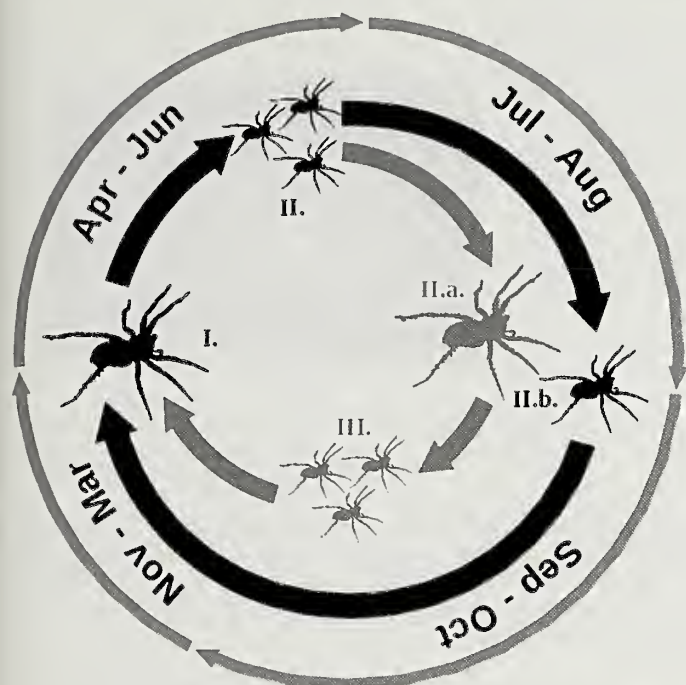


Figure 1.—Phenology of *P. agrestis*; the first adult generation matures between the end of March and April (I.), after which the first wave of progeny hatches in May and June (II.). Some of the spiderlings follow slow development (II.b.) reaching maturity only in the next year, while others develop rapidly, mature and reproduce between August and September (II.a.), giving rise to a new cohort of progeny (III.).

conditions, principal components (PCs) were calculated for May. We also calculated PCs for the given month of sampling. In the PC analyses, we used six weather parameters for each month, measured at the settlement of the sampling location. The spatial detail of available weather data was 10×10 km, therefore we had unique weather data for settlements being at least 10 km apart from one another. The weather parameters were minimum, maximum and mean monthly temperature (Celsius), amount of precipitation (mm), monthly mean of relative humidity and total of sunshine hours in the given month. From the calculated PCA axes, we have used only those with eigenvalues of 1 or higher (Kaiser criterion: Kaiser 1960), which yielded two PCs for May (hereafter, PC1 and PC2 of May) and two for the sampling dates (hereafter PC1 and PC2 of sampling date). The proportions of variance represented by PC1 and PC2 of May were ca. 74 and 17%, respectively. Also, the proportions of variance represented by PC1 and PC2 of sampling-date were ca. 60 and 20%, respectively. PC1 of both May and the sampling date was strongly correlated with all six weather parameters, and PC2 of both May and the sampling date were at least moderately correlated with all weather parameters (see supplementary material for details, online <http://dx.doi.org/10.1636/JoA-S-17-008R2.s1>).

To test, how the calculated PCs for May and for the sampling dates are related to the sampling success of second generation adults in the months between August and November, we have applied non-parametric habitat modeling using HyperNiche v2.30 (McCune & Mefford 2009). In the models, we defined sampling success as response variable, while predictor variables were the calculated principal components for the weather of May and sampling date weather. As additional predictors we also used habitat type (categorical, with levels: arable field, wet meadow, alkaline grassland, rock grassland, disturbed grassy habitat), sampling method (categorical, with levels: pitfall traps or suction sampling) and sampling effort.

Models were acquired by running three model-searching sessions of Local Linear Estimator, using conservative, medium and aggressive over-fitting settings, respectively (3% allowable missing estimates in each). Each session yielded a high number of models, from which the one with the highest cross-validated  $R^2$  value was selected as the best fit, so finally we had one model from each session (i.e., three models in total). To test whether the fitted models are better than could be obtained by chance alone, we have used randomization tests (integrated in HyperNiche) with 100 runs, comparing each model to 100 models with randomly generated predictor values.

In all three best fit models, sampling method and PC1 of May were retained as predictor variables, indicating that out of the tested variables, these consistently explained the variance in sampling success best. Additionally, in the models using medium and aggressive over-fitting settings, PC1 of the sampling date was also retained. All three models explained sampling success significantly better than did randomized predictor values ( $P=0.01$  in case of all models). Based on the models, highest second generation adult abundances were related to a narrow range of early weather conditions in May (see Fig. 2). Similarly, in the models using medium and aggressive over-fitting, a narrow range of sampling date weather conditions was also apparent, at which sampling success peaked (Fig. 2). Regarding the sampling methods, on average pitfall traps collected more spiders per sample compared to suction sampling; estimated sampling success of pitfall traps and suction sampling were  $12.41 \pm 22.97$  and  $1.98 \pm 1.58$  (mean  $\pm$  standard deviation), respectively.

The selected models' consistent retainment of the PC representing weather conditions in May indicates that early conditions strongly influence the abundance of the second adult generation. The relatively narrow range in the values of May PC1 corresponding to high second generation abundance can be regarded as an optimal set of weather conditions, which enable or contribute to the appearance and high abundance of rapidly developing individuals in the populations.

Although our results support that weather conditions during early larval stages contribute significantly to the abundance of rapidly developing spiders, the mechanism in the background remains unclear. Environmental factors may affect postembryonic development directly, for example through providing cues based on which life history decisions can be made (reviewed in Danks 1994). However, they can act indirectly as well, for example due to their effects on prey availability (Hayashi 1988) or metabolism (Gillooly et al. 2001). In years of drought, low prey abundance might limit the opportunities of the spiders because limited prey availability possibly cannot provide sufficient quantity and / or quality of resources for rapid growth. On the other hand, low temperatures during the first larval stages could lengthen developmental time either by reducing the efficiency of different metabolic processes (Brown et al. 2004; Irlich et al. 2009), or simply by decreasing locomotory activity of the animals (Ford 1978), leading to reduced hunting virtue.

Furthermore, differential survival of spiderlings of alternate developmental trajectories could also contribute to the correlation between late summer adult abundance and weather conditions in May. More precisely, it might be possible that the ratio of slowly and rapidly developing spiders (not assessed in this study) is not as strongly related to environmental cues, e.g., due to genetic polymorphism, and the abundance of late summer adults is affected also by their survival throughout the first larval stages. For instance, spiderlings engaging in rapid development have probably higher demand for energy and nutrients, which, if not met, could lead to increased mortality among rapidly developing spiderlings when food is scarce. Therefore, we cannot rule out that late summer abundance of adults, at least in part, is shaped by the differential survival of the two developmental phenotypes during their early ontogeny. However, considering the results of past rearing studies, in which ambient conditions were shown to increase moulting frequency and probability of moulting to adulthood (Kiss & Samu 2002; Kiss 2003), it seems



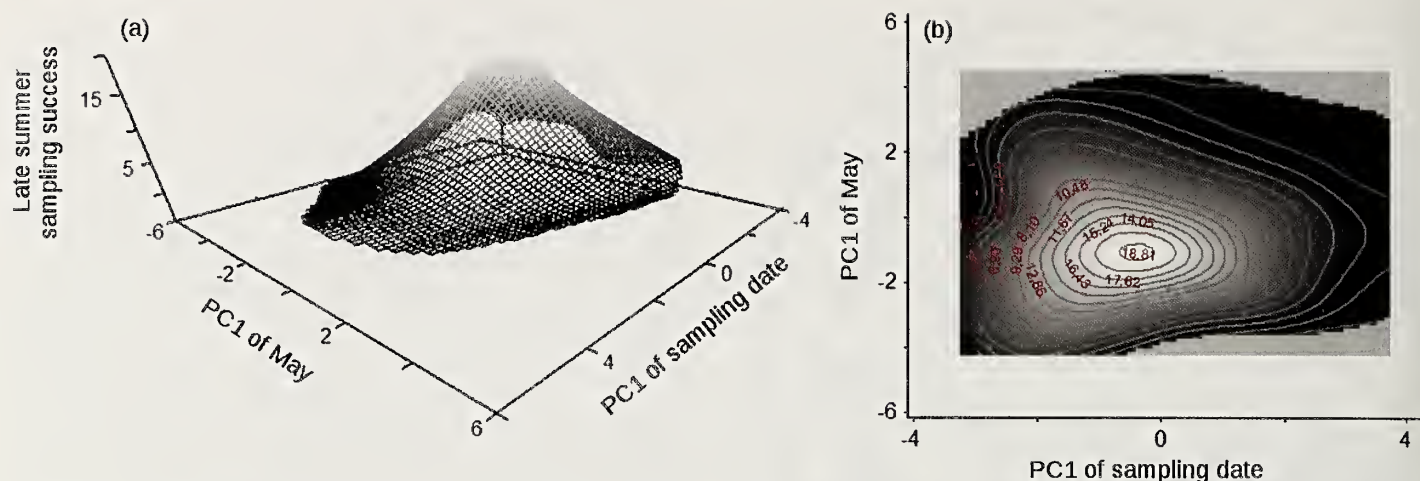


Figure 2.—Sampling success of late summer adults in relation to weather conditions in May and during sampling, visualized on 3D projection plot (a) and contour plot (b). Structural lines on (a) and contour regions on (b) represent the number of adult *P. agrestis* individuals: darker lines / regions correspond to low, while bright lines / regions correspond to higher numbers. On the contour plot (b) gray lines delimit the segments of the response surface of late summer sampling success, and red numbers show the predicted sampling success (i.e., number of adult spiders), in relation to weather conditions in May (PC1 of May) and during sampling (PC1 of sampling date).

likely that weather conditions experienced by the spiderlings in their early ontogeny have a consistent and profound effect on their development.

The result that weather conditions during the month of sampling show similar effect on the abundance of adults suggests that weather also influences sampling success itself, which is not very surprising, since environmental conditions are known to contribute to the activity, and thus the sampling success of epigeic arthropods (e.g., Honěk 1988; Kiss & Samu 2000). Under favourable weather conditions in late summer adult spiders might show increased activity due to increased propensity to forage, or to look for potential mates, leading to an increase in their sampling success. On the other hand, severely adverse conditions might not only decrease their activity, but could also increase mortality, leading to significant reduction in population size, and consequently to low sampling success. We note that because the two sampling methods might represent activity and abundance with different weights, by including both types of data, and also sampling method as a factor in our models, we could base our interpretation of the results on an intermediate estimate of activity and abundance.

In Hungarian *P. agrestis* populations, cohort splitting is a persistent phenomenon (Samu et al. 2011), but its degree is dependent on both the early summer and late summer weather conditions of the given year. This versatile life history strategy of *P. agrestis*, that is unique among congeneric wolf spiders, may represent a special adaptation to climatic conditions in Central Europe, making this species able to benefit from variably occurring favourable periods. Cohort splitting may have preadapted *P. agrestis* to highly changeable agricultural environments, and could be a reason why it has become a successful agrobiont species that attains high abundances in arable habitats (Kiss & Samu 2005).

In conclusion, our results are in accordance with the prediction of our early choice hypothesis, although in this study we cannot rule out that differential survival of the two developmental forms might also contribute to the observed pattern. The exact mechanism by which early weather affects the life histories of *P. agrestis* and evokes cohort splitting remains to be studied. Also, it is likely that not only early weather conditions contribute to this case of cohort splitting, so within- and among brood variation in life histories unrelated to weather conditions should also be considered in future studies. Arguably, retrospective approaches using long term data on

population ecology and high-throughput modeling methods offer valuable insights on population dynamics, and therefore could be valuable tools when studying cohort splitting. The present example of cohort splitting still holds relevant and important questions regarding its background, function and consequences on the spiders' life histories. In the future, common garden tests and linear or multigenerational heritability studies might make it possible to assess the nature and origin of this case of cohort splitting.

#### ACKNOWLEDGMENTS

We owe thanks for the work during the samplings to Ms. Erika Botos, Drs. Csaba Szinetár and Géza Vörös, as they provided invaluable help in field collections. We thank Stefan Sollfors for the original image of *P. agrestis* based on which the figure of phenology was created. We are indebted to Szaboles Lengyel for his aid in the preparation of the analysis in this study, and Zoltán Barta and two anonymous reviewers for their insights and constructive comments on the earlier version of the manuscript. Weather data used in the models was acquired from the homepage of CARPATCLIM Database © European Commission - JRC, 2013 (online at <http://www.carpatclim-cu.org/>). Our work was partially supported by the scholarship of Z. R. providing individual development in the National Talent Programme (NTP-EFÖ-P-15) announced by the Hungarian Human Resources Support Management. F. Samu was supported by NKFIH fund K1 16062.

#### LITERATURE CITED

- Bonte, D. & J. P. Maelfait. 2001. Life history, habitat use and dispersal of a dune wolf spider (*Pardosa monticola* [Clerek, 1757] Lycosidae, Araneae) in the Flemish coastal dunes (Belgium). *Belgian Journal of Zoology* 131:145–157.
- Brown, J.H., J.F. Gillooly, A.P. Allen, V.M. Savage & G.B. West. 2004. Toward a metabolic theory of ecology. *Ecology* 85:1771–1789.
- Callihan, J.L., L.T. Takata, R.J. Woodland & D.H. Secor. 2008. Cohort splitting in bluefish, *Pomatomus saltatrix*, in the US mid-Atlantic Bight. *Fisheries Oceanography* 17:191–205.
- Crowley, P.H. & K.R. Hopper. 2015. Mechanisms for adaptive cohort splitting. *Ecological Modelling* 308:1–13.



- Danks, H.V. 1992. Long life cycles in insects. *Canadian Entomologist* 124:167–187.
- Danks, H.V. 1994. Diversity and integration of life-cycle controls in insects. Pp. 5–40. *In* *Insect life-cycle polymorphism* (H.V. Danks (ed.)). Springer Science+Business Media, Dordrecht.
- David, J.F., M.L. Celerier & J.J. Geoffroy. 1999. Periods of dormancy and cohort-splitting in the millipede *Polydesmus angustus* (Diplopoda: Polydesmidae). *European Journal of Entomology* 96:111–116.
- David, J.F., T. Couret & M.L. Celerier. 1993. The life cycle of the millipede *Polydesmus angustus*: another case of cohort-splitting. *European Journal of Soil Biology* 29:117–125.
- Ford, M.J. 1978. Locomotory activity and the predation strategy of the wolf-spider *Pardosa amentata* (Clerck) (Lycosidae). *Animal Behaviour* 26:31–35.
- Gillooly, J.F., J.H. Brown, G.B. West, V.M. Savage & E.L. Charnov. 2001. Effects of size and temperature on metabolic rate. *Science* 293:2248–2251.
- Gonçalves, S. C., M.A. Pardal, P.G. Cardoso, S.M. Ferreira & J.C. Marques. 2005. Biology, population dynamics and secondary production of *Tylos europaeus* (Isopoda, Tyliidae) on the western coast of Portugal. *Marine Biology* 147:631–641.
- Hayashi, F. 1988. Life history variation in a dobsonfly, *Prothermus grandis* (Megaloptera: Corydalidae): effects of prey availability and temperature. *Freshwater Biology* 19:205–216.
- Honěk, A. 1988. The effect of crop density and microclimate on pitfall trap catches of Carabidae, Staphylinidae (Coleoptera), and Lyeosidae (Araneae) in cereal fields. *Pedobiologia* 32:233–242.
- Hopper, K.R. 1999. Risk-spreading and bet-hedging in insect population biology. *Annual Review of Entomology* 44:535–560.
- Irlich, U.M., J.S. Terblanche, T.M. Blackburn & S.L. Chown. 2009. Insect rate temperature relationships: environmental variation and the metabolic theory of ecology. *American Naturalist* 174:819–835.
- Johansson, F., R. Stoks, L. Rowe & M. De Block. 2001. Life history plasticity in a damselfly: Effects of combined time and biotic constraints. *Ecology* 82:1857–1869.
- Kaiser, H.F. 1960. The application of electronic computers to factor analysis. *Educational and Psychological Measurement* 20:141–151.
- Kiss, B. 2003. Autecology of the wolf spider *Pardosa agrestis* (Westring, 1861). PhD dissertation, University of Veszprém, Hungary.
- Kiss, B. & F. Samu. 2000. Evaluation of population densities of the common wolf spider *Pardosa agrestis* (Araneae: Lycosidae) in Hungarian alfalfa fields using mark-recapture. *European Journal of Entomology* 97:191–195.
- Kiss, B. & F. Samu. 2002. Comparison of autumn and winter development of two wolf spider species (*Pardosa*, Lycosidae, Araneae) having different life history patterns. *Journal of Arachnology* 30:409–415.
- Kiss, B. & F. Samu. 2005. Life history adaptation to changeable agricultural habitats: Developmental plasticity leads to cohort splitting in an agrobiont wolf spider. *Environmental Entomology* 34:619–626.
- Kozáčeková, Z., J.M.T. de Figueroa, M.J. López-Rodríguez, P. Beracko & T. Derka. 2009. Life history of a population of *Protonemura intricata* (Ris, 1902) (Insecta, Plecoptera) in a constant temperature stream in Central Europe. *International Review of Hydrobiology* 94:57–66.
- McCune, B. & M.J. Mefford. 2009. HyperNiche. Non-parametric multiplicative habitat modeling. Version 2.30. MjM Software, Gleneden Beach, OR, USA.
- Moreira, G.R.P. & B.L. Peckarsky. 1994. Multiple developmental pathways of *Agneta capitata* (Plecoptera: Perlidae) in a temperate forest stream. *Journal of North American Benthological Society* 13:19–29.
- Newman, R.A. 1989. Developmental plasticity of *Scaphiopus couchii* tadpoles in an unpredictable environment. *Ecology* 70:1775–1787.
- Newman, R.A. 1992. Adaptive plasticity in amphibian metamorphosis. *Bioscience* 42:671–678.
- Pickup, J. & D.J. Thompson. 1990. The effects of temperature and prey density on the development rates and growth of damselfly larvae (Odonata: Zygoptera). *Ecological Entomology* 15:187–200.
- Post, J.R., M.R.S. Johannes & D.J. McQueen. 1997. Evidence of density-dependent cohort splitting in age-0 yellow perch (*Perca flavescens*): potential behavioural mechanisms and population-level consequences. *Canadian Journal of Fisheries and Aquatic Sciences* 54:867–875.
- Samu, F. 1999. A general data model for databases in experimental animal ecology. *Acta Zoologica Academiae Scientiarum Hungaricae* 45:273–290.
- Samu, F. & C. Szinetár. 2002. On the nature of agrobiont spiders. *Journal of Arachnology* 30:389–402.
- Samu, F., J. Németh, F. Tóth, É. Szita, B. Kiss & C. Szinetár. 1998. Are two cohorts responsible for bimodal life history pattern in the wolf spider *Pardosa agrestis* in Hungary? Pp. 215–221. *In* *Proceedings 17th European Colloquium of Arachnology*, (P.A. Selden (ed.)). Edinburgh.
- Samu, F., C. Szinetár, É. Szita, K. Fetykó & D. Neidert. 2011. Regional variation in agrobiont composition and agrobiont life history of spiders (Araneae) within Hungary. *Arachnologische Mitteilungen* 40:105–109.
- Schaefer, M. 1977. Winter ecology of spiders (Araneida). *Zeitschrift für Angewandte Entomologie-Journal of Applied Entomology* 83:113–134.
- Stearns, S.C. & R.E. Crandall. 1981. Bet-hedging and persistence as adaptations of colonizers. Pp. 371–383. *In* *Evolution Today* (G.G.E. Scudder & J.L. Reveal (eds.)). Hunt Institute for Biological Documentation, Carnegie-Mellon University, Pittsburgh.
- Sunderland, K.D., M. Hassall & S.L. Sutton. 1976. Population dynamics of *Philoscia muscorum* (Crustacea, Oniscoidea) in a dune grassland ecosystem. *Journal of Animal Ecology* 45:487–506.
- Szalai, S., T. Antofie, P. Barbosa, Z. Bihari, M. Lakatos, J. Spinoni et al. 2012. The CARPATCLIM project: Creation of a gridded climate atlas of the Carpathian regions for 1961–2010 and its use in the European Drought Observatory of JRC. ECAC2012, Lodz.
- Townsend, G.D. & G. Pritchard. 1998. Larval growth and development of the stonefly *Pteronarcys californica* (Insecta: Plecoptera) in the Crow's Nest River, Alberta. *Canadian Journal of Zoology* 76:2274–2280.
- Tuljapourkar, S. 1994. Stochastic demography and life histories. Pp. 254–262. *In* *Frontiers in Mathematical Biology* (S.A. Levin (ed.)). Springer, Berlin Heidelberg.
- Watts, P.C. & D.J. Thompson. 2012. Developmental plasticity as a cohesive evolutionary process between sympatric alternate-year insect cohorts. *Hereditas* 108:236–241.

Manuscript received 23 January 2017, revised 31 March 2017.



## SHORT COMMUNICATION

### *Rabidosa rabida* (Walckenaer, 1837) (Araneae: Lycosidae) does not require venom injection to capture prey in the lab

Ryan Stork and Sara Wilmsen: Biology Department, Box 12251, Harding University, Searcy, AR 72149-5615; E-mail: rjstork@Harding.edu

**Abstract.** Spider venom is assumed to be used primarily to subdue larger prey and secondarily in defense. *Rabidosa rabida* (Walckenaer, 1837) is a non-web building, venomous spider. Its feeding behaviors suggest venom may not be as important as previously expected in prey capture and immobilization. We conducted feeding tests to examine the importance of venom injection in prey capture for *R. rabida*. Groups of large crickets were offered to two groups of adult female spiders with either functional or glue blocked venom pores but otherwise functional chelicerae. Our results could not confirm a significant effect of venom availability on prey capture and showed that spiders could immobilize prey without the use of their venom. These results expand upon previous studies suggesting prey capture was possible without the use of the fangs, but prey immobilization required venom. This study suggests our understanding of spider prey capture and venom use is incomplete.

**Keywords:** Chelicerae, fang, prey immobilization

Spiders are the most abundant terrestrial predators and are ecologically important because of the large number of arthropods they consume (Uetz 1992; Foelix 2011; Nyffeler & Birkhofer 2017). Studies of spider predation have mainly focused on the use of webs and venom to immobilize prey and avoid predator injury. For non-web building spiders, venom has been the primary focus of studies on the mechanics of predation. Venom can be defined as a glandular secretion containing molecules that disrupt normal physiological processes, that is delivered from the animal that produces the secretion into a target animal in order to facilitate feeding, defense, escape, or some other fitness-improving practice of the producer (Casewell et al. 2013). Spiders secrete their protein-rich and metabolically costly venoms from glands located within the prosoma. This fluid is then delivered from the gland into the target through the fang. The fangs possess a small, sub-terminal venom pore through which venom is expressed by muscular contraction of the venom glands and ducts. In addition to the venom pore, the fang also possesses cuticular features such as tooth-like projections or serrations and muscles which allow the chelicerae to be used mechanically for manipulation of web and/or prey (Foelix 2011). Other physical factors involved in prey capture, such as adhesive hairs, have been described for spiders (Rovner & Knost 1974; Rovner 1978), but it is still widely assumed that venom is the most important factor affecting any venomous spider's ability to capture prey (Foelix 2011).

*Rabidosa rabida* (Walckenaer, 1837) is found across the eastern half of North America (Brady & McKinley 1994) and occurs in high density and abundances. This spider has a large adult body size and is capable of capturing prey slightly larger than itself (Stork 2011). Indirect benefits for the plants where it hunts nocturnally, such as reduced plant damage due to herbivory, have also been shown for this spider (Schmitz & Suttle 2001). Observations of *R. rabida*'s hunting and prey capture behavior as well as a commonly cited paper (Rovner 1980) initiated interest in the use of venom for prey capture for *R. rabida*. Rovner (1980) examined physical factors involved in prey capture by *R. rabida*, including scopula hairs on the legs, musculature and tooth-like ridges on the chelicera, and use of the basal portion of the chelicera. He suggested that this species is able to use these morphological features to grasp a cricket, but is unable to immobilize prey without the use of the venom from its fangs. The methods used

by Rovner (1980) raise the question of whether it was the lack of venom injection that caused the inability to immobilize prey. In that study, the entire distal portion of the chelicera was sealed into the cheliceral grooves with wax. This resulted in both venom and the ability to naturally manipulate prey with the chelicera being unavailable. In the lab, when *R. rabida* comes into contact with multiple prey items, it will often smash these prey items together into an amorphous mass before consuming them. The observed physical manipulation of prey suggests a reduced need for venom. However, *R. rabida* hunts up in the vegetation, often without a place to chase prey, and this could suggest an increased need for venom (Binford 2001). The speed of the crushing behavior observed in spiders from Arkansas appears to support a prey capture method that would not rely on venom. We tested whether *R. rabida* would be able to capture and consume prey with and without the ability to express venom from its venom pores. We hypothesized that the ability to inject venom would not affect the proportion of prey captured and immobilized by these spiders in the lab.

To test if venom was necessary for all prey capture behaviors, we captured adult female *R. rabida* from a field adjacent to a small body of water just off the public bike trail in Searcy, Arkansas (35.26°N, 91.72°W). The spiders were housed in the lab at Harding University where they were kept in 16 × 14 × 7.5 cm clear plastic boxes on a 14:10 L:D light cycle at 25°C and were provided water *ad libitum* via cotton-stopped shell vials. Once acclimated to the lab for a week, spiders were offered 10 large crickets for 24 hours to standardize their hunger. All live crickets and cricket remains were removed from the boxes after 24 hours. All spiders that ate either 0 or 10 crickets were removed from the test along with any spiders that molted, laid an egg sack, or showed any reduction in coordination or ability to move around its enclosure. Following hunger standardization, we measured the spiders' carapace length, carapace width and mass. The spiders were divided into two groups by ordering the body size from largest carapace length to smallest. We then placed every other spider into the first group and the rest into the second group so that body sizes were distributed equally. In one group, we placed super glue (ethyl cyanoacrylate, Krazy Glue®) over the venom pore of their fangs, filling the pore and blocking the flow of any fluid through the opening. To glue a spider, we placed it into a transparent, plastic sandwich bag and pulled it tight, so that the spider was restrained but



Table 1.—Results of ANOVAs comparing size corrected proportion of prey captured by spiders with their venom pores glued shut and unglued groups of spiders. See text for description of tests 1 and 2.

Source of Variation	Test #1 df	<i>n</i> = 126 spiders			Test #2 df	<i>n</i> = 197 spiders		
		MS	F	<i>P</i>		MS	F	<i>P</i>
Group	1	0.003	1.406	0.238	1	0.003	1.137	0.288
Error	124	0.002			195	0.002		
Power estimate	0.211				0.157			

unharmful. We placed the spider on its back to expose the ventrally pointing chelicerae, and then cut a small hole in the bag just over the chelicerae. A small amount of super glue was placed in a 0.8–1.0 mm capillary tube, which fit snugly over the distal tip of the fang and immersed the fang pore in the glue. When the tube was removed, glue remained, filling the venom pore. After allowing the glue to dry, we observed each fang under a dissecting microscope to ensure the glue filled the venom pore and blocked it completely.

Spiders in the unglued group were restrained the same as the glued group and an empty capillary tube was placed over each fang. Both groups then had the effectiveness of the gluing tested using electrostimulation with a TENS pain relief kit (Medical Products Online Inc.). This battery-operated system provided a burst charge with a pulse width of 80  $\mu$ S and a pulse rate of 120 Hz. Bare lead wires and a drop of tap water were used to allow the point of stimulation to be applied to the sides of the prosoma close to the venom glands of the restrained spider. All spiders recovered quickly and completely from the shocks. Any spider that expressed fluid from the blocked pores was removed from the experiment or re-glued. Following the feeding trial, electrostimulation was again used to check that the pore blockage was not dislodged during feeding and any spiders that expressed venom were removed from analysis. The control group was handled in the same way as the glued group with the exception of the glue application to control for the potential effects of handling on feeding behavior.

Following the gluing procedure, spiders were starved for two weeks to allow for appropriate hunger and venom production. Following two weeks of starvation, the spiders were offered 20 large crickets for 24 hours. Crickets were 20 mm in body length, just under the mean body length of 20.7 mm (SD  $\pm$  1.6) for the spiders we collected during our first test. The proportion of crickets captured, and at least partially consumed, was recorded for each spider. The proportion of prey captured was calculated by dividing the number of killed and partially consumed crickets by the number offered. To scale for spider size, we divided the proportion of prey captured by carapace length. We used carapace length instead of the carapace width, because it allowed us to meet parametric assumptions in this test and has been shown in past work using *R. rabida* from Arkansas to have a significant effect more often than carapace width (Stork 2011). The proportion of prey captured controlled for body size was square-root transformed to meet parametric assumptions. We compared the proportion of prey captured, controlled for body size, between the glued and unglued groups using analysis of variance (*n* = 56 glued and 70 unglued spiders). A power analysis was run in SYSTAT 11.0 (2004) using the smallest group's sample size.

We ran a second feeding test to determine if venom loss during electrostimulation before the feeding test in the unglued group would change the results. No spiders were used in multiple tests. Spiders for the second test were captured a month later in the summer using the same methods and capture location as in the first test. In the second

test, the methods were the same as described above except that electrostimulation was conducted on both groups a week after the feeding trial rather than both before and after. We did this so that the unglued group, which would have lost venom during testing, would not have to regenerate its venom during the period of starvation before the feeding test. If venom regeneration were incomplete, it may have put this group at a prey capture disadvantage and potentially reduced the appearance of any differences between the groups. In both tests, we observed glued fangs under a dissecting microscope before the feeding test, to ensure that the fang pores were completely filled with glue. Another difference in methods in the second test was that the crickets used in the second test were slightly smaller than those in the first test (body length 15–20 mm). Given that spiders in the second test were older and thus larger than spiders in the first test (21.6 mm  $\pm$  SD 2.2), these crickets were relatively smaller. During the second feeding test, 197 spiders were tested. Glued spiders that expressed venom at electrostimulation following the feeding test were removed from the feeding test, leaving 73 spiders that did not express venom. We also tested 124 unglued spiders. The data were analyzed as in the first test. We also made qualitative observations of prey capture behavior.

Spiders that were not able to inject venom showed no significant difference in the proportion of prey captured and killed, corrected for body size, compared to the spiders that were able to inject venom. This was consistent in the first ( $F = 1.406$ ,  $P > 0.23$ , *df* = 1) and second ( $F = 1.137$ ,  $P > 0.29$ , *df* = 1) runs of the test (Table 1; Fig. 1). The power (the likelihood of correctly detecting a difference between the groups) for the first ANOVA was 0.211 for *df* = 1 and *n* = 56. The power of the second ANOVA was 0.157 for *df* = 1 and *n* = 73 (Table 1). To achieve a power of 80%, a sample size of 325 and 623 spiders in each group would be required for the first and second tests respectively.

Observation of prey capture behavior, such as the ability to grab and subdue multiple crickets at one time, did not suggest any difference between spider groups. All spiders were able to grab and subdue prey without any obvious difficulty. Most spiders from each group were able to capture multiple crickets at one time.

Our results show that, in at least some prey capture situations, venom is not vital to *R. rabida* for subduing prey, contrary to what was previously assumed. Our power was very low due to there being almost no difference between the means of each group and large variation in the proportion of prey captured for both groups. This means that a difference could exist that we were unable to show in these tests because our sample sizes were not over 600 spiders. It is possible that venom aids in prey capture, though we were unable to show that here, but it is not necessary for prey capture as even spiders that were unable to express venom were able to capture prey with no apparent difficulty. These results suggest that physical manipulation may be more important than venom in prey capture for *R. rabida*.

Our results contrast with those of Rovner (1980), who found that spiders were unable to immobilize the cricket they captured when the fang was immobilized and venom was not able to be used. We suggest that the inability to subdue prey in Rovner's paper was likely due to the inability to use the entire chelicera, though we did not directly test that here. More work needs to be done on this system to examine previous assumptions and to see if larger, more difficult, or more dangerous prey might require venom for capture by the generalist *R. rabida*.

Rovner (1980) also addressed the question of whether venom allowed for predation on larger prey. Because the spiders were unable to immobilize prey without the fangs, he concluded that venom allowed for capture and ingestion of larger prey (Rovner 1980). This conclusion is called into question by our results, as venom was not necessary to capture and consume prey if the fang was mobile and able to be used in prey immobilization. More recent studies of venom and prey size have shown a link between amount of venom used and



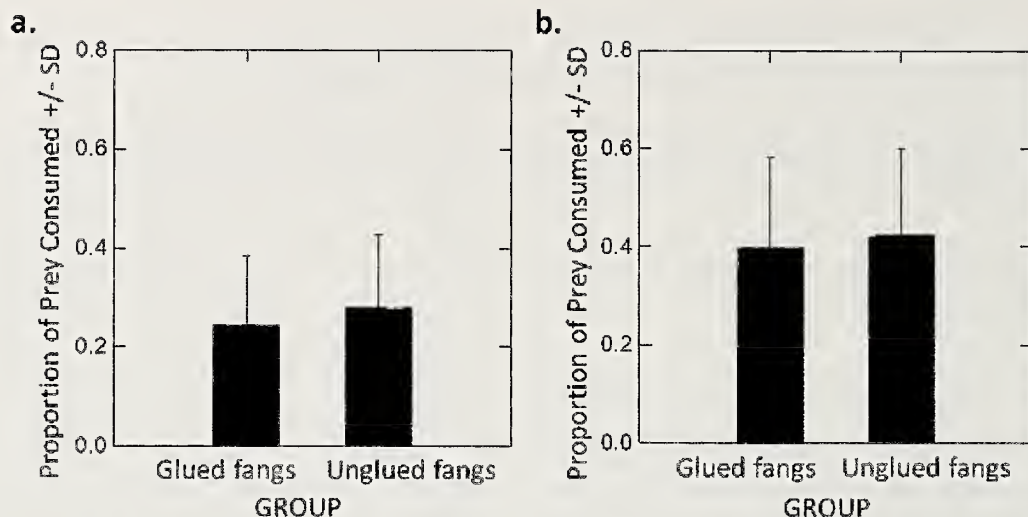


Figure 1.—A comparison of the mean proportion of prey captured and consumed by spiders with and without venom use. (a) First test conducted in early summer. (b) Second test conducted in late summer and with smaller prey size relative to larger spider size.

prey size in *Cupiennius salei* (Keyserling, 1877) (Malli et al. 1998). Other tests have shown that prey size in conjunction with the ease of handling have been found to be more important than size alone (Malli et al. 1999). These studies have advanced our understanding of the role of venom in predation by wandering spiders, but have focused almost entirely on the etcnid *C. salei*, which is found in Eastern Mexico, Guatemala, Belize, and Honduras. These questions have not been applied adequately to other spiders, including those in North America. We would like to see further exploration into the characters affecting prey capture and the role of venom and digestive fluid for *R. rabida* and other families of wandering spiders. A better understanding of the role of venom in prey capture for spiders in general is dependent on diversifying the species used to address these questions and looking at how consistent the dependence on venom is between families (Rovner 1980).

#### ACKNOWLEDGMENTS

We would like to thank the American Arachnological Society Research Fund, the Harding University Biology Department, and the Harding University Margaret M. Plummer Memorial Research Fund for funding this research.

#### LITERATURE CITED

- Binford, G.J. 2001. Differences in venom composition between orb-weaving and wandering Hawaiian *Tetragnatha* (Araneae). *Biological Journal of the Linnean Society* 74:581–595.
- Brady, A.R. & K.S. McKinley. 1994. Nearctic species of the wolf spider genus *Rabidosa* (Araneae: Lycosidae). *Journal of Arachnology* 22:138–160.
- Caswell, N.R., W. Wuster, F.J. Vonk, R.A. Harrison & B.G. Fry. 2013. Complex cocktails: the evolutionary novelty of venoms. *Trends in Ecology and Evolution* 28:219–229.
- Foelix, R. F. 2011. *Biology of Spiders* 3<sup>rd</sup> ed. Oxford University Press, New York.
- Malli, H., H. Imboden & L. Kuhn-Nentwig. 1998. Quantifying the venom dose of the spider *Cupiennius salei* using monoclonal antibodies. *Toxicon* 36:1959–1969.
- Malli, H., L. Kuhn-Nentwig, H. Imboden & W. Nentwig. 1999. Effects of size, motility and paralysation time of prey on the quantity of venom injected by the hunting spider *Cupiennius salei*. *Journal of Experimental Biology* 202:2083–2089.
- Nyffeler, M. & K. Birkhofer. 2017. An estimated 400–800 million tons of prey are annually killed by the global spider community. *The Science of Nature* 104:30.
- Rovner, J.S. 1978. Adhesive hairs in spiders: behavioral functions and hydraulically mediated movement. *Symposium at the Zoological Society of London* 42:99–108.
- Rovner, J.S. 1980. Morphological and ethological adaptations for prey capture in wolf spiders (Araneae: Lycosidae). *Journal of Arachnology* 8:201–215.
- Rovner, J.S. & S.J. Knost. 1974. Post-immobilization wrapping of prey by lycosid spiders of the herbaceous stratum. *Psyche* 81:398–415.
- Schmitz, O. J. & K. Suttle. 2001. Effects of top predatory species on direct and indirect interactions in a food web. *Ecology* 82:2072–2081.
- Stork, R.J. 2011. Intra-specific variation across a small temperature difference in the spider *Rabidosa rabida* (Araneae: Lycosidae) from the mountains of Arkansas. Ph.D. Dissertation Thesis from the University of Texas at Arlington.
- SYSTAT, Inc. 2004. Systat Software Inc.
- Uetz, G.W. 1992. Foraging strategies of spiders. *Trends in Ecology and Evolution* 7:155–159.

*Manuscript received 15 November 2016, revised 19 April 2017.*



## INSTRUCTIONS TO AUTHORS

(revised January 2017)

All manuscripts are submitted online at  
<http://www.editorialmanager.com/arachno>

**General:** The *Journal of Arachnology* publishes scientific articles reporting novel and significant observations and data regarding any aspect of the biology of arachnid groups. Articles must be scientifically rigorous and report substantially new information. Submissions that are overly narrow in focus (e.g., local faunal lists, descriptions of a second sex or of a single species without additional discussion of the significance of this information), that have poorly substantiated observational data, or that present no new information will not be considered. Book reviews will not be published.

Manuscripts must be in English and should use the active voice throughout. Authors should consult a recent issue of the *Journal of Arachnology* for additional points of style. Manuscripts longer than three printed journal pages (12 or more double-spaced manuscript pages) should be prepared as Feature Articles, shorter papers as Short Communications. Invited Reviews will be published from time to time and unsolicited reviews are also welcomed. All reviews will be subject to the same review process as other submissions.

**Submission:** Manuscripts should be prepared in Microsoft Word and then submitted electronically via our online system, *PeerTrack* (<http://www.editorialmanager.com/arachno>). *PeerTrack* will guide you through the step-by-step process including uploading the manuscript and all of its parts. The paper can be uploaded as one piece, with tables, figures, and appendices embedded, or as text, then tables, figures, and appendices, each uploaded individually. Ultimately, *PeerTrack* will assemble all parts of the paper into a PDF that you, as corresponding author, will need to approve before the submission process can be completed. Supplemental Materials (see below) can also be uploaded, but they are not bundled into the PDF.

**Voucher Specimens:** Specimens of species used in your research should be deposited in a recognized scientific institution. All type material *must* be deposited in a recognized collection/institution and the identity of the collection must be given in the text of the manuscript.

**Checklist—Common Formatting Errors** is available as a PDF at <http://www.americanarachnology.org/JOA.html#instructions>

### FEATURED ARTICLES

**Title page.**—The title page includes the complete name, address, and e-mail address of the corresponding author; the title in bold text and sentence case; each author's name and address; and the running head.

**Running head.**—This should be in all capital letters, not exceeding 60 characters and spaces, and placed at the top of the title page. It should be composed of the authors' surnames and a short title. Examples: SMITH—SALTICIDS OF PANAMA; SMITH & CRUZ—SALTICIDS... ; SMITH ET AL.—SALTICIDS...

**Abstract.**—Length: ≤ 250 words for Feature Articles; ≤ 150 words for Short Communications.

**Keywords.**—Give 3–5 appropriate keywords or phrases following the abstract. *Keywords should not duplicate words in the title.*

**Text.**—Double-space text, tables, legends, etc. throughout. Except for titles and headers, all text should be left-justified. Do not add line numbers—they are automatically added by *PeerTrack*. Three levels of heads are used.

- The first level (METHODS, RESULTS, etc.) is typed in capitals and centered on a separate line.
- The second level head begins a paragraph with an indent, is in bold type, and is separated from the text by a period and a dash.
- The third level may or may not begin a paragraph but is italicized and separated from the text by a colon.

Use only the metric system unless quoting text or referencing collection data. If English measurements are used when referencing collection data, then metric equivalents should also be included parenthetically. All decimal fractions are indicated by a period (e.g., 3.141). Include geographic coordinates for collecting locales if possible, using one of the following formats: 0°12'32"S, 29°52'17"E or 0.2089°S, 29.8714°E.

**Citation of references in the text:** Cite only papers already published or in press. Include within parentheses the surname of the author followed by the date of publication. A comma separates multiple citations by the same author(s) and a semicolon separates citations by different authors, e.g., (Smith 1970), (Jones 1988; Smith 1993), (Smith & Jones 1986, 1987; Jones et al. 1989). Include a letter of permission from any person who is cited as providing unpublished data in the form of a personal communication.

**Citation of taxa in the text:** Include the complete taxonomic citation (author, year) for each arachnid genus and/or species name when it first appears in the abstract and text proper. For example, *Araneus diadematus* Clerck, 1757. For Araneae, this information can be found online at [www.wsc.nmbe.ch](http://www.wsc.nmbe.ch). Citations for scorpions can be found in the *Catalog of the Scorpions of the World (1758–1998)* by V. Fet, W.D. Sissom, G. Lowe & M.E. Braunwalder. Citations for the smaller arachnid orders (pseudoscorpions, solifuges, whip scorpions, whip spiders, schizomids, ricinuleids and palpigrades) can be found at [museum.wa.gov.au/catalogues-beta/](http://museum.wa.gov.au/catalogues-beta/). Citations for some species of Opiliones can be found in the *Annotated Catalogue of the Laniatores of the New World (Arachnida, Opiliones)* by A.B. Kury.

**Literature cited.**—Use the following style and formatting exactly as illustrated; include the full unabbreviated journal title. Personal web pages should not be included in Literature Cited. These can be cited within the text as (John Doe, pers. website) without the URL. Institutional websites may be included in Literature Cited. If a citation includes more than six authors, list the first six and add "et al." to represent the others.



- Binford, G. 2013. The evolution of a toxic enzyme in sicariid spiders. Pp. 229–240. *In* Spider Ecophysiology. (W. Nentwig, ed.). Springer-Verlag, Heidelberg.
- Cushing, P.E., P. Casto, E.D. Knowlton, S. Royer, D. Laudier, D.D. Gaffin et al. 2014. Comparative morphology and functional significance of setae called papillae on the pedipalps of male camel spiders (Arachnida, Solifugae). *Annals of the Entomological Society of America* 107:510–520.
- Harvey, M.S. & G. Du Preez. 2014. A new troglobitic ideoroncid pseudoscorpion (Pseudoscorpiones: Ideoroncidae) from southern Africa. *Journal of Arachnology* 42:105–110.
- World Spider Catalog. 2015. World Spider Catalog. Version 16. Natural History Museum, Bern. Online at <http://wsc.nmbe.ch/>
- Roewer, C.F. 1954. *Katalog der Araneae*, Volume 2a. Institut Royal des Sciences Naturelles de Belgique, Bruxelles.
- Rubio, G.D., M.O. Arbino & P.E. Cushing. 2013. Ant mimicry in the spider *Myrmecotypus iguazu* (Araneae: Corinnidae), with notes about myrmecomorphy in spiders. *Journal of Arachnology* 41:395–399.

**Footnotes.**—Footnotes are permitted on the first page, only to give current address or other author information, and at the bottom of tables (see below).

**Taxonomic articles.**—Consult a recent taxonomic article in the *Journal of Arachnology* for style or contact a Subject Editor for Systematics. Papers containing original descriptions of focal arachnid taxa should be listed in the Literature Cited section.

**Tables.**—Each table, with the legend above, should be placed on a separate manuscript page. Only horizontal lines (usually no more than three) should be included. When necessary, tables may have footnotes, for example, to specify the meanings of symbols about particular data.

**Illustrations.**—Original illustrations include photographs, line drawings, maps, and other graphic representations. All should be considered figures and numbered consecutively with other figures. You should ensure that all illustrations, at submission, are at high enough resolution to be useful to editors and reviewers; 300 dpi is usually sufficient.

At the discretion of the Editor-in-Chief, a figure can be rendered in color in the online version but in monochrome in the journal's printed version, or in color in both versions if warranted by the figure's context and content. Most figures will be reduced to single-column width (9 cm, 3.5 inches), but large plates can be printed up to two-columns width (18 cm, 7 inches). Address all questions concerning illustrations to the Editor-in-Chief of the *Journal of Arachnology*: **Deborah R. Smith, Editor-in-Chief** [E-mail: [debsmith@ku.edu](mailto:debsmith@ku.edu)].

**Legends for illustrations** should be placed together on the same page(s). Each plate must have only one legend, as indicated below:

Figures 1–4. *A-us x-us*, male from Timbuktu: 1. Left leg. 2. Right chelicera. 3. Dorsal aspect of genitalia. 4. Ventral aspect of abdomen.

The following alternate Figure numbering is also acceptable:

Figure 1a–e. *A-us x-us*, male from Timbuktu: a. Left leg. b. Right chelicera. c. Dorsal aspect of genitalia. d. Ventral aspect of abdomen.

**Assemble manuscript.**—The manuscript should be assembled in the following sequence: title page, abstract, text, tables with legends, figure legends, figures. As noted above, at the time of submission the paper can be uploaded as one piece, with tables, figures, and appendices embedded, or as text, then tables, figures, and appendices, each uploaded individually.

**Supplemental materials.**—Authors may submit for online publication materials that importantly augment the contents of a manuscript. These may be audio files (e.g., .mp3, .m4a, .aif, .wav), video files (e.g., .mov, .m4v, .flv, .avi), or Word documents (e.g., .doc, .docx) for large tables of data. Consult with the Editor-in-Chief if you are considering submitting other kinds of files. Audio and video files should be carefully edited before submission to eliminate leaders, trailers, and other extraneous content. Individual files may not exceed 10MB; no more than five files may be included as supplemental materials for a manuscript.

Supplemental materials will be considered by reviewers and therefore must be included at the time of manuscript submission. Supplemental materials are published online at the discretion of the editors.

## SHORT COMMUNICATIONS

Short Communications are usually limited to 3–4 journal pages, including tables and figures (11 or fewer double-spaced manuscript pages including Literature Cited; no more than 2 figures or tables). Internal headings (METHODS, RESULTS, etc.) are omitted. Short communications must include an abstract and keywords.

**Page charges.**—Page charges are voluntary, but authors who are not members of the American Arachnological Society are strongly encouraged to pay in full or in part for their articles (\$75 per journal page).

**Proofs.**—The Journal's expectation is that the final revision of a manuscript, the one that is ultimately accepted for publication, will not require substantive changes. Accordingly, the corresponding author will be charged for excessive numbers of changes made in the proofs.

**Reprints.**—Hard copy reprints are available only from Allen Press via EzReprint, a user-friendly, automated online system for purchasing article reprints. If your paper is accepted, prior to its publication you will receive an e-mail containing both a unique URL (SmartLink) from Allen Press/Yurchak Press and information about the reprint order process. Clicking on the SmartLink will take you directly to a web portal where you may place your reprint order. The email will be sent to you from: [reprints@authorbilling.com](mailto:reprints@authorbilling.com). PDFs of papers published in the *Journal of Arachnology* are available to AAS members at the society's web site. They are also available through BioOne ([www.bioone.org](http://www.bioone.org)) and JSTOR ([www.jstor.org](http://www.jstor.org)) if you or your institution is a member of BioOne or JSTOR. PDFs of articles older than one year are freely available from the AAS website.

## COVER ARTWORK

Authors are encouraged to send high quality color photographs to the Editor-in-Chief to be considered for use on the cover. Images should be at least 300 dpi.









## CONTENTS

## Journal of Arachnology

Volume 45

Number 3

## Papers from the 20th International Congress of Arachnology

Sand transport and burrow construction in sparassid and lycosid spiders by Rainer Foelix, Ingo Rechenberg, Bruno Erb, Andrea Albín & Anita Aisenberg .....	255
Exploring the chemo-textural familiarity hypothesis for scorpion navigation by Douglas D. Gaffin & Brad P. Brayfield .....	265
Retreat availability and social influences on retreat sharing in group-living huntsman spiders, <i>Delena lapidicola</i> and <i>Delena cancerides</i> (Araneae: Sparassidae) by Cameron Jones & Linda S. Rayor .....	271
Effect of seasonal photoperiod on molting in <i>Loxosceles reclusa</i> and <i>Loxosceles laeta</i> spiders (Araneae: Sicariidae) by Richard S. Vetter, Linda M. Penas & Mark S. Hoddle .....	277
In the spider nursery: indifference, cooperation or antagonism? by Susan E. Riechert, Jonathan Pruitt & Jennifer Bosco .....	283
A new <i>Liphistius</i> species (Mesothelae: Liphistiidae: Liphistiinae) from Thailand, with notes on its natural history by Varat Sivayyapram, Deborah Roan Smith, Suthon Weingdow & Natapot Warrit .....	287
Revision of <i>Misumessus</i> (Thomisidae: Thomisinae: Misumenini), with observations on crab spider terminology by G. B. Edwards .....	296
A review of Burmese amber arachnids by Paul A. Selden & Dong Ren .....	324

## Featured Articles

An unusual new wolf spider species from the Erg Chebbi Desert in Morocco (Araneae: Lycosidae: Evippinae) by Steffen Bayer, Rainer Foelix & Mark Alderweireldt .....	344
Effects of nectar feeding on cannibalism in striped lynx spiderlings <i>Oxyopes salticus</i> (Araneae: Oxyopidae) by Laurel B. Lietzenmayer & James D. Wagner .....	356
Population structure of the expansive wasp spider ( <i>Argiope bruennichi</i> ) at the edge of its range by Wioletta Wawer, Robert Rutkowski, Henrik Krehenwinkel, Dorota Lutyk, Karolina Pusz-Bocheńska & Wiesław Bogdanowicz .....	361
Pseudoscorpions of the family Cheiridiidae (Arachnida: Pseudoscorpiones) recovered from burial sediments at Pachacamac (500–1,500CE), Perú by Johnica J. Morrow, Livia Taylor, Lauren Peck, Christian Elowsky, Lawrence Stewart Owens, Peter Eeckhout & Karl J. Reinhard .....	370
Three new species of comb-tailed spiders (Araneae: Hahniidae) from a Mexican oak forest with comments on their natural history and sexual behavior by M. Antonio Galán-Sánchez & Fernando Alvarez-Padilla .....	376
Systematics of the spiny trapdoor spiders of the genus <i>Cataxia</i> (Mygalomorphae: Idiopidae) from southwestern Australia: documenting a threatened fauna in a sky-island landscape by Michael G. Rix, Karlene Bain, Barbara Y. Main, Robert J. Raven, Andrew D. Austin, Steven J. B. Cooper & Mark S. Harvey .....	395
Redescription of <i>Geogarypus minor</i> , type species of the genus <i>Geogarypus</i> , and description of a new species from Italy (Pseudoscorpiones: Geogarypidae) by Giulio Gardini, Loris Galli & Matteo Zinni .....	424

## Short Communications

Effect of weather conditions on cohort splitting in a wolf spider species by Zoltán Rádai, Balázs Kiss & Ferenc Samu .....	444
<i>Rabidosa rabida</i> (Walckenaer, 1837) (Araneae: Lycosidae) does not require venom injection to capture prey in the lab by Ryan Stork & Sara Wilmsen .....	448
Instructions to Authors .....	451